



Student Poster Session

2019 IEEE PES General Meeting

Atlanta, GA USA

August 4-8, 2019

Poster Categories:

- Advanced Computational Methods for Power System Planning, Operation, and Control
- Asset Management
- Communication & Control in Energy Systems
- Cyber & Physical Security of the Smart Grid
- Dynamic Performance and Control of Power Systems
- Emerging Software Needs for the Restructured Grid
- Integrating Renewable Energy into the Grid
- Intelligent Monitoring & Outage Management
- Market Interactions in Power Systems
- Operation & Control
- Power Electronics
- Power System Modeling & Simulation
- Smart Cities
- Smart Grid Technology
- Smart Sensors
- Substation and Distribution Automation
- System-Wide Events and Analysis Methods

IEEE PES Student Activities Subcommittee

Dr. Aaron St. Leger, Dr. Valentina Cecchi, Dr. Sridhar Chouhan, Dr. Anthony Deese

Advanced Computational Methods for Power System Planning, Operation, and Control

Poster #	Title	Student Name		UG/Grad
		First	Last	
19STUGM001	Adaptive Trading in the Continuous Intraday Market	Gilles	Bertrand	Grad
19STUGM002	Statistical Interaction Boundary Determination on the Impact of Renewable Energy Resources	Namki	Choi	Grad
19STUGM003	Power System Operations under Data Asymmetry: Towards Learning and Sharing	Vladimir	Dvorkin	Grad
19STUGM004	Application of Load Switching Events in Steady-State Load Modeling in Power Distribution Networks	Alireza	Shahsavari	Grad
19STUGM005	Scalable Optimization Techniques for Market Integration of Highly Distributed Energy Resources	Stephen	Fatokun	Grad
19STUGM006	A Graph Computation based Sequential Power Flow Calculation for Large-Scale ACDC Systems	Wei	Feng	Grad
19STUGM007	Distribution Network Dynamic Reconfiguration Using Reinforcement Learning	Yuanqi	Gao	Grad
19STUGM008	Data-driven Decision Making in Power Systems with Probabilistic Guarantees	Xinbo	Geng	Grad
19STUGM009	Detecting and Locating Smart Grid Cyber Attacks in Real-Time: A Data-driven Approach	Md Abul	Hasnat	Grad
19STUGM010	Estimation of System Inertia using Center of Inertia Frequency Methodology	Seunghyuk	Im	Grad
19STUGM012	Cyberattack-Resilient Load Forecasting with Adaptive Robust Regression	Jieying	Jiao	Grad
19STUGM013	A Two-Stage Algorithm for Optimal Scheduling of Battery Energy Storage Systems for Peak-Shaving	Roozbeh	Karandeh	Grad
19STUGM014	An Enhanced Wide Area Generation Control Scheme under High Renewable Penetration	Christoph	Lackner	Grad
19STUGM015	Synchrophasor Calculation Algorithm Based on Robust State Estimation	Yunting	Li	Grad
19STUGM016	Power System Event Classification using PMU Data in a Deep Learning Platform	Kaveri	Mahapatra	Grad
19STUGM017	Tractable Preventive Stochastic Unit-Commitment for Large Systems with Multiple Line Outages	Farshad	Mohammadi	Grad
19STUGM018	A Data-driven Approach to Predict Size of Cascades using Community Structures in Interaction Graphs	Upama	Nakarmi	Grad
19STUGM019	Tightening QC Relaxations of AC Optimal Power Flow Problems via Coordinate Transformations	Mohammad Rasoul	Narimani	Grad
19STUGM020	Co-Optimized Expansion Planning to Enhance Resilience of the Electrical Infrastructure in Puerto Rico	Cody	Newlun	Grad
19STUGM021	Sufficient Condition for Small-Signal Stability and Construction of Robust Stability Region	Parikshit	Pareek	Grad
19STUGM022	Formulation of a Distributed AC Volt-Var Optimization in Distribution Power Systems	Niloy	Patari	Grad
19STUGM023	Optimal-Probabilistic Coordination of Directional Overcurrent Relays Considering Network Topological Uncertainties	Jiawei	Qi	Grad
19STUGM024	Security Constrained Unit Commitment with Corrective Transmission Switching	Arun Venkatesh	Ramesh	Grad
19STUGM025	Anticipating Impact of Q-Limits for Enhancement of PMU Based Fast Voltage Stability Index	Syed Muhammad Hur	Rizvi	Grad
19STUGM026	Classroom Object for Simulation and Analysis of Power Grid Frequency and Mode Estimates	Pranav	Shrestha	UG
19STUGM027	Enabling Cyberattack-Resilient Load Forecasting through Adversarial Machine Learning	Zefan	Tang	Grad

19STUGM028	Convexified OPF in Multiphase Low Voltage Radial Distribution Networks including Neutral Conductor	Muhammad	Usman	Grad
19STUGM029	MILP-Based Algorithm for the Global Solution of Dynamic Economic Dispatch Problems with Valve-Point Effects	Loïc	Van Hoorebeeck	Grad
19STUGM030	Advanced Distribution Protection for High Penetration of Distributed Energy Resources (DER)	Yaswanth Nag	Velaga	Grad
19STUGM031	A Data-driven Control Method for Operating the Commercial HVAC Load as a Virtual Battery	Jiyu	Wang	Grad
19STUGM032	Chordal Conversion based Convex Iteration Algorithm for Three-phase Optimal Power Flow	Wei	Wang	Grad
19STUGM033	A Stacked Autoencoder Application for Residential Load Curve Forecast and Peak Shaving	Xinan	Wang	Grad
19STUGM034	Data-driven Distributionally Robust Energy Consumption Scheduling of HVAC based on Disjoint Layered Ambiguity Set	Yingjie	Wang	Grad
19STUGM035	Distributed Multi-Functional Finite-Time Secondary Control in Cyber-Physical Microgrid	Yao	Weitao	Grad
19STUGM036	Enabling the Hardware-in-the-loop Co-simulation of Distribution Volt-Var Control through the Optimization of Sub-transmission Voltage Regulation	Fuhong	Xie	Grad
19STUGM037	Blockchain Framework for Peer-to-Peer Energy Trading with Credit Rating	Jiawei	Yang	Grad
19STUGM038	Studying the influence of flexibility provided by aggregated EVs on power system operating risk	Mingzhi	Zhang	Grad
19STUGM212	Indirect Adaptive Control of a Power Distribution System based on Backpropagation of Utility	Hasala	Dharmawardena	Grad

Asset Management

Poster #	Title	Student Name		UG/Grad
		First	Last	
19STUGM039	Energy Portfolio-based Joint Flexibility Scheduling of Coordinated Microgrids	Farhad	Angizeh	Grad
19STUGM040	Performance Evaluation of Fiber Optic Sensors to Measure Moisture in Transformer Insulation	Muhammad	Ansari	Grad
19STUGM041	Finite Element Analysis on On-load Tap Changer (OLTC) Tap Selector Electrical Breakdown Mechanism Caused by Silver Sulphide Corrosion	Sameera	Samarasinghe	Grad
19STUGM042	Transformer Loss of Life Mitigation in the Presence of Energy Storage and PV Generation	Milad	Soleimani	Grad

Communication & Control in Energy Systems

Poster #	Title	Student Name		UG/Grad
		First	Last	
19STUGM043	A Hybrid Systems Approach to Modeling and Analysis of TCL Coordination	Md Salman	Nazir	Grad
19STUGM044	Time Stamp Based IEC 61850 GOOSE Performance Testing	Jan	Westman	Grad
19STUGM045	Scenario-based Optimal Transmission Switching With Uncertain Wind Power	Yuqi	Zhou	Grad

Cyber & Physical Security of the Smart Grid

Poster #	Title	Student Name		UG/Grad
		First	Last	
19STUGM046	Publicly Available Information Driven Cyber Threats in Power Grids Imposed Through IoT of Electric Vehicle System	Samrat	Acharya	Grad
19STUGM047	Impact Assessment of Credible Contingency and Cyber Attack on Australian 14-Generator Interconnected Power System	B M Ruhul	Amin	Grad
19STUGM048	Detecting Line Failures using PMU Time Series for Smart Grids under Cyber-Physical Stresses.	Md Jakir	Hossain	Grad
19STUGM049	False Data Detection in Electric Energy Systems	Ramin	Kaviani	Grad
19STUGM050	Resilient Secondary Frequency Control of Islanded Microgrid in the Presence of Renewable Energy	Mohammad Reza	Khalghani	Grad
19STUGM051	Multistage Game for Smart Grid Security	Shuva	Paul	Grad
19STUGM052	A Simplified Criterion for Identifying a System's Vulnerability to Outage Contingency	Mahdi	Rouholamini	Grad
19STUGM053	Cybersecurity of Smart Inverters in a Distribution System	Chih-Che	Sun	Grad
19STUGM054	Securing Power Distribution Grid Against Power Botnet Attacks	Lizhi	Wang	Grad

Dynamic Performance and Control of Power Systems

Poster #	Title	Student Name		UG/Grad
		First	Last	
19STUGM055	A Discrete Event Theory Based Approach for Modeling Power System Cascading Failures	Wasseem	Alrousan	Grad
19STUGM056	Mode Shape Localization in Inverter-Based Microgrids	Andrey	Gorbunov	Grad
19STUGM057	Flexibility and Stability of an Islanded Microgrid with Smart Loads	Jinrui	Guo	Grad
19STUGM058	Impact of PLL on Harmonic Stability of Renewable Dominated Power System	Indla	Priyamvada	Grad
19STUGM059	Optimal-Probabilistic Coordination of Directional Overcurrent Relays Considering Network Topological Uncertainties	Tongkun	Lan	UG
19STUGM060	Evaluation of High Solar Penetration Impact on Bulk System Stability through a Transmission-Distribution Dynamics Co-simulation	Qinmiao	Li	Grad
19STUGM061	Frequency Control of Decoupled Synchronous Machine Using Koopman Operator Based Model Predictive	Xiawen	Li	Grad
19STUGM062	PMU-based Estimation of the Frequency of the Center of Inertia and Generator Rotor Speeds	Muyang	Liu	Grad
19STUGM063	A New Distributed Voltage Controller for Enabling Volt-Var Support of Microgrids in Grid-Connected Operation	Qian	Long	Grad
19STUGM064	Design and simulation of inertia emulation control for a wind turbine generator	Samaneh	Morovati	Grad
19STUGM065	Distinguishing between Natural and Forced Oscillations in the Power Grid	Herschel	Norwitz	UG
19STUGM066	Visualization the Stability Boundary of Low-Order System to Determine the Transient Stability	Chen	Qi	Grad

19STUGM067	Online Monitoring & Mitigation of Delayed Voltage Recovery in Distribution Networks Using DERs and Controllable Loads	Amarsagar Reddy	Ramapuram Matavalam	Grad
19STUGM068	Data-driven Identification and Prediction of Power System Dynamics Using Linear Operators	Pranav	Sharma	Grad
19STUGM069	Thermostatic load control for frequency regulation considering progressive recovery	Qingxin	Shi	Grad
19STUGM070	An Enhancement in Sum-of-Squares Optimization based Region of Attraction Estimation for Power Systems	Soumyabrata	Talukder	Grad
19STUGM071	Feedforward-Based Accurate Power Sharing and Voltage Control for Multi-Terminal HVDC Grids	Armin	Teymouri	Grad
19STUGM072	Machine-Learning based Advanced Dynamic Security Assessment	Ramin	Vakili	Grad
19STUGM073	Impact of High Penetration of Renewable Resources on Power System Transient Stability	Wenting	Yi	Grad
19STUGM074	Preventive Transient Stability Control of Power Systems with High Level Wind Power	Heiling	Yuan	Grad
19STUGM213	Dynamic Multi-swarm PSO based Tuning of Power System Stabilizer in 12 Bus Power systems	Lili	Wu	Grad

Emerging Software Needs for the Restructured Grid

Poster #	Title	Student Name		UG/Grad
		First	Last	
19STUGM075	A Performace Comparison of Parallel Power Load Flow Implementations	Afshin	Ahmadi	Grad
19STUGM076	Human-centered Electricity Services for the Future Distribution Grid	Athindra	Venkatraman	Grad

Integrating Renewable Energy into the Grid

Poster #	Title	Student Name		UG/Grad
		First	Last	
19STUGM077	A coupled modeling approach for microgrid reliability assessment and system sizing	Ahmed	Abdelsamad	Grad
19STUGM078	Data-Driven Risk Assessment of Wind-Integrated Power Systems via Finite Mixture Models and Importance Sampling	Osama	Ansari	Grad
19STUGM079	Design of a 4 Dimensional Battery Model (4DM) for Improved Remaining Useful Life Assessment of Energy Storage Devices	Bharat	Balagopal	Grad
19STUGM080	Replacement of Synchronous Generator by Virtual Synchronous Generator in the Conventional Power System	Junru	Chen	Grad
19STUGM081	Comparison of RMS and EMT Simulations of a Two-Area System with High Renewable Penetration	Angel	Clark	Grad
19STUGM082	Probabilistic Solar Power Forecasting Using Bayesian Model Averaging	Kate	Doubleday	Grad
19STUGM083	Abnormal Data Filtering Framework for Smart Battery Gauge at Butler's Farm Microgrid	Cong-Sheng	Huang	Grad
19STUGM084	Meeting Onshore Grid Demands through Offshore Wind Integrated VSC Controlled MT-HVDC System	Faria	Kamal	Grad
19STUGM085	Game-Theoretic Modeling for Strategic Regulators in Electricity Market	Jip	Kim	Grad

19STUGM086	Optimal Controller Design for Stabilizing a Power System with Multiple Converter-interfaced Generators	Ryangkyu	Kim	Grad
19STUGM087	Distribution Voltage Regulation Using Combined Local and Central Control Based on Real-Time Data	Min-seung	Ko	Grad
19STUGM088	Optimum Design of Battery-Assisted Photo-Voltaic Energy System for a Commercial Application	Yaze	Li	Grad
19STUGM089	Replicating Real-World Wind Farm SSR Events	Yin	Li	Grad
19STUGM090	Voltage Regulation in Distribution Systems with High Penetration of Renewable Resources	Daniel	Lima	Grad
19STUGM091	Coordinated Control Strategies of PMSG-based Wind Turbine for Smoothing Power Fluctuations	Xue	Lyu	Grad
19STUGM092	Blackstart of DFIG-based Windfarm	Duncan	Maina	Grad
19STUGM093	Impact of Smart Inverters on Dynamic SVR Settings for Distribution Voltage Control	H M Mesbah	Maruf	Grad
19STUGM094	Benefits of Coordinating Voltage Regulators, Capacitors, Smart Inverters, and Demand Response for Distribution Volt-Var Control	Catherine	McEntee	Grad
19STUGM095	A Two-Step Frequency Support Method for Multi-Terminal DC Grids	Mahmoud	Mehrabankhomartash	Grad
19STUGM096	Variable Power Factor DERs and Their Effect on Hosting Capacity	Luther	Miller	UG
19STUGM097	Resource-Mix Variability Mitigation: EWT Based Optimal Sizing/Control of Hybrid Storage System	Abdul Saleem	Mir	Grad
19STUGM098	A Study on Volt-Watt Mode of Smart Inverter to Prevent Voltage Rise with High Penetration of PV System	Jinah	Noh	Grad
19STUGM099	Cooperative Dynamic Demand Response Optimization of a Multistory Building	Chirath	Pathiravasam	Grad
19STUGM100	Interaction between Line Impedance and Inverter Control in Low-voltage Microgrid	Ishita	Ray	Grad
19STUGM101	Performing remote estimations in LV feeders based solely on local monitoring	Valentin	Rigoni	Grad
19STUGM102	Unlocking Linepack Flexibility from Integrated Energy Systems: Convexification Approaches	Anna	Schwele	Grad
19STUGM103	Design and Control of Storage Systems for Voltage Source Controlled Autonomous Microgrids	Lalitha	Subramanian	Grad
19STUGM104	Levelized Cost Analysis of Medium Voltage DC Fast Charging Station	Lisha	Sun	Grad
19STUGM105	Model Predictive Frequency Control of Low Inertia Power Systems	Ujjwol	Tamrakar	Grad
19STUGM106	Optimal Design and Operation Cost of Distributed Energy Resources in a Isolated Microgrid	Fatemeh	Tooryan	Grad
19STUGM107	Improved reactive power sharing between droop controlled inverters in islanded microgrid	Vishal	Verma	Grad
19STUGM108	Active fault management for networked microgrids	Wenfeng	Wan	Grad
19STUGM109	Energy Storage Sizing for Dispatchable Constant Production PV Power Plant	Qianxue	Xia	Grad
19STUGM110	Characterization of Congestion in Distribution Network Considering High Penetration of PV Generation and EVs	Jinping	Zhao	Grad

Intelligent Monitoring and Outage Management

Poster #	Title	Student Name		UG/Grad
		First	Last	
19STUGM111	Natural Hazard Awareness and Sequential Restoration for Distribution Systems and Microgrids	Ogbonnaya	Bassey	Grad
19STUGM112	Reconstruction of Power System Measurements Based on Enhanced Denoising Autoencoder	You	Lin	Grad
19STUGM113	Detecting Behind-the-Meter PV Installation Using Convolutional Neural Networks	Sadegh	Vejdan	Grad
19STUGM114	New Reward and Penalty Scheme for Electric Distribution Utilities Employing Load-Based Reliability Indices	Bo	Wang	Grad
19STUGM115	A Data-Driven Algorithm for Online Power Grid Topology Change Identification with PMUs	Shiyuan	Wang	Grad
19STUGM116	Single-Ended Fault Location for Hybrid Transmission Line using Embedded Artificial Intelligence	Rong	Yan	Grad
19STUGM214	Online Identification Tool for Power System Component Events	Dulip	Madurasinghe	Grad

Market Interactions in Power Systems

Poster #	Title	Student Name		UG/Grad
		First	Last	
19STUGM117	The Optimal Use of Tax Incentives for Wind Power	Alejandro	Castillo	Grad
19STUGM118	Intraday dispatch, energy storage, and the value of re-scheduling in systems with high wind shares	Irene	Danti Lopez	Grad
19STUGM119	Newly Implemented and Proposed Market Products and Reformulations: Stochasticity modeling and flexible ramp products	Mohammad	Ghaljehei	Grad
19STUGM120	Peer-to-Peer (P2P) Energy Exchange in Distribution Networks Considering Network Constraints	Hamed	Haggi	Grad
19STUGM121	Efficient Algorithms for Allocating Payoffs in a Peer-to-Peer Energy Sharing Cooperative Game	Liyang	Han	Grad
19STUGM122	Day-Ahead Bidding of a Pulp & Paper Mill in the Nordic Energy and Reserve Market	Lars	Herre	Grad
19STUGM123	Direct Trade Between Wind Farm and Flexible Load in Competitive Electricity Market	Tingli	Hu	Grad
19STUGM124	Market Mechanism for Energy Storage System based Virtual Inertia	Aravind	Inglalalli	Grad
19STUGM125	Optimal Participation of Price-Maker Battery Energy Storage in Energy and Ancillary Services Markets Considering Degradation Costs	Reza	Khalilisenobari	Grad
19STUGM126	U.S. Electricity Markets as a Model for Broadband Development and Structuring	Evan	McKee	Grad
19STUGM127	Pricing in Peer-to-Peer Energy Trading Using Distributed Optimization Approach	Amrit	Paudel	Grad
19STUGM128	Unbalanced Distribution System Economic Dispatch in a Co-Simulated Environment	Cody	Rooks	Grad
19STUGM129	Decomposable Paradigm for Uncertainty-based Transmission and Distribution Coordinated Economic Dispatch	Shengfei	Yin	Grad
19STUGM130	Shadow Price Formulation and Decomposition for Economic Emission Dispatch	Qiwei	Zhang	Grad

Operations & Control

Poster #	Title	Student Name		UG/Grad
		First	Last	
19STUGM131	Continuous-time Flexible Ramp Scheduling in Forward Power Systems Operation	Avishan	Bagherinezhad	Grad
19STUGM132	To Centralize or to Distribute: A Comparison of Advanced Microgrid Management Systems	Zheyuan	Cheng	Grad
19STUGM133	State Estimation in Distribution Systems with High DER penetration and Heterogeneous Measurements	Chandra Kant	Jat	Grad
19STUGM134	AC Control Optimal Set Point of Embedded VSC HVDC in the Perspective of Converting Loss	Soseul	Jeong	Grad
19STUGM135	A Distributed Energy Management Approach for Residential Demand Response	Xiao	Kou	Grad
19STUGM136	Dynamic Simulation of DFIM-based Pumped Storage Hydro for Pump-Mode Frequency Support	Soumyadeep	Nag	Grad
19STUGM137	Distributed Optimization and Coordination Strategy for Stochastic Economic Dispatch with V2G and G2V	Farnaz	Safdarian	Grad

Power Electronics

Poster #	Title	Student Name		UG/Grad
		First	Last	
19STUGM138	A reverse droop based Distributed control framework for DC distribution systems	Satabdy	Jena	Grad
19STUGM139	Operating Methodology for Hybrid Multi-terminal HVDC to Secure Margin on Extinction Angle	Choongman	Lee	Grad
19STUGM140	Power Density and Reliability Metric Assessment of Thyristor Controlled Rectifiers for AES	Tanvir Ahmed	Toshon	Grad
19STUGM141	Linearized Approach for Dynamic Modeling of Fast Electric Vehicle (EV) Charging Unit	Shuyao	Wang	Grad

Power System Modeling and Simulation

Poster #	Title	Student Name		UG/Grad
		First	Last	
19STUGM142	Impacts of Branch Contingencies: Dynamic Variations in Line Thermal and Electrical Parameters	Forest	Atchison	UG
19STUGM143	Investigation of Relevant Distribution System Representation with DG for VSM Assessment	Alok Kumar	Bharati	Grad
19STUGM144	Worst Case Unavailability Modelling of a Cyber Physical Power System	Suvagata	Chakraborty	Grad
19STUGM145	CVSR-Integrated Meshed Power Grid Analysis	Okan	Ciftci	Grad
19STUGM146	Three Phase Transmission Line Fault Location Based on the Generalized Bergeron Model	Dayou	Lu	Grad
19STUGM147	Stochastic Hosting Capacity in LV Distribution Networks	Matthew	Deakin	Grad
19STUGM148	A New Internal Fault Detection and Classification Technique for Synchronous Generator	Ashish	Doorwar	Grad
19STUGM149	Achieving 100x Acceleration for N-1 Contingency Screening with Uncertain Scenarios using Deep Convolutional Neural Network	Yan	Du	Grad

19STUGM150	Multi-Agent Distributed Control of Integrated Transmission and Distribution Systems with DERs	Inalvis	Alvarez-Fernandez	Grad
19STUGM151	Real-time Physical Test-bed for validation of Event Diagnosis and Generation Estimation in Distribution Network Integrated with Distributed Energy Resources (DERS)	Amir	Gholami	Grad
19STUGM152	Optimal Power Flow Active and Inactive Constraints Identification with Machine Learning	Fouad	Hasan	Grad
19STUGM153	A Fault Zone Identification Scheme for Busbar Using Correlation Coefficients Analysis	Soumitri	Jena	Grad
19STUGM154	Energy Management System for Naval Submarine	Byeongdoo	Jeon	Grad
19STUGM155	A Cost Effective Energy Exchange Strategy to Improve Reliability of Microgrids	Md	Kamruzzaman	Grad
19STUGM156	Bulk Electric Power System Risks from Coordinated Edge Devices	Richard	Kenyon	Grad
19STUGM157	Optimal PMU Placement Using Stochastic Methods	Mirka	Mandich	Grad
19STUGM158	Optimal Model for Integrated Analysis of Transmission and Distribution Systems	Arun Kaarthick	Manoharan	Grad
19STUGM159	Distribution Locational Marginal Prices under Uncertainty	Robert	Mieth	Grad
19STUGM160	Accelerated and Robust Analytical Target Cascading for Distributed Optimal Power Flow	Ali	Mohammadi	Grad
19STUGM161	Measurement-based Parameter Calibration for a Generic Model for Photovoltaic Generations	Jaemin	Moon	Grad
19STUGM162	Generative Adversarial Networks for Real-time Stability Assessment of Inverter-based Systems	Gurupraanesh	Raman	Grad
19STUGM163	Optimal Operation of UCF Campus Grid with Modeling in MGMS and OPAL-RT	Ivelisse	Rivera	UG
19STUGM164	Concepts for Acceptance-Friendly AC-DC Transmission Grids	Samuel	Schilling	Grad
19STUGM165	A Facility for Physical Simulation of High Impedance Faults in Low Voltage Networks	Anwarul Islam	Sifat	Grad
19STUGM166	Optimal Scheduling of Distributed Energy Resources via Convex Relaxation of ACOPF	Zahra	Soltani	Grad
19STUGM167	Power Flow Analysis using Deep Learning Techniques in a Three Phase Unbalanced Distribution Network	Deepak	Tiwari	Grad
19STUGM168	Power System Stability Enhancement by Demand side Management with considering ZIP and induction motor loads	Jaber	Valinejad	Grad
19STUGM169	VSC-HVDC Transmission Line Protection Based on Dynamic State Estimation	Binglin	Wang	Grad
19STUGM170	Forming A Markovian Influence Graph from Utility Line Outage Data to Mitigate Cascading	Kai	Zhou	Grad

Smart Cities

Poster #	Title	Student Name		UG/Grad
		First	Last	
19STUGM171	Feasibility Study of Financial P2P Energy Trading in a Grid-Tied Power	Mohammad Imran	Azim	Grad
19STUGM172	A Bi-Level Optimization Formulation of Multilevel Demand Subscription Pricing	Yuting	Mou	Grad
19STUGM173	An Incentive Mechanism for Motivating Residents to Participate in Peak Shaving	Jing	Tu	Grad

Smart Grid Technology

Poster #	Title	Student Name		UG/Grad
		First	Last	
19STUGM174	Stochastic Optimal Sizing of Micro-Grids Using the Moth-Flame Optimization Algorithm	Abhi	Chatterjee	Grad
19STUGM175	A Residential Community Energy Optimization Scheme with Financial Rewards	Avijit	Das	Grad
19STUGM176	Validation of Transient Conductor Temperature Model for Ampacity Forecasts	Leanne	Dawson	Grad
19STUGM177	A Realistic One-Year Comparison of Priority Service Versus Real-Time Pricing for Enabling Residential Demand Response	Celine	Gerard	Grad
19STUGM178	Voltage stability index ensuring the constancy and pseudo linearity	Jaeyeop	Jung	Grad
19STUGM179	Virtual Synchronous Generator Model of an Inverter-Based Distributed Generator	Anusha	Kandula	Grad
19STUGM180	ACN Research Portal: A Toolbox for EV Charging Research	Zachary	Lee	Grad
19STUGM181	A Measurement-based Model for Contingency Analysis Considering Cascading Failure	Rui	Ma	Grad
19STUGM182	Securing Communications and Deployments for Resilient Control Applications using Edge Computing Technology	Zhijie	Nie	Grad
19STUGM183	A Hybrid Data-Driven Method for Online Power System Dynamic Security Assessment with Incomplete PMU Measurements	Li	Qiaoqiao	Grad
19STUGM184	Assessing the Potential of Large-Scale Energy Storage for Distribution Systems Demand Management	Júlia Beatriz	Ramos da Conceição	Grad
19STUGM185	Distributed Service Restoration in Distribution Networks by DERs Scheduling	Reza	Roofegari nejad	Grad
19STUGM186	Meter and Device Placement for Duke Energy Distribution Circuits	Shelby	Tomassi	UG
19STUGM187	Load Management in a building with BESS and HVAC scheduling	Divya	Vedullapalli	Grad
19STUGM188	Electric Vehicle Aggregator Modeling and Control for Frequency Regulation	Mingshen	Wang	Grad
19STUGM189	A Semi-Supervised Deep Transfer Learning Architecture for Energy Disaggregation	Shengyi	Wang	Grad
19STUGM190	Using Power Transfer Distribution Factors in Subproblems of Distributed Unit Commitment	Shaobo	Zhang	Grad
19STUGM191	Active and Reactive Power Management of Single Phase Distribution Power Inverters Using Droop Control Based on MIMO Identification	Robin	Bisht	Grad
19STUGM192	PMU Measurement based Synchronous Generator Speed Deviation Signals for PSS Controls	Paranietharan	Arunagirinathan	Grad
19STUGM193	Scalable Demand Response Scheme with Limited Information Flow	Pramod	Herath	Grad
19STUGM194	Data-Driven Frequency Sensitivity Analysis for Utility-Scale PV Plants	Ali	Arzani	Grad
19STUGM195	Renewable Distributed Energy Resources Impact on the Macroeconomics Under Net-metering Policy	Mohannad	Alkhrajah	Grad
19STUGM196	Federation based Cyber Physical Security (CPS) Testbed for Wide-Area Protection and Control in Smart Grid	Vivek Kumar	Singh	Grad

Smart Sensors

Poster #	Title	Student Name		UG/Grad
		First	Last	
19STUGM197	Communication-free voltage regulation of distribution power grids	Rayan	El Helou	Grad
19STUGM198	Optimal Control for Load Ensembles in Smart Buildings	Ali	Hassan	Grad

Substation and Distribution Automation

Poster #	Title	Student Name		UG/Grad
		First	Last	
19STUGM199	Automated Switching Operation for Resilience Enhancement of Distribution Systems	Mohammad Mehdi	Hosseini	Grad
19STUGM200	Automated Transformation of IEC 61850 Substation Models to IEC 61499 Applications	Tin	Rabuzin	Grad

System-Wide Events and Analysis Methods

Poster #	Title	Student Name		UG/Grad
		First	Last	
19STUGM201	Prevention of Cascading Failures in Stressed Power System using Energy Functions	Abhishek	Banerjee	Grad
19STUGM202	Machine-Learning based Advanced Situational Awareness: Prediction of Event Propagation	Paroma	Chatterjee	Grad
19STUGM203	An early-recognition algorithm of power systems oscillation detection based on measurement data	Hwanhee	Cho	Grad
19STUGM204	GMD Mitigation Techniques in Power Systems	Pooria	Dehghanian	Grad
19STUGM205	Sequential Detection of Forced Oscillations in Power Systems using the CUSUM Procedure	Sanjay	Hosur	Grad
19STUGM206	An Unsupervised Learning Framework for Event Detection, Type Identification and Localization Using PMUs Without Any Historical Labels	Haoran	Li	Grad
19STUGM207	Power System Fundamental Frequency Estimation Using Unscented Kalman Filter	Cheng	Qian	Grad
19STUGM208	Scalable Coordinated Control of Energy Storage Systems for Enhancing Power System Angle Stability	Mohammadali	Rostami	Grad
19STUGM209	Effective Scenario Selection for Preventive Stochastic Unit Commitment during Hurricanes	Yuanrui	Sang	Grad
19STUGM210	Data Driven Oscillation Source Detection in an Islanded Unbalanced Microgrid Using Innovative Ensemble Learning	Hasan	Ul Banna	Grad
19STUGM211	An Improved Cumulant Method for Probabilistic Load Flow Calculation	Chenxu	Wang	Grad

Adaptive Trading in the Continuous Intraday Market

Gilles Bertrand¹ and Anthony Papavasiliou²

Abstract—Recently, the penetration of uncertain renewable energy has increased in the electricity markets. For this reason, producer needs to correct their position close to real-time if they want to avoid volatile real-time price. The closest option to delivery time is to trade in the continuous intraday market. This market is therefore a good option for assets which wants to value their flexibility. Trading in this market is challenging due to the multistage nature of the problem, its high uncertainty and the fact that decisions need to be made rapidly in order to lock in profitable trades. We model the trading problem as a Reinforcement learning problem. We present how to use policy function approximation in order to simplify this problem. We present some parameters that need to be used in order to parametrize our policy. We show the pertinence of our parametrization by showing that our approach outperforms the method, classically used in the industry, rolling intrinsic of 12.1% (out of sample) on the 165 last days of 2015 and the 366 days of 2016 in the German continuous intraday market.

I. INTRODUCTION

The integration of renewable resources in Germany has recently increased from 18.2% in 2010 to 32.2% in 2016. This increase of renewable production implies that the market requires more flexibility close to real time. Consequently, the German continuous intraday market (CIM) which allows agents to correct their trading positions in the actual day of operations where renewable supply conditions are revealed has become increasingly active. This market is therefore becoming an interesting option for fast-moving assets such as pumped hydro storage to valorize their flexibility.

II. METHODOLOGY

We cast the problem of bidding in the continuous intraday market as a reinforcement learning problem.

A. Motivation for policy function approximation

In order to solve the MDP, we have to find an optimal policy which is a function defining in each state the probability of taking the different actions. This policy should be selected in a set of policy Π in order to optimize the future expected reward as shown in equation 1. In our case, we have an infinite number of states. This make the problem difficult because the set Π is a set of function in infinite dimension. Solving that problem in its initial formulation is therefore untractable. In order to obtain an approximate solution to the problem, we simplify the problem using policy function approximation. Specifically, we

parametrize the policy with respect to a parameter vector θ and optimize on this θ .

$$\max_{\pi \in \Pi} \sum_{t=1}^T \mathbb{E} [R_t(S_t, A^\pi(S_t))] \quad (1)$$

B. Threshold policy

We focus on a policy which is parametrized by buy and sell price thresholds. The threshold policy that we investigate in this paper accepts sell bids if their price is below a buy threshold, and accepts buy bids if their price is above the sell threshold. Therefore, we only need to optimize the thresholds which can be done using the REINFORCE algorithm.

C. Threshold adaptation

Previously, we have introduced the idea of threshold policy in order to trade on the CIM. Having the same threshold at any time step for every day will not perform correctly. Therefore, in order to be adaptive to different situations, we define the threshold as a parametric function of some explanatory variables. We discover that our policy needs to adapt to at least 6 parameters in order to perform correctly (i) the delivery time (ii) the trading day (iii) the remaining time before market closure (iv) the other price on the price curve (v) the reservoir level (vi) the information received during the day.

III. RESULTS

In this section, we compare the results of our method with rolling intrinsic which is a method used in the industry. Our method parameters are learned on the first 165 days of 2015. We compare the two methods out of sample on the rest of 2015 and 2016. Our threshold policy gives a better results in 71% of days. The average profit difference is 12.1%. In figure 1, we show the profit difference per day between our method and rolling intrinsic. This graph shows that the extra profit is coming day by day and is not only due to some days at which we would be really lucky.

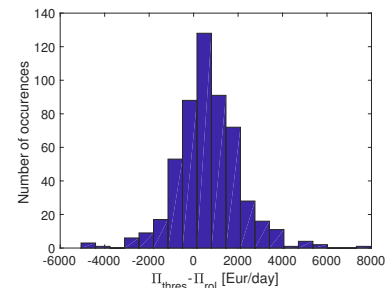


Fig. 1: Distribution of the difference between the profit of the threshold policy and the rolling intrinsic method

¹Gilles Bertrand is with CORE, UCLouvain, Louvain la Neuve, Belgium gilles.bertrand@uclouvain.be

²Anthony Papavasiliou is with CORE, UCLouvain, Louvain la Neuve, Belgium anthony.papavasiliou@uclouvain.be

Statistical Interaction Boundary Determination on the Impact of Renewable Energy Resources

Namki Choi, Hwanhee, Cho, Bohyun Park and Byongjun Lee
Electrical and Electronic Engineering Department
Korea University
Seoul, South Korea

Email: fleminglhr@korea.ac.kr, whee88@korea.ac.kr, wind833@korea.ac.kr and leeb@korea.ac.kr

Abstract— Renewable energy resources are expected to expand in accordance with global due to global environmental concerns and limited resources such as coal, oil and etc. Large penetration of renewable energy resources (wind turbine generators or photovoltaics) to power systems have brought new challenges that have never been experienced before. One of the issues is to make power systems weak. There are many indexes to present how much systems are weak. Weighted Short-Circuit Ratio is usually used to present how weak power systems are considering fully interaction between renewable energy resources. However, large penetration of renewable energy resources is distributed so that it is difficult to define boundary for influence of renewable energy resources. This paper suggests determining boundary for impact of renewable energy resources using correlation coefficient of short circuit current with changing momentary cessation voltage.

Keywords—Renewable energy resources, Control strategy, Faulted power systems, Short circuit current, Boundary of renewable energy resources.

I. KEY METHODS

Momentary cessation is defined in [1] as generator block the active power if point of common coupling voltage is lower than momentary cessation voltage. Renewable energy resources can contribute fault current (approximately 1.2pu) in [2]. Short circuit current of renewable energy resources can be calculated in [3] with changing momentary cessation voltage. There are some buses where changes in short circuit current is similar as momentary cessation voltage is varied. The similarity of changes in short circuit current can be clearly defined by correlation coefficient.

II. RESULTS

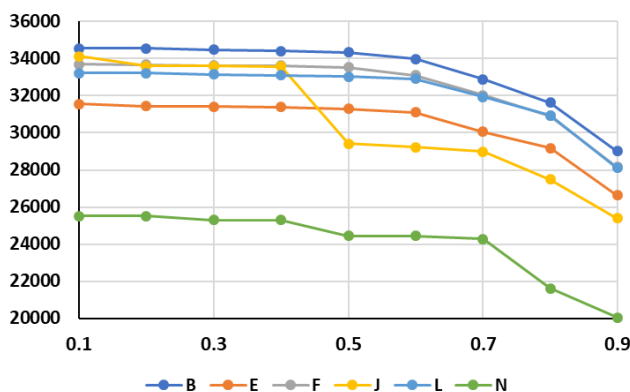


Figure 1 Short circuit current at each faulted bus from changing of momentary cessation voltage.

This work was supported by “Human Resources program in Energy Technology” of the Korea Institute of Energy Technology Evaluation and Planning (KETEP) granted financial resource from the Ministry of Trade, Industry and Energy, Republic of Korea (no. 20174030201820).

Bus name	L	E	F	B	J	N
L	1.0000	0.9987	0.9968	0.9962	0.8176	0.9596
E	0.9987	1.0000	0.9990	0.9986	0.8341	0.9618
F	0.9968	0.9990	1.0000	0.9997	0.8429	0.9670
B	0.9962	0.9986	0.8924	1.0000	0.8457	0.9711
J	0.8176	0.8341	0.9596	0.8457	1.0000	0.8924
N	0.9596	0.9618	0.9670	0.9711	0.8924	1.0000

Figure 2 Correlation coefficient of short circuit current with varying momentary cessation voltage.

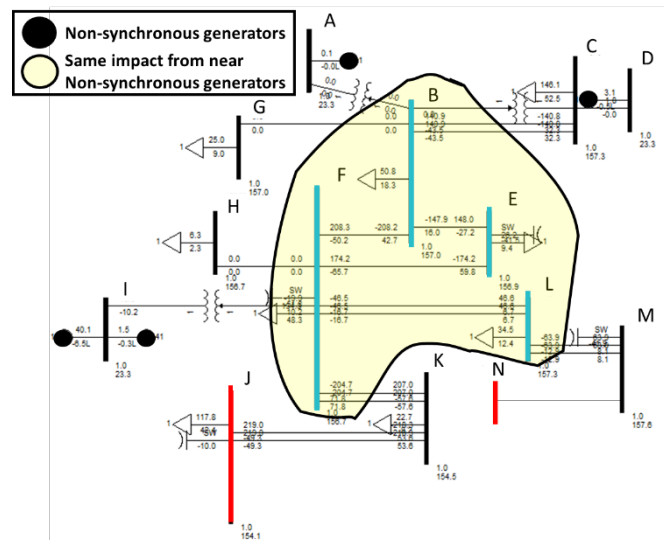


Figure 3 Boundary for same impact of renewable energy sources

III. CONCLUSION

Fault current at faulted buses changed as momentary cessation voltage. From the results, boundary for impact of renewable energy resources could be conservatively determined by correlation coefficient that is greater than 0.99. Those buses with low correlation coefficient has an impact from different non-synchronous generators.

IV. REFERENCES

- [1] IEEE. IEEE Standard for Interconnection and Interoperability of Distributed Energy Resources with Associated Electric Power Systems Interfaces. In IEEE Std 1547-2018 (Revision of IEEE Std 1547-2003), 2018
- [2] Plet, C.A.; Graovac, M.; Green, T.C.; Iravani, R. Fault response of grid-connected inverter dominated networks. In Proceedings of IEEE PES General Meeting, 25–29 July 2010; pp. 1–8.
- [3] Choi, N.; Park, B.; Cho, H.; Lee, B. Impact of Momentary Cessation Voltage Level in Inverter-Based Resources on Increasing the Short Circuit Current. *Sustainability* 2019, *11*, 1153.

Power System Operations under Data Asymmetry: Towards Learning and Sharing

Vladimir Dvorkin, Jalal Kazempour, Pierre Pinson
 Department of Electrical Engineering
 Technical University of Denmark
 Lyngby, Denmark

Abstract—Renewable energy data, such as historical observations or forecasts, is becoming crucial for the operation of modern power systems, as its completeness directly translates into operational efficiency. However, this data is often limited or unevenly distributed among power system agents. We study the connection between asymmetry of renewable energy data among power systems agents and overall system performance. We introduce a distributed algorithm for a look-ahead power dispatch problem based on a dual decomposition, where agents, e.g., generators, integrate private data in their local optimization. The agents receive data in different complexity and from independent data providers. This data is incorporated into agents optimization through chance constraints reformulated in a data-inclusive manner. We design a set of experiments exploring various impacts of data on the overall system performance and on the outcomes for each agent individually. We first show the strong connection between a sample size of agents data and system reliability. The latter tends to reduce in data scarcity. Under this condition, however, we show that the system operation is improved if agents are to learn from or share the data at hand.

Index Terms—Uncertainty, Chance Constraints, Distributed optimization, Power Systems Reliability

SHORT SUMMARY

Each agent (generator) decides its operational decisions, e.g., allocation of its capacity between reserve and energy services, according to the following affine policy:

$$\underline{p}_i \leq p_i - \alpha_i w \leq \bar{p}_i, \quad \forall i, \quad \sum_i \alpha_i = 1,$$

where p_i is a set point of generator i , α_i is the participation factor of generator i in balancing random renewable forecast error w , and \underline{p}_i and \bar{p}_i are capacity limits. The agents integrate their private information on forecast errors which is given by a finite set of samples, e.g., $\mathcal{D}_i = \{w_{i1}, \dots, w_{is}\} \forall i$. Using this data, they estimate the interval of forecast error distribution: $\underline{w}_i := \min\{w_{i1}, \dots, w_{is}\}$ and $\bar{w}_i := \max\{w_{i1}, \dots, w_{is}\}$, respectively, yielding $\underline{w}_i \leq 0 \leq \bar{w}_i$.

Naturally, the complexity of agent data (sample size) may vary. Figure 1 depicts some possible scenarios when agent data complexity is inconsistent. With small data complexity, there is a risk of not capturing the entire range of forecast error realizations, eventually leading to low system reliability and expensive emergency actions. With increasing data complexity, the union of agent sets may suffice to keep the system in balance with high probability, but there is no guarantee of a cost-optimal allocation of units, i.e., less efficient units could be prioritized over more efficient units. With full data

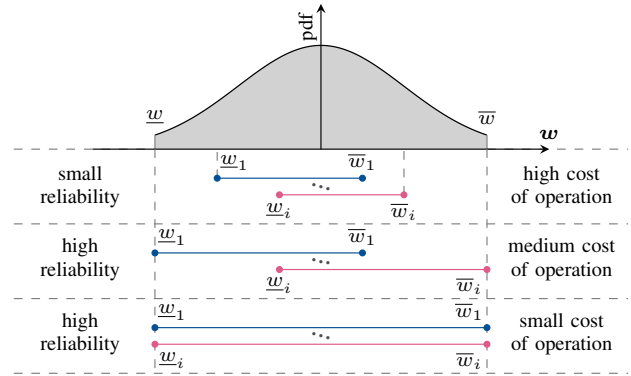


Fig. 1. Relationship between agent data complexity and system operation. The grey area depicts the pdf of the wind forecast error distribution, and blue and red lines show the intervals used in agents optimization problems.

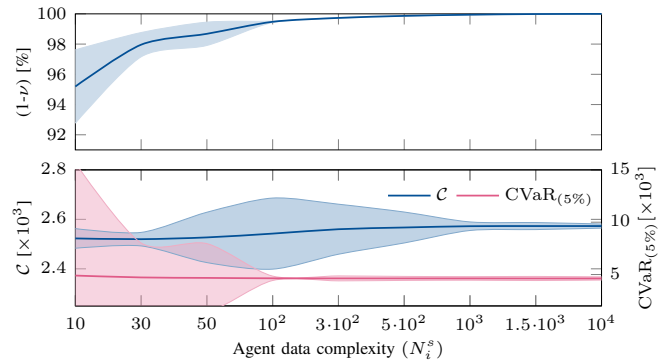


Fig. 2. Impacts of data complexity on reliability ($1 - \nu$, where ν is a generator limits violation level) and cost efficiency (average cost C and cost over 5% of worst-case scenarios $CVaR_{5\%}$). Improved reliability is followed by increasing cost efficiency.

complexity, all units are available to balance the whole range of forecast deviations in a cost-driven manner.

With a set of numerical studies, we analyze the impact of agent data complexity on the reliability of operation and expected dispatch cost. To improve the two indicators under data scarcity, we let agents to learn from data at hand and enhance their knowledge on the underlying distribution. This eventually leads to enhanced operations. Alternatively, data sharing among agents also strengthens operations. Moreover, the agents have incentives for sharing, as their individual performance increases.

Application of Load Switching Events in Steady-State Load Modeling in Power Distribution Networks

Alireza Shahsavari, Mohammad Farajollahi, and Hamed Mohsenian-Rad

Department of Electrical and Computer Engineering, University of California, Riverside, CA, USA

Abstract—A novel event-oriented method is proposed to conduct steady-state load modeling in power distribution systems. It has two fundamental differences with the comparable methods in the literature. First, the type of events are different. Specifically, the existing event-oriented load modeling methods use upstream voltage events as the main enabler for load modeling. In contrast, here we use the load switching events across the distribution feeder itself. Second, the objective of the analysis is different. The existing event-oriented load modeling methods are intended to obtain a ZIP model for the aggregate load of the entire distribution feeder. The application of such feeder-aggregated load models is in analysis of sub-transmission and transmission systems. In contrast, here we seek to obtain a ZIP model for each individual load across the feeder. The application of such individual load models is in the analysis of the distribution system itself, such as with respect to the operation of distributed energy resources. The performance of the proposed method is examined on a test-feeder under various operating scenarios by considering the impact of errors in feeder-head measurements.

Keywords: Event-oriented method, steady-state load modeling, distribution system analysis, load switching events.

I. INTRODUCTION

In this paper, we explore making use of a different type of events and seek to achieve a different load modeling objective. Specifically, we seek to investigate the load switching events on the distribution feeder itself in order to obtain models for the individual loads that exist across the feeder that is being studied. Accordingly, the methodology in this paper is inherently different compared to the existing event-oriented static load modeling approaches.

II. METHODOLOGY

We need to solve a system of equations that comprises circuit models and load models. We start with writing the law of complex power conservation, in terms of complex power and voltage phasor and we write the Kirchhoff's Voltage Law (KVL) for every possible load configuration.

suppose k steady-state measurements are available at the feeder-head corresponding to load switching events, out of which c measurements represent distinct load configurations. We can derive the circuit model in form of equations. In this regard, the total number of equations from the law of complex power conservation and KVL becomes:

$$\# \text{ of Equations in Circuit Model} = (n + 1) c, \quad (1)$$

and the number of corresponding unknowns becomes:

$$\# \text{ of Unknowns in Circuit Model} = n c + \sum_{k=1}^c \sum_{i=1}^n SW_i^{mk}. \quad (2)$$

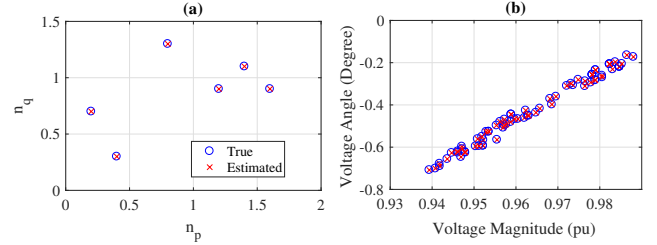


Fig. 1. True versus estimated parameters for the case study in Section IV.A in the absence of measurement errors: (a) load model; (b) voltage phasors.

where, SW_i^{mk} is switched load. Next, we can derive the load model in form of equations. The total number of such equations becomes:

$$\# \text{ of Equations in Load Model} = \sum_{i=1}^n \sum_{k=1}^c SW_i^{mk} - n, \quad (3)$$

and the number of corresponding unknowns becomes:

$$\# \text{ of Unknowns in Load Model} = n. \quad (4)$$

In order to solve the above system of equations, we need the total number of unknowns to be less than or equal to the total number of independent equations, i.e., we need:

$$\begin{aligned} n c + \sum_{i=1}^n \sum_{k=1}^c SW_i^{mk} + n \\ \leq (n + 1) c + \sum_{i=1}^n \sum_{k=1}^c SW_i^{mk} - n. \end{aligned} \quad (5)$$

Accordingly, we can present the following Theorem.

Theorem 1. (a) The minimum number of distinct load configurations in order to solve the system of equations to obtain the individual load models is $c = 2n$. (b) The minimum number of buses in order to allow the proposed event-oriented steady-state individual load modeling approach is $n = 3$.

III. CASE STUDY AND NUMERICAL RESULTS

We investigate the effectiveness of the proposed method to find individual load models on the six buses test feeder. Since the number of buses is $n = 6$, there exist $63 = 2^6 - 1$ possible distinct load configurations for this distribution feeder. From Theorem 1(a), the individual load models can be obtained from any $12 = 2n$ distinct load configurations; Fig. 1(a) shows the true and the estimated individual load model parameters for each individual load. We can see that the proposed method works well on modeling all individual loads. Also, Fig. 1(b) shows the true and estimated voltage phasors of all buses during 12 load configurations.

Scalable Optimization Techniques for Market Integration of Highly Distributed Energy Resources

Stephen Fatokun, *Student Member, IEEE*, Kevin Tomsovic, *Fellow, IEEE*

Abstract—This work presents a scalable method of optimization using the Lagrangian Relaxation (LR) technique. The amount of resources available to most regional markets have greatly increased in recent times. Also, inter-regional market and resource sharing have great potentials to reduce energy cost. The Mixed Integer Programming (MIP) approach guarantees optimum solutions but does not scale well with increase in the number of resources. A DC optimal power flow (OPF) technique is used in this formulation. Line-losses are introduced as heuristics to eliminate the over-commitment problem associated with similar generators in LR. This approach is expected to reduce the simulation time as well as the duality gap, thereby, moving the solution closer to its optimum.

I. INTRODUCTION

The increasing penetration in the power grid of distributed resources like PV, wind, energy storage systems and smaller resources like ‘arbitrage virtual bidding’ has increased the number of resources to consider in the unit commitment problem. Unit commitment now requires longer computational time. At the same forecast uncertainty better managed in the hour ahead (HA) on average. Forecast uncertainty error from renewable energy sources reduces as the dispatch time approaches, hence, HA unit commitment will capture the market better, reducing the required reserves (regulation and contingency). The LR method scales well with increase in units and resources and hence, the choice technique for this work.

II. PROBLEM FORMULATION

Using a DCOPF method and relaxing the coupling constraint, a line loss heuristic for separating similar generators and loads can be used. This is a step closer to a formulation that scales better than MIP for large numbers of resources. The objective function is:

$$\min_{P_{it}, U_{it}} \{ \sum_{t=1}^T \sum_{i=1}^N (a + bP_i + cP_i^2) U_i^t \} \quad (1)$$

Loading constraint:

$$s. t. \quad \sum_{t=1}^T \lambda^t (P_{load}^t + \sum_{j=1}^L (L_{flow}^t(P_{1,2...ng}))^2 R_j - \sum_{i=1}^N P_i^t U_i^t) = 0 \quad (2)$$

Unit limits:

$$U_i^t P_i^{min} \leq P_i^t \leq U_i^t P_i^{max} \text{ for } i = 1..N_{gen} \text{ and } t = 1..T \quad (3)$$

Line limits:

$$-Limit \leq \sum_{i=1}^N GSF_{k-i} \times [G_i - D_i] \leq Limit \quad (4)$$

Lagrangian :

$$L(P, \lambda) = \sum_{t=1}^T \sum_{i=1}^N (a + bP_i + cP_i^2) U_i^t + \sum_{t=1}^T \lambda^t (P_{load}^t + \sum_{j=1}^L (L_{flow}^t(P_{1,2...ng}))^2 R_j - \sum_{i=1}^N P_i^t U_i^t) \quad (5)$$

III. CASE STUDY

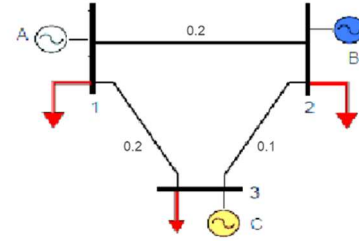


Fig. 1 3-bus System with distributed load

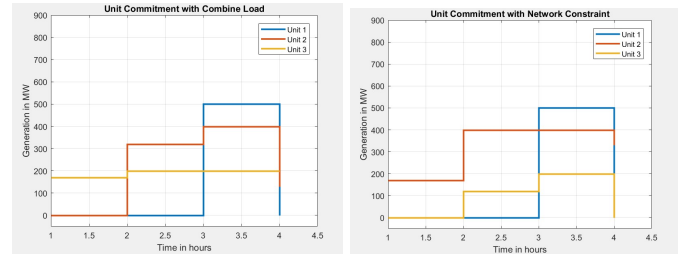


Fig. 2 4 hours commitment and economic ED for 3 generators.

Dispatched for Combine Load and Gen.

	Hour 1	Hour 2	Hour 3	Hour 4
Gen A	0	0	500	0
Gen B	0	320	400	130
Gen C	170	200	200	200
Tot. output	170	520	1100	330
Tot. cost	\$20163			

Dispatch for Distributed Load and Gen.

	Hour 1	Hour 2	Hour 3	Hour 4
Gen A	0	0	500	0
Gen B	170	400	400	330
Gen C	0	120	200	0
Tot. output	170	520	1100	330
Tot. cost	\$21456			

A Graph Computation based Sequential Power Flow Calculation for Large-Scale AC/DC Systems

Wei Feng, Jingjin Wu, Chen Yuan, Guangyi Liu,
Renchang Dai
GEIRI North America Inc
Santa Clara, USA

Qingxin Shi, Fangxing Li
Department of Electrical Engineering & Computer Science
The University of Tennessee
Knoxville, USA

Abstract—This paper proposes a graph computation based sequential power flow calculation method for Line Commutated Converter (LCC) based large-scale AC/DC systems to achieve a high computing performance. Based on the graph theory, the complex AC/DC system is first converted to a graph model and stored in a graph database. Then, the hybrid system is divided into several isolated areas with graph partition algorithm by decoupling AC and DC networks. Thus, the power flow analysis can be executed in parallel for each independent area with the new selected slack buses. Furthermore, for each area, the node-based parallel computing (NPC) and hierarchical parallel computing (HPC) used in graph computation are employed to speed up fast decoupled power flow (FDPF). Comprehensive case studies on the IEEE 300-bus, polished South Carolina 12,000-bus system and a China 11,119-bus system are performed to demonstrate the accuracy and efficiency of the proposed method.

Index Terms—Graph computation, sequential method, AC/DC system, parallel computing, graph partition

I. INTRODUCTION

In this paper, a graph computation based sequential method is proposed to divide the system into blocks and speed up the power flow analysis in each block in parallel for large-scale AC/DC system without compromising accuracy. Firstly, a hybrid system is divided into several sub-systems with graph partition algorithms. The sub-systems are independent and decoupled by DC connections. Then, the power flow analysis of sequential method can be conducted in parallel for each sub-system. Furthermore, graph computation based FDPF is applied to solve power flow in parallel in the sub-system level in each iteration to achieve computation time-saving at the greatest extent.

II. GRAPH COMPUTATION BASED POWER FLOW

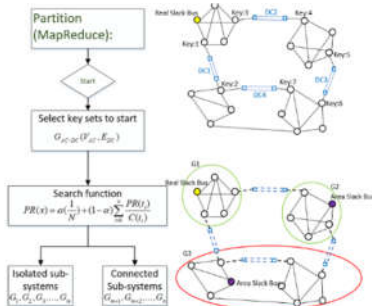


Figure 1. Flow chart of graph partition for hybrid system

The first step is to narrow the partition set to $G_{AC/DC}(V_{AC}, E_{DC})$, which only includes the coupled buses and DC lines. Then, each coupled bus conduct graph partition independently to generate sub-systems with the fewest cut edges except the DC lines. Finally, select new area slack buses in each sub-system to do FDPF. The graph computation based FDPF can be implemented with NPC, which is used in initializing parameters, mismatch vectors and B', B'' matrices, and with HPC, which is used in factorizing LU and solving equations.

III. CASE STUDY AND RESULTS

A. Test cases

Three systems with varied sizes and topologies are tested: the IEEE 300-bus system, an artificial 12,000-bus system, which is developed based on South Carolina 500-bus system, and a China 11,119-bus system.

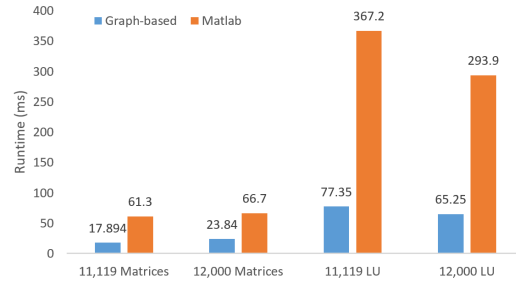


Figure 2. Speed-up gains of graph-based method

TABLE I. TIME OF 12,000-BUS AND 11,119-BUS SYSTEMS (IN MS)

Case	Iterations	1 thread	4 threads	8 threads	16 threads
12,000	2	412.28	212.31	143.25	139.68
11,119	4	946.37	392.25	386.45	375.42
Case	24 threads	32 threads	64 threads	96 threads	128 threads
12,000	136.53	137.12	151.25	157.68	156.43
11,119	362.21	352.49	372.34	376.53	395.43

TABLE II. COMPARISONS OF 11,119-BUS AND 12,000-BUS SYSTEMS (IN MS)

Platform	Case	Total	B', B''	LU
TigerGraph	11,119	352.49	17.894	77.35
	12,000	136.53	23.84	65.25
Matlab	11,119	1491.5	61.3	367.2
	12,000	538.2	66.7	293.9

As shown in Fig. 2, Table I and Table II, it shows that for a hybrid system with over 10,000 buses, the proposed method can save about 75.5% computing time on average.

Dynamic Distribution Network Reconfiguration Using Reinforcement Learning

Yuanqi Gao, Jie Shi, Wei Wang, Nanpeng Yu
 Department of Electrical and Computer Engineering
 University of California, Riverside
 Riverside, California 92507

Email: ygao024@ucr.edu, jshi005@ucr.edu, wwang031@ucr.edu, nyu@ece.ucr.edu

Abstract—Dynamic distribution network reconfiguration (DNR) algorithms perform hourly status changes of sectionalizing and tie switches to reduce network line losses, minimize loss of load, or increase hosting capacity for distributed energy resources. Most of the existing work assumes that the complete set of network parameter information is available to the optimization module. This paper weakens this assumption and solves minimum loss dynamic DNR by formulating the problem as a Markov decision process (MDP) and training an off-policy reinforcement learning (RL) algorithm on a historical data set. In the testing phase, the configuration at any time step is determined with respect to the estimated long-term benefit, which combines network losses and switching actions. To further improve the RL performance, we propose a novel data augmentation method to artificially synthesize more training data for the RL agent. The overall scheme outputs a control policy that reduces the network loss with awareness of the number switching actions it can take. Simulation results on a 16-bus distribution test feeder demonstrate the quality of the RL performance.

Index Terms—Dynamic network reconfiguration, reinforcement learning.

I. INTRODUCTION

Both Federal sponsored programs and market forces are facilitating the wide-spread adoption of smart grid technologies such as the advanced metering infrastructure and remote controllable switches (RCS) [1], which enabled remote data collection and actuation of loads and switches. The minimum loss dynamic distribution network reconfiguration (DNR) algorithms [2] optimize line resistive loss as well as the number of real-time switching actions of RCSs. We propose an RL based technique to solve the minimum loss dynamic DNR problem when the network parameter information is absent. The proposed method only requires a historical configuration, load, and total power loss data set to train the RL algorithm. We also propose a data augmentation method to increase the amount of training data. We show through simulation that the RL algorithm learns a control policy from the historical data set that reduces the network loss in out-of-sample data despite the absence of network parameter information.

II. SIMULATION RESULTS

A. Data Augmentation

The key question in data augmentation is to estimate network loss from nodal injections without knowing net-

work parameters. Fig.1 shows 50 samples from the out-of-sample prediction results of Gaussian process and Monte Carlo dropout methods.

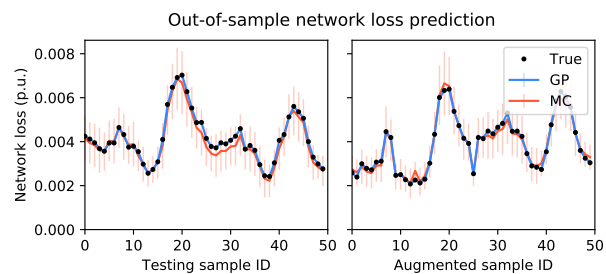


Figure 1. MC and GP out-of-sample prediction

B. Q Learning with Data Augmentation

With data augmentation, the Q learning agent reduces the total operational cost and improves the voltage profile as shown in Fig.2

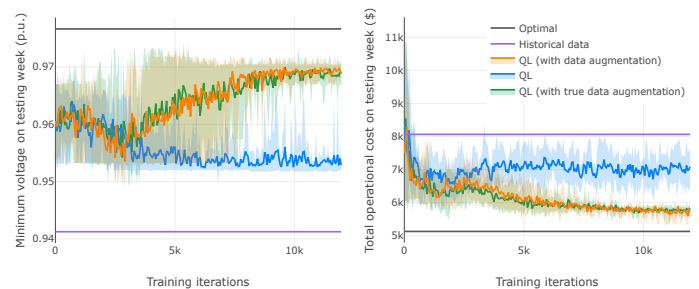


Figure 2. Out-of-sample performance of Q learning for dynamic DNR. The hyperparameters are: neural network: feed-forward (600,190); activation function: ReLU; optimizer: Adam; batch size: 64; discount factor γ : 0.95; copy steps C ($\theta \mapsto \theta^-$): 30

REFERENCES

- [1] N. Yu, S. Shah, R. Johnson, R. Sherick, M. Hong, and K. Loparo, "Big data analytics in power distribution systems," in *2015 IEEE Power Energy Society Innovative Smart Grid Technologies Conference (ISGT)*, Feb 2015, pp. 1–5.
- [2] F. Capitanescu, L. F. Ochoa, H. Margossian, and N. D. Hatziargyriou, "Assessing the potential of network reconfiguration to improve distributed generation hosting capacity in active distribution systems," *IEEE Transactions on Power Systems*, vol. 30, no. 1, pp. 346–356, Jan 2015.

Data-driven Decision Making in Power Systems with Probabilistic Guarantees

Xinbo Geng, *Student Member, IEEE*, Le Xie, *Senior Member, IEEE*,

Abstract—Uncertainties from deepening penetration of renewable energy resources have posed critical challenges to the secure and reliable operations of future electric grids. Among various approaches for decision making in uncertain environments, this paper focuses on chance-constrained optimization, which provides explicit probabilistic guarantees on the feasibility of optimal solutions. Although quite a few methods have been proposed to solve chance-constrained optimization problems, there is a lack of comprehensive review and comparative analysis of the proposed methods. We first review three categories of existing methods to chance-constrained optimization: (1) scenario approach; (2) sample average approximation; and (3) robust optimization based methods. Data-driven methods, which are not constrained by any particular distributions of the underlying uncertainties, are of particular interest. We then provide a comprehensive review on the applications of chance-constrained optimization in power systems. Finally, this paper provides a critical comparison of existing methods based on numerical simulations, which are conducted on standard power system test cases.

I. INTRODUCTION

Real-time decision making in the presence of uncertainties is a classical problem that arises in many contexts. In the context of electric energy systems, a pivotal challenge is how to operate a power grid with an increasing amount of supply and demand uncertainties. The unique characteristics of such operational problem include (1) the underlying distribution of uncertainties is largely unknown (e.g. the forecast error of demand response); (2) decisions have to be made in a timely manner (e.g. a dispatch order needs to be given by 5 minutes prior to the real-time); and (3) there is a strong desire to know the risk that the system is exposed to after a decision is made (e.g. the risk of violating transmission constraints after the real-time market clears). In response to these challenges, a class of optimization problems named “chance-constrained optimization” has received increasing attention in both operations research and practical engineering communities.

II. A SCHEMATIC OVERVIEW OF CHANCE-CONSTRAINED OPTIMIZATION

A schematic overview of solutions to (CCO) and their relationships are presented in Figure 1. Akin methods are plotted in similar colors, and links among two circles indicate the connection of the two methods. The tree-like structure of Figure 1 illustrates the hierarchical relationship of the reviewed methods. Key references of each method are also provided.

III. CONVERTCHANCECONSTRAINT: A MATLAB TOOLBOX

Figure 2 presents the structure and main functions of CCC. Three major methods to solve (CCO) are implemented:

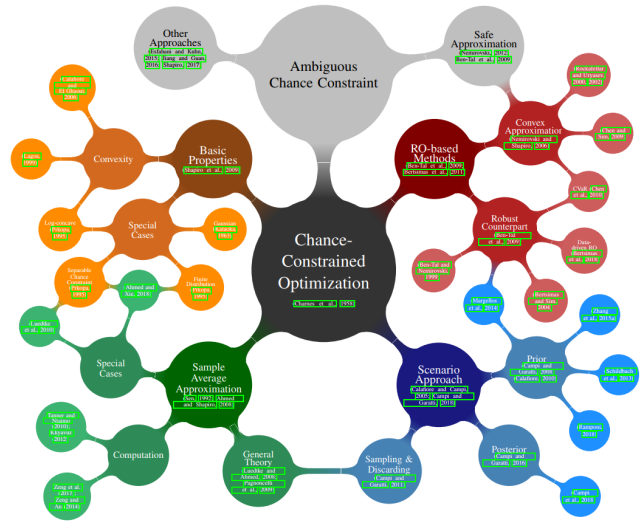


Fig. 1. A Schematic Overview of Existing Methods and Algorithms to Solve Chance-constrained Optimization Problems [1]

scenario approach, sample average approximation and robust optimization related methods. The implementation of RO-related methods is based on the robust optimization module [2] of YALMIP. As illustrated in Figure 2, CCC is interfaced via YALMIP with most existing optimization solvers, e.g. Cplex, Gurobi, Mosek and Sedumi.

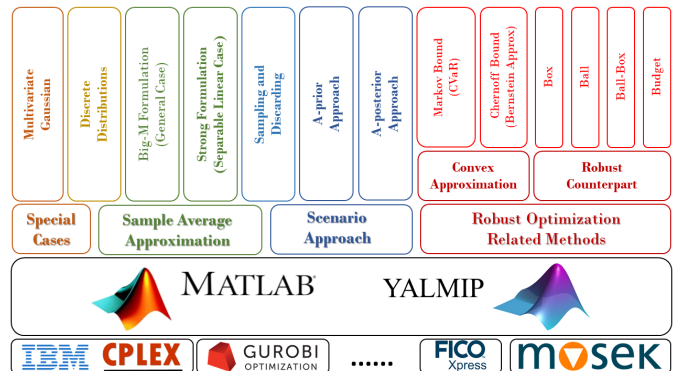


Fig. 2. ConvertChanceConstraint: A Matlab Toolbox

REFERENCES

- [1] X. Geng and L. Xie, “Data-driven decision making with probabilistic guarantees (part i): A schematic overview of chance-constrained optimization.” [Online]. Available: arXiv:1903.10621
- [2] J. Lfberg, “Automatic robust convex programming,” vol. 27, no. 1, pp. 115–129.

Detecting and Locating Smart Grid Cyber Attacks in Real-Time: A Data-driven Approach

Md Abul Hasnat and Mahshid Rahnami-Naeini

Electrical Engineering Department, University of South Florida, Tampa, Florida, USA

hasnat@mail.usf.edu, mahshidr@usf.edu

Abstract—Smart grids being complex cyber-physical infrastructures demand real-time monitoring of their dynamic states. Phasor measurement units (PMUs) are smart metering devices with a high sampling rate, which facilitate visualizing the dynamics of the states with the help of time series corresponding to the system’s parameters and attributes. This work shows the signatures of different cyber-attacks and some physical phenomenons on the PMU time series and the impacts on the correlation among the components’ states. A technique based upon the changes in the instantaneous state correlations is proposed for providing alerts for attacks to the control center’s operators in real-time. The technique will also determine the type of attack and the location of the PMU that is compromised by the attackers.

Index Terms—Cyber attacks, PMU Data, State Correlations, Time series, Smart Grid.

I. INTRODUCTION

Different types of cyber attacks threaten smart grid security and newer types of attacks are being designed every day. Among them, the Denial-of-Service (DoS) attack and Data-replay attacks are very common for any cyber-physical infrastructure and in this work, we try to illustrate their effects on PMU time series. We use MATPOWER 6.0 [1] to run the power flow solution to generate the time series. The daily load profiles from the NYISO [2] are collected and normalized to add to the MATPOWER’s default load to generate the time series.

II. EFFECTS OF ATTACKS ON PMU TIME SERIES

Let, \mathcal{A} be the set of PMUs under cyber attack and \mathcal{S} be the set of PMUs the attackers have access to record data.

The DoS attack can be modeled as the unobservability of the PMU data during the attack duration. Let, $x_i(t)$ be the actual time series of any electrical attribute (e.g. voltage phase angle) of the bus associated with the i -th PMU. In the case of the i -th PMU to be under DoS attack, the time series from this PMU can be represented as:

$$x_{DoS_i}(t) = \begin{cases} n_i(t) & \text{if } t_{start} \leq t \leq t_{end} \\ x_i(t) + n_i(t) & \text{otherwise,} \end{cases} \quad (1)$$

where t_{start} and t_{end} are, respectively, the starting and ending of the DoS attack, and $n_i(t)$ is the Additive White Gaussian Noise signal associated with the i -th PMU. (Fig. 1b)

In data replay attack, the attacker records the data from some of the PMUs that they have access to record the data and replays those past data in the present time to the PMUs under attack:

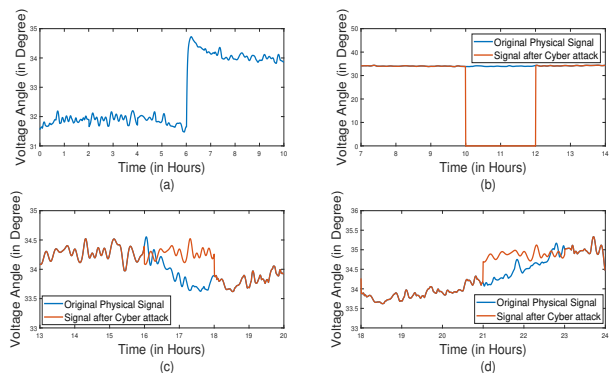


Fig. 1. The effects on the voltage angle time series associated with the PMU at Bus 86: (a) Abrupt load reduction (Hour 6); (b) DoS Attack (Hour 10-12) (c) Replay Attack Hour (16-18) with the past data from the same bus; (d) Replay Attack (Hour 21-23) with past data from Bus 92.

$$x_{Replay_i}(t) = \begin{cases} x_k(t' + t - t_{start}) + n_i(t) & \text{if } t_{start} \leq t \leq t_{end} \\ x_i(t) + n_i(t) & \text{otherwise,} \end{cases} \quad (2)$$

where t_{start} and t_{end} are, respectively, the starting and ending of the replay attack and t' is the starting of the recording time. Here, $i \in \mathcal{A}$ and $k \in \mathcal{S}$. (Fig. 1c for $i = k$ and Fig. 1d for $i \neq k$.)

In our work, we will also simulate some events that can represent physical attacks to observe their effects on the time series and the state correlation profiles to differentiate them from the cyber attacks. For example, Fig. 1d shows the effect of abrupt load change in a bus.

III. DETECTING AND LOCATING ATTACKS

We propose a technique to provide the operator an alert about the cyber attacks on the smart grid and to find the attack locations on the basis of the instantaneous state correlations. We evaluate the correlations of each bus PMU time series with its highly correlated PMUs (to be determined from the historical data) in real time. The onset of the attack can be identified by the dropping of the average correlation of any PMU time series beyond a threshold and the location of the attack can be detected from the identification number of the PMUs for which the average correlations has been dropped.

REFERENCES

- [1] R. D. Zimmerman, C. E. Murillo-Snchez, and R. J. Thomas, *MATPOWER: Steady-State Operations, Planning and Analysis Tools for Power Systems Research and Education*, IEEE Transactions on Power Systems, Volume: 26, Issue:1, Feb. 2011.
- [2] The New York Independent System Operator, Inc[US], <https://www.nyiso.com/>.

Estimation of System Inertia using Center of Inertia Frequency Methodology

Seunghyuk Im
School of Electric Engineering
Korea University
Seoul, Republic of Korea
shyuk1129@korea.ac.kr

Bohyun Park
School of Electric Engineering
Korea University
Seoul, Republic of Korea
wind833@korea.ac.kr

Byongjun Lee*
School of Electric Engineering
Korea University
Seoul, Republic of Korea
leeb@korea.ac.kr

Abstract—As the operation of the conventional generators is replaced by the inverter-based renewable energy source, the kinetic energy of rotating masses in power system is reduced. If the kinetic energy of rotating masses in power system is lowered, Rocof sharply drops when large disturbance occurs such as high-voltage transmission line fault and generator trip. In severe case, recovery from frequency nadir point to frequency operating point in steady state may not be possible. Therefore, in this paper, we apply the center of inertia frequency methodology to Korea power system to estimate the system inertia and derive the appropriate fitting time(dt) for improving the accuracy of the estimated values. Based on these results, we analyze the tendency between the kinetic energy of rotating mass drops due to the penetration of renewable energy, rocof and frequency nadir in the inertia response domain. For further study, the center of inertia frequency methodology has been algorithmized to develop indicator and to build a real-time monitoring system based on PMU measurement.

Keywords—Center of Inertia Frequency, System Inertia, Rocof(Rate of change of frequency), Frequency Nadir, Kinetic Energy of Rotating mass

I. CENTER OF INERTIA FREQUENCY METHODOLOGY

In the Korea power system, there is no measuring equipment in all generators and loads, and it is difficult to measure accurate frequency due to lack of advanced measuring equipment such as PMU. Therefore, in this paper, the center of inertia frequency methodology using the simplified one-bus power system model estimates the system inertia constant.

$$f_{COI} = \frac{\sum_{i=1}^n H_i \cdot f_i}{\sum_{i=1}^n H_i} \quad (1)$$

$$H_{estimation} = \frac{\Delta P}{2 \cdot S_{total} \cdot \frac{df_{COI}}{dt}} \cdot f_n \quad (2)$$

$$H_{system} = \frac{\sum_{i=1}^n H_i \cdot S_{ni}}{S_{total}} \quad (3)$$

$$Error(\%) = \frac{\|H_{est} - H_{sys}\|}{\|H_{sys}\|} \quad (4)$$

The system inertia estimation Eq. (2) is derived by applying the fcoi Eq. (1). The fitting time is derived from the minimum error rate by comparing the estimated value from Eq. (3) with the Eq. (4). The simulation was carried out on the 765kV 2-line fault in the East Coast region of the Korea power system and reflected the generator SPS(Special Protection System). The penetration of renewable energy was conducted in 3 stages of 5,

10, 14GW to analyze the tendency of kinetic energy, rocof and frequency nadir.

II. SIMULATION RESULT

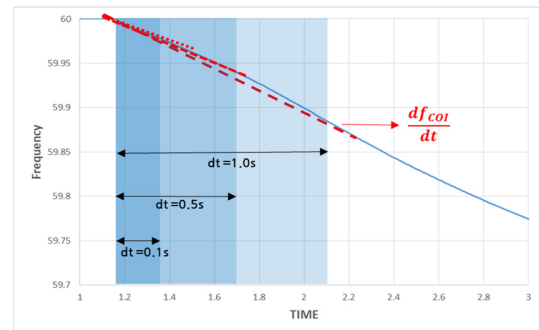


Fig. 1 Center of inertia frequency deviation according to fitting time(dt)

TABLE I. SYSTEM INERTIA ESTIMATION ACCORDING TO FITTING TIME

	Hsys	dt = 0.1 1.95s - 2.05s		dt = 0.5 1.75s - 2.25s		dt = 1.0 1.55s - 2.55s	
		Hest	error%	Hest	error%	Hest	error%
Base	4.90	5.30	8.22%	4.99	1.91%	5.04	2.86%
5GW	4.82	5.41	12.1%	5.06	4.96%	5.06	4.85%
10GW	4.79	5.45	13.6%	5.06	5.67%	4.98	3.86%
14GW	4.78	5.45	13.9%	5.03	5.06%	4.91	2.68%

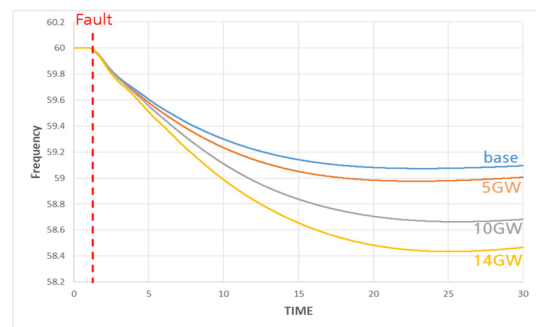


Fig. 2 Frequency deviation due to the renewable energy influence

TABLE II. THE TENDENCY OF KINETIC ENERGY, ROCOF AND NADIR.

	KEsys	KEest	Rocof	Nadir
Base	551GWs	567GWs	-0.1357	59.07Hz
5GW	517GWs	542GWs	-0.1417	58.97Hz
10GW	484GWs	503GWs	-0.1489	58.66Hz
14GW	455GWs	474GWs	-0.1691	58.43Hz

Cyberattack-Resilient Load Forecasting with Adaptive Robust Regression

Jiaying Jiao, Zefan Tang, Peng Zhang, Meng Yue, Chen Chen, Jun Yan

Abstract—Cyberattacks in power systems that alter load forecasting models’ input data have serious, sometimes devastating, consequences. Existing cyberattack-resilient work mainly focuses on enhancing attack detection. Although some outliers can be easily identified, more carefully-designed attacks can escape from being detected and impact load forecasting. We propose a cyberattack-resilient load forecasting approach based on an adaptive robust regression method, where the observations are trimmed based on their residuals and the proportion of the trim is adaptively determined by an estimation of the proportion of contaminated data. In a large-scale simulation study, the proposed method outperforms the standard robust regression in various settings.

I. MAIN RESULTS

Linear regression model was used for load forecasting and attacks were imposed on training data set using random or ramping attack templates. Attack proportion p is a common parameter for both templates. Random attack scale parameter follows Normal(μ , σ^2). Larger scale parameter will change the data value more dramatically. Ramping attack consists of a lot continuous attack intervals. With each interval, the attack scale parameter will increase gradually to the middle of the interval and then decrease with the same rate to the end of the interval. The length of one continuous interval is l and the scale parameter increasing (or decreasing) rate λ_R . Least Squares method (LS) and two robust methods, Huber’s method and Adaptive Least Trimmed Squares method (ALTS) were compared here. LS method doesn’t have robustness and was used as baseline to show the robustness of the other two. Mean Absolute Percentage Error (MAPE) is calculated on validation data set to show the prediction accuracy rate for each method.

Key conclusions: 1) ALTS method is always most robust than Huber’s method under all the settings investigated. It can give almost same prediction accuracy as the situation when there is no attack; 2) Huber’s method will lose robustness quickly when attack data proportion is larger than 20%; 3) When there is no attacks in the training data set, Huber’s and ALTS methods still work and will give the same prediction accuracy rate as the LS method.

This work was supported in part by the National Science Foundation under Grants ECCS-1611095, CNS-1647209 and ECCS-1831811, in part by the Department of Energy Cybersecurity for Energy Delivery Systems (CEDs), and in part by the Office of the Provost, University of Connecticut.

J. Jiao and J. Yan are with the Department of Statistics, University of Connecticut, Storrs, CT 06269, USA.

Z. Tang and P. Zhang are with the Department of Electrical and Computer Engineering, University of Connecticut, Storrs, CT 06269, USA.

M. Yue is with Sustainable Energy Technologies Department, Brookhaven National Laboratory, Upton, NY 11973, USA.

C. Chen is with Energy Systems Division, Argonne National Laboratory, Lemont, IL 60439, USA.

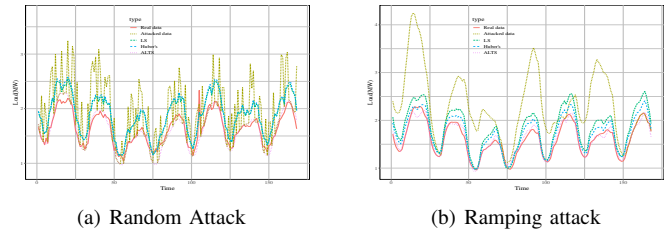


Fig. 1. Visual comparison of different methods. $p = 0.4$, random attack scale parameter $s \sim N(0.5, 0.01)$, ramping attack has length $l = 40$ and $\lambda_R = 0.05$.

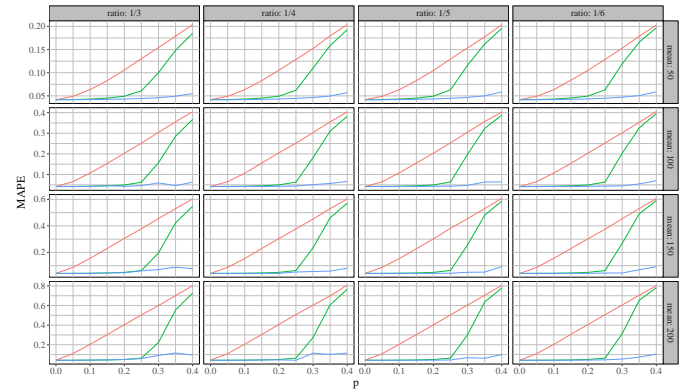


Fig. 2. Average MAPE under random attack along with different attack data proportion. Red line is least square method, green line is Huber’s method, blue line is adaptive method.

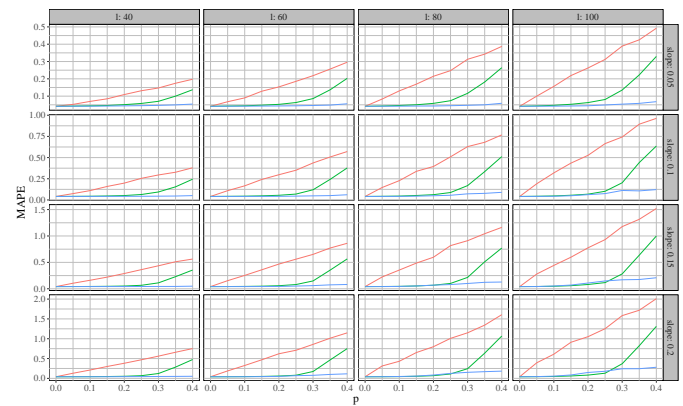


Fig. 3. Average MAPE under ramping attack along with different attack data proportion. Red line is least square method, green line is Huber’s method, blue line is adaptive method.

A Two-Stage Algorithm for Optimal Scheduling of Battery Energy Storage Systems for Peak-Shaving

Roozbeh Karandeh, *Student Member, IEEE*, and Valentina Cecchi, *Senior Member, IEEE*

Department of Electrical and Computer Engineering
University of North Carolina at Charlotte, Charlotte, NC, USA
Email: {rkarande, vcecchi}@uncc.edu

Abstract—This paper presents a two-stage algorithm for optimal energy scheduling of a Battery Energy Storage System (BESS) interfaced with renewable energy sources. Initially, a multivariate linear regression-based estimation of power flow state variables and network active power loss is performed using synthetic data produced from the network model. Thereafter, a linear programming (LP) formulation is used to determine the output power of the BESS for maximum peak-shaving and valley-filling, based on predicted day-ahead demand and solar photovoltaic (PV) output. In comparison with nonlinear approaches, the linearized model would reduce computational complexity and time, while maintaining reasonable accuracy. The linear programming model is solved using MATLAB, and the proposed algorithm is implemented on a real-world distribution feeder modeled in OpenDSS. The results show significant reduction in peak demand, net demand variability, and voltage variability caused by intermittent PV output.

I. BESS SCHEDULING - PROPOSED APPROACH

Given forecasted demand and PV output over 24 hours, the objective is to utilize BESS to minimize the maximum deviation of net demand profile from the average of net demand of the day.

$$\min(\max |P_i^{net} - P_{avg}^{net}|) \quad (1)$$

where

$$P_i^{net} = P_i^d - P_i^{pv} - P_i^{ref} \quad (2)$$

$$P_{avg}^{net} = \frac{1}{N} \sum_{i=1}^N P_i^d - P_i^{pv} - P_i^{ref} \quad (3)$$

$$P_i^d = P_i^L + P_i^{loss}(P_i^{ref}, P_i^L, P_i^{pv}) \quad (4)$$

$$V_{min} \leq V_i^k \leq V_{max}, I_i^l \leq I_{max}^l \quad (5)$$

Equation (4) suggests that the P_i^{loss} is a function of P_i^{ref} , P_i^L and P_i^{pv} and can be calculated through solving power flow, causing the model to become nonlinear. In order to maintain the linearity, a multivariate linear regression-based estimation of required variables is performed using synthetic data produced from the network model.

$$P_i^{loss} = \theta_{p0} + \theta_{p1}P_i^L + \theta_{p2}P_i^{pv} + \theta_{p3}P_i^{ref} \quad (6)$$

$$V_i^k = \theta_{k0} + \theta_{k1}P_i^L + \theta_{k2}P_i^{pv} + \theta_{k3}P_i^{ref} \quad (7)$$

$$I_i^l = \theta_{l0} + \theta_{l1}P_i^L + \theta_{l2}P_i^{pv} + \theta_{l3}P_i^{ref} \quad (8)$$

$$P_i^L = P_i^d - P_i^{loss}(P_i^{ref} = 0, P_i^L, P_i^{pv}) \quad (9)$$

The second stage of the algorithm consists of the linear optimization of objective function (1) taking into account the following BESS technical constraints.

$$-P_{max}^{ch} \leq P_i^{ref} \leq P_{max}^{dis} \quad (10)$$

$$SoC_{min} \leq SoC_i \leq SoC_{max} \quad (11)$$

The linear approximation in (12) is used to estimate State of Charge (SoC).

$$SoC_i = SoC_{i-1} - \left(\frac{P_{i-1}^{ref}}{E_{rated}^b} \times \frac{t_s}{1hr} \times 100 \right) \quad (12)$$

Based on the definition of absolute value, the objective function in (1) is converted to the following form, adding two more constraints.

$$\min Z \quad (13)$$

$$-P_i^{ref} + \frac{1}{N} \sum_{i=1}^N P_i^{ref} - Z \leq -(P_i^d - P_i^{pv}) + P_{avg}^d - P_{avg}^{pv} \quad (14)$$

$$P_i^{ref} - \frac{1}{N} \sum_{i=1}^N P_i^{ref} - Z \leq (P_i^d - P_i^{pv}) - (P_{avg}^d - P_{avg}^{pv}) \quad (15)$$

The proposed algorithm is implemented on a real-world distribution feeder modeled in OpenDSS, resulting in significant reduction in peak demand. Select results are shown in Fig. 1.

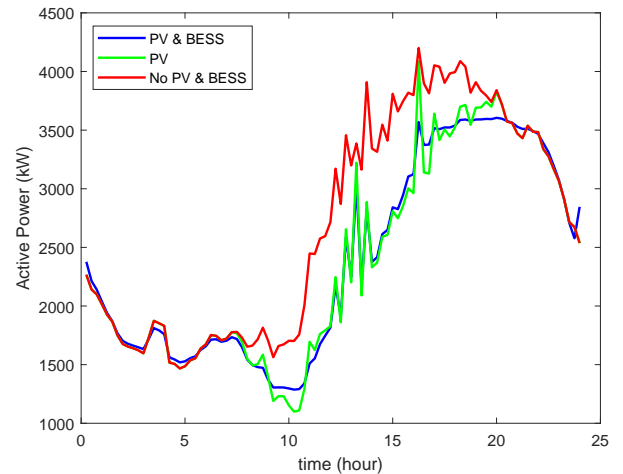


Fig. 1: Demand seen at the substation for three different operating scenarios

An Enhanced Wide Area Generation Control Scheme under High Renewable Penetration

Christoph Lackner, Joe H. Chow, Denis Osipov
Rensselaer Polytechnic Institute
Troy, NY

I. INTRODUCTION

The increased penetration of renewable resources has made frequency regulation and generation control a growing concern for power system operators. Due to the variability of renewable resources and the reduced inertia leading to the deterioration of system frequency response, many control regions expect a need to increase their regulating services and non-spin reserves. Increasing these reserves also increases the total costs of system operation and may elevate locational marginal energy prices. This work addresses the scheduling of energy interchange between control areas to share the reserves in the entire power system. A distributed control architecture is proposed to extend the existing area control error (ACE) concept to allow more cooperation between interconnected control regions. In this scheme, regulation services from different control regions can be pooled such that variability of generation in some cases can utilize reserves in multiple regions resulting in a more economic dispatch of automatic generation control (AGC) resources. This scheme also offers privacy protection as the bid cost of a regulating unit is not seen by operators not in its own control region. This work then introduces a large model of the eastern interconnection (EI) system and shows the effectiveness of the proposed scheme under 50% renewable penetration.

II. PROPOSED ENHANCED WIDE AREA GENERATION CONTROL SCHEME

Traditional AGC systems expect that any area that experiences a loss in generation will make up the lost generation by increasing the output of its generators. However, this is not always the most optimal power dispatch. The optimal power dispatch within can be computed by minimizing the total cost associated with the power necessary to make up for lost generation:

$$\min \text{cost} = \min \sum_i^A c_i(\Delta P_i) \quad (1)$$

subject to the constraint

$$\Delta P = \sum_i^A \Delta P_i \quad (2)$$

where ΔP is the total generation or load change, ΔP_i is the additional power generated in area i , $c_i(x)$ is the cost of producing x MW of additional regulation power in area i , and

A is the set of all interconnected areas. By convention $\Delta P > 0$ indicates an increase in load or decrease in generation.

An extended ACE is proposed as:

$$\text{ACE}_{\text{ext},i} = -\beta_i \Delta f - (\text{IC}_i - \text{IC}_{\text{ref},i} - P_{\text{mod},i}) \quad (3)$$

where

$$P_{\text{mod},i} = P_i - \Delta P \quad (4)$$

for the area that experienced the loss of generation, and

$$P_{\text{mod},i} = P_i \quad (5)$$

otherwise. Using this ACE the proposed scheme uses resources from all interconnected areas to dispatch generation in the most optimal way [1].

III. EASTERN INTERCONNECTION (EI) TEST SYSTEM

A reduced model of the entire US EI is used to validate this scheme. The system contains up to 50% renewable generation. Figure 1 shows a map of this system.

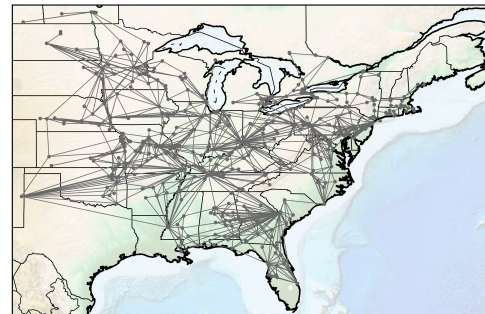


Fig. 1. EI Reduced System.

The system consists of a total of 83 generators in 10 balancing areas. To show the value of the proposed scheme this system is simulated using the CURENT Large Scale Test Bed (LTB) [2] and the additional operating costs after a generation loss in the New England (NE) area are compared.

REFERENCES

- [1] "Wide-Area Automatic Generation Control between Control Regions with High Renewable Penetration," *Proc of IREP*, Aug 2017.
- [2] "CURENT Large-scale Test Bed (LTB) for Innovations in Wide-Area Power System Research," *CURENT NSF DOE Site Visit*, Nov 2017.

Synchrophasor Calculation Algorithm Based on Robust State Estimation

Yunting Li¹, Student Member, IEEE, Yu Liu^{1,2,*}, Member, IEEE and Rui Fan³, Member, IEEE

1. School of Information Science and Technology, ShanghaiTech University, Shanghai, China, 201210

2. Key Laboratory of Control of Power Transmission and Conversion (SJTU), Ministry of Education, Shanghai, 200240

3. Pacific Northwest National Laboratory, Richland, WA, USA, 99354

*Email: liuyu@shanghaitech.edu.cn

Abstract: This paper proposes a novel robust state estimation based method for synchrophasor calculation. With the Tukey's Bi-Square technique, the traditional Weighted Least Square (WLS) based state estimation method is upgraded to the proposed Iteratively Reweighted Least Square (IRLS) based robust state estimation method, to better filter out measurement noise and reject bad data. Extensive numerical experiments demonstrate that the proposed method has higher synchrophasor calculation accuracy compared to existing IEEE C37.118 synchrophasor standard, independent of measurement noise level, bad data level and system frequency.

Key words: robust state estimation, Iteratively Reweighted Least Square (IRLS), synchrophasor calculation, measurement noise, bad data

I. INTRODUCTION

This paper proposed a robust state estimation based synchrophasor calculation algorithm to filter out measurement noise and reject bad data of instantaneous waveform measurements caused by environmental disturbance and physical instrumentation errors. Specifically, the proposed algorithm comes from the traditional Weighted Least Square (WLS) state estimation algorithm, with the weight matrix upgraded to Tukey's bi-square weights. An Iteratively Reweighted Least Square (IRLS) robust state estimation based synchrophasor calculation algorithm method is utilized to minimize the impact of measurement noise and bad data. To validate the effectiveness of the proposed algorithm, the performance of the proposed algorithm is compared to the performance of the existing IEEE C37.118 standard, with different measurement noise level, bad data level and system frequency.

II. ROBUST STATE ESTIMATION

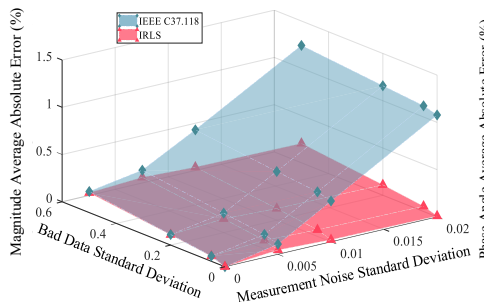


Figure 2. Magnitude Average Absolute Errors at $f=60\text{Hz}$

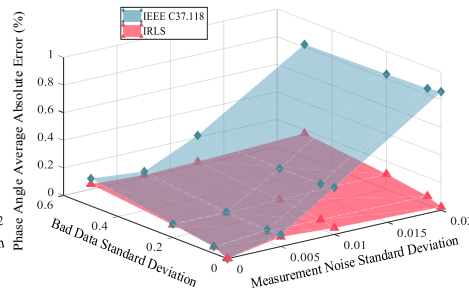


Figure 3. Phase Angle Average Absolute Errors at $f=60\text{Hz}$

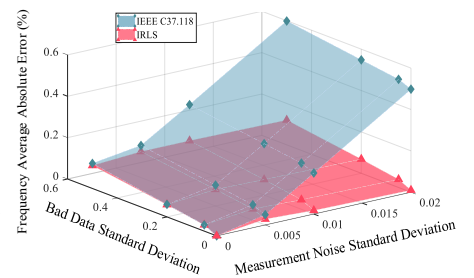


Figure 4. Frequency Average Absolute Errors at $f=60\text{Hz}$

A. WLS State Estimation Based Algorithm

$$\min_x \varepsilon(\mathbf{x}) = \min_x \mathbf{r}^T \mathbf{W} \mathbf{r} \quad (1)$$

$$\mathbf{x}^{(v+1)} = \mathbf{x}^{(v)} + (\mathbf{J}^T \mathbf{W} \mathbf{J})^{-1} \mathbf{J}^T \mathbf{W} (\mathbf{y} - \mathbf{s}(\mathbf{x}^{(v)})) \quad (2)$$

B. Proposed IRLS Robust State Estimation Based Algorithm

$$\mathbf{x}^{(v+1,j)} = \mathbf{x}^{(v,j)} + (\mathbf{J}^T \mathbf{W}^{(j-1)} \mathbf{J})^{-1} \mathbf{J}^T \mathbf{W}^{(j-1)} (\mathbf{y} - \mathbf{s}(\mathbf{x}^{(v,j)})) \quad (3)$$

$$\mathbf{W}_{ii}^{(j)} = \begin{cases} 1 - \left(\frac{\hat{r}_i^{(j)}}{c} \right)^2, & |\hat{r}_i^{(j)}| \leq c \\ 0, & |\hat{r}_i^{(j)}| > c \end{cases} \quad (4)$$

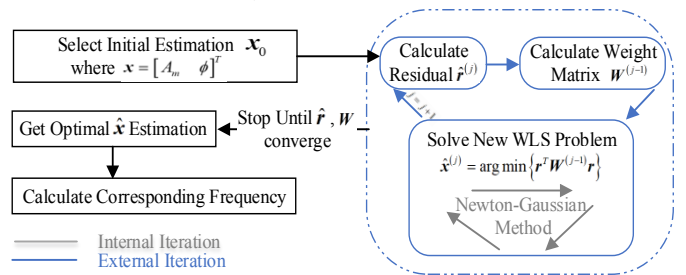


Figure 1. General Steps of IRLS

III. SIMULATION RESULT

Simulation result with different noise and bad data standard deviation are shown in Figure 2, 3, 4.

It can be observed that the plane representing the IRLS based algorithm is lower than or similar as the plane representing the IEEE C37.118 standard based algorithm, which proves that the proposed method has smaller or similar average/maximum absolute errors compared to the IEEE C37.118 standard.

Power System Event Classification using PMU Data in a Deep Learning Platform

Kaveri Mahapatra, *Student Member, IEEE*, Nilanjan Ray Chaudhuri, *Senior Member, IEEE*

Abstract—The proliferation of PMUs brings along challenges to handle a significant increase in the volume of real-time data and also opens up new opportunities for research in this field. This work explores the possibility of applying big data analytics on PMU measurements and highlights the effectiveness of deep neural network (DNN) in the context of power system event classification. The proposed framework considers the most common oscillatory events in power system and data corruptions in these classes of events. The performance of the deep learning platform is evaluated on labeled PMU measurements obtained from simulation of a 16-machine NE-NY system under different operating conditions.

I. BRIEF OVERVIEW

Our goal is to classify different power system events using PMU data on a deep learning platform. In this work, oscillatory events initiated by generator trips, line outages, self-clearing faults are considered as three classes of events. Data corruptions under any of the events is considered as another class of event. A Bidirectional Long Short Term Memory (BiLSTM) based deep neural network (DNN) is utilized for classification using voltage and frequency information of the simulated events. The proposed DNN [1], [2] architecture for event classification consists of 5 layers: i.e. Sequence input layer, BiLSTM layer, fully connected layer, softmax layer, and classification output layer.

II. MAIN RESULTS

We have considered a positive-sequence fundamental frequency phasor model of the 16-machine, 5-area New England-New York system [3] as the test system with PMUs installed at 40 buses. A PMU data rate of 30Hz is assumed. Voltage magnitude measurements at PMU buses are considered as inputs for this experiment. A window of 20 seconds post-disturbance data of those signals are collected from the PMUs during events. In this study, we have considered generator trips, line outages, and self-clearing faults simulated on the test system as disturbances or events. Two operating conditions are created before starting any disturbance.

A. Case-I : Event Classification

Training was done on one operating condition data and testing was done on another operating condition data. In this experiment three classes are Class-(1) self clearing faults (SF), Class-(2) generator outage (GO), Class-(3) line outage (LO).

TABLE I

RESULTS ON CLASSIFICATION OF THREE DIFFERENT TYPES OF DISTURBANCES IN THE SYSTEM, TOTAL EFFICIENCY = 97.8%

Event Type	Class-1 SF	Class-2 GO	Class-3 LO
Correct Prediction	95.8%	100%	100%
Correct Detection	100%	100%	95.5%

B. Case-II : Anomaly Detection

Two types of anomalies are considered for detection which are (1) Bad data Outliers due to noise or measurement errors and (2) Fault injection attack which is a type of anomaly in the data due to cyber intrusion. Training was done on 2/3 of all the examples under each class of event simulated under this operating condition and testing was done on remaining 1/3rd of data.

TABLE II

CONFUSION MATRIX RESULTS ON OUTLIERS DETECTION IN EVENT DATA, CLASS-0: CLEAN EVENT DATA, CLASS-1: CORRUPTED EVENT DATA, TOTAL EFFICIENCY=96.1%

Data type	Target Class-0	Target Class-1	Correct Prediction
Output Class-0	50%	3.9%	92.7%
Output Class-1	0%	46.1%	100%
Correct Detection	100%	92.1%	96.1%

TABLE III

CONFUSION MATRIX RESULTS ON FAULT INJECTION ATTACK DETECTION IN EVENT DATA, CLASS-0: CLEAN EVENT DATA, CLASS-1: CORRUPTED EVENT DATA, TOTAL EFFICIENCY=90.2%

Data type	Target Class-0	Target Class-1	Correct Prediction
Output Class-0	48.9%	8.7%	84.9%
Output Class-1	1.1%	41.3%	97.4%
Correct Detection	97.8%	82.6%	90.2%

III. KEY CONCLUSIONS

Event classification in presence of data corruptions in the context of big data is a challenging problem in presence of oscillations in the system. In this work, we have presented a well-known LSTM based DNN architecture for classification of power system events and data anomalies from PMU observations. Three key observations can be made from the results. First, raw PMU data without any feature extraction is sufficient for training a classifier on a DNN platform. Second, a simple DNN architecture for time series classification can give high accuracy for power system event classification. Third, event data collected under one operating condition can be used for event classification in other operating condition. This implies a DNN framework can also handle lack of training examples or labeled event data. Nevertheless, we can conclude that the event classification problem from limited PMU data, while challenging, has presented us an opportunity to leverage deep learning techniques.

REFERENCES

- [1] S. Hochreiter and J. Schmidhuber, "Long short-term memory," *Neural computation*, vol. 9, no. 8, pp. 1735–1780, 1997.
- [2] MATLAB, "LSTM layer architecture." [Online]. Available: <https://www.mathworks.com/help/deeplearning/ug/long-short-term-memory-networks.html>
- [3] B. Pal and B. Chaudhuri, *Robust control in power systems*, ser. Power electronics and power systems. New York: Springer, 2005.

Tractable Preventive Stochastic Unit-Commitment for Large Systems with Multiple Line Outages

Farshad Mohammadi

Department of Electrical and Computer Engineering
University of Utah
Salt Lake City, Utah
farshad.mohammadi@utah.edu

Mostafa Sahraei-Ardakani

Department of Electrical and Computer Engineering
University of Utah
Salt Lake City, Utah
mostafa.ardakani@utah.edu

Abstract—This work proposes an efficient formulation to solve large-scale stochastic unit commitment with multiple predictable equipment failures. The study is focused on multiple line outages, where standard methods fail the problem efficiently, due to the heavy computational burden. Our algorithm combines the efficient formulation based on generation shift factor and flow canceling transactions and uses iterative optimization to minimize the objective function while the network topology can change at any time. To demonstrate its efficiency, we tested the method to minimize the value of lost load and generation cost in the 2000-bus Texas system, affected by a hurricane. In comparison with the standard B- θ formulation, our algorithm can solve the problem with up to 98% less calculation time and 95% less memory usage.

Keywords— *Stochastic Unit-commitment, preventive optimization, Large-network optimization, Generation dispatch*

I. INTRODUCTION

The Unit Commitment (UC) problem determines the day-ahead schedule of the generators by minimizing the operation cost while satisfying reliability margins. UC is a mixed integer program (MIP), and despite all the recent improvements in MIP solvers, it can still be a challenging problem in the presence of uncertainties. Severe weather conditions can be one source of uncertainty, as it can lead to failure of elements. Traditional reliability requirements are based on deterministic margins that guarantee a minimum required level of operating reserve. However, the deterministic requirements are not efficient in the case of multiple outages. One alternative is stochastic unit commitment (SUC), which solves the problem for multiple possible outage scenarios. SUC, however, is computationally burdensome and cannot be solved within the available time. This study proposes a new model, which is capable of solving the preventive SUC problem for large real-world size network in the presence of many equipment failure scenarios. The following initial targets are considered in our model:

1. The proposed method should be able to solve the SUC within an acceptable computation time and by using minimum hardware requirement for a large-scale real-world network with a representative set of scenarios.
2. As multiple line outages are allowed, the network topology can change over the period of the study. The model should be able to handle changes in the network topology, while load shedding and over-generation are allowed.

II. TEST CASE

To evaluate the performance and validate the accuracy of the proposed method, it is compared with two standard methods (B- θ and PTDF), when they solve the standard unit commitment problem for a large size network. However, we could not compare them when solving SUC as we could not solve any large network with multiple scenarios using standard methods, with the hardware and time we could accept. The selected test case network is a synthetic grid on the footprint of Texas with 2,000 buses, 540 generation units, and 3,206 transmission lines with the possibility of 100 lines outages during [1]. Table 1 represents the results obtained for the standard UC problem. As can be seen in Table 1, the proposed method has the same accuracy as other methods, while it needs much less memory and time.

TABLE 1. BENCHMARK RESULT FOR THE PROPOSED METHOD

Method	B- θ	PTDF	Proposed
Cost Function (\$)	2.019E+7	2.019E+7	2.019E+7
Solution Time (minute)	138	18	2
Required Random Access Memory (Gigabytes)	4	1	0.2

Ten scenarios, which describe ten possible conditions (futures) regarding the uncertainties in the network, are considered to test the performance. The solution time is about four hours, and it consumes less than Five GB of RAM while there is free memory available in the system. The machine we used to run the methods utilizes Intel® Core™ i7-7700 CPU @3.60GHz as processor combined with 16.0 GB of RAM.

III. CONCLUSION

While there are many methods to solve the stochastic unit commitment, none of them is efficiently suitable for large networks and large uncertainty set. In this work, we propose a new formulation that is able to solve the SUC when there is a possibility for the failure of a large number of lines. As one application of the proposed algorithm, we evaluated the preventive SUC a day before a hurricane hits the network. Results showed that it is possible to significantly reduce the lost load and increase system reliability.

IV. REFERENCES

- [1] A. B. Birchfield, T. Xu, K. M. Gegner, K. S. Shetye, and T. J. Overbye, "Grid Structural Characteristics as Validation Criteria for Synthetic Networks," *IEEE Trans. Power Syst.*, vol. 32, no. 4, pp. 3258–3265, Jul. 2017.

A Data-driven Approach to Predict Size of Cascades using Community Structures in Interaction Graphs

Upama Nakarmi, *Student Member, IEEE* and Mahshid Rahnamay Naeini, *Member, IEEE*

Department of Electrical Engineering
University of South Florida, Tampa, FL, USA
unakarmi@mail.usf.edu, mahshidr@usf.edu

Abstract—Cascading phenomenon affects a multitude of networks. In power grids, one mechanism which enables failures to propagate is through transmission line overloading caused by redistribution of power flows during outage conditions. In this study, cascading failures in the transmission network of power grids are studied using interaction graphs. Then, community structures in the interaction graphs are studied to evaluate the role of the grids' components in propagation characteristics of the cascade process. Moreover, community structures of the interaction graphs are utilized for developing a Markov model for predicting the size of cascades. Further, the state variables and transition probabilities of the Markov chain are characterized using the community memberships and overlap/connection among communities. Finally, the asymptotic properties of the community structure-based Markov chains can be utilized to predict the size of cascades.

Index Terms—power grids, cascading failures, interaction graph, community structure, cascade size

I. INTRODUCTION

Cascading failures in the transmission network of power grids can cause huge blackouts and threaten the reliability of the overall grid. In recent years, many studies have been focused on analyzing cascades based on its size. Long term prediction of cascade sizes can be useful in mitigating cascading failures by characterizing contributions of components towards large cascades.

Our preliminary studies in [1] and [2] showed the role of components in the propagation characteristics of cascades based on community structures of the influence-based and correlation-based interaction graphs. We found that failure of overlap/bridge components can spread failures from one community to the other. Additionally, protection of overlap/bridge components can trap failures within communities. Inspired by this trap/spread property of communities, we model the community structures of the interaction graphs into a Markov chain. Then, we study the asymptotic properties of the Markov chain to predict the size of cascades and analyze the role of components in various cascade sizes.

II. PROPOSED METHOD

Using the aforementioned concepts in Section I, we propose a Markov chain $\mathcal{X} = \{X_0, X_1, X_2, \dots\}$ framework to model the cascade size evolution using the community structures in the interaction graphs. $X(t)$ denotes the state of the Markov chain at time $t \geq 0$. The state space $\mathcal{S} = \{s_0, s_1, s_2, \dots\}$ of the Markov chain is dependent on the community structures

of the interaction graphs. Each state s_i of the Markov chain is also associated with two state variables. The first variable reflects the number of components represented by the state. This variable can also be regarded as the current size of the cascade. The second variable tracks the community membership of the state.

Next, we assume two types of state transitions: self-transitions and inter-state transitions. The self-transitions model the scenario when the cascade is assumed to start from the failure of a component that belongs to a single community such that the cascade propagates only within the community itself. Self-transitions show that cascades are likely to be trapped inside communities. The inter-state transitions model the scenario when the cascade starts from the failure of a component belonging to multiple communities (overlap/bridge nodes) such that the cascade propagates to all communities that the component belongs to. Inter-state transitions show that cascades spread between communities. When states encounter self-transitions, both state variables discussed before remain unchanged whereas during inter-state transitions, both state variables will change. The variable that reflects the number of components represented by the state will increment by the size of the state to which it is transiting to. And the variable that tracks the community membership of the state will change into the community membership of the state that it is transiting to. Using these assumptions, the elements $p_{ij}(t)$ of the transition matrix at time t is $P(X_{t+1} = s_j | X_t = s_i)$ and is estimated using the sizes of communities as well as the size of the overlap/bridge nodes among communities. The initial state distribution μ_0 shows the probability of the cascade starting from any of the states and can be characterized based on the size of communities. Thus, given the initial state distributions, asymptotic analysis of the Markov chain can predict the long term cascade size. We expect that cascades that start from failures of overlap/bridge components cause larger cascade sizes compared to cascades that start from components belonging to a single community.

REFERENCES

- [1] U. Nakarmi and M. Rahnamay-Naeini, "Analyzing power grids' cascading failures and critical components using interaction graphs," *IEEE Power and Energy Society General Meeting (PESGM)*, pp. 1–5, 2018.
- [2] U. Nakarmi, M. Rahnamay-Naeini, and H. Khamfroush, "Critical component analysis in cascading failures for power grids using community structures in interaction graphs," *IEEE Transactions in Network Science and Engineering*, 2019 (to appear).

Tightening QC Relaxations of AC Optimal Power Flow Problems via Coordinate Transformations

Mohammad Rasoul Narimani,^{*} Daniel K. Molzahn,[†] and Mariesa L. Crow^{*}

Abstract—Optimal power flow (OPF) is a challenging nonconvex optimization problem that plays a crucial role in power system operation and control. Recently developed convex relaxation techniques provide new insights regarding the global optimality of OPF solutions. The QC relaxation is a promising approach that convexifies nonconvex terms (i.e., trigonometric and product terms) by enclosing them in convex envelopes. The accuracy of the QC relaxation strongly depends on the tightness of these envelopes. We present three improvements which strengthen QC relaxations of OPF problems via coordinate transformations of the power flow equations. These transformations facilitate the development of tighter envelopes for these equations. Comparison to a state-of-the-art QC implementation demonstrates the advantages of these improvements via smaller optimality gaps.

Index Terms—Optimal power flow, QC relaxation, Coordinate transformation

I. OVERVIEW

OPTIMAL power flow (OPF) is a challenging nonconvex optimization problem that plays a crucial role in the operation and control of electric power systems. OPF problems optimize an objective function, such as generation cost, subject to both network physics and engineering limits. Many recent research efforts have developed convex relaxations of OPF problems in order to obtain bounds on the optimal objective values. Convex relaxations are under active development with ongoing efforts aiming to improve the relaxations’ computational tractability and tightness [1]. The quadratic convex (QC) relaxation [2] is a promising approach that uses convex envelopes that enclose the trigonometric functions, squared terms, and products in the polar form of the power flow equations. Figure I provides illustrative examples of convex envelopes for the trigonometric terms.

In [3] and [4], we propose and analyze three improvements for QC relaxations of OPF problems. The first improvement leverages a polar representation of the branch admittances rather than the rectangular coordinate representation that has been used in previous formulations. The second improvement is based on a coordinate transformation via a complex per unit base power normalization that rotates the power flow equations. The associated rotational degree of freedom is exploited to obtain tighter envelopes for the trigonometric functions [3]. The third improvement generalizes the second by applying different coordinate transformations for the power flow equations associated with each line. The additional rotational degrees of freedom are exploited to further tighten the envelopes for the trigonometric functions.

Our proposed “rotated QC” (RQC) relaxation is based on these three improvements. We exploit the degrees of freedom provided by the aforementioned rotational coordinate changes in order to construct tighter convex envelopes for the trigonometric terms. We also perform a statistical analysis using a

Table I
SELECTED RESULTS FROM THE QC AND RQC RELAXATIONS

Test Case	AC (\$/hr)	QC gap (%)	RQC gap (%)
nesta_case3_lmbd	5812.6	0.97	0.86
nesta_case6_ww	3144.0	0.61	0.45
nesta_case30_ieee	205.6	15.06	11.24
nesta_case73_ieee_rts	189764.1	0.03	0.03
nesta_case6_ww_api	273.8	13.14	12.72
nesta_case24_ieee_rts_api	6421.4	8.76	7.14
nesta_case3_lmbd_sad	5959.3	1.38	1.14
nesta_case24_ieee_rts_sad	76943.2	2.74	2.63
nesta_case73_ieee_rts_sad	235241.7	3.24	3.16

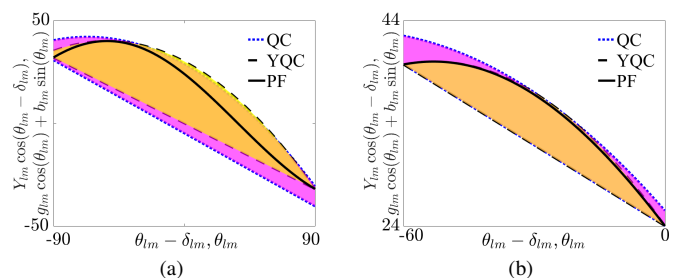


Figure 1. The black solid line represents the $g_{lm} \cos(\theta_{lm}) + b_{lm} \sin(\theta_{lm})$ and $Y_{lm} \cos(\theta_{lm} - \delta_{lm})$ terms, while the blue dotted and black dashed lines show envelopes for these terms, respectively. The area between upper and lower envelopes for $g_{lm} \cos(\theta_{lm}) + b_{lm} \sin(\theta_{lm})$ and $Y_{lm} \cos(\theta_{lm} - \delta_{lm})$ terms are colored by magenta and yellow colors, respectively. The term “YQC” represent RQC with zero rotation angle.

variety of large-scale test cases in order to choose appropriate values for the rotational degrees of freedom [4].

Figure I compares envelopes constructed with our approach versus the original QC relaxation from [2]. Empirical results from the application of QC and RQC relaxations on selected test cases are summarized in Table I. This table shows the advantages of the proposed improvements via smaller optimality gaps (i.e., objective value bounds from the RQC relaxation are closer to the best known objective values from local solvers). Our ongoing work includes further numerical testing and better characterization of the impacts of different choices for the rotational degrees of freedom.

REFERENCES

- [1] D. K. Molzahn and I. A. Hiskens, “A Survey of Relaxations and Approximations of the Power Flow Equations,” *Found. Trends Electric Energy Syst.*, vol. 4, no. 1-2, pp. 1–221, Feb. 2019.
- [2] C. Coffrin, H. Hijazi, and P. Van Hentenryck, “The QC Relaxation: A Theoretical and Computational Study on Optimal Power Flow,” *IEEE Trans. Power Syst.*, vol. 31, no. 4, pp. 3008–3018, July 2016.
- [3] M. R. Narimani, D. K. Molzahn, and M. L. Crow, “Tightening QC Relaxations of AC Optimal Power Flow Problems via Coordinate Transformations,” in preparation for submission to *IEEE Trans. Power Syst.*
- [4] —, “Systematically Rotating Power Flow Equations for Tightening QC Relaxations of OPF Problems,” in preparation for submission to *IEEE Trans. Power Syst.*

^{*}: ECE Dept., Missouri University of Science and Technology.

[†]: ECE Dept., Georgia Institute of Technology.

Co-Optimized Expansion Planning to Enhance Resilience of the Electrical System in Puerto Rico

Cody J. Newlun¹, Armando L. Figueroa², James D. McCalley¹

¹Department of Electrical & Computer Engineering, Iowa State University, Ames, Iowa 50011, USA

²Policy Studies Department, MISO, Eagan, Minnesota 55121, USA

cnewlun@iastate.edu, afigueroa-acevedo@misoenergy.org, jdm@iastate.edu

Abstract—In 2017, the electric infrastructure of Puerto Rico (PR) was devastated by a category 4 hurricane, Hurricane Maria. Therefore, it is of high-interest to re-develop the infrastructure at the generation, transmission, and distribution (GTD) levels to create a hurricane-resilient infrastructure. This work details the methodologies behind developing a more resilient electric infrastructure using a co-optimized expansion planning (CEP) software tool. First, a model of the PR electric power system was developed to perform long-term CEP studies. The CEP tool developed seeks the minimum total cost of the PR system in a 20-year planning horizon while exploring various levels of expansion and resilience investment options. The CEP tool also models the system under extreme events (i.e. hurricanes) to allow for data-driven resilience enhancement decisions. Three infrastructure visions where the amount of distributed generation (DG) penetration varies are used to evaluate the CEP model.

I. MODEL DESCRIPTION

The CEP model developed for the PR system seeks to minimize the total cost while exploring GTD investment decisions. Figure 1 details the structure of the CEP model which has the form of a mixed integer linear program. Figure 2 displays the 3-segment distribution feeder which is used to model the distribution system at the load buses of the system. The corresponding candidate generation technologies and load allocations are also displayed.

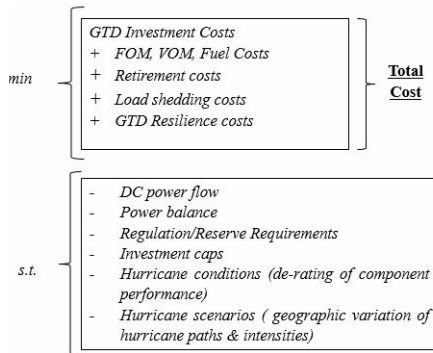


Fig. 1: High-level view of the model developed for PR

To simulate the effects of hurricanes on the island, hurricane wind profiles were developed based on the region of the island and the hurricane path. This data was utilized to develop statistics to "de-rate" the performance of the components in the system during hurricane conditions. Multiple hurricane paths were analyzed to develop characteristic hurricane years within the simulation. Three levels of resiliency were introduced for

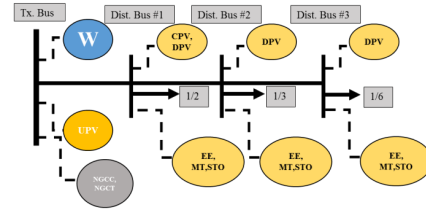


Fig. 2: 3-segment feeder with candidate technologies

candidate GTD technologies. Each resiliency level, denoted standard, semi, and full, have higher probability of surviving a hurricane with increasing costs. By introducing these investment options the model is able to make investment decisions by taking into account the cost of load shed versus the costs of building a more resilient system.

II. RESULTS

Figures 3 and 4 detail the three infrastructure visions and one base case with various amounts of DG penetration. Key findings within this study include the relationship between load shed costs, total costs (investments, retirements, and operational) and resiliency costs.

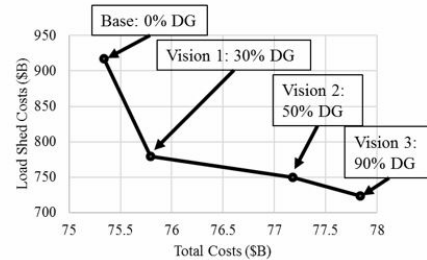


Fig. 3: Plot of load shed costs versus total cost

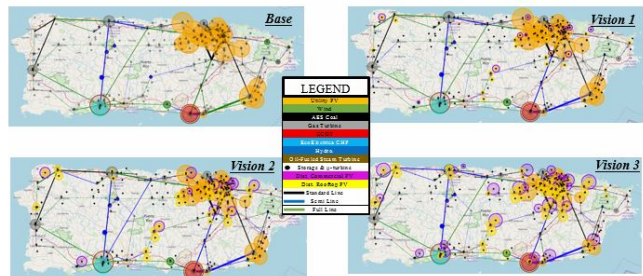


Fig. 4: Visualizations with variations of DG penetrations

A Sufficient Condition for Small-Signal Stability and Construction of Robust Stability Region

Parikshit Pareek¹, Konstantin Turitsyn², Krishnamurthy Dvijotham³, and Hung D. Nguyen⁴

Abstract—This paper focuses on the Differential Algebraic Equation (DAE) formulation of power systems and bridges the gap between the conventional reduced system and the original one using logarithmic norm. We propose a sufficient condition for stability using Bilinear Matrix Inequality and its inner approximation as Linear Matrix Inequality. Another contribution is the construction of robust stability regions in state-space in contrast to most existing approaches trying same in the parameter space. The paper provides a necessary base to develop tractable construction techniques for the robust stability region of power systems.

I. INTRODUCTION

A relation between the reduced form and the associated DAE system has been established using logarithmic norm for small-signal stability assessment. Further, we use this relation to develop a sufficient condition for stability of the DAE system. The robust stability region on which, if there exists any equilibrium point then, the system will be small-signal stable at that equilibrium, has been constructed. The sufficient condition for stability, as a Bilinear Matrix Inequality (BMI) is derived using the logarithmic norm. Then, a convex inner approximation of the BMI has been presented as Linear Matrix Inequality (LMI).

II. MAIN RESULT

The linearized state space model with algebraic constraints:

$$\delta \dot{\mathbf{x}} = A\delta \mathbf{x} + B\delta \mathbf{y}, \quad (1)$$

$$0 = C\delta \mathbf{x} + D\delta \mathbf{y}. \quad (2)$$

The system is small-signal stable if and only if all eigenvalues of the reduced Jacobian lie in the left half plane or $\text{Re}(\lambda(J_r)) < 0$ where $J_r = A - BD^{-1}C$ be the reduced Jacobian matrix.

We define *generalized reduced Jacobian* $F_r = PJ_r$ with $P \in S_n^+$, and *generalized unreduced Jacobian* $F = Z^T J$ which can be written as

$$F = \begin{bmatrix} PA + R^T C & PB + R^T D \\ Q^T C & Q^T D \end{bmatrix}. \quad (3)$$

Here, $Z = \begin{bmatrix} P & \mathbf{0} \\ R & Q \end{bmatrix}$ is an auxiliary matrix consisting of $\mathbf{0} \in \mathbb{R}^{n \times m}$ a null matrix, $R \in \mathbb{R}^{m \times n}$, and $Q \in \mathbb{R}^{m \times m}$.

For the DAE system with a negative logarithmic norm $\mu_p(F) < 0$ characterized by the matrices P, Q, R , the following relation holds:

$$\mu_p(F_r) \leq \mu_p(F). \quad (4)$$

Using affine system matrix expression $J(\mathbf{z}) = J_0 + \sum_k z_k J_k$ for $k = 1 \dots (n+m)$ and $p = 2$, in (4), the BMI for stable region, with ζ as maximum eigenvalue and I representing an identity matrix of size $(n+m) \times (n+m)$:

$$F(\mathbf{z}, Z) + F^T(\mathbf{z}, Z) - \zeta I \preceq 0. \quad (5)$$

To convert the bilinear relation into the linear one, we fix $Z = Z^*$ in the BMI (5). The resultant inner approximated convex stability region, of the non-convex region defined by the BMI (5), obtained as a robust SDP problem for affine perturbation for $\mathbf{z} \in \mathcal{U}$:

$$\begin{aligned} & \text{minimize} && \zeta \\ & \text{subject to} && J(\mathbf{z})^T Z^* + Z^{*T} J(\mathbf{z}) - \zeta I \preceq 0 \end{aligned} \quad (6)$$

If the solution ζ^* of this robust SDP is negative, then the region defined by the set \mathcal{U} is the robust stability region.

III. SIMULATION

The robust stability region using the different condition has been constructed for a 2-bus test system. Fig. 1 depicts the performance of sufficient condition (BMI (5)) with respect necessary and sufficient condition. Fig. 2 shows robust stable space obtained via different conditions.

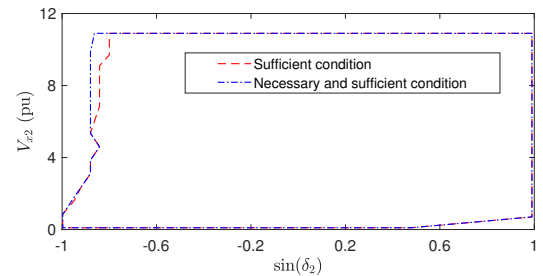


Fig. 1. Performance of sufficient condition (BMI 5) in 2-D state plane

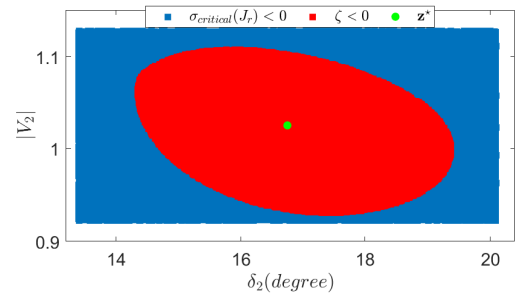


Fig. 2. Stable space in $\delta_2 - |V_2|$ plane using LMI (6)

^{1, 4} are with School of Electrical and Electronics Engineering, Nanyang Technological University, Singapore. e-mail: paree0001@e.ntu.edu.sg.

² is with Department of Mechanical Engineering, MIT, Cambridge, USA

³ is with Google DeepMind, London, UK

Formulation of a Distributed AC Volt-Var Optimization in Distribution Power Systems

Niloy Patari, *Student Member, IEEE*, Anurag. K. Srivastava, *Senior Member, IEEE*

Abstract—Electric utilities have always used a centralized optimization approach to regulate voltage across a distribution feeder. Slow-acting voltage control devices like tap changing regulators and shunt capacitors have done the job so far. However, with increased penetration of distributed energy resources (DERs), voltage control has become exceedingly difficult, mainly due to DERs’ intermittent and variable power injections. IEEE 1547.8 Standard has also strengthened the idea of using DERs as smart inverters to control the point of common coupling (PCC) voltage rapidly using their fast inverter controls. All these make Volt-Var Control (VVC) a large scale optimization problem. Utilities, hence, are looking towards distributed optimization techniques to solve the VVC problem in distribution power grids. This poster presents an overview of how the VVC optimization problem can be presented in a distributed fashion so as to include physical distribution power system constraints properly and also ensuring a global optimal solution for the same.

I. INTRODUCTION

AC Optimal Centralized Voltage Control Formulation:

$$\text{Minimize} : \sum_{i=1}^N w_i (|V_i|^2 - |V_{i,ref}|^2)^2 \quad (1)$$

$$\text{Variables} : S_i^g, V_i \quad (2)$$

$$\text{subject to} : (V_i^l)^2 \leq V_i V_i^* \leq (V_i^u)^2 \quad (3)$$

$$S_i^{gl} \leq S_i \leq S_i^{gu} \quad (4)$$

$$|S_{ij}| \leq S_{ij}^u \quad (5)$$

$$-\theta_{ij} \leq \angle(V_i, V_j^*) \leq \theta_{ij} \quad (6)$$

$$\sum_{(i,j) \in \tau_D} S_{ij} = S_i^{DER} + S_i^g - S_i^d - s_i(t) Y_i^c V_i V_i^* \quad (7)$$

$$Y_i^c = \omega C_i \quad (8)$$

$$S_{ij} = (Y_{ij}^s + Y_{ij}^*) \frac{V_i V_i^*}{T_{ij} T_{ij}^*} - Y_{ij}^* \frac{V_i V_j^*}{T_{ij}} \quad (9)$$

$$T_{ij} = \left(1 + a_{ij} \frac{0.1}{16} \right) \quad (10)$$

$$a_{ij} = \{-16, -15, \dots, 0, \dots, 15, 16\} \quad (11)$$

$$s_i(t) = \{0, 1\} \quad (12)$$

The objective of Centralized AC Optimal Volt-Var Control (ACVVO) problem is to minimize voltage deviations (1,13) along the distribution feeder while satisfying non-linear power flow equations (7-9,14) and power system operational constraints (3-6,15). The tap changing regulator and shunt capacitor constraints are presented in (10-12).

Niloy Patari and Anurag K. Srivastava are with Washington State University, Pullman, WA, 99163 (E-mail: anurag.k.srivastava@wsu.edu).

This work is supported by UI-ASSIST <https://uiassist.org/>

II. A DISTRIBUTED ARCHITECTURE TO SOLVE ACVVO

The basis of Distributed Optimization is to disintegrate the large centralized optimization problem into smaller sub-problems or sub-regions, each of which coordinate with their adjacent sub-regions so as to ensure a global optimal solution. A typical 3 sub-region distributed scenario is shown in Fig. 1. The variables in subproblem j ($j = 1, 2, 3$) are a_j which are composed of intra-problem variables and inter-problem variables (shown in red). The inter-problem variables need to be communicated among sub-problems and form the coordination matrix (18). The power flow equalities (17) and inequalities(19) are composed of intra-problem variables only. A comparison of centralized and distributed ACVVO is shown

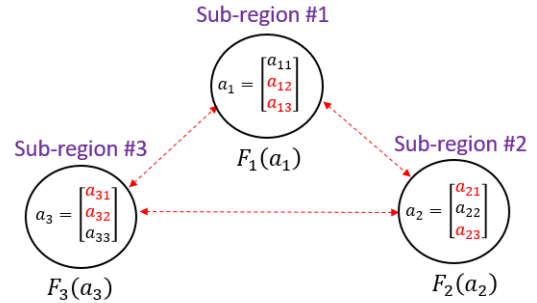


Fig. 1. A 3 Sub-problem Distributed Optimization Scenario

in Fig.2.

$\text{Minimize: } f(y) = \sum_{k \in B} f_k(y) \quad (13)$	$\text{Minimize: } \sum_{j \in P} F_j(a_j) \quad (16)$
$Gy = 0_M \quad (14)$	$G_j a_j = 0 \quad (17)$
$Hy \leq b_M \quad (15)$	$A_j a_j = 0 \quad (18)$
	$H_j a_j \leq b_j \quad (19)$
Centralized Problem Formulation	Distributed Problem Formulation

Fig. 2. Comparison of Centralized and Distributed ACVVO

III. SUMMARY

The Distributed ACVVO Technique should meet the following requirements-

- Should solve ACVVO three phase unbalanced systems with DER operational constraints and integer type constraints (11-12).
- Should converge in polynomial time.
- Convex relaxations if considered must be exact.
- Approximations considered should not deviate much from realistic power system models.

Optimal-Probabilistic Coordination of Directional Overcurrent Relays Considering Network Topological Uncertainties

Jiawei Qi*, Jun Xie†, Xiejin Ling*, Yinhong Li*, *Member, IEEE*, and Tongkun Lan*

* State Key Laboratory of Advanced Electromagnetic Engineering and Technology
Huazhong University of Science and Technology, Wuhan, China

† Central China Electric Power Dispatching and Control Sub-center of State Grid Corporation of China

Email: jw7_hust@hust.edu.cn, xjvhj@163.com, hust_lxj@hust.edu.cn, liyinhong@hust.edu.cn, lantongkun@hust.edu.cn

Abstract—The probability of each network topology occurring in an actual power system is entirely different. The relays coordination considering overall possible topology variations without corresponding probabilities tends to cause unsatisfactory performance of relay settings in operation and even difficulty in determining settings. In this paper, a novel method is proposed for optimal coordination of directional overcurrent relays (DOCRs) considering network topological uncertainties through its probabilistic model. The relays coordination problem is formulated as a multi-objective optimization problem with two objective functions. One is the conventional function that minimizes overall operating time of the relays, and the other is to minimize the probabilities of loss of selectivity under network topology variations. With the proposed method, the settings are satisfactorily determined with the minimum probability of losing selectivity. The method proposed in this paper has been applied to an 8-bus power system, and the results demonstrated the better robustness towards the network topology variations over the prevailing approaches.

Index Terms—Network topological uncertainties, directional overcurrent relays, probabilistic optimization, relay settings, optimal coordination, multi-objective optimization.

I. KEY MODEL

A. Objective Functions

$$\text{Min : } OF_1 = \sum_{i=1}^N \omega_i t_i \quad OF_2 = \sum_{j=1}^M P_j^{\text{loss}} \quad (1)$$

$$t_{i,j} = \frac{0.14 \times TDS_i}{(I_{f_{i,j}}/I_{P_i})^{0.02} - 1} \quad P_j^{\text{loss}} = p_j \times \frac{N_j^{vl}}{N_j} \quad (2)$$

B. Bounds of Variables

$$I_{P_i}^{\text{min}} \leq I_{P_i} \leq I_{P_i}^{\text{max}} \quad (3)$$

$$TDS_i^{\text{min}} \leq TDS_i \leq TDS_i^{\text{max}} \quad (4)$$

$$t_i^{\text{min}} \leq t_{i,j} \leq t_i^{\text{max}} \quad (5)$$

II. KEY RESULTS

It is a tradeoff between operating time and probability of loss of selectivity under different network topologies. Actually, the obtained Pareto optimal frontier could meet such requirements with multiple setting groups provided.

TABLE I

NUMBER OF CONSTRAINTS VIOLATION AND PROBABILITY OF LOSS OF SELECTIVITY FOR RELAY PAIRS UNDER DIFFERENT TOPOLOGIES

Relay Pairs		Case 1		Case 2		Case 3	
PR	BR	N_V	ΣP_{loss}	N_V	ΣP_{loss}	N_V	ΣP_{loss}
1	6	9	0.9038	9	0.9038	2	0.0516
2	1	1	0.0305	1	0.0305	1	0.0305
2	7	4	0.4544	0	0	0	0
3	2	9	0.9446	9	0.9446	0	0
4	3	6	0.1770	2	0.0773	2	0.0773
5	4	9	0.9441	9	0.9441	0	0
6	5	5	0.5199	0	0	0	0
6	14	4	0.4937	0	0	0	0
7	5	5	0.5141	3	0.4449	0	0
7	13	0	0	0	0	0	0
8	7	4	0.4366	2	0.4449	0	0
8	9	3	0.0864	0	0	0	0
9	10	9	0.9484	9	0.9484	0	0
10	11	6	0.1656	2	0.3870	6	0.1656
11	12	9	0.9441	9	0.9441	0	0
12	13	1	0.0305	1	0.0305	0	0
12	14	4	0.4803	0	0	0	0
13	8	9	0.9308	9	0.9308	0	0
14	1	0	0	0	0	2	0.0516
14	9	5	0.4854	0	0	0	0
ΣN_V		102		65		13	

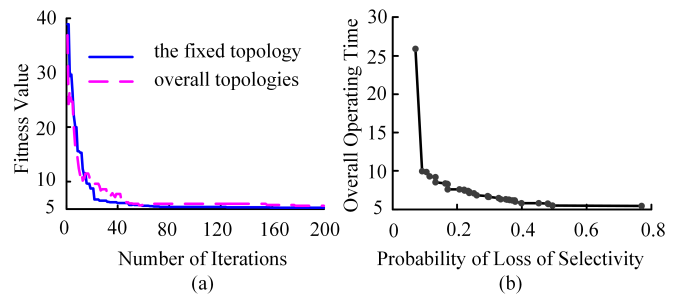


Fig. 1. (a). Convergence of the PSO algorithm considering the fixed topology and overall topology variations respectively; (b). The curve of the Pareto optimal frontier with the solution of the multi-objective optimization problem.

III. CONCLUSION

The results of the case study demonstrate the performance of the proposed optimal-probabilistic coordination method, which is more adaptive to network topology variations in the sense of probabilities of loss of selectivity for relay pairs.

Security Constrained Unit Commitment with Corrective Transmission Switching

Arun Venkatesh Ramesh, *Student Member, IEEE*, and Xingpeng Li, *Member, IEEE*

Abstract-- This Poster emphasizes the importance of including transmission switching to accomplish Flexible Transmission in $N-1$ security-constrained unit commitment (SCUC) model. A $N-1$ SCUC mathematical model implementing a dynamic network in the post-contingency scenario is proposed as opposed to current industry practices of static network in short-term operations. The proposed model is tested and validated on the IEEE 24-bus system. The proposed model results in cost-effective implementation and leads to overall reduced cost, and congestion reduction in the post-contingency scenario.

I. INTRODUCTION

THE advent of multiple national level directives which addresses the requirement for a smarter electrical grid. This includes the development of transmission technologies for optimizing the use of transmission. Currently, switching of power system elements can help independent system operators (ISO) to maintain the system security and reduce operation costs. The infrastructure to perform transmission switching (TS) already exists and this makes it easier to implement without additional investments. However, the use of transmission as a controllable asset today is limited.

The use of TS can improve the market surplus as well as to relieve congestions but also cause significant large system disturbance [1]. Hence, the use of corrective transmission switching (CTS) in post-contingency situations to avoid system disturbance can be a viable option. This mitigates or eliminates the transmission flow violations during contingent scenarios. The current ISO model does not include switching of transmission lines during short-term operations since transmission assets are treated as a static network [2].

II. KEY MODELLING EQUATIONS

Base case modeling of power flow:

$$P_{kt} - b_k(\theta_{nt} - \theta_{mt}) = 0 \quad (1)$$

$$-P_k^{max} \leq P_{kt} \leq P_k^{max} \quad (2)$$

Post-contingency modeling of power flow for non-radial lines:

$$P_{kct} - b_k(\theta_{nct} - \theta_{mct}) + (1 - S_{c,t}^k)M \geq 0 \quad (3)$$

$$P_{kct} - b_k(\theta_{nct} - \theta_{mct}) - (1 - S_{c,t}^k)M \leq 0 \quad (4)$$

$$-P_k^{emax} S_{c,t}^k \leq P_{k,c,t} \leq S_{c,t}^k P_k^{emax} \quad (5)$$

$$\sum_k S_{c,t}^k \leq 1 \quad (6)$$

where line k is defined from bus m to bus n ; c is the contingent line; t denotes the time period; b_k is the susceptance of line; θ_{it}

and θ_{ict} denotes the bus angle and the contingent bus angle for bus i respectively; P_{kt} and P_{kct} denotes the line flow and the contingent line flow respectively; P_k^{max} and P_k^{emax} are the normal limit and the emergency limit of the line respectively; M is a large real number; and $S_{c,t}^k$ is the switching variable of line k for contingency on line c .

III. RESULTS

The IEEE 24-bus system is modified to include congestion in the network during base case solution. The mathematical model is implemented using AMPL and solved using Gurobi solver for a 24-hour (Day-Ahead) load period. The difference in overall cost of $N-1$ SCUC with CTS and $N-1$ SCUC without CTS is used to demonstrate the cost reduction with CTS.

TABLE I. OPERATIONAL COST AND POST-CONTINGENCY CONGESTION COST ANALYSIS IN $N-1$ SCUC

	N-1 SCUC without CTS		N-1 SCUC with CTS
	Limited Emergency Rating	Infinite Emergency Rating	Limited Emergency Rating
Cost (\$)	526839	525018	525018
€	6958	N/A	0

€ denotes the post-contingency congestion cost (\$).

IV. SUMMARY OF RESULTS

The best scenario is represented by infinite transmission capacity in the post-contingency scenario. It is observed that TS of at most one line can alleviate the network congestion in post-contingency scenarios by rerouting power through the network. This results in reduced overall cost and higher transmission capability in the case of a congested network. The use of CTS also avoids system disturbance as the network is unmodified in the base-case.

V. REFERENCES

- [1] X. Li, P. Balasubramanian, M. Sahraei-Ardakani, M. Abdi-Khorsand, K. W. Hedman and R. Podmore, "Real-Time Contingency Analysis With Corrective Transmission Switching," in *IEEE Transactions on Power Systems*, vol. 32, no. 4, pp. 2604-2617, July 2017.
- [2] K. W. Hedman, S. S. Oren and R. P. O'Neill, "A review of transmission switching and network topology optimization," *2011 IEEE Power and Energy Society General Meeting*, San Diego, CA, 2011, pp. 1-7.

Anticipating Impact of Q-limits for Enhancement of PMU Based Fast Voltage Stability Index

Syed M. Hur Rizvi, *Student Member IEEE*
Electrical Engineering and Computer Science
Washington State University
Pullman, USA
Email: syed.rizvi@wsu.edu

Anurag Srivastava, *Member IEEE*
Electrical Engineering and Computer Science
Washington State University
Pullman, USA

Abstract—With power system becoming more stressed everyday it has become more prone to voltage collapse. It is very important to monitor voltage stability of power system in an efficient manner so that operators can be alerted to take corrective measures to reduce the impact of impact of impending voltage collapse. Many indices suitable for real time voltage stability monitoring of power system have been proposed in literature for instance Thevenin based index, L-index and FVSI (based on relative electrical distance). The main objective of all these indices is to give an easily interpretable, local voltage stability index at minimum computational expense. Most of such indices despite being very useful, suffer from one major drawback, which is their discontinuous nature owing to Q-limits of the generators. In case a generator reaches reactive power limits, these indices show sudden jump and sudden change in voltage stability status of the system. In this poster impact of Q-limits on Fast Voltage stability index (FVSI) index is predicted by monitoring the reactive power reserve of nearest generator and the second nearest generator to the monitored load bus. Proposed scheme is applied on WECC 9 Bus System to demonstrate the results.

Keywords—Voltage stability, PMUs, Q-limits, FVSI, Transfer limit

I. INTRODUCTION

Ensuring voltage stability of power system is of utmost importance. This significance has led to lots of research interest in power industry over the years. Traditionally model based schemes like continuation power-flow deployed to estimate the margin of an operating point from voltage stability limit. Continuation power flow and other such schemes based on repetitive power-flow analysis despite being extremely accurate have disadvantage of not being suitable for real-time voltage stability monitoring. To solve this issue many measurement-based voltage stability schemes have been recently proposed in literature. These schemes have advantage of very fast real-time computation of voltage stability index and that makes them attractive despite not being as accurate as their model-based counterparts. One disadvantage associated with measurement-based indices is their discontinuity when generators hit their Q-limits. Whenever a generator hits the Q-limit there is a sudden jump in the voltage stability index. Because of such discontinuity the advantage of extrapolating the index to predict distance to collapse can be hampered. In this poster we introduce a by using reactive power reserve information of two nearest generators to enhance the ability of FVSI to account for generator Q-limits. The results are demonstrated for WECC 9 Bus System but can be applied to any bigger system owing to simplicity of the concept.

Undergraduate Classroom Module for Hardware-in-the-Loop Power System Dynamics Study

Pranav Shrestha, *Student Member, IEEE* and Luke Dosiek, *Member, IEEE*

Department of Electrical and Computer Engineering

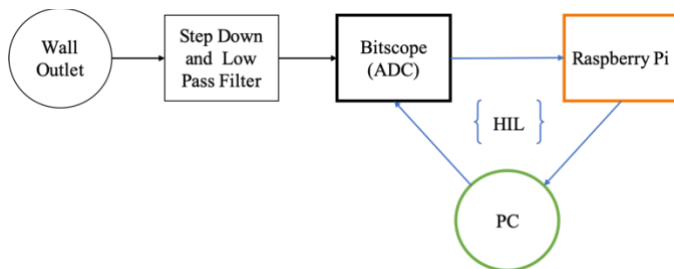
Union College, Schenectady, NY

Abstract— The project includes modules programmed in Python to analyze data and provide easy exercises that students can use to understand concepts in power engineering. It would help with grasping concepts better for students in institutions without expensive industry standard equipment through actual simulation instead of pencil on paper calculations of concepts.

I. INTRODUCTION

Data collected by PMUs are time-synchronized which helps the grid operators to get excellent wide area situational awareness. At the distribution-level, Frequency Disturbance Recorders (FDR) developed by University of Tennessee Knoxville [1] are one of the few PMU devices that have been implemented. Studies have shown system-wide events are observable at this level, and that these low-level voltage variations can be indicators of localized power issues.

The lack of access to commercial PMUs in undergraduate colleges makes the study of topics particular to power grid hard and inaccessible. To include the concepts of power engineering in college level, this project aims to create a power grid monitoring device using ultra low-cost PC. Using this, quick and easy exercises can be designed to let undergraduates learn and interact with real-life data such as the recent Florida event or simulated data that we can create in MATLAB and feed into Raspberry Pi. Hardware-in-a loop (HIL) simulation of such events and their capture is displayed in Figure 1 below.



PC	Raspberry Pi
<ul style="list-style-type: none"> • Option for Simulated or Measured V and $\angle V$ • Create $y = V \cos(2\pi f_0 t + \angle V)$ • Scale for audio and play out of headphone jack • Analyze calculations from Raspberry Pi in real-time 	<ul style="list-style-type: none"> • Reads $V(t)$ • Calculates V and $\angle V$ and frequency • Optional: Calculate mode estimates • Sends estimates to PC

Figure 1: Modules for data collection and simulation

II. OBSERVATIONS

The Raspberry Pi programmed in Python makes it easy to swap out algorithms for phasor estimation or mode estimation from the data supplied either through the PC or the wall outlet.

The playback of simulated and real world archived data through PC using the sound card makes a simple HIL simulation possible. We have also created a program that compares the real data with estimates we receive from the Raspberry Pi. Some example application results are shown below:

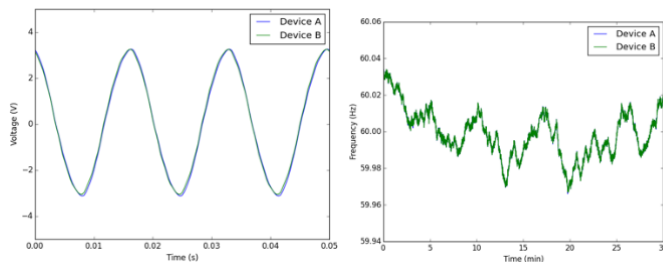


Figure 2: Voltage waveforms captured by each device (left), and extracted frequency estimates (right).

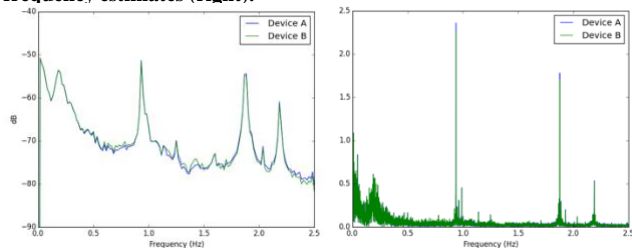


Figure 3: Welch periodograms (left) and FFT (right) of detrended frequency estimates.

REFERENCES

- [1] Z. Zhong, C. Xu, B. Billian, L. Zhang, S. Tsai, R. Conners, V. Centeno, A. Phadke and Y. Liu, "Power System Frequency Monitoring Network (FNET) Implementation", *IEEE Transactions on Power Systems*, vol. 20, no. 4, pp. 1914-1921, 2005.
- [2] D. M. Laverty, R. J. Best, P. Brogan, I. Al Khatib, L. Vanfretti and D. Morrow, "The OpenPMU Platform for Open-Source Phasor Measurements", *IEEE Transactions on Instrumentation and Measurement*, vol. 62, no. 4, pp. 701-709, April 2013

Enabling Cyberattack-Resilient Load Forecasting through Adversarial Machine Learning

Zefan Tang, Jieying Jiao, Peng Zhang, Meng Yue, Chen Chen, Jun Yan

Abstract—In the face of an increasingly broad cyberattack surface, cyberattack-resilient load forecasting for electric utilities is both more necessary and more challenging than ever. This paper addresses the gap by developing an adversarial machine learning (AML) approach. An adversarial training is adopted to increase the robustness of an artificial neural network (ANN) based load forecasting model against cyberattacks. Through adversarial training, the model is trained with not only the clean data, but also malicious data generated by an adversary. To tackle different cyberattack scenarios, an ensemble adversarial training is established, and the parameters selection is evaluated for desired performance.

I. MAIN RESULTS

In this study, the attack is modeled via two parameters: an attack probability p_{te} and a scaling factor λ_{te} . In the adversarial training, the attack model is applied on the input training data with parameters p_{tr} and λ_{tr} . An ensemble adversarial training (EAdv.) is further developed by using a varying λ_{tr} with parameters α and β .

Key conclusions: 1) using different attack configurations in the adversarial training have different impacts when there is no attack, and the impacts can be undesirably large if the configurations are not properly set; and (2) the AML with a proper configuration can strike a balance between enhancing a system’s robustness against cyberattacks and maintaining a reasonable degree of forecasting accuracy under no attack.

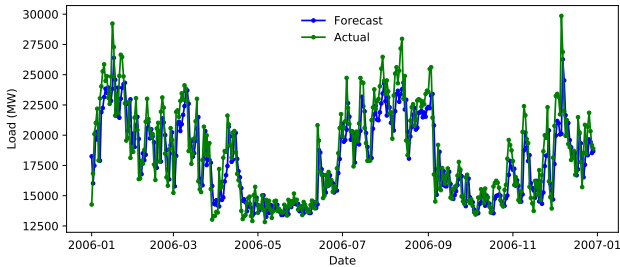


Fig. 1. Comparison results of ANN-based load forecasting and actual values on the testing data throughout 2006.

This work was supported in part by the National Science Foundation under Grants ECCS-1611095, CNS-1647209 and ECCS-1831811, in part by the Department of Energy Cybersecurity for Energy Delivery Systems (CEDs), and in part by the Office of the Provost, University of Connecticut.

Z. Tang and P. Zhang are with the Department of Electrical and Computer Engineering, University of Connecticut, Storrs, CT 06269, USA (e-mail: peng.zhang@uconn.edu).

J. Jiao and J. Yan are with the Department of Statistics, University of Connecticut, Storrs, CT 06269, USA.

M. Yue is with Sustainable Energy Technologies Department, Brookhaven National Laboratory, Upton, NY 11973, USA.

C. Chen is with Energy Systems Division, Argonne National Laboratory, Lemont, IL 60439, USA.

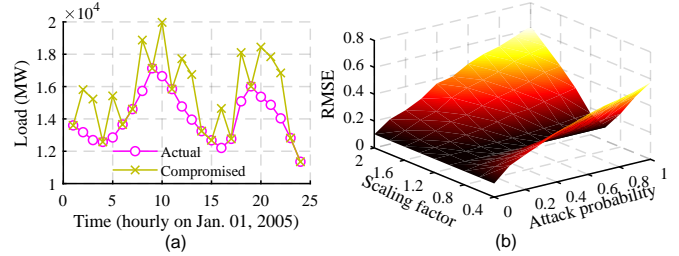


Fig. 2. Impact analysis. (a) An example of the attack model with the data from 1 January when p_{te} is 0.5 and λ_{te} is 1.2. (b) Illustration of cyberattack impact with different p_{te} and λ_{te} .

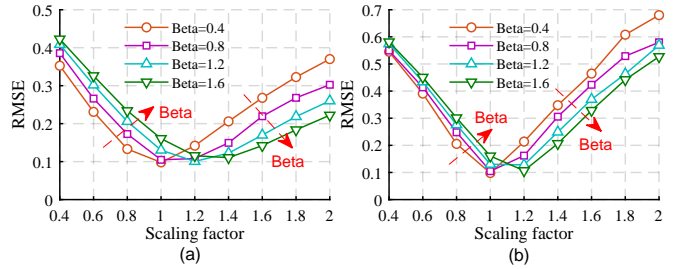


Fig. 3. Comparison results of EAdv. with different β under different attack scenarios when $\alpha = 0.6$ and $p_{tr} = 0.3$. (a) $p_{te} = 0.5$. (b) $p_{te} = 1$.

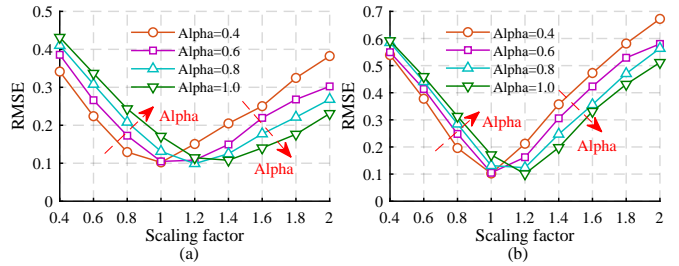


Fig. 4. Comparison results of EAdv. with different α under different attack scenarios when $\beta = 0.8$ and $p_{tr} = 0.3$. (a) $p_{te} = 0.5$. (b) $p_{te} = 1$.

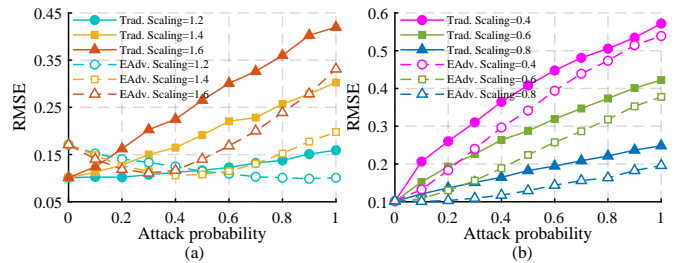


Fig. 5. Comparison results of EAdv. and the traditional ANN under different attack scenarios. (a) $\alpha = 1$, $\beta = 0.8$, and $p_{tr} = 0.3$. (b) $\alpha = 0.4$, $\beta = 0.8$, and $p_{tr} = 0.3$.

Convexified OPF in Multiphase Low Voltage Radial Distribution Networks including Neutral Conductor

Muhammad Usman*, Andrea Cervi, Massimiliano Coppo, Fabio Bignucolo, Roberto Turri
 Department of Industrial Engineering, University of Padova, Padova, Italy
 *muhammad.usman@studenti.unipd.it

Abstract—Optimal power flow problem for low-voltage radial distribution networks including neutral conductor is considered in this paper. The standard semi-definite programming based relaxation, initially proposed for the three-phase networks, is extended to such multi-phase networks by taking into account the coupled phase-neutral power injections. Furthermore, the impact of neutral-ground impedance has also been taken into account. Simulations are carried out on real low-voltage unbalanced distribution networks for the minimization of either slack-bus power injection or power losses objective functions. It has been demonstrated that the proposed approach is numerically exact under a large range of the value of neutral-ground impedance and can be successfully solved by a generic optimization solver such as MOSEK.

I. PROBLEM DESCRIPTION

Semi-Definite Programming (SDP)-based AC-OPF model has gained significant attention in the past few years due to its ability to provide an exact solution of the original non-convex AC-OPF model. However, the developed SDP-model cannot simply be extended to multi-phase Distribution Networks (DNs) by augmenting additional power balance constraints for phase/neutral conductors due to the coupled phase-neutral power injection. Consequently, Correction Current Injection (CCI) based approach is utilized in this paper in order to derive the explicit power injections at each conductor of the network.

II. METHODOLOGY

Based on the CCI approach, the apparent power of a load/DG connected between phase-neutral can be expressed as

$$S_{k(r)}^{*\kappa} = Y_k^\kappa |V_{k(r)}^\kappa|^2 - (\Delta I_{k(r)I\%}^\kappa + \Delta I_{k(r)P\%}^\kappa) V_{k(r)}^\kappa \quad (1)$$

By ignoring CCI terms related to the constant current and constant power injections, and incorporating admittances related to the constant impedance shunt elements into the network admittance matrix, the following SDP-based OPF model for multi-phase DN can be derived.

$$\mathbf{M1} : \underset{\mathbf{X}}{\text{minimize}} f(\mathbf{X}) \quad (2a)$$

subject to

$$\text{Tr}(\Psi_{P,k}^\varphi \mathbf{X}) = 0, \forall \varphi \in \phi_k, k \in N \setminus G \quad (2b)$$

$$\text{Tr}(\Psi_{Q,k}^\varphi \mathbf{X}) - y_{c_k}^\kappa \text{Tr}(\Psi_{V,k}^\varphi \mathbf{X}) = 0, \quad \forall \varphi \in \phi_k, \kappa \in \psi_k, k \in N \setminus G \quad (2c)$$

$$\underline{S}_{g_i} \leq \text{Tr}(\Psi_{P,i}^\varphi \mathbf{X}) \leq \overline{S}_{g_i}, \quad \forall \varphi \in \phi_i, i \in G \quad (2d)$$

$$(\underline{V}_k)^2 \leq \text{Tr}(\Psi_{V,k}^\varphi \mathbf{X}) \leq (\overline{V}_k)^2, \quad \forall \varphi \in \eta_k, k \in N^+ \quad (2e)$$

$$\mathbf{X} \succeq 0 \quad (2f)$$

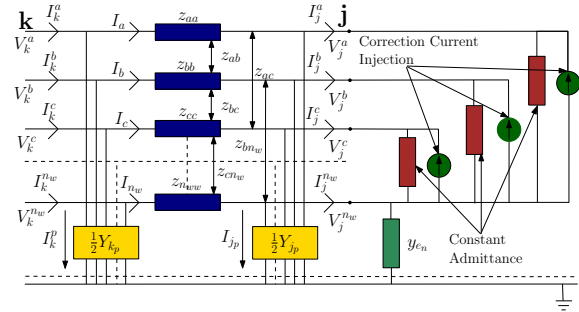


Fig. 1: Distribution network representation with constant load admittances, correction current injections and earthing admittance.

III. RESULTS AND CONCLUSIONS

- A small EVR, in the case of R_{g2} & R_{g3} , indicates the exactness of the proposed approach. However, setting an extremely small value as in the case of R_{g1} provides an ill-conditioned data to the solver which in turn is unable to provide the meaningful results.

Table I: Exactness of the Proposed Approach

Eigenvalue Ratio $ \lambda_2 / \lambda_1 $			
OF ₁ : Minimization of Slack-Bus Power			
Test System	R_{g1}	R_{g2}	R_{g3}
10-bus	0.93	2.75×10^{-6}	4.2×10^{-5}
IT 37-bus	0.0185	5.3×10^{-6}	2.7×10^{-5}
OF ₂ : Minimization of Power Losses			
Test System	R_{g1}	R_{g2}	R_{g3}
10-bus	1.3×10^{-5}	1.5×10^{-5}	2.5×10^{-5}
IT 37-bus	3.1×10^{-6}	1.2×10^{-5}	2.3×10^{-4}

- RMSE indicates that the voltages of the original non-convex AC-OPF problem can be recovered with sufficient accuracy from the solution of the relaxed convex **M1** model.

Table II: Accuracy of the Proposed Approach for $R_g = 1\Omega$

Root Mean Square Error (RMSE)				
OF ₁ : Minimization of Slack-Bus Power				
Test System	$V_A(pu)$	$V_B(pu)$	$V_C(pu)$	$V_N(pu)$
10-bus	7×10^{-4}	1.2×10^{-3}	7×10^{-4}	8×10^{-4}
IT 37-bus	7.9×10^{-4}	7.9×10^{-4}	8.0×10^{-4}	6.3×10^{-4}
OF ₂ : Minimization of Power Losses				
Test System	$V_A(pu)$	$V_B(pu)$	$V_C(pu)$	$V_N(pu)$
10-bus	1.7×10^{-3}	1.5×10^{-3}	1.3×10^{-3}	1.4×10^{-3}
IT 37-bus	3.5×10^{-3}	1.4×10^{-3}	1.0×10^{-3}	1.1×10^{-3}

MILP-Based Algorithm for the Global Solution of Dynamic Economic Dispatch Problems with Valve-Point Effects

Loïc Van Hoorebeek
 ICTEAM
 UCLouvain
 Louvain-la-Neuve, Belgium
 Email: loic.vanhoorebeek@uclouvain.be

P.-A. Absil
 ICTEAM
 UCLouvain
 Louvain-la-Neuve, Belgium

Anthony Papavasiliou
 CORE
 UCLouvain
 Louvain-la-Neuve, Belgium

Abstract—The Dynamic Economic Dispatch (DED) problem consists in satisfying a certain demand for electric power among scheduled generating units over a certain interval of time while satisfying the operating constraints of these units. The consideration of the valve-point effect (VPE) makes the problem more practical but also more challenging due to the non-linear and non-smooth constraints that are required for representing the model. We present a method, based on a sequence of piecewise linear approximations, which produces a feasible solution along with a lower bound on the global solution. In this way, this deterministic approach can trade off the speed which characterizes certain heuristics that are usually used to solve the DED-VPE for a better solution and insights about the problem. The method is applied to a widely used case study and provides a lower solution objective than the best known solution to date.

I. INTRODUCTION

The Economic Dispatch (ED) problem is an important optimization problem in short-term power system planning. It consists in the optimal dispatch of power among scheduled electricity generation facilities in order to meet the system load at a minimal cost. Commonly, the fuel cost functions have been modeled as a smooth quadratic function in the ED problem. Unfortunately, such a model does not reflect the valve-point effect (VPE), i.e., the fact that turbines operating off a valve point run less efficiently due to throttling losses. This significantly affects the output of facilities that are now characterized by a non-smooth and non-convex cost function.

II. PROBLEM DESCRIPTION

The problem of interest (P) can be written in a compact way as the following

$$(P) \quad \min_{p_{it}, s_{it}} \sum_{i=1, t=1}^{n, T} f_i(p_{it}),$$

subject to $(\mathbf{p}, \mathbf{s}) \in D$

where f_i is the fuel cost associated with generator i , p_{it} is the production of each individual generator and s_{it} is the reserve of the generator i at a given time t . A common model of the

fuel cost functions including the VPE is the sum of a smooth quadratic part and a non-smooth rectified sine, i.e.,

$$f_{it}(p_{it}) = a_i p_{it}^2 + b_i p_{it} + c_i + d_i |\sin e_i (p_{it} - p_i^{\min})|, \quad (1)$$

with appropriate parameters a_i, b_i, c_i, d_i, e_i . All operational constraints (ramp, admissible ranges, reserve requirements) and the power balance are included in the set D . As this problem is non-smooth and non-convex, traditional optimization methods may not converge in general.

III. METHOD DESCRIPTION

Instead of solving directly (P), we focus on a surrogate problem (S) that approximates (P) while being easier to solve. The surrogate problem is defined with the piecewise-linear approximations of the cost functions. As the solution of (S), obtained with a commercial solver, can be far from the true solution, the proposed method iterates by increasing the number of knots in an adaptive way: the best solution of the k -th surrogate problem (S) $_k$ is added to the set of knots which defines the piecewise approximation. In this way, any tolerance can be reached by the algorithm given in Figure 1.

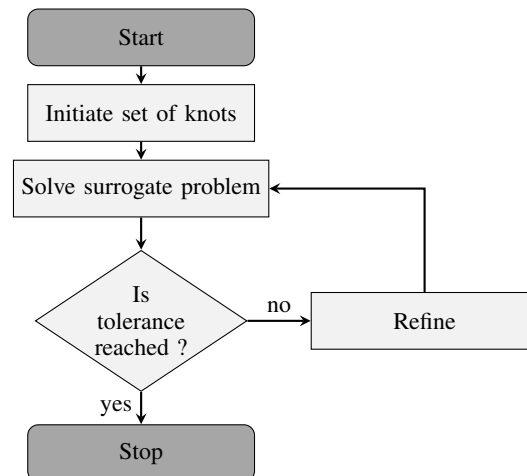


Fig. 1. Flow chart of the algorithm.

Advanced Distribution Protection for High Penetration of Distributed Energy Resources (DER)

Yaswanth Nag Velaga, and P.K.Sen
Department of Electrical Engineering
Colorado School of Mines
Golden, CO

Abstract—With the large amount of distributed energy resources (DER) being added in distribution networks, protection will become a major challenge due to low fault currents and reverse power flows. Present protection schemes that are based on simple over current philosophy will not be adequate. Advanced protection schemes, which can adapt to the changing system configuration is essential. Time-domain based protection that is independent of fault current magnitudes and direction is proposed to enhance the distribution protection.

Keywords— *Distribution Systems, Distributed Energy Resources, Protection, Travelling Wave.*

I. INTRODUCTION

Protection systems are extremely critical for the proper operation of a power grid at all voltage levels. It is important to quickly locate, identify, and isolate the faults in time that will protect grid components, avoid accidents, ensure personnel safety and reduce customer outages. An improper protection action in a transmission system can lead to system wide black outs, cause loss of productivity and damage equipment. There are many examples of that. After the 2003 blackout, a lot of attention has been given to the bulk power system protection.

However, for multiple reasons distribution system protection has not surfaced at the same level of importance. For most part, the power outages are limited in a geographical area involving a smaller number of customers. It still is dominated primarily by the overcurrent relays (50/51 or 50/51G) for both phase and ground fault protections for all feeders and reclosers / sectionalizers and simple fuse protection.

Today, the distribution system is vastly different and changing rapidly with the advancement of DER technologies. As more inverter-based DERs (like rooftop or community PV, battery storage and electric vehicles) are integrated into the distribution grid, these phasor-domain based protection schemes with limited settings capability may become too slow and inadequate to perform all the functions. Moreover, distribution systems with high penetration of DERs also pose other challenges in the proper operation of protection schemes due to the reduction in the fault currents, reverse power flows, arcing faults and loss of ground reference in wye grounded systems. Another challenge is the IEEE 1547-2018 guidelines that dictates the operation of DERs during dynamic conditions. Hence, there is a need for an advanced distribution protection that can adapt to the system configuration and needs.

Current research efforts are focused more on adaptive protection schemes based on phasor domain using different groups of settings. There are limitations to such approach and one of them is the low fault currents (1.2-2pu) from inverters. This can make it challenging for phasor domain-based approaches.

In this proposed research work, time-domain based signatures are studied. Specifically, time-domain based signature, such as, the traveling waves (TWs) that are generated during a fault and propagate in the power lines close to the speed of light. These waves travel fast in the lines and get reflected from buses and other nodes. This information can be used to quickly locate faults, isolate and restore the grid. This travelling wave information can be used in the protection schemes to locate and clear the fault much faster than current methods with low fault currents. This method is suitable for systems with high penetrations of DER with power electronics interface because it does not use directional components or phasor domain current information utilized by the traditional protection schemes.

The principle of travelling wave is well-known and found many applications in power systems analysis especially at the high voltage bulk power systems. However, its applications in distribution network (predominantly 12.47kV, but it could be 25kV) is very limited, if at all. Primary reason is available technology to deal with very short time. Distribution lines are shorter than the transmission lines, limited to below 10 miles.

In order to better protect against faults and other disturbances, time-domain based protection schemes that can be adaptive needs to be developed. Adaptive protection allows the system to make adjustments to the protection coverage based upon varying power conditions. These changes can make the coverage more effective with respect to all real-time conditions that could be present on the system. Electro Magnetic Transient Program (EMTP-RV) is used to model and study the distribution network.

This research work focusses on the broader picture of the distribution protection schemes and addresses various issues and challenges in the distribution network with high penetration of DER.

A Data-driven Control Method for Operating the Commercial HVAC Load as a Virtual Battery

Jiyu Wang and Ning Lu
 Department of Electrical and Computer Engineering
 North Carolina State University
 Raleigh, NC, USA
 jwang49@ncsu.edu

Sen Huang and Di Wu
 Optimization and Control Group
 Pacific Northwest National Laboratory
 Richland, WA, USA

Abstract — This paper presents a data-driven control method for operating the commercial heating, ventilation, and air conditioning (HVAC) load as a virtual battery (VB). Unlike an electric battery, a VB charges/discharges by consuming more/less than its scheduled baseline power. Therefore, while acting as a VB, it is critical for an HVAC load to follow a baseline consumption when no control signal is received and increase/decrease its consumption against the baseline if a charging/discharging signal is received. The HVAC load in a commercial building serves many thermal zones, so each zone can be viewed as a cell in a battery. The total power consumption of the HVAC can be controlled by adjusting the airflow rate of each zone. In this paper, models are presented for approximating the thermal dynamic and the operation of different HVAC components based on measurement data. Then, a control algorithm is proposed for adjusting zonal airflow rate in a commercial building to regulate the total HVAC consumption at desired level. A commercial building located in Richland, WA, is modeled in EnergyPlus to test the performance of the proposed control algorithm for operating the building HVAC load as a VB.

Index Terms— Commercial building, Grid service, HVAC, Virtual battery.

I. INTRODUCTION

Modeling and controlling building loads as virtual batteries (VB) is a novel way to quantify and utilize the flexibility in building operation for grid services [9-10]. Unlike active energy storage systems such as batteries, building loads cannot actually be charged or discharged to supply other loads. Instead, the load can act as a VB by consuming more/less than its scheduled baseline power so that it mimics the battery charging/discharging behaviors. For utilizing building loads as a VB, it is critical for controlling building loads to follow a baseline consumption when no control signal is received and to increase or decrease power consumption against the baseline when a charging or discharging signal is received.

In this paper, a centralized control algorithm is proposed for operating commercial HVAC as a VB by following dispatch signals against the baseline power consumption while maintaining occupants' comfort level within the desired range. To achieve the control accuracy, model are calibrated using building operation data and updated every a few time intervals. By using the model to calculate the airflow rate of each thermal zone, the total HVAC power consumption can be controlled within the target range. To illustrate the control method, a

commercial building located in Richland WA, in its cooling mode is modeled in EnergyPlus to provide the building operational data in a summer month. The baseline following and load following for offsetting duck curve are studied to demonstrate the effectiveness of operating a commercial building HVAC load as a VB.

II. KEY FIGURES

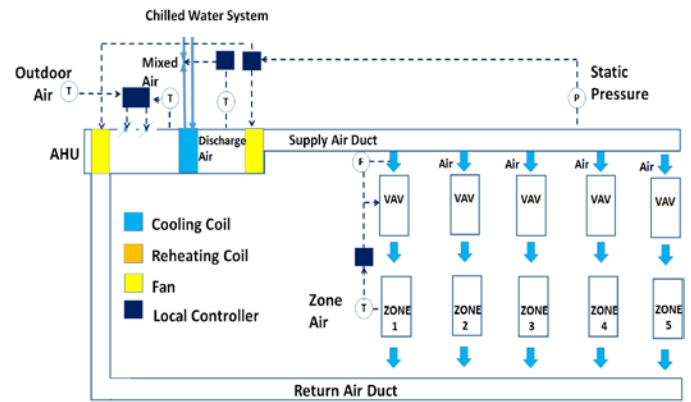


Fig. 1. Configuration of a typical HVAC system in commercial buildings

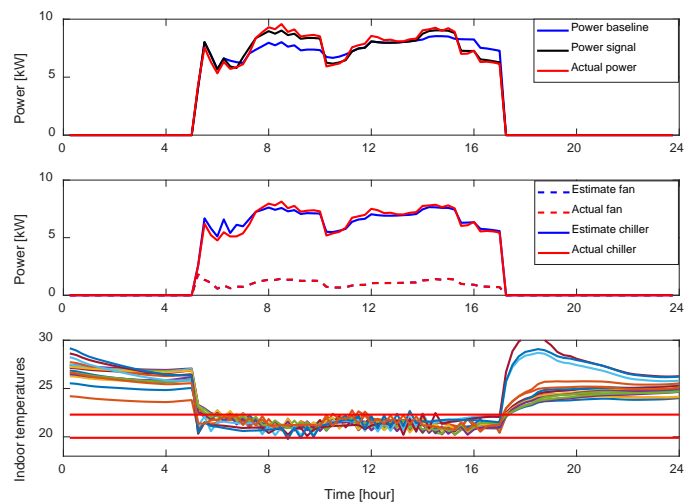


Fig. 2. Load following results for offsetting duck curve power

Chordal Conversion based Convex Iteration Algorithm for Three-phase Optimal Power Flow Problems

Wei Wang¹, *Student Member, IEEE*, Nanpeng Yu, *Senior Member, IEEE*,

Abstract—The three-phase optimal power flow (OPF) problem has recently attracted a lot of research interests due to the need to coordinate the operations of large-scale and heterogeneous distributed energy resources (DERs) in unbalanced electric power distribution systems. The non-convexity of the three-phase OPF problem is much stronger than that of the single-phase OPF problem. Instead of applying the semidefinite programming relaxation technique, this paper advocates a convex iteration algorithm to solve the non-convex three-phase OPF problem. To make the convex iteration algorithm computationally efficient for large-scale distribution networks, the chordal conversion based technique is embedded in the convex iteration framework. By synergistically combining the convex iteration method and the chordal based conversion technique, the proposed three-phase OPF algorithm is not only computationally efficient but also guarantees global optimality when the trace of the regularization term becomes zero. At last, to further improve the computational performance, a greedy grid partitioning algorithm is proposed to decompose a single large matrix representing a distribution network to many smaller matrices. The simulation results using standard IEEE test feeders show that the proposed algorithm is computationally efficient, scalable, and yields global optimal solutions while resolving the rank conundrum.

I. METHODOLOGY AND KEY EQUATIONS

By synergistically combining the chordal conversion method and the convex iteration technique, this paper proposes a new iterative three-phase OPF solution algorithm as follows.

Step 1:

$$\min_X \sum_{l=1}^{N_A} C_l (X_l^{ext}) + \sum_{l=1}^{N_A} w_l Tr(X_l^{ext} W_l^*) \quad (1)$$

s.t.

$$X_l^{ext} \in B^{(l)}, \quad l = 1, 2, \dots, N_A \quad (2)$$

$$X_l^{ext(r)} = X_r^{ext(l)}, \quad l, r = 1, 2, \dots, N_A \quad (3)$$

$$X_l^{ext} \succeq 0, \quad l = 1, 2, \dots, N_A \quad (4)$$

Step 2:

$$W_l = U_j(:, 2 : N_{X_l^{ext}}) U_j(:, 2 : N_{X_l^{ext}})^T \quad (5)$$

where the size of X_l^{ext} is $N_{X_l^{ext}} \times N_{X_l^{ext}}$. U_j is obtained from the singular value decomposition.

$$X_j^{ext} = U_j \Lambda_j U_j^T \quad (6)$$

The computational efficiency of the chordal conversion based convex iteration algorithm depends heavily on the choice of grid partition scheme. A greedy algorithm also developed a to find an appropriate grid partition scheme.

II. KEY RESULTS

As shown in Table I and II, the proposed convex iteration approach achieves the rank-one solutions, i.e., global optimums, for all the test cases.

TABLE I
COMPARISON OF TRADITIONAL METHODS AND THE CONVEX ITERATION METHOD WITH DIFFERENT PRICES FOR DERs

Test system	Prices of three phases (\$/kWh)	Objective value (\$/hour)		
		Powell	Interior Point	Convex Iteration
4-bus test feeder	1/0.5/0.2	3121.9	3121.9	3121.9
	0.9/0.45/0.18	3091.9	3091.9	3086.9
10-bus test feeder	1/0.3/0.6	1229.2	1229.2	1229.1
	0.8/0.24/0.48	1191.4	1191.4	1191.3
13-bus test feeder	0.6/0.3/1	2345.4	2345.4	2345.4
	0.48/0.24/0.8	2290.2	2290.2	2290.2
34-bus test feeder	1/0.9/0.8	832.7	832.7	830.8
	0.9/0.81/0.72	816.5	816.5	815.4
37-bus test feeder	0.6/0.3/1	1740.3	1740.3	1739.5
	0.54/0.27/0.9	1675.9	1675.9	1675.4
123-bus test feeder	1/0.3/0.6	2414.6	2414.5	2413.6
	0.8/0.24/0.48	2205.6	2205.6	2205.0
906-bus test feeder	0.6/0.7/0.5	38.4	38.3	38.2
	0.54/0.63/0.45	37.9	37.9	37.7

TABLE II
COMPARISON OF THE SDP RELAXATION METHOD AND THE CONVEX ITERATION METHOD WITH DIFFERENT PRICES FOR THREE PHASES

Test system	Method	Rank of solution	Objective value (\$/hour)
4-bus test feeder	SDP relaxation	3	3085.6
	convex iteration	1	3121.9
10-bus test feeder	SDP relaxation	7	1216.3
	convex iteration	1	1229.1
13-bus test feeder	SDP relaxation	3	2319.5
	convex iteration	1	2345.4
34-bus test feeder	SDP relaxation	6*	831.8
	convex iteration	1	830.8
37-bus test feeder	SDP relaxation	1*	1739.5
	convex iteration	1	1739.5
123-bus test feeder	SDP relaxation	6*	2413.6
	convex iteration	1	2413.6
906-bus test feeder	SDP relaxation	6*	38.2
	convex iteration	1	38.2

The star symbol, *, represents the highest rank among all partitioned areas.

A Stacked Autoencoder Application for Residential Load Curve Forecast and Peak Shaving

Xinan Wang, *Student Member, IEEE*, Yishen Wang, *Member, IEEE*, Di Shi, *Senior Member IEEE*, Jianhui Wang, *Senior Member IEEE*,

Abstract— For the last ten years, utilities have observed ongoing transitions on consumers’ load curves. The previously flat load curves have more frequently turned into duck-shape. This is jointly caused by the increasing household loads as well as the popularity of rooftop solar photovoltaic. Such load curve transition challenges the operation flexibility of the existing systems and greatly increases the per-MWh energy costs. Peak shaving, in this context, becomes a critical task to demand-side management. Owing to the development of Battery Energy Storage Systems (BESS), numerous peak shaving strategies have been developed and implemented. In this paper, by applying a stacked autoencoder (SAE)-based residential peak load curve forecasting technology, we further lift the peaking shaving capabilities of BESSs to a new level. The proposed strategy takes into account the welfares of both generation-side and demand-side and reaches an optimal balance. A comprehensive case study using smart meter data demonstrates the effectiveness of the proposed method in peak shaving application.

Index Terms—Peak shaving, stacked autoencoder (SAE), BESS, solar photovoltaics, machine learning.

I. BACKGROUND

A study conducted by the California ISO [1] shows the increasing penetration of rooftop solar photovoltaics (PVs), electric vehicles (EVs) and battery energy storage systems (BESS) is driving the net load curve to a duck-neck-shape. Such transition challenges the grid stabilities and increases the per-MWh energy costs. Therefore, demand-side management (DSM) becomes more important than ever.

As one of the most important DSM applications, peak shaving can help to mitigate such issue through demand response [2]-[5] and BESS [7]-[9]. This paper focuses on the BESS-based peak shaving methodology. Three common BESS-based strategies [7]-[9] are summarized in Figure 1. a-c. Figure 1.a is the full-output model, where a BESS supplies peak load until the battery is exhausted. The remaining peak load surge is supplied by the grid. Figure 1.b presents the threshold-

based strategy [8], in which a BESS shaves the load when exceeding a pre-defined threshold. But the performance of the approach is heavily constrained by the limited BESS capacities. In Figure 1.c, BESS provides a conservative constant output to guarantee it can last longer than the peak-hour [9]. All these three strategies try to maximize consumers’ welfares; on the other hand, they all neglect the utilities’ welfares. Figure 1.d. shows an ideal peak shaving strategy, in which BESS’ outputs dynamically follow the peak load curve with a constant mismatch. so that a flatten peak load curve is left to the utility which in other words significantly reduce the peak load volatility. Different from typical time series prediction works [10], the ideal peak-shaving requires a onetime full peak period curve prediction before peak-hour starts. The more accurate the prediction can be the higher peak can be shaved, our proposed SAE-based load curve prediction is detailed discussed in this paper to explain how it achieves a high prediction accuracy.

The biggest challenge for the ideal shaving is to predict an accurate peak load curve before peak-hour starts. Statistical-based load forecasting works [11]-[12] can hardly tackle the uncertainties brought by the residential BESS, PVs and EVs. In addition, feature-based supervised load prediction models like Artificial Neural Network (ANN), Support Vector Regression (SVR) [13]-[15] highly depend on the collected data, such as numerical weather index data and customer behavior analysis data, to reach satisfactory performances. And those data are not always available in practice. In this paper, we propose a machine learning-based load curve regression approach by using the unsupervised stacked autoencoder (SAE) algorithm. In this method, we use SAE to learn a representation of peak load curves from a training set and then encode the data into the SAE and decode it using the latent representation. In summary, the contributions of this paper are as follows:

- Strategically applies SAE to residential peak load forecasting and achieves a promising accuracy;
- Achieves the ideal peak shaving, which takes into account the welfares of both consumers’ and utilities’;
- A detailed performance analysis for the proposed framework is presented to serves as a reference for similar works in the field.

X. Wang and J. Wang are with the Department of Electrical and Computer Engineering, Southern Methodist University, Dallas, TX 75205 USA (Email: xinanw@smu.edu; jianhui@smu.edu;). X. Wang, Y. Wang and D. Shi are with GEIRI North America, San Jose, CA 95134, USA.

This work is funded by SGCC Science and Technology Program under contract no. SGSDYT00FCJS1700676.

Data-driven Distributionally Robust Energy Consumption Scheduling of HVAC based on Disjoint Layered Ambiguity Set

Yingjie Wang*, Yuefang Du†, Chao Duan§, Haotian Xu*, Lin Jiang*

*Dept. of Electrical Engineering and Electronics, The University of Liverpool, Liverpool, UK

†School of Mechanical and Electrical Engineering, UESTC, Sichuan, China

§Dept. of Physics and Astronomy, The Northwestern University, Evanston, USA

Emails: {Yingjie.Wang, hshxu4, ljiang}@liverpool.ac.uk, yuefangdu_liv@163.com, chao.duan@northwestern.edu

Abstract—This paper proposes a distributionally robust optimization approach (DROA) based on a disjoint layered ambiguity set for scheduling the energy consumption of the heating, ventilation and air conditioning (HVAC) system. The uncertainties of the predicted outdoor temperature error and indoor temperature variations that are caused by human activities are taken into account in the energy consumption scheduling of the HVAC based on historical data. The maximum uncertainty set of outdoor temperature is divided into disjoint subintervals and the probabilistic information of these subintervals is obtained to construct a disjoint layered ambiguity set. A nonlinear HVAC’s energy consumption problem is formulated by using the DROA method to deal with these two uncertainties based on a disjoint layered ambiguity set with distributionally robust chance constraints (DRCCs). Simulation results illustrate the effectiveness of the proposed method.

Index Terms—Distributionally robust optimization, energy consumption scheduling, HVAC, demand response.

I. INTRODUCTION

In this paper, a DROA based on the disjoint layered ambiguity set is proposed to deal with the drawbacks of the DROA based on nest layered ambiguity set in [1] and enhance the performance of the energy consumption scheduling of HVAC. Unlike [1], this approach will separate the whole probability distribution of the outdoor temperature into different independent disjoint subintervals, which reduces the effect of interacting of differentiate and decreases the conservatism in programming. As the conservatism in programming is reduced, the user’s electricity cost is decreased as well.

II. KEY EQUATIONS

The objective is to minimise the electricity cost and satisfy customer’s indoor temperature thermal comfort zone by scheduling the energy consumption of HVAC, according to the consumer’s preset comfort indoor temperature zone and the electricity price in Austin, Texas during one of the summer days. Similar to [1], the complete optimization model is formulated with a disjoint layered ambiguity set as follows:

$$\min_{q_t^{ref}} \mathbb{E} \left\{ \sum_{t=1}^T (e_t \cdot q_t \cdot \Delta t) \right\} \quad (1a)$$

$$s.t. (3), (4a) - (4c) \quad (1b)$$

$$\theta^{\min} \leq \theta_t^{ref} \leq \theta^{\max} \quad (1c)$$

where e_t is expressed as the electricity price at time period t . The upper bound and lower bound of the comfortable indoor temperature zone are denoted as θ^{\max} and θ^{\min} , respectively.

III. SIMULATION RESULTS

The simulation results are demonstrated to verify the effectiveness of proposed DROA based on a disjoint ambiguity set.

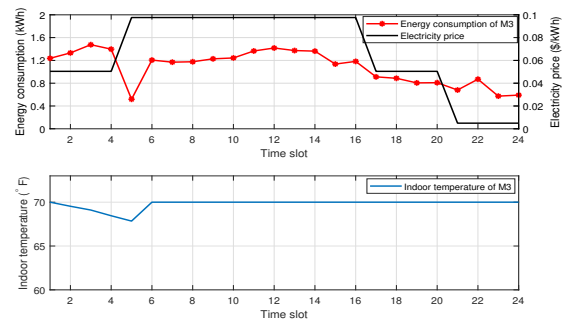


Fig. 1. Energy consumption and indoor temperature for M3

TABLE I
PERFORMANCES OF THE THREE METHODS IN A SCHEDULING CYCLE

Method	Cost (\$)	Num_VioTem	Max_VioTem (°F)	CR (%)
M1	0.9904	0	0	0
M2	0.9311	3	0.0096	6.37
M3	0.9307	1	0.0012	6.42

REFERENCES

- [1] Y.F. Du, L. Jiang, C.Duan, Y.Z. Li and J.S. Smith, “Energy Consumption Scheduling of HVAC Considering Weather Forecast Error through Distributionally Robust Approach,” *IEEE Transactions on Industrial Informatics*, vol. PP, no. 99, pp. 1-11, Jan. 2017.

Distributed Multi-Functional Finite-Time Secondary Control in Cyber-Physical Microgrid

Weitao Yao, *Student Member, IEEE*, Yu Wang, *Member, IEEE*, Yan Xu, *Senior Member, IEEE*,
Tung Lam Nguyen, *Student Member, IEEE*, Xue Feng, *Member, IEEE*

Abstract—In this paper, a novel distributed multi-functional finite-time secondary control strategy is proposed for islanded AC microgrids. The control objective features two key modules: 1) A consensus-based distributed controller aims to achieve frequency restoration and accurate sharing of active power in finite time. 2) A containment-based distributed controller achieves a better trade-off between voltage regulation and reactive power sharing. Finally, a cyber-physical microgrid platform is used to verify the proposed controller's effectiveness considering cases of load variations and voltage boundary changes.

I. CONTROL OBJECTIVES

A. Control Objectives

1. The all DG's frequency can be restored to nominal value and active power can be accurately sharing in finite time.
2. The all DG's voltage can be bounded within a reasonable range and reactive power sharing can also be achieved in finite time

II. PROPOSED MULTI-FUNCTIONAL CONTROL SCHEME

A. For frequency restoration and active power sharing

The neighborhood tracking error of frequency and active power for DG_{*i*} can be calculated as:

$$\delta_i^\omega = \sum_{j \in N_i} a_{ij} (\omega_j - \omega_i) + g_i (\omega^{ref} - \omega_i) \quad (1)$$

$$\delta_i^p = \sum_{j \in N_i} a_{ij} (K_j^p P_j - K_i^p P_i) \quad (2)$$

The control law is designed as follow:

$$u_i^\omega = c_\omega \text{sig}(\delta_i^\omega)^\beta \quad (3)$$

$$u_i^p = c_p \text{sig}(\delta_i^p)^\beta \quad (4)$$

B. For voltage regulation and reactive power sharing

The neighborhood tracking error of voltage and reactive power for DG_{*i*} can be calculated as:

$$\delta_i^V = \sum_{j \in N_i} a_{ij} (V_j - V_i) + \sum_{l \in R_i} b_{il} (V^{bou} - V_i) \quad (5)$$

$$\delta_i^q = \sum_{j \in N_i} a_{ij} (K_j^q Q_j - K_i^q Q_i) \quad (6)$$

The control law is designed as follow:

$$u_i^V = \underbrace{c_{V_1} \text{sig}(\delta_i^V)^{\zeta_1}}_{u_{i_1}} + \underbrace{c_{V_2} \text{sig}(\delta_i^V)^{\zeta_2}}_{u_{i_2}} \quad (7)$$

$$u_i^Q = c_q \text{sig}(\delta_i^q)^{\zeta_1} \quad (8)$$

III. EXPERIMENT RESULT

For load change and voltage boundary change:

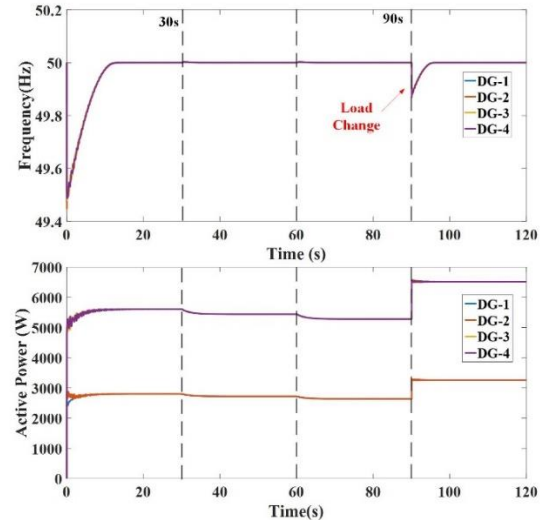


Fig.1 The frequency and active power of each DG in Case 1.

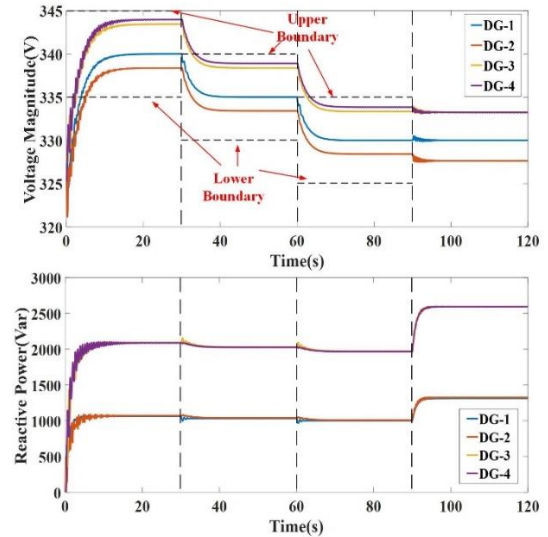


Fig.2 The voltage and reactive power of each DG in Case 1.

Enabling the Hardware-in-the-loop Co-simulation of Distribution Volt-Var Control through the Optimization of Sub-transmission Voltage Regulation

Fuhong Xie ¹, *Student Member, IEEE*, Catie McEntee ², *Student Member, IEEE*, Mingzhi Zhang ³, *Student Member, IEEE*, Ning Lu ⁴, *Senior Member, IEEE*

Dept. Electrical and Computer Engineering, FREEDM System Center
North Carolina State University
Raleigh, NC, 27606, US

Email: ¹fxie2@ncsu.edu, ²cmmcente@ncsu.edu, ³mzhang33@ncsu.edu, ⁴nlu2@ncsu.edu

Abstract — This poster presents a modeling framework of an asynchronous hardware-in-the-loop (HIL) co-simulation platform. This platform can be used to model the dynamic interaction between many small power electronic subsystems connected to a three-phase unbalanced distribution feeder. Subsystem, including microgrid, solar farm, and dynamic composite load, is modeled on the OPAL-RT using eMEGASIM package so that electromagnetic transients of the inverter units can be modeled at a time step of 100 microseconds. The distribution feeder system that subsystems are connected to is simulated using the OPAL-RT ePHASORSIM thus load transients, capacitor switching, and tap-changing events can be simulated. An external distribution volt-var controller will interface the HIL testbed through the Modbus link controlling the voltages on each node and fulfilling the requests from the sub-transmission voltage regulation controller. This HIL testbed can be “connected” to a remote HIL system or hardware through the virtual private network (VPN) links to achieve the co-simulation of control systems located in different geographical locations. The HIL framework allows different distribution controller logic to be developed and tested considering both the subsystem transients, including inverter transients and dynamic responses, and the remote responses from the transmission system and physical hardware. Impacts of communication delay, error, or interruption on the distribution controller can also be modeled and quantified under this framework.

Index Terms — Asynchronous, co-simulation, distribution, OPAL-RT, hardware-in-the-loop, SIMULINK.

I. INTRODUCTION

The integration of microgrids (MGs) significantly increases the flexibility, reliability, and resiliency of power system operation. Microgrids are usually powered by distributed generations (DGs), such as diesel generators, cogeneration through combined heat and power (CHP), photovoltaics (PV) systems. Other distributed energy resources (DERs), such as battery energy storage systems and controllable loads, are often used to help DGs maintain the power balance in normal operating conditions and achieve frequency and voltage stability during outages. Thus, the reliable operation of a microgrid depends on how different DERs control systems

interact with each other under different operation modes.

On the other hand, after the penetration of microgrids increases, the interaction between the microgrids and the main grids are becoming critical to the reliable operation of the main grid. This is because the switching transient of many small DERs and microgrid control systems may start to affect the stability of the main grid operation.

In this poster, an asynchronous hardware-in-the-loop (HIL) co-simulation platform, as shown in Fig. 1, will be presented to model the interaction between DERs and distribution grid. The DER system will be modeled on the OPAL-RT eMEGASIM at a time step of 100 μ s to capture inverter-level transients and dynamic load responses. The distribution grid will be modeled on the OPAL-RT ePHASORSIM at a time step of 10ms to capture switching transients of tap changes, capacitor banks. Communication links between the North Carolina State University (NCSU) HIL system and the remote HIL system or hardware are also established to enable the co-simulation of large-scale, interconnected systems.

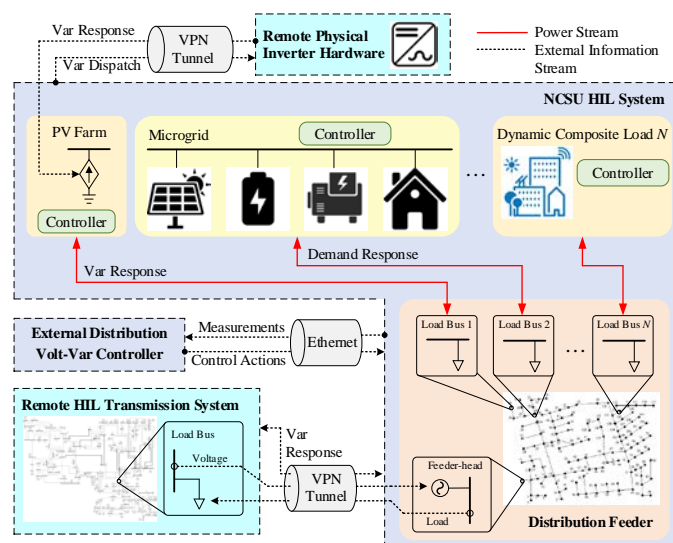


Fig. 1. The architecture of HIL co-simulation platform

Blockchain Framework for Peer-to-Peer Energy Trading with Credit Rating

Jiawei Yang, *Student Member*, IEEE, Amrit Paudel, *Student Member*, IEEE, H B Gooi, *Senior Member*, IEEE
 School of Electrical and Electronic Engineering
 Nanyang Technological University, Singapore
 Email: jiawei003@e.ntu.edu.sg, amrit003@e.ntu.edu.sg, ehbgooi@ntu.edu.sg

Abstract—A peer-to-peer (P2P) energy trading market allows participants to trade their energy with each other directly. In this market, a pricing mechanism can regulate the trading price between traders and a scoring criterion could encourage participants good behaviors. This paper proposes a P2P energy trading model, including a blockchain framework to secure traders information and execute transactions, a two-level pricing mechanism to determine the trading price for each transaction and a credit rating system to improve the quality of the P2P market. The design of these methods to achieve their respective functions and the creation of blockchain are discussed in this paper.

Index Terms—Blockchain, peer-to-peer energy trading, credit rating, distribution network

I. INTRODUCTION

This paper proposes a P2P energy trading model with a proper pricing mechanism to minimize the cost of participants. A credit rating system prevents malicious operations and a blockchain framework ensures the transparency and security of participants. The first objective is to propose a pricing mechanism. Distributed generation in a P2P market allows prosumers to trade their energy, so the price of every unit of energy should be decided by the amount of every participant's generation according to the time slot. This characteristic achieves the consensus with that of the blockchain technology, as the establishment of a new block needs to be approved by the majority of peers. As for the trading market, the prosumers who used to have records of deregulation should be punished by enjoy less priority in the market. To achieve this goal, a credit rating system is applied to secure prosumers' good behaviors and improve the market quality.

II. CREDIT RATING SYSTEM FOR P2P ENERGY TRADING

In the process of trading, a credit rating system plays a significant role because the rating points influence participants' choice directly: Prosumers with higher rating points have more trading choice in transactions. Those with lesser rating points may have no access to trade with those of better offers. This system determines the number of offers or bids a prosumer can collect when it joins the market. Good behaviors of traders can help to increase their credit rating points (CRPs), but their bad behaviors could decrease their CRPs.

The process of transactions is demonstrated in Figure 1.

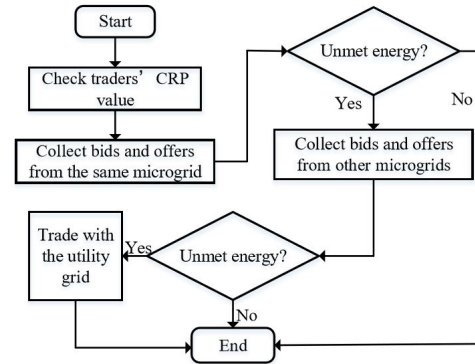


Fig. 1: The process of trading for buyers

A. Smart Contract and Block Creation

In each time slot, after broadcasting trading requirement from the buyers to the P2P network, sellers could respond to every initial participant by providing their energy size and price when they received the trading tokens. Meanwhile, the CRP values of the market participants will be verified by all the peers in the network depending on the criteria of the credit rating system. When the optimal objects are selected, transactions can be operated and terminated between traders. Therefore, the condition of the smart contract to trigger the transaction is that 'the CRP values are verified by all peers and buyer A receives m amount of energy from seller B', after which, the next step 'transfer M number of dollars from A to B' can be triggered automatically. When verified transactions are done, the information of the whole transactions in each time slot is grouped and stored in a new block. This new block is then received by all peers in the network and added to the blockchain. The structure of blockchains for the two-level trading process is demonstrated similarly in Figure 1.

III. CONCLUSION

This paper proposes a P2P energy trading model comprising a two-level pricing mechanism, a credit rating system and a blockchain framework, this proposed model could not only improve the quality of a P2P market, but also provide some flexibility for the market operators to apply more advanced technology into the market.

Studying the influence of flexibility provided by aggregated EVs on power system operating risk

Mingzhi Zhang^{*†}, Lingfeng Wang[†], Ning Lu^{*}

^{*} North Carolina State University, Raleigh, NC 27606 USA Emails:mzhang33@ncsu.edu & nlu2@ncsu.edu

[†]University of Wisconsin-Milwaukee, Milwaukee, Wisconsin 53211, USA Email: l.f.wang@ieee.org

Abstract—A smart charging algorithm is proposed to coordinate the stochastic charging behaviors of large amounts of electric vehicles (EVs). Meanwhile, the potential application of using the flexibility provided by aggregated EVs as operating reserve is also discussed. The available flexibility is estimated based on each EV’s status. Numerical study show this V2G enabled smart charging algorithm can effectively flat the load curve, and the flexibility provided by aggregated EVs as system operating reserve can effectively reduce system operating risk level.

Index Terms—Electric vehicles, flexibility, smart charging, operating risk.

I. V2G ENABLED SMART CHARGING CONTROL

Each EV aggregator can contract a significant number of EVs and work as a coordinator between the end users and market. The capacity of an aggregator is determined by its controlled number of EVs and the flexibility of each car, which depends on users’ behaviors and preferences. Each aggregator can directly control the charging behaviors of each car. By collecting the historical data and users’ preferences, the aggregator can predict its daily energy need and controllable capacity, and it can also monitor the real-time operation of plugged-in EVs and collect related information, like the identification, state of charge (SOC), and user preference settings. The system architecture is shown in Fig. 1.

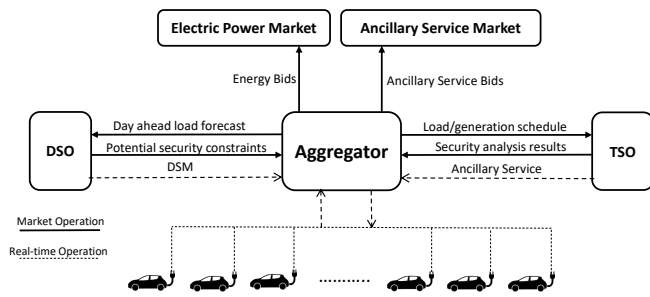


Fig. 1. Smart charging control architecture.

II. CAPACITY ESTIMATION OF FLEXIBILITY PROVIDED BY AGGREGATED EVS

In most cases, providing operating reserve does not affect the normal daily operation of EV, because the operating reserve (contingency reserve) will only be called for in the presence of serious contingencies in power system. Combined with the characteristics of EV, the available operating reserve

capacity is divided into interruptible capacity and V2G capacity. The estimation of operating reserve capacity that provided by an EV aggregator (3000 EVs) is shown in Fig. 2.

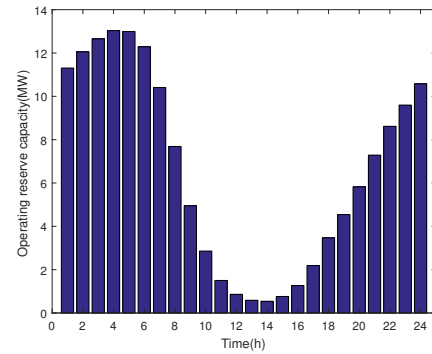


Fig. 2. Operating reserve capacity provided by 3000 EVs in test day.

III. RELIABILITY ANALYSIS WITH OPERATING RESERVE PROVIDED BY AGGREGATED EVS

According to the modified PJM method, the system unit commitment risks (UCR) with or without additional market acquired operating reserve capacity from EV aggregators in the test day can be calculated, the results are shown in Fig. 3.

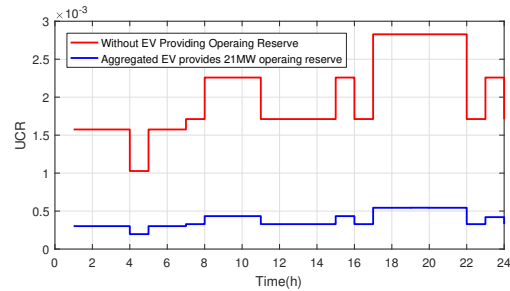


Fig. 3. System UCR with 21MW reserve purchased from aggregators.

IV. CONCLUSION

The V2G enabled smart charging algorithm is proven to be effective in flattening the load curve and transferring the charging load to the night valley hours. Moreover, the flexibility and energy storage characteristics of EVs make it possible to provide operating reserve for the power system.

Indirect Adaptive Control of a Power Distribution System based on Backpropagation of Utility

Hasala Dharmawardena, *Student Member, IEEE* *
 Ganesh K. Venayagamoorthy, *Senior Member, IEEE* * †

*Real-Time Power and Intelligent System Laboratory
 Clemson University, South Carolina, USA

†School of Engineering, University of KwaZulu-Natal, Durban, South Africa
 hasala@ieee.org and gkumar@ieee.org

Abstract—This study describes a method for control of a power distribution system. The method uses back propagation of utility to adapt the controller with the objective to maximize the utility function. It can be applied to control a distribution system in an unknown and dynamic environment. This method requires an accurate model of the system.

Index Terms—Power Distribution System, Adaptive Control, Backpropagation, Neural Networks.

The modern power distribution system requires to operate in a largely unknown and dynamic environment. In order to optimally dispatch and control such a system, the controller needs to learn from its interactions with the environment and dynamically tune its operation.

The control objective (utility) of such a system could also be dynamic by nature. For example, at one point of time power quality could be a dominant requirement, and in another point of time, loss reduction could be the dominant requirement. Therefore, the ideal control framework should be flexible enough to perform optimally in a dynamic environment while ensuring system stability.

The power distribution system is a complex, high-dimensional and non-linear system. This system can be dispatched and controlled by using backpropagation of utility [1], which is a data-driven method for optimization of a dynamic system. This study uses backpropagation of utility to control a simple distribution system. The modified IEEE34 system presented in [2] is used for the case study, since it includes smart inverters that has a controllable reactive power output.

The control system consists of two sub systems; a control network, that mimics the role of a traditional controller, and a Model network, that estimates the plant output. The generic utility function for this study is formulated based on bus voltage deviation (dV), voltage limit violations (α), standard deviation of bus voltage (β), inverter loading (γ), and total system losses (P_{loss}), as shown below. The contribution of each objective to the total utility can be adjusted by changing

This study is supported by the National Science Foundation (NSF) of the United States, under grants IIP #1312260, #1408141 and #1638321, and the Duke Energy Distinguished Professorship Endowment Fund. Any opinions, findings and conclusions or recommendations expressed in this material are those of author(s) and do not necessarily reflect the views of National Science Foundation and Duke Energy.

the corresponding ω value.

$$U = \omega_1\alpha(V) + \omega_2\beta(V) + \omega_3\gamma(Invtload) + \omega_4P_{loss} + \omega_5(dV^2)$$

The control signal is the output from the controller and it is a vector of reactive power injection of the inverters.

The foundation for backpropagation of utility lies in the calculus of variation in classical control theory [3]. Since the controller and the model are both structured as a neural networks, calculus of variation can be applied to change the weights of the controller network to maximize the total utility.

The system is tuned offline using historical data. It is then connected online to control the smart inverters in real time. If system model changes, the controller as well as the model will adapt (online) based on system feedback.

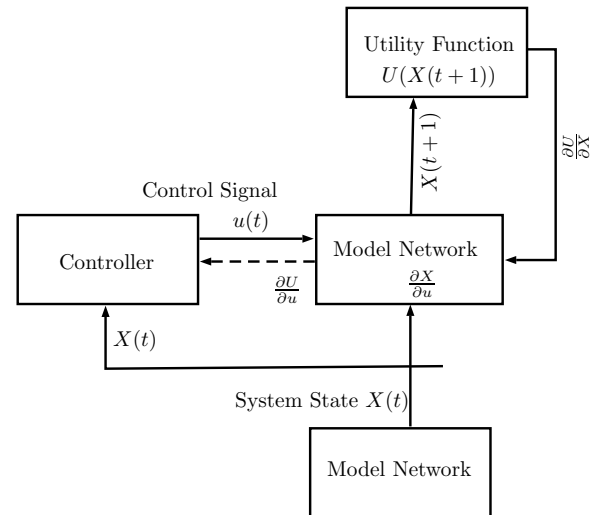


Fig. 1. Backpropagation of utility [1].

REFERENCES

- [1] D. A. White and D. A. Sofge, *Handbook of Intelligent Control: Neural, Fuzzy, and Adaptive Approaches*. Van Nostrand Reinhold Company, 1992.
- [2] H. Dharmawardena and G. K. Venayagamoorthy, "A distribution system test feeder for der integration studies," in *2018 Clemson University Power Systems Conference (PSC)*. IEEE, 2018, pp. 1–8.
- [3] A. E. Bryson, *Applied optimal control: optimization, estimation and control*. Routledge, 2018.

Energy Portfolio-based Joint Flexibility Scheduling of Coordinated Microgrids

Farhad Angizeh, *Student Member, IEEE*, Kien Chau, Khashayar Mahani, and Mohsen A. Jafari, *Member, IEEE*

Abstract—This paper aims at co-optimizing day-ahead operation schedules of distributed energy resources (DER) in a coordinated microgrids (MG) cluster to enhance resiliency. The proposed model strategically integrates the energy flexibility provided by the potential DERs in neighboring MGs, while capturing the joint portfolio flexibilities on an hourly basis scheduling scheme under the Transactive Energy (TE) concept. In this context, the proposed optimization model, which is formulated as a mixed-integer liner programming (MILP) problem, minimizes the total operation cost of the MGs in both normal and emergency cases, where the upstream grid might be unavailable leading the MGs to work in an autonomous mode. In order to reveal the merits of the proposed model, multiple case studies are investigated through the modified IEEE 16-node test feeder, where we decompose the original system to a 6- and 10-node systems denoted by MG 1 and MG 2, respectively. sensitivity analysis is finally conducted to explore the impacts of various DER sizing in optimally scheduling of the coordinated MGs for resiliency purposes under the autonomous mode.

I. INTRODUCTION

Proliferation of utilizing distributed energy resources (DER) in the distribution grids has markedly increased the likelihood of energy interactions, under the recently coined Transactive Energy (TE) notion. Besides, increasing amount of microgrids shows the importance of TE technology, where the positive effects of multiple microgrids including smart energy management, increased resiliency, and reduce residual energy, can be strategically captured. Accordingly, neighboring prosumers¹ and microgrid operators would be able to capture the available joint-flexibilities from the neighbors to procure some or all of their energy demands in both normal and emergency operations. In the latter where the grid reliability is jeopardized, the concept of resiliency encourages various methods of mitigation and recovery plans that decrease the frequency of blackouts and reduce recovery time. We argue that co-optimization of operation schedules of DERs among coordinated microgrids can increase the operation efficiency during extreme events, while capturing the available joint flexibility options.

II. CASE STUDY AND RESULTS

The proposed scheduling model is implemented on the modified IEEE 16-node test system, which is depicted in Fig. 1, where we decompose the original system to a 6- and 10-node systems, namely MG 1 and MG 2 respectively. MG 1 represents a commercial microgrid, while MG 2 encompasses a residential community, where various demand types and corresponding end-users are extracted from [1]. Figs. 2 and 3 illustrate the optimal operation schedule of joint MGs 1 and

2, where the contribution of each DER is observable in both normal and emergency operation modes, where the latter leads the joint MGs 1 and 2 to be autonomously operated.

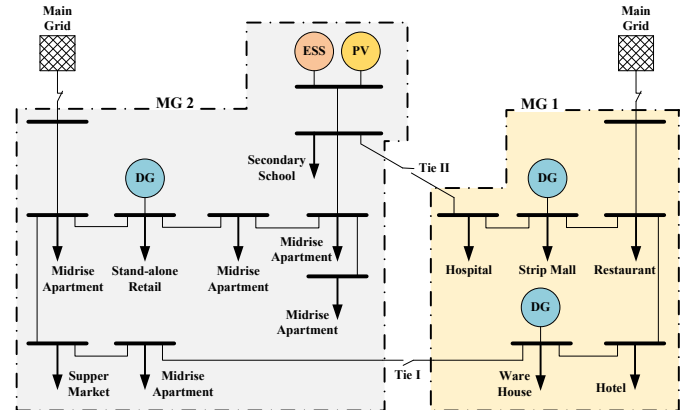


Fig. 1. Modified IEEE 16-node test feeder

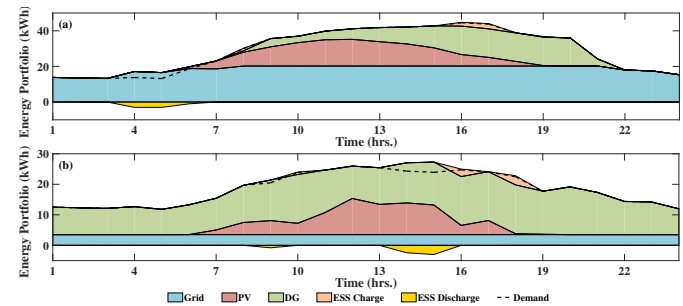


Fig. 2. Optimal normal operation schedule of joint MG 1 and MG 2 in Summer (a): Working day (b): Weekend.

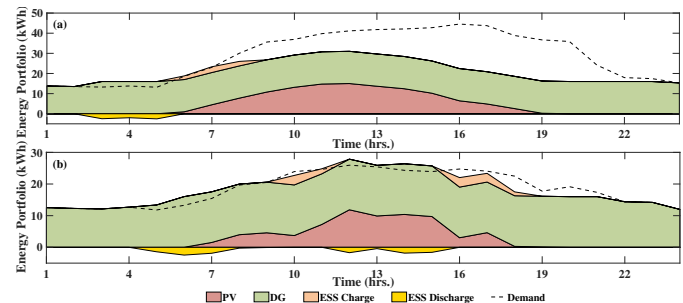


Fig. 3. Optimal autonomous operation schedule of joint MG 1 and MG 2 in Summer (a): Working day (b): Weekend.

REFERENCES

- [1] M. Deru, K. Field, D. Studer, K. Benne, B. Griffith, P. Torcellini, B. Liu, M. Halverson, D. Winiarski, M. Rosenberg *et al.*, "Us department of energy commercial reference building models of the national building stock," 2011.

¹Customers with power generating capabilities

Performance Evaluation of Fiber Optic Sensors to Measure Moisture in Transformer Insulation

Muhammad A. Ansari, Dan Martin, T. K. Saha
 School of Information Technology and Electrical Engineering
 The University of Queensland
 Brisbane, Australia, 4072
 m.ansari, d.martin6@uq.edu.au, saha@itee.uq.edu.au

Abstract—Power transformers have always been a critical asset for a utility. The accurate diagnosis and regular condition monitoring is an essential part of this critical asset management. The evaluation of transformer fleet includes a variety of online and offline measurements, which includes measurement of different parameters such as its temperature, moisture, dissolved gases, oxygen, furanic analysis, partial discharge, winding clamping pressure, sound level, oil flow etc. This paper presents the performance of an online optical fiber sensor for moisture estimation in transformers. The tests are performed on two distribution size transformers of 5 kVA rating, filled with mineral and Envirotemp FR3 insulating fluid, where the optical sensors are installed around the active part of transformers. The advantages and the effectiveness of distributed sensing are discussed against a commercial water activity probe.

Keywords—condition monitoring, power transformer, optical sensors, bragg grating sensors, moisture, water activity

I. MEASUREMENT PRINCIPLE

Fig. 1 presents the working principle of fiber optics sensors.

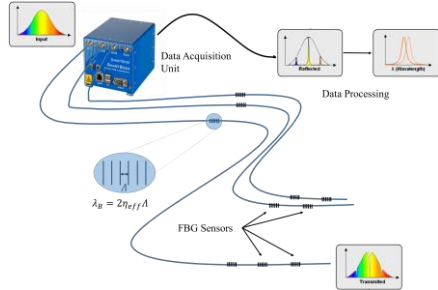


Fig. 1. Fiber Bragg Grating Measurement Principle

II. EXPERIMENTAL SETUP

The transformers are rated at 5 kVA and 2000/230 V and connected in the configuration shown in Fig. 2.

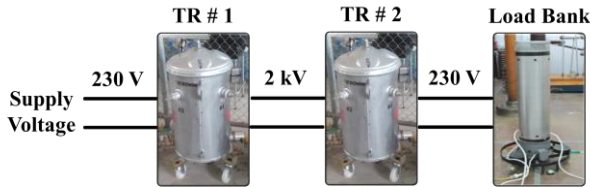


Fig. 2. Schematic Arrangement of Test Transformers

III. CASE I – SINOSOIDAL THERMAL LOADING

1) Mineral Oil Filled Transformer:

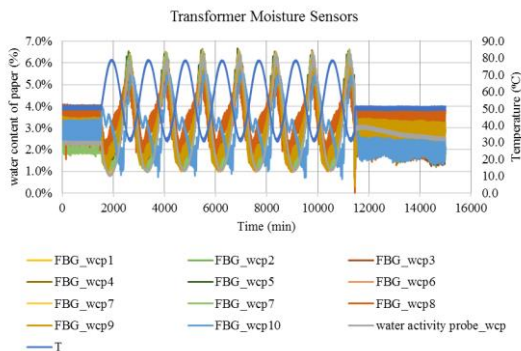


Fig. 3. Mineral Oil Transformer Sensors Measurements during Sinusoidal Loading

2) Vegetable Oil Filled Transformer:

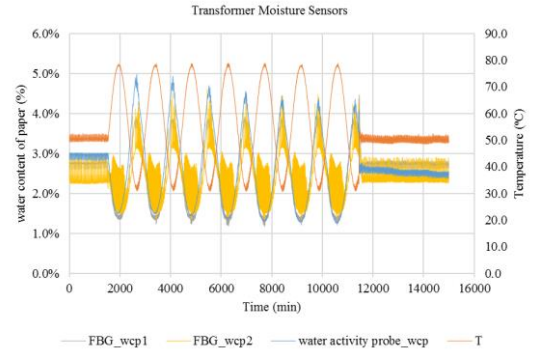


Fig. 4. Vegetable Oil (FR3) Transformer Sensors Measurements during Sinusoidal Loading

IV. CASE II – STEP THERMAL LOADING

1) Mineral Oil Filled Transformer:

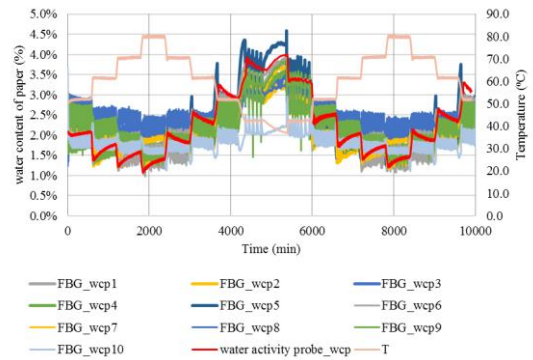


Fig. 5. Mineral Oil Transformer Sensors Measurements during Step Loading

2) Vegetable Oil Filled Transformer:

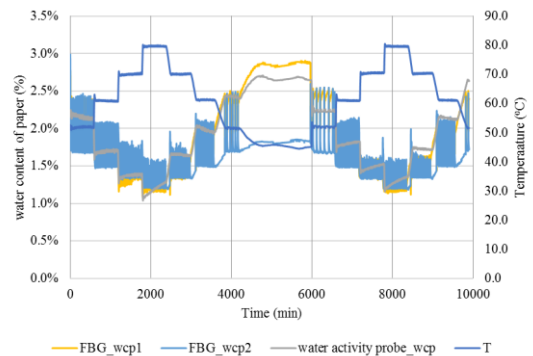


Fig. 6. Vegetable Oil (FR3) Transformer Sensors Measurements during Step Loading

Finite Element Analysis on On-load Tap Changer (OLTC) Tap Selector Electrical Breakdown Mechanism Caused by Silver Sulphide Corrosion

S. Samarasinghe, L. Naranpanawe, D. Martin, H. Ma and T. K. Saha

Power and Energy Systems Research Group, School of Information Technology and Electrical Engineering
The University of Queensland, Australia

Abstract— An on-load tap changer (OLTC) is the main moving part of a power transformer, and is designed to maintain the voltage without interruption. OLTCs are experienced to many stresses during operation. Therefore, it is important to have an understanding on failures mechanisms to protect assets from catastrophic failures. This paper discusses one particular failure mode taking place in an OLTC tap selector, which is when the silver used to coat the contacts reacts with corrosive sulphur compounds dissolved in the insulating oil. As a result, a thin layer of silver sulphide is formed on the selector’s contacts. Due to mechanical forces applied on this layer it flakes off and forms conductive particles suspended in the oil. Consequently, the dielectric strength of the oil can be reduced due to these particles, and the flashover can destroy the transformer. In this paper finite element modeling of a tap selector is used to study the impact of silver sulphide on the electric field in between tap selector contacts. Breakdown voltage test results are used to validate the simulation outputs.

Keywords— Condition monitoring, finite element modeling, On-load tap changer, Power transformer, Silver sulphide.

I. INTRODUCTION

The aim of the work presented in this paper is to understand the impact of silver sulphide corrosion on OLTC failures, using laboratory investigations and FEM modeling. In this paper, FEM is used to simulate OLTC tap selector. Then, the effect of different particle locations and distribution is studied using the FEM model. Simulation data is analyzed and used to establish conclusions with the aid of electric breakdown test results.

II. KEY RESULTS

As shown in Fig. 1, it can be seen that breakdown voltage rapidly decreases with the increase of sulphur particle content in mineral oil.

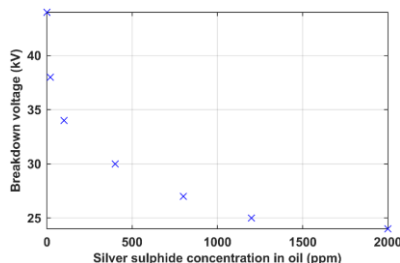


Figure 1. Variation of breakdown voltage with added silver sulphide

Also, as shown in Fig.2 FEM results shown that, presence of a silver sulphide particle enhances the electric stress between two electrodes. Moreover, it was observed that particle location, distribution and concentration are the key factors which influencing the silver sulphide based OLTC failure (see Fig 4-5).

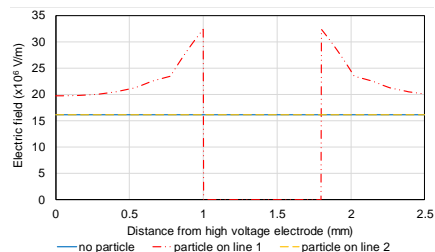


Figure 2. Electric field distribution between electrodes with and without silver sulphide particle

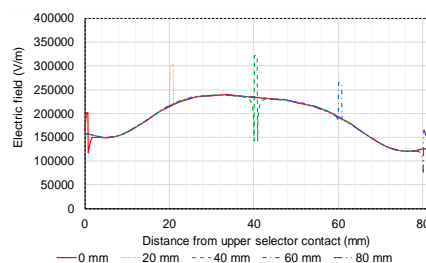


Figure 3. Electric field variation between selector contacts due to vertical particle movement

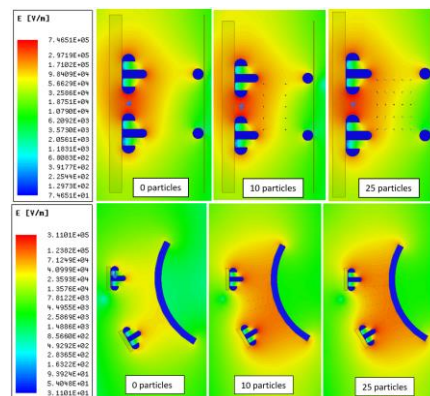


Figure 11. Variation of electric field due to particle distribution (between vertically adjacent and horizontally adjacent selector contacts)

III. CONCLUSIONS

Oil breakdown voltage tests indicated that the presence of silver sulphide can significantly reduce electric breakdown voltage of transformer oil. FEM analysis confirmed that the increase of the electric field due to the presence of silver sulphide particles is the root cause of the decrease in oil breakdown voltage. FEM analysis also indicated an OLTC with silver sulphide particles is more likely to fail due to arcing between vertically adjacent contacts. Moreover, factors like particle location, concentration and distribution has significant influence of the electric stress distribution.

Transformer Loss of Life Mitigation in the Presence of Energy Storage and PV Generation

Milad Soleimani
 Student Member, IEEE
 Electrical and Computer Engineering Department
 Texas A&M University
 College Station, Texas, USA
 soleimani@tamu.edu

Mladen Kezunovic
 Life Fellow, IEEE
 Electrical and Computer Engineering Department
 Texas A&M University
 College Station, Texas, USA
 kezunov@ece.tamu.edu

Abstract—The impacts of high penetration of these equipment on distribution transformers loss of life are quantified employing a probabilistic approach, Monte Carlo simulation is utilized to model the stochastic behavior of EVs. The needed data for the city of College Station including temperature, irradiance and load data are collected from different sources. The impacts on the life of transformer is illustrated and it is shown how battery energy storage with different capacities could mitigate the EVs’ loss of life impact on the transformers. Finally, a risk analysis and economic method to evaluate risk and payback period for different scenarios is proposed.

Keywords— *loss of life, energy storage, risk assessment, photovoltaic generation.*

I. INTRODUCTION

Although electric vehicles (EVs) provided a promising solution to decrease greenhouse gases emission and fossil fuel consumption, the increase in EV penetration may put the assets of the distribution system under an accelerated ageing risk. One possible solution to mitigate the impacts of the high penetration of EVs is employing battery energy storage systems (BESS). In decision-making process, considering transformer loss of life may have conspicuous impact. The remainder explains the employed data, risk analysis and economic methodology and results are presented.

II. IMPLEMENTED SYSTEM

An optimization formulation is developed for the purpose of peak shaving. The load, PV generation and temperature data are obtained from OpenEI, PVWatts Calculator and Iowa Environmental Mesonet respectively. The nominal power of the transformer is 63KVA and PV system size is 10KW. The building load is connected to the same bus as PV panel, battery storage, and EV charging station. The EV demand is generated using the flowchart shown in Figure 1.

III. TRANSFORMER AGEING AND RISK ASSESMENT

For quantifying the transformer loss of life, the method proposed in IEEE Standard C57.91 is used. The loss of life of the transformer for various scenarios of utilizing PV and BESS is calculated and the results shown that BESS can have a considerable effect on the loss of life mitigation. Then, 300 hundred different battery capacities are considered and the impact of the battery size on the loss of life mitigation is discussed. Risk matrix is an effective method for quantitative risk analysis. In this method, different criteria are defined and

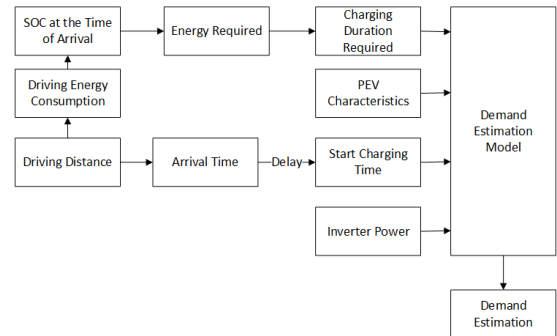


Figure 1. EV demand estimation flowchart.

associated with terms such as “low” and “high” for the risk as shown in TABLE I. The results of the risk analysis is illustrated in Figure 2. Finally, an economic model using net present value (NPV) and equivalent annual cost (EAC) is proposed to evaluate the impact of considering transformer loss of life on the decision making process.

IV. CONCLUSION

The impact of employing BESS and PV to mitigate transformer loss of life and its risk is studied. It is shown that considering loss of life can have considerable effect on economic calculations of the mitigation measures.

TABLE I. RISK MATRIX FOR TRANSFORMER LOSS OF LIFE

Severity	Probability				
	Rare	Occasional	Probable	Frequent	Likely
Insignificant	Low	Low	Low	Low	Low
Normal	Low	Low	Low	Medium	Medium
Critical	Medium	Medium	Medium	High	High
Severe	High	High	High	Extreme	Extreme
Catastrophic	Extreme	Extreme	Extreme	Extreme	Extreme

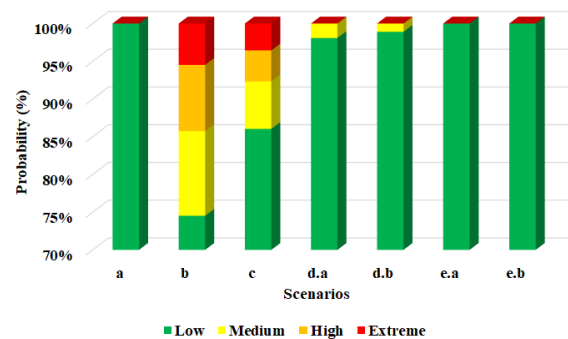


Figure 2. Risk of loss of load for different scenarios.

A Hybrid Systems Approach to Modeling and Analysis of TCL Coordination

Md Salman Nazir, *Member, IEEE*, and Ian A. Hiskens, *Fellow, IEEE*

Abstract—Coordinated control of thermostatically controlled loads (TCLs), such as air-conditioner, water-heaters and refrigerators, can balance fluctuations from renewables, reduce peak demand and provide voltage support. Various coordination techniques exist, such as set-point variation, randomized switching and Transactive energy coordination. While the aggregate dynamics of TCLs can be captured using continuous-time models, the control updates typically occur at relative slow discrete intervals (minutes range). Hence, a hybrid dynamical system representation is proposed to accurately capture the overall continuous/discrete dynamics and to systematically study the performance of proposed control strategies. Analysis techniques based on Lyapunov (energy) functions for switched systems provide important insights into the impact of different control strategies.

Index Terms—Hybrid systems; Thermostatically controlled loads (TCLs); Demand response; Oscillations.

I. MODELING AND ANALYSIS

The aggregate dynamics of TCLs can be captured using continuous time models whereas control actions through price signals or set-point changes typically occur at discrete intervals. Hence, the overall dynamics can be captured using a hybrid systems representation as follows,

$$\dot{x}(t) = A(t)x(t), \quad (\text{continuous dynamics})$$

$$x(t^+) = \phi_u(x(t^-)), \quad (\text{discrete switchings})$$

$$y(t) = Cx(t), \quad (\text{output})$$

where $x(t)$ represents the TCL states, matrix $A(t)$ captures the natural dynamics and can be time-varying, ϕ_u is a mapping function capturing the effect of the control actions and $y(t)$ is the aggregate power consumption [1].

Assume that TCLs are coordinated based on price signals, π^{clr} . Fig. 1 shows the aggregate power consumed under fixed price levels. It is observed that

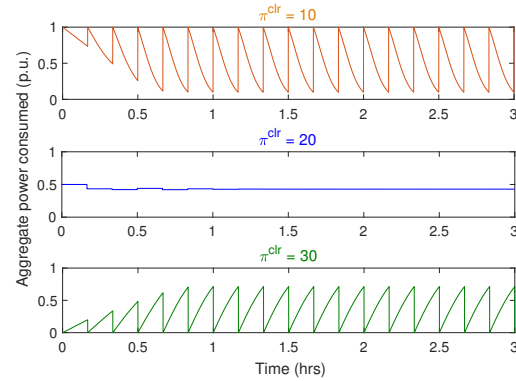


Fig. 1. Aggregate power consumed under different π^{clr} .

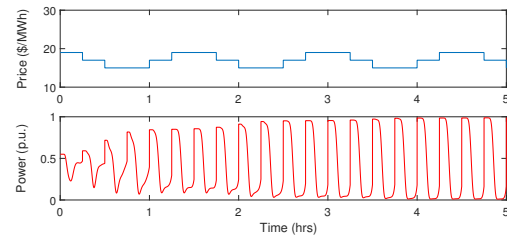


Fig. 2. Response to periodically fluctuating signals.

at low and high values of π^{clr} the TCL aggregate demand can be highly oscillatory. Furthermore, Fig. 2 shows that growing oscillations can be induced under periodically fluctuating price signals.

With the hybrid systems representation, the system behavior is analyzed using Lyapunov (energy) functions and results related to switched systems. This provides insights into system characteristics, such as bounds on price variations and aggregate demand changes and suitable control update intervals. The impacts on power systems are also captured.

REFERENCES

- [1] M. S. Nazir and I. A. Hiskens, "A Dynamical Systems Approach to Modeling and Analysis of Transactive Energy Coordination," in *IEEE Transactions on Power Systems*, 2018.

The authors are with the Department of Electrical Engineering and Computer Science, University of Michigan, Ann Arbor, MI, USA. Emails: mdsnazir@umich.edu, hiskens@umich.edu.

The authors gratefully acknowledge the contribution of the U.S. National Science Foundation through grant ECCS-1810144.

Time Stamp Based IEC 61850 GOOSE Performance Testing

Jan Westman, Dr. Ramtin Hadidi, Dr. Curtiss Fox
 Department of Electrical and Computer Engineering
 Clemson University
 Clemson, SC USA

jwestma@clemson.edu, rhadidi@clemson.edu, fox8@clemson.edu

Abstract— The IEC 61850 set of standards was first published in 2003 with the objective of promoting interoperability of substation intelligent electronic devices (IEDs) across vendors and creating a substation communication protocol that decreased the cost of implementing and integrating substation communication systems. This poster demonstrates performance testing of the IEC 61850 Generic Object Oriented Substation Event (GOOSE) message type on a simple Ethernet network. Thus, a hardware testbed was created using digital relays and a test procedure developed for collecting time stamp data from GOOSE messages for the analysis of end-to-end data transmission between network IEDs.

Keywords— IEC 61850, GOOSE, Protocol Testing

I. TEST SET-UP

Two Schweitzer 651R-2 Recloser Controls (the IEDs under test) are connected to a network composed of a single Software Defined Network (SDN) switch (the network under test). A workstation PC is also connected to the SDN to provide the user interface for configuring the GOOSE protocol on the IEDs and for analyzing the time stamp data. In addition, a Schweitzer Satellite Synchronized Clock is used to provide high accuracy IRIG-B time synchronization to the IED system clocks.

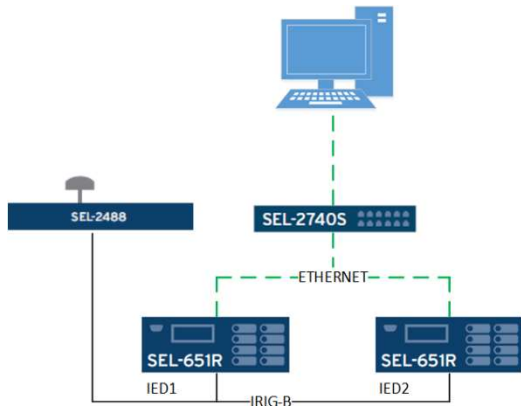


Fig. 1. Hardware Test System

The test begins by initiating the publication of a binary data point from one IED to the network. The subscribing IED will receive the binary value, invert it, and publish the inverted value back to the network. The first IED will receive the inverted binary value and by inverting that value and publishing back to

the network, the process can repeat allowing many time stamped messages to be created quickly.

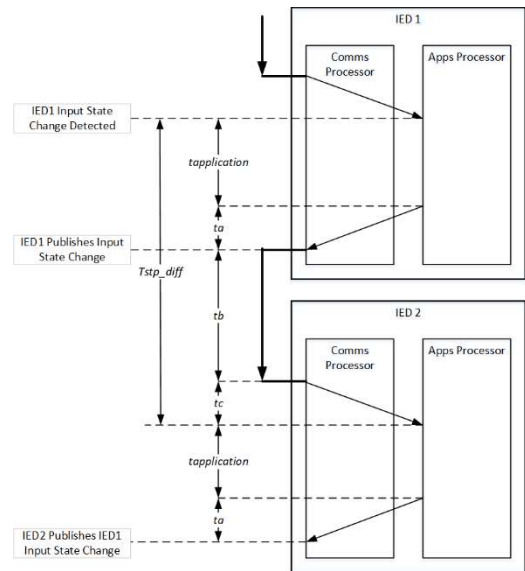


Fig. 2. GOOSE Transmission Timing Diagram

The GOOSE message time stamps are collected using Wireshark, a free open-source packet analyzer software. The difference between time stamps of consecutive messages indicates the total time taken for data to be sent from one IED to the other.

II. RESULTS

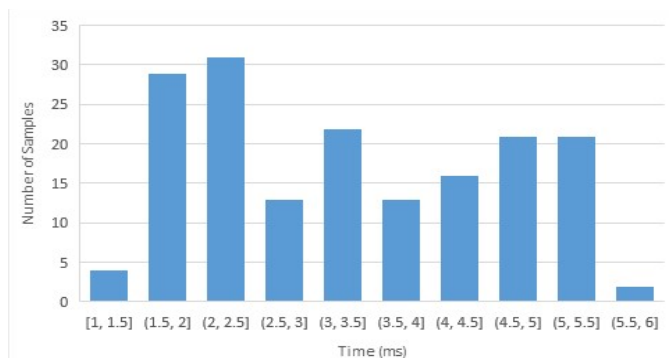


Fig. 3. End-to-End Data Transmission Time

Scenario-based Optimal Transmission Switching With Uncertain Wind Power

Yuqi Zhou

Electrical and Computer Engineering
The University of Texas at Austin
Austin, USA

Grani A. Hanasusanto

Operations Research and Industrial Engineering
The University of Texas at Austin
Austin, USA

Hao Zhu

Electrical and Computer Engineering
The University of Texas at Austin
Austin, USA

Abstract—Optimal transmission switching is a transmission planning strategy that can help save dispatch cost by switching system topology. With higher penetration of distributed energy resource (DERs) like wind energy, power system planning and operation under the uncertainty can be challenging. In this work, optimal transmission switching decision making under wind energy uncertainty is investigated. A two-stage stochastic program is proposed and Monte Carlo simulation approach based on sample average approximations is applied, the problem can then be formulated as a mixed integer linear program. The proposed scenario based method minimizes the total operation cost for the two-stage stochastic problem and can help with optimal transmission switching decision making under uncertain wind penetration.

Index Terms—Optimal transmission switching, wind power, Monte Carlo, sample average approximation

I. INTRODUCTION

Optimal transmission switching (OTS) has been investigated in recent years and proved to be able to save operation cost by switching line status [1], [2]. We apply a two-stage stochastic program on the OTS considering the uncertainty based on the wind prediction, where the scenarios of uncertain wind generation will have an impact on the first stage decision.

II. METHODOLOGY

Two-stage stochastic program has a variety of applications in energy planning [3]. In this work, the two-stage problem that involves optimal transmission switching decision making is formulated as a two-stage stochastic integer program:

$$\min_{\theta_1, x, f_1, z_1} c^T x + \mathbb{E}_{\mathbb{P}}[Q(\theta_1, x, f_1, z_1, \xi)] \quad (1)$$

where $Q(\theta_1, x, f_1, z_1, \xi)$ is the optimal value of second-stage problem:

$$Q(\theta_1, x, f_1, z_1, \xi) = \min_y c^T y \quad (2)$$

s.t. $Tx + Wy \leq h$

Under the assumption that random vector ξ has finite number of realizations, the two-stage problem can be represented as:

$$\min c^T x + \frac{1}{S} \sum_{i=1}^S c^T y^s \quad (3)$$

s.t. $x \in \mathcal{X}$

$T_s x + W_s y_s \leq h_s, s = 1, \dots, S$

where the decision variables are $\theta_1, x, f_1, z_1, \xi, y_1, \dots, y_s$, and S is the number of scenarios generated.

III. KEY RESULTS

The two stage stochastic program has been implemented with YALMIP and solved with CPLEX solver. The test results with IEEE 14 bus system as shown in Fig. 1 and TABLE I indicate the feasibility of the proposed method.

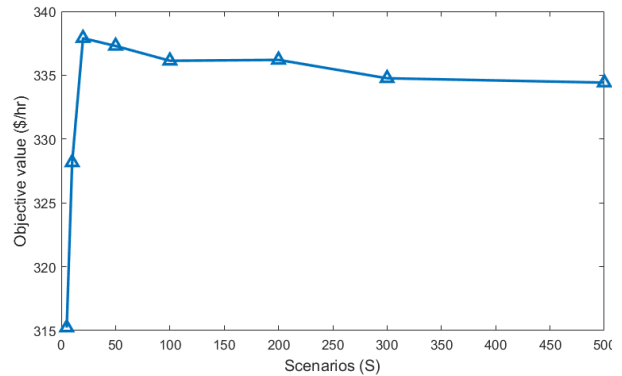


Fig. 1. Monte Carlo Simulation.

TABLE I
COMPARISON OF OPERATION COST

	Switching lines	Total cost C
Optimal power flow without OTS	-	\$371
OTS with deterministic wind power	[9;11;20]	\$324
OTS with uncertain wind power	[9;11;13]	\$334

REFERENCES

- [1] E. B. Fisher, R. P. O'Neill, and M. C. Ferris, "Optimal transmission switching," *IEEE Transactions on Power Systems*, vol. 23, no. 3, pp. 1346–1355, 2008.
- [2] F. Qiu and J. Wang, "Chance-constrained transmission switching with guaranteed wind power utilization," *IEEE Transactions on Power Systems*, vol. 30, no. 3, pp. 1270–1278, 2015.
- [3] C. Ordoudis, V. A. Nguyen, D. Kuhn, and P. Pinson, "Energy and reserve dispatch with distributionally robust joint chance constraints," Tech. Rep., 2018.

Publicly Available Information Driven Cyber Threats in Power Grids Imposed Through IoT of Electric Vehicle System

Samrat Acharya, IEEE, Student Member, Yury Dvorkin, IEEE, Member, Ramesh Karri, IEEE, Senior Member
 Department of Electrical & Computer Engineering
 Tandon School of Engineering
 New York University
 New York, USA
 {ssa495, dvorkin, rkarri}@nyu.edu

Abstract—Demand-side cyberattacks in the power grid are catching the attention of concerned researchers and utilities, because of the proliferation of internet of things (IoT) of high-power demand-side devices- such as electric vehicles (EVs). On the grid end, the trend of publicizing information about grid infrastructures and its operation has been increasing lately. A cyber attacker’s meticulous study of the public information, both of grid-side and demand-side, can be detrimental. In this paper, power grid model incorporating demand-side cyberattack, which relies on the public information of power grid and EVs available over the internet, will be presented. The cyberattack will be formulated as a problem of optimal reallocation of eigenvalues of the power grid model, with an intent to destabilize the grid. A case will be developed based on Manhattan, NY, USA will be presented.

Index Terms—Cybersecurity in power grids, eigenvalues placement, electric vehicles, publicly available information.

I. INTRODUCTION

Cyber alarms have started buzzing in modern power grid portfolios, particularly because of a large scale deployment of internet of things (IoT) in both grid and demand sides. Furthermore, IoT deployed in demand-side relatively impose greater threat than the grid side because of the diversified and distributed nature of demand-side devices, and the greater need of user interfaces [1], [2]. The potentially large scale impact of grid-side cyberattacks led the researchers and concerned parties focus mostly on grid-side cyberattacks. However, demand-side cyberattacks deploying electric vehicles (EVs) are being focused lately in the literature. Because of an exponential global growth in EVs number, significant increase in the battery capacity of EVs and charging capacity of electric vehicle supply equipment (EVSE), and ever increasing internet interfacing of EV system, EV system has been evolving as a profound attack vector in demand-side cybersecurity domain of power grids.

II. IOT IN EV SYSTEM

Fig.1 presents the network intricacies within an EV system which can broadly be grouped into communication interfaces of EV and EVSE. The interfaces are defined between EVSE/EV and N(wireless network), G(grid), and S(central server of EV/EVSE). An attacker can hack into these interfaces and

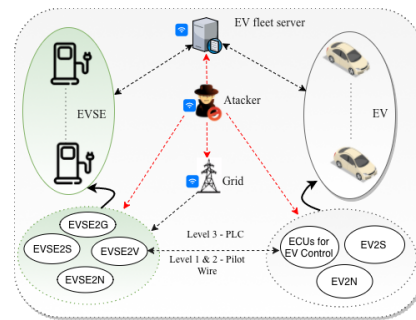


Fig. 1. Simplified layout of communication among EVs, EVSEs and grid.

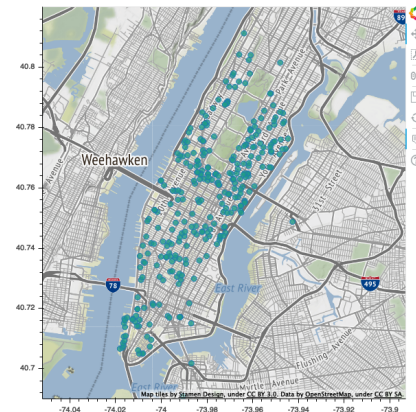


Fig. 2. EVSE distribution in Manhattan, NY.

potentially change the pattern of power consumption of EVSE, and hence destabilize the normal operation of power grids. Fig. 2 depicts the publicly available locations of EVSE in Manhattan, NY, USA.

REFERENCES

- [1] Dvorkin, Yury, and Siddharth Garg. "IoT-enabled distributed cyber-attacks on transmission and distribution grids." 2017 North American Power Symposium (NAPS). IEEE, 2017.
- [2] Soltan, Saleh, Prateek Mittal, and H. Vincent Poor. "BlackIoT: IoT botnet of high wattage devices can disrupt the power grid." 27th USENIX Security Symposium (USENIX Security 18). 2018.

Impact Assessment of Credible Contingency and Cyber Attack on Australian 14-Generator Interconnected Power System

B M Ruhul Amin
 School of Engineering
 Macquarie University
 Sydney, NSW 2109, Australia
 ruhul.amin@students.mq.edu.au

M. S. Rahman
 Dept of strategy and innovation
 AEMO
 Melbourne, VIC 3000, Australia
 msrahman@ieee.org

M. J. Hossain
 School of Engineering
 Macquarie University
 Sydney, NSW 2109, Australia
 jahangir.hossain@mq.edu.au

Abstract—This paper analyses the impacts of credible contingency and an event of cyber attack on the dynamic performance of a real large-scale interconnected power grid. Any credible contingency, for example, short circuit fault or unnatural behaviour of protective devices due to cyber intrusion could create catastrophic consequences and even complete blackout to the power systems. In order to protect power systems against cyber events, it is necessary to analyse the impacts of both faults and cyber attacks on the dynamic behaviour of the power system to identify cyber events from credible contingencies. In this paper, a simplified model of an Australian 14-generator interconnected system is considered as a testbed and MATLAB/Simulink Simpowersystems Toolbox is used for the analyses. A real-life incident of faults has considered as case study and an event of a cyber attack on protection relay function is simulated to explore the possible similar impacts on the same page. The systematic analyses of different properties of the system will help to design the detection and counter measure techniques to ensure the system is protected from cyber threats.

Index Terms—credible contingency, cyber attack, interconnected power grid.

I. INTRODUCTION

According to the Australian Energy Market Commission (AEMC), natural events such as single or double phase faults in the transmission line, loss of single generator from the grid are considered as credible contingencies. All contingencies except credible events are referred to non-credible contingency events [1].

In this paper, the dynamic performance analyses of credible events and cyber attacks are performed in a simplified model of South East (SE) Australian power grid which validate the practical aspect of this research. Unlike Europe or USA, the Australian grid is a linear, long interconnected system. For convenience, the complete model is divided into 5 interconnected areas which represent the Australian Central Territory (ACT)/Snowy Hydro(SH), New South Wales (NSW), Victoria (VIC), Queensland (QLD) and South Australia (SA) regions.

II. SIMULATION RESULTS

In this case study, a remote switching attack is imposed in the single phase and three-phase relays of Queensland and New South Wales Interconnector (QNI) at 10.0 s.

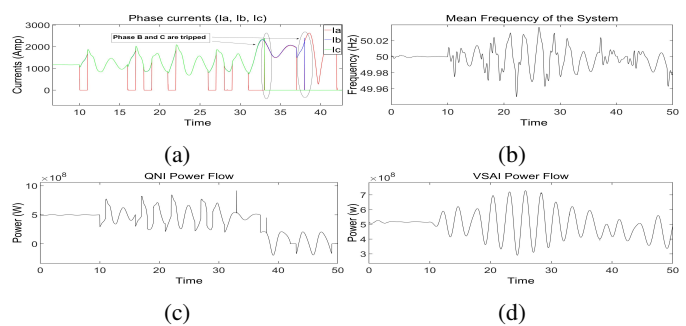


Fig. 1: System Response (switching attack in phase A of QNI): (a) Phase currents in relay, (b) System frequency, (c) Active power flow in QNI, (d) Active power flow in VSAI

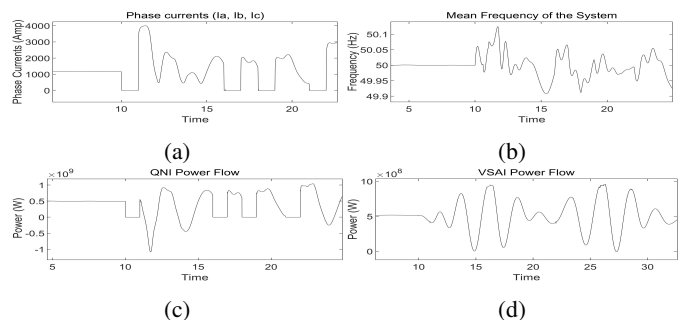


Fig. 2: System Response (switching attack in all phases of QNI): (a) Phase currents in relay, (b) System frequency, (c) Active power flow in QNI, (d) Active power flow in VSAI

III. CONCLUSION

The research outcomes demonstrate the severity of cyber attacks in the power grid than the credible contingencies. The dynamic behavior of the system parameters also show distinct patterns for credible events and cyber attacks.

REFERENCES

- [1] AEMC. [Online]. Available: <https://www.aemc.gov.au/energy-system/electricity/electricity-system/security>

Detecting Line Failures using PMU Time Series for Smart Grids under Cyber-Physical Stresses

Md Jakir Hossain and Mahshid Rahnamy-Naeini

Electrical Engineering Department, University of South Florida, Tampa, Florida, USA

mdjakir@mail.usf.edu, mahshidr@usf.edu

Abstract—The critical inter-dependency of smart grids on the cyber layer (communication, control and computational components) does not just have the latent to upsurge smart grid reliability and resilience, but also provides adversaries with the opportunities to interrupt power delivery. Thus, smart grids exhibit new vulnerabilities to cyber and physical stresses such as joint cyber and physical attacks. In this study, a joint cyber-physical attack is considered in which an adversary damages some lines physically (physical attack) and prevents the information flow from the attacked zone to the control center to tamper the observability of the grid and mask the physical failure (cyber attack). The goal of the presented work is to evaluate if and under what scenarios the PMU time series available from outside of the attacked zone can be used to estimate the state of the components in the attacked zone and expose the line failures in real-time. To do so, several advanced multivariate time-series prediction methods (Recurrent Neural Network (RNN), Long Short-Term Memory (LSTM), etc.) will be applied to the simulated PMU time series. The dynamic state estimation in this study is a data-driven approach and does not use models as traditional power system state estimation. The IEEE 118 test case will be used to show scenarios that the state of the lines can be estimated with minimum error as well as the lines that are difficult to estimate their state and thus may require more protection.

Index Terms—Line outages, PMUs, Cyber-physical attacks, Dynamic state estimation, Smart-grid security, RNN, LSTM.

I. INTRODUCTION

Smart-grid is a cyber-physical system which is becoming more and more equipped with cyber elements for wide-area monitoring, communication and control which also exhibit new vulnerabilities to cyber threats. Successful attacks that exploit these emerging technologies may interrupt power by triggering automated PMU control schemes through subversion of synchronized timing systems or may be by gaining unauthorized access to cloud-based PMU information to coordinate attack timing etc.

When cyber-attacks occur jointly with physical attacks or failures in the power grid, they could have even more serious impacts and cause large-scale blackouts with severe societal and economic consequences [1-2]. Modern wide area monitoring systems integrated with PMUs gives high precision time synchronized measurements of system phasors. With the help of data analytic and machine learning these time series provides opportunities to expose, recognizing and investing these threats in appropriate cyber-security countermeasures. Which may decrease the likelihood of attacks and guarantee that these technologies are only used to endorse grid reliability rather than abolish it.

II. METHODS

The goal is to utilize the PMU time series from outside the masked zone and the historical measurements before the joint cyber-physical event to quickly estimate the state of the transmission lines and expose the physical failure in the process. These PMU time series make it a multivariate time series prediction problem, which may be analyzed using advanced machine learning based multivariate time series prediction models like RNNs and LSTM etc.

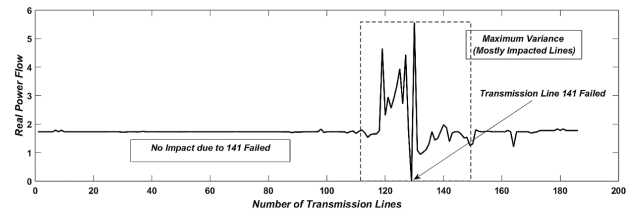


Fig. 1: Impact on line flow of every transmission line of IEEE 118 bus system after line 141 failed.

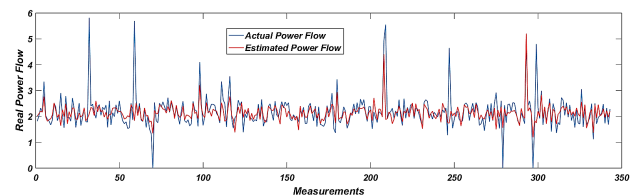


Fig. 2: Power flow of transmission line 141 during various measurements.

III. RESULTS AND CONCLUSION

Fig. 1. shows the impact of a single line (for example line 141) on the other lines of the IEEE-118 bus system. From where we could see that not all the lines equally effected, thus we could implement feature selection and dimensionality reduction for increased computational speed. Fig. 2. shows that estimation capability of linear prediction model during joint cyber-physical stress. From here we may expect that advanced multivariate time-series prediction model such RNN, LSTM, etc. will provide much better prediction power.

REFERENCES

- [1] Md Jakir Hossain and Mahshid Rahnamy-Naeini, Line Failure Detection from PMU Data after a Joint Cyber-Physical Attack, IEEE Power and Energy Society General Meeting 2019, Georgia, USA.
- [2] S. Soltan, M. Yannakakis and G. Zussman, "Power Grid State Estimation Following a Joint Cyber and Physical Attack," in IEEE Transactions on Control of Network Systems, vol. 5, no. 1, pp. 499-512, March 2018.

False Data Detection in Electric Energy Systems

Ramin Kaviani

Arizona State University, Tempe, AZ

Kory W. Hedman

Arizona State University, Tempe, AZ

Abstract— In this study, a real-time detection mechanism to detect false data injection attacks against energy management systems is proposed. Prior studies have shown that certain cyber-attacks can bypass conventional bad data detectors (BDD) and remain undetectable. Therefore, a reliable and intelligent detection mechanism, which can flag malicious behavior, is imperative. This study proposes a detection mechanism to enhance the existing BDDs. It is developed based on the fundamental knowledge of the laws of physics in the electric grid. The main contribution of this detection mechanism is the leveraging of power system domain insight to identify an underlying exploitable structure in the attacker problem, which enables the prediction of the attacker's behavior. The approach is tested on IEEE systems.

Keywords—cyber attacks; false data injection attack; cyber attack detection

I. INTRODUCTION

Extensive usage of cyber layers in power system monitoring and controlling exposes the system to cyber-attacks. A false data injection (FDI) based attack, or FDIA, is a class of cyber-attacks that tries to maliciously change the measurements and perturb the state estimation process by targeting the BDD's vulnerability [1]. Obviously, this would be an easy task for the attackers to spoof BDDs since they are not looking for the attackers; rather, the BDD is looking for some natural driven events: measurement errors, faulty equipment, etc. Various researchers have proposed a false-data injection attack that falsifies load measurements in the grid in such a way that is not detected by traditional state estimator bad data detectors [2]. To design a better bad data detector, in this study, the core problem of load shifting attack problem is investigated and utilized. The subsequent work is not a substitute to prior attack detection methods; rather, it is a significant complement and it is also an approach that can be used by itself.

II. METHODOLOGY

A. Detection method

The simplest way to develop a clear insight to the structure of the core problem of a load-shifting attack problem is to start with the concept of power transfer distribution factor (PTDF). Considering the concept of shift factors, there is a very clear way to determine the optimal way to change a line's flow relative to the flexibility in the resources (Loads at buses) throughout the system. For instance, consider the condition in which the attacker wishes to overload the line from bus 3 to bus 5 in the six-bus test case in Figure 1.

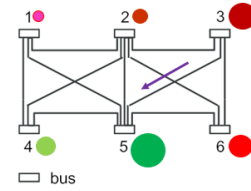


Figure 1. 6-Bus test case diagram with critical buses identified for line 3-5

Table 1 demonstrates two vectors for the net injection changes at all six buses in the system that are samples from a normal distribution. One vector is an attack vector while the other is not; the one that is an attack is simply arranged in such a way that there is an overload caused on the line 3-5. This is the basic technique of an unobservable attack: have the deviations fall into the potential spectrum of generally accepted noise but have the preferred values be at preferred buses.

Table 1. Two random load deviations vectors for 6-Bus test case: ordered by bus number

Bus	Shift Factor	Vector 1 (MW)	Vector 2 (MW)
1	0	-0.456	-0.932
2	0.0622	-0.127	0.954
3	0.289	1.136	1.143
4	0.0183	-0.564	-2.051
5	-0.1207	-0.751	1.519
6	0.1526	0.762	-0.633

In Figure 1, red dots in this figure are where the attacker wishes to have a positive change in net injection (larger and darker: larger in magnitude change); the green dots are where he/she wishes to have a negative change in net injection (smaller and lighter: smaller in magnitude change). Therefore, an index is proposed based on the changes on the most sensitive locations in the system to flag all set of malicious changes.

III. CONCLUSION

The proposed detection mechanism uses power systems domain insights to find the most sensitive locations of the system with respect to their impacts on a targeted asset.

REFERENCES

- [1] Y. Liu, P. Ning, and M. K. Reiter, "False data injection attacks against state estimation in electric power grids," in Proceedings of the 16th ACM Conference on Computer and Communications Security, ser. CCS '09. New York, NY, USA: ACM, 2009, pp. 21–32.
- [2] J. Liang, L. Sankar, and O. Kosut, "Vulnerability analysis and consequences of false data injection attack on power system state estimation," IEEE Transactions on Power Systems, vol. 31, no. 5, pp. 3864–3872, 2016.

Resilient Secondary Frequency Control of Islanded Microgrid in the Presence of Renewable Energy

Mohammad Reza Khalghani, *Student Member, IEEE*, Jignesh Solanki, *Senior Member, IEEE*, Sarika Solanki, *Senior Member, IEEE*, and Arman Sargolzaei, *Member, IEEE*,

Abstract—Load Frequency Control (LFC) of islanded microgrids equipped with primary and standard secondary control has become challenging. One of the main challenges of frequency control is induced by man-made and natural cyber disruptions of metering and communication infrastructures. These anomalies can create undesired responses which in turn cause performance degradation and even unstable operation. Vulnerable operation of microgrids to false data injection (FDI) and time delay interruption are proved. Therefore, it is essential that these anomalies are identified and their adverse effects are mitigated from the microgrid. We developed a two-layer resilient controller based on optimal regulator joint with a improved Stochastic Unknown Input observer (SUIO) to address both the cyber disruptions and uncertainties of renewable sources and load.

Index Terms—Load Frequency Control, Islanded Microgrid, Stochastic Unknown Input Observer, Optimal Control, False Data Injection, Time Delay Interruption.

I. INTRODUCTION

THE interconnection of distributed generation, energy storage and load and their interface with communication infrastructure creates microgrids. Microgrids can be operated islanded, where the major objective is to maintain the balance between sources and loads owing to no energy support from the main grid. The basic control strategy for microgrids is the hierarchical control, including primary control (droop control) and secondary control (compensating the frequency deviations caused by primary control) and tertiary control. Primary control response is the immediate adjustment of power output by the governor. Since we also intend to properly employ other energy sources (than governor-based or droop-based energy sources, e.g. batteries), secondary control is adopted, which is a supervisory control and utilizes measurements and communication systems, to guarantee frequency deviation is eliminated. This cyber-interface embedded in secondary control make the microgrid prone to all types of cyber intrusions. Hence we need to design a resilient approach for secondary control of microgrids.

There are three general types of cyber interruptions that can potentially jeopardize microgrids, including FDI, Denial of Service, Time Delay interruption to measurements. If false data is injected to the microgrid measured data or actuators, a misleading control response will be imposed to the microgrid. Also, time-delay introduced to the data exchanged with the measurements can cause a oscillatory control response for the microgrid. The frequency response for the microgrid with different time delays τ_d exposed to the data exchanged between measurements and control center is shown in Figure 1. Examining Figure 1, as the time delay increases, we have more

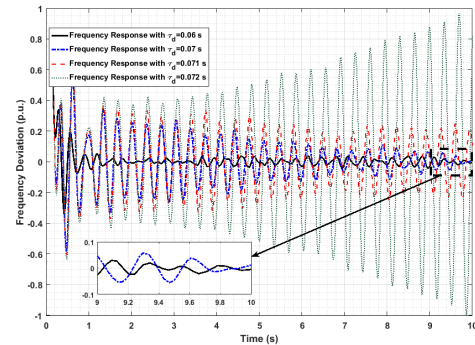


Fig. 1: Time-delay effect on frequency response

the oscillatory frequency response. Therefore, it is necessary to equip the secondary control with a resilient methodology.

II. THE PROPOSED CONTROL STRATEGY

We must design a LFC based on an optimal feedback regulator and observer to optimally and resiliently operate LFC. The observer is an improved type of Unknown Input Observer to be robust against FDI, time-delay introduced to measurements and measurement noise. The LFC model of a microgrid can be presented in state-space representation as below:

$$\begin{cases} \dot{x}(t) = A_c x(t) + B_c u(t) + Dd(t) + w(t) \\ y(t) = Cx(t) + v(t) \end{cases} \quad (1)$$

where $d(t)$ indicates FDI to the microgrid actuators, and $v(t)$ and $w(t)$ indicate measurement and actuator noises. Using the proposed control methodology, the control input $u(t) = K\hat{x}(t)$ is designed such that it can address both cyber interruptions of FDI and delay. K is an optimal control gain obtained to optimally manage the energy sources in the microgrid. The control strategy is illustrated in Figure 2.

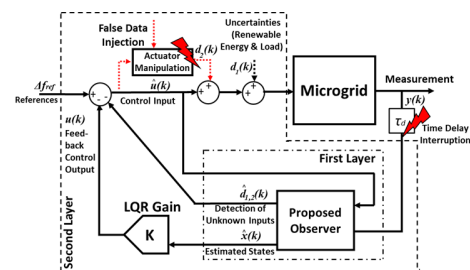


Fig. 2: The proposed control strategy

Multistage Game for Smart Grid Security

Shuva Paul and Zhen Ni

Department of Electrical Engineering and Computer Science
 South Dakota State University, Brookings, SD 57006, United States
 Email: {shuva.paul, zhen.ni}@sdstate.edu

Abstract—In this work, we propose a new solution for a multi-stage game in power system. The game is formulated and conducted between the attacker and the defender based on reinforcement learning. The aim is to identify the optimal attack sequences given certain objective (e.g., transmission line outages). Different from a one-shot game, the attacker here learns a sequence of attack actions applying for the transmission lines. The defender protects a set of selected lines. After each time step, the cascading failure will be measured, and the line outage will be used as the feedback for the attacker to generate the next action. The performance is evaluated on standard IEEE test system. We show that the proposed solution can identify optimal attack sequences under certain attack objective and enhances the power system protection scheme.

I. KEY EQUATIONS

A modified reinforcement learning framework is used in this multistage sequential game to define the attacker and the defender [1]. The attacker intends to maximize the future discounted rewards whereas the defender intends to minimize them. We consider only deterministic cases while implementing reinforcement learning. From the attacker’s perspective, the Q -value is

$$Q_{att}(s, a, d) = R_A(s, a, d) + \gamma \sum_{s' \in S} V_{att}(s') \quad (1)$$

and the corresponding value function is defined as

$$V_{att}(s) = \max_{a \in A} \min_{d \in D} \sum_{a \in A} \sum_{d \in D} Q_{att}(s, a, d) \quad (2)$$

where V_{att} is denoted as the attacker’s expected long-term reward for optimal strategies at the initial state s and $Q_{att}(s, a, d)$ as the expected long term rewards for taking action a against defender’s taken action d . $R_A(s, a, d)$ represents the attacker’s reward due to action a and d at state s . γ is the discount factor which helps the agent to focus on long term or short term rewards. s' represents the next state. Similarly we can define the defender’s Q -function and value function as well. Here, the defender is a passive player and it’s policy is pre-defined throughout the learning procedure. To initiate the attack, a threat/attack model is adopted from [2]. In this model topological information from a typical power system is used. We calculate the overloads due to the attacks in the transmission lines using time delayed overcurrent relay. Transmission line switching (physical attack) is considered as the attack scheme in this work. In this game, the attack success is measured based on the total number of line outages. This total number of line outages includes targeted transmission

lines and cascading failures. If the attack is successful, the attacker is assigned positive reward and the defender is assigned negative reward, and vice versa.

II. KEY RESULTS

For IEEE 39 bus system, we conduct the multistage sequential game between the players. First, we use [1, 2, 3] as the defender’s pre-defined protection set. Then we conduct 100 independent runs containing 8000 episodes in each runs. We consider, the attack objective as 30% transmission line outage (14 out of 46 transmission lines).

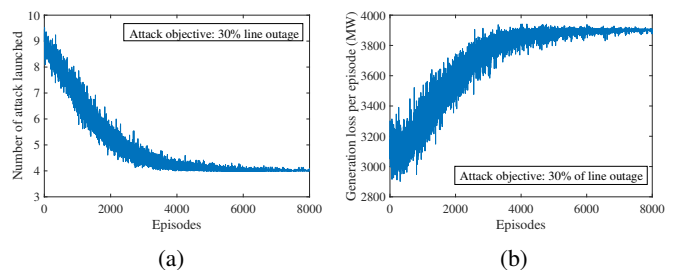


Figure 1: Convergence of the attacker’s number of actions for IEEE 39 bus system (average of 100 runs). The defender’s protection set is $\langle 1, 2, 3 \rangle$. (a) The number of attack actions and (b) Convergence of generation loss due to the attacker’s action.

Figure 1a shows the convergence curve for the attacker’s number of actions to reach the Nash equilibrium point. We found that the attacker needs to take minimum four actions to reach the line outage threshold (30%). Figure 1b shows the convergence curve for generation loss. There are multiple optimal action sequences that the agent can learn from the gaming process. Such as, attacking line $\langle 8, 29, 10, 13 \rangle$ gives the total outages of $\langle 1, 3, 7, 8, 10, 12, 13, 18, 19, 21, 22, 23, 29, 31 \rangle$. From the results, the power system operator is suggested to protect the learned optimal action sequences, which are the most critical lines in this benchmark system.

III. CONCLUSION

In this work, we find the most critical transmission lines from IEEE 39 bus system in an adversarial gaming environment. Adjusting the defender’s protection scheme based on the attacker’s learned policy enhances the system security.

REFERENCES

- [1] Z. Ni and S. Paul, "A Multistage Game in Smart Grid Security: A Reinforcement Learning Solution," *IEEE Transactions on Neural Networks and Learning Systems*, DOI: 10.1109/TNNLS.2018.2885530
- [2] M. J. Eppstein and P. D. Hines, "A random chemistry algorithm for identifying collections of multiple contingencies that initiate cascading failure," *IEEE Transactions on Power Systems*, vol. 27, pp. 1698–1705, Aug 2012.

A Simplified Criterion for Identifying a System's Vulnerability to Outage Contingency

Mahdi Rouholamini, Caisheng Wang, *Senior Member, IEEE*, Carol Miller

Wayne State University, Detroit, USA

Abstract—In this paper, a simple and effective criterion is proposed based on the reserve constraint in power system operations. The objective of this index is to determine if there exist any potential combinations of generation units that satisfy the reserve adequacy constraint in case of outage contingency, without having to deal with the model optimization i.e., economic dispatch / unit commitment. The proposed criterion is indeed a pre-condition to evaluate the model's feasibility and is useful regardless of the order and the type (simultaneous or consecutive) of the contingency.

Index Terms—generation sector; outage contingency; power system restorability; reserve constraint

I. METHODOLOGY AND KEY EQUATIONS

Equation (1) and (2) express a common $N-1$ contingency condition and the power balance constraint in a typical power system, respectively.

$$\sum_{\substack{i=1 \\ i \neq j}}^N u_i \cdot (P_i^{max} - P_i) \geq u_j \cdot P_j \quad (1)$$

$$\sum_{i=1}^N u_i \cdot P_i = D \quad (2)$$

In the following some algebraic manipulation is performed to derive the proposed contingency criterion.

$$\left(\sum_{i=1}^N u_i \cdot P_i^{max} - \sum_{i=1}^N u_i \cdot P_i \right) - u_j \cdot (P_j^{max} - P_j) \geq u_j \cdot P_j \quad (3)$$

$$N \left(\sum_{i=1}^N u_i \cdot P_i^{max} - D \right) - \sum_{j=1}^N u_j \cdot P_j^{max} + \sum_{j=1}^N u_j \cdot P_j \geq \sum_{j=1}^N u_j \cdot P_j \quad (4)$$

$$\sum_{i=1}^N u_i \cdot P_i^{max} \geq \frac{N}{(N-1)} D \quad (5)$$

$$\sum_{i=1}^N u_i \cdot P_i^{max} \geq \frac{n}{(n-1)} D, \quad n = \sum_{i=1}^N u_i \quad (6)$$

Now (6) is generalize to cover higher-order sequential outage contingencies. For the sequential outage of m units (i. e., $\underbrace{-1 - 1 - \dots}_{-m}$), (6) changes into (7).

$$\sum_{i=1}^N P_i^{max} \geq \frac{N}{N-m} D \quad (7)$$

For the simultaneous loss of m units, (1) needs to be rewritten as:

$$\sum_{\substack{i=1 \\ i \notin S_m}}^N (P_i^{max} - P_i) \geq \sum_{j \in S_m} P_j \quad (8)$$

The total number of combinations that S_m comprises is C_N^m .

$$C_N^m = \frac{N!}{m!(N-m)!} \quad (9)$$

Now, we write out (8) for all the possible m -combination of units from N units and then get the sum of all the terms. This will lead to (10):

$$\frac{(N-1)!}{m!(N-m-1)!} \left[\left(\sum_{i=1}^N P_i^{max} \right) - D \right] \geq \frac{(N-1)!}{(m-1)!(N-m)!} D \quad (10)$$

After some manipulation:

$$\sum_{i=1}^N P_i^{max} \geq \left(\frac{N}{N-m} \right) D \quad (11)$$

Equation (11) states that (7) remains valid regardless of the type of contingency (be it simultaneous or consecutive). It is interesting to note that the denominator of R always remains as the same as the order of the contingency. It is claimed that (11) is a simple but effective criterion developed to determine if a power system is vulnerable to $N-m$ outage contingency.

A. Nomenclature

Indices	
i	Index for generating unit.
j	Index for lost generating unit
Binary variables	
u_i	Commitment state of unit i . Equal to 1 if unit is on and to zero if it is not.
Continuous variables and parameters	
D	System demand (MW)
m	Index for outage contingency ($m=0$ for normal operation).
n	Number of total committed units (online)
N	Number of total units (be on or off).
P	Scheduled generation of a unit in the pre-contingency state (MW).
P^{max}	Unit maximum generation output (MW).
S_m	The set of all the possible combinations of the simultaneous loss of m units.

Cybersecurity of Smart Inverters in a Distribution System

Chih-Che Sun
 Energy Systems Innovation Center
 Washington State University
 Pullman WA, USA
 chih-che.sun@wsu.edu

Ruoxi Zhu
 Power and Energy Center
 Virginia Tech
 Blacksburg VA, USA
 ruoxi@vt.edu

Chen-Ching Liu
 Power and Energy Center
 Virginia Tech
 Blacksburg VA, USA
 ccliu@vt.edu

Abstract— To enable large scale deployment of renewable energy, utilities must implement wide-area communication to allow remote control of these devices. Smart inverters are adopted to provide digital communication interfaces for real-time control and monitoring. However, the deployment of Information and Communications Technology (ICT) also brings cyber security concerns in a smart grid. In this research, a signature-based Intrusion Detection System (IDS) is proposed to detect cyber intrusions for smart inverters in a distribution system. The technique of Timed Failure Propagation Graph (TFPG) is used for the detection algorithm to generate attack index numbers, representing the likelihood of cyber attacks. This work has been validated by the Cyber-Power System (CPS) simulation platform at Virginia Tech (VT).

Keywords— Distributed energy resources, cyber security, smart inverter, intrusion detection system, cyber-physical system security

I. INTRODUCTION

At the third quarter of 2018, the installed solar energy in the U.S. has reached 60 GW. However, the high penetration of Distributed Energy Resources (DERs) has also raised questions regarding cyber security of the power grid. In this work, an on-line detection system [1] is proposed to identify suspicious abnormal behaviors that deviate from regular operations of a smart inverter. For example, smart inverters should provide three control modes (i.e., off, maximum power point, and constant voltage) to handle different voltage levels on a feeder by complying with the IEEE 2030.5 standard. Each control mode has a unique pattern to manipulate the power output of a smart inverter. Any violations of the default manipulation are considered anomalies. The defined anomaly types are correlated by the TFPG [2] model and transformed into an attack table. It uses chronological relations among anomaly events to list the possible attack paths in a smart inverter. By comparing the similarity between detected anomalies and possible attack paths in the attack table, the proposed IDS is able to determine the likelihood of a cyber attack. Fig. 1 shows an example of TFPG models for cyberattacks in a DER system. A software based CPS platform has been developed at VT. DIGSILENT PowerFactory is used as a power system

This research is supported by U.S. National Science Foundation under the award number ECCS-1824577 at Virginia Tech, a Collaborative Project with Ohio State University.

simulation tool. The embedded OPC communication provides an interface between the cyber system and the power system, providing a co-simulation environment for the cyber-physical system.

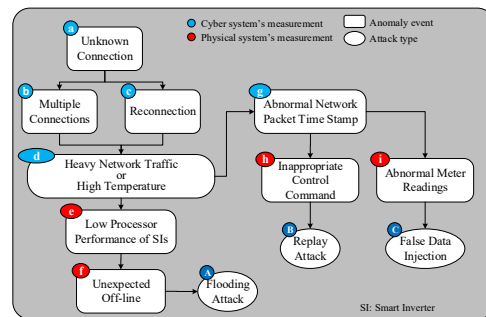


Fig. 1. Intrusion processes of a DER system based on TFPG model.

II. TEST CASE

In the test attack scenario, attackers launch a flooding attack to a smart inverter in IEEE 13-Node Distribution Feeder. The voltage regulation function of a PV system is disabled for study of the impact on smart inverter attacks. In Fig. 2, the voltage levels dropped to approximately 0.9 p.u. at each feeder. Since Node 650 is directly connected to the utility substation, the voltage impact is minimal at the node.

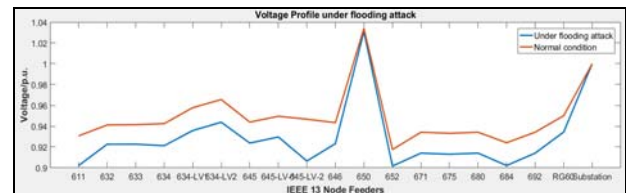


Fig. 2. Comparison of voltage profiles with and without a flooding attack.

REFERENCES

- [1] C. C. Sun, R. Zhu and C. C. Liu, "Cyber Attack and Defense for Smart Inverters in a Distribution System" in *CIGRE D2 Colloquium 2019*, Helsinki, FIN, 2019.
- [2] S. Abdelwahed, G. Karsai, N. Mahadevan, and S.C. Ofstun, "Practical Implementation of Diagnosis Systems Using Timed Failure Propagation Graph Models," in *IEEE Trans. Instrumentation and Measurement*, vol. 58, no. 2, pp. 240–247, Feb. 2009.

Securing Power Distribution Grid Against Power Botnet Attacks

Lizhi Wang, Lynn Pepin, Yan Li, Fei Miao, Amir Herzberg, Peng Zhang and Christopher Leigh

Abstract—Power Botnet Attacks are introduced as a new class of cyber-physical attacks against power system. A botnet is a collection of internet-facing devices that are compromised and controlled by a malicious hacker. We propose this attack utilizing a botnet of high-wattage internet-facing devices, which we call Power Botnet. The fundamental characteristics of Power Botnet Attacks are explained. We conduct vulnerability analysis of OLTC transformers under Power Botnet Attack. Here, we define four different attack strategies. Simulations on the modified IEEE 123-bus system using OpenDSS demonstrate the effect of the proposed attack strategies. The results reveal the mechanism of Power Botnet Attacks and highlight the importance and complexity of defending power systems against Power Botnet attacks. And then we use deep learning methods to detect these attacks. We show successful detection for these attacks and give the locational detection results of power botnet.

Index Terms—Cyber Security, Power Botnet, Load altering attack, Machine Learning, Attack Detection

I. INTRODUCTION

A single device controlled by an attacker is known as a **bot**. When such a device is capable of demanding high load, we call it a **power bot**, and we call the collection of such power bots a **power botnet**. High wattage devices such as air conditioners and water heaters are connected to the power-grid and are not part of the infrastructure of the power company. Vulnerabilities in many IoT devices that could allow attackers to remotely control them, usually via the Internet. As stated, this is called a bot, and a large number of internet-facing high-wattage bots controlled by a single hacker is known as a power botnet. Attackers can utilize a power botnet to exert a coordinated load change in power grid, performing attacks such as by synchronously switching on or off quantities of high wattage devices or changing the set-points synchronously. We call such an attack a *power botnet attack*.

Moving towards defense against this class of attacks, it can be beneficial to be able to detect them. This is a new class of attacks, and the objectives and methods vary. Unlike traditional botnets[?], which usually perform short-term denial-of-service attacks by brute force, a power botnet attack can be successful with subtle and small influences, making it hard to detect. Machine learning method can be leveraged to detect Power Botnet Attack.

II. ATTACK STRATEGIES, RESULTS OF ATTACK AND DETECTION

- 1) Random Attack: Attacker Goal:Random attack strategy is employed by this greedy attacker. The attacker aims at causing power failure through manipulating all the IoT devices that he can access.
- 2) Aggressive Attack Attacker Goal:The goal of the attacker is to manipulate the IoT devices frequently and fast wear down the OLTC devices. The attacker aims

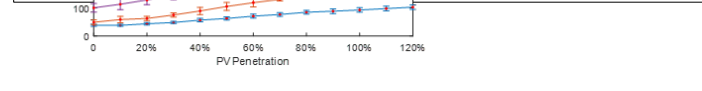
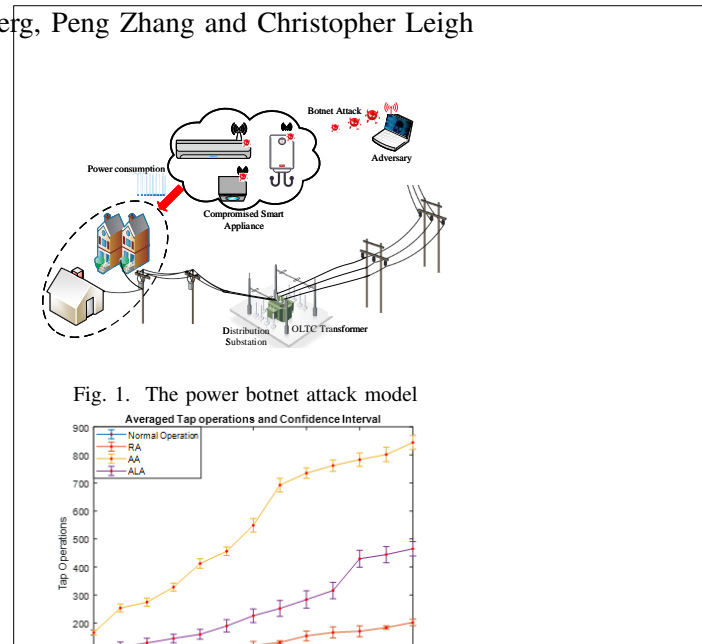


Fig. 2. The attack effect on OLTC tap changing

at causing tap operations as much as possible while considering the vulnerable scenario.

- 3) Targets targeted Attack Attacker Goal:The goal of the attacker is to cause tap change frequently while manipulating small amount of devices.
- 4) Anti-locating Attack Attacker Goal:The goal of the attacker is to avoid being located once being detected. The attacker will change the attacked nodes from the primary and secondary side of the OLTC every time the attacked are launched and meanwhile adopt the strategy 3) to attack the power distribution grid

III. CONCLUSION

Power botnet attacks on power distribution grid and detection results based on deep learning were analysed. Our simulation results show that manipulating different percentages of power botnets can wear down OLTC in different times.

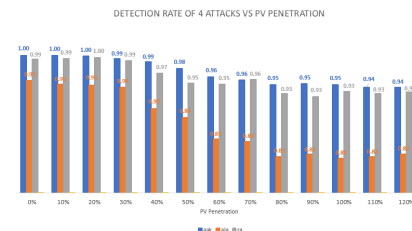


Fig. 3. Detection of three different kinds of attacks

A Discrete Event Theory Based Approach for Modeling Power System Cascading Failures

Wasseem H. Al-Rousan, Caisheng Wang, Feng Lin
 Department of Electrical and Computer Engineering
 Wayne State University
 Detroit, USA

Abstract—For a power system cascading failure, the failure propagates through a sequential tripping of the components in the network. As a result, a complete or partial shutdown may occur. Although many models were developed to understand the failure propagation mechanism, the joint dynamics between discrete sequential tripping and continuous power flow has not been fully evaluated. Further study is needed in this area to develop an abstract higher model, which captures the systems flow dynamics. This paper introduces a new approach for studying the cascading failure and develops a model that translates the power system into an Automata based on the components operational modes. Based on a Discrete Event Systems (DES) approach, the overall system is analyzed. Cascading failure is then defined in a DES framework, and supervisory control strategies are introduced as a solution to mitigate cascading failures. Additionally, an illustrative example for the proposed approach is presented. Finally, the proposed modeling approach is simulated by combining continuous power flow study and DES tools in a unified framework.

Keywords—Cascading failure, discrete-event systems, hybrid simulation.

I. DES MODEL OF CASCADING FAILURE

We model each component in a power system by an automaton, also called finite state machine (FSM) in the framework of DES. The operational modes of a component are modeled as (discrete) states. The transitions from one state to another are modeled as events. This automaton model will be used later to design a control strategy/policy to mitigate cascading failures. Formally, an automaton is a 5-tuple

$$H = (Q, \Sigma, \delta, q_o, Q_m) \quad (1)$$

Transmission line, Load and Generator automata models are illustrated in Fig. 1.

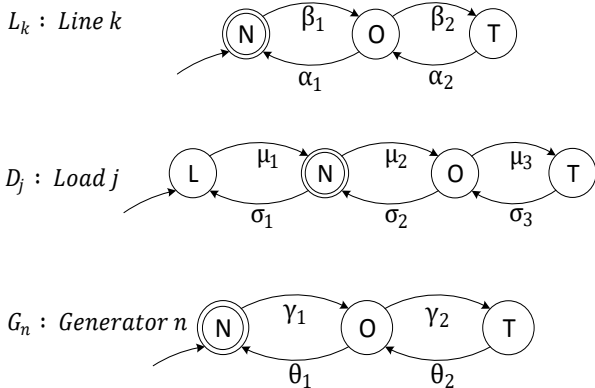


Fig. 1. Transmission line, load and generation unit modeled as automata.

A. Mitigating cascading failures using DES approach

Formally, let F^1, F^2, \dots, F^i be a sequence of failure state sets in H . Then a cascading failure can be described by

$$q^1 \xrightarrow{s_1} q^2 \xrightarrow{s_2} q^3 \dots q^i \xrightarrow{s_i} q^{i+1} \quad (2)$$

where $q^2 \in F^1 \wedge q^3 \in F^2 \dots \wedge q^{i+1} \in F^i$ and $s_1, s_2 \dots s_i$ denotes a sequence of events. Fig. 2 illustrates a cascading failure in a system, where the strings of tripping and overloading events evolve through states of failures.

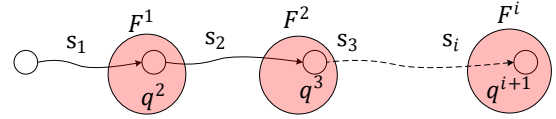


Fig. 2. Sequence of failure states presented in DES.

For a sequence of events that leads to a failure, described by $s_i = \sigma_1 \sigma_2 \dots \sigma_n$. Then a sequence $s_i = \sigma_1 \sigma_2 \dots \sigma_n$ is controllable if and only if

$$(\exists i \in \{1, 2, \dots, n\}) \sigma_i \in \Sigma_c \vee (\exists \sigma' \in \Sigma_f) (\exists q' \in Q) \delta(q_i, \sigma', q')$$

Fig. 3 illustrates preempting a sequence of events s_i by σ' .

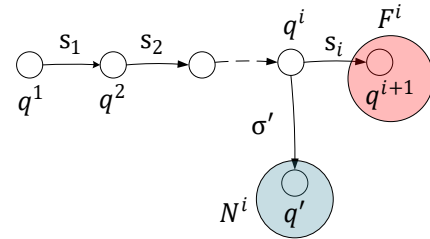


Fig. 3. Pre-empting state of failure by forcing an event (σ').

If a sequence in a cascading failure is controllable, then a controller called supervisor can be designed and used to mitigate the failure. Formally, a supervisor, denoted by S is a mapping

$$S: L(H) \rightarrow 2^{\Sigma_c} \times 2^{\Sigma_f} \quad (3)$$

II. SIMULATION MODEL

We propose a model that has a modular basis, in a way that each node or bus in the power system is represented by an automaton. To implement the model, the events for each bus from the automata of individual components are constructed.

$$H_i = L_1 \parallel L_2 \parallel G_1 \quad (4)$$

Mode Shape Localization in Inverter-Based Microgrids

Andrey Gorbunov *Student Member, IEEE*, and Jimmy Chih-Hsien Peng *Member, IEEE*
 Department of Electrical & Computer Engineering,
 The National University of Singapore
 gorbunov@u.nus.edu, jpeng@nus.edu.sg

Abstract—While transmission systems experience critical inter-area oscillations, oscillations of inverter-based could be local. An inverter-based system could be represented by a graph where nodes correspond to inverter connections and edges represent electric lines. This representation would allow the parameterization of the topological properties (e.g., connectivity) of the system by the graph spectrum. Using this, we could infer how the topology of the system affects the stability without relying on numerical simulations. In other words, we could find the relationship between poles of a dynamic model and eigenvalues an admittance matrix. This analysis provides the conceptual explanation as to why certain clusters of inverters have a higher impact on stability.

Index Terms—coherency analysis, invert-based systems, microgrids, power systems stability and control, small signal stability.

I. INTRODUCTION

To illustrate localization, consider the system depicted in Fig. 1. The system consists of two areas, where each area has two inverters. We turn to the well-known two-area network to understand the dynamics of the local and inter-area oscillations. In this case, the synchronous generators are replaced by inverter systems.

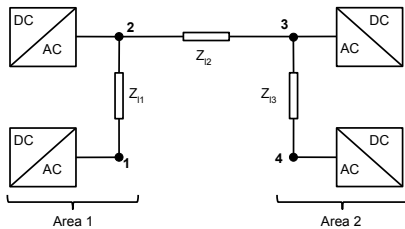


Fig. 1. The two-area system

We assume that all inverters are participating in power-sharing and voltage regulation, i.e., are in the grid-forming operation mode. The control is implemented through the following frequency and voltage droop static droop characteristics,

$$\omega = \omega_{set} - mP, \quad (1a)$$

$$V = V_{set} - nQ. \quad (1b)$$

Where ω_{set} is the reference setting of the frequency controller and V_{set} is that of the voltage controller; M is the frequency

droop coefficient, N is the voltage droop coefficient; P, Q - filtered measurements of real and reactive power consequently.

Also, we assume that the impedance of the line 2-3, Z_{l2} , connecting the two areas is much higher than those inside each area, Z_{l1}, Z_{l3} . Thereby, the network is clearly separated into two clusters, and we wish to determine which area dominantly influences stability. For doing this, we compute the eigenvalues associated with the dominant modes of the linearized model and the same are plotted in Fig. 2. It may be observed that there are three dominant modes (pole-pairs). These modes correspond to oscillations among four inverters. The noteworthy fact is that the most critical mode corresponding to the closest to the imaginary axis pole is associated with Area 2. Therefore, only inverters 3 and 4 determine the stability of the whole system. The localization of critical modes has not been observed in the transmission level where usually critical modes correspond to low-frequency inter-area modes while local modes (associated with Area 1 and Area 2 in our case) are well damped. This observation motivates us to investigate the power sharing properties in inverter-based systems.

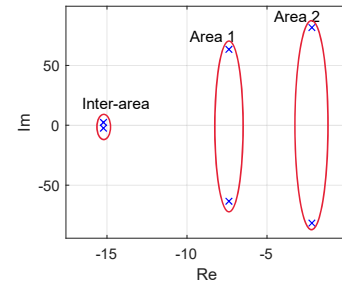


Fig. 2. Dominant poles of the two-area system

II. KEY RESULT

We make plausible assumptions on the same $\frac{R}{X}$ ratios for all lines and the same $\frac{m}{n}$ proportional power sharing for each inverter. With these assumption mode shapes of linearized model coincide with the eigenvectors of the (re-weighted) admittance matrix Y . Besides, the critical modes correspond to higher eigenvalues of Y . Specifically, in the two-area system, we could find the criteria for Y eigenvector localization using the perturbation analysis that gives the following:

- $Z_{l2} \ll Z_{l1}, Z_{l3}$
- $Z_{l1} \neq Z_{l3}$

Flexibility and Stability of an Islanded Microgrid with Smart Loads

Jinrui Guo, Balarko Chaudhuri
 Imperial College London, United Kingdom
 j.guo16@imperial.ac.uk
 b.chaudhuri@imperial.ac.uk

Shu Yuen Ron Hui
 The University of Hong Kong, Hong Kong
 Imperial College London, United Kingdom
 ronhui@eee.hku.hk

Abstract—Flexibility in demand could be realized through an electric spring (ES) connected in series of the loads forming the so-called smart loads (SLs). This flexibility could improve frequency regulation in islanded microgrids with converter-interfaced distributed generators (DGs) working in grid forming mode. It is observed that there could be a trade-off between the extent of frequency deviation reduction and the dynamic response of the whole system when choosing the droop gains of SLs. To find out the root cause behind, the linearized state space model of an islanded microgrid is extended to include the dynamics of a SL with a series-shunt converter arrangement in its voltage compensator. It is shown that the dynamics of the DC link and the control loops of the series and shunt converters of the SL dictates the lower limit of its droop gain for stable operation. The modal analysis also reveals that SLs have marginal influence on low frequency oscillations that are typically associated with the droop control of the converter-interfaced DGs.

Index Terms—Smart load, electric spring, stability, microgrid, frequency regulation

I. PERFORMANCE VS. STABILITY

The test system considered here is an islanded microgrid with two identical converter-interfaced DGs with normal local loads and one SL connected via two line segments. An overview control scheme of the SL is given in Fig. 1.

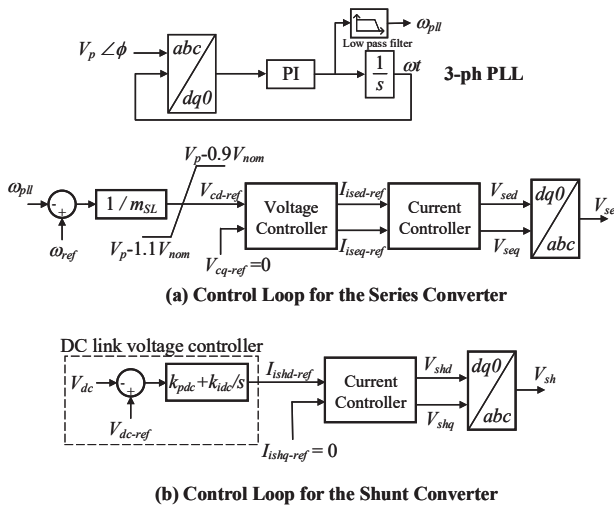


Fig. 1. Control of series and shunt converter of a smart load (SL)

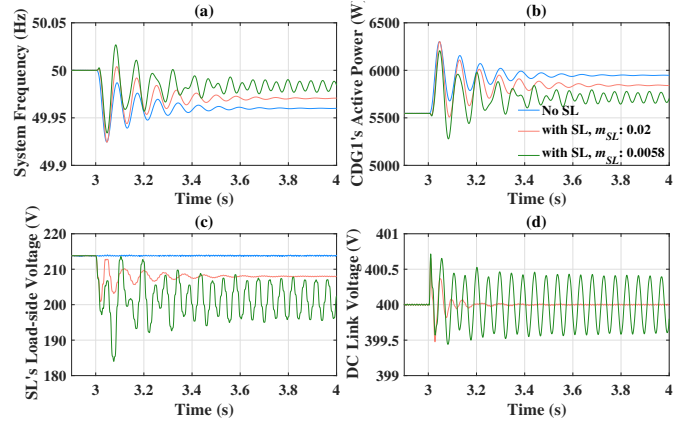


Fig. 2. Dynamic response of (a) microgrid frequency; (b) Active power output of CDG1; (c) RMS value of SL's load voltage; (d) DC-link voltage

It can be seen from Fig. 2 that with lower droop gains, the frequency deviation would decrease however at the expense of a more oscillatory dynamic response. Also dynamic response for low droop gains reflects two interleaved modes.

II. KEY RESULTS OF MODAL ANALYSIS

The eigenvalue traces of Modes 1 and 2 as the droop gain is varied between 0.001 to 0.1 can be seen below. Mode 1 (around 12 Hz) denotes the mode mainly associated with the droop control of DGs while Mode 2 (about 22 Hz) is more related with the voltage and current controllers of SL's both converters and DC link dynamics.

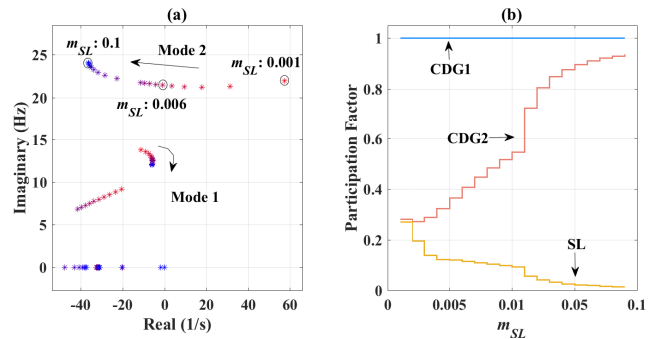


Fig. 3. Root locus and participation factor with droop gain of SL varying between 0.001 and 0.1

Impact of PLL on Harmonic Stability of Renewable Dominated Power System

Indla Rajitha Sai Priyamvada
 Electrical Engineering Department
 Indian Institute of Science
 Bangalore, India
 indlap@iisc.ac.in

Sarasij Das
 Electrical Engineering Department
 Indian Institute of Science
 Bangalore, India
 sarasij@iisc.ac.in

Abstract—For reliable operation of power system, the system should be stable not only in the fundamental domain but also in harmonic domain. Power electronic converters of renewable energy (RE) generators inject harmonics into the power systems. So, at higher RE penetration levels, study of power system stability in harmonic domain i.e. harmonic stability is required. The Phase Locked Loop (PLL) affects the dynamic behavior of power electronic converters in harmonic domain also. This work analyzes the impact of PLL on the harmonic stability of renewable dominated power systems. A small signal state space model is developed for PLL in harmonic domain to analyze the behavior of PLL. The obtained state space model is a periodic Linear Time Varying (PLTV) system, making the state space model of the whole power systems also a PLTV system. As the obtained state matrix is periodic in nature, the concept of time varying eigen-values is employed to analyze the harmonic stability. Impact of PLL parameters on harmonic stability is analyzed using a modified IEEE 39 Bus system. The impact of RE penetration on harmonic stability is also analyzed.

I. KEY EQUATIONS

A. Phase Locked Loop Model in Harmonic Domain

The state space model of PLL for harmonic stability analysis can be obtained as (1). The small signal model of PLL is a Periodic Linear Time Varying (PLTV) System with period T .

$$\begin{bmatrix} \Delta \dot{\delta}_{pll} \\ \Delta \dot{x}_{pll} \end{bmatrix} = \begin{bmatrix} K_p a(t) & 1 \\ K_i a(t) & 0 \end{bmatrix} \begin{bmatrix} \Delta \delta_{pll} \\ \Delta x_{pll} \end{bmatrix} + b(t) \begin{bmatrix} K_p \\ K_i \end{bmatrix} \Delta V_n \quad (1)$$

where, n denotes the harmonic order of interest; V_n denotes the peak of n^{th} harmonic frequency voltage; $a(t) = -V_{n0} \cos((n-1)wt + \delta_n - \delta_{pll0}) - V_1$; $b(t) = \sin((n-1)wt + \delta_{pll0} - \delta_1)$; $V_{q0}, V_{n0}, \delta_{pll0}$ are initial values of V_q, V_n, δ_{pll} ; K_p and K_i are the PI parameters of PLL. Δx_{pll} is a state variable of PLL; $a(t)$ and $b(t)$ are periodic with time period T .

$$a(t+T) = a(t); b(t+T) = b(t); T = \frac{1}{(n-1)\omega} \quad (2)$$

B. Harmonic Stability Analysis

The small-signal model for power systems can be written in a compact form as $\Delta \dot{X} = A(t)\Delta X$. $A(t)$ will be periodic with the same period as that of PLL model i.e. $A(t+T) = A(t)$. The dynamics of the power system in harmonic frequency domain is analyzed using time varying eigen-values.

This work was presented in IEEE Power Electronics, Drives and Energy Systems (PEDES) Conference-2018.

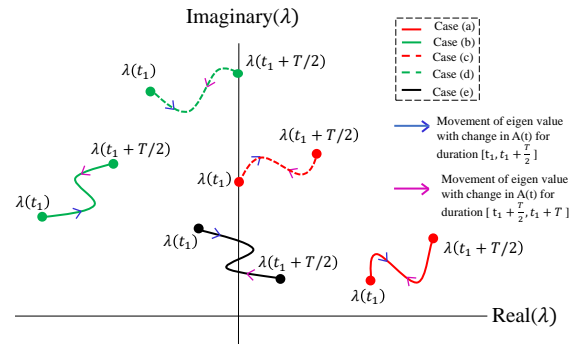


Fig. 1. Possible cases of eigen-values with periodically varying $A(t)$

II. KEY RESULTS

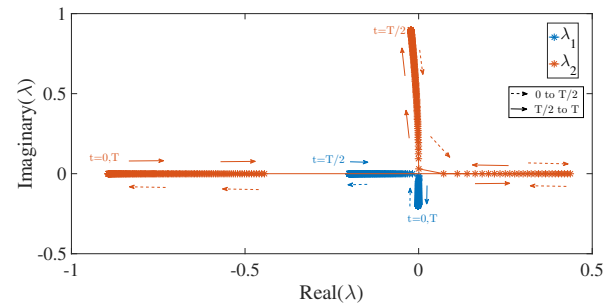


Fig. 2. Variation of the eigen-values in one time period

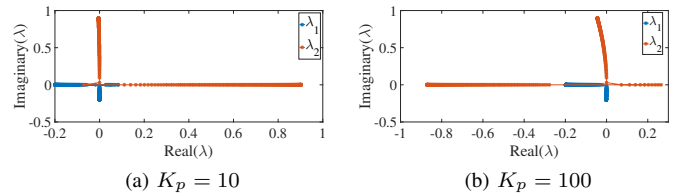


Fig. 3. Impact of K_p on harmonic stability

- To carry out the analysis, the IEEE 39 bus system is modified in order to achieve 60% renewable penetration.
- The time period of $A(t)$ is obtained as $T = 0.53 \text{ ms}$ for 6^{th} harmonic frequency.
- As K_p is increased or K_i is decreased, the eigen-values stay in left half plane for longer duration improving the stability of power system in harmonic domain.

Optimal-Probabilistic Coordination of Directional Overcurrent Relays Considering Network Topological Uncertainties

Jiawei Qi*, Jun Xie†, Xiejin Ling*, Yinhong Li*, *Member, IEEE*, and Tongkun Lan*

* State Key Laboratory of Advanced Electromagnetic Engineering and Technology
Huazhong University of Science and Technology, Wuhan, China

† Central China Electric Power Dispatching and Control Sub-center of State Grid Corporation of China

Email: jw7_hust@hust.edu.cn, xjvhj@163.com, hust_lxj@hust.edu.cn, liyinhong@hust.edu.cn, lantongkun@hust.edu.cn

Abstract—The probability of each network topology occurring in an actual power system is entirely different. The relays coordination considering overall possible topology variations without corresponding probabilities tends to cause unsatisfactory performance of relay settings in operation and even difficulty in determining settings. In this paper, a novel method is proposed for optimal coordination of directional overcurrent relays (DOCRs) considering network topological uncertainties through its probabilistic model. The relays coordination problem is formulated as a multi-objective optimization problem with two objective functions. One is the conventional function that minimizes overall operating time of the relays, and the other is to minimize the probabilities of loss of selectivity under network topology variations. With the proposed method, the settings are satisfactorily determined with the minimum probability of losing selectivity. The method proposed in this paper has been applied to an 8-bus power system, and the results demonstrated the better robustness towards the network topology variations over the prevailing approaches.

Index Terms—Network topological uncertainties, directional overcurrent relays, probabilistic optimization, relay settings, optimal coordination, multi-objective optimization.

I. KEY MODEL

A. Objective Functions

$$\text{Min : } OF_1 = \sum_{i=1}^N \omega_i t_i \quad OF_2 = \sum_{j=1}^M P_j^{\text{loss}} \quad (1)$$

$$t_{i,j} = \frac{0.14 \times TDS_i}{(I_{f_{i,j}}/I_{P_i})^{0.02} - 1} \quad P_j^{\text{loss}} = p_j \times \frac{N_j^{vl}}{N_j} \quad (2)$$

B. Bounds of Variables

$$I_{P_i}^{\text{min}} \leq I_{P_i} \leq I_{P_i}^{\text{max}} \quad (3)$$

$$TDS_i^{\text{min}} \leq TDS_i \leq TDS_i^{\text{max}} \quad (4)$$

$$t_i^{\text{min}} \leq t_{i,j} \leq t_i^{\text{max}} \quad (5)$$

II. KEY RESULTS

It is a tradeoff between operating time and probability of loss of selectivity under different network topologies. Actually, the obtained Pareto optimal frontier could meet such requirements with multiple setting groups provided.

TABLE I

NUMBER OF CONSTRAINTS VIOLATION AND PROBABILITY OF LOSS OF SELECTIVITY FOR RELAY PAIRS UNDER DIFFERENT TOPOLOGIES

Relay Pairs		Case 1		Case 2		Case 3	
PR	BR	N_V	ΣP_{loss}	N_V	ΣP_{loss}	N_V	ΣP_{loss}
1	6	9	0.9038	9	0.9038	2	0.0516
2	1	1	0.0305	1	0.0305	1	0.0305
2	7	4	0.4544	0	0	0	0
3	2	9	0.9446	9	0.9446	0	0
4	3	6	0.1770	2	0.0773	2	0.0773
5	4	9	0.9441	9	0.9441	0	0
6	5	5	0.5199	0	0	0	0
6	14	4	0.4937	0	0	0	0
7	5	5	0.5141	3	0.4449	0	0
7	13	0	0	0	0	0	0
8	7	4	0.4366	2	0.4449	0	0
8	9	3	0.0864	0	0	0	0
9	10	9	0.9484	9	0.9484	0	0
10	11	6	0.1656	2	0.3870	6	0.1656
11	12	9	0.9441	9	0.9441	0	0
12	13	1	0.0305	1	0.0305	0	0
12	14	4	0.4803	0	0	0	0
13	8	9	0.9308	9	0.9308	0	0
14	1	0	0	0	0	2	0.0516
14	9	5	0.4854	0	0	0	0
ΣN_V		102		65		13	

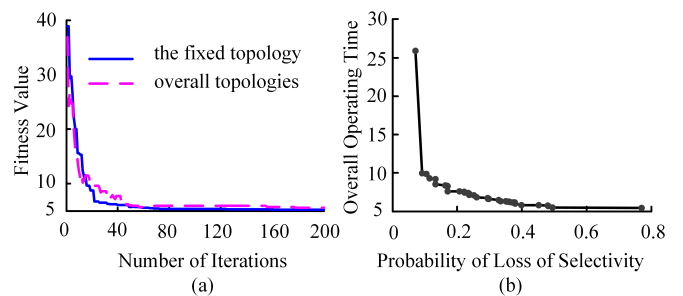


Fig. 1. (a). Convergence of the PSO algorithm considering the fixed topology and overall topology variations respectively; (b). The curve of the Pareto optimal frontier with the solution of the multi-objective optimization problem.

III. CONCLUSION

The results of the case study demonstrate the performance of the proposed optimal-probabilistic coordination method, which is more adaptive to network topology variations in the sense of probabilities of loss of selectivity for relay pairs.

Evaluation of High Solar Penetration Impact on Bulk System Stability through a Transmission-Distribution Dynamics Co-simulation

Qinmiao Li, *Student Member, IEEE*, Shrirang Abhyankar, *Member, IEEE*

Abstract—Currently, utilities are greatly interested in understanding the interactions between power transmission and distribution, particularly those that impact bulk power stability, as the penetration of distributed energy resources increases. In this paper, we present a transmission and distribution dynamic co-simulation to assess the impacts of increasing distributed photovoltaic (DGPV) penetration on bulk power stability. This method uses a non-iterative coupling algorithm to link the separate dynamic simulators for transmission and distribution systems. We carry out case studies of an IEEE 14-bus transmission system with IEEE 8500-node distribution feeders for disturbances such as loss of generation, faults on the transmission and distribution under different PV penetration levels.

Keywords—Co-simulation, Dynamics, Distributed Energy Resources

I. DYNAMIC CO-SIMULATION METHODOLOGY

A. T-D Dynamics Modeling and Information Exchange

The transmission system model can be represented by equations (1)-(2) and we can also model the distribution system in the form of equations (3)-(4):

$$\dot{x}_T = f_T(x_T, y_T, u_T) \quad (1)$$

$$0 = g_T(x_T, y_T, u_T) \quad (2)$$

$$\dot{x}_D = f_D(x_D, y_D, u_D) \quad (3)$$

$$0 = g_D(x_D, y_D, u_D) \quad (4)$$

The consistency of boundary variables for TSS and DSS are referred to as boundary conditions. They can be represented by equations (5) and (6) for transmission and distribution systems, respectively:

$$0 = h_T(u_T, r(y_D)) \quad (5)$$

$$0 = h_D(u_D, s(y_T)) \quad (6)$$

$$r(y_D) = S_{T,+} \quad (7)$$

$$s(y_T) = V_{D,abc} \quad (8)$$

B. Interfacing Algorithm

The interfacing algorithm, as illustrated in Fig. 1, is a non-iterative algorithm. At every time-step, the DAEs for the transmission and distribution systems are separately computed with the inputs from last time-step. Then the boundary variables are updated.

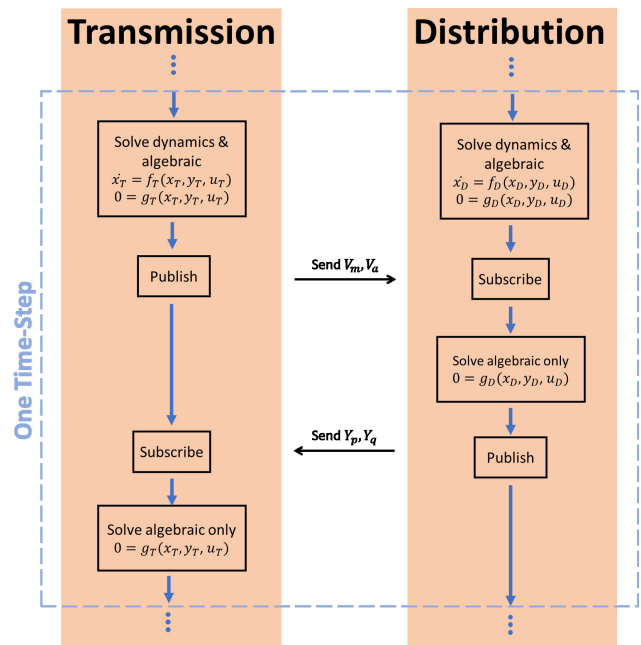


Fig. 1: Flowchart for the coupling algorithm

II. KEY SIMULATION RESULTS

In this section, we demonstrate the simulation results of the frequency response in the IEEE 14-bus system under different PV penetration levels.

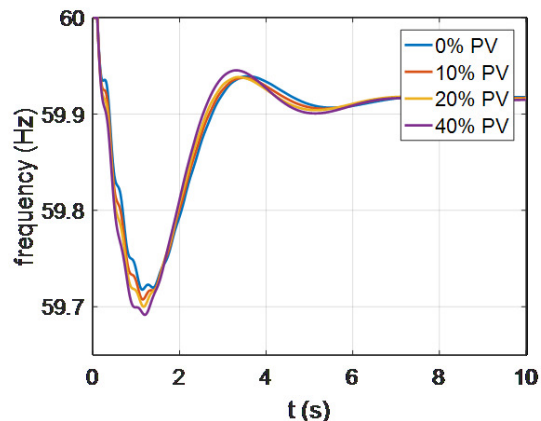


Fig. 2: System frequency responses under different PV penetration levels

This work was funded under the Grid Modernization Lab Consortium (GMLC) project Development of Integrated Transmission, Distribution, and Communication (TDC) Models.

Frequency Control of Decoupled Synchronous Machine Using Koopman Operator Based Model Predictive

Xiawen Li

Jaime De La Ree

Department of Electrical and Computer Engineering
Virginia Polytechnic Institute and State University
Blacksburg, U.S.

xiawenli@vt.edu

Chetan Mishra

Dominion Energy

Richmond, U.S.

Chetan.Mishra@dominionenergy.com

Abstract—Conventional generators have been retired or replaced by renewable energy because of the utility long-standing goals. However, instead of decommissioning the entire plant, the rotating mass can be utilized as a storage unit to mitigate the frequency issues due to these changes in the grid. The goal is to design a control utilizing the retired machine interfaced with the grid through a back to back converter referred to as decoupled synchronous machine system (DSMS) to damp frequency oscillations. However, in a practical setting, it is often not possible for a utility to obtain access to the detailed state equations of such devices from the vendor making the addition of another layer of control a challenging problem. Therefore, a purely data driven approach to nonlinear control design using Koopman operator based framework is proposed for this application. The effectiveness of the proposed system is demonstrated in the Kundur two-area system.

Keywords—Frequency Control, Koopman operator, Model predictive control.

I. KEY METHODOLOGY AND EQUATIONS

The system to be controlled in Fig. 1 is a classical input-output system which comprised of the proposed DSMS and the external power grid. In order to design the external controller, we first use Koopman operator to obtain the linear representation of the controlled system. Consider a generic input-output nonlinear system given in (1), its future dynamic can be found by the nonlinear function f and the current dynamic in the original state space M . Then we apply the lifting function g in (2) to lift M to a higher-dimensional space H such that the system dynamics can be predicted by the Koopman operator K in a linear manner. nd is the number of delay embeddings.

$$f(y_i, u_i) = (y_{i+1}, u_{i+1}) \quad f, y_i, u_i \in M \quad (1)$$

$$g_i(y_i, u_i) = z_i = [y_i, u_i, \dots, y_{i+nd}, u_{i+nd}, \|y_i\|_2, \text{constant}] \quad (2)$$

$$z_{i+1} = Kz_i \quad K, z_i \in H \quad (3)$$

Koopman operator-based Model predictive control (KMPC) is proposed as the external controller. According to the latest and previous frequency values, KMPC seeks for the optimal solution to obtain the 60Hz frequency. The solution is then sent to DSMS as the active power reference.

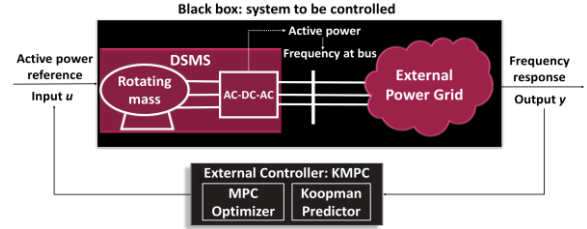


Fig. 1. DSMS system diagram

II. KEY RESULTS

The system was tested in Kundur two-area system with generator 3 replaced in Fig. 2. The algorithm has 0.1468% RMSE (see Fig. 3). DSMS (system C) has better performance than the traditional system (system A) while the system with RESs (system B) behaves the worst in both Fig. 4 and Fig. 5.

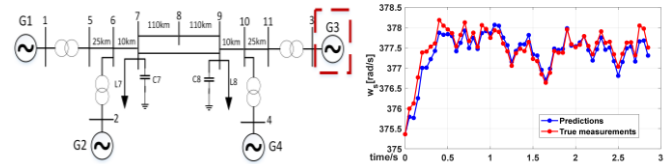


Fig. 2. Kundur two-area system

Fig. 3. Prediction v.s. measurement

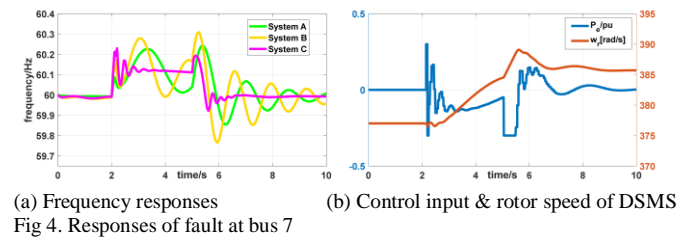


Fig 4. Responses of fault at bus 7

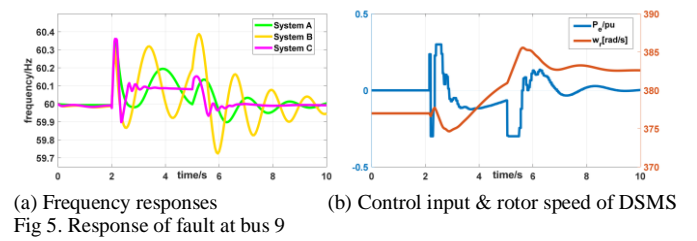


Fig 5. Response of fault at bus 9

PMU-based Estimation of the Frequency of the Center of Inertia and Generator Rotor Speeds

Muyang Liu, *Student Member, IEEE*, Álvaro Ortega, *Member, IEEE*, Federico Milano, *Fellow, IEEE*
 School of Electrical and Electronic Engineering, University College Dublin, Ireland
 muyang.liu@ucdconnect.ie, {alvaro.ortegamanjavacas, federico.milano}@ucd.ie

Abstract—The paper compares a variety of on-line approaches based on PMUs to estimate the angular speed of individual synchronous machines as well as of the center of inertia. These approaches involve the solution of an optimization problem or a Weighted Least Square problem and are based on the frequency divider formula. The case study is based on a dynamic 1,479-bus model of the all-island Irish system with inclusion of stochastic wind speed, noise and time-varying PMU measurement delays. The scenarios studied in the paper allow identifying the key features of the considered estimation approaches. A thorough discussion on the impact of measurement delays and system size is also provided.

I. INTRODUCTION

On-line estimations of synchronous machine rotor speeds and of the frequency of the Center of Inertia (COI) are meaningful to Transmission System Operators (TSOs). This paper compares the accuracy and robustness of conventional estimation approaches with the novel alternatives through several real-world scenarios.

II. ESTIMATION THEORY

1) Synchronous Machine Rotor Speed Estimation:

- Optimization Problem (OPT):

$$\begin{aligned} \min_{(e_B, \Delta\omega_G)} \quad & J = \frac{1}{2} e_B^T \mathbf{W} e_B \quad (1) \\ \text{s.t.} \quad & \mathbf{0} = \mathbf{B}_{BG} \Delta\omega_G + \mathbf{B}_{BB} (\Delta\tilde{\omega}_B + e_B) : \mu_B, \end{aligned}$$

- Weighted Least Square (WLS):

$$\Delta\omega_G^* = (\mathbf{D}^T \mathbf{D})^{-1} \mathbf{D}^T \Delta\tilde{\omega}_B = \mathbf{D}^+ \Delta\tilde{\omega}_B, \quad (2)$$

2) Estimation of the Frequency of COI:

$$\omega_{COI} = \xi^T \omega_B + \alpha, \quad (3)$$

III. CONCLUSION

More measures imply better accuracies in the frequency estimation, in real-world applications, factors such as Phasor Measurement Unit (PMU) measurement delays and system size and/or topology, might lead to the break-even point where the accuracy is compromised if too many measures are used. TSOs should always choose estimation approaches with the full considerations of power system features and the potential impact from measurement delays to fulfil the required accuracy with fewer measures.

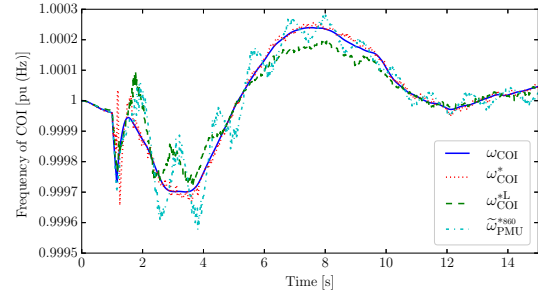


Fig. 1: AIITS undergoing a three-phase fault – estimations of the frequency of the COI. ω_{COI} : actual frequency of the COI; ω_{COI}^* : eq. (3) with all measures available; ω_{COI}^{*L} : eq. (3) with loss of the measures of the North-Ireland sub-area system; $\tilde{\omega}_{PMU}^{*860}$: measured frequency at the pilot bus.

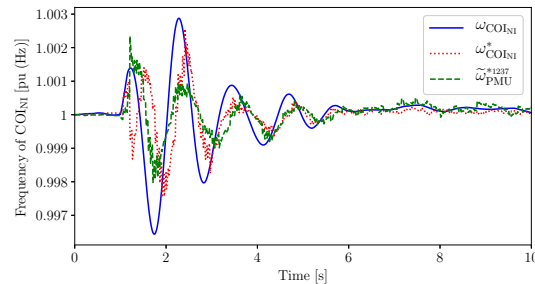
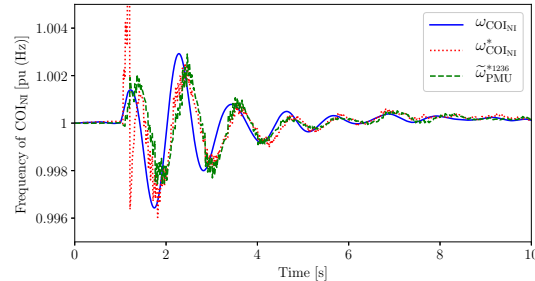


Fig. 2: AIITS undergoing a three-phase fault – estimations of the frequency of the COI of the North-Ireland sub-area system. Upper panel: all measures available; lower panel: loss of measure at bus 1236. $\omega_{COI_{NI}}$: actual frequency of the sub-area COI; $\omega_{COI_{NI}}^*$: estimation by means of eq. (3); and $\tilde{\omega}_{PMU}^{*1236(1237)}$: frequency measured at bus 1236 (1237).

A New Distributed Voltage Controller for Enabling Volt-Var Support of Microgrids in Grid-Connected Operation

Qian Long, Hui Yu, David Lubkeman, Srdjan Lukic
 Department of Electrical & Computer Engineering
 North Carolina State University
 Raleigh, NC, USA
[qlong2, hyu11, dllubkem, smlukic}@ncsu.edu](mailto:{qlong2, hyu11, dllubkem, smlukic}@ncsu.edu)

Abstract — Voltage support is one of ancillary services that can be provided by grid-connected microgrids. This paper presents a new microgrid-level voltage controller to enable microgrids to contribute to distribution system voltage regulation. Like the Volt-Var control of the smart inverters, the proposed controller makes sure that the voltage and reactive power flow at microgrid point of common coupling (PCC) follows a proportional relationship. To increase flexibility and avoid centralized computation, a distributed controller design is developed using the distributed averaging algorithm in order to achieve reactive power sharing among multiple distributed energy resources (DERs) within the microgrid. A large signal analysis is performed to study the stability and dynamic characteristics of the closed-loop system. Simulation results show that the proposed controller is effective in providing voltage regulation for distribution systems with multi-microgrid architecture.

I. INTRODUCTION

Volt-Var control is well-known as a localized proportional voltage control strategy for inverter-based DERs. Inspired by this local control, a new proportional voltage controller is proposed in this paper to enable grid-connected microgrids to provide voltage regulation at point of common coupling (PCC) in a similar way as smart inverter Volt-Var control. The distributed version of the proportional voltage controller is developed using the distributed averaging algorithm such that multiple DERs within a microgrid are coordinated with respect to reactive power capacity. The proposed control is referred to as distributed proportional voltage control (DPVC). It is also shown in the paper that the DPVC supports multi-microgrid architecture in a distribution system.

II. DPVC DESIGN

A. Proportional Voltage Controller Design

The objective of the proportional voltage controller is to enable microgrids to regulate voltage at microgrid PCC based on the proportional setting, which is similar to the Volt-Var setting of smart inverters. To achieve this, the proposed proportional voltage controller is formulated as

$$k \frac{d\Omega}{dt} = -d(V_{PCC} - V^*) - (Q_{PCC} - Q^*) \quad (1)$$

where k is the voltage controller gain and Ω is the voltage control variable for DER reactive power injection; d is the proportional gain that determines the Volt-Var response at microgrid PCC; V_{PCC} and V^* are microgrid PCC voltage magnitude and microgrid PCC nominal voltage; Q_{PCC} and Q^*

are reactive power measurement and nominal reactive power flow in three phases at microgrid PCC.

B. Distributed Implementation of Proportional Voltage Control

The distributed averaging algorithm is integrated with the proposed proportional voltage control to achieve reactive power sharing among multiple DERs in a distributed manner. The DPVC is defined as

$$\begin{cases} k_i \frac{d\Omega_i}{dt} = -d(V_{PCC} - V^*) - (Q_{PCC} - Q^*) - \gamma_i \\ \gamma_i = \sum_{j=1}^n b_{ij} \left(\frac{Q_i}{Q_{iavail}} - \frac{Q_j}{Q_{javail}} \right) \end{cases} \quad (2)$$

where k_i and Ω_i are the DPVC control gain and DPVC control variable for DER i ; d is the DPVC proportional gain; b_{ij} is the communication link between DER i and DER j ; Q_i , Q_{iavail} , Q_j and Q_{javail} are the reactive power output and available reactive power capacity for DER i and DER j , respectively.

III. KEY RESULTS

As Fig. 2 shows, without proper microgrid control for voltage support, the system has low voltage operating point and could potentially experience undervoltage issues especially when there is load step up, such as at MG2 PCC. The proposed voltage controller is able to enable microgrids to provide extra 2% voltage regulation for the distribution system after being activated.

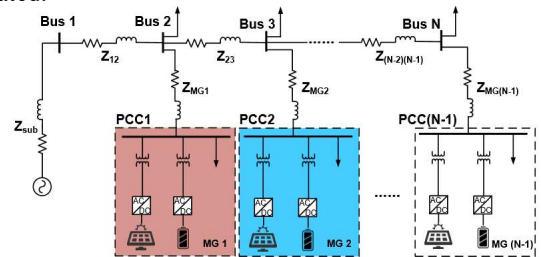


Figure 1. Radial distribution feeder with interconnection of multi-microgrids

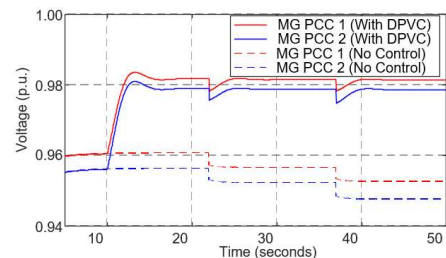


Figure 2. Microgrid PCC voltage magnitude with and without control

Design and simulation of inertia emulation control for a wind turbine generator in a microgrid

Samaneh Morovati, Andrew R. Wintenberg, Yichen Zhang, Seddik M. Dejoudi, Kevin Tomsovic
 Electrical Engineering and Computer Science Department, The University of Tennessee
 [Smorovat, awinten1, yzhan124, mdjouadi, ktomsovi]@tennessee.edu

Abstract— Frequency performance is a critical issue for islanded micro grids, which generally have low inertia. This paper proposes two types of inertia emulation control methods for a diesel wind system. The objective is for the speed of the diesel generator to track a typical reference to achieve a desired frequency response. To achieve inertia emulation, reduced order models, balanced truncation and Hankel reduction technique are used to obtain an easy to implement low order controllers. Comprehensive numerical results show that designed inertia can be emulated resulting in accurate frequency responses.

Keywords—Wind turbine generator, model reduction, balance truncation method, Hankel model reduction

I. INTRODUCTION

Diesel generators are very popular resources for powering microgrids in remote locations. Coupled with wind generation, lack of inertia has become a critical issue because wind turbine generators are converter-interfaced and do not respond to frequency variations due to their decoupled rotor and grid side converter controllers [1]. Regarding this issue, an inertia emulation strategy was proposed in [2] for a diesel-wind system. The model reference control concept has been used to achieve precise inertia emulation. Ref. [3] proposes a model reference control based inertia emulation strategy, which was implemented on the IEEE 33 node based microgrid. In this paper, we provide two different types of model reduction techniques and compare their robustness according to measuring H_∞ norm with full order model. Comprehensive numerical result show that desired frequency response and precise inertia emulation is achieved by using H_2 / H_∞ mixed controller and PI controller.

II. KEY RESULTS

The structure of the control method used is based on the mixed H_2 / H_∞ state feedback control method. The selective model analysis (SMA) based model reduction has been used in [3] and employed to design the controller. In this paper, balanced truncation and Hankel model reduction techniques that have better results according to the H_∞ norm of the error as shown in table I and Fig.2 are used.

TABLE I. H_∞ norm comparison of reduced order models

Reduction method	H_∞ norm
SMA	1.0691
Balance truncation	0.2408
Hankel reduction	5.4206×10^{-4}

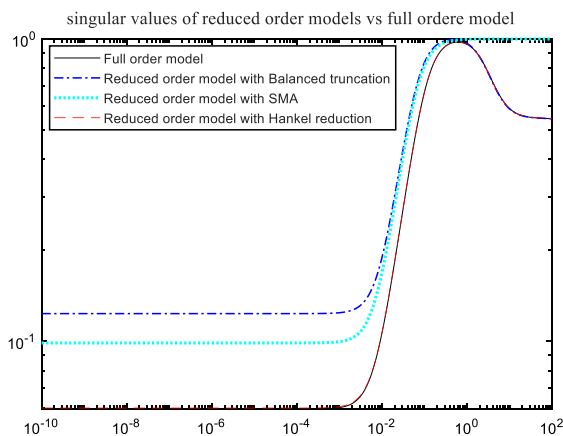


Fig. 1. Singular values of reduced order models and full order model

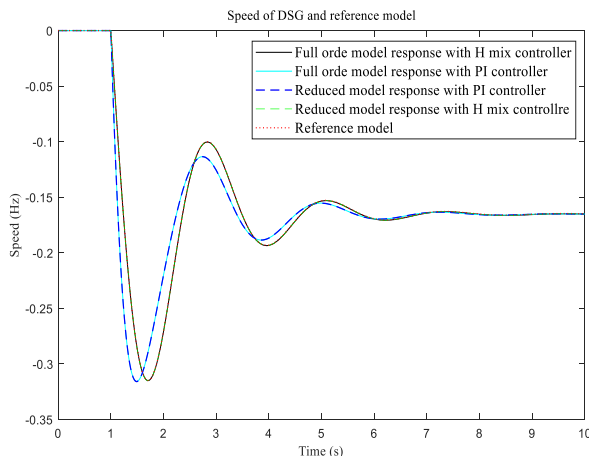


Fig. 2. Speed of diesel synchronous generator and reference model

REFERENCES

- [1] Hector Pulgar-Painemal, Yajun Wang, and Horacio Silva-Saravia. "On inertia distribution, inter-area oscillations and location of electronically-interfaced resources." *IEEE Transactions on Power Systems* 33, no. 1 (2018): 995-1003
- [2] Yichen Zhang, Alexander Melin, Seddik Djouadi, and Mohammed Olama. "Performance guaranteed inertia emulation for diesel-wind system feed microgrid via model reference control." In *2017 IEEE Power & Energy Society Innovative Smart Grid Technologies Conference (ISGT)*, pp. 1-5. IEEE, 2017.
- [3] Yichen Zhang, Yichen, Alexander M. Melin, Seddik M. Djouadi, Mohammed M. Olama, and Kevin Tomsovic. "Provision for guaranteed inertial response in diesel-wind systems via model reference control." *IEEE Transactions on Power Systems* 33, no. 6 (2018): 6557-6568

Distinguishing Between Natural and Forced Oscillations in the Power Grid

Herschel Norwitz, *Student Member IEEE*

Department of Electrical, Computer, and Biomedical Engineering
 Union College
 Schenectady, NY, USA
 norwitzh@union.edu

Luke Dosiek, *Member IEEE*

Department of Electrical, Computer, and Biomedical Engineering
 Union College
 Schenectady, NY, USA
 dosiekl@union.edu

Abstract— Currently, power grids experience false alarms due to localized and isolated issues that produce a measurable oscillation. As electrical engineers, we care if those oscillation are natural or forced. We care because typically, when looking at the flow of power in the system, it should be relatively constant within some ambient operating parameters. When the grid starts to oscillate it serves as a warning that something could be very wrong and that the whole grid is at risk of going down. The objective of this research is to find a way to experimentally determine between natural and forced oscillations, thus decreasing false alarms.

Keywords—forced oscillations, mode meter, dynamometer, simulation, system identification

I. INTRODUCTION

What are natural and forced oscillations? A helpful way to understand them is through examples. First consider natural oscillations. One way to see this is when a tree falls down on a power line. When this happens, the modified grid may be less damped than the original, which can lead to low frequency oscillations [1]. Another way of putting it is that it sends a sort of shock to the system that then generates a transient response. If the system is healthy this shock appears as a bleep on the monitors. However, if the system is unhealthy it will appear to oscillate and grow until the circuit breakers open up and the power grid goes down.

On the other hand, forced oscillations can occur when a piece of equipment breaks, or some part of the hardware was not properly constructed. For example, consider a steam valve. If this component breaks, it can enter a limit cycle in which it bounces back and forth between fully on and fully off. When the frequency of this process approaches the power grid's natural frequencies, it results in a resonance that can be measured from further away on the grid itself. This often leads people to think the system is becoming unstable when it is not. The oscillations due to these issues are not a real threat to the grid in and of themselves; the real risk is that they are sending out false alarms that, over time, could result in laxness with protocol and seriousness. This could be catastrophic when a real problem occurs, and the grid is in real risk of going down.

Example simulated power grid frequency is shown in Fig. 1, in which power system forced oscillations begin at the 20s mark. If it is not known that that oscillation is from a bad controller, one could think it is evidence of an unstable system.

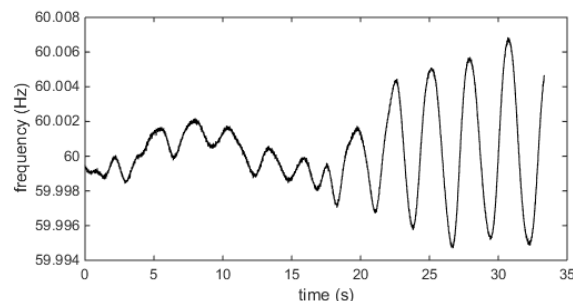


Fig 1: Example simulated frequency data. Forced Oscillation begins at 20s.

II. PROCEDURE

Currently, the detection of and the distinguishing between natural and forced oscillations has been achieved in simulations. For this research, we will use a dynamometer to generate real world oscillation data to validate the simulation results. Specifically, the dynamometer will be controlled so that it represents a cyclic load to the lab power distribution system, indeed cyclic loads are a known cause of forced oscillations [2]. The overall procedure is as follows:

1. Program the dynamometer to have a cyclic load that varies in magnitude and frequency. Frequencies will be chosen both near and far from the grid's natural frequencies.
2. Capture actual distribution-level (wall outlet) voltage from elsewhere in the lab building.
3. Analyze the captured voltages to detect oscillations and classify as forced.
4. Compare results with known oscillation parameters from the dynamometer, assess algorithm performance and, edit as necessary.

REFERENCES

- [1] Prasertwong, Komkrit & Nadarajah, Mithulananthan & Thakur, Devbratta. (2010). Understanding Low-Frequency Oscillation in Power Systems. International Journal of Electrical Engineering Education. 47. 10.7227/IJEE.47.3.2.
- [2] S. A. N. Sarmadi and V. Venkatasubramanian, "Inter-Area Resonance in Power Systems From Forced Oscillations," in IEEE Transactions on Power Systems, vol. 31, no. 1, pp. 378-386, Jan. 2016.

Visualization the Stability Boundary of Low-Order System to Determine the Transient Stability

Chen Qi, *student member, IEEE*

MOE Key Lab of Power Transmission and Power Conversion and Control
Shanghai Jiao Tong University, Shanghai, China 200240

Abstract—The conventional direct method of transient stability studies adopts the energy function to estimate the stability region. However, the accuracy of the energy function method is relatively low, which is reflected by its conservativeness. Theoretically, the transient stability boundary of a stable equilibrium point is the union of the stable manifolds of the unstable equilibrium points on the boundary, which provides a method to accurately depict the stability region. In this work, the transient stability regions of low-dimension dynamic systems (two-order and three-order) are visualized using this idea. The depicted stability regions are able to reveal some characteristics of the system transient stability. For higher-order system, it is hoped that there will be a method to decouple it into lower-order systems and thus, the transient stability may thus be precisely determined.

I. INTRODUCTION

According to the nonlinear dynamic system theory [1], one method to depict the stability boundary of a stable equilibrium point (SEP) \bar{x}_s in a system can be summarized as:

- 1) Obtain the unstable manifolds of the unstable equilibrium points (UEPs) and find the ones whose unstable manifold contains the trajectories which go to the \bar{x}_s .
- 2) Find the union of the stable manifolds of the UEPs discovered in the last step, which should form the stability boundary of the SEP \bar{x}_s .

With the help of numerical integration, this method is very suitable for the low-order system to visualize the accurate stability boundary, which will be shown in the following sections.

II. TWO-ORDER DROOP CONTROLLED INVERTER

Considering a droop controlled inverter is connected with the ideal grid, then the system dynamics can be expressed by the following two-order differential equations.

$$\begin{cases} \dot{\delta} = m(P_{set} - P_e) \\ \dot{E} = n(Q_{set} - Q_e) + K_e(E_r - E) \end{cases} \quad (1)$$

An energy function can be constructed according to the system dynamic model, which is omitted in this abstract. Fig. 1 respectively shows the stability boundary estimated by the energy function, and the stability boundary obtained as the stable manifolds of the surrounding UEPs. It can be seen that with the above mentioned method, the precise stability boundary is visualized, which is a better depiction than the stability boundary estimated by the energy function.

III. THREE-ORDER SYNCHRONOUS MACHINE

Conventionally, synchronous machines adopt the classical two-order model in transient stability analysis. When the voltage

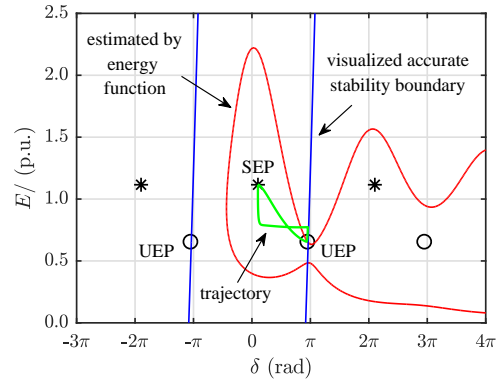


Figure 1. Stability boundary of the droop controlled inverter.

control is considered, a three-order model can be formed, as shown in (2).

$$\begin{cases} \dot{\delta} = \omega - \omega_0 \\ \dot{\omega} = \frac{1}{J} \left[\frac{P_{set}}{\omega} - \frac{P_e}{\omega} - D(\omega - \omega_0) \right] \\ \dot{E} = n(Q_{set} - Q_e) + K_e(E_r - E) \end{cases} \quad (2)$$

Similarly, the visualized stability boundary of the system is shown in Fig. 2. With this visualized stability boundary, the system stability can be easily determined by examining whether the trajectory goes out of the stability region. This provides a fast and accurate approach to judge the transient stability.

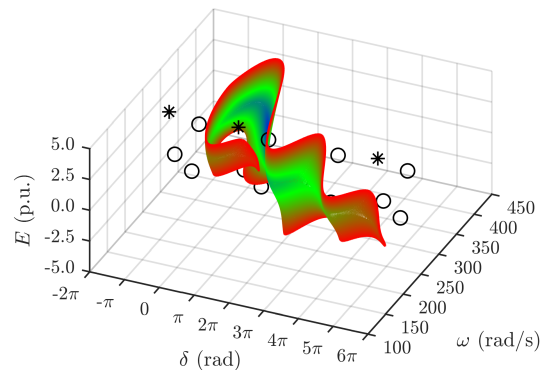


Figure 2. Stability boundary of the synchronous machine.

REFERENCES

- [1] H.-D. Chiang, *Direct methods for stability analysis of electric power systems: theoretical foundation, BCU methodologies, and applications*. John Wiley & Sons, 2011.

Online Monitoring & Mitigation of Delayed Voltage Recovery in Distribution Networks Using DERs and Controllable Loads

Amarsagar Reddy Ramapuram Matavalam, *Student Member, IEEE*, and Venkataramana Ajjarapu, *Fellow, IEEE*.

Abstract—This paper proposes an online method to monitor and mitigate fault induced delayed voltage recovery (FIDVR) phenomenon in distribution systems using μ PMU measurements in conjunction with a Reduced Distribution System Model (RDSM). The recovery time estimated from a dynamic analysis of the FIDVR is used to monitor its behavior and a linear optimization is formulated to control air conditioner loads and DER reactive power injection to mitigate the FIDVR severity. The RDSM is made up of several sub-models, each of which is analogous to the Composite Load Model (CLM) with selected parameters. The linear formulation in combination with the RDSM reduces the computation time, enabling online execution. Simulated μ PMU measurements from the IEEE 37 node distribution system connected to the IEEE 9 bus system under various fault scenarios are used to evaluate the proposed methodology. The resulting mitigation schemes are validated using combined transmission-distribution system simulations, thereby demonstrating that μ PMU measurements along with the RDSM enable FIDVR mitigation by optimal control of reactive power injection from DERs with minimal load disconnection.

Index Terms—Delayed Voltage Recovery, Reduced Order Models, Phasor Measurement Unit, Load and DER Control, Distribution Voltage Stability.

I. INTRODUCTION

IN today's ever evolving power grid, advanced monitoring and control schemes to mitigate abnormal grid behavior such as short term voltage instability are vital for the reliability. The phenomenon of short term voltage stability deals with the behavior of the power system in the first few seconds after a disturbance. A special case of interest is the Fault Induced Delayed Voltage Recovery (FIDVR) phenomenon which occurs in regions where the 1ϕ induction motor (IM) load portion is more than 30% [1]-[2]. FIDVR is a precursor to short term voltage instability since the generator excitation and the transmission lines are stressed due to motor stalling, thus increasing the risk of cascading. FIDVR is mainly observed in systems with a moderate proportion of 1ϕ IM loads, which are present mainly in air conditioner (A/C) loads. After a large disturbance (fault, etc.), these motors can stall and draw ~ 6 times their nominal current, leading to the depression of the system voltage for several seconds (>15 sec).

Two types of methodologies have been proposed in literature

to mitigate the FIDVR phenomenon – supply side methods (injection of dynamic VARs via SVC, etc.) and demand side methods (disconnection of loads using measurements, etc.). Utilities usually employ the supply side solution by determining the amount and location of the SVCs and STATCOMs during the offline planning phase [3][4]. These methods use contingency sets along with extensive time domain simulations to ensure that FIDVR is mitigated over a wide range of operating conditions. The widespread adoption of Phasor Measurement Units (PMUs) by utilities has led to the development of measurement based methods to estimate the severity of FIDVR in real-time and take appropriate control actions to prevent further voltage reduction [5][6][7].

Until recently, distribution systems (DS) have lacked high-quality real-time measurement data. There has been a compelling motivation for using advanced measurement data from accurate, high resolution devices in distribution networks [8]. High-precision micro phasor measurement units (μ PMUs), when tailored to the particular requirements of power distribution, can support a range of monitoring, diagnostic and control applications [8]. They can also enable a new approach for managing distribution systems, particularly in the presence of significant renewable penetration [9] and can reveal phenomenon that were not usually thought to occur in distribution systems. In fact, it was recently shown from μ PMU measurements that FIDVR occurred more frequently in distribution systems than transmission systems (TS) [10].

To mitigate FIDVR in distribution systems, [11][12][13] have proposed utilizing the reactive support from DER inverters based on voltage reduction at the inverter. However, as FIDVR phenomenon is driven by the load dynamics, targeted load control in regions with large motor stalling will lead to a faster recovery. This approach is adopted in this paper where we demonstrate that the μ PMU measurements provide sufficient visibility to identify and localize motor stalling in distribution systems. Furthermore, by analyzing the dynamics of FIDVR, we are able to estimate the recovery time from measurements to enable improved mitigation schemes by targeted control of A/C smart thermostats and DERs. These targeted schemes are shown to mitigate FIDVR with lesser load control than widespread disconnections throughout the system.

A. R. Ramapuram Matavalam, R. Venkatraman and V. Ajjarapu are with the Department of Electrical and Computer Engineering, Iowa State University, Ames, IA 50011 USA. (e-mail: amar@iastate.edu, rvenkat@iastate.edu & vajjarap@iastate.edu).

The authors were supported from National Science Foundation grants and Department of Energy grants and are grateful for their support.

Data-driven Identification and Prediction of Power System Dynamics Using Linear Operators

Pranav Sharma, Bowen Huang, Umesh Vaidya, Venkatramana Ajjarapu
 Department of Electrical and Computer Engineering, Iowa State University, Ames, Iowa, USA

Abstract—We propose linear operator theoretic framework involving Koopman operator for the data-driven identification of power system dynamics. We explicitly account for noise in the time series measurement data and propose robust approach for data-driven approximation of Koopman operator for the identification of nonlinear power system dynamics. The identified model is used for the prediction of state trajectories in the power system. The application of the framework is illustrated using an IEEE nine bus test system.

I. KEY CONCEPTS

A. Robust approximation of Koopman operator

We have a random dynamic system of form $x_{t+1} = T(x_t, \xi_t)$. For such a discrete dynamical system we can define Koopman linear operator, given any $h \in \mathcal{F}$, $\mathbb{U} : \mathcal{F} \rightarrow \mathcal{F}$ is defined by

$$[\mathbb{U}h](x) = \mathbf{E}_\xi[h(T(x, \xi))] = \int_W h(T(x, v))d\vartheta(v)$$

Consider snapshots of state variables subjected to various processes and measurement noises $X = [x_0, x_2, \dots, x_M]$. We define $\mathcal{D} = \{\psi_1, \psi_2, \dots, \psi_K\}$ as the observables on x_k . Define vector valued function $\Psi : X \rightarrow \mathbb{C}^K$ as

$$\Psi(x) := [\psi_1(x) \quad \psi_2(x) \quad \dots \quad \psi_K(x)] \quad (1)$$

Here, Ψ lift the system from state space to feature space. Any function $\phi, \hat{\phi} \in \mathcal{G}_{\mathcal{D}}$ can be written as

$$\phi = \sum_{k=1}^K a_k \psi_k = \Psi \mathbf{a}, \quad \hat{\phi} = \sum_{k=1}^K \hat{a}_k \psi_k = \Psi \hat{\mathbf{a}} \quad (2)$$

Here the objective is to minimize this residue for all possible pair of data points $\{x_m + \delta, x_{m+1}\}$. Using (2) we have:

$$\Psi(x_k + \delta x_k) \hat{\mathbf{a}} = \Psi(x_{k+1}) \mathbf{a} + r.$$

Our aim is to find \mathbf{K} , finite approximation of Koopman operator that maps \mathbf{a} to $\hat{\mathbf{a}}$, i.e., $\mathbf{K}\mathbf{a} = \hat{\mathbf{a}}$, and minimize the the residue term, r . The robust optimization can be written as a min – max convex optimization problem, as follow:

$$\min_{\mathbf{K}} \max_{\delta \mathbf{G} \in \Delta} \| (\mathbf{G} + \delta \mathbf{G}) \mathbf{K} - \mathbf{A} \|_F \quad (3)$$

where $\mathbf{K}, \mathbf{G}_\delta, \mathbf{A} \in \mathbb{C}^{K \times K}$ and $\delta \mathbf{G} \in \mathbb{R}^{K \times K}$ is the new perturbation term characterized by uncertainty set Δ which lies in the feature space of dictionary function.

B. Design of robust predictor in power system

Based on the robust optimization formulation (3), we have systematic way of tuning the regularization parameter. Here regularization term implies that the operator framework can fit into data driven predictor design. We first approximate the transfer operator using training data. Let \bar{x}_0 be the starting

point for trajectory prediction. The initial condition from state space is mapped to the feature space, i.e., $\bar{x}_0 \implies \Psi(\bar{x}_0)^\top =: \mathbf{z} \in \mathbb{R}^K$. Using Koopman operator system propagates as $\mathbf{z}_n = \mathbf{K}^n \mathbf{z}$. From this we can obtain the trajectory in state space, as $\bar{x}_n = C \mathbf{z}_n$. Here matrix C is obtained as the solution of the following least square problem:

$$\min_C \sum_{i=1}^M \| x_i - C \Psi(x_i) \|_2^2 \quad (4)$$

II. RESULTS

In order to understand the implications of developed robust prediction and identification algorithm for power system, we consider IEEE 9 bus test case.

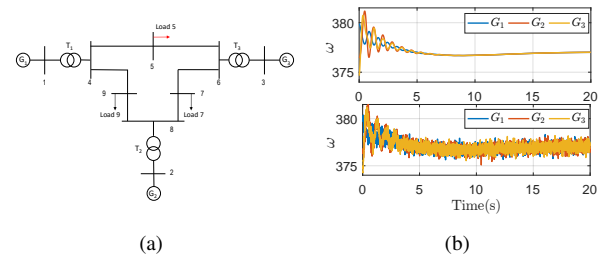


Fig. 1. (a) IEEE 9 bus system, (b) Post fault frequency measurement for purely deterministic measurement and measurement corrupted with ambient noise of 20 dB

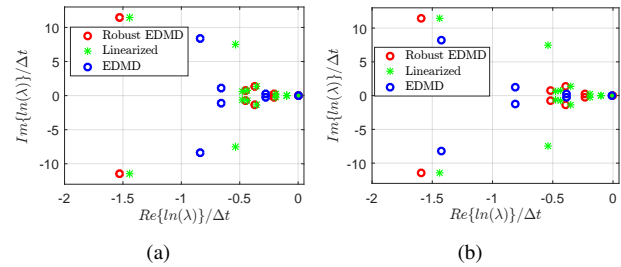


Fig. 2. System mode identification using Robust EDMD and EDMD (a) For ambient noise of SNR 20 dB (b) For ambient noise of SNR 17 dB

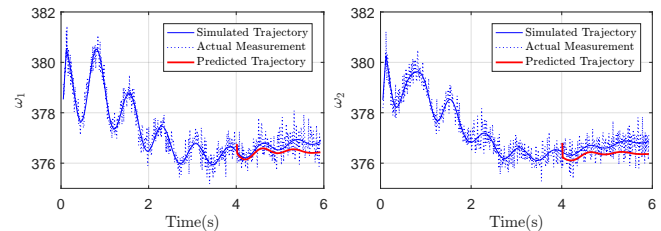


Fig. 3. Generator Angular Speed prediction for noisy measurement

Thermostatic Load Control for System Frequency Regulation Considering Progressive Recovery

Qingxin Shi, Fangxing Li
 University of Tennessee, Knoxville
 Dept. of Electrical Engineering and Computer Science
 Knoxville, TN, United States

Abstract—This project proposes a thermostatic load control (TLC) strategy for primary and secondary frequency regulation, in particular, using heating, ventilation and air-conditioning (HVAC) units and electric water heaters (EWHs). First, daily demand profile modeling indicates that these two loads are complementary in the daytime and can provide a relatively stable frequency reserve. Second, the progressive load recovery is specifically considered in the control scheme. The proposed control strategy can organize a large population of thermostatic loads for the provision of a frequency reserve. Consequently, the requirement of a spinning reserve is reduced.

Index Terms-- Thermostatic load control, frequency regulation, demand profile, load recovery, electric water heater, HVAC.

I. MODEL OF DAILY DEMAND PROFILES

The demand profiles of EWHs and HVACs are necessary input for the dynamic TLC strategy. Based on the one-order thermal transfer model, the combined demand profile of 25,000 EWHs and 25,000 HVACs is obtained, as is shown in Fig. 1. We can observe that the power of EWHs and HVACs are complementary during 7:00 - 20:00 and the loads can provide a continuously sufficient frequency reserve.

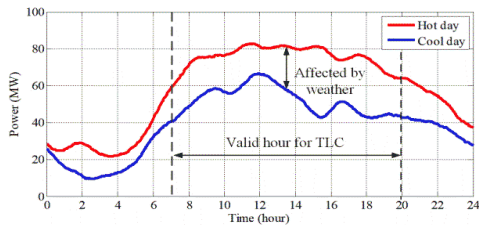


Fig. 1. EWH and HVAC load as frequency reserve on a hot and cool day.

II. SERIFICATION STUDY

In the proposed TLC strategy, EWHs participate in PFR and HVACs participate in SFR.

A. EWHs for Primary Frequency Regulation

TLC is designed to emulate the frequency droop control of turbine governors. At time instant t , the target load reduction $P_{PFR}(t)$ is computed by

$$P_{PFR}(t) = \begin{cases} 0, & \text{if } \Delta f(t) \geq \Delta f_{db} \\ -k_p \Delta f(t), & \text{if } \Delta f(t) < \Delta f_{db} \text{ and } 0 \leq t \leq t_{nadir} \\ -k_p \Delta f(t_{nadir}), & \text{if } t > t_{nadir} \end{cases} \quad (1)$$

B. HVACs for Secondary Frequency Regulation

Step 1: When the SFR is activated, each ON device is switched off with a specified probability p_{off} that is sent from the aggregator. Each ON device makes a switching-off decision according to the random number $r \sim U(0, 1)$. If $r \leq p_{off}$, the device is switched off; otherwise it remains on.

Step 2: After T_{SFR} , the activated devices are switched on. Their temperature settings are raised by $\Delta\theta_{a,s}$ for a duration of $(T_{A,off} - T_{SFR})$. Since $\theta_a(t)$ can be measured by the thermometer in the HVAC, $\Delta\theta_{a,s}$ is given by

$$\Delta\theta_{a,s} = \theta(t_{SFR0} + T_{SFR}) - \theta(t_{SFR0}) \quad (2)$$

Within a narrow deadband, $\theta_a(t)$ changes linearly with t . $T_{A,off}$ is estimated by

$$T_{A,off} = \left(\theta_{a,db} / \Delta\theta_{a,s} \right) \cdot T_{SFR} \quad (3)$$

III. SIMULATION STUDY

In order to verify the proposed method, the IEEE RTS 24-bus dynamic system is simulated in this study. The frequency response of a generator outage is shown in Fig. 2.

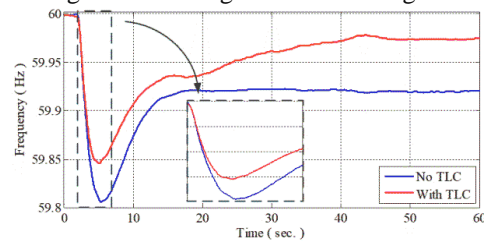


Fig. 2. Frequency & generation response of ASFR model.

Additionally, the wind/solar power decrease also challenges the system frequency. The response of this disturbance is shown in Fig. 3.

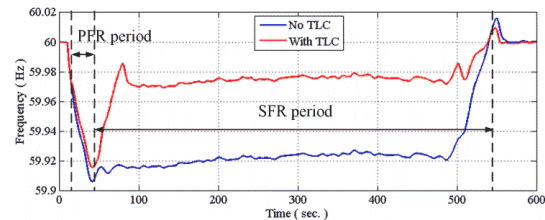


Fig. 3. Response of TLC under PV penetration.

In conclusion, the 25,000 EWHs and HVACs can increase the system frequency to the 59.96 Hz deadband by the proposed TLC strategy whether in peak hours or off-peak hours.

Feedforward-Based Accurate Power Sharing and Voltage Control for Multi-Terminal HVDC Grids

Armin Teymouri, Ali Mehrizi-Sani
 Washington State University
 Pullman, WA, USA
 armin.teymouri@wsu.edu,
 mehrizi@wsu.edu

Abstract—

This poster presents a power sharing and voltage control scheme for multi-terminal HVDC (MTDC) grids. A generalized hierarchical droop-based controller is designed to control the DC-side voltages and dispatched powers within a single control loop. To improve the steady state performance of the MTDC grid, a feedforward mechanism is proposed. This mechanism makes the current controller of the voltage-sourced converters (VSC) in the MTDC grid independent of the AC-side load conditions. The performance of the proposed scheme is evaluated under several case studies. A comparison between the proposed controller and traditional controllers is also made with time-domain simulations in PSCAD/EMTDC simulation software. Results show that the proposed scheme can successfully control the real powers and DC voltages while having a stable performance during AC-side load changes.

Keywords— Droop control, feedforward control, multi-terminal HVDC, real power sharing, voltage-sourced converter.
Introduction (Heading 1)

I. Introduction

Multi-terminal direct current (MTDC) systems are a potentially feasible solution, both economically and technically, for the integration of renewable energy sources and the connection of different AC grids with different frequencies. Voltage-sourced converters (VSC) and line-commutated converters (LCC) are two common power converters used in MTDC systems. Several advantages of VSC over LCC, such as independent and flexible real and reactive power control, black start capability, no commutation failure, and smaller footprint, have made the VSC-based MTDC a dominant solution. However, there are still challenges regarding DC voltage regulation and power flow control in the operation of VSC-MTDC systems.

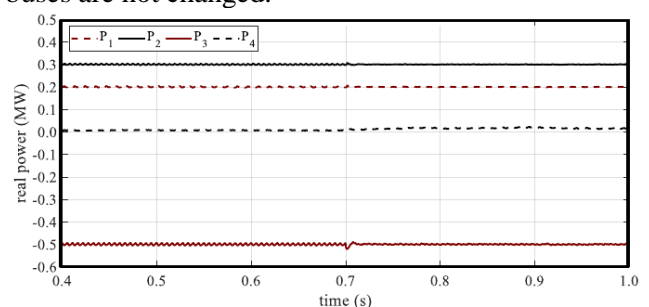
Different methods are proposed to control the voltage and power in MTDC systems. The most common method to control the DC-side voltages is the master-slave control. In this method, one converter is responsible for the voltage control while other converters control their power. However, this method has a low reliability since a single failure can corrupt the voltage regulation. This method also relies on fast communication of

the remotely measured signals to the master converter.

Voltage droop is an alternative to master-slave control. Voltage droop distributes the voltage regulation responsibility between several converters while the power is controlled by the remaining converters based on their droop coefficients. However, this method has some disadvantages such as the DC-side voltage imbalance, overloading in converters, and instability caused by load changes on the AC side. Although extensive research studies are performed on MTDC voltage control, none of them addresses the inaccuracies in the DC voltage regulation and power sharing caused by a load change on the AC-side terminal. To mitigate this shortcoming, this poster proposes an improved voltage regulation and accurate power sharing scheme that, unlike the available literature, can maintain the desired voltage and power values after a large load is added to the AC terminals of the MTDC converters. The proposed method is implemented using a generalized droop-based controller.

I. Sample Results

This part compares the real power tracking results of a 4-terminal system as a result of a sudden load change in an AC terminal. The poster compares this result with the result of a system that does not have the feedforward loop. It will be seen that the system without the feedforward cannot track the load change. At $t=0.7s$, a 1.5 MW load is added to terminal 4. It is seen that the real powers are not changed, as the set points of the buses are not changed.



Machine-Learning based Advanced Dynamic Security Assessment

Ramin Vakili, *Student Member, IEEE*, and Mojdeh Khorsand, *Member, IEEE*
 School of Electrical, Computer and Energy Engineering, Arizona State University, Tempe, AZ, USA
rvakili@asu.edu and mojdeh.khorsand@asu.edu

Online situational awareness plays a critical role in the resilient smart electric grid due to the increase in uncertain and unforeseen events, e.g., stochastic nature of renewable resources and distributed energy resources (DERs) and cyber-attack threats. Operation of modern electric grids near to their security limit can result in reduced stability margin, which makes them vulnerable to severe disturbances and can lead to static/dynamic instability and cascading outages and blackouts. Therefore, online monitoring of the static/dynamic stability of modern power systems is known to be one of the most important tasks to prevent blackouts [1].

Wide Area Measurements (WAMS) using synchronized phasor measurement units (PMUs) are being widely used in the WECC system to provide a wide range of application such as situational awareness for operational decision making. Eastern Interconnection Phasor Project (EIPP) provides new opportunities to deploy the measurements from PMUs in real-time analysis to evaluate system dynamic performance [2]. Using this online information provided by PMUs, online Dynamic Security Assessment (DSA) can provide operators with accurate security classification decisions following various possible contingencies. However, there are many hurdles associated with conventional DSA methods such as time-domain (T-D) simulation (consisting of solving a set of non-linear differential equations) and transient energy functions methods. The computational complexity of analyzing $N-k$ contingencies, dynamic change in transmission topology during contingency propagation in the system due to relay operation, and the massive size of power system make such methods too slow to satisfy the online DSA needs [3]. The advancements made in power system monitoring provide an overwhelming amount of data, which can be efficiently used for operational decision-making. Utilizing this data and its underlying patterns, machine learning (ML) algorithms has proven to be an effective tool for analysis of modern power systems stability.

This paper develops ML-based methods, which use the results of extensive offline simulations or historic data of different contingencies to train machine learning algorithms, in order to predict dynamic stability of the system following any type of contingencies. The output of these algorithms then can be used to trigger emergency control and remedial actions after the occurrence of severe contingencies if the trained method predicts an impending instability. This paper presents a comparison between different machine learning algorithms to be used in online DSA including Support-Vector Machines (SVM) with linear and gaussian kernels, decision tree, and random forest. Accuracy, training time, precision, recall, and F1 score of these methods are compared. Also, this paper analyses the impacts of using feature selection methods like Principal Component Analysis (PCA) in accuracy and training time of the learning methods. The number of principle component to be used, and the optimal values of SVM parameters, namely C and kernel scale, are achieved using both a grid search algorithm and heuristic methods; a comparison between these two methods is

provided in Table I. Figure 1 shows the accuracy achieved for various C and kernel scale using a grid search algorithm.

The proposed method is tested on the WECC 179-bus system considering different operation conditions and topologies. Different types of contingencies including three-phase, two-phase, and single-phase-to-ground line faults followed by removing transmission line(s) and/or generator outage(s) ($N-1$, $N-2$, and $N-3$) have been simulated using Transient Stability Assessment Tool (TSAT) software to provide a comprehensive data base for training the algorithms. A comprehensive comparison between the performances of different machine learning algorithms is provided in Table I.

Table I. Performance comparison of different machine learning algorithms

Method	Accuracy (%)	Training time(s)	F1 Score
SVM with linear kernels	94.17	3	0.96
SVM with Gaussian Kernels (heuristic kernel scale)	93.33	0.23	0.95
SVM with Gaussian Kernels (grid search for kernel scale)	97.5	0.2	0.97
SVM with Gaussian Kernels (3 features used)	97.5	3.48	0.96
Decision Tree	95.83	0.15	0.97
Decision Tree with PCA (three features)	93.33	0.19	0.94
Random forest	98.33	2.98	0.99

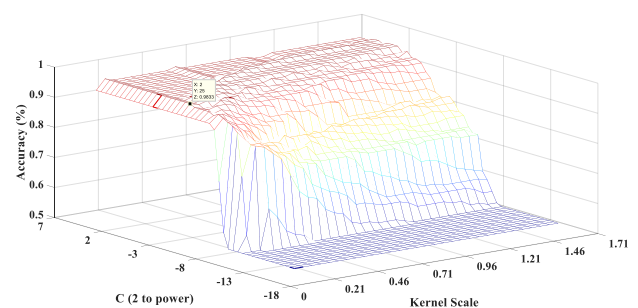


Fig. 1. Accuracy of the proposed SVM with Gaussian kernels with changes in C and Kernel scale parameters

REFERENCES

- [1] Y. Xu, Z. Y. Dong, K. Meng, R. Zhang and K. P. Wong, "Real-time transient stability assessment model using extreme learning machine," in *IET Generation, Transmission & Distribution*, vol. 5, no. 3, pp. 314-322, Mar. 2011.
- [2] Kai Sun, S. Likhate, V. Vittal, S. Kolluri and S. Mandal, "An online dynamic security assessment scheme using phasor measurements and decision trees," *IEEE Power and Energy Society General Meeting - Conversion and Delivery of Electrical Energy in the 21st Century*, Pittsburgh, PA, 2008.
- [3] M. He, J. Zhang and V. Vittal, "Robust online dynamic security assessment using adaptive ensemble Decision-Tree learning," *IEEE Transactions on Power Systems*, vol. 28, no. 4, pp. 4089-4098, Nov. 2013.

Impact of High Penetration of Renewable Resources on Power System Transient Stability

Wenting Yi, David J. Hill and Yue Song
 Department of Electrical and Electronic Engineering
 The University of Hong Kong, Hong Kong, China
 Email: wtyi, dhill, yuesong@eee.hku.hk

Abstract—Environmental concerns and technology development are driving power systems to a new stage where the increased penetration of renewable energy resources (RES) is replacing the conventional fossil fuel-based power plants. This transition brings the sustainable and ecological credentials but at the same time involves the major challenge of low-inertia systems, unfamiliar dynamics of electronics-interfaced generations as well as their regulation and interaction with the rest of the system. In this paper, by virtue of graph theory, cutset properties are explored and applied to transient stability analysis in high RES penetrated power systems. First, the relationship of transient stability and the critical cutsets are studied and explained theoretically. Second, two indexes, i.e., Cutset index (CI) and Improved cutset index (ICI), are investigated and compared for identifying the vulnerable cutset as well as estimating the critical energy for determining stability region. Different RES penetration levels are explored from 0 to 100% with different network size, topology and dynamics. Numerical studies are conducted on large-scale IEEE test systems as well as nine open-source synthetic transmission systems. Simulation results show that the increased penetration of RES can affect system stability and the specific influence depends on the penetration levels, system structures and the RES replacement.

I. INTRODUCTION

With emerging requirements for renewable portfolio standards, limits on greenhouse gases, and energy conservation measures, environmental issues and sustainable concerns have inspired higher penetration of renewable resources (RES) in power systems. Higher penetration of RES possess the advantages of more environmental friendly and ecological sustainably. Yet, these intermittent renewable resources pose challenges to power systems in terms of system planning, modelling, operating and dynamic performance especially consider the low-inertia characteristics of inverters. The questions that remain to be answered relate to what extent can RES penetrate into systems before there is a stability problem. It's reasonable to study them scientifically as related at least to system structure and stability type. In this paper, we study the impact of RES and network structure on transient stability.

II. KEY EQUATIONS AND CONCEPTS

The overall system dynamics can be described by

$$M_i \ddot{\theta}_i + D_i \dot{\theta}_i + \sum_{j \in N_i}^n B_{ij} \sin(\theta_i - \theta_j) = P_i. \quad (1)$$

This model also has applicability when RES penetration is taken into consideration. In summary:

- For the synchronous generators, $M_i > 0$ denotes the inertia constants, $D_i > 0$ denotes the steam and mechanical damping, and P_i is the active power generation at bus i ;
- For the inverter-based generators, $M_i = 0$ because there is no inherent inertia, $D_i > 0$ denotes the frequency coefficient, and P_i is the inverter-based power generation;
- For the loads, similar to the inverters, $M_i = 0$, $D_i = -P_{Li} > 0$ denotes the frequency coefficient, and $P_i = -P_{Li}$ denotes the power consumption at bus i .

III. KEY RESULTS

Our analysis has been applied to both the standard IEEE test systems as well as nine newly developed synthetic grids.

A. IEEE test systems

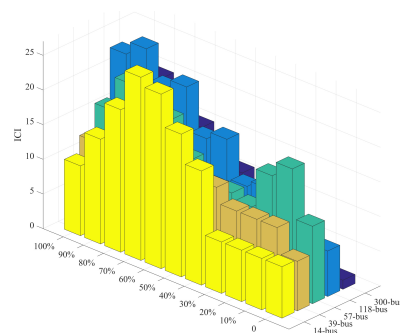


Fig. 1. The system ICI when RES penetration increases from 0 to 100%

B. Synthetic networks

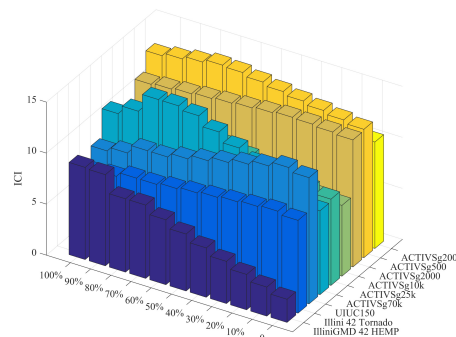


Fig. 2. The system ICI when RES penetration increases from 0 to 100%

Preventive Transient Stability Control of Power Systems with High Level Wind Power

Heling Yuan, Yan Xu

School of Electrical and Electronic Engineering
Nanyang Technological University
Singapore
HELING001@e.ntu.edu.sg
XUYAN@ntu.edu.sg

Abstract—High level wind power penetration has significantly affected the dynamic behavior of power systems. Due to its uncertainty and intermittency, conventional generators need to compensate wind power variation constantly. Based on trajectory sensitivity and Extended Equal Area Criterion (EEAC) method, this paper proposes a new approach to optimize power dispatch with wind power variation while maintaining the transient stability of the system. With the least power rescheduling, the system can be transient stable even though wind power output changes significantly. The proposed method is validated on the New-England 10-machine 39-bus system by using commercial simulation software TSAT. The results show good performance on the robustness, effectiveness and computational efficiency of the approach.

Index Terms—Transient stability control, Wind power, Trajectory sensitivity, Stability margin, EEAC.

I. INTRODUCTION

Modern power system has been dramatically penetrated by renewables due to its environmental and financial benefits. In this paper, a computationally efficient method is proposed for generation rescheduling to balance wind power variation as well as ensure transient stability. The objective is to use least generation redispach to stabilize the system while compensating wind power variation. Critical machines and non-critical machines wind power balancing strategy is applied since it is the most sensitive to transient stability according to [9]. Based on EEAC method, stability margin could be calculated. By applying trajectory sensitivity, critical machines and non-critical machines could be recognized. Then, transient stability control is formed by bounding stability margin larger than zero, which is a linear programming problem.

The proposed method is validated on the New England 10-machine 39-bus system by using commercial and industrial grade simulation software.

II. KEY EQUATIONS AND COMPUTATION PROCESS

$$\min - \sum_{i \in S^-} \Delta P_{G_i} \quad (1)$$

$$\text{s.t. } \Delta P_{G_i} \geq 0, \quad i \in S^+ \quad (2)$$

$$\Delta P_{G_j} \leq 0, \quad j \in S^- \quad (3)$$

$$\sum_k \Delta P_{G_k} + \Delta P_w = 0, \quad \forall k \in \{S^- \cup S^+\} \quad (4)$$

$$\sum_k \Phi_k(\eta, P_{Gk}) \Delta P_{Gk} + \eta_0 \geq 0 \quad (5)$$

$$P_{Gk}^{\min} \leq P_{Gk}^0 + \Delta P_{Gk} \leq P_{Gk}^{\max} \quad (6)$$

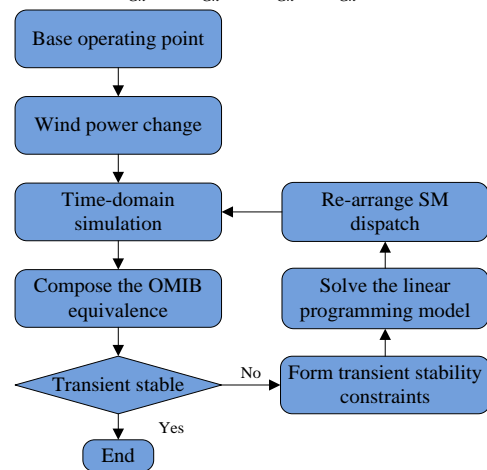


Fig.1. Computation flowchart of the proposed approach

III. KEY RESULTS

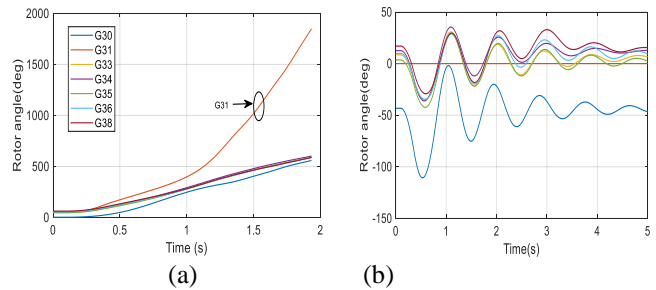


Fig.3. Rotor angle trajectories for C1: (a) unstable (before optimization); (b) stable (after optimization)

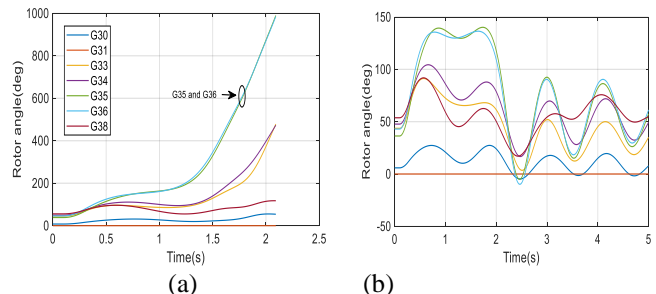


Fig.4. Rotor angle trajectories for C2: (a) unstable (before optimization); (b) stable (after optimization)

Dynamic Multi-swarm PSO based Tuning of Power System Stabilizer in 12 Bus Power systems

^{1,2}Lili Wu, *Student Member, IEEE*, ^{1,3}Ganesh K. Venayagamoorthy, *Senior Member, IEEE*,

⁴Ronald G. Harley*, ²Jinfeng Gao

¹Real-Time Power and Intelligent Systems Laboratory,

Holcombe Department of Electrical and Computer Engineering, Clemson University, Clemson, SC 29634, USA

²School of Electrical Engineering, Zhengzhou University, Zhengzhou, China.

³Eskom Centre of Excellence in HVDC Engineering, University of KwaZulu-Natal, Durban, South Africa

⁴School of Electrical and Computer Engineering, Georgia Institute of Technology, Atlanta, USA

lwu2@g.clemson.edu, gkumar@ieee.org, rharley@ece.gatech.edu and jfgao@zzu.edu.cn

Abstract—This paper demonstrates the tuning of power systems stabilizers for a 12-bus power system, operating at different line contingency conditions. A speed-frequency based lead-lag power system stabilizer (PSS) is used in this work. The problem of selecting the stabilizer parameters is converted to a simple optimization problem with generators speed deviation based objective function, which is solved by a dynamic multi-swarm particle swarm optimization (DMPSO) algorithm. The objective function allows the selected stabilizer parameters to have minimum generator speed deviation. The effectiveness of the stabilizers tuned using the suggested technique, in enhancing the stability of power systems under contingencies.

Index Terms--Power system stability, PSO, PSS tuning, speed deviation, line contingency

I. INTRODUCTION

The power system is experiencing great change, at the same time, facing more challenges. The introduction of controls and special protection systems raises the possibility of misoperation of protections and cascading failures. Moreover, because of economic benefits and the transmission expansion, the power systems have been forced to operate close to the stability limit. In recent years, with the development of artificial intelligence (AI), several approaches based on AI have been applied to the power system stability and security problem [1]. The PSO algorithms has attracted the attention of researchers in the field of AI since its application. It is clearly seen that PSO algorithm is a powerful tool for optimization problem solving in power system stability.

Power system stabilizer helps to improve the damping characteristics of a synchronous generator under disturbance as well as foreseeable contingencies. The tuning of power systems stabilizers using DMPSO for a 12-bus power system is proposed in this study. DMPSO is a kind of local versions of PSO with small size dynamic sub-swarms [2]. This DMPSO with local search performs well when solving large scale global optimization problem.

II. DMPSO BASED PSSs PARAMETER TUNING

In this study, a 12-bus power system is used to illustrate the design of the PSSs using DMPSO. The test power system in Fig.1 includes 4 generators, 6 transformers and 12 buses.

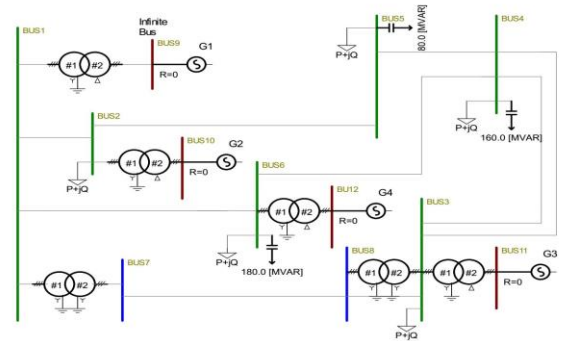


Figure1. 12-bus test power system

A speed-frequency based lead-lag PSS is used in this work. The optimization fitness function is defined as generators speed deviation in this study, which is shown in the formula:

$$J = \sum_{G_n=1}^m \sum_{t=t_0}^{t_2/\Delta t} (\Delta\omega_{G_n}(t) \times A \times (t - t_0) \times \Delta t)^2 \quad (1)$$

where $m=4$ here, G_n is the generator number, $\Delta\omega_{G_n}$ is the speed deviation of generator G_n . t_0 and t_2 are the simulation time, A is the weighting factor, Δt is the speed signal sampling period.

REFERENCES

- [1] Lili Wu, et al. "On Artificial Intelligence Approaches for Contingency Analysis in Power System Security Assessment." 2018 IEEE Power & Energy Society General Meeting (PESGM). IEEE, 2018.
- [2] Liang J J, Sugathan P N. "Dynamic multi-swarm particle swarm optimizer with local search", *Evolutionary Computation*, In *Proc. The 2005 IEEE Congress on. Ieee*, vol 1, pp. 22-528.

A Performance Comparison of Parallel Power Load Flow Implementations

Afshin Ahmadi, *Student Member, IEEE*

Melissa C. Smith, *Senior Member, IEEE*, E. Randolph Collins, *Senior Member, IEEE*

Holcombe Department of Electrical and Computer Engineering

Clemson University, South Carolina 29631

{aahmadi, smithmc, collins}@clemson.edu

Abstract— Power system planning and control has become a challenging issue in presence of renewable energy due to the intermittent nature of these resources. Many utilities across the world have installed Phasor Measurement Units (PMUs) to allow real-time monitoring of the power grid status, and as a result, quicker response to external disturbance. However, existing computer applications are unable to handle high velocity and volume of these data and deal with troubling events. Parallel processing is a key solution to address these challenges. In this study, we have developed two parallel versions of Newton-Raphson (N-R) power flow based on Open Multi-Processing (OpenMP) and Intel Math Kernel Library (Intel MKL). Experimental results were obtained by testing these implementations on several real-world and synthetic power system test cases. Results show that parallel processing can significantly reduce the execution time of N-R algorithm.

Keywords—Power Flow Analysis; Parallel Programming; Performance Comparison; Newton-Raphson Method;

I. INTRODUCTION

Parallel computing can be achieved by either utilizing a single machine with multiple CPU cores or using multiple machines and distributing the workload among them. The former is called shared-memory parallel computing model and the latter is named distributed parallel computing model. This study makes use of OpenMP technique to develop a parallel version of the N-R algorithm on shared-memory computers. On the other hand, Intel MKL features highly optimized, threaded, and vectorized math function, which we used in another parallel implementation to perform a comparison with the simple OpenMP version.

II. KEY ALGORITHMS

The following algorithm shows the general steps of N-R in solving the power flow problem.

Algorithm 1. N-R Power Flow Code

1	Form admittance matrix	Simple/Nested
2	Initialize V and evaluate $F(X_0)$	Multiple Funcs.
4	While ($iter \leq iter_{max}$) and ($tol \geq \epsilon$) {	
5	Calculate partial derivatives of power injection	
6	Create Jacobian matrix (J)	Nested loop
7	LU factorization to Solve the Linear System	Nested loop
8	Update voltage magnitudes and angles	Nested loop
9	Build power mismatch vector and find its norm	For loop
10	Iter++	Nested loop
11	}	For loop
13	Return	

III. OPENMP IMPLEMENTATION

Fig. 1 briefly summarizes the OpenMP directives usage for both task and loop - level parallelization. Any OpenMP directive starts with #pragma omp.

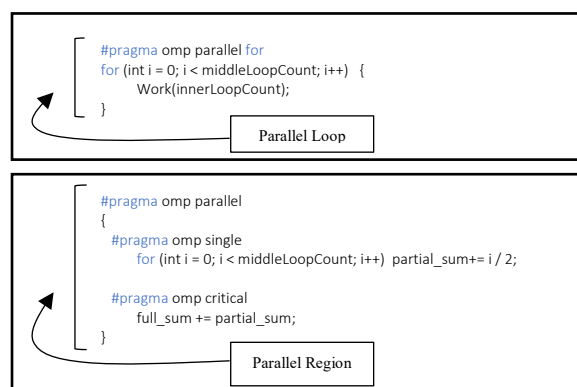


Fig. 1: OpenMP Parallelization

IV. KEY RESULTS

Fig. 2 shows the speedup of the two aforementioned parallel implementations for several power system cases. The running time of the sequential version was selected as the reference to calculate the speedup.

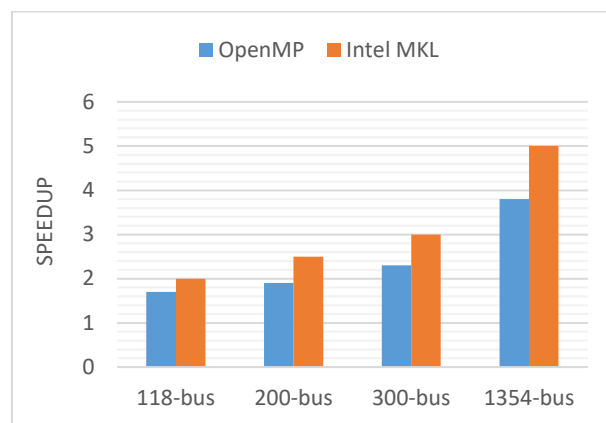


Fig. 2: Speedup by utilizing 4-Cores

Human-Centered Electricity Services for the Future Distribution Grid

Athindra Venkatraman, *Student Member, IEEE*, Le Xie, *Senior Member, IEEE*

Abstract—Technological advancements on the distribution grid, and reduced costs of grid-edge infrastructure have resulted in a push for increased penetration of such devices at the end-user level. These innovations at the grid edge threaten utility revenues, since the existing utility business model treats electricity as a commodity, and are based on volumetric throughput of power. With the inevitable penetration of grid-edge technologies causing increased capital and maintenance costs for utilities over and above the loss of revenue due to reduced throughput, it is clear that a new business model is required. The objective of this paper is to propose the idea of electricity as a service. This is done by formulating a rate design mechanism that evaluates the ‘impact’ of each end-user based on their power consumption patterns, and assign a fixed cost (a grid access fee) for each end-user to compensate the utility company for using its grid infrastructure.

I. INTRODUCTION

The rise of demand-side power generation through rooftop solar PV and other DERs implies that large-scale investments in bulk power generation units and transmission infrastructure will be significantly lower than in the past few decades. The amount of energy transacted at the end-user level is increasing, yet the total amount of transmission-level bulk energy transactions may be decreasing. [1].

The innovation of control, communication and computing capabilities that come with many of the grid edge devices can be used favorably by the utility company to maintain the performance of electricity services. The business question lies in how to properly incentivize the decentralization of technology solutions for a conventional grid. (Fig. 1)

II. WHY A NEW UTILITY BUSINESS MODEL?

In preparation for a decentralized, ‘grid-edge’ future, utilities need to embrace this change and recalibrate their business practices to not only survive the paradigm shift, but to thrive in the new system and be instrumental in helping it attain its maximum potential. A shift away from the volumetric approach of charging a \$/kWh volumetric throughput of power is thus required - the utility revenue must be decoupled [2] from the throughput incentive, otherwise it will be in the utility’s interests to maximize power flow through its lines.

III. NEW UTILITY RATE DESIGN - GRID ACCESS FEE

We consider the case of a deregulated market with retail electric choice, where the Transmission Delivery Utility (TDU) must be compensated for the usage of its grid infrastructure, and the Retail Energy Provider (REP) for the volumetric consumption of the consumer. A fixed grid-access fee is introduced, completely replacing the traditional “small

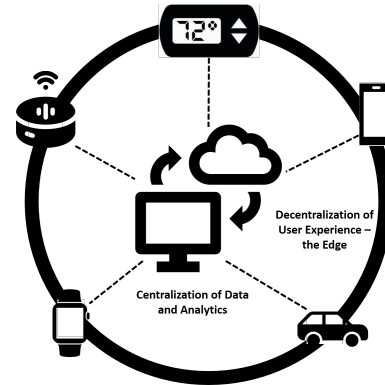


Fig. 1. User Experiences more distributed and towards the ‘Edge’ (DERs, Smart Devices); Centralization of Analytics (Cloud Services, Data centers)

fixed + large volumetric” structure of utility pricing. This grid-access fee is customer-specific, and evaluates each end-user’s ‘impact’ on the grid. This ‘impact’ is measured by considering the consumer’s *variability* and *magnitude* of consumption.

A comparison of the existing and new rate design mechanisms is depicted in Figure 2.

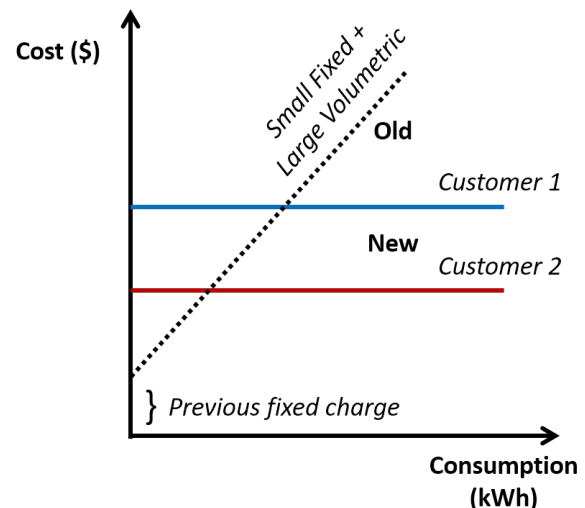


Fig. 2. Old vs New Cost Curve for Utility Revenue - The end-user compensates the utility for using its grid infrastructure

REFERENCES

- [1] EIA - *Annual Energy Outlook*, 2019, <https://www.eia.gov/outlooks/aeo/>.
- [2] L. Wood, R. Hemphill, J. Howat, R. Cavanagh, S. Borenstein, J. Deason, and L. C. Schwartz, “Recovery of utility fixed costs: Utility, consumer, environmental and economist perspectives,” *Tech. Rep.*, 06/2016 2016.

A Coupled Modeling Approach for Microgrid Reliability Assessment and System Sizing

Ahmed Abdelsamad, *Student member*, David Lubkeman, *Fellow, IEEE*
North Carolina State University

Abstract—For continuous power-serving applications, a microgrid is designed to maintain supplying load for a certain proportion of the year at the lowest cost of investment through minimum component sizes. Previously, reliability assessment is either accounted for by scheduling and applying faults or by designing an oversized system to aim for a 100% reliability. In this work, the economical aspect is assessed while maintaining the energy security targets and assessing stochastic system failures. A new MG optimal sizing methodology based on Particle Swarm Optimization (PSO) is proposed. A system reliability target constraint is considered and estimated using sequential modeling based on Monte Carlo Simulation (MCS). Model is applied to a commercial case study supplied by a PV system, lead-acid batteries and a diesel generator.

I. METHODOLOGY FRAMEWORK

In this work, a MG cost minimization objective function is solved using PSO. The optimization work is coupled to a sequential-based reliability assessment model as shown in Fig. 1. The cost function considers the investment costs of MG components and the cost of unreliability. A target of maximum Loss of Energy Expectation (LOEE) index is implemented as the reliability constraint in the problem.

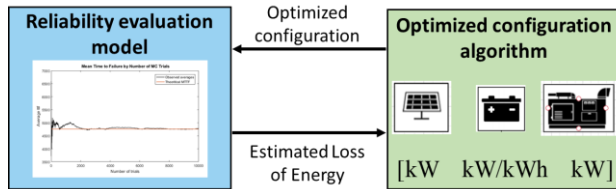


Figure 1 - Modeling framework

A. Reliability assessment

Reliability evaluation is executed using sequential modeling. Sequential MC is a very powerful technique to effectively estimate the reliability of a complex power system. Reliability assessment model input is the MG configurations suggested by the sizing model. The model runs the assessment for the number of Monte Carlo trials required to achieve stable results and converges. In this study, the loss of energy (LOE) is calculated on a yearly basis at each simulation trial. As in Eq. 1, the Energy not Served (ENS) is incremented for each year and stored as the LOE of the simulation year. The expected value of the loss of energy is then calculated

$$LOE = \left[\sum_{i=1}^{8760} ENS(i) \right]_N \quad (kWh) \quad (1)$$

$$LOEE = \frac{1}{NS} \sum_{j=1}^{NS} LOE(j) \quad (kWh / y) \quad (2)$$

B. Optimization problem statement

In this work, the optimization variables are the sizes of MG components and the LOEE as expressed in Eq. 3. The methodology is based on finding the best sizes of components that minimize the initial capital and maintain a cap on the yearly cost of not serving simultaneously. The heuristic approach, particle swarm optimization (PSO), suggests a population of configurations (particles). This process initially starts with a

random population, then through several iterations and runs the population gets updated by approaching the optimal solution. Constraints are aimed to satisfy the load to the highest level possible while maintaining a specific reliability target.

$$\text{Minimize } f(\text{Cost of investment} + \text{Cost of unreliability}) \quad (3)$$

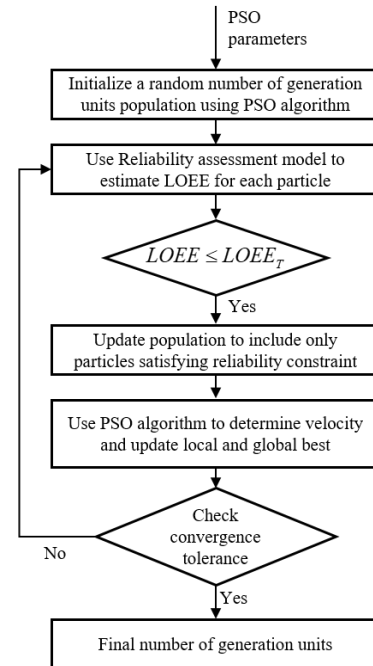


Figure 2 - PSO optimization algorithm

II. KEY RESULTS

The proposed framework is tested with a commercial application. Results in Table 1 show that the model suggests increasing PV system size to utilize the storage system. If cost of not serving is high enough, upgrading the existing capacities is economically viable. Fig. 3 represents experimentation on battery sizing and backup fuel-based units. Results assert that battery upgrading will improve reliability until reaching the optimal size for the system. On the other hand, system can be 100% reliable by adding an additional backup diesel generator.

Table 1 – Optimal renewable capacities for different reliability targets

LOEE target (kWh/y)	Generation units			Total capacity (kW)	LOEE (kWh/y)	Cost function (\$)
	PV 30kW	ESS 192kWh	DG 36kW			
-	1	1	1	84	4104	449,880
2000	2	1	1	26	1804	375,880
1000	3	1	1	144	400	364,600
200	3	2	1	162	81	378,270

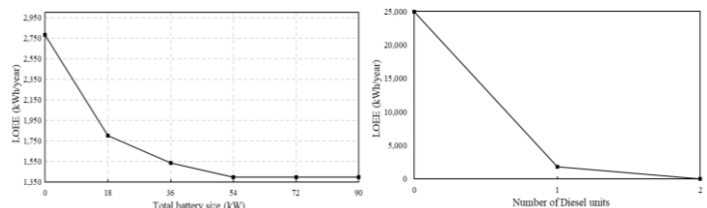


Figure 3 – Impact of upsizing ESS and adding a backup DG on LOEE

Data-Driven Risk Assessment of Wind-Integrated Power Systems via Finite Mixture Models and Importance Sampling

Osama Aslam Ansari, *Student Member, IEEE*, and C. Y. Chung, *Fellow, IEEE*
Department of Electrical and Computer Engineering, University of Saskatchewan, Canada

Abstract— In this work, a novel framework for operational risk assessment of wind-integrated composite power systems is presented. The short-term uncertainty of wind generation is modeled via finite mixture models (MMs). The proposed data-driven wind generation model is integrated into a cross-entropy (CE)-based importance sampling (IS) Monte-Carlo simulation (MCS) technique to evaluate operational risk indices at HL-II. The results verify the superiority of the proposed framework both in terms of accuracy and computational performance.

Index Terms— Cross entropy, importance sampling, operational risk, Monte-Carlo simulation, uncertainty modeling

I. KEY IDEA

THE increasing penetration of highly stochastic wind generation in modern power systems could significantly endanger the operational reliability and security of power systems. This necessitates the development of computationally-efficient simulation tools that can evaluate the operational risk indices of wind-integrated power systems. The existing approaches have two significant drawbacks [1]. First, these techniques model wind speed instead of wind generation and thus incorporate the inaccuracies of wind power curve. Second, parametric and unimodal probability distribution functions (PDFs) are adopted which cannot model the complex statistical features of wind speed or wind generation. To this end, this work proposes the use of finite mixture models (MMs) to model the short-term uncertainty of wind generation. This data-driven uncertainty model is then included in a cross-entropy (CE)-based importance sampling (IS) Monte-Carlo simulation technique to evaluate the short-term risk indices [1].

II. MODEL

Using the MMs, the conditional PDF for wind generation in a particular hour ($f_w(g^w|g_0^w)$) is estimated as

$$f_w(g^w|g_0^w) = \sum_{k=1}^{K(g_0^w)} \pi_k(g_0^w) \Psi_k(g^w|\theta_k(g_0^w)) \quad (1)$$

where g^w is the wind generation in a particular hour, g_0^w is the wind generation in the hour prior to give a n hour. π_k and Ψ_k are the k th mixing proportion and mixture PDF, respectively. K is the number of mixtures and θ_k is the parameter for k th mixture. Note that the MM parameters (π_k , θ_k , and K) are conditioned on wind generation in previous hour to capture temporal correlation. By capturing the multimodality of wind generation's PDF, the MMs accurately model the uncertainties of wind generation in the operational domain.

III. KEY RESULTS AND KEY CONCLUSIONS

The case studies are performed on a modified 24-bus IEEE reliability test system (RTS). The penetration of wind

generation is set to 23.5%. Real wind generation data from a wind farm in Swift Current, Saskatchewan, Canada is employed. Fig. 1 pictorially depicts the superiority of the proposed MMs-based modeling of wind generation. On comparing Fig. 1(a) and Fig. 1(c), it can be observed that the proposed approach correctly captures the statistical features of wind generation.

Table I shows the operational risk indices evaluated for different values of initial wind generation. Consider the results for the interval [0.4, 0.6). The risk obtained from the proposed method is lower than that of unimodal PDF. This is because the unimodal PDF is unable to capture a second mode of high wind generation state (see, Fig. 1(b) and Fig. 1(c)). This high wind generation state contributes to lower risk index.

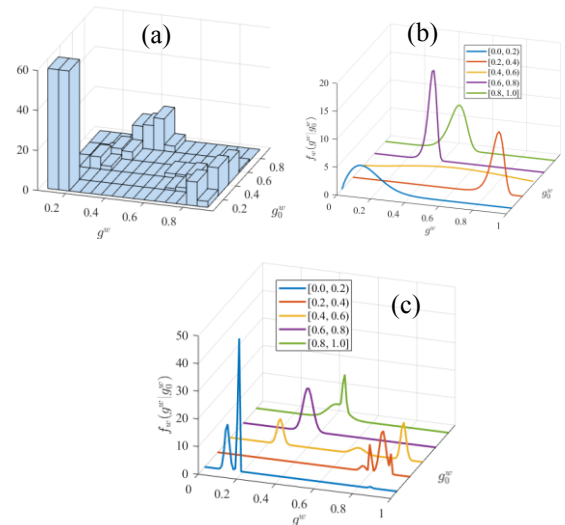


Fig. 1 (a) The histogram of wind generation in two hours, (b) a unimodal PDF fitted to the histogram, (c) proposed MM fitted to the histogram.

TABLE I
OPERATIONAL RISK INDICES FOR DIFFERENT APPROACHES

Initial Wind Generation	Proposed Method	Unimodal PDF
[0.0, 0.2)	1.0573 E-5	1.4194 E-5
[0.2, 0.4)	8.4011 E-7	8.1962 E-7
[0.4, 0.6)	8.3473 E-7	1.0939 E-6
[0.6, 0.8)	1.5907 E-6	1.7563 E-6
[0.8, 1.0)	3.4178 E-8	4.5665 E-7

REFERENCES

- [1] O. A. Ansari, and C. Y. Chung, "A hybrid framework for short-term risk assessment of wind-integrated power systems," *IEEE Trans. Power Syst.*, 2019 (Early Access).

Design of a 4 Dimensional Battery Model (4DM) for Improved Remaining Useful Life Assessment of Energy Storage Devices

Bharat Balagopal, Cong Sheng Huang, Mo-Yuen Chow
 Department of Electrical & Computer Engineering
 North Carolina State University, Raleigh, NC, USA
 emailEmail:{bbalago, chuang15, chow}@ncsu.edu

Abstract—The Remaining Useful Life (RUL) of an energy storage device provides insights into the duration of usability of the device before it needs to be replaced. While most commercially available technology are able to identify the RUL using statistical methods, few are able to provide the user information regarding the reason behind the decrease in the RUL. Providing this insight to the user will enable them to utilize their energy storage devices more appropriately and thereby obtain a greater return on their investment.

Index Terms—Remaining Useful Life (RUL), energy storage, battery, modelling

I. INTRODUCTION

The usage of energy storage devices has been rapidly increasing over the past decade. This increase in usage can be attributed to the development of better technology that has higher energy and power density with smaller sizes. However, with the improvement in technology, there are also complications that arise in terms of identifying the operating status of these devices and their maintenance schedules. Energy storage vendors provide battery management systems with their batteries, but there is a significant gap between the information that these battery management systems provide vs. the requirement of the end user, especially in large scale energy storage devices. Most battery management systems (BMSs) provide users with the State of Charge (SOC) and some provide information regarding the State of Health (SOH). While these information are important to the end user, they are more interested in understanding how to use their batteries so that they can get the highest return on their investment while not compromising on the application that they are using the batteries for. This information is often missing from the BMSs provided by vendors. The RUL is highly dependent on a number of factors the most important of those factors is the utilization pattern. Since different utilization patterns impact the degradation of the battery differently, a 4 Dimensional First Principle Based Degradation Model (4DM), 3D with time, was developed to study the impact different operating conditions have on the degradation of the battery and its components. This model would provide key insights to better utilization and when tied with the Equivalent Circuit Model (ECM), can provide real-time information on appropriate battery utilization for improved RUL.

II. KEY FIGURES

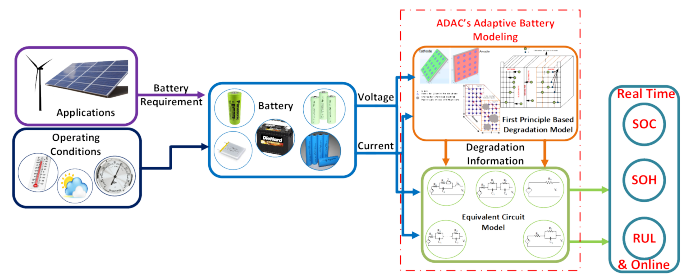


Fig. 1. Real-time, online and accurate RUL Assessment using a comprehensive 4D model and the ECM

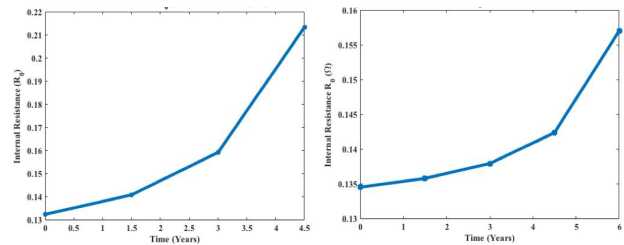


Fig. 2. R_0 for concentration and conductivity degradation

III. CONCLUSION

Using the information from the 4DM it is possible to determine the impact different operating conditions have on battery component degradation and these phenomena can be translated into the change in parameter values in the ECM. For example, II shows the change in the R_0 of the ECM for concentration and conductivity degradation due to calendar aging. It can be seen that the change in R_0 for concentration degradation is four times higher than for conductivity degradation. This information could be used as an example to gauge the kind of degradation a particular operating condition has on the performance and RUL of the battery and thus provide meaningful feedback to the user on appropriate utilization of the battery to prolong the RUL.

Replacement of Synchronous Generator by Virtual Synchronous Generator in the Conventional Power System

Junru Chen, *IEEE Student Member*, Muyang Liu, *IEEE Student Member*, Terence O'Donnell, *IEEE Member*

Abstract--Virtual synchronous generator (VSG) has been proposed to mimic the synchronous generator in terms of voltage establishment and provision of virtual inertia from electric energy storage. It thus facilitates increased power electronics connected renewable penetration while maintaining the system stability. Besides virtual inertia, a well-functioning VSG also includes frequency droop control and voltage regulation, which corresponds to the turbine governor and automatic voltage regulation in the synchronous generator (SG). This leads to the question of whether such a VSG can fully replace the SG in the conventional power system and achieve 100% power electronics generation penetration. This poster tries to answer this question by first comparing SG and VSG and then replacing all of the SG by VSG in the IEEE 39-bus system under the assumption of the infinite electric energy storage capacity. The results verify that the VSG has the same function as SG and the system remains stable under 100% VSG penetration.

I. INTRODUCTION

The increase in renewable generation reduces the inertia of the power system, with potential impacts for the system stability. In order to greatly increase the use of renewables while maintaining system stability, these power electronics connected generation sources must move from being purely grid feeding to grid forming. With this goal in mind, virtual synchronous generator (VSG) control has been proposed to provide frequency support by emulating the swing equation dynamics in the control of grid connected converters.

However, although the main function of SG and VSG can be set to be identical, their physical differences ultimately mean they have different behaviors. Considering the difference, this poster contributes to firstly compare the SG and VSG in the system level performance and secondly analyze the possibility of 100% power electronics generation penetrations.

II. DEVICE COMPARISON

Fig. 1 presents the comparison of the VSG versus SG, where the function parts, i.e. voltage control, governor and inertia are identical, but the physical parts are different. SG relies on electromagnetic and electromechanical interactions, which has the corresponding transient and sub-transient dynamics. VSG itself has dynamics associated with the voltage source converter controls (inner current outer voltage control) and the output

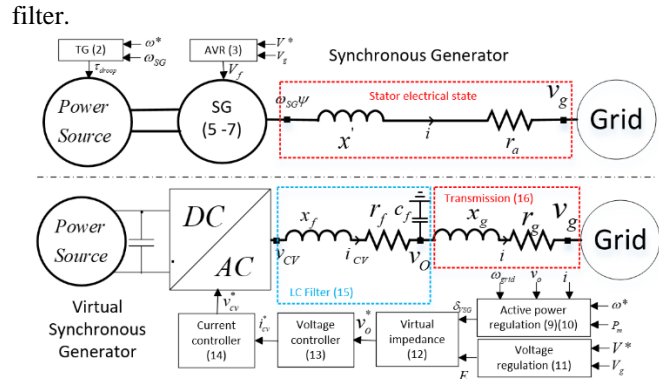


Fig. 1. Structure: VSG vs. SG

III. 100% POWER ELECTRONICS GENERATION PENETRATIONS

The tested system is IEEE 39-bus system. The SG is fully replaced by the VSG with identical settings and capacity. Fig. 2 presents the system behaves after the contingency, G10 lost.

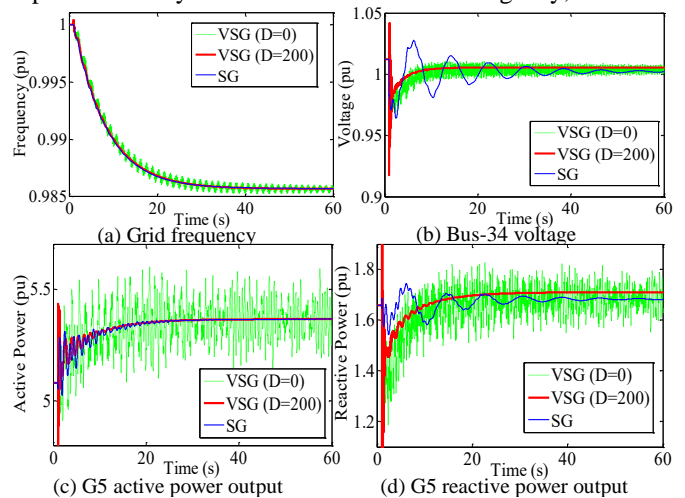


Fig. 2. 100% Wind Penetration (D: damping)

- 1) VSG has similar performance as the SG in terms of primary frequency and voltage regulation, which indicates that VSG can provide the same inertia into the system as the SG.
- 2) The SG tends to have more severe sub-transient than VSG, which leads to worse voltage performance.
- 3) The parameter in VSG is adjustable while in SG is not. A proper designed VSG, thus, is supposed to have better performance than SG.

Comparison of RMS and EMT Simulations of a Two-Area System with High Renewable Penetration

Angel Clark*, Pinaki Mitra†, Nicklas Johansson‡, and Mehrdad Ghandhari*

*Department of Electric Power and Energy Systems, KTH Royal Institute of Technology, Stockholm, Sweden

†ABB, FACTS, Västerås, Sweden

‡ABB, Corporate Research, Västerås, Sweden

Abstract—The objective of this research is to analyze the effect of different factors on the transient, small-signal and frequency stability of the two-area, four-generator test system with very high penetration of converter-based non-synchronous generation (NSG). Equivalent EMT simulations will be performed in PSCAD that were previously executed as RMS simulations in PowerFactory. The results of the EMT and RMS simulations can then be compared to determine if the RMS model and simulations are sufficient to accurately describe converter behavior.

Keywords—transient stability, small-signal stability, angle stability, frequency stability, renewable generation

I. INTRODUCTION

The increase of installed power electronics-based non-synchronous generation (NSG) coupled with the decrease of conventional forms of synchronous generation (SG) has led to a growth in renewable penetration. System operators already experience challenges and are forced to curtail renewable generation or set stringent instantaneous penetration limits. As countries look towards cleaner forms of generation, the amount of installed NSG is predicted to increase, while conventional sources are predicted to decrease due to retirement and economic factors. Based on the current converter technology, it is expected that this will have several impacts on power systems. First, the rate of change of frequency (ROCOF) will increase following a disturbance leading to larger frequency deviations from the decrease in system inertia. Due to the current limitations of the converter, the system wide short circuit current will be lower. This will cause a decrease in reactive power support as well as a larger challenge to detect faults. Also, the decrease of synchronizing torque will cause more rapid changes in voltage phase angle. The primary goal of this work is to obtain greater insight to the power system stability issues that arise in systems with high penetration of NSG. Also, another key objective is to formulate an accurate modeling approach to study such stability issues.

II. PROPOSED METHODOLOGY

A. RMS Simulations

A comprehensive set of analysis using RMS simulations has been conducted in PowerFactory on the two-area, four-generator test system [1] with integrated NSG connected by power converters (Fig.1), for both transient and small-signal stability. The converter used was based on the standard PowerFactory converter model. The objective was to analyze the effect that the

following factors had on both the transient and small-signal stability:

- NSG Penetration Level
- Distribution of NSG
- Voltage Control Settings of NSG

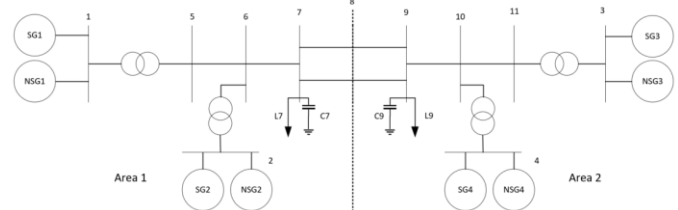


Fig. 1. Two Area System with converter-based NSG

B. EMT Simulations

RMS or phasor-based simulations have a large time step, generally around 1 ms and are effective for quickly simulating large systems. However, due to the phasor representation, it can only capture transients with respect to the fundamental frequency. RMS simulations can be limiting because they are unable to fully represent the fast switching converter behavior. Alternatively, EMT simulations have a time step that is generally less than 100 μ s and the system is modeled with detailed differential and algebraic equations. EMT simulations can fully capture converter behavior but have a long computational time. Therefore, EMT simulations are only performed for systems with a limited number of buses.

By performing an EMT analysis of a small system with varying penetration of NSG, further insight into the system behavior can be gained. The proposed work is to model the two-area, four-generator test system including converter-based NSG as an EMT model in PSCAD. The same simulations that have been done in PowerFactory will be executed in PSCAD to study the effect that penetration level, distribution of NSG and voltage control settings of NSG have on the transient, small-signal and frequency stability of the system. Further, comparison of the EMT and RMS simulation results will validate if the RMS model is able to effectively capture the converter behavior.

REFERENCES

- [1] P. Kundur, "Power System Stability and Control", EPRI, McGraw-Hill, 1993, pages 813-816.

Probabilistic Solar Power Forecasting Using Bayesian Model Averaging

Kate Doubleday, William Kleiber, and Bri-Mathias Hodge

I. INTRODUCTION

Bayesian model averaging (BMA) [1], a method from meteorology literature, is adapted to calibrate numerical weather prediction (NWP) ensembles for hourly probabilistic solar power forecasts up to a day-ahead. Probabilistic forecasts can inform adaptive reserves and stochastic or robust unit commitment/economic dispatch models. However, NWP ensembles often have bias and under-dispersion – in this case, over-estimation of sunniness and under-estimation of uncertainty.

Additionally, by directly forecasting solar power rather than irradiance, the probability distribution should account for “clipping,” when a plant’s output is truncated at or below its AC power rating, \mathcal{P} . This poster presents a two-part model to correct ensemble under-dispersion and account for clipping.

II. BAYESIAN MODELING AVERAGING

In BMA, the predictive probability density function (PDF) of solar power y is a mixture of conditional PDFs, $h_k(y|f_k)$, one for each forecast f_k in an ensemble of K members, weighted with a non-negative weight w_k , where $\sum_k w_k = 1$:

$$p(y|f_1, \dots, f_K) = \sum_{k=1}^K w_k h_k(y|f_k)$$

For this application, an appropriate PDF for $h_k(y|f_k)$ is the beta PDF (β): the forecasted power should obey a lower bound of zero and an upper bound at \mathcal{P} . Power can be normalized by \mathcal{P} onto $[0,1]$, the interval where the beta distribution is defined. By including the probability of clipping P_{clip} above a threshold of $\lambda = 0.995$, $h_k(y|f_k)$ is modeled as:

$$h_k(y|f_k) = \frac{P_{clip}(y|a_k)}{(1-\lambda)\mathcal{P}} \mathbb{1}[y \geq \lambda\mathcal{P}] + \frac{(1-P_{clip}(y|a_k))}{\int_0^\lambda \beta(\frac{x}{\mathcal{P}}|[b_k, c_k])dx} \frac{\beta(\frac{y}{\mathcal{P}}|[b_k, c_k])}{\mathcal{P}} \mathbb{1}[y < \lambda\mathcal{P}],$$

where $\mathbb{1}$ is the indicator function, and a , b , and c are parameters used to model the clipping probability, the beta mean, and beta variance, respectively, as a function of the forecast.

The authors are with the University of Colorado Boulder, Boulder, CO, 80309 USA. K. Doubleday and B.-M. Hodge are also with the National Renewable Energy Laboratory (NREL), Golden, CO 80401. This work was authored in part by NREL, operated by Alliance for Sustainable Energy, LLC, for the U.S. Department of Energy (DOE) under Contract No. DE-AC36-08G028308. Funding provided by DOE’s Office of Energy Efficiency and Renewable Energy under Solar Energy Technologies Office Agreement Number 33505. The views expressed in the article do not necessarily represent the views of the DOE or the U.S. Government.

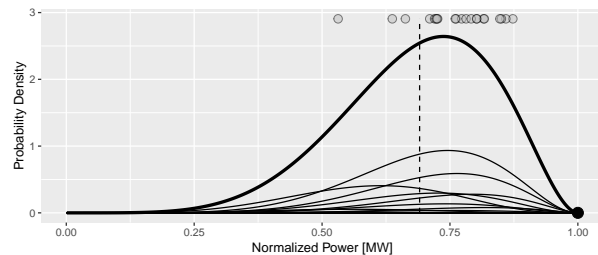


Fig. 1. Illustration of a BMA forecast. The shaded dots indicate the ensemble members, and the thin black lines are the corresponding weighted PDFs. The thick line is the sum, $p(y|f_1, \dots, f_K)$, and the dotted line is the observed power. At this time, the forecast probability of clipping is 0 (black dot).

Respectively, these are fit through logistic regression, linear regression, and maximum likelihood estimation along with the member weights w_k on a historical training set.

III. RESULTS & CONCLUSIONS

The method above was evaluated with historical data from 3 days in July 2018 from a utility-scale plant in Texas, using 21-member ensemble. The model parameters were trained using a time-of-day window, using 1-hour ahead forecast and observation data from the same hour of the day from the past 14 days, plus a 25-day window centered on the same date in the previous year. An example mid-day probabilistic forecast compared to the observed power is shown in Fig. 1.

The BMA forecast was compared to a linear interpolation (LI) among the ensemble members to evaluate sharpness, continuous ranked probability score (CRPS), and Brier score of the 5th percentile, to test accuracy of the distribution tails. Table I shows similar CRPS values, though the BMA has better tail accuracy while not being as sharp as the LI forecast. This illustrates that the LI forecast is too sharp at the expense of accuracy, while BMA post-processing can help alleviate these issues, including improved modeling of the distribution tails.

TABLE I
AVERAGE PERFORMANCE OF FORECAST POWER, NORMALIZED FOR PRIVACY. ALL METRICS ARE NEGATIVELY ORIENTED (LOWER IS BETTER).

	Sharpness	CRPS	Brier 5 th
LI	0.181	0.113	0.279
BMA	0.266	0.107	0.141

[1] A. E. Raftery, T. Gneiting, F. Balabdaoui, and M. Polakowski, “Using Bayesian model averaging to calibrate forecast ensembles,” *Monthly Weather Review*, 133(5): 1155–1174, 2005.

Abnormal Data Filtering Framework for Smart Battery Gauge at Butler’s Farm Microgrid

Cong-Sheng Huang, Bharat Balagopal and Mo-Yuen Chow

Electrical and Computer Engineering, North Carolina State University, Raleigh, U.S.A.

Email: chuang15@ncsu.edu, bbalago@ncsu.edu, chow@ncsu.edu

Abstract— Battery Energy Storage Systems (BESS) are key components in microgrids for reliable operations. Most battery SOC estimation algorithms are developed assuming the measured battery data are trust-worthy. However, the measured battery data contains multiple types of abnormal data, resulting in poor SOC estimation accuracy and causing detrimental effect on the BESS safety and the microgrid stability. Learning from a microgrid testbed, an abnormal data filtering framework for the Smart Battery Gauge (SBG) at Butler’s farm microgrid is proposed for accurate SOC estimation in real-world BESS applications.

Index Terms— abnormal data filtering, battery energy storage system (BESS), microgrid, State-of-Charge (SOC).

I. INTRODUCTION

Microgrid is envisioned to be the future of electric grid. As defined by the Department of Energy (DOE), the microgrid can be disconnected from the main grid and operates autonomously [2]. Battery energy storage systems (BESS) play a key role in microgrids by serving as energy reservoirs. However, they are hazardous to improper operations, which is mainly a result of inaccurate SOC estimation. Numerous SOC estimation algorithms had been proposed, but assume the load current and terminal voltage measured from the battery are trust-worthy, thus the SOC estimation error is purely caused by the error from the battery model approximation. However, the field data acquired from the real-world BESS applications contains abnormal data and mainly results in inaccurate SOC estimation. Learning from the Butler’s farm microgrid, a real-time abnormal data filtering framework to filter the abnormal data in the BESS applications is proposed.

II. SMART BATTERY GAUGE

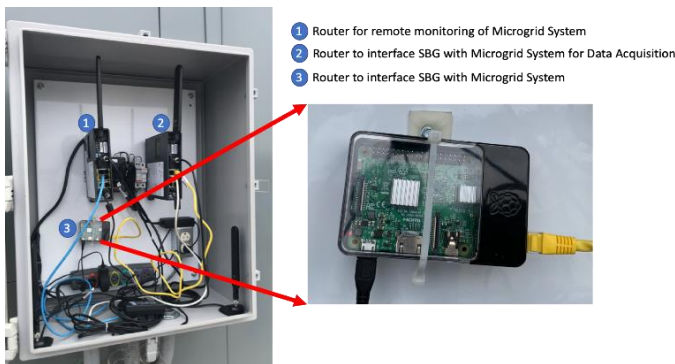


Fig. 1. SBG implemented at the microgrid testbed.



Fig. 2. The BESS located at a microgrid testbed.

III. KEY FIGURES

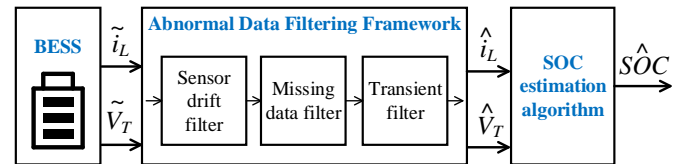


Fig. 3. The flow chart of the data pre-processing framework.

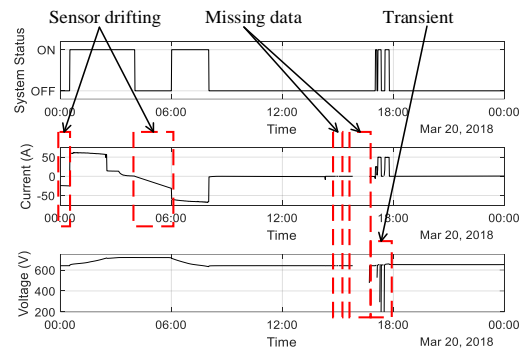


Fig. 4. A battery use case which contains three typical abnormal data.

IV. CONCLUSION

The abnormal data causes poor SOC estimation, as investigated from the Butler’s farm microgrid. In a typical operation day in spring, the mean absolute SOC estimation error is 3.2% and the maximum SOC estimation error is 79.9%. Adopting the proposed abnormal data filtering framework, the SOC estimation accuracy is significantly improved: the average SOC estimation error is 1.3% and the maximum SOC estimation error is 8.55%. The results show that the proposed abnormal data correction framework is able to effectively detect and filter the abnormal data and thus improves the SOC estimation accuracy for reliable microgrid operation.

Meeting Onshore Grid Demands through Offshore Wind Integrated VSC Controlled MT-HVDC System

Faria Kamal, *Student Member, IEEE*
 University of North Carolina at Charlotte
 Charlotte, USA
 fkamal@uncc.edu

Badrul Chowdhury, *Senior Member, IEEE*
 University of North Carolina at Charlotte
 Charlotte, USA
 B.Chowdhury@uncc.edu

Abstract—This paper focuses on the power sharing amongst the Voltage Source Converters (VSC) in a Multi-Terminal High Voltage DC (MT-HVDC) system. A four terminal VSC-HVDC system is modeled in PSCAD/EMTDC that connects two Offshore Wind Farms (OWF) with two onshore grids via VSCs which share the available power based on the voltage droop. In addition, the paper compares the total losses on both AC and DC side as the power injection from OWF is changed due to converter outage and changes in the wind speed. A cost comparison has been presented where the line, converter, transformer losses and the generator fuel costs have been considered.

Index Terms—HVDC, voltage droop, VSC, power sharing, offshore wind farm (OWF)

I. PROPOSED ALGORITHM

The flowchart shown in Fig. 1 represents an algorithm to determine the droop gains of the two P-V Droop controlled VSC stations connecting two grids, as the available generation varies.

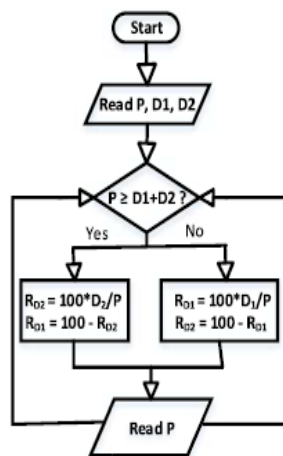


Fig. 1: Algorithm for finding the droop gain.

Here, P is the total available power from the OWFs, $D1$ and $D2$ are the minimum demands, and R_{D1} and R_{D2} are the converter droop gains of Grid 1 and Grid 2, respectively. It is assumed that the grids have unequal minimum demands. Initially, the total power imported from OWF is equally supplied to the two grids (Case 1). The proposed algorithm first determines if the total power import is still enough to supply the total minimum demand ($D1+D2$). If it is enough (Case 2), then the minimum demand of the grid that is farther away from the active converter station is met. However, if the total generation is less than the total minimum demand (Case 3), the minimum demand of the nearby grid is met first.

II. TEST SYSTEM AND SIMULATION

Fig. 2 shows the modified CIGRE B457 system. The converter stations B2 and E1 connects the two OWFs, B3 connects Grid 1 and F1 connects Grid 2 (455 MW). It is assumed that Grid 1 had a minimum demand $D1 = 130$ MW, and Grid 2 has a minimum demand $D2 = 70$ MW. The remaining loads are met by the local generators in the grids.

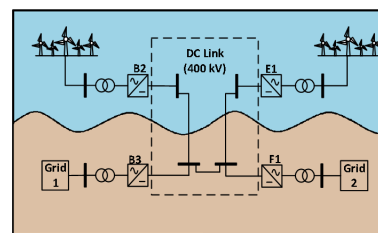


Fig. 2: Modified CIGRE B457 System.

Fig. 3 depicts the power flow at the four converter stations. Before 3.5 s, equal power was being shared by two grids (P_{B3}) and (P_{F1}). After E1 is lost at 3.5 s, only the OWF at B2 exports power (P_{B2}). Therefore, Grid 2 is supplied its minimum demand $D1$ (70 MW), and the remaining power is supplied to Grid 1. However, at 4.1 s the wind speed drops. When total OWF generation is less than $D1+D2$ (At 11 s), Grid 1 is supplied its minimum demand $D2$ (130 MW). The remaining power is sent to Grid 2. Table I represents the cost

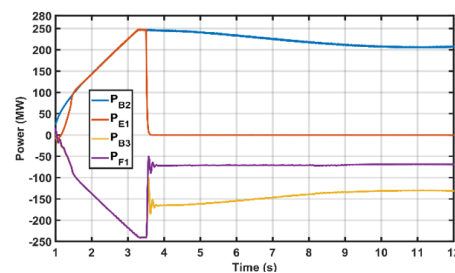


Fig. 3: Power at HVDC Converter Stations.

comparison among three cases. The converter and line loss costs are calculated using 30\$/MWh price, where as the local generator costs are calculated using generator cost curves.

TABLE I: Cost Comparison

Case	Time (s)	Supply from OWF (MW)	Total Cost (\$)
1	3-3.5	492	485.4
2	6-6.5	<233.8	1362
3	11-11.5	<210	1367

The table reflects the benefits of having the maximum power being supplied from the OWFs.

Game-Theoretic Modeling for Strategic Regulators in Electricity Market

Jip Kim

Dept. of Electrical and Computer Engineering
New York University
New York, USA
jipkim@nyu.edu

Yury Dvorkin

Dept. of Electrical and Computer Engineering
New York University
New York, USA
dvorkin@nyu.edu

Abstract—This paper proposes a game-theoretic approach to model regional competition of multiple regulatory bodies (policymakers) within a wholesale electricity market, while pursuing an individual renewable goal. We first formulate a regulator’s planning problem as a mathematical program with equilibrium constraints (MPEC) considering feed-in tariffs and tradable green certificates as renewable support schemes. To tackle the uncertainties of renewable generation, we adopt chance constraints which ensure power output limits of controllable units are met with a given probability. Then we extend our model in a competitive environment where multiple regulators (leaders) are tied in a single wholesale market (common follower). As a solution technique, multiple MPECs of regulators are reformulated as an equilibrium problem with equilibrium constraints (EPEC) and chance constraints are converted into deterministic second-order conic (SOC) constraints. Finally, we validate our model in ISO New England (ISO NE) 8-zone test system.

Index Terms—strategic regulator, game theory, renewable portfolio standard, multi-leader common-follower game

I. MODEL SUMMARY

Neighboring states of the U.S. have different renewable goals but tied in a single wholesale electricity market. For example, ISO NE system has 8 zones governed by 6 states with different renewable goals as shown in Fig. 1. To appropriately model this regulatory environment, we first formulate multi-regulators within a single wholesale electricity as multiple MPECs with regulator’s planning problem in the upper-level and the common wholesale electricity market in the lower-level. Since such multiple MPECs are not tractable, we exploit the KKT optimality conditions and duality as solution techniques to convert the problem into equilibrium problem with equilibrium constraints (EPEC) as shown in Fig. 2.

REFERENCES

- [1] D. Krishnamurthy, W. Li, and L. Tesfatsion, “An 8-zone test system based on iso new england data: Development and application,” *IEEE Transactions on Power Systems*, vol. 31, no. 1, pp. 234–246, 2016.
- [2] G. L. Barbose, “U.S. renewables portfolio standards: 2018 annual status report,” 2018.

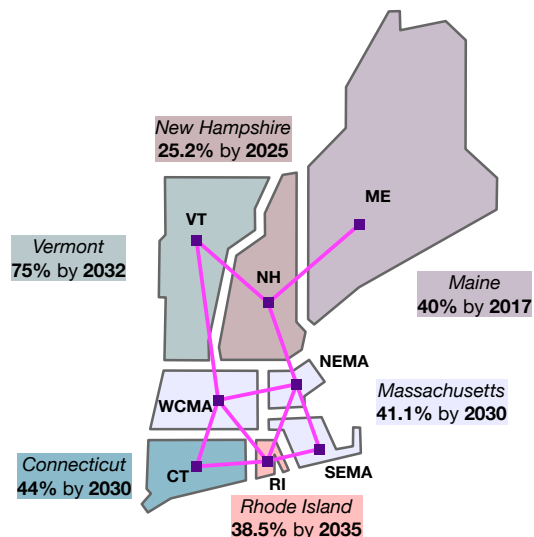


Fig. 1: ISO New England 8-zone test system with renewable portfolio standard goals [1], [2]

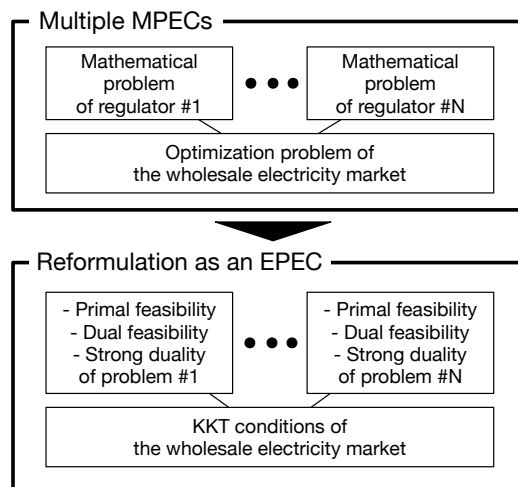


Fig. 2: Proposed model and reformulation structure

Optimal Controller Design for Stabilizing a Power System with Multiple Converter-interfaced Generators

Ryangkyu Kim
 Dept. of Electrical and Electronic
 Engineering
 Yonsei University
 Seoul, Republic of Korea
 ryangkyu0730@yonsei.ac.kr

Youngho Cho
 Hyundai Electric
 Seoul, Republic of Korea
 cyh_0228@hanmail.net

Kyeon Hur
 Dept. of Electrical and Electronic
 Engineering
 Yonsei University
 Seoul, Republic of Korea
 khur@yonsei.ac.kr

Abstract—This paper performs optimization-based controller design to avoid control interaction among multiple converter-interfaced generators (CIGs). To assess the control interaction between CIGs, an impedance-based stability analysis. Parameter sensitivity is performed to determine which control parameter has more influence on the stability, and particle swarm optimization is utilized to adjust the control parameters to enhance the stability with computational efficiency. Simulation results demonstrated that the proposed tuning procedure helps ensure the stability of the test case even if a CIG is disconnected from the grid.

Keywords—converter-interfaced generation (CIG), system stability, impedance-based stability, particle swarm optimization (PSO)

I. INTRODUCTION

Impedance-based stability analysis is an applicable method to assess the stability of a CIG-connected grid [1]. The important part in this analysis is to obtain the CIG impedance that is observed from the Point of Common Coupling (PCC). In particular, the CIG malfunctions or maintenance should be carefully considered in the tuning process as a CIG disconnection may result in impedance changes in the system, waveform distortion, and instability. To tune the control parameters, particle swarm optimization (PSO) is one of the attractive methods due to its implementation and computational advantages [2].

II. IMPEDANCE-BASED STABILITY ANALYSIS

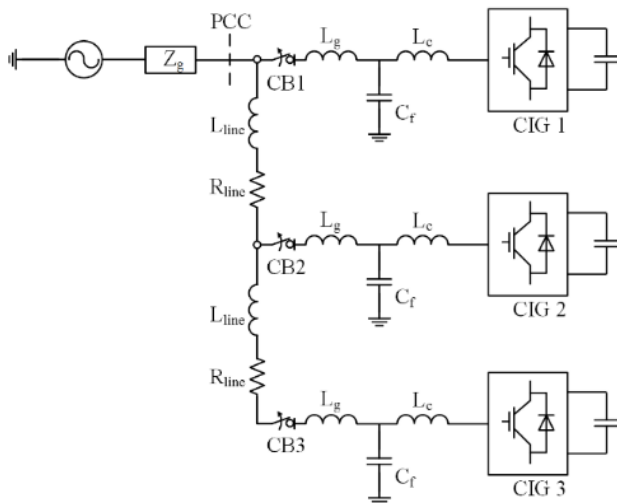


Fig. 1. Equivalent model of CIGs. This model consists of CIG admittance and current sources.

A. Equivalent Impedance and Analysis

Fig. 1. Illustrates equivalent model for a number of CIGs connected in cascade. When the total admittance of the CIG side at PCC is addressed as Y_{eq} , the current flowing into the grid can be obtained as follows:

$$I_{grid} = \frac{Y_g}{Y_g + Y_{eq}} I_{con} - \frac{Y_{eq}}{Y_g + Y_{eq}} I_{src} \quad (1)$$

Where Y_g is the admittance of the source impedance, I_{con} is the total current generated by the CIGs, and I_{src} is the current generated by the grid.

B. PSO for CIG Parameter Tuning

For the application of PSO in a stability assessment, the objective function is defined as follows:

$$f_{obj} = \text{Max} \left(\text{Real} \left(\text{Pole} \left(\frac{1}{Y_g + Y_{eq}} \right) \right) \right) \quad (2)$$

III. CASE STUDY AND RESULT

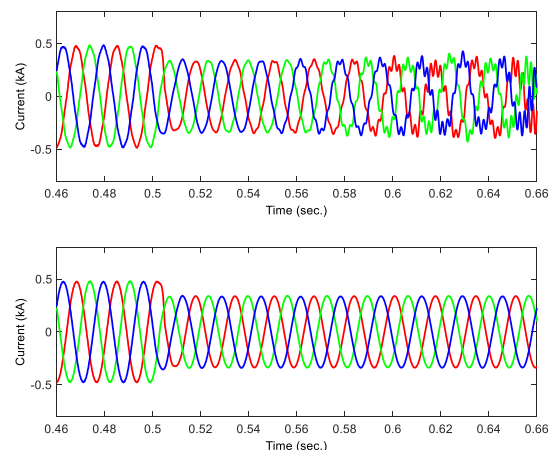


Fig. 2. The above waveforms of current flowing into grid when CIGs are disconnected from grid at 0.5s and 0.65s. The below waveforms after PSO parameter tuning.

REFERENCES

- [1] J. Sun, "Small-signal methods for ac distributed power systems-a review," IEEE Trans. Power Electronics, vol. 24, pp. 2545–2554, November 2009.
- [2] K. Y. Lee and M. A. El-Sharkawi, "Modern Heuristic Optimization Techniques: Theory and Applications to Power Systems," Wiley, 2008.

Distribution Voltage Regulation Using Combined Local and Central Control Based on Real-Time Data

Min-seung Ko, Sae-hwan Lim, Jae-kyeong Kim, and Kyeon Hur
 School of Electrical and Electronic Engineering
 Yonsei University
 Seoul, South Korea
 kms4634500@yonsei.ac.kr and khur@yonsei.ac.kr

Abstract—This paper proposes a control architecture that hierarchically combines a central and a local control to overcome individual weaknesses as well as to effectively and continuously regulate the voltage in the distribution systems under multiple PVs. The central control calculates the accurate references based on the periodic measurements in real-time, by considering the multiple target buses to improve the computational efficiency. With the determined references, the local control provides fast response to the voltage deviation during the computation of the central control. Therefore, the combined method can maintain continuously the voltage within the control range, and simultaneously minimize the active power curtailment. The performance of the proposed scheme is investigated by the simulation results on the modified IEEE 34-bus distribution feeder.

Keywords—Distributed generation, photovoltaic systems, power control, reactive power control, voltage control.

I. KEY EQUATIONS AND RESULTS

When reactive power compensation (RPC) is used, the central control finds a set with the objective function given by

$$100 \times \min \left(\frac{Q_{s,m} - |\Delta Q_m|}{Q_{s,m}} \right). \quad (1)$$

It is definite that regulation methods other than RPC is needed when

$$|V_j - V_t| > \sum_m (Q_{s,m} \cdot \mathbf{K}_{VQ}(j, m)). \quad (2)$$

As an alternative of RPC, OLTC or active power curtailment (APC) should be used with RPC. Tap operations of OLTC can be represented as

$$Tap = \begin{cases} Tap + 1 & \text{if } \Delta Comp_{over} \geq \Delta Comp_{low} \\ Tap - 1 & \text{if } \Delta Comp_{low} \geq \Delta Comp_{over} \end{cases} \quad (3)$$

where

$$\begin{aligned} \Delta Comp_{over} &= (V_{bus,h} - V_{T,U}) / \sum_m (Q_{s,m} \cdot \mathbf{K}_{VQ}(h, m)) \\ \Delta Comp_{low} &= (V_{T,L} - V_{bus,l}) / \sum_m (Q_{s,m} \cdot \mathbf{K}_{VQ}(l, m)) \end{aligned} \quad (4)$$

In case of APC, a set is chosen with the objective function as

$$\min \left(\sum_m \Delta P_m \right). \quad (5)$$

Chosen set in the central control is delivered to each PVs and the local control activates. Local control covers the computation time of central control and continuously regulates the voltage against the deviation. Volt-Watt-Var (VWV) curve represented in Fig. 1 determines the output of PVs during the local control.

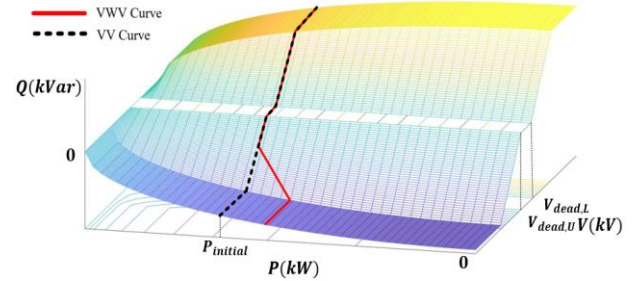


Figure 1. Schematic diagram of VWV curve in 3-dimensions.

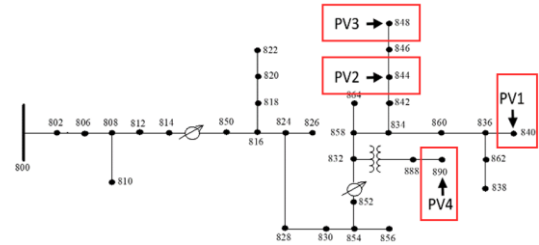


Figure 2. Modified IEEE 34-bus distribution feeder

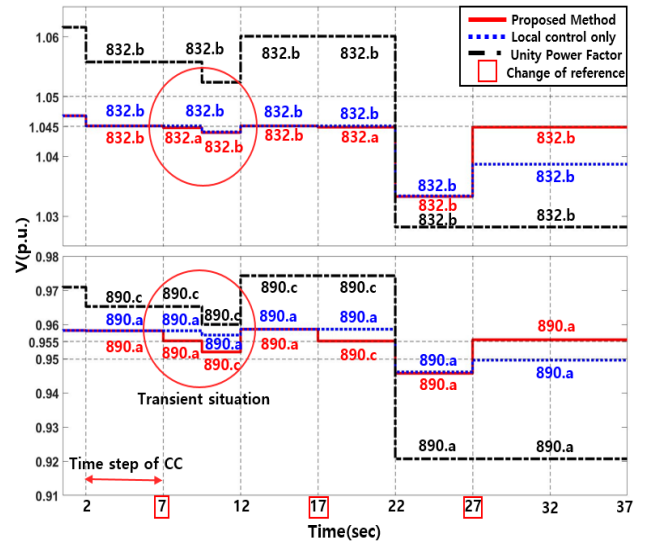


Figure 3. Comparison of the highest and the lowest voltage using the propose method and the local control only.

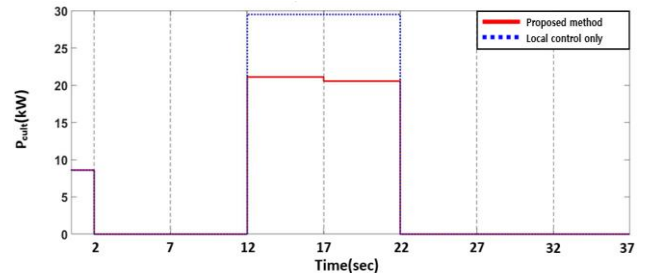


Figure 4. Total amount of the active power curtailment of PVs.

Optimum Design of Battery-Assisted Photo-Voltaic Energy System for a Commercial Application

Yaze Li, *Student Member, IEEE*, and Jingxian Wu, *Senior Member, IEEE*

Department of Electrical Engineering, University of Arkansas, Fayetteville, AR 72701

Abstract—This paper focuses on the optimum design of a battery-assisted photo-voltaic (PV) system by using real world data from commercial users. Specifically, we identify the size of PV panels, the capacity of battery energy storage system (BESS), and the optimum scheduling of BESS charging/discharging, such that the long-term average cost, including both energy cost and system cost, can be minimized. The optimum designs are performed by considering the overall cost of the PV system, which usually accounts for a big amount of initial investment, and the aging effects of batteries and solar panels. Practical considerations, such as calendar aging and cycling aging of batteries, inflation of utility cost, and interest rates for investments required for system construction, are considered in the study. The problem is formulated as a mixed integer non-linear programming (MINLP) problem over a time horizon on the order of years to capture the aging effects, whereas almost all existing works on PV system designs consider much shorter time horizons on the order of days or months. The MINLP is transformed into mixed integer linear programming (MILP) and solved by the branch-and-bound (B&B) algorithm. Applying the newly developed algorithms on real-world data from a commercial user in San Francisco reveals that the system achieves the break-even point at the 62nd month and a 38.5% reduction in utility bills.

I. PROBLEM DESCRIPTION

In order to accurately capture the impacts of aging, we propose to formulate the optimization problem by covering the entire life cycles of solar panels and BESS. The problem can be formulated as

$$\begin{aligned} \min_{q_c, q_d, n_s, n_b} \quad & C_E + C_D + C_S & (1) \\ \text{s.t.} \quad & & (2) \\ q^{net}(i) = q^{ld}(i) - q^{sol}(i) + q_c(i) - q_d(i) & & (3) \\ q^{sol}(i) = n_s q_0(i) \gamma_s^{m-1} & & (4) \\ s(i+1) = s(i) + q_c(i) \gamma_e - \frac{q_d(i)}{\gamma_e} & & (5) \\ 0 \leq q_c(i) \leq n_b Q_c \tau & & (6) \\ 0 \leq q_d(i) \leq n_b Q_d \tau & & (7) \\ 0 \leq s(i) \leq n_b S [1 - \alpha(m-1)^{0.75} - \beta \sqrt{m-1}] & & (8) \\ n_s \leq N_s, & & (9) \\ n_b \leq N_b, & & (10) \\ n_s, n_b \in \mathbb{Z}_+, & & (11) \end{aligned}$$

In the objective function (1), C_E is the energy charge, C_D is the demand charge proportional to the peak power each month, C_S is the cost of the system. Constraint (3) represents

TABLE I: Total utility bill under different configurations

System	Battery-assisted PV	PV-only
Utility bill (\$)	4,347,943	5,075,923
Reduction (\$)	2,719,900	1,991,920
System cost (\$)	1,299,000	768,000
Break-even point (month)	62	51
Electricity bill without PV (\$)	7,067,843	

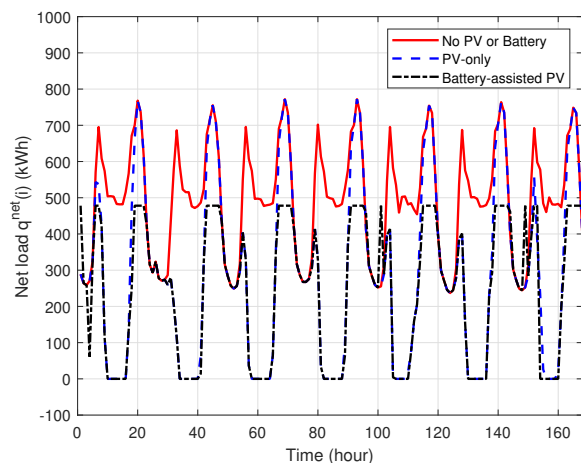


Fig. 1: Snap shots of 1-week energy usage in the first weeks of June.

the net energy purchased from the grid during the i -th hour, where $q^{ld}(i)$ is the load, $q^{sol}(i)$ represents the amount of renewable energy calculated by (4), $q_c(i)/q_d(i)$ are the amount of energy charged/discharged constrained by (6) and (7), Q is the maximum charging/discharging rate of one battery. Constraints (5) and (8) correspond to the constraints imposed by the battery, where $s(i)$ the state-of-charge (SOC) of all batteries, γ_e is the charging/discharging efficiency, S is the capacity of one battery. n_b/n_s are the number of batteries and solar panels, respectively constrained by their maximums.

II. KEY RESULTS

The proposed optimum design of the battery-assisted PV system ($n_b = 90$, $n_s = 120$) can achieve a 38.5% reduction in utility bills in Table I.

Fig. 1 has a significant peak shaving phenomenon after using batteries.

Replicating Real-World Wind Farm SSR Events

Yin Li, Student Member, IEEE, Lingling Fan, Senior Member, IEEE, Zhixin Miao, Senior Member, IEEE
 Department of Electrical Engineering
 University of South Florida, Tampa, United States

Abstract—In 2017, the transmission system of Electric Reliability Council of Texas (ERCOT) reported three sub-synchronous resonance (SSR) events which had the same cause and three different consequences. This project will build a testbed to replicate these real-world events for investigation. The replication results will match the real-world records including magnitudes and resonance frequencies. The replication testbed is built in MATLAB/Simpowersystems based on the information of the real system. The challenge of replication is the collect and combine fragmented information from public reports generated by energy companies and transmission companies. Relying on implication and assumptions, we are able to replicate the real events using the built testbed.

I. INTRODUCTION

From August 2017 to October 2017, three SSR events were recorded by ERCOT [1]. These three events happened in the same transmission system as shown in Fig. 1. The voltage level of main transmission line is 345 kV. Six wind plants are integrated at three stations. The series compensation line is employed to connect Cenizo and Del Sol. Two end stations are connected to the main grid. The causes for three events are marked in Fig. 1. Due to SSR, Plant 3 and 4 were tripped in Event 1 while Plant 1 and 2 were tripped in Event 2. However, there was not wind plant tripped in Event 3.

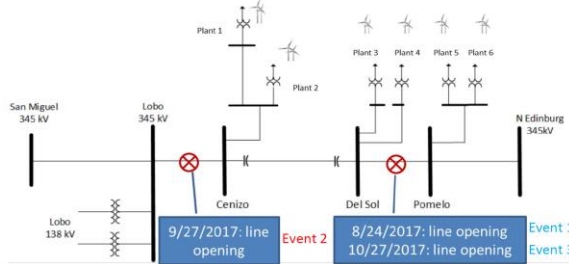


Figure 1: the configuration of the generator system

Fig. 2 shows the real-world records in three events including the instantaneous currents and their frequency spectrum. Three events were caused by the same reason but the resonance during these events had the different consequences, especially Event 1 and 3. It is puzzling to see Event 1 and 3, with the same line tripped, led to one case that SSR is severe enough being detected by the protection device and the other case that is less severe. We also noticed that in Event 3, more wind power was generated compared to that in Event 1.

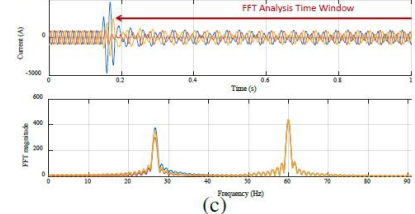
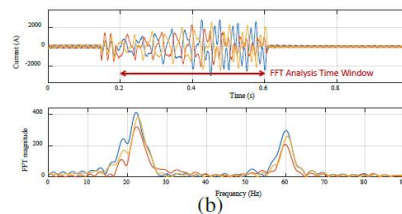
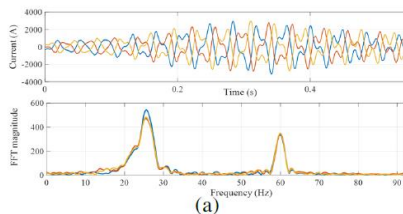


Fig. 2: Recorded real-world data. Event 1 (a): 25.6 Hz. Event 2 (b): 22.5 Hz. Event 3 (c): 26.5 Hz.

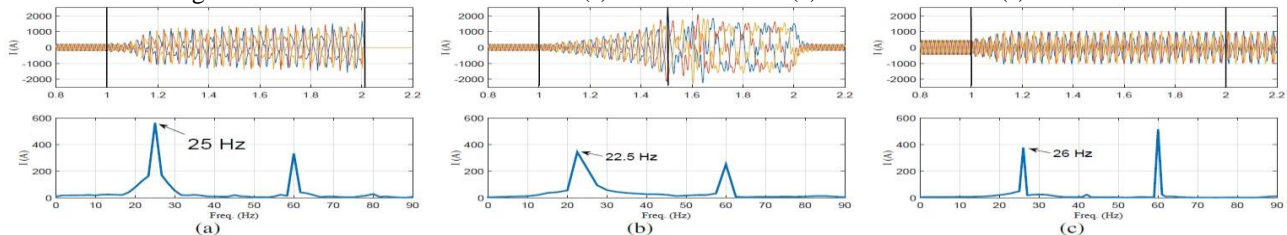


Fig. 4: Simulation results based on the testbed. Event 1 (a); Event 2 (b); Event 3 (c).

II. TESTBED PARAMETERS CONFIGURATION

The transmission line information was collected based on the public project reports [2] and [3]. According to [2], the transmission line is 156 miles from Lobo to North Edinburg and the total reactance of two series capacitor is 48 Ω . [3] provides the map of this real system. Based on the portion of each part, the length between two stations is estimated. The additional line from San Miguel to Lobo is found from other report. The impedance of each line is calculated using the per unit length impedance.

For wind farm parameters, the name of each wind plant can be found from the public project reports of utilities. Then, we can find the detailed information about each wind plant including capacity, the number of wind turbines, and types by searching their names in public wind power database. Fig. 3 shows the topology of the testbed including all of found parameters.

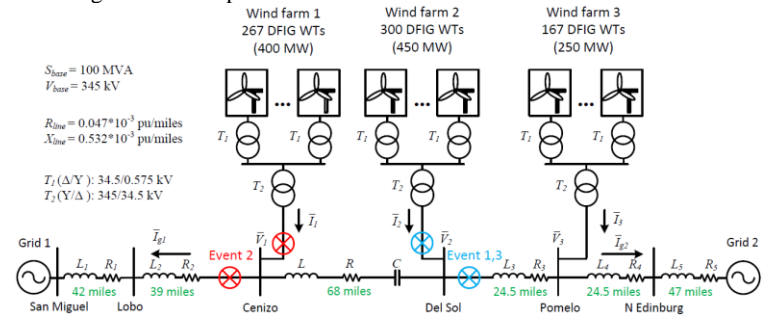


Figure 3: the configuration of the generator system

Besides above parameters, how many wind turbines online and wind speed at each event affect the generated wind power and SSR stability as well but they are unknown. For these two factors, we tuned their values to match the simulation results with the recorded data. The basic rules are: the larger number of wind turbines increases the oscillation frequency and the magnitude of fundamental component; the faster wind speed makes the ratio of SSR component to the fundamental one smaller. With the fine-tuned factors and found parameters, the replication results were generated by the detailed testbed and presented in Fig. 4.

III. REFERENCE

- [1] S. H. Huang and Y. Gong, South Texas SSR. ERCOT Meeting, May, 2018.
- [2] Rio Grande Valley Projects. Electric Transmission Texas, 2016.
- [3] New ETT 345-kV lines begin delivering power to LRGV. Electric Transmission Texas, 2016

Voltage Regulation in Distribution Systems with High Penetration of Renewable Resources

Daniel F. Lima and José C. M. Vieira

Department of Electrical and Computer Engineering, São Carlos School of Engineering
University of São Paulo, USP
São Carlos, Brazil
daniel.ferreira.lima@usp.br, jose.vieira@ieee.org

Abstract—Short-duration voltage variations throughout distribution systems with high level of Distributed Energy Resources (DER) penetration may become more frequent, thus novel voltage regulation strategies are going to be decisive in allowing a reliable operation of these systems. This paper aimed at providing a novel strategy of voltage regulation for distribution systems with high penetration of DER, without relying in installing extra components such as voltage meters or communication systems. The strategy used an optimization process to obtain the setpoint of voltage regulators that keeps the voltage throughout the system within acceptable values, even if the output of a renewable resource sudden varies. The results showed that the strategy can assist satisfactorily at regulating the voltage in a distribution system with high penetration of renewable resources.

Index Terms-- Distributed energy resources, renewable energy resources, short-duration voltage variation, voltage regulator.

I. INTRODUCTION

The addition of generators in distribution systems might increase the voltage at the generators' and load nodes. Since the voltage regulators purpose is to regulate voltage when slow and gradual changes occur in the consumers demand, they are not suitable for sudden variations caused by the intermittent generation profile of some renewable energy resources.

In this paper, a decentralized methodology that requires no extra real-time measurements is proposed. To achieve that, the setpoints of voltage regulators are adjusted in such a way the voltage levels throughout the distribution system are always maintained at an acceptable range, even when there are sudden voltage variations caused by the renewable resources. So, even if the output of the renewable resources quickly changes, no overvoltage or undervoltage occurs at any node. The methodology models the voltage regulation as an optimization problem. The solution is obtained offline and can be done by a variety of optimization methods. In this paper the Compact Genetic Algorithm was chosen due to its simple implementation.

II. METHODOLOGY

Potential solutions to the problem are created by the algorithm using a Probability Vector. These solutions are compared with each other and the one that is better at solving the problem (lower objective function) is selected to adjust the Probability Vector. The potential solutions in this strategy are the voltage setpoints of voltage regulators, varying between 0.90 p.u. and 1.10 p.u. Maximum and minimum generator's power outputs are used to model the uncertainty of renewable resources.

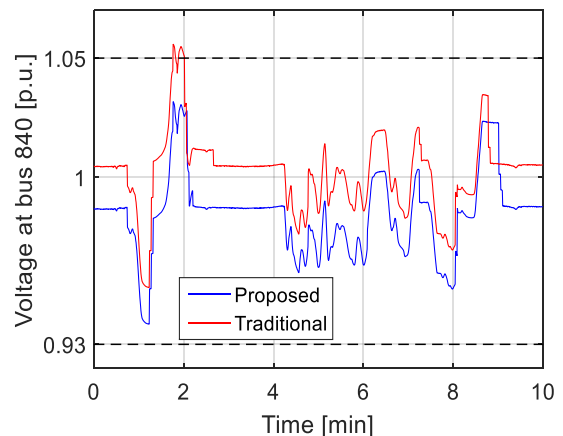


Figure 1. RMS voltage from phase "A" at node 840 in a scenario with high penetration of renewable resources.

III. CONCLUSIONS

The proposed strategy successfully found solutions that minimized the voltage violations in distribution systems with high penetration of renewable resources. Even if the power output of the renewable resources quickly changes, no overvoltage or undervoltage occurred at any node. The proposed strategy can regulate the voltage in distributions system with uncertain generators' power outputs without the need of extra monitors, so it is possible to be implemented in current distribution systems without a considerable financial burden.

This study was financed by the National Council for Scientific and Technological Development (CNPq) and by the São Paulo Research Foundation (FAPESP) – Grant #2015/04147-1.

Coordinated Control Strategies for PMSG-based Wind Turbine Smoothing Power Fluctuations

Xue Lyu¹, Jian Zhao², Youwei Jia¹, Zhao Xu¹, Kit Po Wong³

¹dept. Electrical Engineering, The Hong Kong Polytechnic University, Hong Kong, China

²dept. Electrical Power Engineering, Shanghai University of Electric Power, Shanghai, China

³dept. Electrical and Electronic Engineering, The University of Western Australia, Perth, Australia

Abstract—High penetration of wind energy in the modern power system exposes the need of smoothing the fluctuating output power in an effective and conducive way. In this context, this paper proposes two novel control strategies that utilize the self-capability of permanent magnet synchronous generator based wind turbine to realize power smoothing. The first strategy pursues to offer power smoothing support via simultaneous utilization of DC-link voltage control, rotor speed control and pitch angle control. The second control strategy seeks to coordinate the three concerned individual control schemes in a hierarchical manner, where the power smoothing tasks are allocated to individual control modules or their combinations dynamically in line with WT's operation status. Both two strategies are able to provide power smoothing support by fully exploiting wind turbine's self-capability, whereas the second strategy has the merits on 1) reducing the activation frequency of pitch angle control, and 2) enhancing wind energy harvesting. Case studies of the proposed control strategies are carried out to compare and verify their effectiveness in achieving power smoothing.

Keywords—Permanent magnet synchronous generator(PMSG), power smoothing, simultaneous control, hierarchical control.

I. INTRODUCTION

In the last decades, wind energy has exhibited a dramatic increase due to energy crisis and environmental issues. Though wind energy is a clean and efficient resource, high penetration of wind power can lead to detriment of power quality due to its uncertain and intermittent nature[1-3]. In industry, the variable speed wind turbines (VSWTs) are widely utilized due to their high efficiency and low cost. However, the nonsynchronous grid connection of VSWTs and their free-running operation mode intensifies output power fluctuations and thereby threaten the power system security. In particular, fast fluctuation of wind power output can result in frequency variation, system instability [4-6], variation of reactive power loss and voltage flicker at the point of common coupling (PCC) to the main grid [7]. In addition, wind power fluctuations lead to other technical and economic issues. For example, wind power fluctuations result in less operational efficiency of thermal units as discussed in[8]. Generally, power reserve would be increased to counterbalance wind power fluctuations, which consequently result in higher reservation cost[9]. Furthermore, high wind penetration may require high transmission capacity, which in turn increases the transmission losses[10]. It is straightforward that wind power fluctuations bring about more operational challenges especially in the islanded power systems, of which the inertia is low and the system is weak. In this context, smoothing power fluctuations can be quite beneficial to the islanded power systems.

In order to ensure system operation security and reliability, smoothing the wind power fluctuation is desirable especially for islanded systems which have limited power reserve. The fluctuated power can seemingly be alleviated owing to the intrinsic temporal and spatial coupling in one or more wind farms. However, such aggregation effect is naturally flawed with limited smoothing capability considering volatile wind direction and fixed location of wind turbine (WT) installation [11]. In this sense, it is still worthy of further investigation of advanced control to exploit individual WT's full potential of power smoothing. Thus far, this research direction has attracted wide attention in both industry and academia over the last decade, which can be categorized into two classes. The first class is to utilize energy storage system (ESS) to store the excessive energy and release back once needed. In [12], an ultra-capacitor (UC) bank and a lithium-ion battery bank (LB) are utilized to mitigate the short-term and long-term wind power fluctuation, respectively. Other ESSs such as flywheel and upper conducting magnetic energy storage (SMES) have also been considered in [13-17]. Nevertheless, such approaches inevitably involve additional investments. Distinguished from the previous approaches that rely on additional ESS, the second class is aimed to delve into the greatest potential of the WT itself for power smoothing. This type of strategies is advantageous over ESSs based ones owing to less investment cost and maximum utilization of the existing resources of WT. Such resources comprising of the following three aspects can be synthesized as the self-capability of WTs for power smoothing.

The first resource lies in the energy harvesting capability through pitch angle adjusting. An effective pitch angle control can directly affect the active power output of WTs. To achieve such control objective, fuzzy logic pitch controllers are reported in [18, 19] to smooth wind power fluctuations under below-rated wind speed conditions. Those controllers are reported to be robust and easy to be implemented. However, it is noted that the wind energy harvesting efficiency is low since the curtailed wind power is directly discarded. In addition, frequent activation of pitch angle adjustment will inevitably increase mechanical stress and fatigue of WTs.

Another resource that can be utilized to smooth out wind power fluctuation is the kinetic energy (KE) stored in the rotational rotor [20-22]. When the smoothing command is received, the rotating mass releases or absorbs excessive energy via rotor speed deceleration/acceleration. To establish the relationship between smoothing command and rotor speed, a fuzzy PID controller is proposed in [22] to replace the conventional speed controller. In [21], the frequency deviation is introduced to the controller by utilizing KE. Even though the operating point of WT is shifted away from maximum power point (MPP) when rotor speed control is adopted, it has an advantage as compared to pitch angle control in energy

Blackstart of DFIG-based Windfarm

Duncan Kaniaru Maina, Mohammad Javad Sanjari,
 Department of Electrical and Computer Engineering
 University of Auckland
 Auckland, New Zealand

Nirmal-Kumar C. Nair
 Department of Electrical and Computer Engineering
 University of Auckland
 Auckland, New Zealand

Abstract—This paper explores the possibility of starting DFIG-based windfarms in preparation of network restoration with the use of an emergency diesel generator set (DGS). The windfarm substation is assumed to be composed of the diesel gen-set, synchronous condenser and a dump load. Pitch control, different from the one used during high wind speeds, is modeled and incorporated in this scheme to control speed of rotor during 2 processes: switching on of RSC and stator resynchronization to the grid. Results, from simulation in MATLAB/SIMULINK, show successful starting of DFIG windfarm and subsequent autonomous operation with the synchronous condenser (SC) providing reference voltage after the DGS has been switched off.

DFIG. This slows down the rotor speed thus speed control is enforced to return it to the speed required for resynchronization. SW3 is closed after the rotor speed nears 1 pu after which the outer loop controls of the RSC (MPPT and Pitch control) are activated to resume normal DFIG operation.

This study assumes a windfarm (Fig. 2) consisting of 4 such DFIGs simultaneously energized by the DGS, followed by transition to windfarm autonomous operation with the DGS switched off and SC used to provide reference voltage.

I. MODEL DESCRIPTION

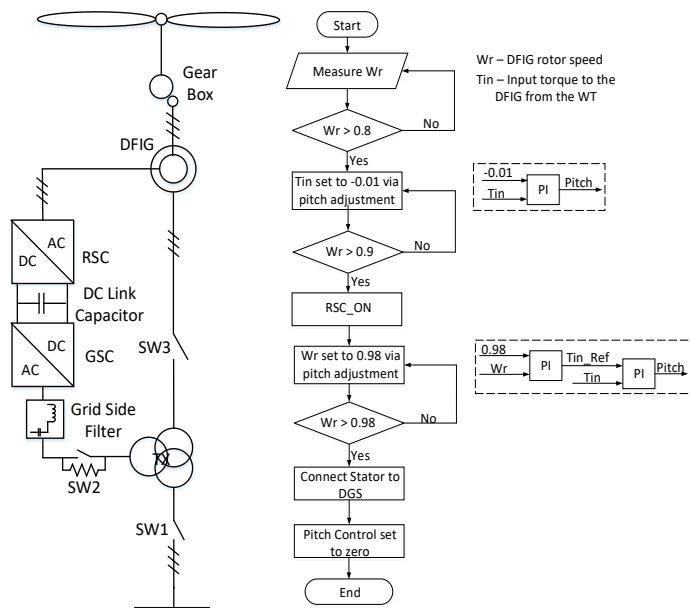


Figure 1. DFIG WECS Starting Model and Pitch Control Algorithm

SW1 (Fig. 1) is closed to pre-charge the dc link with the GSC and RSC being off during this stage. Pre-charging resistors are bypassed by closing SW2 after which the GSC is turned on with the required dc link voltage as the reference point. Whilst this is ongoing (dc link charging), assuming the wind speed is above the cut-in speed, the DFIG rotor can be rotated by the wind turbine. After the rotor speed attains a speed above 0.9 pu, the RSC converter is switched on to provide excitation current to the

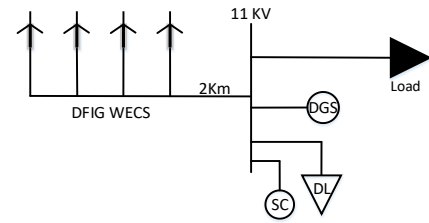


Figure 2. DFIG based Windfarm

II. KEY RESULTS/CONCLUSION

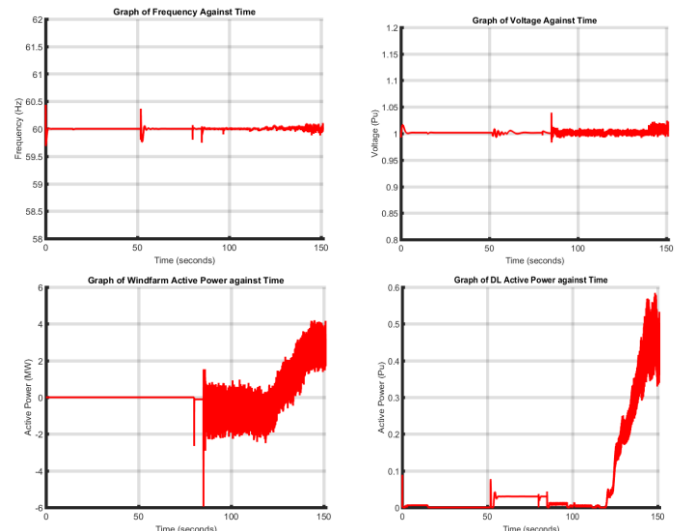


Figure 3. Frequency, voltage, Windfarm output and DL absorption during windfarm starting.

There is a possibility of using DFIG windfarms during the initial stage of restoration if wind is forecasted to be available. Future work by the author is focusing on windfarm cable, transformer and auxiliaries energization before DFIG starting.

The authors acknowledge funding support to carry out this research from MBIE, New Zealand's National Science Challenge-Resilience to Nature's Challenges and in particular the project on Electricity Distribution Resilience Framework informed by West Coast Alpine Fault Scenario; University of Auckland under Faculty Research Development Fund (FRDF) Grant 3709539 and QuakeCoRE New Zealand Centre of Earthquake Resilience

Impact of Smart Inverters on Dynamic SVR Settings for Distribution Voltage Control

H M Mesbah Maruf, *Student Member, IEEE*
 University of North Carolina at Charlotte
 Charlotte, USA
 hmaruf@uncc.edu

Badrul H. Chowdhury, *Senior Member, IEEE*
 University of North Carolina at Charlotte
 Charlotte, USA
 B.Chowdhury@uncc.edu

Abstract—A dynamic step voltage regulator (SVR) setting for an active distribution system in the presence of distributed photovoltaic (PV) systems is proposed to mitigate unnecessary tap operations during high PV variability period. Classical voltage regulating devices, such as on load tap changers (OLTC), SVR, and capacitor banks should be properly controlled and coordinated to improve power quality, and overall system efficiency while interacting with the smart inverter functions. The proposed dynamic regulator settings require unidirectional communication links from the distribution management system (DMS) to update its controller setpoints on a timely fashion based on the solar and load forecasts to achieve the desired voltage profile throughout the feeder. In addition, voltage violation duration reduction and lower network losses can be attained. The proposed scheme is tested on a modified PV integrated IEEE-123 bus test system to evaluate the performance under different system loading conditions and varying smart inverter functions.

Index Terms—Regulator control settings, smart inverter function, voltage control, distributed PV

I. PROPOSED DYNAMIC REGULATOR SETTINGS

Fig. 1a represents a simple circuit showing active and reactive power injection by the PV connected at the end of the line. If V_1 is the bus voltage of the regulator secondary terminal, the line voltage drop during forward active power flow is given by:

$$\Delta V = \frac{R_1(P_{L2} - P_{PV2}) + X_1(Q_{L2} \pm Q_{PV2})}{V_2} \quad (1)$$

Here, active and reactive power generation from PV is represented by P_{PV2} and Q_{PV2} , respectively. Load consumption at bus 2 is denoted by P_{L2} and Q_{L2} . If $P_{L2} - P_{PV2} > 0$ and $Q_{L2} - Q_{PV2} > 0$, then the current transformer (CT) of the regulator controller reads the exact current that is responsible for the voltage drop in the line segment $R_1 + jX_1$. Here, it is considered that line drop compensation (LDC) is enabled and the regulator is fictitiously controlling V_2 . In Fig. 1b, the current flow caused by $P_{X2} = P_{PV2} - P_{L2} > 0$ and $Q_{X2} = Q_{PV2} - Q_{L2} > 0$ is not seen by the regulator CT (if V_4 is the target bus) though they are contributing to the line voltage drop. For example, current flow caused by $P_{X2} + jQ_{X2}$ is added with the current carrying $P_1 + jQ_1$ minus the line loss (in line segment from bus 1 to 2), and the total current is responsible for the line voltage drop for the downstream segment(s). The desired secondary terminal voltage of the regulator should be computed using the exact current flow responsible for the line voltage drops. However, the regulator controller triggers necessary tap operations by calculating the line voltage drop from the CT reading, which only considers the current carrying $P_1 + jQ_1$. Here, it has been assumed that

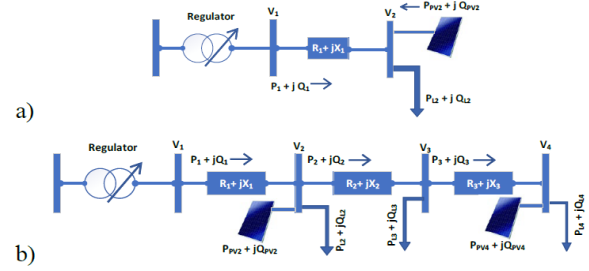


Fig. 1: Voltage drop caused by PV active and reactive power injection.

there is no reverse power flow caused by the PV at bus V_4 (e.g. $P_{L4} - P_{PV4} > 0$, and $Q_{L4} - Q_{PV4} > 0$). The impact of DER active and reactive power injection on the individual bus voltages can be measured by the voltage sensitivity matrix. For a distribution feeder with k -buses, the voltage rise/drop in a certain bus caused by the PV injections on the other buses can be calculated using the sensitivity matrix shown in (2).

$$\begin{bmatrix} \Delta V_1 \\ \vdots \\ \Delta V_k \end{bmatrix} = \begin{bmatrix} \frac{\delta V_1}{\delta P_1} & \cdots & \frac{\delta V_1}{\delta P_k} \\ \vdots & \ddots & \vdots \\ \frac{\delta V_k}{\delta P_1} & \cdots & \frac{\delta V_k}{\delta P_k} \end{bmatrix} \begin{bmatrix} \Delta P_1 \\ \vdots \\ \Delta P_k \end{bmatrix} + \begin{bmatrix} \frac{\delta V_1}{\delta Q_1} & \cdots & \frac{\delta V_1}{\delta Q_k} \\ \vdots & \ddots & \vdots \\ \frac{\delta V_k}{\delta Q_1} & \cdots & \frac{\delta V_k}{\delta Q_k} \end{bmatrix} \begin{bmatrix} \Delta Q_1 \\ \vdots \\ \Delta Q_k \end{bmatrix} \quad (2)$$

As the DER locations are assumed to be known by the DMS, regulator target bus voltage dependencies can be easily calculated using the sensitivity matrices. In addition, PV smart inverter functions (e.g. Volt-var, Volt-watt, constant pf etc.) decide active power curtailment and reactive power injection/absorption which also impacts the sensitivity matrices. Using fixed regulator settings can result in miss/unnecessary tap operations and sometimes voltage violations as the line voltage rise/drop caused by downstream DER injection are ignored by the regulator controller. If the remotely regulated bus is m , then voltage rise/drop at the target bus caused by z -downstream DER injections can be calculated from (2).

$$\Delta V_m(t) = \sum_{i=1}^z \frac{\delta V_m}{\delta P_i} \Delta P_i(t) + \frac{\delta V_m}{\delta Q_i} \Delta Q_i(t) \quad (3)$$

If the regulator controller parameters are selected to maintain the regulated bus voltage V_L^* at 120 V scale, then the updated voltage setpoint considering the DER impacts should be:

$$V_L^*(t) = V_L(t-1) + \sum_{i=1}^z \frac{\Delta V_m(t)}{V_{LL}/\sqrt{3}} * 120 \quad (4)$$

With this updated target voltage V_L^* almost the desired voltage profile can be achieved with the exact current seen by the regulator CT.

Benefits of Coordinating Voltage Regulators, Capacitors, Smart Inverters, and Demand Response for Distribution Volt-Var Control

Catie McEntee, David Mulcahy, Ning Lu
 FREEDM Systems Center
 North Carolina State University
 Raleigh, NC, USA
 cmmcente@ncsu.edu

Abstract— This study explores the benefits of coordinating voltage regulators (VRs), capacitors, photovoltaic smart inverters (PVSI), and customer demand response (DR) for volt-var control (VVC) on unbalanced distribution systems. The VVC algorithm studied uses a Voltage Sensitivity Matrix (VSM) in a mixed-integer nonlinear program to choose the least-cost combination of control actions that successfully brings all voltages within desired voltage limits, maintains an acceptable power factor at the top of the feeder and minimizes changes in voltage between time periods [1]. The VVC is implemented in several case studies, each employing a different subset of possible control devices. Preliminary analysis shows that coordinating the actions of all the available devices on a feeder can reduce operational costs and improve voltage control when compared to cases using only traditional devices or only smart inverters.

I. INTRODUCTION

Increased DER penetration can exacerbate voltage issues on distribution feeders, but also offers opportunities for distribution system operators to more precisely and efficiently control voltage. [1] presents a centralized VVC scheme which can coordinate voltage regulators, capacitors, demand response, and smart inverters to find an acceptable voltage solution at the least cost. Each of the control devices has different advantages and limitations. Voltage regulators are costly to install and are only placed in a few locations along the feeder, but they offer fine voltage control within .00625 pu. Overuse of voltage regulators, which can occur on circuits with high PV penetration, can reduce the lifetime of those devices. Capacitors are cheaper but only offer large step changes in reactive power injection. Controllable loads are widely distributed across the feeder which allows them to correct voltage issues at specific locations, but their overuse can be costly and impact customers. Smart inverters can also be widely distributed and offer fine control of both real and reactive power, but reactive power injected by smart inverters through transformers can increase losses, and active power

curtailment can be undesirable. Implementing a VVC scheme that coordinates all these devices to use the best resources depending on the situation adds complexity and requires increased investment in robust communication infrastructure to all devices. The benefits in terms of both voltage control and cost must be explored to justify implementation of this type of VVC.

II. CASE STUDIES

Six cases are run using different subsets of control devices as enumerated in table II. All cases use the VVC in [1] except the locally controlled VR and capacitor case, which is used as the base case. Each case is run on a large (1200 nodes) three-phase unbalanced distribution feeder with 4 voltage regulators, one capacitor, and 418 residential PV systems with a combined maximum capacity equal to the peak feeder load. The maximum voltage violation magnitude (MVVM), number of voltage violations (NVV) and total operational cost for each case are compared to show how each device impacts the voltage control capability and operational cost of the VVC scheme.

TABLE II. CASE STUDY RESULTS

Control Devices Used	MVVM (p.u.)	NVV	Cost (\$)
VR and Capacitor, locally controlled	.0434	2451	112.60
VR and Capacitor	.0166	1277	24.10
PVSI only	.0377	28549	1501.74
PVSI and DR	.0392	22595	4776.63
PVSI, VR and Capacitor	.0088	475	9.08
PVSI, VR, DR, and Capacitor (All)	.0086	474	9.07

III. REFERENCES

- [1] Catie McEntee, David Mulcahy, Jiyu Wang, Xiangqi Zhu, Ning Lu, "A VSM-Based DER Dispatch MINLP for VoltVAR Control in Unbalanced Power Distribution Systems," Accepted by *IEEE Power Engineering Society General Meeting*, 2019. IEEE, 2019.

A Two-Step Frequency Support Method for Multi-Terminal DC Grids

Mahmoud Mehraban, *Student Member, IEEE*, Maryam Saedifard, *Senior Member, IEEE*, Santiago Grijalva, *Senior Member, IEEE*,
Georgia Institute of Technology

Abstract—This paper proposes a two-step frequency support method for a Multi-Terminal DC (MTDC) grid. Subsequent to a disturbance in an AC area, the disturbed area converter station utilizes a $P-f$ droop, while the converter stations of the undisturbed AC areas use $P-V$ droops. An algorithm is proposed by which the disturbed area converter station switches its control mode from $P-f$ droop to $P-V$ droop during the disturbance. The proposed algorithm determines the droop constant of the $P-V$ droop and the time to switch the controller mode such that the power transferred to the disturbed area is maximized, while the power constraint of each AC area converter station and the DC voltage limit are taken into consideration. A wind farm inertia support is embedded in the proposed frequency support method by which subsequent to any disturbance, the share of each wind farm power in the inertia support can be predetermined by the MTDC operator. The performance and effectiveness of the proposed frequency support method are evaluated by time-domain simulation studies on a 5-bus MTDC grid. The study results confirm the superiority of the proposed method over the conventional one in terms of the speed of frequency recovery and post-disturbance frequency deviation.

Keywords—Multi-terminal DC (MTDC) systems, Frequency support, wind farms inertia support

I. INTRODUCTION

Following a disturbance in an AC area, a $P-f$ droop is exploited for the disturbed AC area converter station while a $P-V$ droop for each undisturbed AC area converter station is used. The structure of the proposed frequency support is modified such that not only can the MTDC grid operator determine the share of each wind farm in the inertia support but also the amount of power received by the AC grid can be maximized. Performance and effectiveness of the proposed controller is evaluated and confirmed by time-domain simulation studies on a MTDC grid interconnecting three AC areas and two wind farms in the PSCAD/EMTDC software environment.

II. THE PRINCIPLES OF THE PROPOSED FREQUENCY SUPPORT

Following a disturbance at $t = 0$ s, two time intervals with different droops for the disturbed area are considered. Table I summarizes the proposed frequency support method and compares it with the conventional one. It can be inferred that the conventional method does not change any of the droops during the disturbance.

Assuming that the wind speed variation is negligible during the disturbance, the block diagram of proposed inertia support

TABLE I: $P-V$ and $P-f$ droops for the conventional and proposed methods within different time intervals.

Method	Area	$0 \leq t < t_1$	$t_1 \leq t$
Proposed	Area _i	$P_i = P_i^{ref} - k_{fi} \Delta f_i$	$P_i(t) = P_i(t_1) + k_{vi}(V_{DCi}(t_1) - V_{DCi}(t))$
	Area _j	$P_j = P_j^{ref} + k_{vj} \Delta V_{DCj}$	$P_j = P_j^{ref} + k_{vj} \Delta V_{DCj}$
Conventional	Area _i	$P_i = P_i^{ref} - k_{fi} \Delta f_i$	$P_i = P_i^{ref} - k_{fi} \Delta f_i$
	Area _j	$P_j = P_j^{ref} + k_{vj} \Delta V_{DCj}$	$P_j = P_j^{ref} + k_{vj} \Delta V_{DCj}$

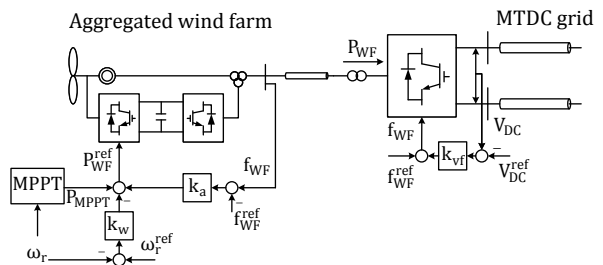


Fig. 1: Schematic diagram of the inertia support controller used for the wind turbines.

for the wind farms embedded in the proposed frequency support is shown in Fig. 1.

III. KEY RESULTS

The results of simulations on a test system that includes a 5-bus MTDC grid, which transfers the power generated by two wind farms to three asynchronous AC areas.

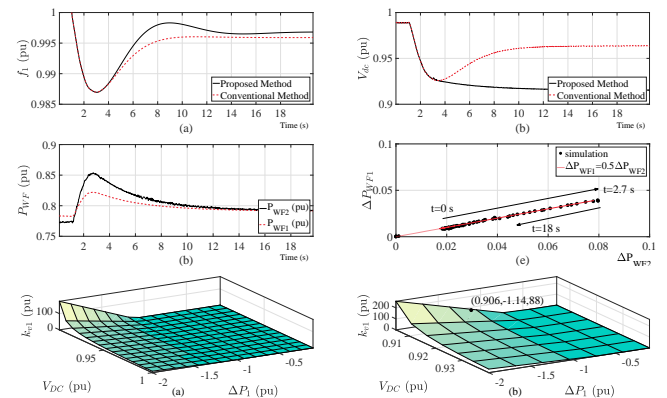


Fig. 2: Key results of the proposed frequency support: (a) Frequency of the disturbed AC area, (b) DC voltage of the MTDC grid, (c) Wind farm powers, (d) Power change of wind farm 1 versus power change of wind farm 2, and (e, f) Minimum droop gain without and with considering constraints, respectively.

Variable Power Factor DERs and Their Effect on Hosting Capacity

Luther Miller, *Student Member, IEEE*, Mahmoud Kabalan, *Member, IEEE*

Abstract— This paper explores the possibility of an increase in Hosting Capacity on utility feeders with variable power factor DERs. Hosting capacity is the ability for a utility power distribution system (feeder) to connect renewable Distributed Energy Resources (DERs) to the grid. Hosting capacity has become a focus for utilities as many seek to implement more DERs for environmental and economic benefits. A feeder's hosting capacity is dependent on national regulatory standards for high and low voltage as well as other factors such as frequency variation and protective device limits. The recently updated IEEE 1547-2018 utility standards regarding DER interconnection highlights a requirement that all newly connected DERs shall be capable of varying their power factor to provide greater output control. A feeder was simulated in the OpenDSS power software and the effects of both standard and variable power factor DER was analyzed in low voltage and high voltage scenarios. The resulting data showed that high and low voltage was more effectively controlled with the variable power factor DER than with today's standard fixed power factor DER. Due to Hosting Capacity's heavy reliance on voltage stability, it can be inferred from the simulation results that the introduction of variable power factor DER shall have a positive effect on hosting capacity for utility feeders.

Index Terms— Hosting capacity, distributed energy resources, software, distribution, reactive power

I. METHODOLOGY

IEEE 1547-2018 states “DER shall be capable of injecting reactive power (over-excited) and absorbing reactive power (under-excited) for active power output levels” [1]. The DER must be able to inject as little reactive power as 44% of the rated apparent power output and absorb as little reactive power as 25% of the apparent power output.

The OpenDSS coding and simulation software developed by the Electric Power Research Institute (EPRI) was selected to perform power system simulations. Both high and low voltage simulations must be performed for each DER scenario to capture a complete image of variable output DER and its effects on a feeder's hosting capacity. A load flow operation within OpenDSS is able to output the voltage, amp and power data that is required for feeder analysis to Microsoft Excel spreadsheets.

To create an accurate feeder simulation, data provided by a local utility was used to determine the distribution line and system characteristics. A single-line diagram similar to the map shown in Fig. 1 including system voltage, line lengths, line material and impedances, load buses and fuses was translated into OpenDSS code.

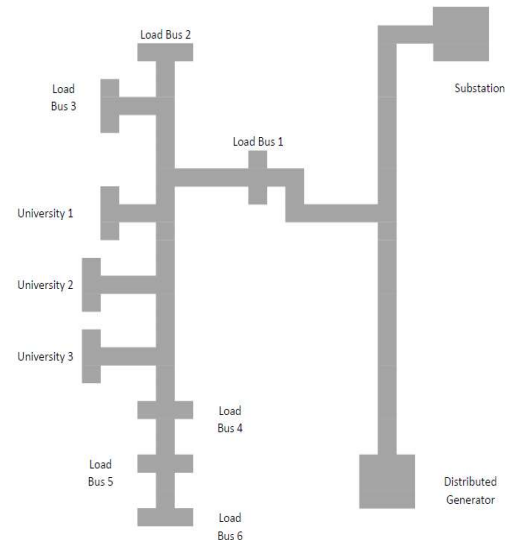


Fig. 1: Feeder outline

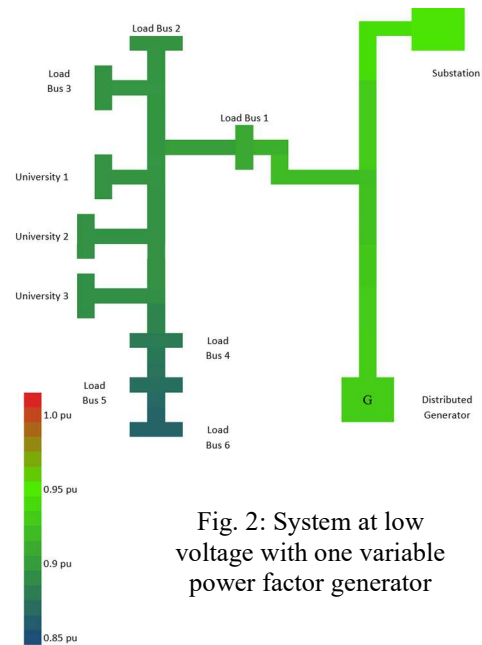


Fig. 2: System at low voltage with one variable power factor generator

REFERENCES

- [1] *IEEE Standard for Interconnection and Interoperability of Distributed Energy Resources with Associated Electric Power Systems Interfaces*, IEEE Std. 1547-2018, February 2018

Resource-Mix Variability Mitigation: EWT Based Optimal Sizing/Control of Hybrid Storage System

Abdul Saleem Mir¹ and Nilanjan Senroy², *Senior Member, IEEE*

Abstract—Temporal diversity via resource-mix is supposed to alleviate issues of adequacy and stability associated with complimentary renewable sources like wind and solar. However, variability/intermittency is still associated with resource-mix generation. Empirical wavelet transform (EWT) based ‘role-dividing-strategy’ (RDS) is proposed/ devised for imbalance power allocation hybrid storage system to mitigate these issues. The proposed scheme exploits the complimentary characteristics of the battery and the ultracapacitor, with battery and ultracapacitor in charge of middle and high frequency power fluctuations of the power imbalance respectively. Based on role dividing strategy, the optimal sizing strategy for ultracapacitor bank and the battery is devised accordingly to ensure balanced flow of energy and maximum utilization of hybrid storage system (HSS) without any overloading condition thereby making the power from resource mix dispatchable. The energy/power rating of HSS needed to make power from resource mix dispatchable is significantly lower the power/energy ratings of HSS required to make solar and wind dispatchable separately. An actual site data of wind and solar power has been used for case studies.

I. INTRODUCTION

Main objectives and associated advantages addressed are listed below:

- To make renewables dispatchable and, improve power system reliability, temporal diversity by mixing complementary NCES like wind and solar has been suggested. To address associated issues of intermittency/variability the use of HSS is proposed.
- Empirical wavelet transform (EWT) based RDS has been proposed for power allocation of individual storage units of the HSS. The rationale of using EWT over other signal processing techniques is its accuracy.
- Based on EWT decomposition of the NCES power, a sizing methodology for individual HSS units (battery and ultracapacitor modules) has been proposed.
- Actual wind and SPV data from a resource-mix site has been used for case studies.

II. EMPIRICAL WAVELET TRANSFORM (EWT) ALGORITHM

Sequential steps of EWT decomposition algorithm :

- 1) Compute the Fourier-transform (\mathcal{F}) of the power command $x(t)$ to be analyzed.
- 2) Use EWT equations to compute the inner products for signal analysis.
- 3) Reconstruct the IMFs using inverse Fourier-transform.
- 4) Divide the reconstructed IMFs into three groups: low frequency components for BES power $P_{BS}(t): [f_{min} f_{max}]$, high frequency components for ultracapacitor power $P_{UC}(t): [f_{max} \infty]$ and trend component for scheduling: $x_0(t) = P_{mix}^{sch}: [0 f_{min}]$.

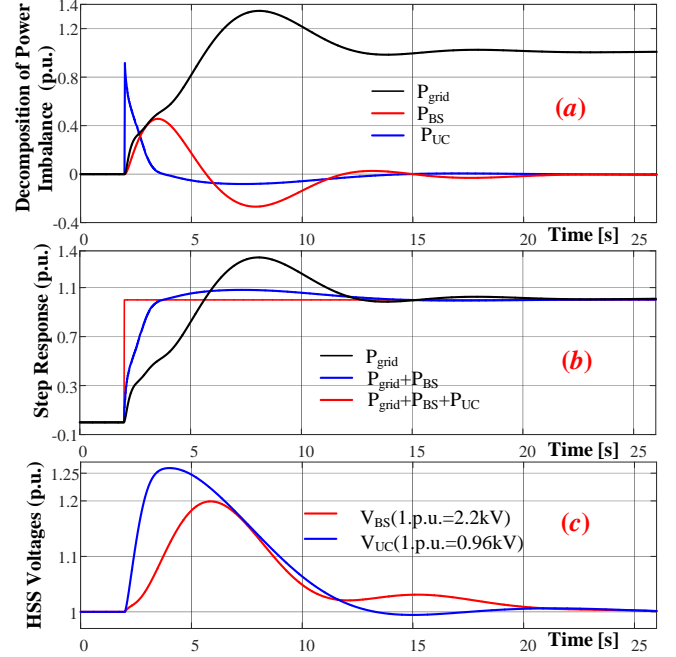


Fig. 4. Illustration of power allocation strategy

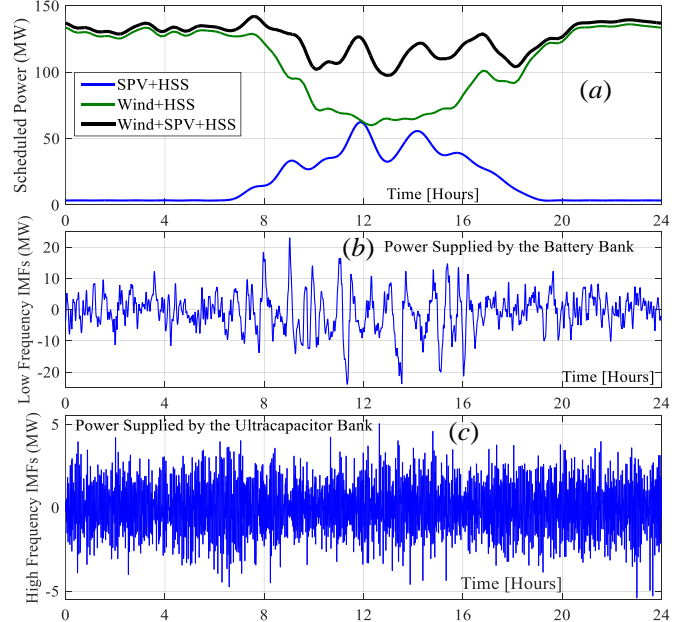


Fig. 8. Decomposition of combined power of wind and solar via EWT.

TABLE I: COMPARISON OF HSS SIZING FOR DIFFERENT SCENARIOS

Storage Size		Solar	Wind	Solar+Wind
Battery Bank	Power (MW)	21.1	15.3	22.2
	Energy (MWh)	117.2	84.5	134.4
UC Bank	Power (MW)	3.121	6.00	5.50
	Energy (kWh)	4.663	7.28	6.584

A Study on Volt-Watt Mode of Smart Inverter to Prevent Voltage Rise with High Penetration of PV System

Jinah Noh
School of Electrical & Electronic Engineering
Yonsei University
Seoul, Korea
njah8712@yonsei.ac.kr

SeokJu Kang
School of Electrical & Electronic Engineering
Yonsei University
Seoul, Korea
ksj8343@yonsei.ac.kr

Jaewoo Kim
School of Electrical & Electronic Engineering
Yonsei University
Seoul, Korea
clog10@yonsei.ac.kr

Jung-Wook Park
School of Electrical & Electronic Engineering
Yonsei University
Seoul, Korea
jungpark@yonsei.ac.kr

Abstract—The penetration of renewable energy sources (RESs) into power systems is increasing, causing problems with power systems. In particular, increases in the output power of RESs cause reverse power flow and voltage rise, which may exceed the upper limit of the grid voltage. To solve these problems, research on control methods for RESs is being conducted to minimize their influence on the grid. This paper proposes a smart inverter control strategy to prevent voltage rise caused by RESs. Specifically, using a method to set parameters for Volt-Watt (VW) mode, the voltage profile of each bus is checked and voltage rise resulting from the injection of active power is prevented. To identify voltage rise problems caused by high penetration of photovoltaic (PV) systems and to confirm the effect of the method proposed in this paper, a simulation test is carried out using the IEEE 30 bus-test system.

Keywords—Energy management system, photovoltaic systems, power curtailment, voltage rise, volt-watt control

I. INTRODUCTION

This paper presents a method for setting voltage parameters for the Volt-Watt (VW) function of Smart Inverter (SI) to prevent power system voltage rise due to high PV penetration.

II. BACKGROUND

The SI operating in VW mode changes the active power based on the voltage at the point of common coupling (PCC). Point arrays that set the active power corresponding to each voltage reduce the active power output at voltages beyond the upper limit value.

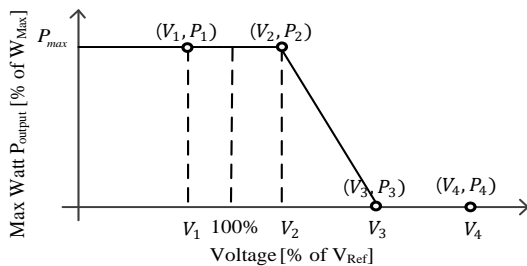


Fig. 1. Curve of VW mode

III. KEY FIGURES

Fig. 2 shows the method for setting the V_{ref} , V_2 , and V_3 of VW curve.

This work was supported in part by Korea Electric Power Corporation (Grant number: R18XA06-80) and in part by the Power Generation & Electricity Delivery Core Technology Program of the Korea Institute of Energy Technology Evaluation and Planning (KETEP) granted financial resource from the Ministry of Trade, Industry & Energy, Republic of Korea (No. 20171220100330).

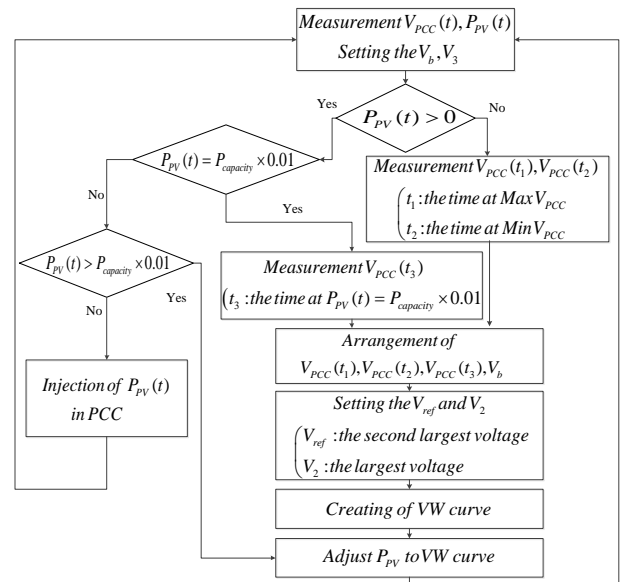


Fig. 2. Flow chart for VW mode

IV. SIMULATION RESULTS

Fig. 3 shows that the voltage width for the proposal model is lower when compared to base case because voltage rise is prevented due to the variation of PV power. The results show that the method employed for parameter setting for VW mode control is effective.

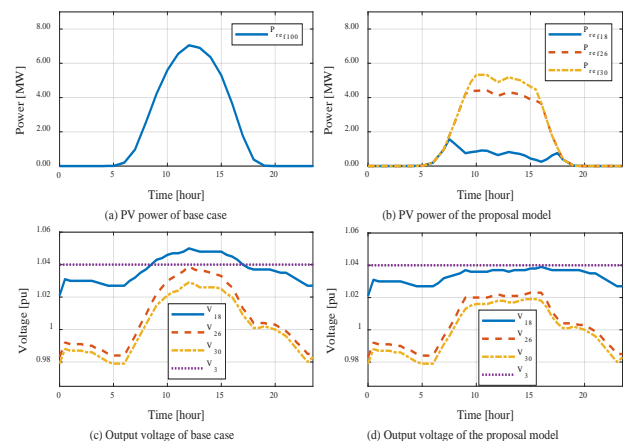


Fig. 3. Comparison of the proposal model and base cases

REFERENCES

- [1] IEC 61850-90-7 — Communication networks and systems for power utility automation - Part 90-7: Object models for power converters in distributed energy resources (DER) systems, International Electrotechnical Commission, IEC, Geneva, Switzerland, Feb. 2013.

Cooperative Dynamic Demand Response Optimization of a Multistory Building

Chirath Pathiravasam, *Student Member, IEEE*, Ganesh K. Venayagamoorthy, *Senior Member, IEEE*

Real-Time Power and Intelligent Systems (RTPIS) Laboratory

The Holcombe Dept. of Electrical and Computer Engineering

Clemson University, SC 29634, USA

Emails: chirathd@ieee.org, gkumar@ieee.org

Abstract –High proliferation of distributed energy resources (DER) demand controllability in the electricity end-use. Demand response is a one of the solutions to mitigate variability of the distribution system. Multistory buildings with substantial solar power generation have the opportunity of controlling their demand to reap benefit in a real-time pricing scheme. Thermostat controlled loads offer a high controllability in scheduling as the flexibility is higher than other loads. In this study, dynamic demand response of HVAC units of the building is considered. Solar power generation and a real-time electricity price signal are evaluated to optimize the HVAC schedule of the building.

Index Terms— demand response; HVAC; energyplus; co-simulation; renewable energy;

I. INTRODUCTION

The power system is confronting a complex set of changes and challenges, including: aging infrastructure, change in the generation mix, growing penetration of variable renewable energy sources, low or negative energy growth, climate change and widespread adoption of distributed energy resources. The modern power grid should be resilient to threats posed by these challenges. Demand response (DR) is identified as an effective solution for this conundrum. The low initial and operational costs of demand response makes it an attractive option to absorb system dynamics of the modern electric grid.

Heating, ventilation and air conditioning (HVAC) can be considered as the end use with the highest potential in demand response participation. This is due to the frequency of its operation, power rating and the flexibility in the desired operating conditions. HVAC units could absorb as well as reduce power usage with minimal disruption of consumer comfort. Essentially, the thermal capacity of a building could be regarded as a thermal energy storage which could be utilized to reduce the effects of an intermittent energy generation such as solar power. The total thermal energy of the buildings can be utilized by a DR aggregator to maximize the revenue, firm variable renewable energy capacity, participate in regulation markets, shave the peak and participate in secondary & tertiary frequency controls.

The objective of this project is to optimize the dynamic demand response of a multistory building with rooftop solar power generation. A real-time price is used as an input to the optimization. The building is modeled in energyplus platform and a matlab-energyplus co-simulation is performed to run the system. Binary particle swarm optimization (BPSO) based algorithm is used to schedule HVAC units in the building in each minute (Fig. 2).

II. KEY FIGURES



Fig 1. A multistory building with rooftop solar power.

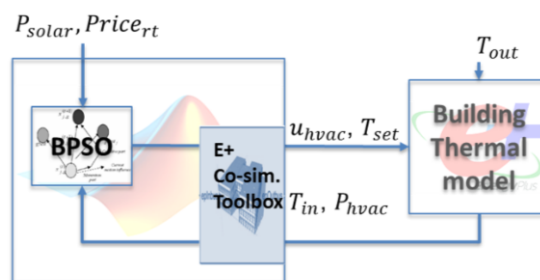


Fig 2. Matlab-energyplus co-simulation platform.

REFERENCES

- [1] Q. Hu, F. Li, X. Fang and L. Bai, "A Framework of Residential Demand Aggregation With Financial Incentives," in *IEEE Transactions on Smart Grid*, vol. 9, no. 1, pp. 497-505, Jan. 2018.
- [2] P. U. Herath *et al.*, "Computational Intelligence Based Demand Response Management in a Microgrid," in *IEEE Transactions on Industry Applications* (early access).

Interaction between Line Impedance and Inverter Control in Low-voltage Microgrid

Ishita Ray, *Student Member, IEEE*
 Bredesen Center for Interdisciplinary Research and Graduate Education
 The University of Tennessee
 Knoxville, TN

Leon M. Tolbert, *Fellow, IEEE*
 Min H. Kao Department of Electrical Engineering and Computer Science
 The University of Tennessee
 Knoxville, TN

Abstract— With increasing penetration of renewable sources and interest in microgrids, much research effort has been directed into improving the power sharing and synchronization capabilities of inverters connected to stiff grids. However, weaker grids completely formed and fed by inverter-connected sources will also be more commonplace in the near future. While some insights gained from the literature on grid-connected inverters are useful in such grids, they also have their own unique challenges. Hence, it is worthwhile to study not only the interaction between inverters but also the impact of other elements of the microgrid on inverter control. This work focuses on the impact of varying line impedance on inverter behavior. For this analysis, the data was collected by simulating an inverter-dominated microgrid using Opal-RT and Simulink. Each inverter can be operated in voltage-control (Vf), current control (PQ, or droop control (Pf-QV) mode. Each control mode was tested at several different X/R ratios as well as three different power levels. This analysis presents interesting observations regarding the behavior of and interaction between inverters by varying X/R ratios.

Keywords—microgrid, line impedance, X/R ratio, inverter control

I. SIMULATION MODEL

The Simulink model for an inverter-dominated microgrid was first built and tested in Simulink. Then, it was converted into an Opal-RT model for faster simulation and rapid data collection. The microgrid model is made up of one battery and one PV array connected through individual inverters to a ZIP load. The data was collected for a combination of power levels (1kW/1kvar, 5kW/5kvar, and 10kW/10kvar), control modes (as shown in Tab.1), and X/R ratios (5.0, 2.0, 1.0, 0.5 and 0.2).

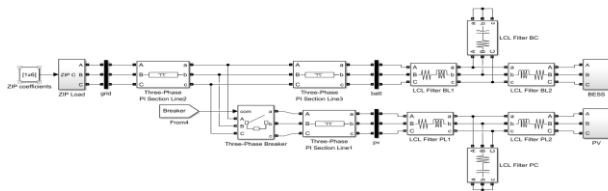


Fig. 1. Simulink model of inverter-dominated microgrid

TABLE I. COMBINATION OF INVERTER CONTROL MODES FOR EACH CASE

Control Mode	BESS	PV
Vf/PQ	Vf Control	PQ Control
Vf/Vf	Vf Control	Vf Control
Droop	Pf-QV Droop	Pf-QV Droop

II. OBSERVATIONS

The data showed that changing the line impedance did, in fact, have an impact on phase error, inverter starting, power sharing, inverter impedance and P-Q coupling. A couple of these results are presented in this section.

A. Equal Output Impedance for Vf and PQ Controlled Inverters

Almost all of the results for inverters in Vf/PQ and Vf/Vf modes were identical. This can be seen in Fig. 2, where the Vf/PQ curves are barely visible as they are overlapped by the Vf/Vf curves. This identical behavior suggests that the output impedance of the PV inverter in PQ and Vf mode is the same, in spite of their disparate control structures.

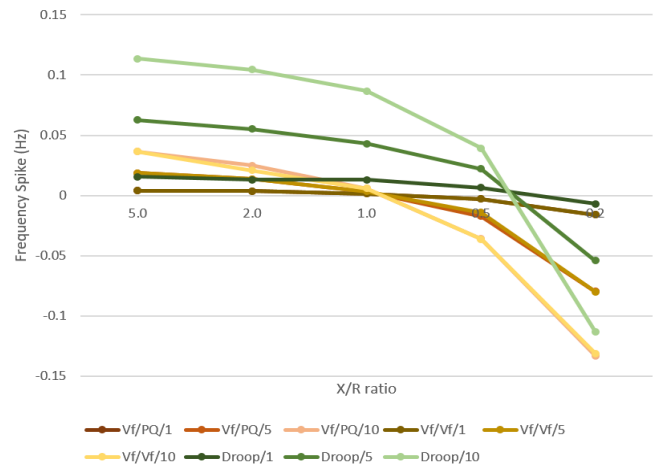


Fig. 2. Impact of varying X/R ratio on phase error (frequency spike)

B. Impact of X/R Ratio on Phase Error

Fig. 2 shows the effect of changing line impedance on the initial phase error when PV is connected to the common AC point. The phase error decreases with increasing line resistance up to a minimum point and then increases in a different direction. The minimum point is reached when the line impedance matches the inverter output impedance for each control case. Droop controlled inverters have a higher output resistance which shifts the point of minimum phase error to a lower X/R ratio.

Performing remote estimations in LV feeders based solely on local monitoring

Valentin Rigoni, *Student Member*, IEEE, and Andrew Keane, *Senior Member*, IEEE
 University College Dublin
 Dublin, Ireland
 valentin.rigoni@ucdconnect.ie; andrew.keane@ucd.ie

Abstract— The increasing adoption of domestic-scale distributed generation is likely to have technical impacts on low voltage (LV) feeders. Consequently, the observability of key system variables is crucial for the identification of statutory limits violation. The problem is that most LV feeders do not have a widespread monitoring/communication infrastructure. Therefore, traditional centralized State Estimation cannot be deployed in the near-term. The latter results in the need for decentralized solutions, focused on practicality and cost-effectiveness, that provide an alternative to utilities. This poster introduces a novel decentralized technique that enables to estimate, from every customer location, remote system variables based solely on local measurements. It consists of solving a maximum likelihood estimation algorithm where full observability is achieved by means of pseudo-measurements.

Keywords—LV networks, smart grids, State estimation

I. METHODOLOGY

The current operating state of a network can be identified with State estimation (SE) [1]. It is a well-known technique used to determine the most likely state of a system based on the network model and a set of m measurements. Assuming errors to have a Gaussian distribution, the latter can be accomplished by solving the maximum likelihood estimation (MLE) in (1):

$$\min \sum_i^m \left(\frac{z_i - E(z_i)}{\sigma_i} \right)^2 \quad (1)$$

where $E(z_i)$ and σ_i are the expected value and the standard deviation of the i th measurement, z_i , respectively. Typically, $E(z_i)$, is expressed as a non-linear power flow equation relating the system state variables to z_i .

Accounting for the lack of full monitoring in LV feeders, some centralized methods have suggested the partial use of pseudo-measurements to achieve full observability [2]. Here, we propose a totally decentralized SE algorithm, solvable autonomously at the location of each customer point of connection (CPOC); where actual monitoring is restricted to the measurement of the local CPOC voltage and the active and reactive power injections of the local DG unit. Therefore, pseudo-measurements (derived from statistical models) are used for $E(z_i)$ and σ_i of the non-monitored demand of all customers. Furthermore, remote DG units' power injections are deduced from those of the local one.

II. RESULTS & DISCUSSION

The method is implemented on a real 3-phase European residential LV feeder with a total of 83 single-phase customers. It is illustrated in Fig. 1, where the dots represent houses and the triangle the head of the feeder. Every house is considered to have a photovoltaic panel (PV) with a fixed power factor regulation. The solar irradiance of all PVs is

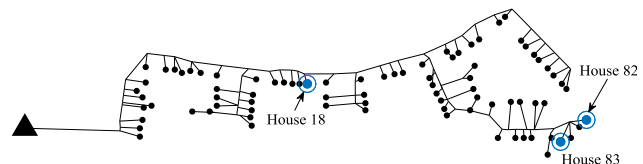


Fig. 1. Real residential LV feeder

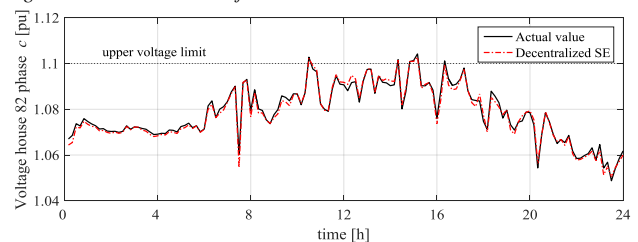


Fig. 2. House 82 phase c actual and estimated voltages – Local monitoring at house 18 phase c

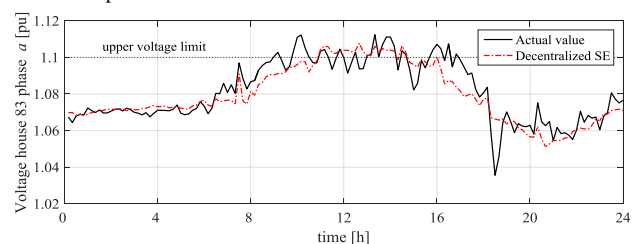


Fig. 3. House 83 phase a actual and estimated voltages – Local monitoring at house 18 phase c

assumed to be uniform given the reduced geographical extension of the feeder. During simulations, local measurements are considered to have no error.

Fig. 2 shows the actual voltage profile for house 82 phase c (end of the feeder) together with the estimations obtained locally from house 18 phase c . The estimations obtained from the proposed method result in a good match for the actual voltage profile; with errors in the order of 1×10^{-3} pu. Nonetheless, as seen in Fig. 3, if the remote house is connected to a phase different from that of the local CPOC, results show a greater gap. Nonetheless, the trend of the voltage increment due to PV generation is still captured. The same accuracy observed in Fig. 2 can be obtained if the local voltage measurement is extended to all 3 phases.

Overall, the obtained results show that local measurements and adequate pseudo-measurements can be enough to provide a reliable estimation of the system state. This combined with its autonomous implementation, places the methodology as a valid alternative to centralized schemes. Future work should expand on integrating a decentralized DG regulation strategy.

REFERENCES

- [1] A. Abur and A. Gomez Exposito, *Power System State Estimation: Theory and Implementation*. 2004.
- [2] A. Angioni, T. Schlösser, F. Ponci, and A. Monti, "Impact of pseudo-measurements from new power profiles on state estimation in low-voltage grids," *IEEE Trans. Instr. Meas.*, vol. 65, no. 1, pp. 70–77, 2016.

Unlocking Linepack Flexibility from Integrated Energy Systems: Convexification Approaches

Anna Schwele, Jalal Kazempour, Pierre Pinson

Center for Electric Power and Energy, Technical University of Denmark, Kgs. Lyngby, Denmark
 {schwele, seykaz, ppin}@elektro.dtu.dk

Abstract—A holistic view of the energy system can help unlock power systems flexibility from interfacing with other energy carriers. Utilizing operational flexibility from the existing energy networks can foster the integration of uncertain and variable renewable power production. We model an integrated energy dispatch to reveal the maximum potential of linepack, i.e., energy storage in pipelines, as a source of flexibility for the power system. To account for both energy transport and linepack in the pipelines in a computational efficient manner, we explore convex quadratic relaxations and linear approximations for the nonlinear and nonconvex formulation of flow dynamics. Flexibility is quantified in terms of system cost compared to a dispatch model that either neglects linepack or assumes infinite storage capability.

I. INTRODUCTION

Apart from ensuring technical feasibility of short-term operations, accounting for the natural gas network unlocks its inherent flexibility in order to facilitate the integration of renewables and deal with uncertainties and variability from large-scale wind power penetration. Our work evaluates social value of short-term operational flexibility that the network can provide to the electricity system. This requires a proper coordination between systems, accurate modeling of flow dynamics, and efficient solution methods.

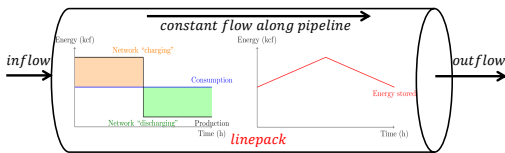


Fig. 1. Linepack as energy storage in pipeline

II. COMBINED ENERGY DISPATCH

The combined energy dispatch from [1] can assess the ability of natural gas networks to react to changes in the power sector due to intermittent renewables and is supposed to reveal the maximum potential of energy storage in the pipelines as sources of flexibility for the power system. The nonconvex co-optimization problem aims at minimizing the total cost of operating the power and natural gas systems. The model contains constraints pertaining to the power and to the natural gas system as well as constraints coupling both systems. We compare second-order cone relaxation and outer linear approximation of the highly nonconvex gas flow constraint, see Fig. 2.

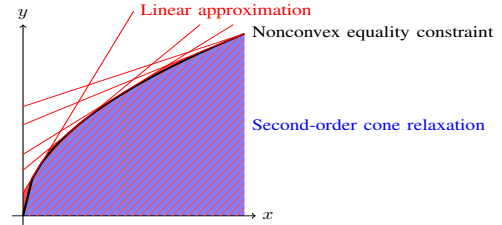


Fig. 2. SOC relaxation and outer linear approximation

III. RESULTS

Fig. 3 shows the total system cost for both convexification approaches under different levels of wind power penetration. The flexibility revealed from the pipelines decreases the total system cost by 2% and 1% on average for relaxation and approximation models, yielding on average a cost saving equal to 25.5% and 13.1% of that in the ideal storage case.

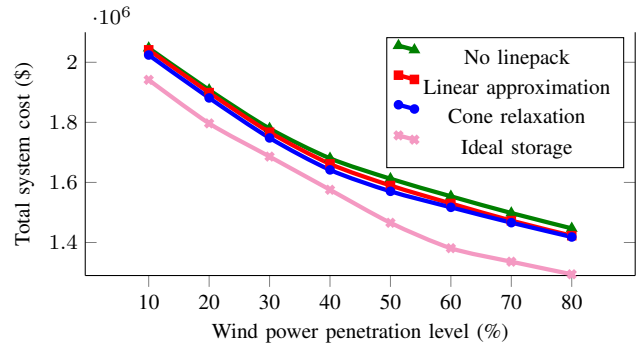


Fig. 3. Total system cost as a function of wind power penetration

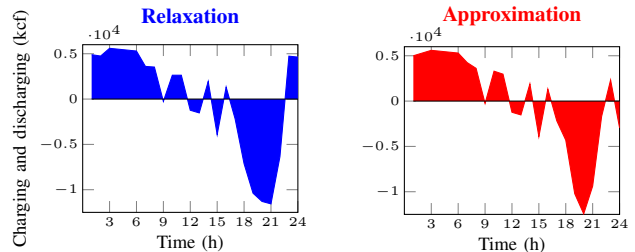


Fig. 4. Hourly charging/discharging profile of linepack storage

REFERENCES

- [1] A. Schwele, C. Ordoudis, J. Kazempour, and P. Pinson, "Coordination of Power and Natural Gas Systems: Convexification Approaches for Linepack Modeling," in *13th IEEE PES PowerTech Conference*. IEEE, 2019.

Design and Control of Storage Systems for Voltage Source Controlled Autonomous Microgrids

Lalitha Subramanian
Student Member, IEEE

Vincent Debusschere
Member, IEEE

Hoay Beng Gooi
Senior Member, IEEE

Abstract—Self-sustainable autonomous microgrids with 100% converter-connected generation are most suitable for powering remote areas without impacting the environment. This work focuses on the regulation aspect of such islanded microgrids by sizing and controlling energy storage systems to support the renewable energy-based microgrids. Each generation unit in the microgrid acts as a voltage-source that contributes to the regulation, wherein the regulation is achieved by a modified droop control that emulates the inertia property of synchronous machines. The size of energy storage systems that support this task is estimated and the designed storage and control are validated with the help of real-time simulation.

I. SUMMARY OF RESULTS

The increasing trend of using converter technologies is taken as the inspiration to power a small, decentralized, and self-sustainable power system. A regulation control scheme based on droop control is adopted and modified to serve as an inertia support to the 100% converter-connected system shown in 1. The storage requirement to meet a given set of steady-state conditions and stability criteria is estimated as shown in table I.

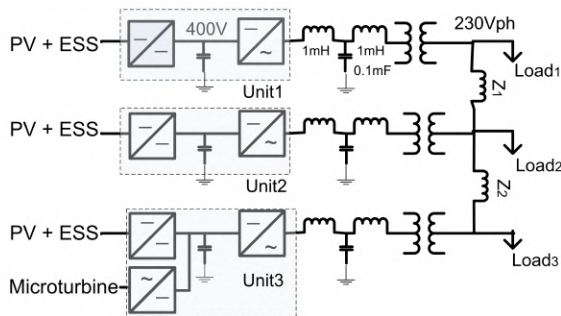


Fig. 1: Schematic of the autonomous microgrid.

TABLE I: ESS Sizing for PFR and IR

PFR sizing		IR sizing	
m_{ess}	0.0036 p.u.	J_{ess}	2 p.u.
Δf_{lim}	± 0.2 Hz	$RoCoF_{lim}$	± 0.5 Hz/s
P_{ess}	24.3 kW	P_{ess}	270 kW
E_{ess}	12.22 kWh	E_{ess}	2.43 kWh
Δf	0.204 Hz	Δf	0.32 Hz
$RoCoF$	0.55 Hz/s	$RoCoF$	0.3 Hz/s
f_{min}	49.52 Hz	f_{min}	49.76 Hz

The microgrid simulation results with droop and inertia control supported by the estimated size of storage is given in fig.

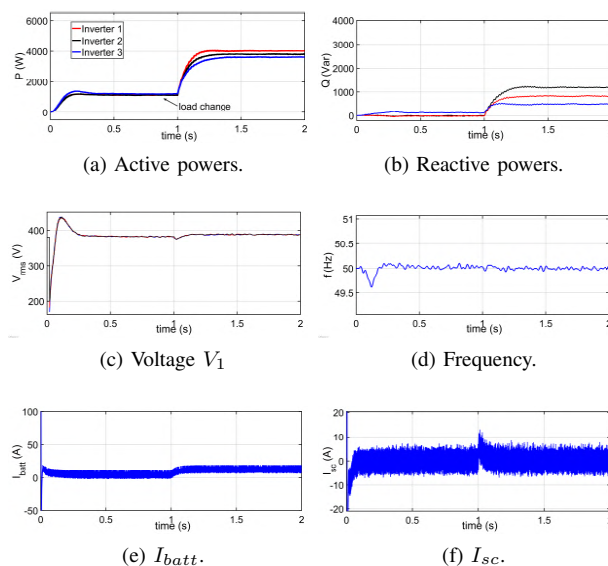
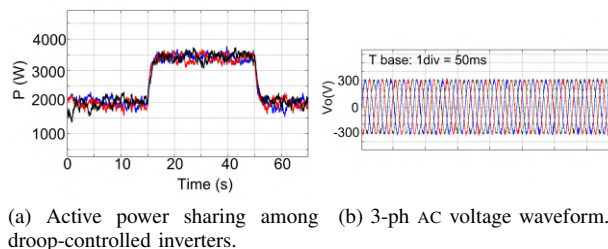


Fig. 2: Inverter waveforms with modified droop control.



(a) Active power sharing among droop-controlled inverters. (b) 3-ph AC voltage waveform.

Fig. 3: Realtime validation of droop control.

2. When the PV current varies due to the solar irradiance, the battery kicks in to balance the power. The simulation results presented in this section are verified in offline simulation and in real-time simulation with OPAL-RT as shown in fig. 3.

II. CONCLUSION

The storage design procedure to perform the PFR, i.e. droop control and the IR, i.e. the VI control for a voltage-source controlled islanded microgrid have been discussed. This work finds its application in remote areas with no access to grid supply and where fossil fuel based generators may not be encouraged.

Levelized Cost Analysis of Medium Voltage DC Fast Charging Station

Lisha Sun, David Lubkeman, Mesut Baran
 Dept. of Electrical and Computer Engineering
 North Carolina State University
 Raleigh, USA

Abstract—With improvements in wide-band gap power electronics technology, it is becoming feasible for a DC fast charging station to connect directly to the distribution primary medium voltage (MV) service. This paper provides a comparative levelized cost analysis of a novel MV DC fast charger to commercial 480V DC fast charger technology. The advantages of the MV DC fast charger include a higher efficiency, a considerable reduction in weight and volume, and savings in eliminating the step-down transformer. In order to compare the operational cost of these DC charger options, the impact on system losses and peak demand are quantified through quasi-static time-series distribution feeder simulation. Based on this, the levelized cost of energy is estimated for two ownership models: utility-owned (DC as a service) and customer-owned. The results indicate that the utility-owned MV DC fast charger has the lowest levelized cost of energy based on the example feeder system analyzed.

Index Terms—Charging station, DC fast charger, Electric vehicle, Levelized cost of energy, Medium voltage DC fast charger

I. DC FAST CHARGER AND MODELLING METHOD

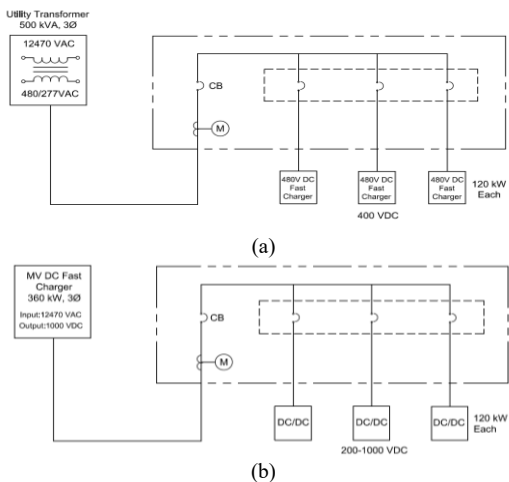


Figure 1. DC Fast Charging Station Diagram (a) 480V Connected DC fast charger (b) MV DC fast charger.

II. FEEDER SIMULATION RESULTS

TABLE I. DC FAST CHARGING STATION YEARLY SIMULATION RESULTS

Category	EV Load MWh	Energy MWh	Peak kW	Total Loss MWh	Line Loss MWh	Dist. XFMR Loss MWh	FC XFMR Loss MWh	FC Loss MWh
Base	0	23,385	6,933	682	82	600	-	-
480V FC	462	23,950	7,034	787	86	600	17	85
MV FC	462	23,869	7,015	707	85	600	NA	21
480V FC - Base	462	564	100	105	4	0	17	85
	NA	2.4%	1.4%	15.5%	0.6%	0.0%	2.5%	12.4%
MV FC - Base	462	484	82	25	3	0	NA	21
	NA	2.1%	1.2%	3.6%	0.5%	0.0%	NA	3.1%
480V - MV	0	80	18	81	1	0	17	63

III. LEVELIZED COST ANALYSIS

TABLE II. UTILITY-OWNED FC LEVELIZED COST OF ENERGY ANALYSIS RESULTS (DC AS A SERVICE)

Cost Worksheet		MV FC	480V FC
Labor	Installation	\$ 28,728	\$ 47,880
	Drawing, Permit, Site Visit etc.	\$ 4,484	\$ 4,484
Materials	Charger Cost (360kW)	\$ 176,400	\$ 176,400
	Meter, Circuit Breaker, Wire, Conduit etc.	\$ 3,606	\$ 3,084
	Transformer	\$ -	\$ 17,500
Other	Concrete Work	\$ 2,520	\$ 4,200
Total Front Cost		\$ 215,737	\$ 253,548
Operation Cost (year)	Network Fees	\$ 140	\$ 140
	Regular Maintenance	\$ 700	\$ 700
	Extra Loss (\$50/MWh)	\$ 1,050	\$ 5,100
	Extra Demand (\$100/kW)	\$ 8,200	\$ 10,100
Total Operation Cost Each Year		\$ 10,090	\$ 16,040
Life-time Cost for 15 Years		\$ 292,483	\$ 375,549
Annualize Cost per Year at 10%		\$ 38,454	\$ 49,375
Charger Cost per kWh		\$ 0.083	\$ 0.107
Cost of Energy per kWh		\$ 0.05	\$ 0.05
Levelized Cost of Energy \$/kWh		\$ 0.13	\$ 0.16

Model Predictive Frequency Control of Low Inertia Power Systems

Ujjwol Tamrakar[†], Timothy M. Hansen,
and Reinaldo Tonkoski
South Dakota State University
Brookings, South Dakota, USA

David A. Copp
Sandia National Laboratories
Albuquerque, New Mexico, USA

Abstract—In low inertia power systems, fast-frequency control strategies are desired to maintain frequency stability. A model predictive control (MPC) approach is proposed to maintain the frequency stability of low inertia power systems such as microgrids. Using a simple predictive model, MPC computes control actions by recursively solving a finite-horizon, online optimization problem that satisfies peak power output and ramp-rate constraints.

I. KEY EQUATIONS

The set $\mathcal{T} := \{t, t + \tau, \dots, t + T - \tau\}$ is defined as the discrete times in the finite-forward time horizon. T is defined as the length of the time horizon, which is a multiple of the time step τ . Defining $x_k = [\Delta\omega_k \ \Delta\dot{\omega}_k]^\top$ as the discrete states of the system, the proposed MPC formulation will take the following form [1]:

$$\text{minimize } J = \sum_{k=t}^{t+T-\tau} (x_k^\top Q x_k + \Delta p_k^\top R \Delta p_k) \quad (1a)$$

$$+ x_{t+T}^\top Q^f x_{t+T}$$

subject to

$$x_{k+\tau} = A x_k + B \Delta p_k \quad \forall k \in \mathcal{T}, \quad (1b)$$

$$|\Delta p_k| \leq P_{max} \quad \forall k \in \mathcal{T}, \quad (1c)$$

$$\|\Delta p_{k+\tau} - \Delta p_k\|_\infty \leq S \quad \forall k \in \mathcal{T}, \quad (1d)$$

where $\Delta\omega$ and $\Delta\dot{\omega}$ are change in frequency and the rate-of-change-of-frequency (ROCOF), A and B are the discretized state-space matrices of the system. J is the cost-function to be minimized, and Q and R are the weighting matrices. The weighting matrix Q can be used to penalize poor system performance (i.e., to penalize change in frequency and/or ROCOF), while matrix R is used to penalize the control effort. Similarly, Q^f is a terminal cost weighting matrix.

II. KEY FIGURES

The simulation setup used is illustrated in Fig. 1. The MPC formulation was implemented using CVXGEN. The weighting parameter values used were $Q_{11} = 0.7$, $Q_{22} = 0.5$ and $R = 0.0001$.

III. KEY RESULTS

Figure 2 shows the reduction in the frequency and ROCOF of the system with the MPC controller for a step change in the load. Both the constrained and the unconstrained cases are highlighted. For the constrained operation the peak power output of the inverter is limited to 0.15 p.u. which accordingly leads to higher excursions in the frequency and the ROCOF.

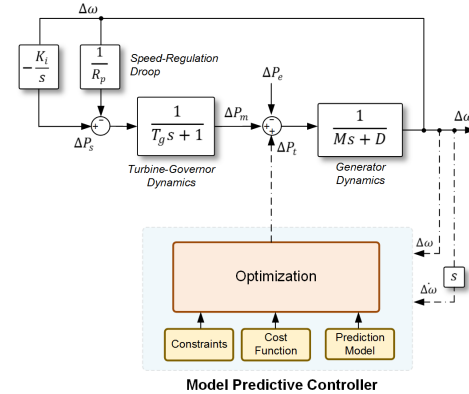


Fig. 1: Simulation setup for model predictive frequency controller implementation.

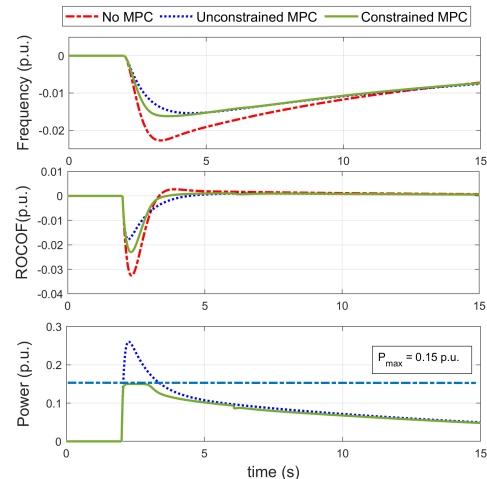


Fig. 2: Constrained and unconstrained MPC for frequency control.

IV. CONCLUSIONS AND FUTURE WORK

A model predictive frequency controller was able to provide fast-frequency control while respecting the physical constraints of the inverter. In the future the computational feasibility and the effect of MPC parameters like prediction and control horizons on the performance will be analyzed.

REFERENCES

- [1] U. Tamrakar, D. A. Copp, T. M. Hansen, and R. Tonkoski, "Model Predictive Frequency Control of Low Inertia Microgrids," in *28th IEEE International Symposium on Industrial Electronics*, accepted 2019, to appear.

Optimal Design and Operation Cost of Distributed Energy Resources in a Isolated Microgrid

Fatemeh Tooryan, Edward R. Collins

Holcombe Department of Electrical and Computer Engineering Clemson University, Clemson, SC 29634, USA

ftoorya@clemson.edu, collins@clemson.edu

Abstract—To extract maximum potential benefits from the Distributed Energy Resources (DERs), the optimal planning of such sources has always been a topic of great interest. This poster presents the design, operation and dispatch strategy for the hybrid system of Photovoltaic (PV), Wind Turbine (WT), Battery Energy Storage (BES) and Micro-turbine (MT) for isolated microgrid. First, models of all component are developed. Then, optimization algorithm that minimizes the Annual Present System Cost (APSC), the total system loss and optimizing the voltage profile along the feeders are developed to find the allocation of DERs.

Index Terms—Annual Present System Cost (APSC), battery energy storage (BES), dispatch strategy, microgrids, optimization

I. INTRODUCTION

Distributed Energy Resources (DERs) have been receiving increasing attention over the past decade considerably as alternatives to centralized generation. A microgrid is technically a low voltage distribution network that integrates DERs. The DERs' benefits are highly location sensitive in nature, which needs to be factored into these cost studies. This poster presents the design procedure, operation and dispatch strategy of a hybrid system of PV, WT, BES and MT in isolated microgrid. The optimal sizes and locations of DERs in islanded microgrid are determined. Annual Present System Cost (APSC), which contains Annual Initial Cost(AIC), Annual Operation Maintenance Cost (AOMC), annual Replacement Cost (ARC), Annual Loss Cost (ALC) and Annual Fuel Cost (AFC) are minimized subjected to the microgrid's configuration and operation constraints to achieve optimal allocation. The priority for supplying the load demand is in the order of renewable energy resources (WT and PV), BES then MT respectively. The design process is verified by extensive simulations. In the microgrid, the optimum location is determined by considering total system loss and voltage profile of the buses.

II. KEY EQUATIONS

A. Problem Formulation

$$APSC = AIC + AOMC + ARC + ALC + AFC \quad (1)$$

1) **Annual Initial Cost (AIC):**

$$AIC = \left(\frac{(1 + \alpha)^y - 1}{\alpha \times (1 + \alpha)^y} \right) \times I_C \quad (2)$$

2) **Annual Operation and Maintenance Cost (AOMC):**

$$AOMC = \left(\frac{(1 + \alpha)^y - 1}{\alpha \times (1 + \alpha)^y} \right) \times OP_C \quad (3)$$

3) **Annual Replacement Cost (ARC):**

$$ARC = \sum_{n=1}^{\gamma} \frac{1}{(1 + \alpha)^{Ld \times n}} \times R_C \quad (4)$$

4) **Annual Loss Cost (ALC):**

$$ALC = \left(\frac{(1 + \alpha)^y - 1}{\alpha \times (1 + \alpha)^y} \right) \times \gamma_1 \times \sum_{t=1}^{8760} Loss(t) \quad (5)$$

5) **Annual Fuel Cost (AFC):**

$$AFC = C_f \times \sum_{t=1}^{8760} a \times P_{MT}(t) + b \times P_{MTR}(t) \times S(t) \quad (6)$$

III. KEY RESULTS

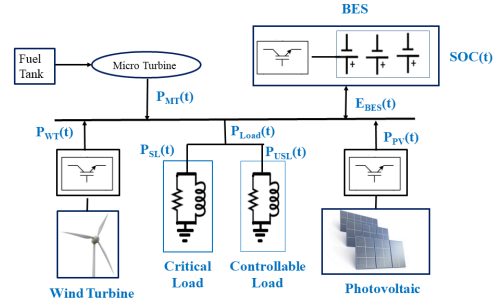


Fig. 1: Isolated microgrid system

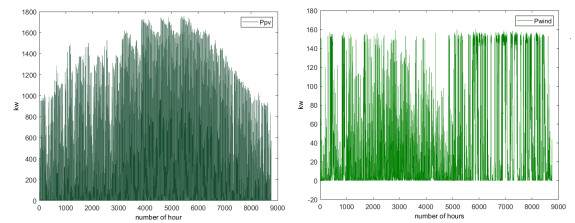


Fig. 2: WT and PV output power

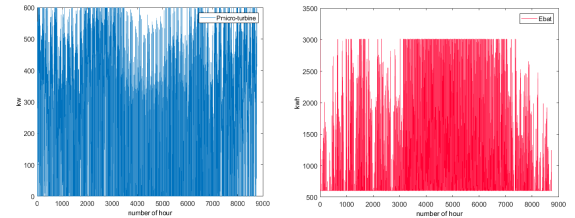


Fig. 3: BES and MT output power

Improved Reactive Power Sharing Between Droop Controlled Inverters In Islanded Microgrid

Vishal Verma, *Student Member, IEEE*, Sarika K. Solanki, *Senior Member, IEEE*,
and Jignesh Solanki, *Senior Member, IEEE*

Abstract—Generally, a droop control is used for power sharing among DGs in islanded microgrid. Problem of reactive power sharing among distributed generators (DGs) when using droop strategy as primary control is studied here. It has been observed that droop control strategy results in proper sharing of real power but reactive power sharing among DGs deteriorates. A modified droop strategy is proposed here that improves the reactive power sharing between distributed generators (DGs) without any secondary controller. Advantage of this droop strategy is that it only uses local measurements.

Index Terms—Distributed Generators, droop control, primary control, islanded microgrid.

I. INTRODUCTION

DURING the past decade or few DGs have attracted a number of researchers due to recent advancements in their control and their plug and play feature. Control of these DGs, such as wind, photovoltaics etc. refers to the control of power converter through which they are connected to the microgrid. Control hierarchy of these DGs can be divided into three stages, namely, primary control, secondary control, and tertiary control [1].

Each control scheme have their own advantages. Such as secondary and tertiary control for proper power sharing, strictly regulating the voltage, power management etc. but it requires a communication link. On the other hand, improper power sharing of frequency and voltage from their set point are drawbacks of primary control but this type of control does not require any communication link and can be used in islanded microgrid. Droop control and VSG control are widely used primary control strategies to control islanded microgrid. Here authors investigate reactive power sharing due to droop control; the conventional droop control to improve the reactive power sharing among DGs.

To overcome the drawbacks of conventional primary control in LV microgrid and improve the system stability, a P-f droop can be used. Line impedance can be made inductive by adding a virtual output impedance to the primary control and thus a P-f droop can be used in such cases.

To overcome shortcomings such as improper power sharing, use of secondary controller [2], and use of evolutionary algorithms, this paper proposes a simplified droop strategy which just uses an offset in reactive power droop to improve the reactive power sharing between DGs.

II. AN IMPROVED DROOP CONTROL FOR PROPER REACTIVE POWER SHARING

The control strategy developed is carried out in dq-frame instead of abc-frame.

$$\omega = \omega_{ref} - m_P P \quad (1)$$

$$V_d = V_{d_{ref}} - m_Q Q + k_P v_d i_q \quad (2)$$

Where k_P is the new droop coefficient which helps in decoupling P from Q. The proposed approach modifies the d-axis voltage, which eventually helps in better reactive power sharing, by adding an offset from the instantaneous real power ($v_d i_q$).

III. RESULTS

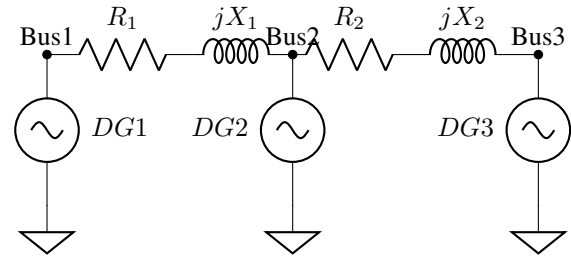


Fig. 1. Islanded microgrid

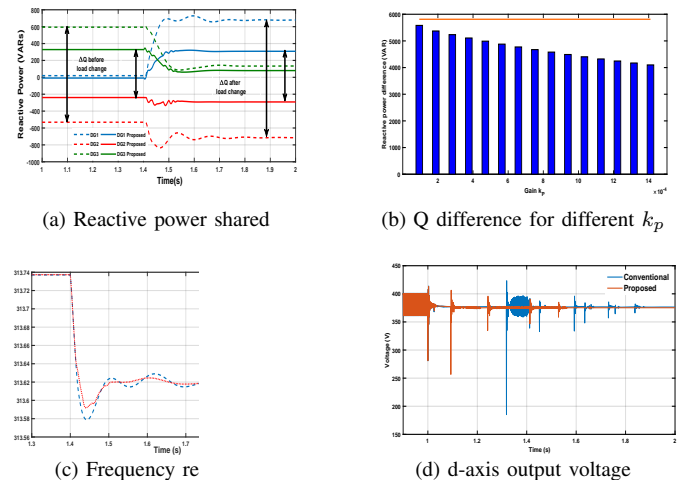


Fig. 2. Response to step change in load at Bus1

REFERENCES

- [1] Joan Rocabert, Alvaro Luna, Frede Blaabjerg, and Pedro Rodriguez. Control of power converters in ac microgrids. *IEEE transactions on power electronics*, 27(11):4734–4749, 2012.
- [2] Zishun Peng, Jun Wang, Daqiang Bi, Yuxing Dai, and Yeting Wen. The application of microgrids based on droop control with coupling compensation and inertia. *IEEE Transactions on Sustainable Energy*, 9(3):1157–1168, 2018.

Active Fault Management for Networked Microgrids

Wenfeng Wan, *Student Member, IEEE*, Yan Li, *Student Member, IEEE*, Bing Yan, *Member, IEEE*, Mikhail A. Bragin, *Member, IEEE*, Jason Philhower, *Senior Member, IEEE*, Peng Zhang, *Senior Member, IEEE*, and Peter B. Luh, *Life Fellow, IEEE*

Abstract—This paper presents Active Fault Management for Networked Microgrids (AFM-NM) to manage microgrids during faults. First, AFM-NM is formulated as an online optimization problem so that customized objectives and constraints can be conveniently added to the formulation. Second, the coordination of each microgrid’s AFM is enabled by the Surrogate Lagrangian Relaxation (SLR) method to allow distributed computation with guaranteed convergence.

Keywords—active fault management (AFM), networked microgrids (NMs), faults, ride through

I. INTRODUCTION

NETWORKED microgrids (NMs) are able to provide resiliency benefits by sharing power during extreme events and further improving reliability for critical loads. One challenge of fault management is occurrence of undesirable variables: large currents into the main grid, and double-frequency power ripples. The second challenge of NMs’ fault management is achievement of convergent coordination among a cluster of individual microgrids.

II. PROPOSED METHOD

To address the above two challenges, AFM-NM (Fig. 1) is first formulated as an online optimization problem, which supports plug-and-play. Second, an efficient and reliable SLR method is offered as an AFM-NM solver (Fig. 2). Within SLR, after relaxing system constraints, the resulting relaxed problem is decomposed into N subproblems, each subproblem belonging to each microgrid’s AFM. Comparison results with a conventional ride-through method show AFM-NM achieves desirable trade-offs between different objectives. Comparison with centralized AFM demonstrates distributed AFM-NM ensures convergence and accuracy (Table I).

TABLE I
COMPARISON BETWEEN DIFFERENT FAULT MANAGEMENT METHODS

Methods	Fault current contribution	Power ripples
Distributed AFM-NM	0.00%	4.77%
Conventional ride-through method	13.55%	12.77%
Centralized AFM	0.00%	5.75%

This work was supported in part by the National Science Foundation under Grants ECCS-1611095, CNS-1647209 and ECCS-1831811, and in part by the Office of the Provost, University of Connecticut. All authors are with the Department of Electrical and Computer Engineering, University of Connecticut, Storrs, CT 06269, USA (e-mail: peng.zhang@uconn.edu).

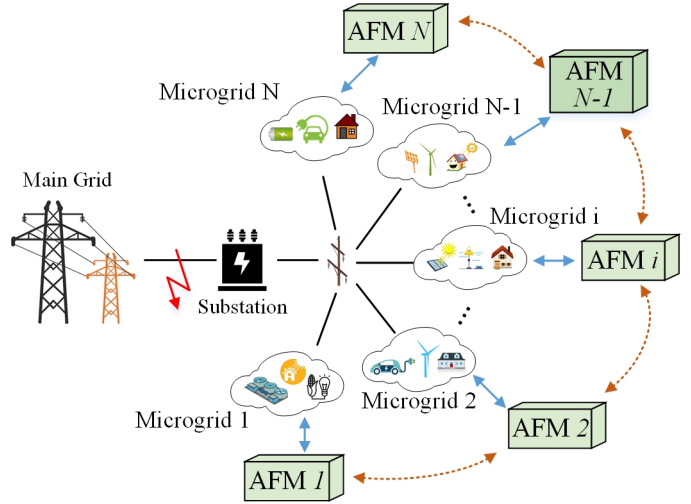


Fig. 1. Schematic of AFM for N networked microgrids (NMs).

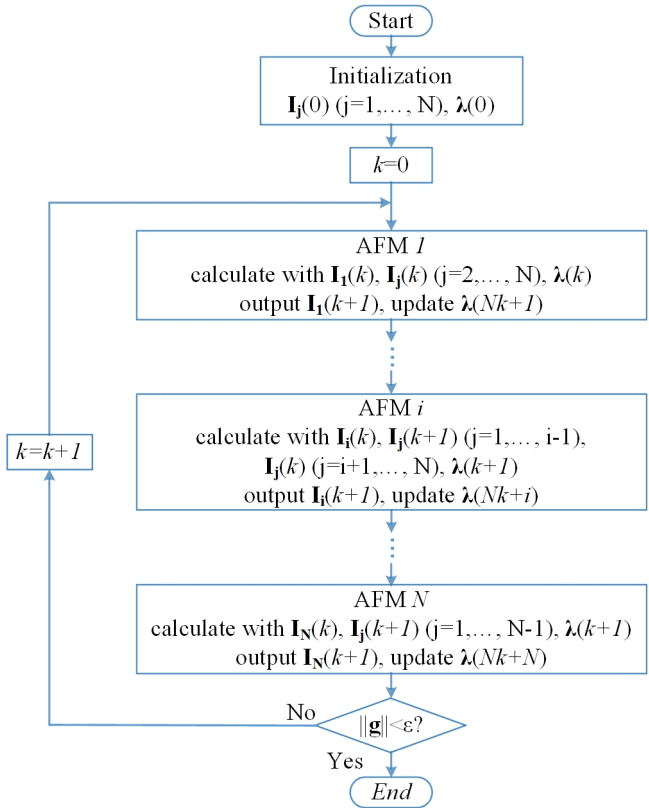


Fig. 2. AFM-NM’s computation process.

Energy Storage Sizing for Dispatchable Constant Production PV Power Plant

Qianxue Xia, *Student Member, IEEE*, Maryam Saeedifard, *Member, IEEE*, and Suman Debnath, *Member, IEEE*

Abstract— This paper presents a novel optimal sizing algorithm for the energy storage system (ESS) of a grid-connected PV solar farm, located in Pittsburg, CA, by minimizing the total annual cost. The algorithm involves time series simulations using one-year data where the “PV+ESS” system is designed to be dispatchable. Two-day simulation scenarios are performed to find the best suitable predominated intervals for constant power output. The results of two-day simulations will be confirmed by one-year simulation scenarios with the same power generation configuration. This paper also includes one-year simulation for the hourly generation pattern of the PV plant.

Index Terms—Energy storage, grid integration, large-scale Photo Voltaic (PV) plant, power generation scheduling.

I. PROBLEM FORMULATION

THIS paper proposes and compares the methods for battery sizing of a large-scale PV system; it also described how the constant steps of power generation for a PV farm can be achieved and implemented. In two-day simulation scenarios, the PV system seeks to optimally operate the PV+ESS over a time horizon of two days. The system produces constant power within each time interval at different power levels. The number of time intervals is determined by several factors including the market electricity price and PV generation. The generation patterns considered in this work are:

- The n interval constant power output configuration ($nICPO$) defines a P_{Grid} , which is the output of the PV+ESS system, consisting of n different power steps throughout the day, $n=1,2,\dots,23$.
- The hourly constant power output ($HCPO$) configuration represents P_{Grid} with hourly varied constant generation output.

The two-day simulation averages the PV output within each hour throughout summer and winter. Summer is chosen to be from April to October and winter is defined from November to March according to the fluctuation of locational marginal prices (LMP).

II. CASE STUDIES

The simulation results for different generation patterns are presented in Table 1. This table contains the optimal size of ESS and the simulation time for different power pattern configurations. One $4ICPO$, two $5ICPO$ with different time interval and $6ICPO$ configurations are studied. Compared to other configurations, the $5ICPO2$ is within the range of ESS size determined by the calculation of baseload generation while providing more redundant and better suitable generation pattern. Thus, $5ICPO2$ is chosen to be the optimum configuration for Pittsburg. The designed constant power output for each

time interval is shown in Table 2. The variations of the outputs through 24 hours in summer and winter are illustrated in Figure 1. The total revenue of the integrated PV system with ESS presented in Table 2 is \$4,836,681 for this 100 MW PV power plant.

Table 1: Two-day simulation results for Pittsburg

Power pattern configurations	Optimum size of ESS (MWh)	Simulation time (s)
$4ICPO$ – Pittsburg	275447	0.047
$5ICPO1$ – Pittsburg	90625.7	0.047
$5ICPO2$ – Pittsburg (different time interval)	91701.2	0.078
$6ICPO$ – Pittsburg	48937.2	0.047

Table 2: Two-day simulation results for $5ICPO2$ in Pittsburg

Objective function value: \$4,836,681.9	
Grid Revenue: \$6,021,514.5	
Cost of Battery: \$1,690,800.0	
Power capacity of Battery: 33.3 MW	
P_1 : 0 MW	P_6 : 0.942 MW
P_2 : 9.659 MW	P_7 : 1.400 MW
P_3 : 60.925 MW	P_8 : 54.767 MW
P_4 : 17.403 MW	P_9 : 26.555 MW
P_5 : 0 MW	P_{10} : 0 MW

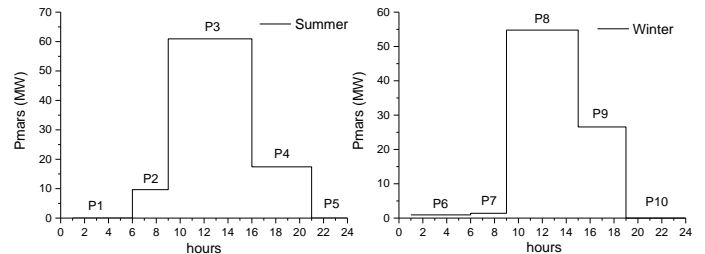


Figure 1: Output power level for optimum configuration pattern in Pittsburg.

The $HCPO1$ and $HCPS2$ represent two different hourly constant power step configurations. By setting different upper limits of battery state of energy, the capacity of battery will be different. From Table 3, ESS size for $HCPO2$ is 91,700 MWh, which is close to the two-day simulation. The $5ICPO$ under one-year simulation has the longest simulation time and this shows the advantage of two-day simulation.

Table 3: One-year simulation results for Pittsburg

Power pattern configuration	ESS size (kWh)	Simulation time (s)
$5ICPO$ – Pittsburg	11,419,500	31.895
$HCPO1$ – Pittsburg	110,000	1.703
$HCPO2$ – Pittsburg	91,700	1.64

Numerical simulations demonstrate the effectiveness of the proposed algorithm and confirms the designed PV+ESS system is capable of providing constant stable power to the grid.

Characterization of Congestion in Distribution Network Considering High Penetration of PV Generation and EVs

Jinping Zhao¹, *Student Member, IEEE*, Ali Arefi¹, *Senior Member, IEEE*, Alberto Borghetti², *Fellow Member, IEEE*, Javid Maleki Delarestaghi¹, *Student Member, IEEE*, GM Shafiullah¹, *Senior Member, IEEE*

¹School of Engineering and Information Technology, Department of Electrical Engineering, Energy and Physics, Murdoch University, Perth, Australia, Jinping.zhao@murdoch.edu.au, Ali.arefi@murdoch.edu.au

²Department of Electrical, Electronic, and Information Engineering, University of Bologna, Bologna, Italy

Abstract—This paper at first discusses the limitations of traditional congestion definition, then characterizes congestion and congestion management procedures in distribution network. Besides, metrics of congestion both in short-term and long-term horizon are proposed. Simulation tests on IEEE-33 bus distribution test system illustrate the impacts of the presence of PV generation and EV charging station on violations of current and voltage limits that are the two main reasons for congestion. An effective control algorithm of PV units and EV charging stations can play an essential role in the mitigation of congestions.

Keywords – congestion, congestion management, distribution network, electric vehicle, photovoltaic

I. CHARACTERIZATION OF CONGESTION

Congestion management (CM) is an important guarantee for safe, stable, efficient operation of whole system. A sequence of the typical objectives of CM methods in distribution networks is to:

- meet the requirements of voltage quality in terms of magnitude and balance degree;
- give priority to important customers, especially when the capacity of flexibilities is limited;
- generate an optimal scheduling and network configuration in different circumstances to maximize the benefits for customers, power utility and network;
- propose backup scheme as a response to failures.

II. PROPOSED METRICS OF CONGESTION

Short-term metrics or metrics for a daily operational congestion contain the congestion probability, duration, electricity price changes caused by congestion, and the congestion level. These short-term metrics will build up the long-term metrics. Long-term metrics (monthly, seasonally or yearly calculated) refer to the total congestion frequency and duration, average congestion levels (both for current violations and voltage violations), congestion costs and total required energy in congested areas.

III. SIMULATION RESULTS

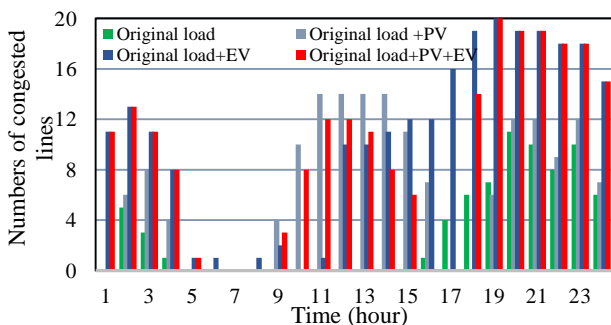


Fig. 1 Numbers of congested lines from 1:00 to 24:00

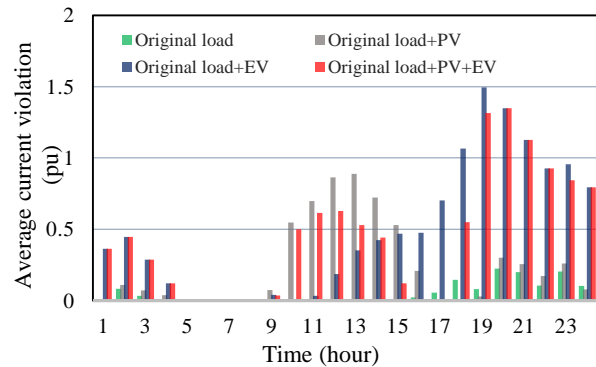


Fig. 2 Hourly average of current violations during a day

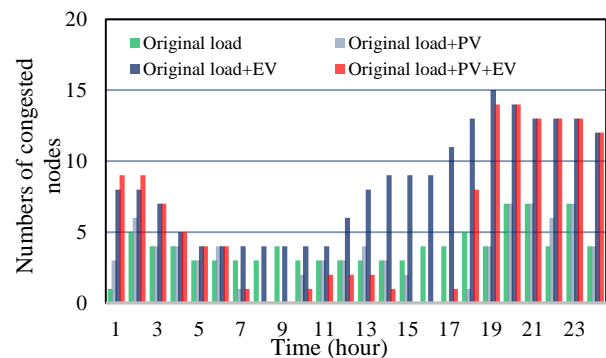


Fig. 3 Numbers of congested nodes from 1:00 to 24:00

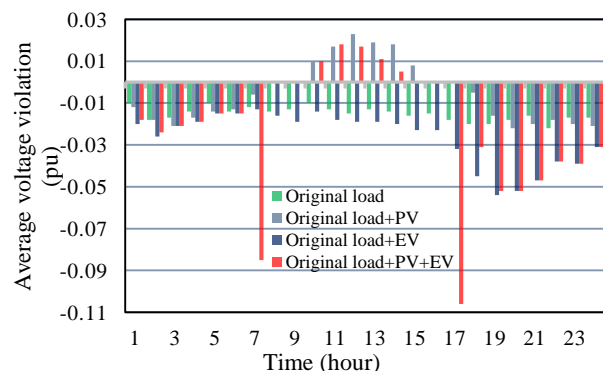


Fig. 4 Average voltage violation from 1:00 to 24:00

IV. CONCLUSION

In this paper, we outline the specific characteristics of congestion events and the typical metrics to assess the adequacy of CM approaches in distribution networks. The simulation test illustrates the effects of different combination of load, PV production and the charging of EVs on congestions. The results suggest that congestion area increase to a great degree by considering also voltage violation in addition to overcurrent conditions.

Natural Hazard Awareness and Sequential Restoration for Distribution Systems and Microgrids

Ogbonnaya Bassey, Karen L. Butler-Purry
Texas A&M University, College Station TX, USA

Chen Chen, Bo Chen, Shijia Zhao, Jianzhe Liu, Yichen Zhang
Argonne National Laboratory, Lemont IL, USA

Abstract— The major stages of natural hazard awareness for pre-event and post-event damage is presented. The information obtained from the post-event damage analysis can be used to implement an emergency restoration scheme by the formation of autonomous microgrids. Operation considerations during black start restoration for droop-controlled autonomous microgrids are highlighted and simulation of a small test system is presented.

Keywords—Hazard awareness, restoration, droop control, microgrid, black start

I. NATURAL HAZARD AWARENESS

Natural hazard awareness, which refers to pre-event failure probability analysis and post-event damage assessment in this work, can be carried out in 3 major steps: (1) Generate weather metric of extreme weather events; (2) Prepare fragility model of test systems which describes the behavior of electric components in test system under extreme weather events; (3) Acquire damage status of components in test system subject to specific extreme weather events.

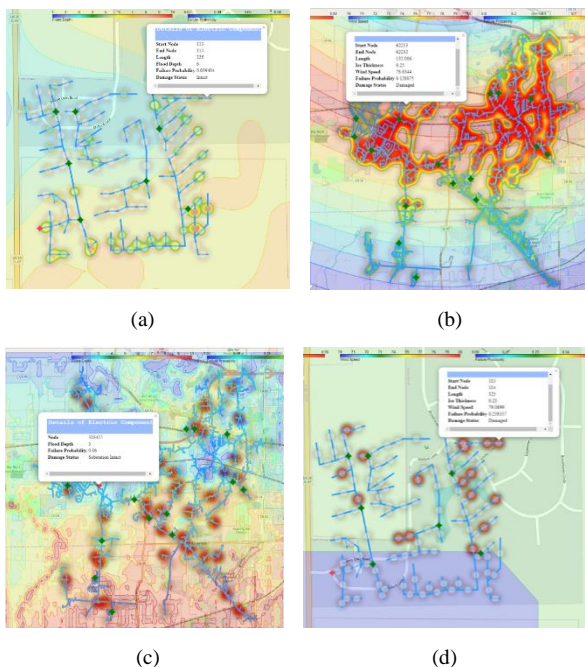


Fig. 1. Damage status and failure probability of IEEE-123 bus test system and a large-scale test system. a): Failure probability of IEEE-123 bus test system under flood; b): Failure probability of large-scale system under winter storm; c): Damage status of large-scale system under flood; d): Damage status of IEEE-123 bus test system under winter storm

II. RESTORATION BY FORMATION OF AUTONOMOUS MICROGRIDS

Formation of multiple microgrids could help in restoring different parts of an affected system after a natural disaster. Each of the formed microgrids is expected to share loads, maintain frequency and voltage profile in the islanded system.

Selecting the droop settings is a compromise between sensitivity and stability as high droop co-efficient improves sensitivity while reducing the stability margin and vice versa.

III. SIMULATION RESULT

Figs. 2 and 3 show some responses during the black start restoration of a small autonomous microgrid.

Sequence 1: DG 1 and DG 2 are turned on at 0 seconds together with load 1.

Sequence 2: Load 2 is restored at 3 seconds.

Sequence 3: At 6 seconds, DG 3 is connected to the system via some synchronization check for matching the voltage magnitude and phase at the point of interconnection and the droop settings are updated.

Notice the sustained oscillation resulting from increasing the frequency droop coefficients in Figs. 2b and 3b.

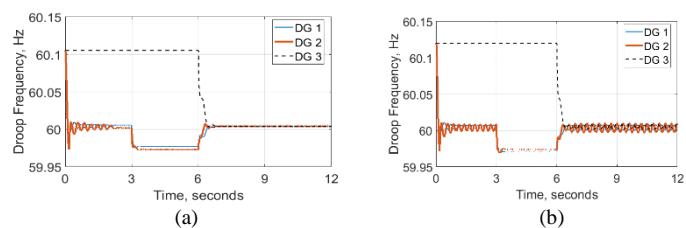


Fig. 2. (a) Droop frequency for DG 1, 2 & 3 with online synchronization of DG 3 at 6 seconds (b) Same as a, with all frequency droop coefficients increased by 14.3%

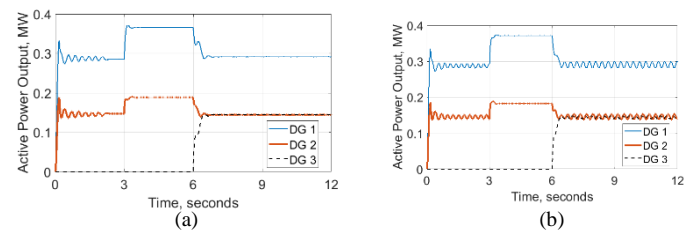


Fig. 3. (a) Active power output of DG 1, 2 & 3 with online synchronization of DG 3 at 6 seconds (b) Same as a, with all frequency droop coefficients increased by 14.3%

Reconstruction of Power System Measurements Based on Enhanced Denoising Autoencoder

You Lin, Jianhui Wang, and Mingjian Cui

Southern Methodist University

Abstract: This paper presents a new solution for reconstructing missing data in power system measurements. An Enhanced Denoising Autoencoder (EDAE) is proposed to reconstruct the missing data through the input vector space reconstruction based on the neighbor values correlation and Long Short-Term Memory (LSTM) networks. The proposed LSTM-EDAE is able to remove the noise, extract principle features of the dataset, and reconstruct the missing information for new inputs. The paper shows that the utilization of neighbor correlation can perform better in missing data reconstruction. Trained with LSTM networks, the EDAE is more effective in coping with big data in power systems and obtains a better performance than the neural network in conventional Denoising Autoencoder. A random data sequence and the simulated Phasor Measurement Unit (PMU) data of power system are utilized to verify the effectiveness of the proposed LSTM-EDAE.

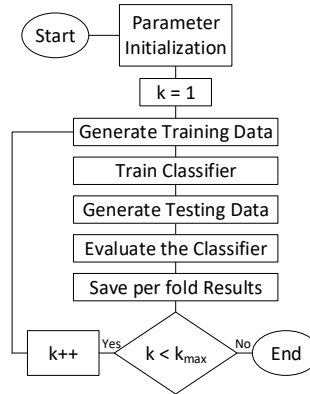
Keywords—Power system measurements, data reconstruction, Enhanced Denoising Autoencoder, Long Short-Term Memory network

Detecting Behind-the-Meter PV Installation Using Convolutional Neural Networks

Sadegh Vejdán, *Graduate Student Member, IEEE*, Karl Mason, Matthew Reno, and Santiago Grijalva, *Senior Member, IEEE*

Abstract—As the costs of behind-the-meter (BTM) PV systems are decreasing, more customers are expected to install them. Increased penetration of PV installations can cause numerous challenges in the distribution feeders and utilities must know the installed PVs in their territory for reliable planning and operation. However, many utilities do not have enough visibility on the actual installed PVs due to many challenges such as the growing number of unauthorized PV installations and updating the authorized PV databases. In this paper, a data-driven classification method is proposed for detecting BTM PV installation using convolutional neural networks and synthetic net load profiles generated from AMI data. The impact of training data parameters, such as the size, temporal resolution and label errors on the accuracy and computational time of the method is studied and characterized. The proposed method help utilities detect BTM PV systems and update their databases automatically. Simulation results provide valuable insights on the optimally-trained classifier with the minimum data requirements that result in the most accurate and yet computationally efficient input data parameters.

- CNN trained for 200 epochs using RMSprop optimization.
- 50-fold cross validation



Index Terms—Behind-the-meter solar energy, classification, convolutional neural networks, PV detection, synthetic data generation.

I. PROPOSED METHODOLOGY

THE proposed methodology consists of three main components as shown in Fig. 1.

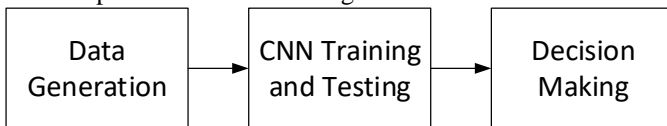


Fig. 1 Components of the proposed methodology

A. Data Generation

In order to create large datasets for training and testing the CNN, databases of residential load measurements and residential PV production were combined in a combinatorial manner to create a range of customer net load profiles with different irradiance profiles and PV sizes.

$$NetLoad_{n(l,s,p)} = Load_l - r_s \times ScalingFactor_{s(l,p)} \times PV_p \quad (1)$$

B. CNN Training and Testing

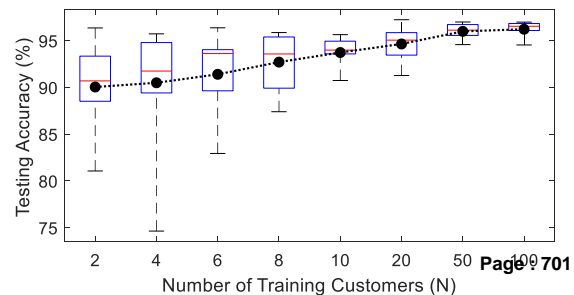
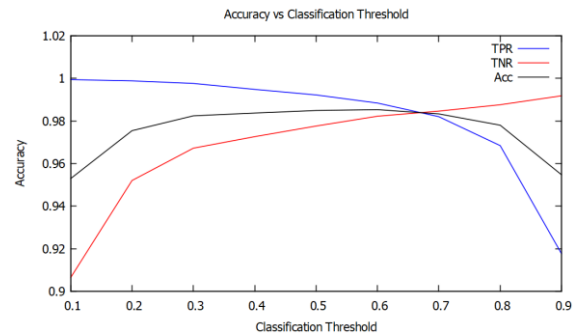
- Input: daily net load profile.
- Output: probability of PV (1 = PV installed, 0 = no PV).
- Architecture: convolutional layer, max pooling, convolutional layer, max pooling, fully connected layer (100), fully connected layer (1).

C. Decision Making

Once all the days of a customer’s net load profile are classified as either 1, “with PV”, or 0, “No-PV”, we have to decide whether the customer has PV or not given the daily estimated labels.

$$Label_n = \begin{cases} 1 & \text{if } \frac{1}{N_d} \sum_d Label_{n,d} \geq th \\ 0 & \text{o.w.} \end{cases} \quad (2)$$

II. SIMULATION RESULTS



New Reward and Penalty Scheme for Electric Distribution Utilities Employing Load-Based Reliability Indices

Bo Wang, Jorge A. Camacho, Gary M. Pulliam, Amir H. Etemadi and Payman Dehghanian

Abstract—Electric distribution utilities are required to continuously deliver reliable electric power to their customers. Regulatory utility commissions often practice reward and penalty schemes to regulate reliability performance of utility companies annually with respect to a desired performance targets. However, the conventional regulation procedures are commonly founded based on the customer-based standard reliability indices which are not able to discern the service characteristics behind the electric meters and, hence, fail to holistically characterize the actual impact of electricity interruption. This paper proposes a new method to evaluate the load-based reliability indices in power distribution systems using Advanced Metering Infrastructure (AMI) data. Furthermore, we introduce a reward/penalty regulation scheme for utility regulators to provide a reliability oversight using the proposed load-based reliability metrics. The new load-based reliability metric and the reward/penalty scheme proposed bring about superior advantages as the distribution grids become further complex with a high penetration of distributed energy resources (DERs) and enabled microgrid flexibilities. Numerical analyses on different settings with and without microgrid considerations reveal the applicability and effectiveness of the proposed approach in real-world scenarios.

Index Terms—Advanced metering infrastructure (AMI), load forecasting, reliability assessment, smart grids, utility regulation.

I. THE PROPOSED UTILITY REGULATION MODEL

A utility consists of hundreds of feeders. So utility reliability is determined by reliability characteristics of its feeders. We classify feeders of the utility with different reliability requirements, and regulate these feeders based on the contract of the feeders assigned between utilities and public utility commissions.

Feeders with AMI can calculate ASIFI, ASIDI and ASSDI. We use PF which contains these reliability indices to penalize utilities.

$$PF = IR(1 - \alpha)(CI - 1) \quad (1)$$

We introduce composite index (CI) to represent the difference between the expected reliability level and real reliability level.

$$CI = W_1 \left(\frac{ASIFI}{ASIFI_0} \right) + W_2 \left(\frac{ASIDI}{ASIDI_0} \right) + W_3 \left(\frac{ASSDI}{ASSDI_0} \right) \quad (2)$$

where W_1 , W_2 and W_3 are the weights that utilities place on each index and weights add up to one. $ASIFI_0$, $ASIDI_0$, and $ASSDI_0$ are expected values set by utility regulators.

The customer reliability premium can be calculated as

$$B_{RP} = IEAR \cdot G \quad (3)$$

TABLE I
PROPOSED UTILITY REGULATION SETTINGS

$ASIDI'$	Reliability Level	Reward or Penalty
$< TL_0$	high	fixed PF
$TL_0 \leq ASIDI' < TU_0$	medium	PF
$\geq TU_0$	low	PF and C_c

II. KEY RESULTS

We regulate utilities with advanced metering infrastructure (AMI) by first calculating the $ASIDI'$ of each feeder. To examine the effectiveness of using $ASIDI'$, we simulate the interruptions of the two feeders. The $ASIDI'$ calculated using load forecasting method is compared with the simulated ASIDI. Then we evaluate the reliability of each feeder based on Table I.

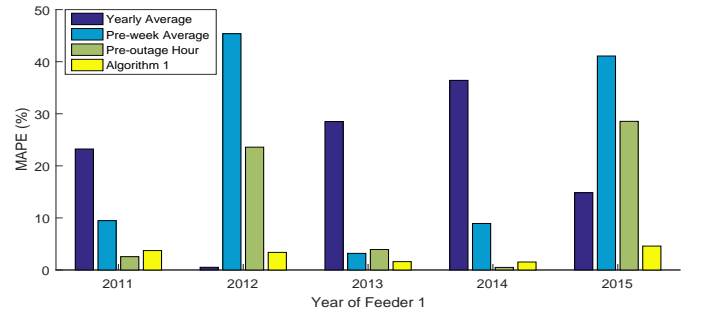


Fig. 1. Prediction error of the ASIDI index for Feeder 1. Simulated ASIDI from year 2011 to 2015 are 32.63, 16.09, 2.44, 3.64, and 0.31 (hours).

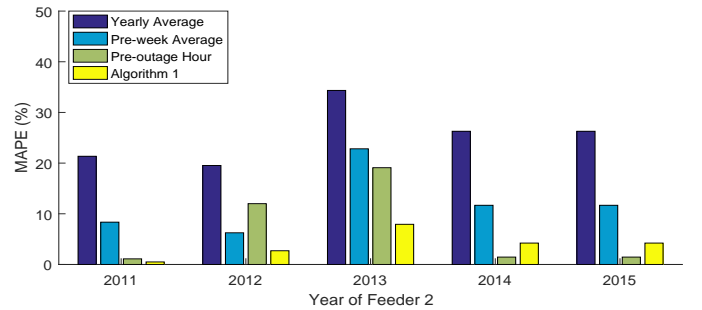


Fig. 2. Prediction error of the ASIDI index for Feeder 2. Simulated ASIDI from year 2011 to 2015 are 9.66, 13.62, 2.55, 4.49, and 0.67 (hours).

A Machine Learning Approach to Detection of Geomagnetically Induced Currents in Power Grids

Shiyuan Wang, *Student Member, IEEE*, Payman Dehghanian, *Member, IEEE*, Li Li, *Student Member, IEEE*, and Bo Wang, *Student Member, IEEE*

Abstract—Geomagnetically induced currents (GICs) in power grids are mainly caused by geomagnetic disturbances especially during solar storms. Such currents can potentially cause negative impacts on power grid equipment and even damage the power transformers resulting in a significant risk of blackouts. Therefore, monitoring GICs in power systems and developing solutions to mitigate their impacts before rising to a certain threatening level is urgently in need. Monitoring GICs is quite a challenge and costly, as they usually appear in forms of DC components in the high voltage transmission lines, which are barely accessible through transformers. By examining the measured currents from the current transformers (CTs), this paper proposes a framework to detect GICs in power transmission systems through a hybrid time-frequency analysis combined with machining learning technology. Simulated results verify that the proposed approach can promisingly estimate GICs in power systems during a variety of grid operating conditions.

Index Terms—Convolutional Neural Network (CNN); feature extraction; geomagnetic disturbance (GMD); geomagnetically induced current (GIC); harmonics; wavelet transform (WT).

I. WAVEFORM MODELING AND KEY EQUATION

When a transformer is injected with different levels of GICs, the harmonic magnitude curves will differ significantly as it is shown in Fig.1 and Fig. 2

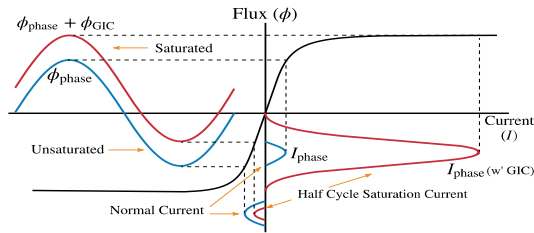


Fig. 1. Half-cycle saturation of a single-phase transformer due to GICs.

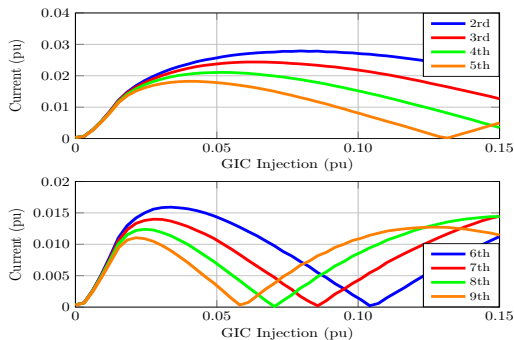


Fig. 2. Excited harmonic current components in different levels of GICs.

$$x(t) = A_1 \cos(\omega_1 t + \phi_1) + \underbrace{\sum_{h=2}^H A_h \cos(\omega_h t + \phi_h)}_{\text{Harmonic Components}} \quad (1)$$

$$X_g(\omega_h | a, b) = \frac{A_h}{\sqrt{a} C_{gN}} \int_{-\infty}^{\infty} \frac{d^N}{dt^N} \cos(\omega_h t + \theta_h) \cdot e^{-\frac{(t-b)^2}{2a^2}} dt$$

$$= \frac{A_h \omega_h^N}{\sqrt{(N-1)!}} \cos(\omega_h b + \theta_h + \frac{N\pi}{2}) e^{-\frac{a}{2} \omega_h^2} \quad (2)$$

II. FEATURE EXTRACTION & GIC DETECTION BY CNNs

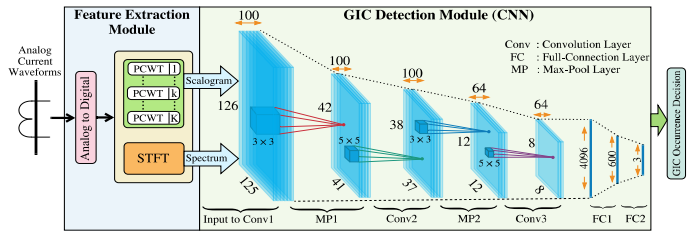


Fig. 3. The general architecture of the proposed framework for GIC detection in power grids.

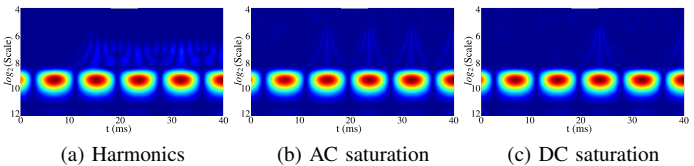


Fig. 4. Extracted features of test waveform: (a) polluted with random harmonics; the AC (b) and DC (c) saturation level is 0.01pu; all events start at t=10ms.

TABLE I
SIMULATED TEST WAVEFORM PARAMETER SPECIFICATION & ACCURACY PERFORMANCE OF THE TEST RESULTS

Test Case	Saturation Type		
	AC	DC	NO
Saturation level	0.001pu-0.15pu	0.001pu-0.15pu	0
Harmonic Distortion	0.5 %-10 % THD; random choose up to 50 th order		
Out-of-Band	10Hz to 120Hz; level 0.01pu-0.1pu		
Nonlinear Load	1% to 20% of total load		
Signal to Noise Ratio	30dB applied to all generated signal		

GIC (pu)	0-0.03	0.03-0.06	0.06-0.09	0.09-0.12	0.12-0.15	Overall
Hybrid*	73.93%	82.70%	85.15%	86.85%	87.02%	82.50%

III. CONCLUSION

Experiments demonstrated that the proposed analytics achieved a high accuracy for online detection of GICs under different operating conditions.

Single-Ended Fault Location for Hybrid Transmission Line using Embedded Artificial Intelligence

Rong Yan, Guangchao Geng, Guoqiang Zeng, and Quanyuan Jiang

Abstract—Fault line identification, phase selection, and exact location play a significant role in power system daily protection and maintenance. The idea of this work is to construct a novel framework summarized as “train in the cloud and infer on the edge”, deploying the fault-location task on the edge of data source for distributed inference instead of sending measured data to a centralized cloud. To achieve this goal, a modified long short-term memory (LSTM) network is trained in the cloud, covering various fault scenarios. Meanwhile, the trained model is imported on a small embedded artificial intelligence (e-AI) module equipped in fault recorder of the substation, in order to infer fault information using local single-ended measurements in real time. The performance of the proposed method is tested for various fault scenarios with satisfactory results in real time.

Index Terms—Embedded artificial intelligence (e-AI), fault location, edge computing, long short-term memory (LSTM)

I. INTRODUCTION

FAULT location plays an important role in power system protection and daily maintenance. There is always a trade off between location accuracy and data acquisition cost (e.g., data communication time, measurement equipment cost) using state-of-the-art methods like steady-state phasor-based or traveling wave-based approaches for hybrid transmission line: overhead line combined with cable. In this paper, a single-ended fault location framework shown in Fig. 1 is proposed for a hybrid transmission line.

II. PROPOSED METHOD

We designed an modified LSTM network for fault location accurately. Meanwhile, model trained in the cloud is imported to an a module embedded near the data source (such as fault recorder), and infer the fault location in real time, using local voltage and current measurements. Contributions are as follow:

- 1) Embedded artificial intelligence (e-AI) concept is introduced into power system applications, and employed to process a large amount of local collected voltage and current measurements for fault-location without latency.
- 2) The idea of “train in the cloud and infer on the edge” is proposed. By this way, trained model is downloaded from the cloud regularly to the e-AI module, instead of sending measured data to the cloud in real time.

This work was supported by the National Natural Science Foundation of China (51677164) and Fundamental Research Funds for the Central Universities (2018QNA4018).

R. Yan, G. Geng and Q. Jiang are with the College of Electrical Engineering, Zhejiang University, Hangzhou, Zhejiang 310027, China (email: {yanrong052, ggc, jqy}@zju.edu.cn). G. Zeng is with the College of Engineering, Carnegie Mellon University, Pittsburgh, PA 15213, USA (email: guoqianz@andrew.cmu.edu). Guangchao Geng is the corresponding author.

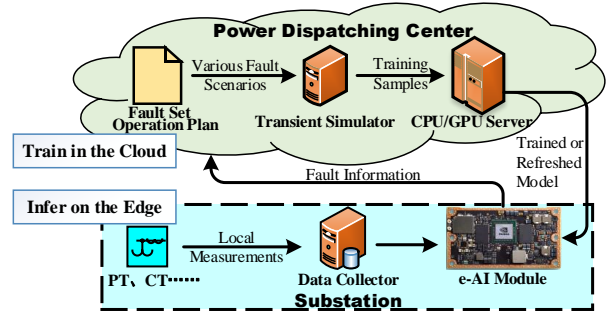


Fig. 1. Framework of the proposed method.

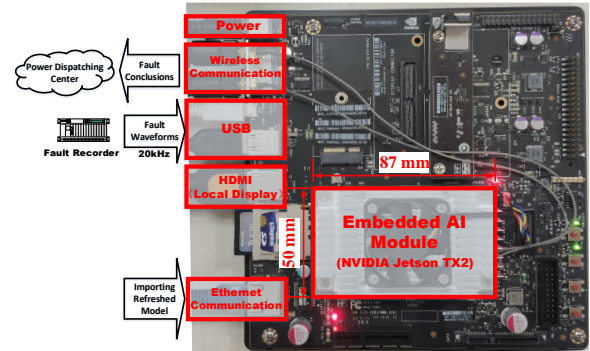


Fig. 2. An embedded AI edge device: NVIDIA Jetson TX2 module.

III. CASE STUDY

A 500-kV, 50Hz hybrid transmission-line system is employed to test the proposed method. Modified LSTM model is constructed with Keras and TensorFlow. Inference task is tested on NVIDIA Jetson TX2 Module shown in Fig. 2. The test results can be seen in Table I and Fig. 3.

TABLE I
PERFORMANCE INDICES EVALUATION OF FAULT LINE IDENTIFICATION, PHASE SELECTION AND EXACT LOCATION

Classification Task				Regression Task			
Indices		Line Identification	Phase Selection	Indices		Exact Location	
Error Rate	Training	0	0.06%	Absolute Error	Training	Avg	0.106 km
	Testing	0	0.32%		Testing	3σ	0.622 km
Time	Training	15.19 s/epoch		18.76 s/epoch			
	Testing	0.11 ms/sample		0.11 ms/sample			
Model Size			215 KB	207 KB			

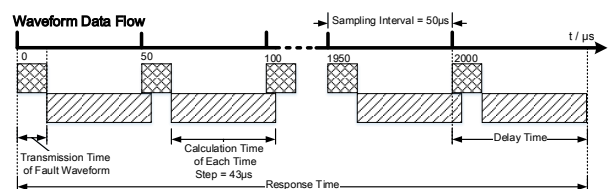


Fig. 3. Timing diagram of the proposed method.

Online Identification Tool for Power System Component Events

¹Dulip Madurasinghe, *Student Member, IEEE*, ¹Paranietharan Arunagirinathan, *Student Member, IEEE*,

^{1,2}Ganesh K. Venayagamoorthy, *Senior Member, IEEE*

¹Real-Time Power and Intelligent Systems Laboratory,

Holcombe Department of Electrical and Computer Engineering, Clemson University, Clemson, SC 29634, USA

²Eskom Centre of Excellence in HVDC Engineering, University of KwaZulu-Natal, Durban, South Africa

dtmadurasinghe@ieee.org, parani@ieee.org and gkumar@ieee.org

Abstract—The smart grid (SG) enable the possibility to implement real-time situational awareness (SA) through synchronized measurements by utilizing the fully connected communication backbone. Generation units and the successful operation of the geographically distributed transmission network and its components are critical for the reliable operation of the power system. The transmission network is the bridge between bulk generation and distribution system. These critical component outages can occur due to number of reasons, which may be led to partial or complete blackout of the power system. Accurate identification of these events are critical. PMU measurement based event identification is investigated. A redundant monitoring tool of these critical components integration with existing identification system increase the surety of the component event identification.

Index Terms-- cyber physical systems, phasor measurement units, smart grid, transmission lines, generators

I. INTRODUCTION

The conventional power system is rapidly changing towards a SG that is comprised with utility scale renewable generations, distributed energy sources (DES), energy storages units, electrified transportation, demand response (DR) schemes, demand side management, etc. Phasor measurement units (PMU) are introduced in the power system to achieve higher rate synchronized phasor measurements. Intelligent controls are implemented to control the dynamic power system in a stable condition maintaining the quality power supply. Successful system control depends on the accurate SA. One aspect of the SA is the power network topology (i.e. power system components status).

In this study PMU based event identification approaches are investigated. Three separate identification approaches are tested as shown in the Fig.1. Two of them are focused on the transmission network component events. YBUS-I approach utilize the property of the admittance matrix changes respective to branch event. NN-I approach identify the branch event with a pre-trained identifier. The generator event identifier, GEN-I is based on the PMU measurements of the generator terminal. All these three approaches integrated to a single identification tool and the component events are visualized through MATLAB based graphical user interface (GUI) as shown in Fig. 2.

II. KEY FIGURES

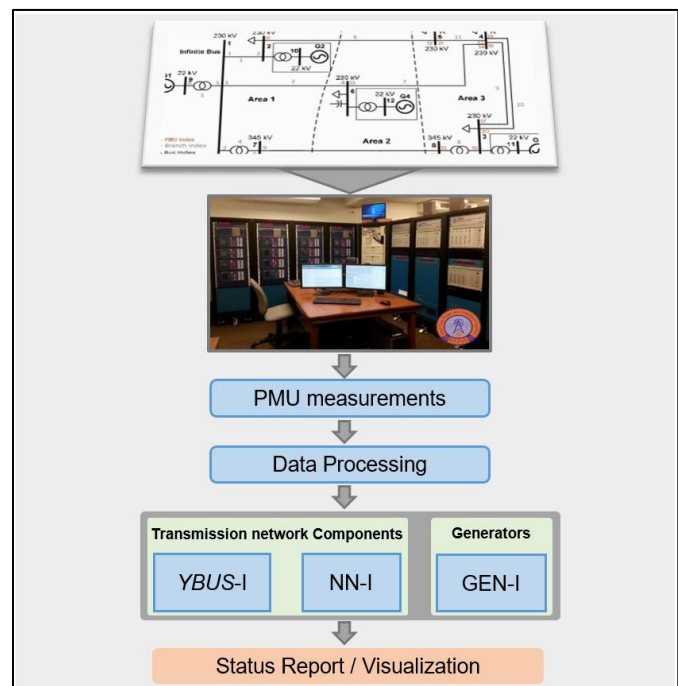


Figure 1. Identification tool testing procedure

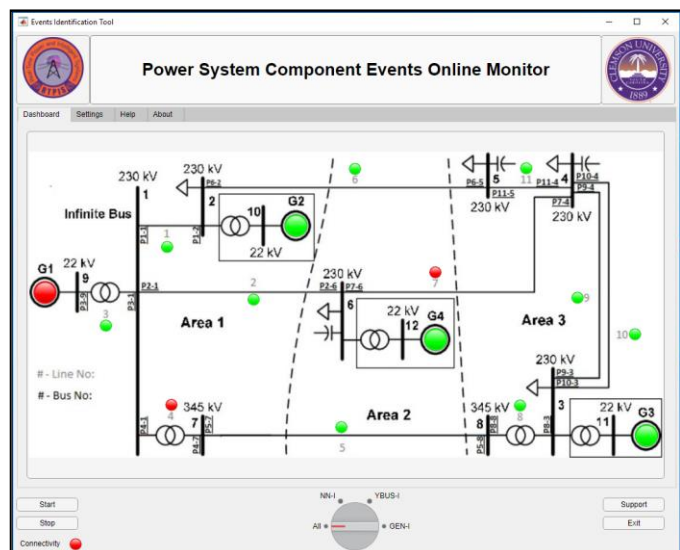


Figure 2. Power system component events identification tool app

The Optimal Use of Tax Incentives for Wind Power

Alejandro Castillo-Ramírez
 Group of Efficient Energy Management
 Universidad de Antioquia
 Medellín, Colombia
 alcara50@gmail.com

Diego Mejía-Giraldo
 Department of Electrical Engineering
 Universidad de Antioquia
 Medellín, Colombia
 diego.mejia@udea.edu.co

Abstract—We present a methodology that computes the optimal use of tax incentives for wind power facilities in US. The Consolidated Appropriations Act of 2016 reauthorized Investment Tax Credit (ITC) and Production Tax Credit (PTC) for wind power. Our methodology minimizes the Present Value of Income Tax (PVIT) for a firm that invest in a single wind facility. Results shows the optimal use of ITC and PTC for a base case scenario. Sensitivity analysis was developed to assess the impact of capacity factor ρ and tax rate α . Main findings indicated that PTC must be preferred at higher levels of power generation, and PVIT could be zero even when tax rate is positive.

I. TAX OPTIMIZATION MODEL

We have constructed a linear programming model aimed to minimize the PVIT of the firm computed as the discounted sum of tax payments. To do so, decision variables like yearly ITC, yearly PTC, and yearly tax loss, must be strategically management to derive the optimal solution. A key constraint required to enable use of ITC is that tax liability of a particular year should be greater than the ITC claimed that particular year. Annual tax liability requires taxable income, which is computed as the difference between gross profit and allowable depreciation. In years where ITC is not claimed, taxable income is not constrained and can be even negative (tax loss). Tax losses are modeled in a way they can be used in the future to offset and/or reduce tax payments.

II. NUMERICAL RESULTS

Model tests have been focused on the tax incentives granted to the wind facilities. The Act of 2016 provides tax credits (TC) to the wind facilities that are being constructed in the year 2019 [1]. Particularly, wind facilities may elect to claim a tax credit between ITC and PTC. Whereas the ITC allows wind developers to deduct investment up to 12%, the PTC gives them up to 9.2 cents per kWh. The optimal use of ITC and PTC is showed in Fig. 1. Also, capacity factor ρ and tax rate α were analyzed to compute their impact on the resulting optimal tax strategies and PVIT as depicted in Fig. 2 and Fig 3.

III. CONCLUSIONS

This work describes an optimization-based strategy to apply tax incentives in the context of the Act of 2016 in the US. Regulatory constraints are considered in the formulation, which

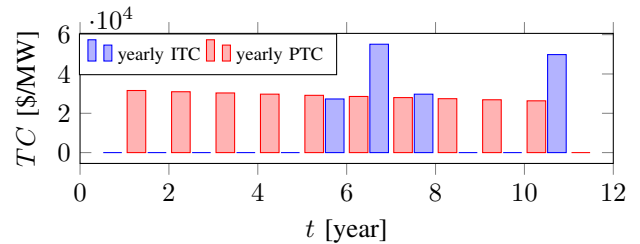


Fig. 1. Optimal use of ITC and PTC

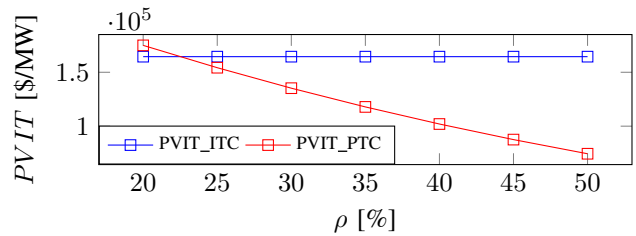


Fig. 2. PVIT vs ρ

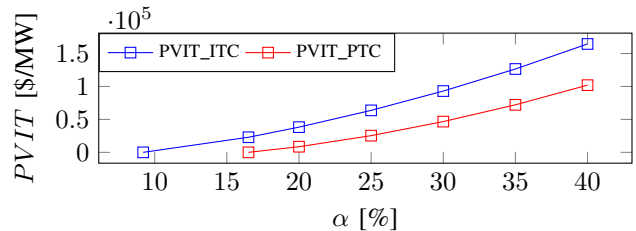


Fig. 3. PVIT vs α

cause nontrivial results in the way tax credits are employed. Also, the optimal selection between PTC and ITC depends on the capacity factor of the wind project. In fact, large capacity factor makes PTC the most profitable incentive. We also found that managing in an optimal manner incentives and tax loss, tax payments can be reduced even to zero throughout projects life time below certain tax rate.

REFERENCES

- [1] T. Mai, W. Cole, Wesley, E. Lantz, C. Marcy, B. Sigrin, "Impacts of federal tax credit extensions on renewable deployment and power sector emissions," National Renewable Energy Laboratory, Golden, CO, NREL/TP-6A20-65571, Feb. 2016.

Intraday dispatch, energy storage and the value of re-scheduling in systems with high wind shares

Irene Danti Lopez and Damian Flynn
 School of Electrical and Electronic Engineering
 University College Dublin, Ireland

Maël Desmartin and Marcelo Saguan
 Électricité de France R&D
 Paris, France

Abstract—The combination of increasing uncertainty and decreasing flexibility, brought about by growing shares of wind and solar power, require a re-thinking of the way in which power systems are modelled and operated. In systems with high wind and solar power shares, standard modelling and operational practices may not make the best use of the available flexibility, nor will they necessarily yield an accurate calculation of the value of flexibility providers such as energy storage. In this paper, we compare how dispatch decisions and operating costs differ between perfect foresight, day-ahead-only and intraday dispatch unit commitment simulations.

Index Terms—unit commitment, energy storage, intraday dispatch

I. INTRODUCTION

Unit commitment and economic dispatch (UCED) models lie at the core of power system planning and operations. Traditionally, these were constructed using a perfect foresight approach, where the role of forecast uncertainty remained marginal and did not often require intraday updates to reflect updated forecasts in demand, wind and/or solar power. It is the combination of increased uncertainty and flexibility requirements, brought about by the growing shares of wind and solar power, that requires a re-assessment of the detail included and the structure of UCED models. In high renewable energy systems, it is no longer certain that perfect foresight or day-ahead-only dispatches will make best use of the flexibility available, nor will they necessarily yield the least-cost solution. Moreover, these approaches may give misleading results regarding the value of highly flexible, energy-limited, resources, such as energy storage.

II. METHODOLOGY AND KEY FINDINGS

Kohala, a system cost minimisation model was developed. The market structures considered in this study are illustrated in Figure 1 and the key findings are presented in Figure 2. The results indicate that:

- In high wind power scenarios, perfect foresight approaches will likely underestimate the need/value of energy storage and peaking plant as flexibility providers.
- Intraday dispatch, on the other hand, requires less corrective actions at the balancing phase due to the frequent forecast updates, lowering the reliance on energy storage and peaking units.
- Fast and flexible units provide significant value to the system when operating in day-ahead-only dispatch, given

that these are efficient at correcting forecast errors in the balancing phase.

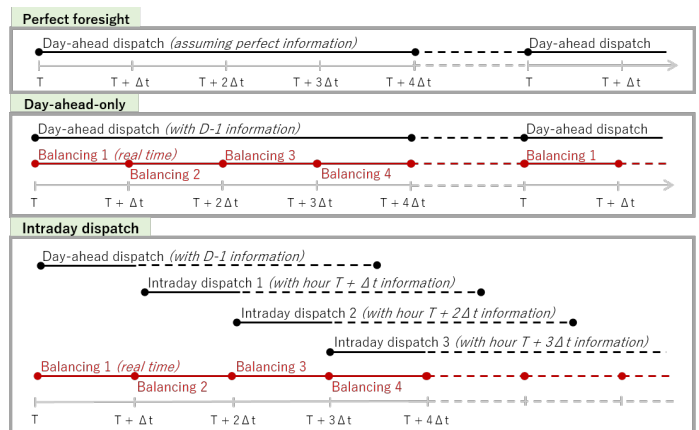


Fig. 1: Illustration of the perfect foresight, day-ahead only and intraday dispatch approaches in Kohala

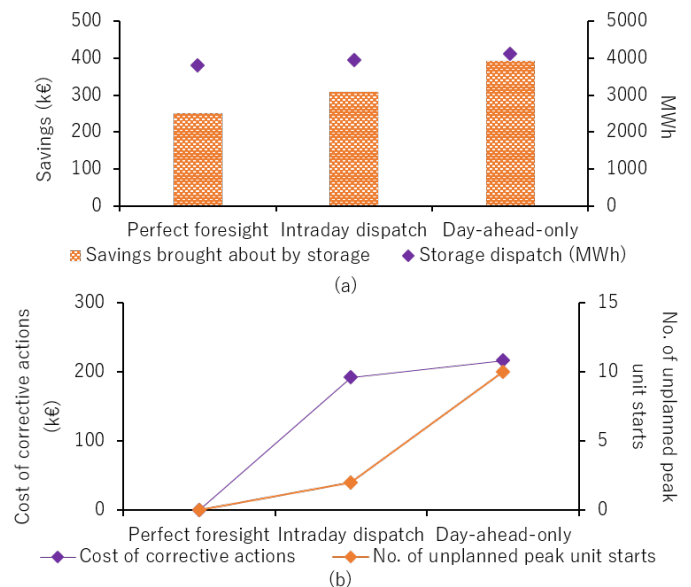


Fig. 2: (a) Savings brought by energy storage and (b) cost of corrective actions and peak unit starts in the three operation modes considered

Newly Implemented and Proposed Market Products and Reformulations: Stochasticity modeling and flexible ramp products

Mohammad Ghaljehei, *Student Member and IEEE*, Mojdeh Abdi-Khorsand, *Member*
 School of Electrical, Computer, and Energy Engineering, Arizona State University, Tempe, AZ 85287, USA
 Email: mghalje@asu.edu and mojdeh.khorsand@asu.edu

Modern day market management systems (MMS) continue to evolve due to the new resource mix and the intention to improve system reliability and security. For example, in recent years, independent system operators (ISOs) have introduced new market products, i.e., flexible ramp products (FRPs), to account for extreme ramp events that are imposed on the system due to the evolving resource mix (e.g., renewables) [1]. There are also proposals to transition the market auction models from a deterministic structure to a stochastic program in order to better prepare for uncertain events [2]. Overall, questions remain regarding how to best reflect these essential changes in market models (reformulation) while considering their impact on the corresponding market settlements. This paper focuses on two aforementioned market changes, i.e., FRP design and implications of uncertainty modeling strategies for contingency events.

Market design and pricing implications of contingency modeling: In first part of the paper, an extensive study is performed in order to analyze impacts of contingency modeling strategies on market settlement and pricing. Following models have been investigated in this study: (i) deterministic models with proxy reserve requirements with appropriate out-of-market corrections, (ii) contingency modeling using participation factors, e.g. line outage distribution factors, and (iii) corrective action optimization via a two-stage extensive form stochastic unit commitment. The simulation results are performed on the IEEE 118-bus system. Fig. 1 shows market settlements obtained from different contingency modeling strategies.

Moreover, for the extensive form stochastic security-constrained unit commitment models, the choice of minimizing cost of normal operating condition as the objective function is compared with minimizing expected cost of normal and contingency conditions. The realized cost during contingency and inaccurate estimation of probabilities are among the investigated topics. Figure 2 provides a comparison between the two choices of objective function.

Enhancement of FRPs in DA market: In second part of the paper, a comprehensive study is conducted to: (a) propose a novel method to enhance formulation of FRP in day-ahead (DA), and (b) design corresponding market settlement policies that accurately reflect value of flexibility. The main contributions are listed below:

- Strategies to identify needed amount of FRPs.
- Effects of the unit commitment status on FRPs in DA framework.
- Modeling FRPs in DA market to capture both hourly and 15-min ramping requirements (see Fig. 3 that shows there can be cases, e.g., cases I and II, where the hourly ramp requirement cannot accommodate 15-minute variability and uncertainty).
- Deliverability modeling of FRPs in DA markets.

More specifically, we want to present an FRP formulation that not only ensures post-deployment deliverability of FRPs,

but also immunizes the DA solutions against intra-hour 15-minute net load variability and uncertainty while keeping the scheduling framework based on an hourly basis.

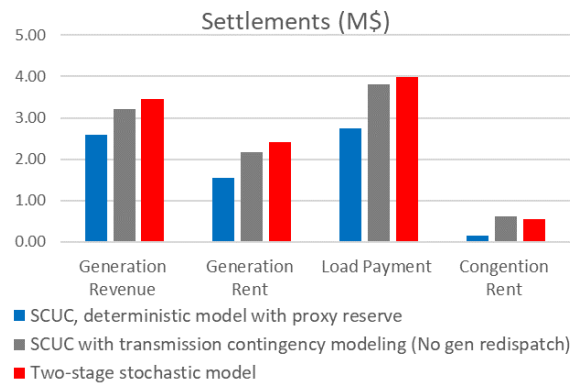


Fig. 1: Market settlements obtained from different contingency modeling strategies.

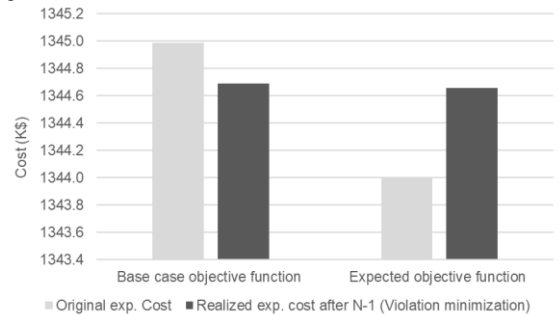


Fig. 2: Comparing the market solutions of stochastic SCUC with base case objective function and expected objective function.

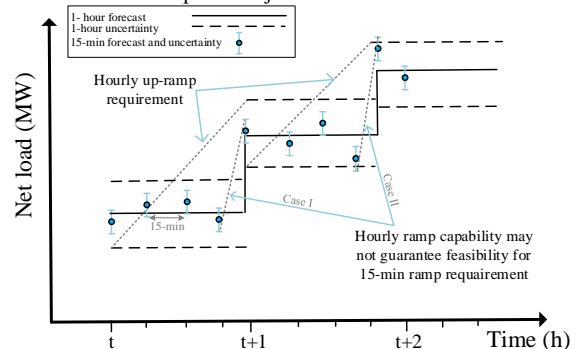


Fig. 3. Hourly FRP versus 15-minutes variability and uncertainty.

[1] California ISO, "Flexible ramping product," Revised Draft Final Proposal, December 17, 2015.

[2] J. Zhao, T. Zheng, E. Litvinov, and F. Zhao, "Pricing schemes for two-stage market clearing models," FERC Conference on Increasing Efficiency through Improved Software.

Peer-to-Peer (P2P) Energy Exchange in Distribution Networks Considering Network Constraints

Hamed Haggi, *Student Member IEEE*, Wei Sun, *Member IEEE*

Department of Electrical and Computer Engineering, University of Central Florida, Orlando, FL USA

hamed@ece.ucf.edu, sun@ucf.edu

Abstract—Distributed energy resources (DERs) and information, communication technologies (ICTs) have transformed the traditional electricity consumers into proactive consumers, named as "prosumers". The energy exchange between consumers and prosumers can be enabled through Peer-to-Peer (P2P) energy sharing. In this paper, a new framework for P2P energy exchange between prosumers and consumers is proposed with the goal of benefit maximization of peers considering network constraints. Based on sensitivity factors such as voltage, power loss, power transfer distribution factor (PTDF), the aforementioned framework ensures the network constraints and prevents any violation in normal operation of distribution systems.

Index Terms—Blockchain technology, Distribution market, Peer-to-Peer (P2P) energy exchange

I. INTRODUCTION

The integration of DERs such as rooftop solar panels, energy storage systems, and electrical vehicles, together with the ICT devices, has been transforming traditional consumers into proactive consumers, known as "prosumers". The energy exchange between consumers and prosumers in a local energy market could be enabled through Peer-to-Peer (P2P) energy trading. There are three different structures of P2P markets in the literature: 1) Full P2P market (decentralized market), in which the peers agree on a transaction for a certain amount of energy and price without supervision of a central entity; 2) Community based market (centralized market), in which both prosumers and consumers send their requests for selling or buying energy to a central entity, like community managers, local aggregators in microgrids, etc., and then start the energy transition; 3) Hybrid P2P market, which is the mix of the aforementioned two markets. P2P markets can be considered for distribution systems consisting of multiple microgrids with several local aggregators and active/passive users willing to exchange energy with each other. How to exchange energy under P2P concept while considering the network physical constraint in a multi-microgrid distribution network is a preminent challenge.

II. PROPOSED FRAMEWORK

In this paper, a new framework of P2P market is developed, as shown in Fig. 1. It is assumed after self-consumption, prosumers/consumers can sell/buy (surplus) energy by sending their requests to local aggregators (LAG) considering the delivery time and amount of energy. Auction-based models are used to match offers and bids. In order to facilitate the transactions, recent technologies such as blockchain can be

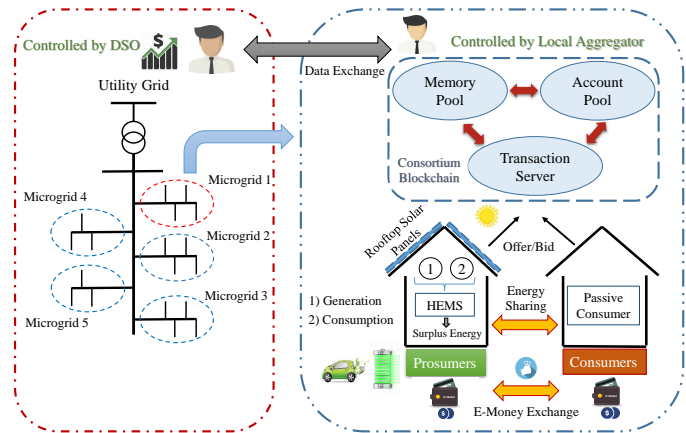


Fig. 1. The proposed structure of P2P market

used. As P2P market participants only share limited data with each other, consortium blockchain is the best option, which consists of account pool, transaction server, and memory pool. Account pool is to require each participant to become an official entity through registration in a trusted authority for smart contracts. The transaction server is responsible for collecting the energy requests from prosumers and consumers, which can be accessed by LAG. Memory pool is responsible to keep the transaction records in blocks of blockchain. Once the price matching completed, LAG checks the last transaction block for both prosumer and consumer from memory pool.

Besides checking the amount of electronic money (e-money), LAG will ensure the secure energy exchange and prevent any violation by checking through sensitivity factors. If both financial and physical checks are approved, prosumers can send energy to consumers in the microgrid. However, if two prosumers in different microgrids want to trade energy between each other, the upper layer of proposed framework will enable distribution system operator (DSO) to check the energy transition by obtaining data from LAGs. Considering the power loss and congestion, if the distance of two peers in different microgrids is further away, DSO sends a signal to LAGs and inform prosumer and consumer that the transaction will not be approved due to non cost-effective of long-distance power delivery. At this stage, instead of being a prosumer, the consumer has the option to buy energy from utility grid. The price of energy can be determined by the distributional locational marginal pricing (DLMP) defined by DSO.

Efficient Algorithms for Allocating Payoffs in a Peer-to-Peer Energy Sharing Cooperative Game

Liyang Han, Thomas Morstyn, Constance Crozier, Malcolm McCulloch

Department of Engineering Science, University of Oxford, Oxford, UK

{Liyang.Han, Thomas.Morstyn, Constance.Crozier, Malcolm.McCulloch}@eng.ox.ac.uk

Abstract—Among the various peer-to-peer energy sharing schemes proposed in recent studies, one cooperative game theoretic model stands out by incorporating energy storage units along with other distributed energy resources in the model, and detailing a clear payoff structure to incentivize prosumers to cooperate their energy resources. The nucleolus has been proven to be a stabilizing payoff allocation, which guarantees that no players can make a higher profit outside of the grand coalition. However, as the size of the game increases, the computation of the nucleolus becomes intractable. This work explores existing estimation methods such as sampling and clustering to reduce the model’s computational complexity, and proposes a new method that uses K-means clustering to identify critical samples to estimate the nucleolus for up to 50 players with high accuracy and within a reasonable amount of time.

Index Terms—Cooperative game theory, K-means clustering, nucleolus, prosumers, peer-to-peer

I. PROPOSED METHOD

A. Peer-to-Peer Cooperative Game Formulation

We index each prosumer by i and the *grand coalition* by $i \in \mathcal{N} := \{1, 2, \dots, N\}$. Assuming the electricity import price r_t^{im} (£/kWh) is higher than the electricity export price r_t^{ex} (£/kWh) for all timesteps ($t = 1, 2, \dots, R$), we can schedule all the energy storage (ES) units’ operation within coalition \mathcal{T} to minimize the *coalitional energy cost*, defined as $G(\mathcal{T})$:

$$G(\mathcal{T}) = \min \sum_{t=1}^R \sum_{i \in \mathcal{T}} \left\{ r_t^{im} [p_{it} + \mathbf{b}_{it}]^+ + r_t^{ex} [p_{it} + \mathbf{b}_{it}]^- \right\}$$

where p_{it} is the net energy consumption (positive) or generation (negative) (kWh) without ES, and the variables are $\mathbf{b} \in \mathbb{R}^{N \times R} := \mathbf{b}_{it}$: ES charge (+) or discharge (−) energy (kWh), subject to the ES power, energy, and cycle constraints. We also define operation $[z]^{+(-)} = \max(\min)\{z, 0\}$.

We define the value of a coalition \mathcal{T} as the energy cost savings obtained by forming the coalition: $v(\mathcal{T}) = \sum_{i \in \mathcal{T}} G(\{i\}) - G(\mathcal{T})$. The *nucleolus* $\mathbf{u} \in \mathbb{R}^N$ is a payoff allocation whose entry u_i represents the payment to prosumer i , where $\sum_{i \in \mathcal{N}} u_i = v(\mathcal{N})$, and $u_i \geq v(\{i\})$, $\forall i \in \mathcal{N}$. The *nucleolus* \mathbf{u} is also stabilizing: $\sum_{i \in \mathcal{S}} u_i \geq v(\mathcal{S})$, $\forall \mathcal{S} \subset \mathcal{N}$.

B. Nucleolus Estimation with K-Means Identified Sampling

We first adopt a stratified random sampling method to estimate the nucleolus. Each stratum P_{il} is a group of coalitions, all of which contain player i and are of size l . A fixed number of coalition samples are then taken randomly from each stratum to estimate the nucleolus. After being tested against the full nucleolus calculation for 14 players, a sample size of 3 from each stratum, with a standard error of estimation

of merely 0.35%, is selected as the benchmark to validate the results of other estimation methods for larger games.

In the proposed method, we use K-means clustering to identify critical samples. Based on each prosumer’s energy profile in the grand coalition, we separate them into K clusters $cl_{\mathcal{K}} := \{cl_1, cl_2, \dots, cl_K\}$, with clustering assignment $f : f(i) = j \mid i \in cl_j, \forall i \in \mathcal{N}$. For each prosumer $i \in \mathcal{N}$, we define the set of coalitions of clusters that do not contain i as $\mathcal{U}_i = \{cl_{\mathcal{U}} \mid cl_{\mathcal{U}} \subseteq (cl_{\mathcal{K}} \setminus cl_{f(i)})\}$. Then we add Prosumer i back into all the coalitions in \mathcal{U}_i and obtain the critical coalition samples $\mathcal{S} := \{\mathcal{T} \mid \mathcal{T} = cl_{\mathcal{U}} \cup \{i\}, \forall cl_{\mathcal{U}} \in \mathcal{U}_i, \forall i \in \mathcal{N}\}$. \mathcal{S} is then used to estimate the nucleolus.

II. KEY RESULTS AND DISCUSSION

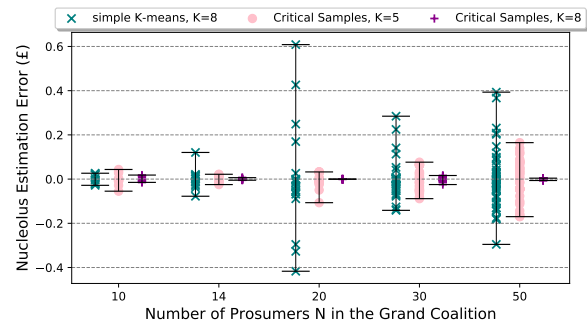


Fig. 1: Sampling Benchmarked Nucleolus estimation for a 24-hour P2P game

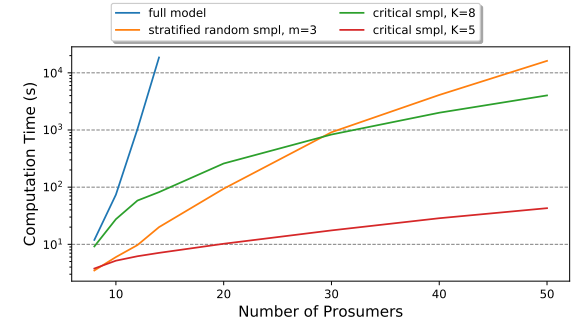


Fig. 2: Nucleolus estimation computation time for a 24-hour P2P game

We test our proposed method using load and PV data from the Customer-Led Network Revolution trials. Fig. 1 shows that the proposed method yields very similar nucleolus estimations as the stratified random sampling benchmark, and that increasing K improves the estimation accuracy. Fig. 2 demonstrates the time savings from the proposed method. With $K = 8$, the computation time becomes significantly shorter than the benchmark when the number of players exceeds 30. The $K = 5$ case, despite its higher estimation errors, shows the potential to scale up the game to hundreds of players.

Day-Ahead Bidding of a Pulp & Paper Mill in the Nordic Energy and Reserve Market

Lars Herre, *Student Member, IEEE*, Federica Tomassini, Lennart Söder, *Senior Member, IEEE*

Abstract—Due to increased use of variable renewable energy sources, more capacity for balancing reserves is required. Non-generating resources such as large industrial consumers can arbitrage energy prices and provide reserves by exploiting the inherent flexibility in selected industrial processes. A large enough industrial consumer can capitalize on this flexibility through optimized bidding in electricity markets. In this work, the day-ahead cost minimization problem of a risk-averse pulp and paper mill (PPM) is formulated as a two-stage stochastic optimization problem, considering the thermal and electrical constraints of the PPM. The bids in the energy and primary frequency reserve markets are optimized subject to price uncertainty. The results of a case study in Sweden display a significant economic benefit in exploiting the flexibility of the steam accumulator. The expected cost of the pulp and paper mill resulting from different strategies are compared and the risk adversity of the PPM is investigated. We show that frequency containment reserve offers can significantly improve the profitability of the PPM.

Index Terms—pulp and paper mill, ancillary services, frequency regulation reserves, industrial demand response

I. INTRODUCTION

The Nordic TSOs recognize in Demand Response (DR) one of the most promising solutions to the current challenges that the power system is facing [1]. In Sweden, there exist 4,500 MW of flexible demand, out of which 51% is found in the industrial sector [2], mainly the pulp and paper (PP) industry. Within the Swedish energy intensive industries, the PP firms are responsible for about 52% of the whole energy consumption [3]. The literature identifies the largest source of flexibility in the pulp production process in the refiners, due to the high utilization and rated capacity. Slowing down the refining process, however, would lead to degraded quality of the pulp. A lower quality of the pulp results inevitably in a worse quality of the paper. For this reason we will not consider flexibility from the refiners in this paper, and instead focus on flexibility from a steam accumulator. The day-ahead cost minimization problem of a risk-averse pulp and paper mill (PPM) is formulated as a two-stage stochastic problem, considering energy and primary frequency reserve markets. The results display a significant economic benefit in exploiting the flexibility of the steam accumulator.

II. CONSIDERED ELECTRICITY MARKETS

Nord Pool is the nominated electricity market operator in Norway, Sweden, Finland, Denmark, Estonia, Latvia and Lithuania with 15 price areas. Nord Pool operates the day-ahead spot market (*Elspot*) and intra-day market (*Elbas*) and publishes relevant information on their website [4]. Besides the wholesale market, electricity can be traded in long term contracts (futures and bilateral contracts) or in the short

term markets (balancing markets). The balancing markets are single-buyer markets that are operated by the Transmission System Operator (TSO) of the respective country. Market players that are responsible for imbalances are invoiced ex-post the day after operation. In figure Fig. 1 the different markets and their time line are illustrated. In this work, we

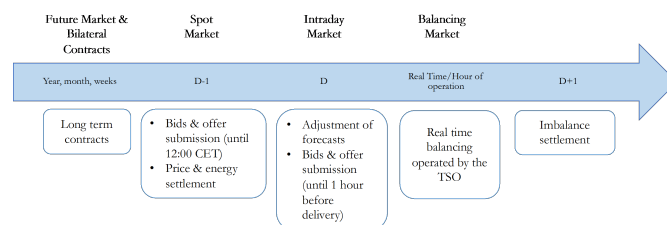


Fig. 1. Electricity and Balancing market time line

examine a PPM that participates in the DA energy spot market and FCR-N market, and - being a Balance Responsible Party (BRP) - implicitly in the imbalance settlement.

III. FLEXIBILITY SOURCE

The most energy intensive process has been identified as the pulp production in the refiners. Therefore, previous literature was focused on the refiners for providing reserve capacity. However, a variation in the power consumption, and thus the rotational speed of the refiners would affect the quality of the produced pulp (in terms of granularity). The quality of pulp, in turn, would inevitably be reflected on the quality of paper. However, it is important to maintain the quality of paper constant and at a high level. Therefore, we focus on the electric boilers and steam accumulator.

REFERENCES

- [1] Statnett, "Challenges and Opportunities for the Nordic Power System," Statnett, Tech. Rep., 2016. [Online]. Available: <https://www.svk.se/en/about-us/news/european-electricity-market/report-challenges-and-opportunities-for-the-nordic-power-system/>
- [2] L. Söder, P. D. Lund, H. Koduvere, T. F. Bolkesjø, G. H. Rossebø, E. Rosenlund-Soysal, K. Skytte, J. Katz, and D. Blumberga, "A review of demand side flexibility potential in Northern Europe," *Renewable and Sustainable Energy Reviews*, vol. 91, no. March, pp. 654–664, 2018. [Online]. Available: <https://doi.org/10.1016/j.rser.2018.03.104>
- [3] Swedish Energy Markets Inspectorate, "Measures to increase demand side flexibility in the Swedish electricity system Abbreviated version," Swedish Energy Markets Inspectorate, Tech. Rep., 2017. [Online]. Available: https://www.ei.se/PageFiles/308322/Ei_{_}R2017_{_}10.pdf
- [4] Nord Pool AS, "Historic Market Data," October 2018. [Online]. Available: <http://www.nordpoolspot.com/historical-market-data/>

Direct Trade Between Wind Farm and Flexible Load in Competitive Electricity Market

Tingli Hu, *Student Member, IEEE*, Caisheng Wang, *Senior Member, IEEE*

School of Electrical and Computer Engineering, Wayne State University, Detroit, Michigan 48202

Email: tinglih@wayne.edu, cwang@wayne.edu

Abstract—Wind farms in a competitive electricity market may suffer from economic losses due to the intermittent nature of wind power. This paper proposes a solution by establishing direct trade between a wind farm and a flexible load. Unlike traditional cooperation scheme, the benefits of wind farm and flexible load are considered individually. Each participant of the trade considers the other's reaction to its decision and adjust its strategy until both sides are satisfied. Uncertainties of wind power generation, energy market prices, and the rest loads are considered. To solve the model, L-shaped method and Lagrangian Relaxation are adopted to decompose the problem. Study cases show that the revenue of the wind farm and the cost of the flexible load can be improved compared with the case when there is no direct trade.

I. POSTER OVERVIEW

Maximizing profit is the objective of a wind farm. For a wind farm that has a plan to trade outside market with flexible load, its source of profit comes from the day-ahead electricity market, real-time electricity market, and the dealing outside market. The objective can be expressed as follows

$$\max_{\lambda_{wt}, W_{dt}, W_{rt}^s, W_{ct}^s} \sum_{t \in T} d_t \left\{ P_{wt} \lambda_{wt} + \lambda_{dt} W_{dt} + \sum_{s \in S} p^s [\lambda_{rt}^s (W_{rt}^s - W_{dt})] \right\} \quad (1)$$

The objective of a flexible load is to minimize its energy cost as expressed in (2). The objective function consists of four parts: 1) the cost of power from direct trade with a wind farm; 2) the cost of power in day-ahead market; 3) the expected cost of power in real-time market; and 4) the extra cost of shifting its production plan.

$$\min_{P_{wt}, P_{dt}, P_{rt}^s} \sum_{t \in T} d_t \left\{ \lambda_{wt} P_{wt} + \mu_{dt} P_{dt} + \sum_{s \in S} p^s [\mu_{rt}^s (P_{rt}^s - P_{dt}) + c (P_{wt} + P_{rt}^s - P_{0t})_+ + h (P_{0t} - P_{wt} - P_{rt}^s)_+] \right\} \quad (2)$$

By including the complicating constraint in the cost function as a penalty, the model of the flexible load can be decomposed into sub-problems for each individual time intervals:

$$L_t(\pi) := \min_x \lambda_{wt} P_{wt} + \mu_{dt} P_{dt} + \sum_{s \in S} p^s [\mu_{rt}^s (P_{rt}^s - P_{dt}) - \pi^s (P_{wt} + P_{rt}^s) + c P_{1t}^s + h P_{2t}^s] \quad (3)$$

In the direct trade, the wind farm is a price setter and the factory is a price responder. They cooperate at the same time they game with each other. The process of how they make decisions is described below

Algorithm 2. solve a cooperation problem

- 1 choose $W_{rt}^s = 0 \forall t$ and s ;
- 2 choose $\lambda_{wt} \leq \mu_{dt} \forall t$;
- 3 solve the factory model and compute its cost over T ;
- 4 by results of step 3, solve the wind farm model and obtain its total revenue over T ;
- 5 if a constraint is violated with updated parameters, go to step 3, otherwise go to step 2 with different λ_{wt} ;
- 6 compare and determine a proper wind power price that is acceptable for wind farm and factory.

Some experiment results are shown below:

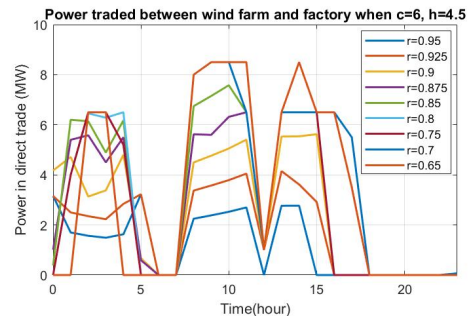


Fig. 1. Power traded between wind farm and factory, $c = 6$ and $h = 4.5$

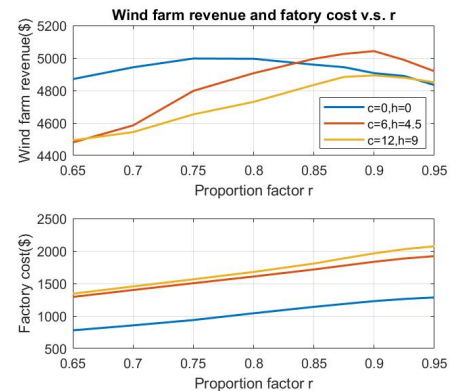


Fig. 2. Revenue of the wind farm and cost of the factory during one day

Market Mechanism for Energy Storage System based Virtual Inertia

Aravind Ingalalli, Timothy M. Hansen, and Reinaldo Tonkoski
 South Dakota State University, Brookings, SD 57007
 Email: aravind.ingalalli@sdstate.edu

Abstract—Different Federal Energy Regulator Commission (FERC) orders have provided the opportunity for battery energy storage systems (ESSs) to participate in markets. The ability to be a fast-ramping generator or load allows ESSs to provide different grid services. This paper proposes a framework for ESSs to participate in virtual inertia services and build market mechanisms for offered services. The economic value of ESSs can be further increased by pragmatically participating in markets and services considering operational and degradation aspects. To analyze the system transient response during disruptive events, a detailed power system model is developed. Using model reduction technique equivalent reduced order model that retains the transient response is used for analytical computation of transient performance parameters. Reduced models are also suitable for real-time deployment, and hence are key for providing ESS services and taking emergency control actions. The effectiveness of the proposed framework will be examined in WSCC (Western System Coordinating Council) 9-Bus system.

Index Terms—Battery energy storage systems, power system resilience, electricity markets.

I. INTRODUCTION

Synchronous generators, which have rotational inertia, traditionally dominated the bulk generation of power systems. Rising greenhouse gas (GHG) levels have encouraged investments in renewable energy sources (RES), the majority of which are intermittent in nature. RESs are often interfaced to the grid through inverters, not providing inertial response. As the deployment of RES increases, there is a decline in mechanical system inertia, leading to larger frequency variations or even instability. Recent advances in battery energy storage systems (ESSs), with new regulations and market frameworks, have facilitated the integration of ESSs in the U.S. bulk electric grid. Along with services like regulation, load following, and energy shifting, ESSs can also support the inertial response of the grid. Even though a future low-inertia grid is likely, the conventional frequency regulation process has not been updated to allow new market mechanisms for inertial services. ESSs can make use of their fast-ramping characteristic, inverters, and control algorithms to mimic the inertia of a conventional system and provide *virtual inertia* (VI), as illustrated by Fig. 1.

II. PROPOSED FRAMEWORK

A framework to assess economic viability of ESSs to improve low-inertia grid stability still needs to be designed. During disruptive events, frequency nadir (FN), and rate of change of frequency (ROCOF) are the primary performance parameters that define the transient behaviour of the power

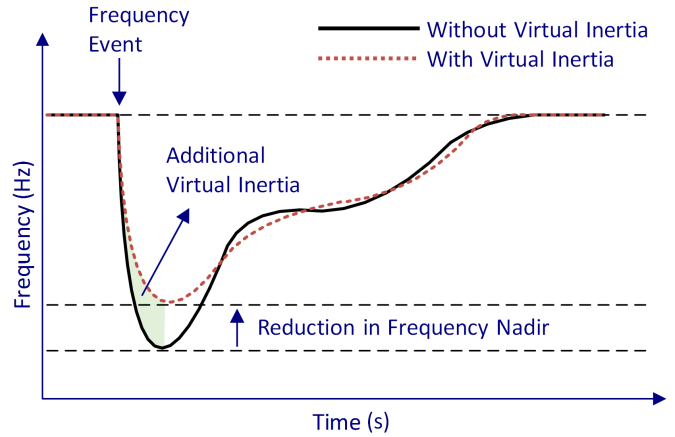


Fig. 1. Comparison of frequency response between a system with low inertia and a system with additional virtual inertia.

system with a given inertia constant (M), generation (P_G) and load profiles (P_L). The proposed framework for estimating the economic value of ESS in maintaining the stability of the low-inertia grid is depicted in Fig. 2.

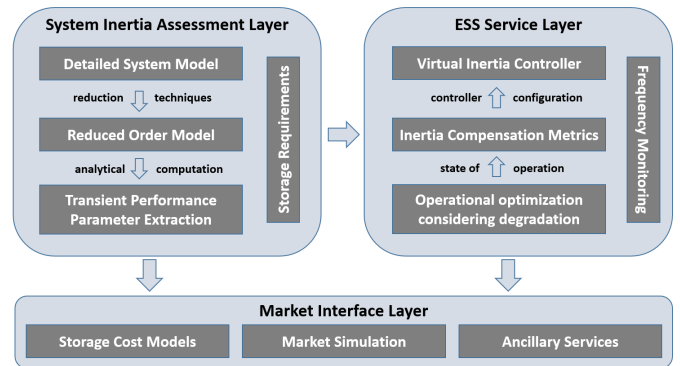


Fig. 2. Overall structure of the framework for estimation of economic value of storage participation in VI market.

Each of the layers of the proposed framework aim to provide a model with the respective objectives described as below.

- System inertia assessment layer for capturing the transient behavior: $[FN, ROCOF] = \mathcal{F}(\Delta P_G, \Delta P_L, M)$
- ESS service layer for improving the transient behavior: $[\Delta FN, \Delta ROCOF] = \mathcal{F}(FN, ROCOF, Degradation)$
- Market interface layer for estimating the economic value: $[\$Cost] = \mathcal{F}(\Delta FN, \Delta ROCOF, \Delta Degradation)$

Optimal Participation of Price-Maker Battery Energy Storage in Energy and Ancillary Services Markets Considering Degradation Costs

Reza Khalilisenobari
Arizona State University, Tempe, AZ

Meng Wu
Arizona State University, Tempe, AZ

Abstract—Motivated by the need of assessing the impact of stacked battery energy storage (ES) services on various market operations, an optimization framework is proposed to coordinate the operation of a utility-scale price-maker ES in the energy, reserve and performance-based regulation markets while considering the cost of battery cells degradation. The entire problem is formulated as a bi-level optimization process, where ES is modeled as a price-maker in real-time (RT) energy, reserve, and regulation markets, but a price-taker in day-ahead (DA) energy market, due to the size and liquidity of DA markets. In the upper level (UL) problem, ES owner maximizes its revenue from participating in multiple markets while considering its operating costs and limits. The lower level (LL) problem is a joint optimization of energy, reserve and regulation in the RT, simulating the joint market clearing process of independent system operators (ISOs). The advantages of the proposed framework include: 1) Doing portfolio management for a ES over various markets; 2) Investing effect of a price-maker ES on each market; 3) Considering degradation cost in the bi-level bidding strategy problem.

Index Terms—Battery energy storage, bidding strategy, price-maker, bi-level optimization

I. MODEL FORMULATION

A. Upper Level Problem

The objective function of the UL problem can be written as following:

$$\max \sum_t \sum_i R_{i,t}^{DA} + R_{i,t}^{RT} + R_{i,t}^{Rs} + R_{i,t}^{Rg,C} + R_{i,t}^{Rg,M} - DgC_{i,t} \quad (1)$$

In (1), i is the index of each ES unit, t is the time interval index, R represents the revenue of ES from participating in DA energy market and RT energy, reserve and regulation markets, and DgC is the battery's degradation cost function. ES revenue from each market is calculated by multiplication of market clearing price (MCP) and the scheduled power. The MCPs and scheduled power of RT energy, reserve, and regulation markets are obtained from the LL optimization problem. For the performance-based regulation market, there exist two components for the regulation capacity (Rg, C) and regulation mileage (Rg, M) which are affected by the unit performance. The degradation cost is modeled by a simplified linear function of charged and discharged power. Note that it models less cost for regulation signals as they cause shallower charging cycles and less degradation. Constraints of UL problem are mainly limits of output power and state of charge. It is assumed

that ES owner can perfectly estimate DA price. The decision variables for this UL profit maximization problem, including ES power exchange in DA market and ES offers in various RT markets, serve as inputs to the LL market clearing problem.

B. Lower Level Problem

$$\min \sum_t \left[\sum_i C_{i,t}^{ES,RT} + C_{i,t}^{ES,Rs} + C_{i,t}^{ES,Rg,C} + C_{i,t}^{ES,Rg,M} + \sum_j C_{j,t}^{O,RT} + C_{j,t}^{O,Rs} + C_{j,t}^{O,Rg,C} + C_{j,t}^{O,Rg,M} \right] \quad (2)$$

The objective function of the LL co-optimization is shown in (2), where $C_{i,t}^{ES,\cdot}$ and $C_{j,t}^{O,\cdot}$ represent the cost for procuring various market products from ES units and other market participants, respectively. Optimal ES offers for various markets, obtained from the UL problem, serve as inputs for calculating $C_{i,t}^{ES,\cdot}$. Operating limits of the market participants, performance-based regulation limits and system requirements for each product are three main groups of LL problem constraints. The dual variables of the third group of LL constraints are MCPs that are used for revenue calculation in UL.

II. CASE STUDY

Fig. 1 shows the exchanged power of a ES in various markets in a three-bus test system over 12 consecutive hours.

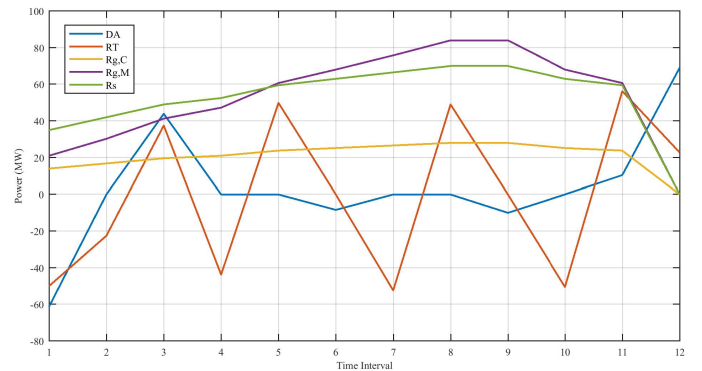


Fig. 1. Simulation results of a test system.

U.S. Electricity Markets as a Model for Broadband Development and Structuring

Evan McKee, *Student Member, IEEE*, and Fanxing Li, *Fellow, IEEE*
University of Tennessee, Knoxville

Abstract—The United States electricity market is a deregulated market that uses limited government control to bring reliable service to customers at a reasonable price. The transmission and distribution of electricity is controlled by supervised monopoly, while market participants are able to compete at the generation and retail levels. Resiliency, affordability, and open access are maintained largely because electricity is considered a necessity. By contrast, the market for broadband internet managed by U.S. telecom companies enjoys a high level of privatization and sparse government regulation, with a few large players and high barriers to entry. Should society in the 21st century deem internet a necessity, the organization and regulation of the electricity market may prove useful as a model for government intervention in these markets. A mock arrangement of such an industry is imagined and described here, and challenges to adoption are explored. The regulation and maintenance of U.S. electricity is a success story with regards to the level of government oversight, and one that could be repeated in other industries as societal demands warrant.

I. INTRODUCTION

Electricity began as a luxury good available only to the very wealthy. As technology made electricity more affordable, state and federal governments decided electricity was a necessity and facilitated its adoption with consumer-friendly policies for maximum coverage. Electricity represents the most recent American commodity converted to a utility.

Although electricity markets vary across the country, certain regulatory structures are common. Most markets are vertically de-integrated so that generation, transmission, and distribution are handled by different companies. This is to ensure fair access to small players at the generation and distribution levels. Fig. 1 shows a typical U.S. electricity market. At the transmission level, most ISOs and RTOs are nonprofits subject to FERC governance.

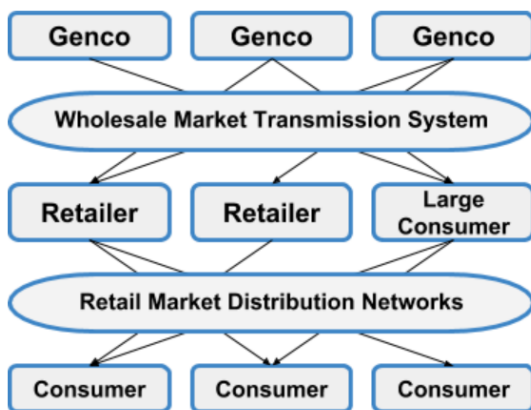


Fig. 1. Retail competition model of electricity market according to Hunt and Shuttleworth (1996).

In the telecommunications industry, infrastructure development is so expensive that large players can be tempted to recoup their efforts by exerting monopolistic or collusive power. The FCC has difficulty preventing price gouging, because transmission and distribution are maintained by the same few internet service providers (ISPs).

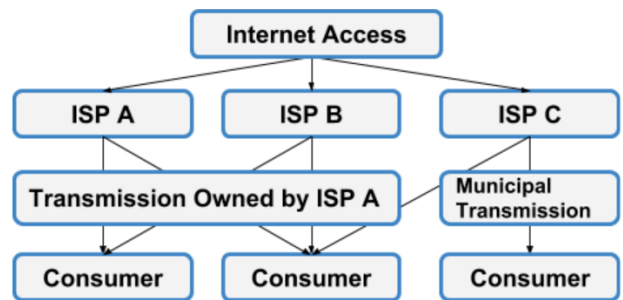


Fig. 2. Current model of the U.S. telecommunications market.

In the proposed vertically de-integrated model, one company is given regulated monopoly access to a geographic region to establish a broadband or fiber optic network, but is restricted in selling directly to consumers. Instead, small retailers rent access to the transmission line and maintain relatively less expensive distribution networks. The price is regulated at the transmission level and small players gain market access.

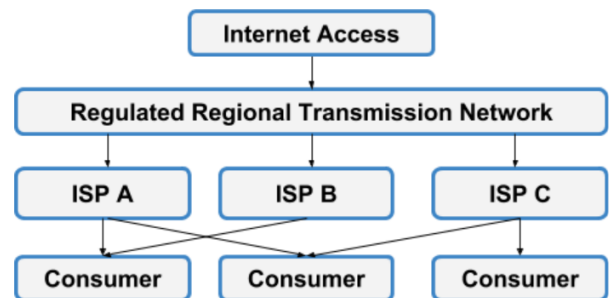


Fig. 3. Proposed vertically de-integrated model.

II. KEY RESULTS

The proposed model is able to use the regulatory lessons of the electricity market to mitigate price and competition issues in the U.S. broadband market, but creates challenges of its own. Even if this model were utopian and support for universal broadband were unanimous, there are significant transition barriers between the current system and the new one. The model described might be more suitable for undeveloped markets instead of established ones.

Pricing in Peer-to-Peer Energy Trading Using Distributed Optimization Approach

Amrit Paudel, *Student Member, IEEE*, Hoay Beng Gooi, *Senior Member, IEEE*
Nanyang Technological University, Singapore

Abstract—A peer-to-peer (P2P) energy trading model is considered as one of the suitable models to manage local energy trading in a community microgrid. The pricing mechanism is crucial in P2P energy trading because energy price is a key factor in determining the benefits of local energy trading. Designing a proper pricing scheme maintaining the privacy of the participants is a challenging task. This work proposes a novel privacy preserving pricing mechanism for P2P energy trading in a community microgrid with prosumer and consumer households. An alternating direction method of multiplier (ADMM) based distributed approach is proposed to determine the energy price. The proposed method solves the energy pricing problem for P2P energy trading with minimal exchange of information among the agents participating in the trading. The simulation results have shown the proposed distributed approach of energy pricing in P2P energy trading is feasible.

I. INTRODUCTION

A proper pricing mechanism is necessary to facilitate the energy trading between prosumers and consumers in the P2P energy market. The pricing mechanism is crucial in P2P energy trading because energy price is a key factor in determining the benefits of local energy trading. The pricing mechanism should be computationally efficient and set with a defined objective of the trading. Each participant in the P2P market is an independent entity. They have their own set of private information which they do not want to reveal it to the public. Modeling the user's behavior with limited information is difficult. Therefore, designing a proper pricing scheme maintaining privacy is a challenging task.

II. SYSTEM MODEL

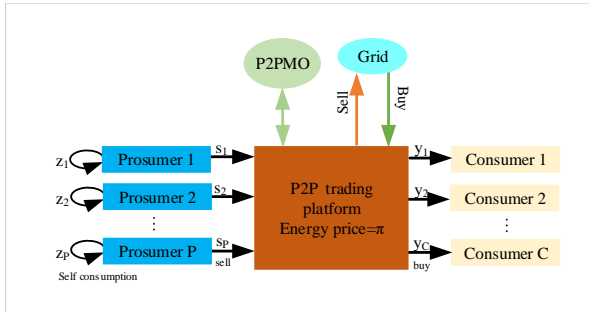


Fig. 1. P2P energy trading platform

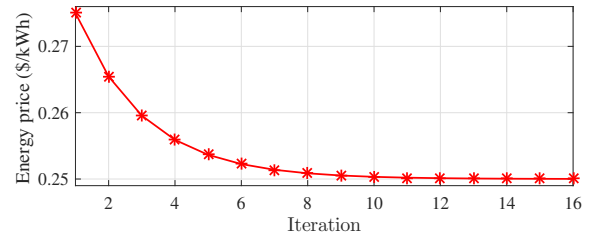


Fig. 2. Convergence characteristics of P2P energy price

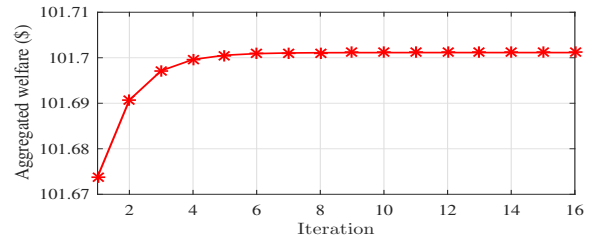


Fig. 3. Aggregated welfare of the community microgrid

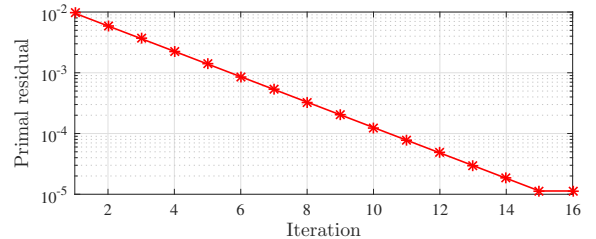


Fig. 4. Primal residual at each iteration

III. CASE STUDY

IV. CONCLUSION

The proposed method is applied to a small community microgrid with consumers and prosumers having PV systems. Then, the convergence of our ADMM-based distributed approach is verified with numerical results. The simulation results have shown the proposed distributed approach of energy pricing in P2P energy trading is feasible.

Unbalanced Distribution System Economic Dispatch in a Co-Simulated Environment

Cody Rooks, *Student Member, IEEE*, and Fangxing Li, *Fellow, IEEE*
 Department of Electrical Engineering and Computer Science
 The University of Tennessee
 Knoxville, TN 37996
 {crooks2, fli6}@utk.edu

Abstract—The multitude of grid devices available for a distribution system operator create a challenging economic dispatch problem. Some devices are dispatchable, while others are not and can exhibit intermittent characteristics. Also of challenge in a distribution system is its inherently unbalanced operation, which must necessarily be taken into account. In this work, the economic dispatch problem is solved for a distribution system operator in a co-simulated environment, where an agent-based network simulator is paired with a linear programming-based optimizer.

Keywords—distribution system operator, economic dispatch, co-simulation, electricity markets

I. BACKGROUND

Similar to the challenges faced by an Independent System Operator (ISO), a microgrid or distribution system operator (DSO) will attempt to balance a portion or all of its load in an economically optimized way [1]. In other words, it will attempt to solve the economic dispatch problem in its own domain. A DSO has several different types of distributed energy resources (DERs) at its disposal. These DERs will take the form of dispatchable generators (e.g., microturbines), non-dispatchable generators (e.g., solar PV) and curtailable load (e.g., thermal energy storage). The availability of many of these resources is difficult to forecast and fluctuate significantly throughout the day. Capacity and energy forecasts typically become more accurate and valid the closer they are to the dispatch time. For these reasons, a co-simulated approach is taken, where the economic dispatch problem is solved in comparatively shorter iterations. The benefits of this approach are: a more realistic study and consequently more practical results, as well as a more readily-deployable solution. Further, while most previous work in this area assumes balanced operation, this work models unbalanced system operation.

II. SYSTEM MODELLING

The optimizer must rely on approximated system models in order to calculate appropriate decision variables. For the network model, Reduced DistFlow [2] equations are used, which are shown in the figure below.

$$\begin{aligned}
 P_{i+1} &= P_i - r_i(P_i^2 + Q_i^2)/V_i^2 - p_{i+1} \\
 Q_{i+1} &= Q_i - x_i(P_i^2 + Q_i^2)/V_i^2 - q_{i+1} \\
 V_{i+1}^2 &= V_i^2 - 2(r_i P_i + x_i Q_i) + (r_i^2 + x_i^2)(P_i^2 + Q_i^2)/V_i^2 \\
 p_i &= p_i^p - p_i^q & q_i &= q_i^p - q_i^q \\
 P_{i+1} &= P_i - p_{i+1} \\
 Q_{i+1} &= Q_i - q_{i+1} \\
 V_{i+1} &= V_i - (r_i P_i + x_i Q_i)/V_i^2
 \end{aligned}$$

Figure 1. Reduced DistFlow equations

Each phase in the distribution system is described by its own set of DistFlow equations. Additional inequalities are added in to ensure the system does not become too unbalanced. A linearized home model is also used to approximate home thermal energy storage capacity.

III. CO-SIMULATION ENVIRONMENT

The co-simulated environment is built from a number of open-source tools, including GridLAB-D, HELICS and Python. In the developed environment, the optimizer receives state information from the network simulator, which it uses to run an optimization program. The decision variables are sent back as set points to the network simulator, which continues its trajectory over a prescribed amount of time. This process iterates in multi-minute intervals.

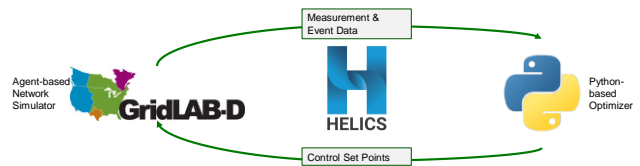


Figure 2. Co-Simulation Environment

IV. CASE STUDY

The approach is tested on the IEEE 13 bus distribution system, diagrammed in Figure 3. Results show that the operator is able to minimize its cost over the course of the day utilizing both imports from the main substation, as well as DERs in its own domain.

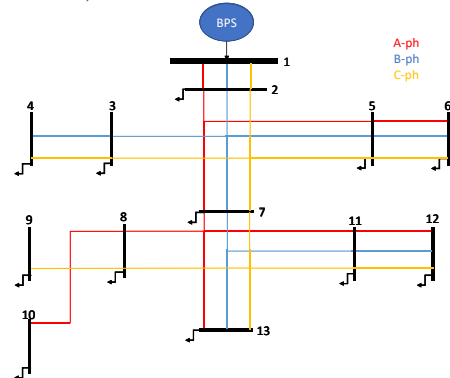


Figure 3. IEEE 13 bus system

REFERENCES

- [1] R. Masiello, J.R. Agüero, “Sharing the Ride of Power,” IEEE Power and Energy Magazine, vol. 14, issue 3, pp. 70-78, 2016.
- [2] Wu, F.F., “Network reconfiguration in a distribution system for loss reduction and load balancing,” IEEE Transactions on Power Delivery, 1989, 4, 1401-1407.

Decomposable Solution Paradigm for Uncertainty-based Transmission and Distribution Coordinated Economic Dispatch

Shengfei Yin, *Student Member, IEEE*, Jianhui Wang, *Senior Member, IEEE*, and Zhengshuo Li, *Member, IEEE*,
 Department of Electrical and Computer Engineering, Southern Methodist University, TX, USA

Zusammenfassung—This paper proposes a two-stage formulation and its solution paradigm for the coordinated economic dispatch of transmission and distribution (T-D) market. The first stage concerns the benefits for transmission system operator (TSO), which transfers the optimal power injection with locational marginal prices (LMPs) via the boundary node to the active distribution system operators (DSOs), whereas DSOs in the second stage return their optimal nodal power demand back to the TSO. In the distribution network, not only conventional dispatchable distributed generators but the uncertainties of renewable energy and volatile demands are considered, which are tackled via stochastic programming approach in the second stage. The proposed framework can be effectively solved by a generalized multi-cut L-shaped method. Numerical experiments on test systems support the efficacy of this paradigm.

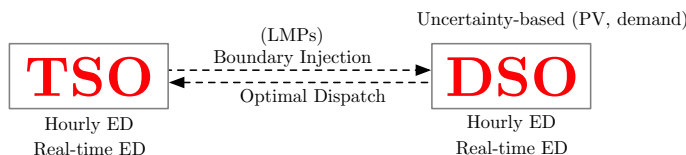
Index Terms—Coordinated T-D markets, renewable and demand uncertainty, stochastic programming, nested L-shaped method.

I. INTRODUCTION

The coordination between transmission and distribution (T-D) networks has raised great attention these days along with the wild growth of lower-level uncertainties from the increasing penetration of renewable energy. Decentralized transactive optimization method has undertaken wide discussion for the future's market paradigm. In this paper, a decentralized market structure is proposed for the T-D coordination, with consideration of multiple uncertainties drawn from the renewable energy and elastic demand. The validation of this structure is performed via solving an uncertainty-based T-D coordinated day-ahead economic dispatch (ED) model. Since the problem is stochastic, we generalize the multi-cut L-shaped method to enhance the decomposition of the structure and the efficiency of the solution.

II. PROPOSED MARKET STRUCTURE

Below shows the coordination between TSO and DSO in terms of ED problem in the market. The communication between TSO and DSO is limited to LMP and boundary injection, which ensures the operator's confidentiality and the system's decentralizing structure.



III. KEY MODELS

A. Master Problem for TSO

$$\min_{\mathbf{P}_{g^T}, \mathbf{s}_{d^T}} \text{TC}$$

subject to

$$\mathbf{P}_{g^T} - \mathbf{F}_{s\ell^T} + \mathbf{F}_{r\ell^T} = \mathbf{D}_{d^T} - \mathbf{s}_{d^T}$$

operational constraints, DC power flow

The TSO's master problem is not uncertainty-based and adopts DC power flow for industrial practice. TC represents the TSO's cost; \mathbf{P} , \mathbf{F} and \mathbf{s} denote active power generation, line flow and load curtailment, respectively.

B. Subproblem for DSO

$$\min_{\mathbf{P}_{g^D}, \mathbf{s}_{d^D}} \sum_i \mathbb{E}_\omega \{v_i \text{DC}_i\}$$

subject to

$$\mathbf{P}_{g^D, i} + \mathbf{P}_{r^D, i}(\omega) - \mathbf{F}_{s\ell^D, i} + \mathbf{F}_{r\ell^D, i} = \mathbf{D}_{d^D, i}(\omega) - \mathbf{s}_{d^D, i}, \quad \forall i$$

operational constraints, SOCP-based AC power flow

The DSO's subproblem is stochastic in terms of renewable generation ($\mathbf{P}_{r^D, i}(\omega)$) and elastic demand ($\mathbf{D}_{d^D, i}(\omega)$). ω and i denote the number of scenarios and distribution systems respectively. The L-shaped cuts are sent from DSO's ED to TSO's ED. Second-order cone programming (SOCP) based AC power flow is adopted for DSOs.

IV. KEY RESULTS AND CONCLUSION

IED_1	TS	Costs:	\$76913.86
		ADG₁	ADG₂
	Power Mismatch	14.8%	28.1%
	Generation Costs	\$6043.27	\$9652.77
	Received LMP	17.91	17.91
IED_1	TS	Costs:	\$64146.11
		ADG₁	ADG₂
	Power Mismatch	3.6%	6.8%
	Generation Costs	\$6243.71	\$9643.86
	Received LMP	13.44	13.44
$TDCEd$	TS	Costs:	\$63392.43
		ADG₁	ADG₂
	Power Mismatch	0%	0%
	Generation Costs	\$6236.84	\$9662.21
	Received LMP	13.90	13.90

Other figures and tables are omitted here and will be presented in the poster. This table shows the result on a 22 bus TS + 2ADG system, which validates the necessity of designing T-D coordinated market paradigm.

Shadow Price Formulation and Decomposition for Economic Emission Dispatch

Qiwei Zhang, *Student Member, IEEE*, Fangxing Li, *Fellow, IEEE*

Abstract—Power system multi-objective optimization problems have been investigated for years. Numerous models are developed and algorithms are proposed to improve the computation efficiency. However, the lack of discussion on the sensitivity analysis will prevent the intrinsic information of the problem itself from being revealed. In this paper, a sensitivity matrix formulation method for power system multi-objective problem is proposed and applied to economic emission dispatch problem (EED). Furthermore, an emission related locational marginal price is proposed to relate the emission trade and electricity market, according to the sensitivity on the emission generation. In the end, a thorough sensitivity analysis of EED is performed on IEEE 30 bus system to investigate the influence of resources on operation cost and pollutions

Index Terms— Multi-objective optimization, Shadow price decomposition, Sensitivity matrix, Economic emission dispatch

I. PROBLEM FORMULATION

) Objective functions

➤ Operation costs minimization

$$Fc_i(P_{G_i}) = a_i + b_i P_{G_i} + c_i P_{G_i}^2 \quad (1)$$

where P_{G_i} is the power generation of the generator i , $Fc_i(P_{G_i})$ is the total fuel cost for the generator i , and a_i , b_i , and c_i are fuel cost coefficients of the generator i .

Then, the overall system operation cost is defined in (2)

$$Fc = \sum_{i=1}^N Fc_i(P_{G_i}) \quad (2)$$

where N is the generator counts in the system. Fc represents the overall system operation cost.

➤ Pollution minimization

$$E_i(P_{G_i}) = \alpha_i + \beta_i P_{G_i} + \delta_i P_{G_i}^2 \quad (3)$$

where α_i , β_i , and δ_i are emission coefficients of the generator i .

(2) Constraints

➤ Power balance constraint:

$$\sum_{i=1}^N P_{G_i} = \sum_{i=1}^{N_L} P_{L_i} \quad (4)$$

where N_L is the total number of loads. The power balance constraint is equality constraint. The sum of electricity from generators must be equal to the sum of the distributed loads.

➤ Generator output limits

$$P_{G_i}^{Min} \leq P_{G_i} \leq P_{G_i}^{Max} \quad \forall i \quad (5)$$

The generation of each generator must be within its lower and upper limit to secure the generator operation. $P_{G_i}^{Min}$ and $P_{G_i}^{Max}$ are the minimum and maximum value respectively.

➤ Transmission line limit

$$|P_k| \leq P_k^{Lim} \quad k=1,2,3,\dots,N \quad (6)$$

where N is the total number of transmission lines, and P_k^{Lim} is the flow limit at line k .

II. MAIN METHODOLOGY

A. Shadow price decomposition

C_b is defined as the optimal basis's coefficients in the composite objectives.

$$[v, \kappa_k] = C_b * B^{-1} \quad (7)$$

Then by substituting C_b , the shadow price can be expressed as (15). W is the weight matrix, and G is the coefficient matrix.

$$[v, \kappa_k] = W * G * B^{-1} \quad (8)$$

$$V = G * B^{-1} \quad (9)$$

$$[v, \kappa_k] = W * V \quad (10)$$

Therefore, the relationship between the composite shadow prices and model parameters is established. The decomposed shadow price will be defined as (10)

III. CASE STUDY

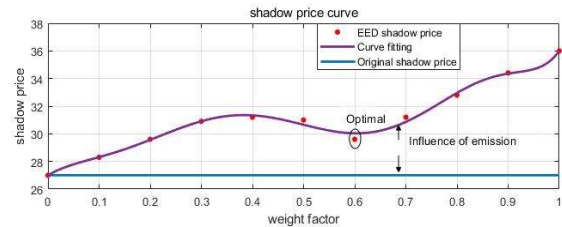


Fig.1. Composite shadow price

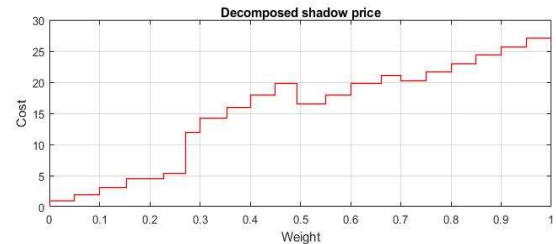


Fig. 2. Weighted decomposed shadow price for fuel cost

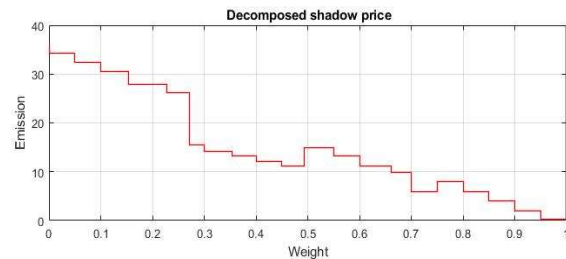


Fig. 3. Weighted decomposed shadow price for emission

Continuous-time Flexible Ramp Scheduling in Forward Power Systems Operation

Avishan Bagherinezhad, Masood Parvania
 Department of Electrical and Computer Engineering
 University of Utah, Salt Lake City, UT 84112

Emails: {avi.bagherinezhadsowmesaraee, masood.parvania}@utah.edu

Abstract—This paper proposes a novel continuous-time optimization model for co-optimizing the energy, regulation and flexible ramp services in forward markets. The proposed model accurately models the power and ramping requirements of each market product and ensures that they are carefully allocated to generating units based on their available power and ramping capacity. Therefore, the proposed model ensures the coordination of services provided by generating units based on both power and ramping requirement of the services. A function space method is then proposed that converts the proposed continuous-time model into a mixed-integer linear programming (MILP) problem. The numerical results, conducted on the IEEE Reliability Test System, demonstrates the effectiveness of the proposed model in ensuring simultaneous delivery of different services in the system.

I. INTRODUCTION AND METHODOLOGY

Large-scale integration of renewable energy sources (RES) and the associated variability and uncertainty of RES increases the real-time deviation of net-load (load minus RES) from the forecast values. The emergent deviation of forward resource scheduling models calls for additional resources to provide adequate power and ramping capacity in real-time operation. In this regard, California independent system operator (CAISO) and Midcontinent independent system operator (MISO) has introduced flexible ramp products to provide more flexibility in real-time operation. Integrating and scheduling flexible ramp products in electricity market have introduced operational challenges that have been the topic of multiple research works in the past few years. The current discrete-time models for scheduling flexible ramp products do not provide an appropriate platform to model the ramping of resources that may result in schedules that are not deliverable and are in conflict with the energy and reserve schedules of resources. As an alternative modeling approach, continuous-time optimization models provide an accurate view of ramping in power systems operation, where ramping is defined as an explicit decision variable that is equal to time derivative of continuous-time power trajectory of resources. The current models, have focused on energy markets and have not explored the application in scheduling flexible ramp services. The proposed continuous-time optimization model to co-optimize the energy, regulation and flexible ramp services provided by generating units in forward (e.g., day-ahead) power systems operation. The paper models the up and down flexible ramping capacity provided by generating units as explicit continuous-time decision variables and ensures the deliverability of ramp-

ing capacity by reserving the respective energy requirement in generation capacity constraints of units. In addition, regulation up and down capacity of generating units are modeled by continuous-time variables and their respective ramping requirement is accounted for in the ramping constraints of units. A function space method is then proposed to solve the problem that converts the continuous-time problem into a mixed-integer linear programming (MILP) problem, which enables the system operators to ensure the adequate provision of power and ramping requirements of their systems.

II. RESULTS HIGHLIGHTS

We adopt IEEE Reliability Test System to investigate the efficiency of the proposed model. The hourly day-ahead load and solar generation data of CAISO are scaled down to 2850MW and 5% of the net-load trajectory is considered as regulation requirements. Further, CAISO's net-load data in real-time dispatch (RTD) is utilized to calculate the up and down flexible ramp requirements of the system. The results show that the co-optimizing forward market with regulation and flexible ramp products (case2) accurately models the power and ramping trajectories and provide more flexibility as illustrated in ramping capacity allocation Figs.1.

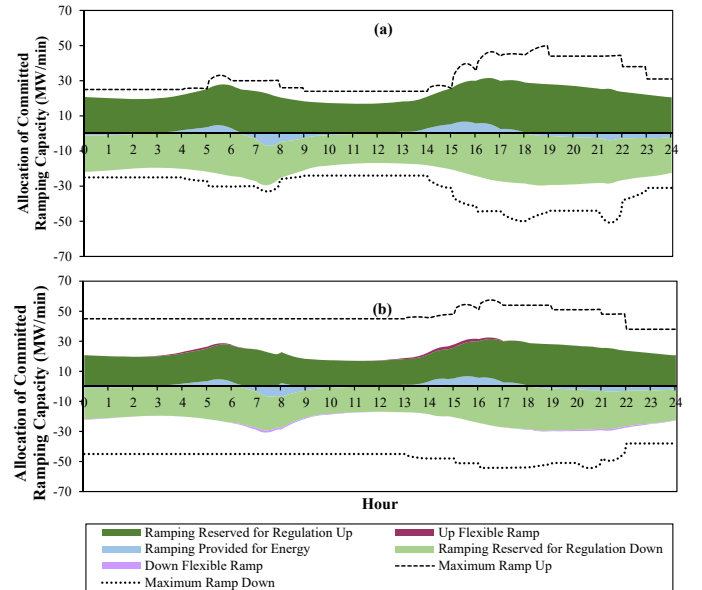


Fig. 1. Ramping Capacity Allocation in a) Case 1, b) Case 2.

To Centralize or to Distribute: A Comparison of Advanced Microgrid Management Systems

Zheyuan Cheng and Mo-Yuen Chow
 Department of Electrical and Computer Engineering
 North Carolina State University
 Raleigh, NC, USA
 Email: {zcheng3, chow}@ncsu.edu

Abstract—The advanced microgrid is envisioned to be a critical part of the future smart grid because of its local intelligence, automation, interoperability, and distributed energy resources (DER) hosting capability. The enabling technology of advanced microgrids is the microgrid management system (MGMS). In this article, we discuss and review the concept of the MGMS and state-of-the-art solutions regarding centralized and distributed MGMSs in the primary, secondary, and tertiary levels, from which we observe a general tendency toward decentralization.

Index Terms—Microgrid, Energy Management System, and distributed control.

I. INTRODUCTION

Both centralized and distributed MGMS includes three control hierarchies: primary, secondary, and tertiary.

A. Primary Control

The primary control directly interacts with the devices in the microgrid and responds to system dynamics and transients. For the centralized MGMS, the concentrated control and master/slave control techniques are typically used to realize power sharing. In the distributed MGMS framework, the distributed control algorithms typically utilize consensus-based communication, distributed observers, or droop control techniques to simplify the communication network, reduce or eliminate communication traffic, and enhance the scalability.

B. Secondary Control

The MGMSs secondary control is responsible for the economical and reliable operation of the microgrid. The main control functions include the automatic generation control and the microgrid EMS. In a centralized MGMS framework, the MGCC first performs a load and renewable generation day-ahead forecast, then collects the required information from every component to solve the day-ahead energy scheduling problem. For the distributed MGMS framework, the concept of the multiagent system (MAS) is primarily used to model the microgrid. More recent works adopted the concepts of distributed optimization and consensus network.

C. Tertiary Control

Tertiary control is the highest MGMS level. It coordinates with neighboring microgrids, DERMSs, and DMSs. For centralized control, tertiary control is typically recognized as a

subsystem of the utility distribution management system (DMS). For distributed control, techniques such as the consensus algorithm and gossip-based algorithm are frequently used to coordinate the MGs and solve the global optimization in a distributed way.

II. COMPARISON: CENTRALIZED VS. DISTRIBUTED

A. System Reliability

In this case study, we adopted a general reliability assessment methodology based on the sequential Monte Carlo simulation method. Overall, the simulation results indicate that, using controllers with the same level of reliability, the system with the distributed MGMS can achieve an 86% lower SAIFI and a 78% lower EENS.

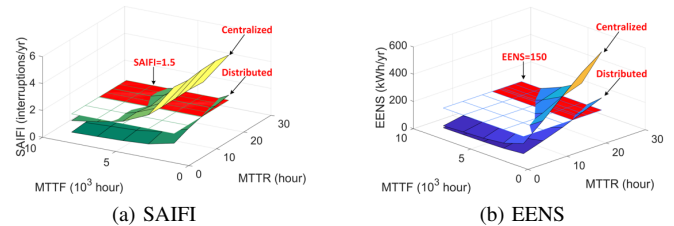


Fig. 1. The reliability indices for various configurations.

B. Resilience Against False Data Injection Attacks

In Fig. 2, we demonstrated that when node 3 is compromised and sends out false information at iteration 600, the attack-resilient distributed controlled system can detect the attack; mitigate the effects; and finally recover from the attack.

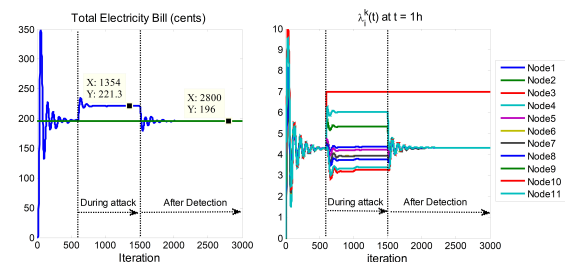


Fig. 2. The convergence evolution of the scheduling result under a fault attack.

State Estimation in Distribution Systems with High DER penetration and Heterogeneous Measurements

Chandra Kant Jat

Department of Electrical and
Computer Engineering
Michigan Technological University
Houghton, Michigan 49931

Sumit Paudyal

Department of Electrical and
Computer Engineering
Michigan Technological University
Houghton, Michigan 49931

Abstract—Correct knowledge of the network topology and system states is critical for reliable and optimal operation of power distribution grids. Modern distribution grids have significant level of dispatchable energy resources including electric vehicles and distributed storage. The uncertainty of these flexible devices also bring the uncertainty in the estimation of system states. The increased uncertainty needs to be tackled by adjusting weights associated with the corresponding measurements. This task is further challenged by the variety of measurements. Remote Terminal Units (RTU), Advanced Metering Instruments (AMI), and micro Phasor Measurement Units (μ PMUs) coexist in modern distributions systems. Therefore, Distribution System State Estimator (DSSE) with the capability to handle flexible resources and heterogeneous data need to be realized. This work presents an outline of state-of-the-art distribution system state estimation and key challenges associated with existing methods. An integral approach with heterogeneous measurements based on the three-phase model of distribution system will be presented.

I. INTRODUCTION

State Estimation (SE), in general, is the process of estimating system states with some knowledge about the system and measurements. In the context of power system, these states could be bus voltage magnitude and phase angles, whereas the measurements can be active and reactive power injections, branch flows (power and/ or current) and bus voltage. The relationship between measurement and the states is non-linear. Correct knowledge of the systems states is critical for any control or resource management decision. Given the importance, it is quite a mature technology in transmission network [1]. A proactive distribution grid with high penetration of distributed energy resources (DERs) and controllable loads, renewed the interest in the field of distribution system state estimation[2], [3]. Direct use of transmission state techniques to distribution may not always work due to some peculiarities of distribution system, such as, less observability, low X/R ratio, mutual coupling, and unbalanced in nature [1]. The key challenges associated with the state estimation in context of distribution system are:

- Network topology identification.
- Uncertainty of DERs and flexible loads.
- Presence of heterogeneous (asynchronous) data.

Here, we make an attempt to develop an integrated DSSE algorithm which addresses the above mentioned challenges.

A general sequential approach for state estimation using heterogeneous measurements is illustrated in Fig. 1. Here, the network topology will be considered to be known based on which a three-phase model of the distribution network will be developed. Depending upon measurement data, weights are assigned to DER measurements. A state estimation based on Weighted Least Square Error will be first tested without utilizing PMU data. The developed state estimates will be further updated with sparse μ PMU data with timed average value for error reduction and improving estimation accuracy.

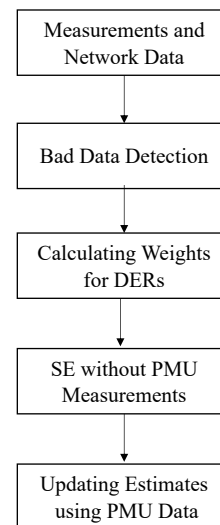


Fig. 1. General flow chart of the planned DSSE.

REFERENCES

- [1] K. Dehghanpour, Z. Wang, J. Wang, Y. Yuan, and F. Bu, "A survey on state estimation techniques and challenges in smart distribution systems," *IEEE Transactions on Smart Grid*, vol. 10, pp. 2312–2322, March 2019.
- [2] A. Primadianto and C.-N. Lu, "A review on distribution system state estimation," *IEEE Transactions on Power Systems*, vol. 32, no. 5, pp. 3875–3883, 2017.
- [3] C. Muscas, M. Pau, P. A. Pegoraro, and S. Sulis, "Uncertainty of voltage profile in pmu-based distribution system state estimation," *IEEE Transactions on Instrumentation and Measurement*, vol. 65, pp. 988–998, May 2016.

AC Control Optimal Set Point of Embedded VSC HVDC in the Perspective of Converting Loss

Soseul Jeong
Department of Electrical Engineering
Korea University
Seoul, South Korea
jss928@korea.ac.kr

Sungwoo Lee
Department of Electrical Engineering
Korea University
Seoul, South Korea
kswvoice@korea.ac.kr

Gillsoo Jang
Department of Electrical Engineering
Korea University
Seoul, South Korea
gjang@korea.ac.kr

Abstract— VSC (Voltage Sourced Converter) HVDC (High Voltage Direct Current) which is in the spotlight in world power system can control AC voltage through reactive power output. Control of the converter can also affect the opposite voltage according to the distance between the two PCC (Point of Common Coupling) bus. Unnecessary conversion loss may occur depending on the AC voltage Setpoint. This paper analyzes the Q output by Setpoint of both converters and proposes the optimal AC voltage Setpoint of Embedded HVDC in terms of conversion loss.

Keywords—VSC, HVDC, AC voltage control, setpoint, PSS/UDM (User Defined Model)

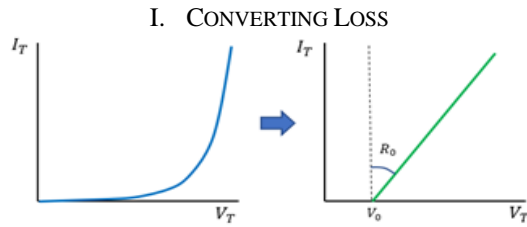


Figure 1. Linearization of VI Character of IGBT

According to the criteria of IEC 62751, conversion loss of VSC is classified into 9 categories in total. Assuming that only the conduction loss of the device is present, the average conduction loss per hour can be as follows.

$$P_T = V_T * I_{Tav} = V_0 * I_{Tav} + R_0 * I_{Trms}^2 \quad (1)$$

The current flowing through the device is as follows.

$$I_t(t) = \frac{I_{dc}}{3} \pm \frac{I_{ac}\sqrt{2}}{2} * \sin(\omega t) \quad (2)$$

Assuming that the first term of Eq. (1) is ignored, one device conversion loss is as follows.

$$P_{conloss} = R_0 * \left[\left(\frac{I_{dc}}{3} \right)^2 + \left(\frac{I_{ac}}{2} \right)^2 \right] \quad (3)$$

II. VAC OPTIMAL SETPOINT

Suppose that converter 1 of Embedded HVDC controls Vac at 1.01 pu and outputs -Q in the region where overvoltage occurs. At this time, the PCC bus of converter 2 is 0.99 pu. If converter 2 controls Vac setpoint to 1.01pu, + Q will be output. As the voltage of the converter 1 PCC bus increases by the +Q of converter 2, converter 1 outputs an additional -Q to keep the voltage at 1.01 pu.

The relationship between P and Q output and AC current on one bus line is as follows.

$$I_{ac} = \frac{P-jQ}{V_{ac}^*} \quad (4)$$

If the value of Q increased when the voltage is relatively constant, the magnitude of the ac current increases and the loss increases due to Equation (3). If the voltage of the converter 2, which is formed when the converter 1 performs the Vac control alone, is set to the Vac setpoint of the converter 2, the Q output can be reduced as much as possible, which is the optimum Vac setpoint in terms of the conversion loss.

III. CASE STUDY

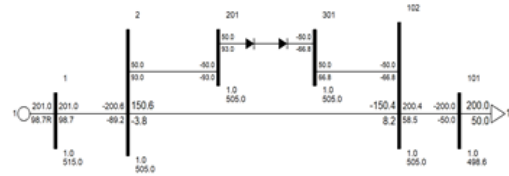


Figure 2. PSS/E Simulation Test System

Table I. Test System Parameter

S_base		300MVA
V_base		120kV
Vdc_base		250kV
PCC bus Voltage (When no Q)	Conv 1	1.0151 p.u
	Conv 2	1.0017 p.u
Num of VSC Submodule (1arm)		100
Submodule R ₀		0.005 Ohm

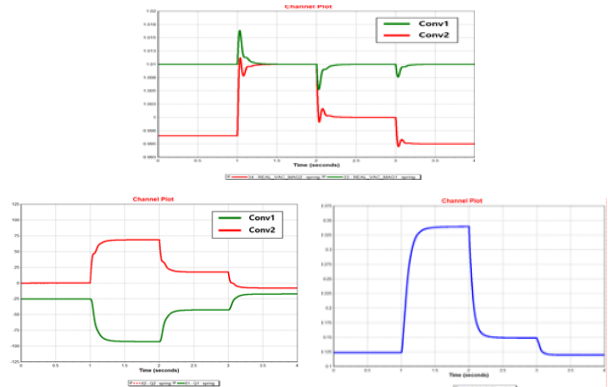


Figure 3. Vac, Q output, Converting loss at different Vac Setpoint

A Distributed Energy Management Approach for Residential Demand Response

Xiao Kou, Fangxing Li
 Dept. of Electrical Engineering and Computer Science
 University of Tennessee, Knoxville
 Knoxville, TN, 37996, USA
 {xkou1, fli6}@utk.edu

Jin Dong, Michael Starke, Jeffery Munk, Teja Kuruganti,
 Helia Zandi
 Oak Ridge National Laboratory
 Oak Ridge, TN, 37831, USA
 {dongj, strakemr, munkjd, kurugantipv, zandih}@ornl.gov

Abstract—The implementation of residential demand response (DR) comes with the challenges of controlling and coordinating domestic appliances for peak shaving. However, existing residential energy management systems are mostly designed for a single house or a small-scale system and cannot be extended for large-scale applications. To address this issue, in this poster we present a hierarchical control scheme to coordinate large-scale residential demand response. The proposed algorithm determines the responsive load operation strategies in a distributed manner by leveraging local home energy management systems (HEMS). Furthermore, only the DR reward price and aggregated load information are being exchanged between the upper and lower levels to reduce communication and computational burdens.

Keywords- distributed computation; home energy management system (HEMS); HVAC; load aggregator; residential demand response; water heater.

I. INTRODUCTION

Today and into the future, there is an increasing need to examine opportunities of shifting electrical energy consumption to improve load factor or the peak-to-average ratio (PAR). According to the U.S. Energy Information Administration, the PAR of electricity consumed in the United States has been increasing for the past few decades [1]. A growing PAR leads to traditionally higher cost for upgrading and maintaining the infrastructures. While energy storage, is a potential distributed energy resource that could provide this needed energy shift, building loads such as heating, ventilation, and air conditioning (HVAC) and water heating can also provide support through thermal energy storage of a building envelope. This could potentially be a lower cost solution compared to large energy storage systems [2].

Existing demand response (DR) research has primarily focused on deployments for industrial customers [3]. These customers tend to have large loads that are more easily targetable with energy management systems. However, residential load accounts for 37% of the total electricity consumption in the United States (2013) and suggest a significant missed opportunity [4]. Still, challenges to energy shifting for residential loads do exist. Unlike industrial load, the residential load is composed of numerous low-power home appliances. In addition, the electricity consumption habits of residential customers are highly varied and dynamic.

Many efforts have been dedicated to investigate the load controls and optimizations in residential networks. However,

from the literature, it is observed that most studies treated the total electricity consumption as a fixed value and assumed that responsive load demand could be shifted without considering comfort factors such as indoor or water temperatures. Furthermore, these approaches require massive information exchange and may not be scalable for large-scale applications. To solve these problems, a new approach is proposed and the main contributions of this paper are: 1) a distributed control scheme with a centralized aggregator to reduce the computational complexity and ensure its feasibility for large-scale applications, 2) customers only need to report aggregated load amount so that all DER parameters, objectives, and constraints remain private, 3) rather than modeling the entire population, the central aggregator is only responsible for updating the incentive variables, 4) users’ discomfort index and the temperature constraints for HVAC and water heater are included into consideration.

II. FLOWCHART OF THE PROPOSED ALGORITHM

The flowchart of the overall process is plotted in Figure 1.

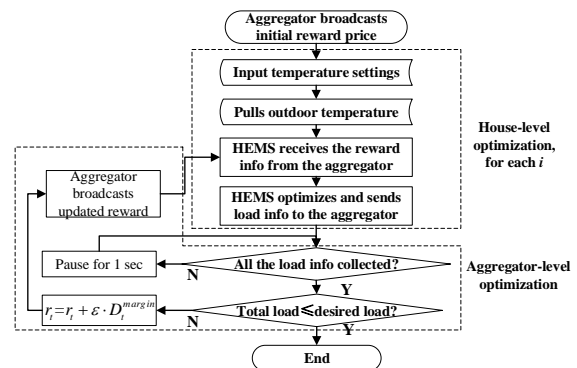


Figure 1. Flowchart of proposed distributed approach.

REFERENCES

- [1] U.S. EIA, “Peak-to-average electricity demand ratio rising in New England and many other U.S. regions,” [Online] available: <https://www.eia.gov/todayinenergy/detail.php?id=15051>.
- [2] C. Li, X. Yu, W. Yu, et al., “Efficient computation for sparse load shifting in demand side management,” *IEEE Transactions on Smart Grid*, vol. 8, no. 1, pp. 250-261, Jan. 2017.
- [3] M. Starke, N. Alkadi, and O. Ma, “Assessment of industrial load for demand response across US regions of the western interconnect,” Oak Ridge National Laboratory, ORNL/TM-2013/407, 2013.
- [4] U.S. EPA, “Electricity consumers,” [Online] available: <https://www.epa.gov/energy/electricity-customers>.

Dynamic Simulation of DFIM-based Pumped Storage Hydro for Pump-Mode Frequency Support

Soumyadeep Nag, Kwang. Y. Lee
 Dept. of Electrical and Computer Science
 Baylor University
 Waco, TX, USA
 {soumyadeep_nag, kwang_y_lee}@baylor.edu

D.Suchitra
 Dept. of Electrical Engineering
 SRM University
 Chennai, India
 such1978@yahoo.com

Vineet Mediratta
 Dept. of Power System Engineering
 University of Petroleum and Energy Studies
 Dehradun, India
 vmediratta@ddn.upes.ac.in

Abstract— This poster displays the ability of the DFIM-based PSH to provide the required support to frequency disturbances due to large output variation of high voltage (HV) grid connected solar farms during pump mode operation. It is found that the nonlinearities of a centrifugal load connected to the grid can be accommodated by the use of model reference adaptive control (MRAC) system. Using MRAC, speed reference tracking can be improved significantly. Also, an algorithm has been investigated to supervise speed reference generation for the DFIM so as to enhance the rate of change of frequency (ROCOF). Together these algorithms provide faster frequency support.

Index Terms—Doubly-fed induction machine, variable speed pumped hydro, model reference adaptive control, nonlinear systems, frequency control.

I. KEY CONCEPTS

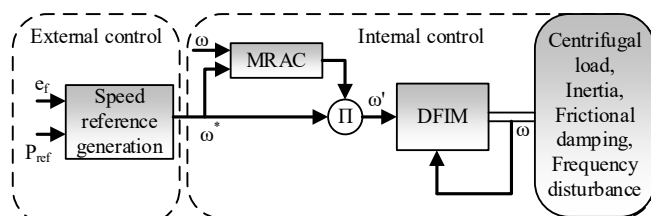


Fig. 1. Schematic diagram of proposed external and internal control DFIM based PSH.

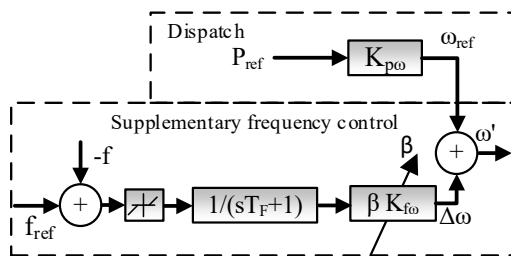


Fig. 2. Adaptive droop based external control for set-point generation based on frequency error.

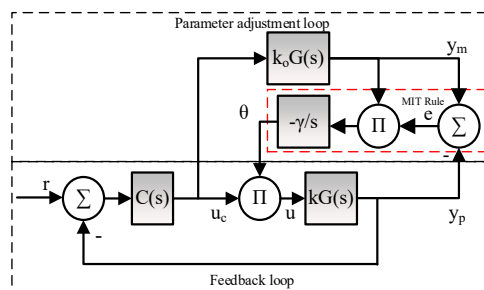
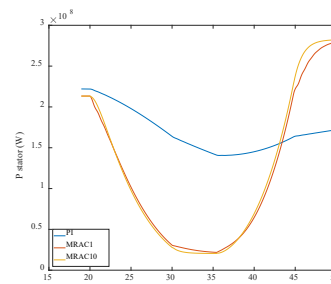
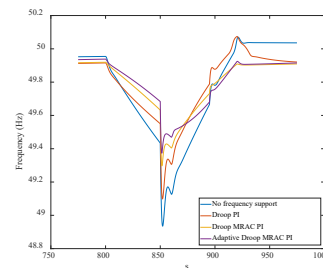


Fig. 3. Internal control for set-point tracking MRAC with MIT rule.

II. KEY RESULTS



(a)



(b)

Fig. 4. (a) Power absorbed by the pump as the speed is varied. (b) system frequency

Distributed Optimization and Coordination Strategy for Stochastic Economic Dispatch with V2G and G2V

Farnaz Safdarian, *Student Member, IEEE*, and Amin Kargarian, *Member, IEEE*

Abstract—Network-constrained economic dispatch (NCED) problem, which takes into account the random mobility of electric vehicles (EV) and additional variables corresponding to each EV’s charge/discharge cycles, is large scale, complex and computationally expensive. To reduce the computational burden associated with this optimization problem, distributed optimization is introduced. Thousands of EVs are considered over the scheduling horizon in order to take advantage of parallel computing and achieve reduced solution time. A ramp-constrained NCED is formulated for each sub-horizon while the connections between subproblems are modeled as shared variables/constraints. In order to coordinate the subproblems and find the optimal solution for the entire operation horizon, auxiliary problem principle (APP) with an efficient initialization strategy is proposed. The proposed method is employed to solve a week-ahead NCED on a 6-bus and IEEE 118-bus test systems. The results are compared with those of a centralized approach and effectiveness of the proposed method in reducing the solution time is verified.

I. INTRODUCTION AND MOTIVATION

The increasing popularity of electric vehicles (EV) is creating new challenges for modern power system operation and planning. EVs are not just a load on the system; vehicle-to-grid (V2G) integration enables bi-directional power flow. The integration of thousands of plug-in electric vehicle (PEV) fleets, considering their random behavior, and defining new variables for each PEV’s charge/discharge makes the size of an economic dispatch problem, much larger and the solution time grows non-linearly with problem size. Distributed optimization algorithms are introduced to reduce the computational burden of solving these large-scale optimization problems. Geographical decomposition approaches are presented in the literature for large operation problems. However, since electric vehicles are randomly moving from one bus to another, the problem cannot easily be decomposed over geographical areas.

II. RESULTS

It is proposed to decompose large problems into a master mixed-integer programming (MIP) problem with several linear programming (LP) subproblems and use Benders cuts for scenario reduction. In order to further alleviate the computational burden and reduce the solution time, time decomposition is applied. The proposed distributed algorithm is employed to solve a week-ahead NCED problem on a 6-bus and the IEEE 118-bus systems.

TABLE I

EV FLEET TRAVEL CHARACTERISTICS

PEV Fleet No.	Number of PEVs	First Trip				Second Trip			
		Departure		Arrival		Departure		Arrival	
		Time	Bus	Time	Bus	Time	Bus	Time	Bus
1	3400	6:00	5	8:00	1	17:00	1	19:00	5
2	2000	7:00	4	8:00	2	16:00	2	17:00	4
3	1000	5:00	4	7:00	2	16:00	2	18:00	4
4	1600	5:00	6	6:00	3	17:00	3	18:00	6
5	2000	7:00	5	9:00	3	18:00	3	20:00	5

A. 6-Bus System

TABLE II EV FLEET CHARACTERISTICS FOR 6-BUS

PEV Fleet No.	Min Cap. (MWh)	Max Cap. (MWh)	Min Charge /Discharge (kW)	Max Charge /Discharge (MW)	a (\$/MW2)	b (\$/MW)	c (\$/h)
1	13.152	65.76	7.3/6.2	24.8/21.08	0.17	8.21	0
2	10.96	54.8	7.3/6.2	14.58/12.4	0.20	8.21	0
3	5.48	27.4	7.3/6.2	7.29/6.2	0.41	8.21	0
4	8.768	43.84	7.3/6.2	11.67/9.92	0.25	8.21	0
5	10.96	54.8	7.3/6.2	14.58/12.4	0.20	8.21	0

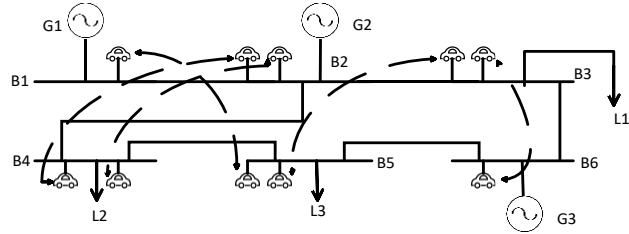


Fig. 1. Six-bus test system.

TABLE III

RESULTS OF 6-BUS SYSTEM

Algorithm	Iteration	relative error	Time (s)
Centralized	-	-	0.18
Distributed	1+1	1e-12	0.14

B. IEEE 118-Bus System

TABLE IV

EV FLEET CHARACTERISTICS FOR IEEE 118-BUS SYSTEM

PEV Fleet No.	Min Cap. (MWh)	Max Cap. (MWh)	Min Charge /Discharge (kW)	Max Charge /Discharge (MW)	a (\$/MW2)	b (\$/MW)	c (\$/h)
1	131.52	986.4	7.3/6.2	24.8/21.08	0.57	27.35	0
2	109.6	822	7.3/6.2	14.58/12.4	0.68	27.35	0
3	54.8	411	7.3/6.2	7.29/6.2	1.36	27.35	0
4	87.68	657.6	7.3/6.2	11.67/9.92	0.85	27.35	0
5	109.6	822	7.3/6.2	14.58/12.4	0.68	27.35	0

TABLE VIII

RESULTS OF IEEE 118-BUS SYSTEM

Algorithm	Iteration	relative error	Time (s)
Centralized	-	-	3.08
Distributed	3+1	1e-08	1.37

III. CONCLUSION

Adding PEV fleets will impose additional operation constraints, but has benefits for supplying critical demands in specific locations and times. We proposed a horizontal decomposition algorithm to divide an ED problem over the scheduling time horizon. The interdependencies, originating from intertemporal constraints of generating units, were modeled by introducing the concept of overlapping time intervals. APP with the introduction of a suitable initialization strategy is proposed. The simulation results showed that the proposed method reduced the computation time of ED for the 6-bus system by 22% and for the IEEE 118-bus system by 55%. We observed that as the size of the problem increases, the distributed algorithms show better performance compared to the conventional centralized method.

A reverse droop based Distributed control framework for DC distribution systems

Satabdy Jena¹, Narayana Prasad Padhy²
 Department of Electrical Engineering
 Indian Institute of Technology Roorkee, India
 sjenal@ee.iitr.ac.in¹, nppeefee@iitr.ac.in²

Abstract—A distributed control paradigm based on reverse droop primary controller is established to formulate a control framework for the problem of achieving voltage regulation and proportionate load current sharing in a DC microgrid scenario. The adjustment/correction factors for the DC voltage is generated by the secondary control layer wherein the voltage and current observers process the neighboring agents’ dataset to effectively regulate the DC voltage. The proposed control achieves faster dynamics as compared to a conventional V-I droop controller thereby enabling improved transient and steady state dynamics. The controller is subjected to various test cases like plug-n-play capability, switched networks, remote and local load changes, resiliency to communication delays, etc. in order to investigate its robustness to disturbances and uncertainties. A low voltage DC microgrid test-system with underlying buck converters with dispatchable energy source inputs is employed to validate the aforementioned features. The paper considers the functioning of the microgrid test-bench under various load dynamics such as constant power loads (CPLs) and resistive loads.

I. KEY FIGURES

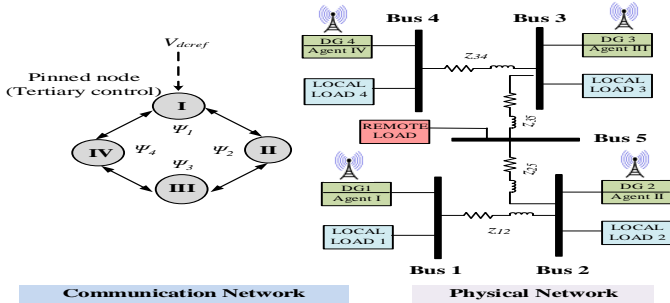


Fig. 1: DC Microgrid Testbed

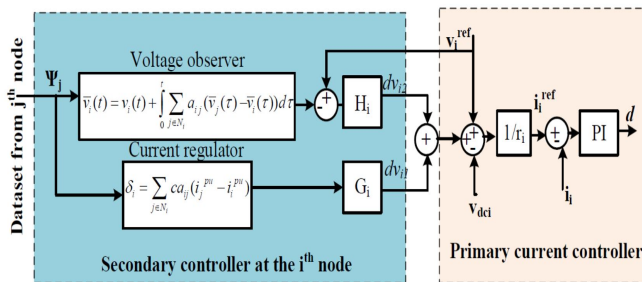


Fig. 2: Proposed IV droop controller with secondary distributed control

II. KEY RESULTS

[H]

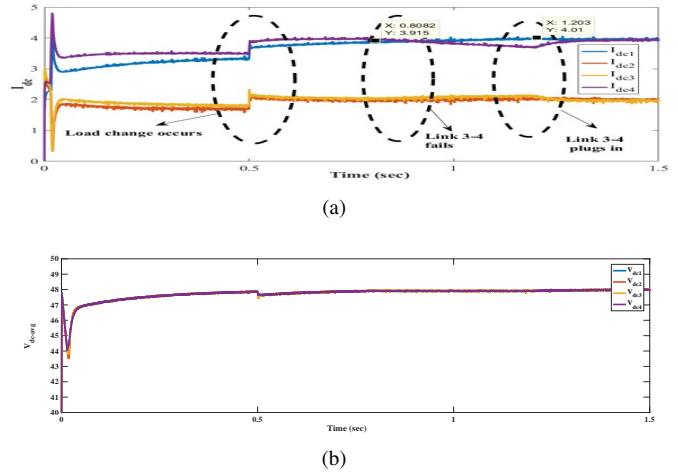


Fig. 3: (a) Load current sharing during Converter 4 failure occurs (b) DC average voltages

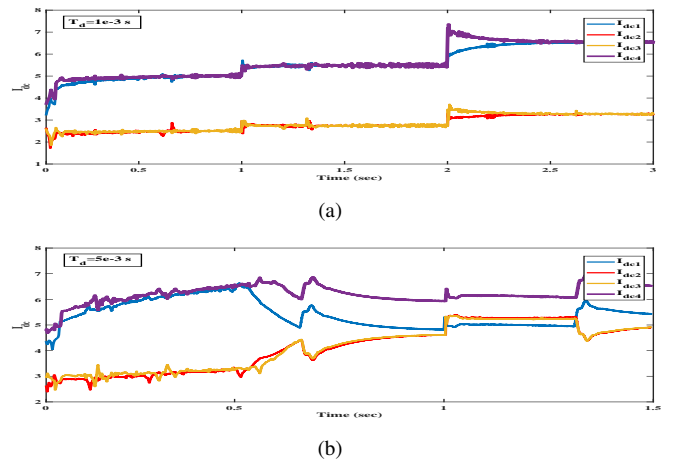


Fig. 4: Performance assessment under time-delay (a) 1 ms (b) 5 ms

III. CONCLUSION

The work investigates the functioning of I-V based primary droop controller annexed with secondary distributed layer, using a sparse communication network, for an autonomous DC microgrid of 48 V under various test scenarios.

Operationg Methodology for Hybrid Multi-terminal HVDC to Secure Margin on Extinction Angle

Choongman Lee
School of Electrical and
Electronic Engineering
Yonsei University
Seoul, South Korea
cmlee@yonsei.ac.kr

Jeehun Lee
School of Electrical and
Electronic Engineering
Yonsei University
Seoul, South Korea
cmlee@yonsei.ac.kr

Jae. W. Shim
Department of Energy
Engineering
Inje University
Kimhae, South Korea
jaewshim.inje@gmail.com

Kyeon Hur
School of Electrical and
Electronic Engineering
Yonsei University
Seoul, South Korea
khur@yonsei.ac.kr

Abstract—This paper provides the relationship between extinction angle of line-commutated converter (LCC) and power of modular multilevel converter (MMC) power in hybrid multi-terminal HVDC (MTDC) system. Based on this relationship, it introduces the methodology to secure the extinction angle margin by adjusting the power bypassing through MMC. We exploit the power share between LCC and MMC to meet the demand in the receiving end for extension of extinction angle, consequently it reduces the risk of commutation failure. The number of operation of the on-load tap changer (OLTC) can be reduced by proposed methodology. A dynamic simulation demonstrates the efficacy of the proposed strategy using real-time simulator (RTS)

Keywords—Commutation failure, extinction angle, gamma margin, hybrid multi-terminal HVDC, on-load tap changer

I. INTRODUCTION

Line-commutated converter (LCC) consisting of the thyristor valves is characterized as uncontrollable switching off nature. High DC current or low AC voltage cuts down the extinction time, resulting in commutation failure in LCC inverter which may lead the significant impact on the power system. In order to avoid this problem, high voltage DC (HVDC) operators generally set up minimum extinction angle including a certain value of margin for safe commutation. The introduced hybrid multi-terminal HVDC (MTDC) transmission system, which takes advantages of LCC and modular multilevel converter (MMC) technology, is also faced with identical problem. In this regard, this letter unfolds the way to manage extinction angle utilizing MMC power to circumvent commutation failure.

II. HYBRID MTDC SYSTEM

Hybrid MTDC system has emerged as a promising solution for bulk power transmission over a long distance, wind farm integration into a grid, and so on. In this paper, we consider the hybrid MTDC system, tapping voltage-sourced converter (VSC)—especially MMC—station on the LCC HVDC as shown in Fig. 1.

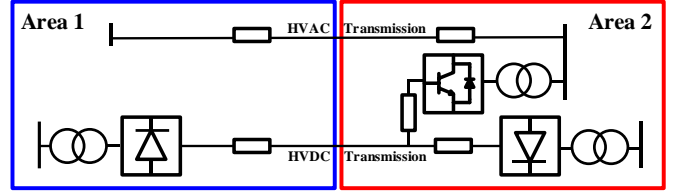


Fig. 1 Schematic of hybrid MTDC(LCC and MMC) system over two areas.

III. KEY EQUATIONS AND FIGURES

We clarify mathematical foundation of MMC operation contributing to extinction angle margin. Through the simulation, we verify that the extinction angle margin is extended due to sharing power between MMC and LCC inverter. In addition, the number of operation of the OLTC, may cause a disturbance on AC system and HVDC converters, can be reduced by proposed method.

$$P_{demand} = P_{inv} + P_{mmc} \quad (1)$$

$$\begin{aligned} P_{mmc} &= P_{demand} - P_{inv} \\ &= P_{demand} - V_{d,ref} I_{d,inv} \\ &= P_{demand} - V_{d,ref} \frac{V_{doi} \cos \gamma_{ref} - V_{d,ref}}{R_{ci}} \end{aligned} \quad (2)$$

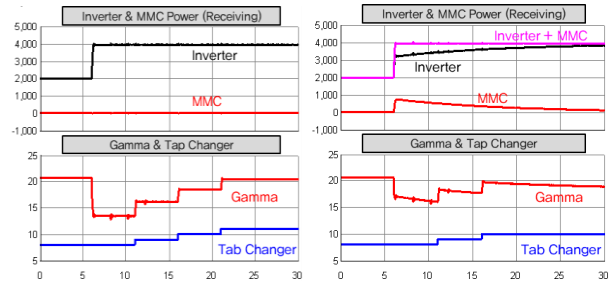


Fig. 2 LCC HVDC Power, MMC Power(red line), Extinction angle and OLTC Status.

Power Density and Reliability Metric Assessment of Thyristor Controlled Rectifiers

Tanvir Ahmed Toshon
 FAMU-FSU College of Engineering
 Tallahassee, FL
 tt15b@fsu.edu

M. O. Faruque
 FAMU-FSU College of Engineering
 Tallahassee, FL
 faruque@caps.fsu.edu

R R Soman
 ZS Associates
 Princeton, New Jersey
 rsoman@fsu.edu

Abstract—This paper presents a robust design strategy followed by pertinent metrics production for a twelve pulse thyristor controlled rectifier specifically for MVDC (Medium Voltage DC) systems in All Electric ships (AES). System level design exercises through the application of full factorial design method reveal the parameters for a power densed and reliable converter. Scaling relations in between converter parameters and output metrics are derived and presented in this paper. Overall, this approach is expected to enhance early stage ship design study through smart ship systems design (S3D).

Index Terms—MVDC, TCR, S3D, Power Density, Reliability, Scaling laws

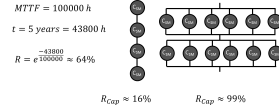


Fig. 2: Capacitor arrangement based reliability calculation

TABLE I: SLDF and ELDF with their levels

Factor type	Factor Names	Level 1	Level 2	Level 3	Level 4	Level 5
SLDF	DC Bus Voltage (kV)	6	12	18	30	N/A
	Fundamental Frequency (Hz)	60	120	180	240	300
ELDF	Voltage Ripple (%)	1	2	3	4	5
	s factor (m/s)	0.2	0.5	0.75	1	1.3

I. INTRODUCTION

This paper develops metrics such as power density and reliability for a thyristor controlled rectifier through a design exercise. One way to formulate and evaluate such robust design exercises is the full factorial experiment. Infeasible designs are eliminated in each iteration through Signal to Noise Ratio (SNR) based evaluation until it narrows the design space to a few best choices of parameters. One important outcome from such methodology is scaling relation between the metrics and parameters.

II. DEVELOPMENT OF METRICS

An algorithm is developed and implemented in matlab script which sizes all the components of TCR and evaluates the power density for the converter as shown in Fig. 1. Fig. 2 shows one example for reliability calculation with

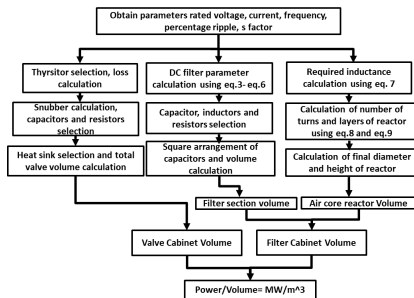


Fig. 1: Flow chart for MW/m^3 evaluation process

series/parallel connection of capacitors for a given R value.

III. RESULTS

TABLE II: Response Matrix

	Voltage Ripple	S factor
Level 1	6.04	9.87
Level 2	9.33	10.06
Level 3	10.97	10.17
Level 4	11.84	10.33
Level 5	12.44	10.20
Maximum Occurs at	Level 5	Level 4

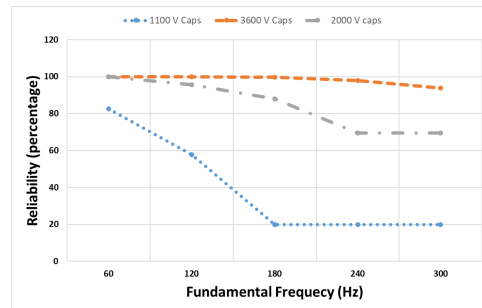


Fig. 3: Reliability with varying frequency and capacitors

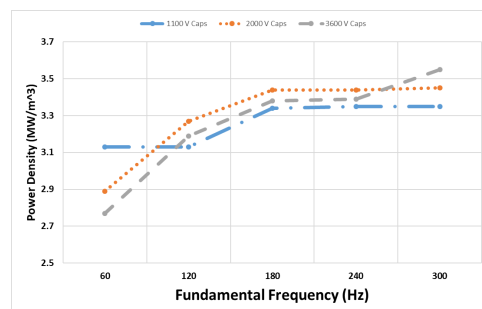


Fig. 4: MW/m^3 with varying frequency and capacitors

Linearized Approach for Dynamic Modeling of Fast Electric Vehicle (EV) Charging Unit

Shuyao Wang
CURENT, Department of EECS
The University of Tennessee
Knoxville, TN, USA
swang67@vols.utk.edu

Fred Wang
CURENT, Department of EECS
The University of Tennessee
Oak Ridge National Laboratory
Knoxville, TN, USA
fred.wang@utk.edu

Leon M. Tolbert
CURENT, Department of EECS
The University of Tennessee
Oak Ridge National Laboratory
Knoxville, TN, USA
tolbert@utk.edu

Abstract—In order to examine the grid impacts for high penetration of electric vehicle (EV) charging, a dynamic model of a fast EV charging unit is proposed based on the linearization approach, and then simplified by selective modal analysis (SMA). The dynamic performance at the rectifier DC link voltage control time scale is considered. The simulation results verify that the proposed simulation model is accurate in terms of the power consumption.

I. INTRODUCTION

The importance of accurate modeling of power electronic interfaced loads have been emphasized considering that more and more loads have power electronic interfaces. The modeling of fast electric vehicle (EV) charging unit is studied in this paper due to its increasing penetration and large power consumption. A reduced order linearized dynamic model of the EV charger is proposed at the time scale of DC link voltage control. The highly simplified model has decreased the model complexity so that it can be utilized in large scale power system simulation studies.

II. EV CHARGER LOAD MODEL DESCRIPTION

A. EV Charger State Space Model

A fast EV charger topology is illustrated in Fig. 1, which includes a three phase active front end rectifier and a dc-dc converter. The constant current (CC) and constant voltage (CV) mode are widely used in the battery charging process and the charging mode is selected according to the state of charge (SoC) of the battery. Here the time scale of the rectifier dc link voltage control loop is considered, so the inner current loop is represented by a first-order system due to its high control bandwidth. The Shepherd model is used for the battery modeling. Accordingly, the EV charger load performance is characterized by a 7th order state space model, which is expressed in (1).

$$\begin{aligned}
 \dot{I}_{dref} &= (V_{dc,ref} - V_{dc})K_{IV} - \frac{K_{PV}}{C_{dc}}(I_{dc} - I_L) \\
 \dot{V}_{dc} &= \frac{1}{C_{dc}}(I_{dc} - I_L) \\
 \dot{I}_d &= \frac{1}{T_{eq}}(I_{dref} - I_d) \\
 \dot{I}_q &= \frac{1}{T_{eq}}(I_{qref} - I_q) \\
 \dot{D}_b &= K_i \left(\frac{i_{batt,ref}}{i_{batt,base}} + \frac{i_{batt}}{i_{batt,base}} \right) + \frac{K_p}{i_{batt,base}} i_{batt} \\
 \dot{i}'_L &= \frac{v_{dc,buck} - v_{batt}}{L} \\
 i_{batt} &= -\frac{b_{para}}{CC_1 b_{series}} (i'_L + i_{batt})
 \end{aligned} \tag{1}$$

B. Model Simplification

The EV charger operating in CC mode and CV mode are analyzed respectively. The battery SoC is almost constant at the time scale of 0.1s, which yields to a constant terminal

voltage across the battery as well as a constant current consumption. Thus, a constant dc current load connected at the rectifier dc side is used to replace the dc-dc converter and battery. Therefore, the original EV charger model has been simplified to a 4th order state space model.

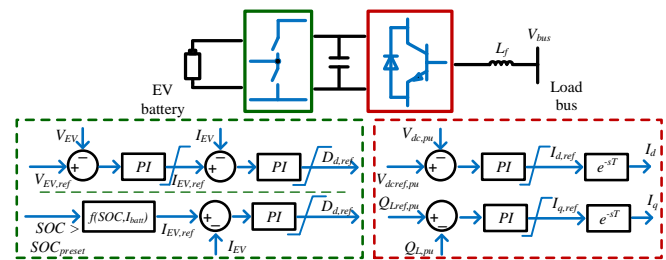


Fig. 1. Topology and control algorithm of the fast EV charging unit.

It is proved based on the sensitivity analysis that the state variables I_{dref} , V_{dc} of the linearized 4th order EV charger model have more significant effect during system transients compared with the other two state variables. So the 4th order model has been simplified to a 2nd order state space model based on selective modal analysis (SMA). Accordingly, the linearized EV charger load active and reactive power consumption are characterized in (2):

$$\Delta P = \frac{\partial P}{\partial V}(s)\Delta V + \frac{\partial P}{\partial I_L}(s)\Delta I_L, \Delta Q = \frac{\partial Q}{\partial V}(s)\Delta V + \frac{\partial Q}{\partial I_L}(s)\Delta I_L \tag{2}$$

III. KEY RESULTS

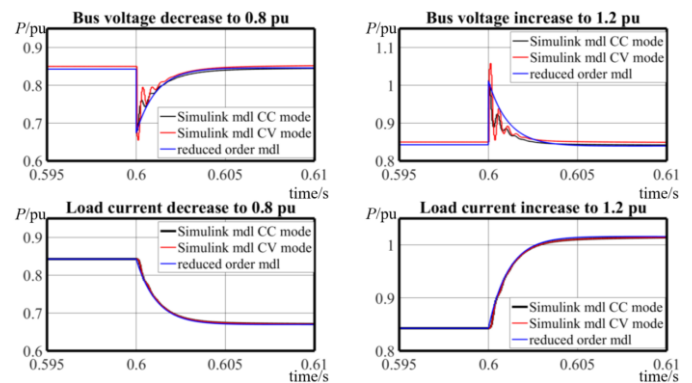


Fig. 2. Load dynamic performance during power network disturbance.

The EV charger model is simulated and compared with a corresponding detailed model built in Simulink. Fig. 2 illustrates the load power response when there is an increase or decrease at the load bus voltage and load current consumption. The linearized reduced order EV charger model presents a good agreement with that of the detailed model built in Simulink within the linear operating region, and it can be incorporated in power system studies examining the impact of EV fast chargers.

Impacts of Branch Contingencies: Dynamic Variations in Line Thermal and Electrical Parameters

Forest Atchison, Mahbubur Rahman, Valentina Cecchi
 University of North Carolina at Charlotte
 Charlotte, NC USA

Abstract- During a branch outage, the remaining lines experience changes in line current which impact the thermal and electrical conditions of the lines. The non-static heat balance equation (HBE) from IEEE std. 738 is used to determine the time to reach the thermal limit of a line in case of line outages. However, this approach cannot consider the impact of outage on voltage stability conditions and assumes the post-contingent line current as constant. This work proposes a method to combine the non-linear algebraic power flow equations and the difference equations from the non-static HBE to consider the dynamic coupling between the line electrical and thermal parameters. This proposed approach is capable of determining a more realistic representation of the time to reach the new steady-state conductor temperature or the thermal or voltage stability limit of a transmission system.

I. POSTER OVERVIEW

During a branch outage in a transmission network, branch currents on the other lines are impacted as the same amount of load needs to be delivered with fewer branches. This change in line currents in one or more branches introduces changes in line conductor temperatures (T), which in turn affect line impedances, and therefore, line currents. The line current continues to change until the T of each line reaches a new steady-state. Therefore, the assumption of a constant post-contingent line current is no longer valid. This variation in line impedance, and therefore in line current, has a direct effect on the thermal and voltage stability limits, and on the critical time to reach the limit or the new steady state condition.

In order to capture the variation in line currents, this work incorporates the non-static Heat Balance Equation (HBE) with the non-linear algebraic power flow equations to form a system of algebraic - discrete equations. The proposed approach can be used to determine the critical power transfer limiting factor of a system during a contingency, as well as to define the critical time to reach the power transfer limiting factor or the new steady state conditions. Noticeable differences are observed when the results from the proposed method are compared to the conventional approach to determine the line thermal limits. A temperature-dependent power flow approach is also used in this work to consider the impacts of weather conditions and conductor temperature on line impedances, as in figure 1.

When applied to a 2-bus 2-line power system, the difference in variation in line current after a branch outage between the proposed method and the conventional HBE approach is seen in Fig. 2. The consequence of this variation in line current impacts the increase in T differently than in a typical HBE approach, as seen in Fig. 3.

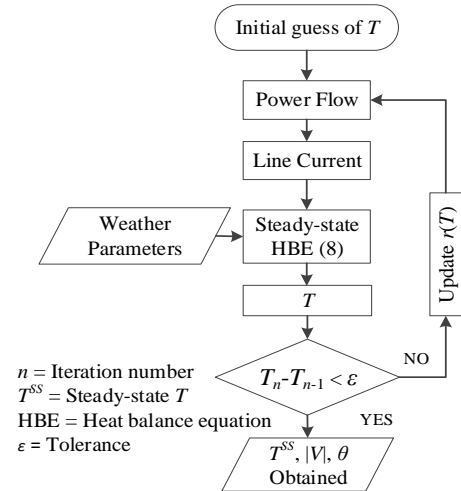


Figure 1: Temperature-dependent power flow

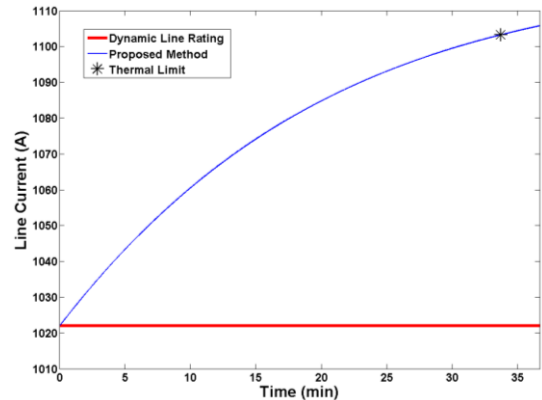


Figure 2: Branch 1 current – after branch 2 outage

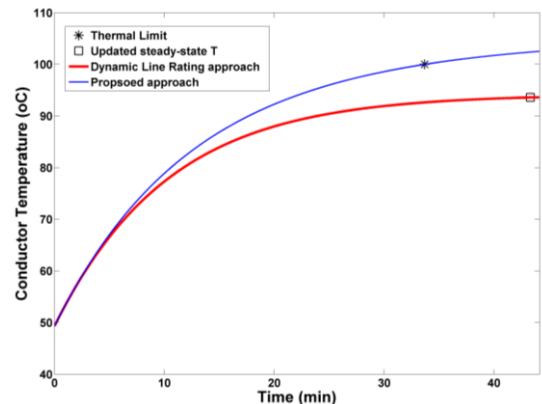


Figure 3: Branch 1 conductor temperature

This work was supported in part by the National Science Foundation award #1509681 “A Novel Electric Power Line Modeling Approach: Coupling of Dynamic Line Ratings with Temperature-Dependent Line Model Structures.”

Investigation of Relevant Distribution System Representation with DG for VSM Assessment

Alok Kumar Bharati and Venkataramana Ajjarapu

Department of Electrical and Computer Engineering,
Iowa State University,
Ames, Iowa, USA – 50011.

alok@iastate.edu ; vajjarap@iasate.edu

Abstract— This poster emphasizes the importance of including the unbalance in the distribution networks for stability studies in power systems. The distribution system is evolving rapidly with high proliferation of distributed energy resources (DERs); these are not guaranteed to proliferate in a balanced manner and uncertainty resulting due to these DERs is well acknowledged. These uncertainties cannot be captured or visualized without representing the distribution system in detail along with the transmission system. We show the impact of proliferation of DERs in various 3-phase proportions on voltage stability margin through T&D co-simulation. Higher percentage of net-load unbalance (NLU) in distribution system aggravates the stability margin of the distribution system which can further negatively impact the overall stability margin of the system

Keywords— T&D Co-simulation, Voltage Stability Margin, VSM, Unbalanced Distribution System, Distributed Generation (DG), Equivalent Feeder Impedance, Net-Load Unbalance (NLU)

I. OVERVIEW

THE power system is a large complex network of various components that are geographically spread in the form of transmission and distribution sub-systems. For accurate voltage stability margin assessment in the presence of large DER penetration, there is a need to represent the distribution system with sufficient detail. Net-Load Unbalance (NLU) is determined and is used to demonstrate the relation between NLU and the voltage stability margin of the system. Relevant representation of the distribution system is important for accurate assessment of the voltage stability margin of the system. With the proliferation of DERs in the distribution system, there is no/minimal control over how these DERs are proliferating in the three phases which can affect the NLU thereby affect the VSM of the system. We have used T&D co-simulation to demonstrate its need as the equivalent distribution feeder cannot capture the complete system details for VSM studies. DERs can be controlled to reduce the NLU and thereby improve the stability margin of the system.

We define the net-load unbalance as percentage:

$$P_{avg} = \frac{P_A + P_B + P_C}{3} \quad (1)$$

$$U_i = \frac{P_i - P_{avg}}{P_{avg}} \quad \forall i = A, B, C \quad (2)$$

$$NLU = \max(|U_i|) \times 100 \% \quad \forall i = A, B, C \quad (3)$$

Where,

P_A, P_B, P_C

The net-loads on phases A, B, C.

$NLU \%$

Percentage of maximum net-load unbalance.

II. KEY RESULTS

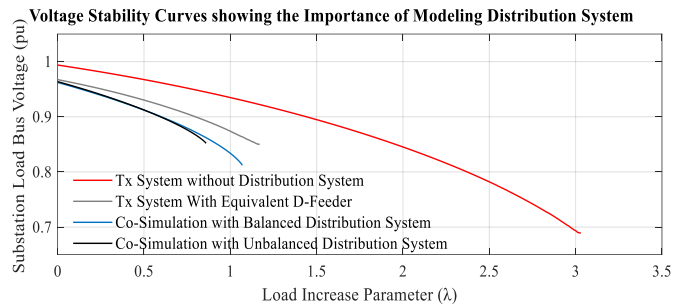


Fig. 1. Voltage Stability Curves with Various Method of Simulations: IEEE 9-Bus Transmission + IEEE 4-Node Distribution System

The study is extended to the IEEE 123-bus distribution system. The loads are modeled with ZIP profile [ZIP] = [0.4 0.3 0.3]. The total load on the 3 phases A, B, C are 45.44 MW, 29.28MW and 36.96 MW respectively. 40%, 60% and 80% DG of the total load is added in various proportions in the 3 phases.

TABLE I. IMPACT OF DG OPERATING IN VVC MODE VERSUS UPF MODE ON LOAD MARGIN- IEEE 9 –BUS T + 123-BUS D-SYSTEM

Total DG Penetration	DG Distribution across 3-Ø (% A,% B,% C)	Net-Load Unbalance (%)	Load Margin/ VSM (MW)	
			DG in VVC Mode	DG in UPF Mode
40% DG (44.67 MW)	50, 10, 50.3	17.80	273.49	243.86
	40,40,40	25.53	267.69	240.61
	55, 55, 10	48.73	260.80	237.81
	10, 62, 61	88.05	241.38	231.75
60% DG (67 MW)	60, 60, 60	25.53	299.17	256.44
	72, 25, 72	41.47	290.05	258.93
	77, 77, 25	85.93	284.66	254.14
80% DG (89.34 MW)	25, 85, 85	134.85	260.10	240.98
	90, 50, 90	17.80	317.48	271.28
	80, 80, 80	25.53	316.60	268.83
	95, 95, 50	147.93	296.81	269.24
	52, 100, 100	200.00	294.25	254.48

Worst Case Unavailability Modelling of a Cyber Physical Power System

Suvagata Chakraborty and Visvakumar Aravinthan
 Department of Electrical Engineering and Computer Science
 Wichita State University
 Wichita, Kansas, 67260
 sxchakraborty@shockers.wichita.edu

Abstract—This paper analyses the impact of unavailability of physical layer, communication layer and decision making layer in a cyber-enable power system. Worst case scenario due to unavailability of three layers and the incorporated worst case probability due to communication delay for the cyber physical system in presence of cyber-attack is modelled and compared with the expected reliability of the system.

I. INTRODUCTION

Cyber physical power system is a combination of traditional physical network, communication network and information layer for decision making functions. The introduction of sensors and communication network made it possible for real time decision making in a cyber power system. The physical layer consists of sensors (fault detectors) and commanding executing devices (switches) which are connected to the commutation layer by means of communication channel [1]. The communication layer consists of relays to transmit this data or measurement which in turn used to make decision layer functions. The study of the unavailability of these three layers in a centralized distribution system therefore studied in this work as show in Fig. 1. Since availability of communication layer and information are interdependent and have lower failure rate compare to the physical system, hence a worst case study will provided a better refection on the importance of this work.

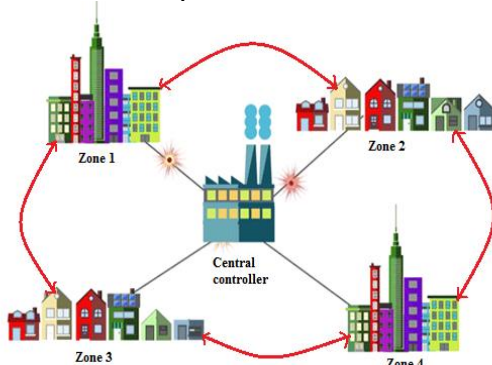


Fig. 1: A substation-centered mesh connected communication

II. MODEL DEVELOPMENT

The initial model was developed to incorporate communication link failure with that of fault detector and remote switch failure probability [2]. Updated probabilities for fault detector and switch including link failures are given in equation 1 and 2. The decision layer function is obtained based on the information received for the communication layer. Communication delay due to latency or congestion will impact the decision making function and hence the communication delay can be used to model the decision function. The nodes at each relay at different congestion level is therefore analyzed to model for the unavailability of decision layer. Also error induced due to cyber-attack by

making wrong switching decision or operation is also included in the model.

$$q_{fi_new} = q_{fi} + (1 - q_{fi})q_{linkfi} \quad (1)$$

$$q_{Si_new} = q_{links2} + (1 - q_{links2})q_{S2} \quad (2)$$

$$q_{linkfi} = q_{linkfi} + (1 - q_{linkfi})q_{delay} \quad (3)$$

$$q_{links2} = q_{links2} + (1 - q_{links2})q_{delay} + (1 - q_{linkfi}) + (1 - q_{linkfi}) + (1 - q_{linkfi})q_{swit_err} \quad (4)$$

Expected probability of unsuccessful operation incorporated by communication delay and decision error can be obtained by substituting equation (3) and (4) in equation (1) and (2), where q_f, q_s are the probabilities of unsuccessful operation of fault sensor and switch, respectively. q_{linkfi}, q_{linksi} ($i = 1, 2, 3, 4$) are the probabilities of unsuccessful connection of fault detector and switch links. q_{delay}, q_{swit_err} are the probabilities failure due to communication delay and switching error due to decision manipulation by cyber-attack.

III. ANALYSIS AND RESULT

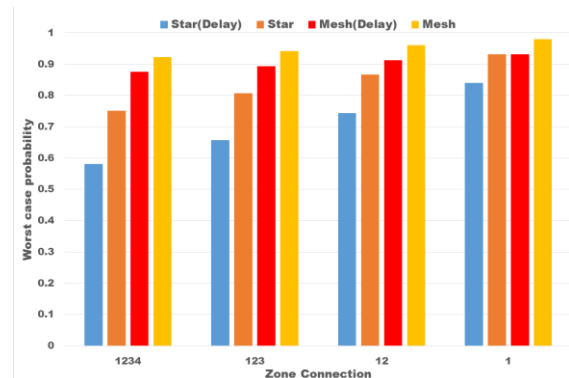


Fig. 2: Comparison of probabilities of different communication infrastructure with and without delay for centralized distribution system.

IV. CONCLUSION

Comparison among zone connection probabilities in Fig. 2 reveals that centralized star connection with communication delay and switching error has the lowest and mesh without delay has the highest worst-case communication probability.

REFERENCES

- [1] V. Aravinthan *et al.*, "Reliability Modeling Considerations for Emerging Cyber-Physical Power Systems," *2018 IEEE International Conference on Probabilistic Methods Applied to Power Systems (PMAPS)*, Boise, ID, 2018, pp. 1-7. J. Clerk Maxwell, *A Treatise on Electricity and Magnetism*, 3rd ed., vol. 2. Oxford: Clarendon, 1892, pp.68-73.
- [2] S. Chakraborty, T. Balachandran and V. Aravinthan, "Worst-case reliability modeling and evaluation in cyber-enabled power distribution systems," *2017 North American Power Symposium (NAPS)*, Morgantown, WV, 2017

CVSR-Integrated Meshed Power Grid Analysis

Okan Ciftci¹, Student Member, IEEE, Kevin Tomsovic¹, Fellow, IEEE, Aleksandar Dimitrovski², Senior Member, IEEE and Zhi Li³, Member, IEEE

¹Department of Electrical Engineering and Computer Science, The University of Tennessee, Knoxville, TN, 37996, USA

²Electrical and Computer Engineering Department, The University of Central Florida, Orlando, FL, 32816, USA

³Oak Ridge National Lab., Oak Ridge, TN, 37830, USA

ociftci@vols.utk.edu

Abstract—The distribution systems during peak consumption hours max experience overloading of the transformers, particularly, in such dense areas like downtowns. This paper proposes an optimization and control approach based on using a continuously variable series reactor (CVSR) to control power flow in the meshed distribution grid. The CVSR is used to regulate the reactance on the primary side of transformer to control power distribution among transformers in order to relieve overloading scenarios. This approach can allow a system to avoid transformer upgrades. After determining the specifications of the device, an optimization problem is formulated to identify location and settings to relieve overloads.

Keywords—Variable series reactor, power flow, control, optimal location, sensitivity analysis, transformer.

I. INTRODUCTION

A continuously variable series reactor (CVSR) is a unique device which is a series line reactor for controlling power flow in meshed power system grids. A concept of this device is a continuous modulation of line reactance by controlling the magnetization in a ferromagnetic core. Illustration of a CVSR is shown in Figure 1. The target application of this device is power flow control in meshed electric power systems [1, 2]. In this work, the CVSR regulates the reactance of transformer, which in turn controls the power flow. In dense-downtown areas, such as New York City, the electrically closer transformer(s) supplies the power for any load increment. To avoid overloading of a transformers, a CVSR device can be used to regulate reactance on the primary side of transformer and hence control power flow through the transformer. Increasing the reactance of the transformer will decrease the power flow and overloading can be prevented. Therefore, normal operation of the system will be sustained without equipment upgrades. Depending on the transformer capacity in kVA and loading conditions, a CVSR size and requirement can be determined. A few ohms is generally enough to significantly reduce loading. Determining the exact specifications of a possible CVSR leads to the next step where optimal location and setting can be determined.

Simulations are conducted on the IEEE 342-Node Low Voltage Test System [3], which represents a typical large urban center. Transformer sensitivity analyses are carried out to determine the impedance and size of the CVSR. Below, Table I and II provide the sensitivity analysis of Transformer-23 in this standard network. Results show that in this network a few ohms can relieve as much of 20% of the loading.

II. KEY FIGURES

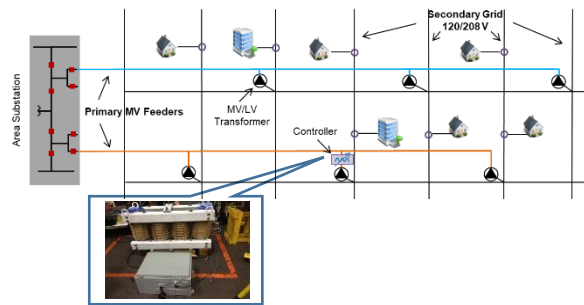


Fig. 1: CVSR device and its application in the meshed power grid

TABLE I. SENSITIVITY ANALYSIS OF TRANSFORMER-23 WHILE REGULATING THE REACTANCE IN OHMS (0.5 OHM/INTERVAL)

	Reactance(Ohm)	Reactance(%)	Power Flow(kVA)	kVA Difference
Normal Situation	8.5219	4.474	716.9	20.6
	9	4.725	696.3	19.2
	9.5219	5	677.1	16.8
	10	5.251	660.3	19.2
	10.5219	5.525	641.1	

TABLE II. SENSITIVITY ANALYSIS OF TRANSFORMER-23 WHILE REGULATING THE REACTANCE IN PERCENTAGES (0.1%/INTERVAL)

	Reactance(Ohm)	Reactance(%)	Power Flow(kVA)	kVA Difference
Normal Situation	9.141	4.8	690.9	7
	9.3314	4.9	683.9	7
	9.5219	5	676.9	6.8
	9.7123	5.1	670.1	6.6
	9.9027	5.2	663.5	

REFERENCES

- [1] M. Young, A. Dimitrovski, Z. Li, Y. Liu, and R. Patterson, "Continuously variable series reactor: Impacts on distance protection using CCVTs," in *2015 IEEE Power & Energy Society General Meeting*, 2015: IEEE, pp. 1-5.
- [2] X. Zhang, K. Tomsovic, and A. Dimitrovski, "Security constrained multi-stage transmission expansion planning considering a continuously variable series reactor," *IEEE Transactions on Power Systems*, vol. 32, no. 6, pp. 4442-4450, 2017.
- [3] K. Schneider, P. Phanivong, and J.-S. Lacroix, "IEEE 342-node low voltage networked test system," in *2014 IEEE PES General Meeting| Conference & Exposition*, 2014: IEEE, pp. 1-5.

Three Phase Transmission Line Fault Location Based on the Generalized Bergeron Model

Dayou Lu, *Student Member, IEEE*, Yu Liu, *Member, IEEE* and Xiaodong Zheng, *Member, IEEE*

Abstract: Accurate fault location technique minimizes the power outage time and operating costs. This paper proposed a three-phase transmission line fault location scheme based on the generalized Bergeron model. Three phase instantaneous voltage and current measurements at two terminals of the line are required. Compared to traditional Bergeron model based fault location scheme, the proposed method does not need the assumption of geometrically symmetric transmission lines and works for arbitrary transmission line parameters. Numerical experiments demonstrate that the proposed generalized Bergeron model based method has higher accuracy compared to the traditional Bergeron model based method.

Key words: fault location, generalized Bergeron model, three phase transmission line model

I. INTRODUCTION

The traditional Bergeron model deals with the single phase transmission line and expresses the relationship among voltages and currents at terminals of the line. For three phase system, the mode decomposition is usually used applied to decoupled the system into three independent single line, thus the assumption of geometrically symmetry line is required.

This paper proposes a generalized Bergeron model for three phase coupled transmission line fault location. This model does not require the assumption of geometrically symmetry line and works for arbitrary parameter matrices. The considered line model is constructed with coupled inductance and capacitance and decoupled resistance parameters. The Bergeron form solution of voltage distribution is calculated in time domain for voltage method fault location. With the fault location function, the fault location results calculated with proposed method is compared to those calculated with traditional Bergeron model through simulation.

II. FORMULATION OF GENERALIZED BERGERON MODEL AND FAULT LOCATION

Consider a three-phase transmission line with terminals 1 and 6, the first step of derivation is to analytically solve the voltages and currents of a lossless three phase transmission line, then the resistance is lumped in terminals and midpoint of the line. The generalized Bergeron model is expressed as follow equations,

$$\begin{aligned} \sum_{n=1}^3 M_{jn} i_{1n}(t) &= u_{1j}(t) - u_{6j}(t - \tau_j) - \sum_{p=n}^3 N_{jp} i_{6n}(t - \tau_j) \\ &- R_j X_j / 2 \cdot \left[u_{6j}(t) - \sum_{n=1}^3 M_{jn} i_{6n}(t) - u_{6j}(t - \tau_j) - \sum_{n=1}^3 N_{jp} i_{6n}(t - \tau_j) \right] \\ &+ R_j Y_j / 2 \cdot \left\{ u_{6(j+1)} \left[t + (\tau_{(j+1)} - \tau_j) / 2 \right] - \sum_{n=1}^3 M_{(j+1)n} i_{6n} \left[t + (\tau_{(j+1)} - \tau_j) / 2 \right] \right. \\ &\left. - u_{6(j+1)} \left[t - (\tau_{(j+1)} + \tau_j) / 2 \right] - \sum_{n=1}^3 N_{(j+1)n} i_{6n} \left[t - (\tau_{(j+1)} + \tau_j) / 2 \right] \right\} \\ &- R_j Z_j / 2 \cdot \left\{ u_{6(j+2)} \left[t + (\tau_{(j+2)} - \tau_j) / 2 \right] - \sum_{n=1}^3 M_{(j+2)n} i_{6n} \left[t + (\tau_{(j+2)} - \tau_j) / 2 \right] \right. \\ &\left. - u_{6(j+2)} \left[t - (\tau_{(j+2)} + \tau_j) / 2 \right] - \sum_{n=1}^3 N_{(j+2)n} i_{6n} \left[t - (\tau_{(j+2)} + \tau_j) / 2 \right] \right\} \end{aligned} \quad (1)$$

With the generalized Bergeron model, calculated the voltage distribution with currents and voltages at one terminal,

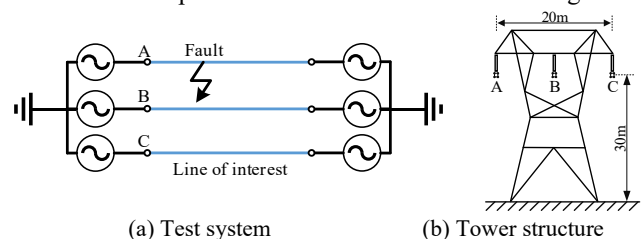
$$u_6(t) = M i_6(t) - U_6(t) \quad (2)$$

In (2), $i_6(t)$ and $U_6(t)$ are only dependent by the voltages and currents at terminal 1. Calculate the voltage distributions with measurements at each terminal, the fault location is afterwards calculated as the zero point of fault location function,

$$f(x) = \sum_{t=t_1}^{t_2} |u_{1x}(x, t) - u_{6x}(x, t)| \quad (3)$$

III. SIMULATION RESULTS

The example test system is a 500-kV two-machine system with a 300 km transmission line, the test system and the considered three-phase tower structure are shown in Figure 1.

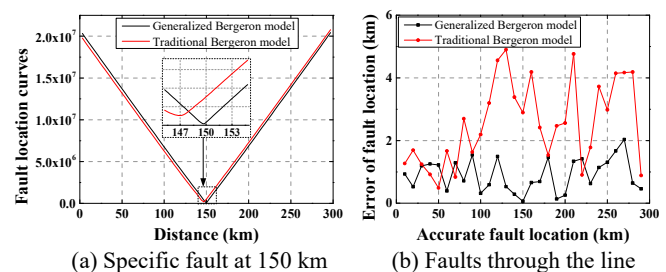


(a) Test system

(b) Tower structure

Figure 1. Simulation model

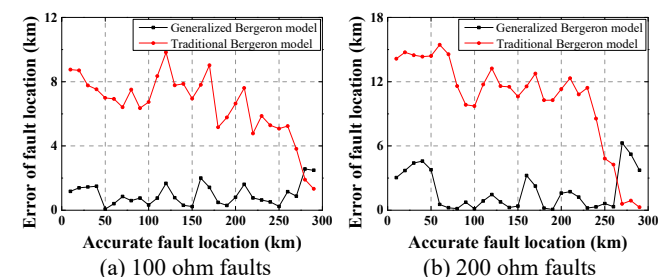
The fault location results with an A-G fault occurs at 150 km and a group of fault cases occur distributed through the line with 0.1 ohm fault resistance are shown in Figure 2. Two groups of high fault resistance cases with fault resistance as 100 and 200 ohm respectively are shown in Figures 3.



(a) Specific fault at 150 km

(b) Faults through the line

Figure 2. Comparison between the proposed method and the traditional method, 0.1 ohm A to G faults



(a) 100 ohm faults

(b) 200 ohm faults

Figure 3. Comparison between the proposed method and the traditional method, high impedance A to G faults through the line

The simulation results show that the fault location errors with proposed generalized Bergeron model is smaller than those calculated with traditional Bergeron model especially in high fault resistance cases.

Stochastic Hosting Capacity in LV Distribution Networks

Matthew Deakin, Constance Crozier,
Thomas Morstyn, and Malcolm McCulloch
Department of Engineering Science
University of Oxford, Oxford, UK

Dimitra Apostolopoulou
Department of Electrical & Electronic Engineering
City, University of London, London, UK

Abstract—We propose a computationally efficient method for stochastic hosting capacity analysis of LV distribution networks. The proposed method only considers load flow solutions with an active constraint, reducing the computational burden significantly. This is facilitated by using a linear load flow, leading to a linear program formulation with a closed form solution. The computational efficiency of the scheme is demonstrated to be an order of magnitude faster than a naïve linear load flow formulation.

I. INTRODUCTION

Hosting capacity is defined as the level of penetration that a particular technology can connect to a distribution network without causing power quality problems. In this work, we study the impact of solar photovoltaics (PV) on voltage rise in low voltage distribution networks.

In most cases, the locations and sizes of the PV are not known in advance, so hosting capacity Φ must be considered a random variable. Most hosting capacity methods study the problem considering a large number of scenarios, many of which provide little additional information.

II. APPROACH

We take a different approach, studying only those cases where voltage constraints are active (a fixed voltage’ method). This results in a reduction in the number of scenarios by an order of magnitude compared to a fixed-power’ based search method (see Fig. 1).

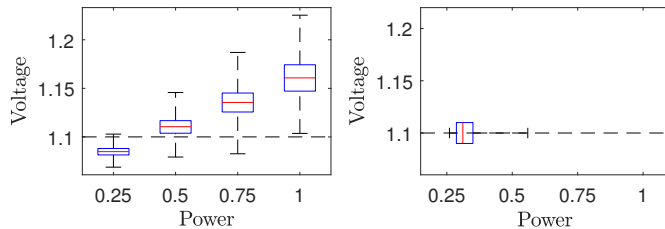


Fig. 1. ‘Fixed power’ (l) and proposed ‘fixed voltage’ (r) calculation methods.

The fixed power method is found using the ‘bisection’ method to find the hosting capacity, requiring a number of iterations. The fixed voltage does not iterate, resulting in the computation time being reduced by an order of magnitude (Table 1).

TABLE I
COMPARISON OF TIMINGS AND ESTIMATED HOSTING CAPACITIES FOR THE FIXED POWER AND FIXED VOLTAGE METHODS

Feeder	Fixed power			Fixed voltage	
	Iterations	Time, s	$\Phi_{5\%}$, kW	Time, s	$\Phi_{5\%}$, kW
EU LV	8	5.30	15.0	0.80	15.3
N1.1	11	6.95	91.4	0.77	92.4
N2.1	23	102.83	228.4	5.57	230.1
N3.1	10	15.49	115.2	1.82	115.5
N4.1	10	1.20	120.2	0.17	120.5

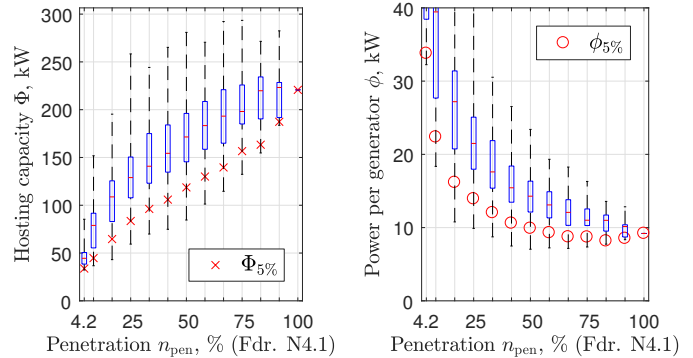


Fig. 2. The hosting capacity of a feeder as a function of the number PV generators installed

To illustrate the flexibility of the method, the hosting capacity is studied as a function of the number of generators connected (Fig. 2). This demonstrates that assumptions about the penetration level will have a large impact on the conclusions drawn for a given network.

III. RESULTS & CONCLUSIONS

The fixed-voltage hosting capacity method will equip DSOs with the ability to rapidly study hosting capacity in a computationally efficient manner, which is paramount considering the large number of LV feeders. Given recent policy shifts, in future it may be that relatively fewer PV systems connect, but the PV systems that connect are larger. We have illustrated that this method is ideally suited to study these types of problems. Finally, this approach lends itself to the tools of linear algebra; further analysis is left as future work.

A New Internal Fault Detection and Classification Technique for Synchronous Generator

Ashish Doorwar, *SIEEE*, Bhavesh Bhalja, *SMIEEE*, and Om P. Malik, *LFIEEE*

Abstract-- A new internal fault detection and classification technique for synchronous generators is presented. First, the presence of an abnormal/fault condition is detected based on the Negative Sequence Component (NSC) of neutral end current. Thereafter, the internal fault and abnormal/external-fault conditions are discriminated by utilizing the instantaneous phase angle between the NSCs of the terminal voltage and current. Subsequently, the internal fault is classified based on phase angle between NSCs of terminal voltage and neutral end current along with the zero sequence component of the neutral end current. Efficacy of the proposed scheme has been verified on a Phase Domain Synchronous Machine model developed on the Real Time Digital Simulator (RTDS®). The results derived from various fault data sets show that the proposed technique is able to effectively distinguish between internal and external faults including special cases such as current transformer saturation, overloading and unbalance condition. Further, it provides added capability of detecting and identifying inter-turn faults irrespective of the winding configuration of the generator. Comparative assessment of the proposed scheme in terms of detection time and incorporation of different types of faults with the existing techniques proves its superiority.

I. INTRODUCTION

In order to overcome the deficiencies in many of the earlier schemes, a new internal fault detection and classification technique based on negative sequence components (NSCs) of voltage and current is presented in this paper.

II. PROPOSED METHODOLOGY

A flowchart of the proposed scheme is shown in Fig. 1

III. MODELLING OF SYNCHRONOUS GENERATOR USING RTDS

A single line diagram of the developed simulation model of the generator is shown in Fig. 2.

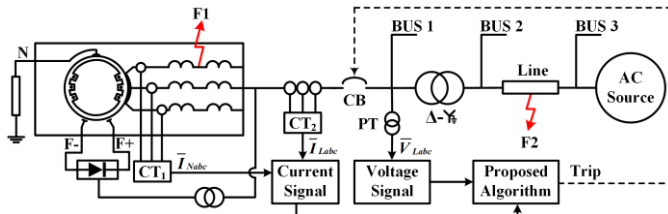


Fig. 2 Single line diagram of the simulation model developed in RTDS®.

This research work is supported in part by Council of Scientific & Industrial Research (CSIR), Ministry of Science & Technology, Govt. of India, New Delhi, India under Project Grant No.: 22/701/15/EMR-II.

Ashish Doorwar and Bhavesh R. Bhalja are with EE Dept., Indian Institute of Technology Roorkee, Roorkee – 247667, Uttarakhand, India. (e-mail: ashish.doorwar@gmail.com, bhaveshbhalja@gmail.com)

Om P. Malik is with the ECE Dept., University of Calgary, Calgary, AB T2N 1N4 Canada (e-mail: maliko@ucalgary.ca).

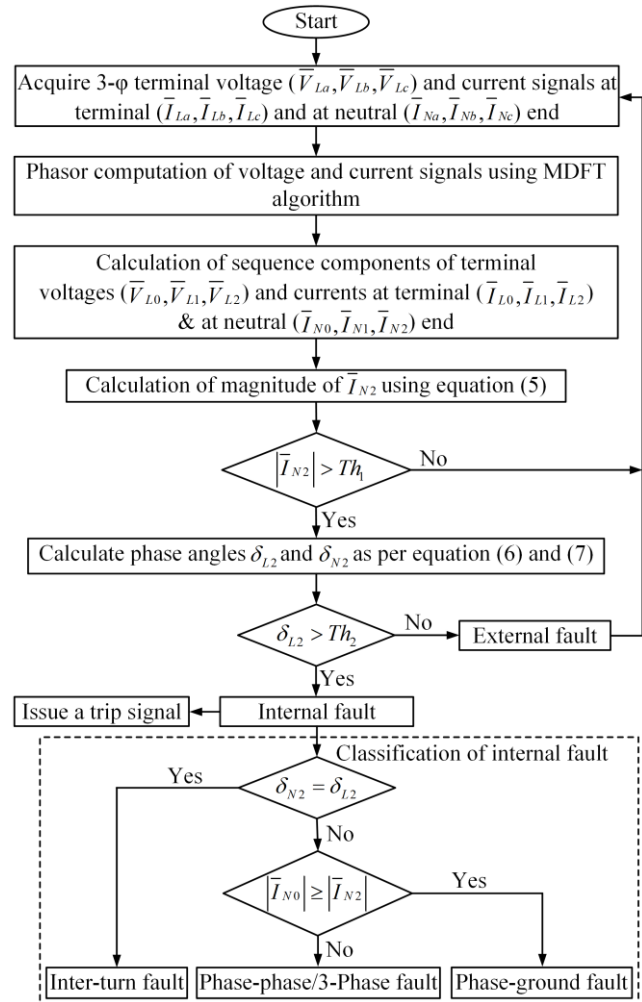


Fig. 1 Flowchart of the proposed algorithm.

IV. RESULTS AND DISCUSSION

TABLE I
COMPARATIVE ANALYSIS OF THE PROPOSED SCHEME

Scheme Parameter	Harmonic [12]-[13]	ANN [19]	NF [22]	WT [24]	MM [28]	Proposed Scheme
P-G	✓	✓	✓	✓	✓	✓
P-P	✗	✓	✓	✓	✓	✓
P-P-P	✗	✓	✓	✓	✓	✓
Inter-turn	✗	✗	✓	✓	✗	✓
Average ROT (ms)	One cycle	12.0	18.035	20	6.2	5.6
Special condition	continuous sub-harmonic source and generator loading dependent	Large training data	65% accuracy for Inter-turn fault	Valid for only split-phase winding	Reliant on SG loading	Independent of SG's winding structure and

Achieving 100x Acceleration for N-1 Contingency Screening with Uncertain Scenarios using Deep Convolutional Neural Network

Yan Du, *Student Member, IEEE*, Fangxing Li, *Fellow, IEEE*,
 Jiang Li, *Senior Member, IEEE*, Tongxin Zheng, *Senior Member IEEE*

Abstract—The increasing penetration of renewable energy makes the traditional N-1 contingency screening highly challenging when a large amount of uncertain scenarios need to be combined with contingency screening. In this letter, a novel data-driven method, similar to image-processing technique, is proposed for accelerating N-1 contingency screening of power systems based on the deep convolutional neural network (CNN) method for calculating AC power flows under N-1 contingency and uncertain scenarios. Once the deep CNN is well trained, it has high generalization and works in a nearly computation-free fashion for unseen instances including topological changes such as in the N-1 cases, as well as uncertain renewable scenarios. The proposed deep CNN is implemented on several standard IEEE test systems to verify its accuracy and computational efficiency. The proposed study constitutes a solid demonstration of the considerable potential of the data-driven deep CNN in future online applications.

Index Terms—AC power flow, deep convolutional neural network (deep CNN), data-driven, N-1 contingency screening.

I. INTRODUCTION

The increasing penetration of renewable energy into the bulk power system has aggravated the concern of system operation security under N-1 contingency. The main challenge for N-1 contingency screening under uncertainty is the extreme model complexity in case of large-scale power systems, combined with many uncertain scenarios. The main issue with the traditional model-based methods is the huge number of power flow runs, which poses great computational burden that prevents their online applications even with proper model simplification. To address this issue, in this letter we present a novel data-driven method, similar to image processing, for accelerating N-1 contingency screening under multiple uncertain scenarios. The deep convolutional neural network (deep CNN) is utilized as a regression tool for AC power flow calculation. Once the deep CNN is well trained, it is expected to have high generalization for unseen power flow cases and can improve the computational efficiency by around 100 times as compared with the conventional model-based methods in N-1 contingency screening. It should be noted that the solution can deal with topological change under N-1 contingency without the need of additional trainings.

II. DEEP CNN-BASED POWER FLOW CALCULATION

In the N-1 contingency screening problem, the deep CNN is proposed as a regression tool to automatically generate AC power flow (ACPF) results based on the known system parameters. Deep CNN is applicable for ACPF calculation because power system state variables, i.e., the bus voltage magnitude and bus voltage angle, are also sparsely connected

like image pixels. The deep CNN structure is shown in Fig. 1.

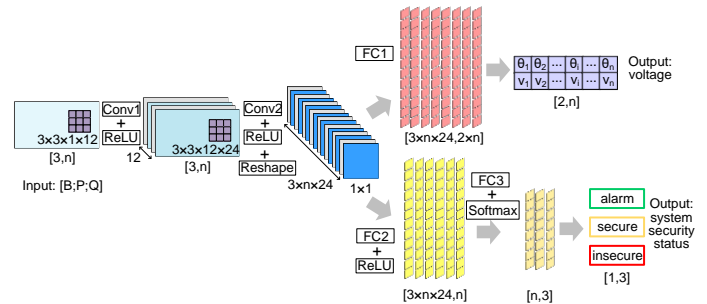


Fig. 1. Deep CNN structure for N-1 contingency screening using image-processing-like technique

III. CASE STUDY

The proposed image-processing-like, deep CNN models for ACPF calculation under N-1 contingency are tested on the IEEE 9, 30, 57, 118, and 300-bus systems, WECC 181-bus system, and European 1354-bus system to verify its accuracy and computing efficiency.

TABLE I AC POWER FLOW RESULTS OF DEEP CNN

Case	No. of samples		Errors		Training time(s)	Classification Accuracy
	Training	Test	θ	v		
9	2419	1037	4.8e-3	7.6e-4	10.33	98.94%
30	4262	1066	1.5e-3	4.0e-4	27.09	97.37%
57	3364	1443	5.0e-3	1.5e-3	52.26	99.24%
118	3027	1298	7.0e-3	2.5e-4	60.33	100%
181(WECC)	2557	1096	4.9e-2	3.0e-3	66.02	97.45%
300	3471	1488	4.8e-2	1.8e-3	152.77	99.53%
1354 (Eu.)	3985	1709	1.3e-2	1.7e-3	1594.83	97.66%

TABLE II TEST TIME COMPARISON

Case	Test size	Test time (s) (deep CNN)	Test time (s) (model-based)	Acceleration ratio
9	1037	0.076	10.83	142.5
30	1066	0.077	12.92	168
57	1443	0.099	22.2	224
118	1298	0.106	29.97	283
181(WECC)	1096	0.116	26.89	232
300	1488	0.189	55.10	292
1354(Eu.)	1709	0.666	59.71	90

IV. CONCLUSIONS

In this work, a data-driven approach is proposed to achieve over 100 times acceleration for N-1 contingency screening under uncertain scenarios. An image-processing-like technique is proposed to utilize the deep CNN as an efficient regression method to fit AC power flow model, and then to automatically generate power flow results for system security evaluation with considerable accuracy. The high computational efficiency of deep CNN makes it a desirable tool for real-time security assessment applications as well as other related power system studies.

Multi-Agent Distributed Control of Integrated Transmission and Distribution Systems with DERs

Inalvis Alvarez-Fernandez, and Wei Sun
 Department of Electrical and Computer Engineering
 University of Central Florida
 Orlando, Florida, United States
alvarezfernandez@knights.ucf.edu, sun@ucf.edu

Abstract—With the growth of smart grid technologies and the increasing number of distributed energy resources (DERs), the distribution network has become more complex and dynamic. This work focuses on creating an integrated transmission and distribution model in order to capture the dynamics of the distribution network. The transmission and distribution networks are modeled in OpenDSS with Python co-simulation. Parallel programming is used to execute the simulations of distribution systems simultaneously and provide information back to the transmission system which adjusts based on the various distribution systems' statuses. The distribution systems with the high penetration of DERs, such as PV, are intermittent and affected by voltage events at the substation. Therefore, multi-agent distributed control and optimization are implemented in the distribution system level. The transmission network is able to adjust to any changes in the distribution networks increasing/reducing generation.

Keywords— DERs, integrated transmission and distribution, parallel processing, multi-agent distributed control.

I. INTEGRATED T&D ARCHITECTURE

The integrated transmission and distribution (T&D) architecture was modeled and simulated using co-simulation of Python and OpenDSS. The transmission model is based on the IEEE 14-bus system. Three distribution systems are modeled: IEEE 8,500-node, 11,000-node (IEEE 8,500 + EPRI Circuit 7), and 100,000-node system (12 of IEEE 8,500). Loads in transmission system were analyzed to determine real and reactive power values, which resembled the total real and reactive power of the various distribution systems. Once the buses were identified, the distribution systems are allocated to each bus individually.

Python was used to interface with OpenDSS and facilitate the usage of parallel processing in solving the power flow of each distribution system. The algorithm is formulated as follows. The snapshot power flow of transmission system is solved, and the voltage at each bus connected with distribution systems are saved. Each distribution system is assigned one process whose parameters are voltage levels, circuit name and process number. Once each process is established, they start and execute simultaneously. The various sizes and complexity of distribution systems cause the power flow to solve in shorter or longer time. Thus, the algorithm waits for the convergence of all distribution systems before sending the real and reactive power values at the substation back to the

transmission bus. A text file is generated containing the P and Q at the substation after each power flow solution with respect to the transmission voltage. The power flow of transmission system is then solved again with the updated parameters. The algorithm loops through this process until the $\Delta V \leq 0.0001$.

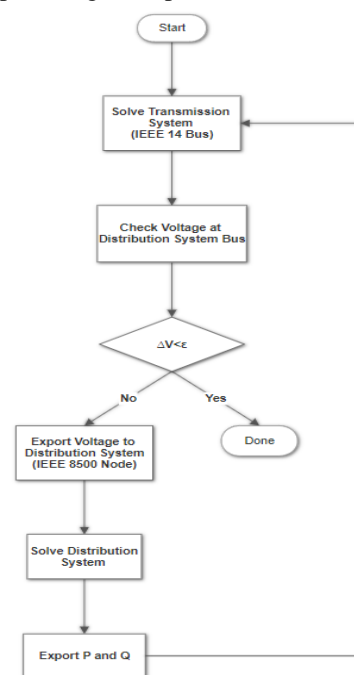


Figure 1: Integrated T&D Architecture

II. SIMULATION RESULTS

Simulation is performed with and without distributed control in one of distribution systems. Multi-agent distributed control is implemented in OpenDSS and added in the 11,000-node circuit. Two large-scale PVs with total capacity of 12MVA (about 21% penetration) are added to the circuit. Furthermore, the performance of parallel and sequential simulations is compared.

Table 1: Results of Parallel Simulation with Distributed Control

Ite	85k Nodes			100k Nodes			11k Node		
	V Bus 13	P	Q	V Bus 14	P	Q	V Bus 10	P	Q
1	0.9495	10045.50	2789.08	0.9493	144611.00	21991.70	0.9495	43876.60	18296.40
2	1.0318	11550.70	2980.46	1.0316	143813.00	16719.00	1.0318	48006.10	21204.90
3	1.0267	11473.90	2982.72	1.0265	143808.00	16662.80	1.0266	47968.50	21131.10
4	1.0268	11476.40	2982.69	1.0266	143801.00	16625.40	1.0268	47969.80	21133.30
5	1.0268	11475.30	2982.70	1.0266	143804.00	16641.70	1.0267	47969.20	21132.30

**Real-time Physical Test-bed for validation of Event
Diagnosis and Generation Estimation in Distribution Network
Integrated with Distributed Energy Resources (DERS)**

Amir Gholami, Anurag Srivastava
EECS Department of Washington State University
Email: amir.gholami@wsu.edu

Abstract—To guarantee the reliable power supply, the expected operation of all the components in the power system is critical. Failure in protection devices can result in multiple conflicting alarms at the power grid operation center and complex events analysis to manually find the root cause of the observed system state. If not handled in time, it may lead to the propagation of the faults/ failures and make the damage even worse. With availability of the synchronized measurements from micro phasor measurement units (Micro PMUs), real-time system monitoring, and automated failure diagnosis is feasible. With multiple adverse events and possible data anomalies, complexity of the problem will be escalated.

I. INTRODUCTION

Power is delivered to the customers using the transmission system, and thus the key factor to have a reliable power supply in demand point, is to have a secure and reliable delivery method. One important element in distribution network, by means of which the goal of having a clean and renewable generation is possible is to install distributed energy resources (DERs) within the distribution system.

Generally-speaking, the distance protection of the transmission lines is a set of current and voltage transformers, protective relays, circuit breakers, and batteries. Any type of fault in any of the aforementioned components may lead to the propagation of the fault to the other parts of the system, as a result of which it may end up with a black-out, which is kind of disaster as far as the damage to the system and the restoration effort and money are concerned.

In order to address this issue, in this work the standard IEEE 123 node test feeder have been studied and the system modeling and test cases have been simulated using the Gridlab-d distribution modeling software.

Firstly, the 123-node system is to be modeled and examined in terms of the steady state power flow convergence. Further on, some case studies of integration of distributed energy resources with the remaining loaded and unloaded nodes of the system have been theoretically investigated.

In the next step, in order for the analysis to be completed in real time, the model of the system has been built-up in Hypersim (Fig. 2) and the developed case studies for different DER generation scenarios implemented in the model. Then using the OPAL-RT real-time simulation, the cases have been implemented and the real time results have been extracted.

As the final step of this work, the acquired data from the micro phasor measurement units (Micro PMUs) of the system have been collected and analyzed using the event detection algorithm which is developed.

Parallel to this work, to implement a more sophisticated test cases in a bigger standard power transmission system, the IEEE 123-node test system is chosen and modeled in OPAL-RT. Using the real time simulation, some more complex test cases have been implemented in this system and the resiliency of the system have been examined.

Optimal Power Flow Active and Inactive Constraints Identification with Machine Learning

Fouad Hasan, *Student Member, IEEE*, and Amin Kargarian, *Member, IEEE*

Abstract—A combined supervised classification+regression learning based algorithm is proposed to identify active and inactive sets of inequality constraints solely based on nodal power demand information in this work. Inactive constraints are removed to reduce the size of OPF. This reduced optimization problem can be solved within a much smaller time frame and requires less computational resources.

Index Terms— Optimal power flow, active constraints, feasible region, machine learning, confusion matrix.

I. INTRODUCTION

OPTIMAL power flow (OPF) is one of the main energy management functions that is solved every 5 minutes.

Recently, the application of machine learning to OPF has seen increased interest. Majority of the recently published papers aim at a direct estimation of OPF solution by machine learning algorithms. This potentially degrades the optimality and reliability of the estimated OPF solution and make operators reluctant to deploy them for real power systems operation. However, this letter presents a combined supervised classification+ regression learning based algorithm to identify active and inactive bus voltage and line flow constraints for the ACOPF problem with the aim of reducing the size of OPF. The simulation results show that the proposed algorithm has an accuracy of 99% for active and inactive inequality constraints classification.

II. INACTIVE CONSTRAINTS DETECTION

The target is to predict constraints status using only nodal demand values. $f(x)$ is the objective function, $h_v(x)$ and $h_{pl}(x)$ are respectively the set of bus voltage and branch flow inequality constraints, χ denotes the feasible region of all other equality and inequality constraints except $h_v(x)$ and $h_{pl}(x)$, and x is the set of decision variables.

$$\begin{aligned} & \min f(x) \\ \text{s.t. } & h_v(x) \leq 0 \quad \& \quad h_{pl}(x) \leq 0, \text{ where } x \in \chi \end{aligned} \quad (1)$$

For the purpose of training, a dataset is prepared with 25000 random and 1000 rational demand scenarios. For each demand sample, OPF is solved and Karush-Kuhn-Tucker (KKT) multipliers are used to identify active and inactive bus voltage constraints ($A(h_v(x))$) and branch flow constraints ($A(h_{pl}(x))$).

The input of the trained regression learners is nodal demand D and their outputs are predicted power generated, \tilde{P}_g and \tilde{Q}_g by each unit. However, net injection \tilde{NI} at each node is used as input to trained classifiers and the output of classifier one is active bus voltage constraints ($\tilde{A}(h_v(x))$) and the second

classifier predicts active branch flow constraints ($\tilde{A}(h_{pl}(x))$). They will be used to formulate a reduced OPF problem as follows:

$$\begin{aligned} & \min f(x) \\ \text{s.t. } & \tilde{A}(h_v(x)) \leq 0 \quad \& \quad \tilde{A}(h_{pl}(x)) \leq 0, \text{ where } x \in \chi \end{aligned}$$

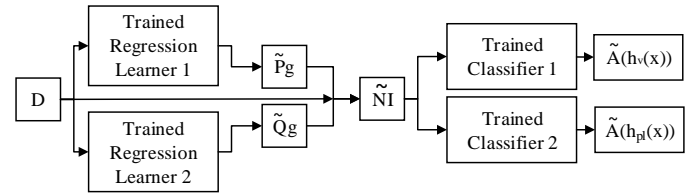


Fig. 1. Block diagrams of the trained learners' utilization procedure.

III. NUMERICAL RESULTS

Active constraints are labeled as '1' and inactive constraints are labeled as '0'. To test, 100 new scenarios are generated each containing 236 bus voltage constraints and 372 branch constraints. Thus, there are 23,600 voltage constraints and 37,200 constraints for all 100 test scenarios.

Figure 2a represents the confusion matrix for voltage constraints, and Fig. 2b illustrates the confusion matrix for branch flow constraints. Green blocks in the first row show that 96.9% of bus voltage constraints and 99.5% of branch constraints are true negative that means they are correctly predicted to be inactive. Green blocks in the second row depict that 2.1% and 0.5% of voltage and branch constraints are true positive, which means they are correctly predicted to be active. As shown in the third row of the confusion matrices, no misclassification is observed for branch flow constraints. 1.0% of voltage constraints are misclassified out of which 0.49% is false positives and 0.51% is false negatives (orange colored blocks in Fig .3). KKT multipliers corresponding to false negatives are near zero. So, they have little impact on the OPF feasible region.

Predicted class	Target Class			Predicted class	Target Class		
	0	1			0	1	
0	22883 96.9%	117 0.51%	99.1% 0.9%	0	37000 99.5%	0 0.0%	100% 0.0%
1	100 0.49%	500 2.1%	83.3% 16.7%	1	0 0.0%	200 0.5%	100% 0.0%
	99.5% 0.5%	81.0% 19.0%	99% 1.0%		100% 0.0%	100% 0.0%	100% 0.0%
	0	1			0	1	
	Target Class				Target Class		

Fig. 2. Confusion matrices for a) voltage constraints and b) branch constraints.

IV. CONCLUSION

The results showed that a very small fraction (less than 1%) of voltage and branch constraints are active and omitting all inactive constraints by the proposed algorithm reduces the size of OPF problem significantly.

A Fault Zone Identification Scheme for Busbar Using Correlation Coefficients Analysis

Soumitri Jena*, Bhavesh R. Bhalja*, S. R. Samantaray†

*Department of Electrical Engineering, Indian Institute of Technology Roorkee, Uttarakhand, India

†School of Electrical Sciences, Indian Institute of Technology Bhubaneswar, Odisha, India

Email: sjena@ee.iitr.ac.in, bhaveshbhalja@gmail.com, srs@iitbbs.ac.in

Abstract—This paper proposes a new busbar protection scheme based on the analysis of correlation coefficients between the current waveforms of all lines connected to the busbar. The cross-correlation coefficients between current waveforms of each line in moving windows are calculated in a phase segregate manner with respect to a reference line. It's performance has been evaluated by modelling an existing 400-kV Indian substation in PSCAD/EMTDC software package. The proposed scheme is able to provide ultra-high-speed protection for the busbar. It's stability has been tested against a wide range of external faults. It also solves the problem of CT saturation which is the biggest challenge in conventional low-impedance busbar differential protection schemes (87B).

Keywords—busbar protection, cross correlation coefficient, bus zone identification, CT saturation.

I. INTRODUCTION

In terms of sensitivity and security, busbar protection is one of the difficult aspects of power system protection. As the connection point of number of incoming and outgoing transmission lines and various substation equipment, a bus fault has the same disastrous effect as that of a large number of simultaneous faults. In large substations, busbar protection zone is usually divided into multiple zones. An internal bus fault, in this case, will disturb only a smaller part of the substation and fewer components will be affected. High-speed tripping during bus fault is one of the most important requirements of busbar protection as it limits the widespread damage. This has created a paradigm shift in the industry to reduce the relay tripping time rather than developing new arc extinction methods for circuit breakers.

II. PROPOSED SCHEME AND RESULTS

Often used in statistical mathematics, the correlation coefficient (ρ_{xy}) shows the measure of linear relationship between two variables x and y , where, $-1 < \rho_{xy} < +1$. In case of a perfect positive correlation, it's value remains 1. Conversely, for a complete negative correlation it's value remains -1. If the variables can not be linearly related then the value remains 0. In other terms, this coefficient defines the degree of similarity between two coefficients. In order to measure the similarity between a set of variables $X, Y, \{(x_1, y_1), \dots (x_n, y_n)\}$, ρ_{XY} is calculated as follows:

$$\rho_{XY} = \frac{\sum_{i=1}^n (x - \bar{x})(y - \bar{y})}{\sqrt{\sum_{i=1}^n (x - \bar{x})^2} \sqrt{\sum_{i=1}^n (y - \bar{y})^2}} \quad (1)$$

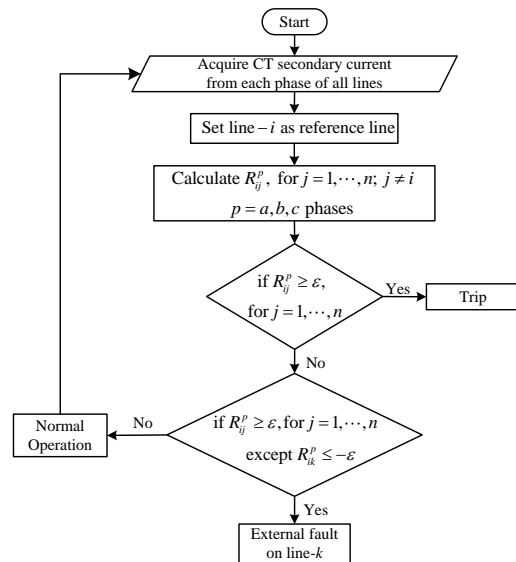


Fig. 1. Flow chart of the proposed scheme.

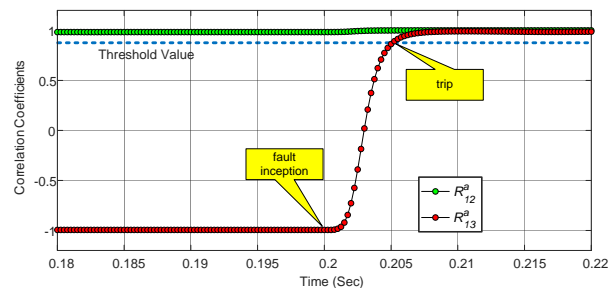


Fig. 2. Correlation coefficients during single line to ground fault on busbar.

III. CONCLUSION

This paper presents a new fault zone identification scheme for busbar by analyzing correlation coefficients. The proposed scheme uses moving windows of one cycle CT secondary current signals of all lines connected to the busbar to calculate the correlation coefficients. The correlation coefficients are compared to a threshold value to decide the fault zone. The proposed scheme has been verified against a wide range of fault scenarios where it remains reliable during internal busbar faults and maintains stability in case of external faults even with CT saturation. Moreover, in terms of response time, the proposed protection scheme is on par with modern busbar protection schemes.

Energy Management System for Naval Submarine

Byeongdo Jeon, *Student Member, IEEE*, and Mojdeh Khorsand, *Member, IEEE*

School of Electrical, Computer, and Energy Engineering, Arizona State University, Tempe, AZ 85287, USA

Email: byeongdoo.jeon@asu.edu and mojdeh.khorsand@asu.edu

An optimal energy scheduling is essential procedure in an isolated environment such as naval submarines, all electric boats. The conventional naval submarines include diesel-electric propulsion system. The diesel generators are used to charge the batteries when the submarine is at the surface or at snorkeling depth. This is the most dangerous time as it may make the submarine easily detectable by acoustic and non-acoustic sensors of enemy assets. This imposes a significant concern for the conventional submarines including for boats with fuel cells. By reducing the snorkeling time through entire mission period, the submerged endurance will be enhanced due to optimal energy schedule. This paper introduces an optimal energy management algorithm and tool for submarines with various energy resources such as lithium-Ion batteries, diesel generators, and fuel cells. Energy supply and demand sources for a conventional submarine is shown in Figure 1.

An energy management system (EMS), which optimally schedule submarines' available energy resources for the duration of each mission, can substantially reduce the need for excessive snorkeling and reduces the danger of being exposed to enemies. The flexibility of energy consumption for the mission period, mission's purpose and plans, and available energy resources should be simultaneously considered in the optimal energy management model to enhance efficiency and reduce the risk of being exposed. The proposed EMS can serve as a supervisory tool to submarine officers to identify hourly, daily, and weekly generation and consumption schedule for the duration of the mission. Such EMS tool can be enhanced to account for the emergency and risky events in order to support submarine officers to make critical decisions at sea.

The proposed model is aimed at minimizing the snorkeling time while accounting for operational limitations and availability of resource for the duration of the mission.

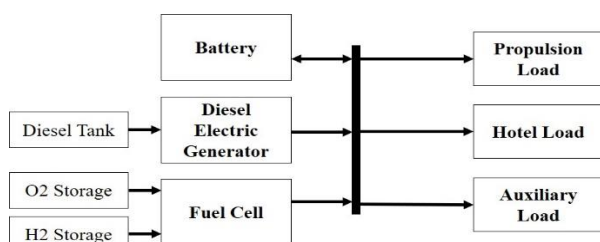


Fig. 1. Power system of the conventional submarine.

In this study, an EMS is design for a generic 3000 Ton class conventional submarine. By considering physical installable spaces, the diesel electric generator system, fuel cells, and batteries are modeled on board. The proposed EMS accounts for subordinate systems, e.g., pressurized air and hydraulic system. Therefore, all the energy sources in the submarine are managed systematically by EMS as shown in Figure 2.

For further study, the model is applied to various military missions including but not limited to surveillance and information gathering, anti-submarine warfare, attack of land targets. Depend on the given mission, the energy scheduling will be modified to satisfy its criteria.

The objective of the model is to minimize the snorkeling time as (1).

$$\text{minimize: } \sum_{t \in T} u_{s,t} \quad (1)$$

Where $u_{s,t}$ is snorkeling binary variable. Power Balance Constraint of the system as (2).

$$P_{s,t} + P_{f,t} - P_{b,t} = L_{p,t} + L_{h,t} + L_{a,t} \quad (2)$$

Where, $P_{s,t}$, $P_{f,t}$, $P_{b,t}$ are power supply from diesel gen-set, fuel cell, and battery. $L_{p,t}$, $L_{h,t}$, $L_{a,t}$ are propulsion, hotel, and auxiliary load respectively. The propulsion load can be expressed as (3).

$$L_{p,t} = 0.0026 \cdot \left(\frac{D}{1000}\right)^2 \cdot \left(\frac{u}{1.852}\right)^3 \quad (3)$$

Where, D is a displacement of sea water for submarine and u is maneuver speed in knot.

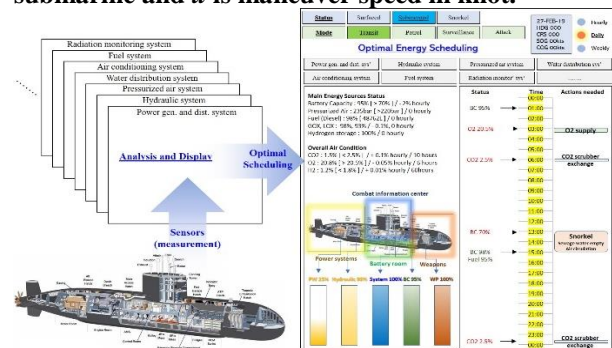


Fig. 2. EMS for Optimal Energy Scheduling.

REFERENCES

- [1] R. Burcher, and L. Rydill, Concepts in Submarine Design. Cambridge Ocean Technology Series, Cambridge: Cambridge University Press, 1994.
- [2] J. Buckingham, C. Mimeche, T. Hardy, and C. Mimarest, "Submarine Power and Propulsion - Application of Technology to Deliver Customer Benefit," *UDT Europe* 2008, June, pp. 1-17, 2008.
- [3] P. C. Ghosh and U. Vasudeva, "Analysis of 3000T Class Submarines Equipped with Polymeric Electrolyte Fuel Cells," *Energy*, vol. 36, no. 5, pp. 3138-3147, 2011.

A Cost Effective Energy Exchange Strategy to Improve Reliability of Microgrids

Md. Kamruzzaman, *Student Member, IEEE*, and M. Benidris, *Member, IEEE*

Department of Electrical and Biomedical Engineering, University of Nevada, Reno, NV 89557, USA

Emails: mkamruzzaman@nevada.unr.edu and mbenidris@unr.edu

Abstract—This paper proposes a cost effective energy exchange strategy for energy storage devices (ESDs) to improve reliability of microgrids. The proposed strategy starts with evaluating the minimum storage level of ESDs based on expected loss of load duration (ELOAD) and expected loss of load (ELOL) indices. This minimum storage level will be used only during power supply interruption to avoid load curtailments. In addition, a controlled charging/discharging strategy beyond the minimum storage level of ESDs is introduced to reduce cost for electricity consumption. In this strategy, the ESDs are charged at low price periods without creating energy deficiency and discharged at high price periods of electricity supply. Also, owners of ESDs can participate in the electricity market after satisfying their own demand at high price periods. This will reduce cost for electricity consumption. Therefore, the proposed strategy would be effective in both improving the reliability of microgrids and reducing cost for electricity consumption. The developed method is demonstrated on a microgrid through several case studies. Monte Carlo simulation is used to evaluate the reliability indices.

Index Terms—Cost reduction, energy storage devices, microgrid, reliability.

I. KEY EQUATIONS

A. Expected Loss of Load Duration

Expected loss of load duration (ELOAD) for each interruption is calculated by using the following equation [1].

$$ELOAD = \frac{\left(\sum_{n=1}^N T_n \right)}{N} \quad (1)$$

where N is the total number of interruption for a given period of time and T_n is the duration at n^{th} interruption.

B. Expected Loss of Load (ELOL)

The ELOL of microgrid is calculated by using the following introduced equation.

$$ELOL = \frac{\left(\sum_{i=1}^N L_n \right)}{N} \quad (2)$$

where L_n is the total loss of load at n^{th} interruption. In this work, $ELOAD$ and $ELOL$ are calculated from grid side.

In the proposed strategy, it is considered that the minimum storage of ESDs should be sufficient to compensate for the $ELOL$ during interruptions. Therefore, $ELOAD$ and $ELOL$ are used to determine the minimum storage level of ESDs, which would be supplied only at interruption condition to improve reliability of the microgrids.

II. KEY RESULTS

In this work, the proposed method is demonstrated on a microgrid presented in [2]. The load profile is constructed based on the IEEE Reliability Test System [3] and Monte Carlo simulation is used to evaluate the reliability indices.

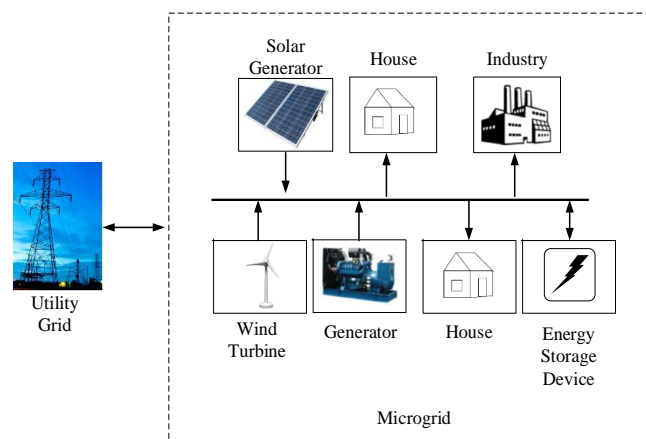


Fig. 1. Energy exchange diagram of Microgrid

TABLE I
RELIABILITY INDICES OF THE CONSIDERED MICROGRID

	LOLP	LOLE (hr/yr)	LOLF (Occ/yr)	ELOAD hr	ELOL kw
Case I	0.00204	17.84	3.26	5.47	27.18
Case II	1.14E-06	0.01	0.004	2.5	15.04

* Case I = without ESDs & Case II = with ESDs

The minimum storage level of ESDs for the considered microgrid is calculated by multiplying the $ELOAD$ and $ELOL$ of Case I which is 148.72 kWh.

REFERENCES

- [1] T. Yuting, A. Bera, M. Benidris, and J. Mitra, "Stacked revenue and technical benefits of a grid-connected energy storage system," *IEEE Transactions on Industry Applications*, pp. 1–10, 2018.
- [2] H. Daneshi and H. Khorashadi-Zadeh, "Microgrid energy management system: A study of reliability and economic issues," in *Power and Energy Society General Meeting, 2012 IEEE*, San Diego, CA, USA, Nov. 2012, pp. 1–5.
- [3] P. M. Subcommittee, "IEEE reliability test system," *IEEE Transactions on Power Apparatus and Systems*, vol. PAS-98, no. 6, pp. 2047–2054, Nov. 1979.

Bulk Electric Power System Risks from Coordinated Edge Devices

Richard Wallace Kenyon*, *Student Member, IEEE*, Jeffrey Maguire, Elaina Present, Dane Christensen, *Member, IEEE*, and Bri-Mathias Hodge, *Member, IEEE*

Abstract—With cloud connected residential air conditioners, the potential for widespread coordinated control is present. Using the NREL ResStock program for load allocation and PSLF for dynamic simulations, a bulk power system study was performed on the Western Interconnection investigating the potential impacts of such coordinated control on the bulk electric power system.

Index Terms—residential air conditioning, cloud connected edge devices, coordinated control, western interconnect, bulk power system, PSLF

I. INTRODUCTION

BY the end of 2019, it is expected that over 50% of US households will be smart [1] - meaning they will have two or more cloud connected products installed. There are over 17 million connected thermostats deployed in the U.S. today (and this is expected to grow to 25 million by 2019) [2], each of which operates a residential air conditioner (RAC), the single most dominant load in capacity of the residential sector. Hacked edge devices were used to launch a large-scale denial of service attack on the bulk internet in 2016 and edge devices were used in a Ukrainian power grid outage due to hacking; widespread coordinated control is proven. We set out to study the potential impact of the coordinated control of cloud connected RACs on the Western Interconnect (WI) bulk electric power system.

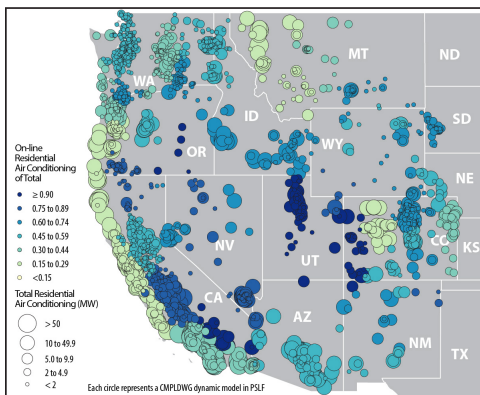


Fig. 1. Distribution of aggregate RAC in the WECC, with associated online percentages based on ResStock modeling from August 25, 2012 weather data.

II. CASE STUDY

The National Renewable Energy Laboratory (NREL) ResStock tool was used to locate aggregate RAC load on the WI

All authors are with the National Renewable Energy Laboratory, Golden, CO 80401 USA e-mail: first.last@nrel.gov. * Corresponding Author

21,000 bus Positive Sequence Load Flow (PSLF) model at over 3,000 dynamic composite load models (CMPLDWG) (see Fig. 1). Two power flow cases and associated dynamic models from the Western Wind and Solar Integration Study (WWSIS) Phase 3, that of heavy summer (HS) and light spring (LSP) conditions, were used to analyze the impact of coordinated RAC control across the WECC. Fig. 2 shows the system wide frequency response for three different controllable fractions of cloud connected RACs in the HS case.

Controllable (%)	LSP Online (MW)	HS Online (MW)	Max (MW)
10	350	1150	2650
20	700	2300	5300
30	1050	3450	7950

TABLE I
AGGREGATE RAC TOTALS FOR HS & LSP CASES.

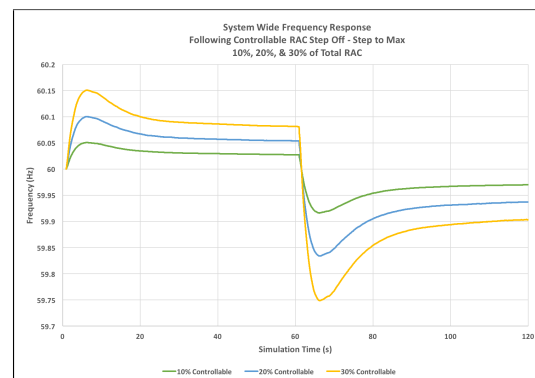


Fig. 2. Center of Inertia frequency response of WI following controllable RAC step off with subsequent full step on for the HS case.

III. CONCLUSION

The results of the HS case study result in system wide frequency deviations from nominal contained within permissible boundaries. For the LSP case, with a larger component of potential RAC load verse total system load, larger frequency deviations occur. An investigation into cascading impacts on distributed generation ride through following load step induced voltage fluctuations accompanies the full report.

REFERENCES

- [1] 2017 tech growth exceeds expectations. Consumer Technology Association. [Online]. Available: <https://www.cta.tech/News/Press-Releases/2017/July/2017-Tech-Growth-Exceeds-Expectations-Industry-Re.aspx>
- [2] Smart thermostat market report. Mordor Intelligence. [Online]. Available: <https://www.mordorintelligence.com/industry-reports/smart-thermostat-market>

Optimal PMU Placement Using Stochastic Methods

Mirka Mandich, Tianwei Xia, Kai Sun
 Department of Electrical Engineering and Computer Science
 University of Tennessee, Knoxville, USA

Abstract—Phasor Measurement Units (PMUs) collect high-precision voltage and current data in order to monitor the performance of a power system. However, it is expensive to implement PMUs on every bus within a power system. Optimal PMU placement (OPP) becomes necessary to minimize the number of PMUs implemented while maintaining full observability of the network. This paper considers the resiliency of bus connections when optimizing PMU placement. First, a graphical and mathematical model is developed. Next, techniques from chance constrained programming are adapted to create a stochastic model in which N-1 contingency is considered. Finally, by applying stochastic programming techniques, the model is tested with the 73-Bus IEEE 1996 Reliability Test System (RTS-96).

Index Terms—Integer Linear Programming, N-1 Contingency, Optimal PMU Placement, RTS-96, Stochastic Methods.

APPLYING STOCHASTIC METHODS TO OPP

Two variables are introduced to traditional OPP modeling in this paper. The variable $\eta_{i,j}$, inspired by chance constrained programming, represents the resiliency of the connection between buses i and j . If a connection frequently experiences failures (e.g. $\eta_{6,9}$ in Fig. 1) placing PMUs on neighboring buses may improve network observability during a failure.

The variable $\alpha_{i,j}$ represents the user-selected confidence interval for each connection. Selecting a low α value improves affordability by decreasing the number of PMUs needed to satisfy the constraint equations. Selecting a large α increases system observability and improves resilience.

This stochastic model was developed into a MATLAB program for the RTS-96. First, users select an α value. Next, Monte Carlo simulations are ran using realistic stochastic η values. Finally, OPP solutions are identified and the minimum number of PMUs for each simulation is plotted.

STOCHASTIC GRAPHICAL MODEL

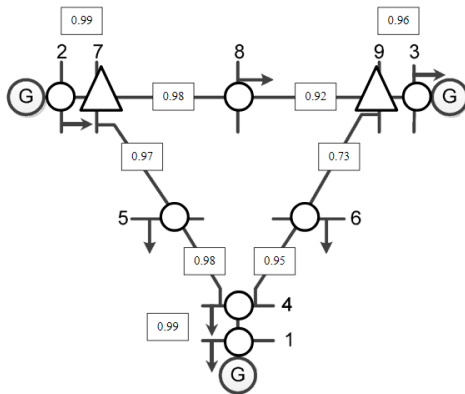


Fig. 1. Modified IEEE 9-Bus with sample η values

STOCHASTIC MATHEMATICAL MODEL

Conditions:

- $a_{i,j} = 1$ If buses i and j are connected
- 0 Otherwise
- $x_i = 1$ If bus i has a PMU
- 0 Otherwise
- $y_{i,j} = 1$ If zero-injection bus i or j has a PMU
- 0 Otherwise
- $z_i = 1$ If bus i is zero-injection
- 0 Otherwise
- $\eta_{i,j} = 1$ Always successful (e.g. $\eta_{1,1}$)
- η Success rate (e.g. $\eta_{6,9} = 0.73$)
- 0 Line outage (e.g. $\eta_{1,2}$)
- $\alpha_{i,j} = 1$ Always confident
- α Confidence interval (e.g. 0.95 or 2)
- 0 Never confident

Objective Function:

$$\min \sum_{i=1}^n x_i$$

Constraints:

$$f_i = \sum_{i=1}^n a_{i,j} \eta_{i,j} x_i + \sum_{i=1}^n a_{i,j} \eta_{i,j} z_i y_{i,j} \geq \alpha_{i,j}$$

$$z_i = \sum_{i=1}^n a_{i,j} y_{i,j}$$

Constraints for Modified IEEE 9-Bus (Fig. 1):

$$f_1 = \eta_{1,1} x_1 + \eta_{1,4} x_4 \geq \alpha_1$$

$$f_2 = \eta_{2,2} x_2 + \eta_{2,7} x_7 + \eta_{2,7} y_{2,7} \geq \alpha_2$$

$$f_3 = \eta_{3,3} x_3 + \eta_{3,9} x_9 + \eta_{3,9} y_{3,9} \geq \alpha_3$$

$$f_4 = \eta_{4,4} x_4 + \eta_{4,1} x_1 + \eta_{4,5} x_5 + \eta_{4,6} x_6 \geq \alpha_4$$

$$f_5 = \eta_{5,5} x_5 + \eta_{5,4} x_4 + \eta_{5,7} x_7 + \eta_{5,7} y_{5,7} \geq \alpha_5$$

$$f_6 = \eta_{6,6} x_6 + \eta_{6,4} x_4 + \eta_{6,9} x_9 + \eta_{6,9} y_{6,9} \geq \alpha_6$$

$$f_7 = \eta_{7,7} x_7 + \eta_{7,2} x_2 + \eta_{7,5} x_5 + \eta_{7,8} x_8 + \eta_{7,7} y_{7,7} \geq \alpha_7$$

$$f_8 = \eta_{8,8} x_8 + \eta_{8,7} x_7 + \eta_{8,9} x_9 + \eta_{8,9} y_{8,9} \geq \alpha_8$$

$$f_9 = \eta_{9,9} x_9 + \eta_{9,3} x_3 + \eta_{9,6} x_6 + \eta_{9,8} x_8 + \eta_{9,9} y_{9,9} \geq \alpha_9$$

$$z_7 = y_{2,7} + y_{5,7} + y_{7,8} + y_{7,7} = 1$$

$$z_9 = y_{3,9} + y_{6,9} + y_{8,9} + y_{9,9} = 1$$

Optimal Model for Integrated Analysis of Transmission and Distribution Systems

Arun-Kaarthick Manoharan
 Dept. of Electrical Engineering and Computer Science
 Wichita State University
 Wichita, Kansas, 67260
axmanoharan@shockers.wichita.edu

Visvakumar Aravinthan
 Dept. of Electrical Engineering and Computer Science
 Wichita State University
 Wichita, Kansas, 67260
visvakumar.aravinthan@wichita.edu

Abstract—The integrated analysis of transmission and distribution systems gained momentum due to the increased interest in analyzing the interdependencies and interactions between the two systems, as it might play a crucial role in cases with significant penetration of distributed generation and variable loads. This work proposes an optimal framework for performing the combined analysis of transmission and distribution system.

I. INTRODUCTION

The first step in developing an integrated analysis is to develop a procedure to combine transmission and distribution system. As shown in figure 1, coupling can be either full or partial. A fully coupled co-simulation is where the combined transmission and distribution system is modeled together and analyzed. This a very challenging task as it involves a lot of

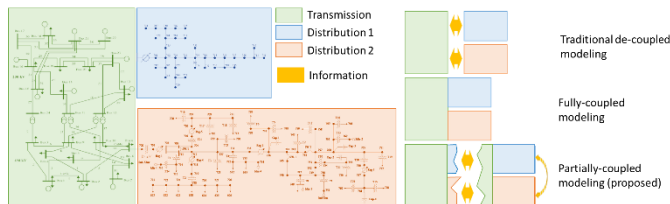


Figure 1 Framework for Integrated Analysis of T and D

variables. In [1] Velaga et al. try to model the entire system as an unbalanced three phase system. Singhal et al [2] come up with an iterative integration procedure where both the systems have separate optimal power flow analysis. Although this way of fully coupled co-simulating will be more accurate, due to the complex nature of this analysis, the implementation becomes tedious. Thus, the need for a lesser complex partially coupled model with desired accuracy becomes crucial.

II. PARTIAL COUPLING MODEL

The main problem to be addressed in developing a partially coupled model, is the transferring of parameters that are represented in single phase in the transmission and in three phases in distribution power flow studies. We propose the idea of developing the interconnection relation based on concept of three sequence power flow developed by Abdel-Akher et al in [3]. The procedure starts with performing power flow analysis on distribution side resulting in an unbalanced substation node voltage (V_D) and current (I_D). Then equations (1)-(3) to find negative(V_2) and zero (V_0).sequence of it.

$$I_{012} = A^{-1} * I_D \quad (1)$$

$$I_0 = Y_0 V_0 \quad (2)$$

$$I_2 = Y_2 V_2 \quad (3)$$

Finally run AC power flow on transmission system whose stopping criteria will be to attain a voltage that will go in as positive sequence and satisfy (4).

$$V_T = V_0 + V_1 + V_2 \quad (4)$$

This way the fluctuations on the unbalanced distribution system can be matched using single phase representation of transmission system

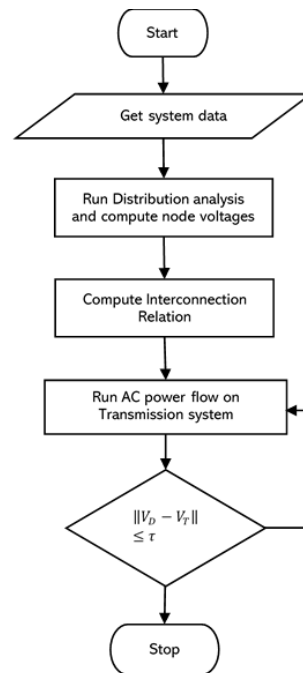


Figure 2 Proposed coupling procedure

REFERENCES

- [1] Velaga, Yaswanth Nag, et al. "Transmission-Distribution Co-Simulation: Model Validation with Standalone Simulation." 2018 North American Power Symposium (NAPS). IEEE, 2018.
- [2] Singhal, Nikita G., and Kory W. Hedman. "An integrated transmission and distribution systems model with distribution-based LMP (DLMP) pricing." North American Power Symposium (NAPS), 2013. IEEE, 2013.
- [3] Abdel-Akher, Mamdouh, Khalid Mohamed Nor, and AH Abdul Rashid. "Improved three-phase power-flow methods using sequence components." IEEE Transactions on power systems 20.3 (2005): 1389-1397.

Distributional Locational Marginal Prices under Uncertainty

Robert Mieth, *Student Member, IEEE*, and Yury Dvorkin, *Member, IEEE*.

Abstract—Distributional locational marginal prices (DLMPs) have been shown an efficient concept to incentivise optimal investment and operation of distributed energy resources in low-voltage distribution systems. This work proposes an uncertainty-aware pricing framework for distribution markets using chance constraints and presents a comprehensive analyses of the resulting prices. Using convex duality theory DLMPs that internalize the stochasticity of renewable generation resources, risk tolerance of the distribution system operator, as well include energy, balancing, and voltage support services are obtained. The resulting prices for scheduled active power procurement and balancing participation are itemized by their local and global components. The presented analyses shows the successful internalization of the uncertain operational conditions and reveals the discrepancy between local and global decisions under uncertainty.

I. MOTIVATION

Nodal electricity pricing has been shown to reflect physical and economical constraints on power system operations and to support the efficient allocation of energy resources. With the proliferation of distributed energy resources (DERs) in low-voltage distribution systems and their inherent volatility, lack of controllability and low marginal cost the existing economic signals are distorted. To overcome these distortions distributional marginal prices (DLMPs) have been proposed to incentivize optimal DER investments and operation in low-voltage distribution systems.

Existing DLMP concepts disregard the stochasticity of renewable generation resources and, therefore, the resulting prices do not provide proper incentives to efficiently cope with balancing needs. This work fills this gap and derives uncertainty-aware DLMPs and analyzes their composition to improve the understanding of those pricing signals.

II. MODEL AND METHODOLOGY

We use a chance constrained (CC) AC-OPF model to represent a distribution system with renewable generation resources. With a well-known representation of chance constraints as second order conic (SOC) constraints, we obtain a deterministic, convex equivalent of the CC AC-OPF model. The proposed program minimizes expected system cost subject to the respective nodal energy balances, voltage limits and power flow constraints as functions of the uncertain net-injections and balancing participation and provides probabilistic guarantees on those constraints. By applying convex duality theory we obtain DLMPs that internalize the stochasticity of renewable generation resources, risk tolerance of the distribution system operator, as well include energy, balancing, and voltage support services.

III. KEY RESULTS

Result 1 (Influence of uncertainty on DLMPs). Figure 1 shows the distribution of DLMPs with and without uncertainty in a 15-bus radial test-feeder. We see that not including uncertainty leads to prices for scheduled active power that are systematically too low. The proposed DLMPs internalize the necessary security margins for safe real-time operations.

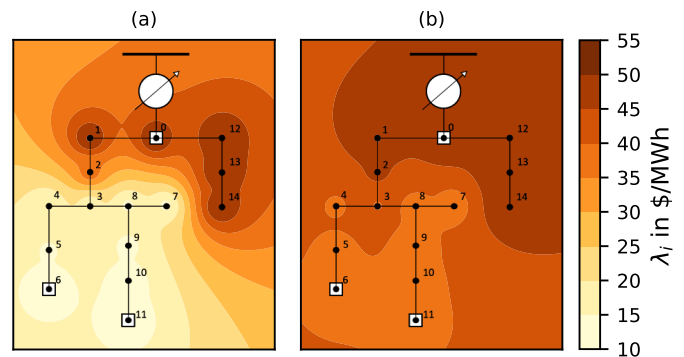


Fig. 1. Values of λ_i for the 15-bus system (a) without uncertainty and (b) with uncertainty.

Result 2 (Decomposition of scheduled power prices). Given a radial distribution system the price for scheduled active power at each node can be itemized by the price at the ancestor node, the price for reactive power at the same node and the ancestor node as well as a term reflecting the congestion of the line towards the node. We show that those prices are independent from the price for balancing participation.

Result 3 (Decomposition of balancing participation price). There exists a single system-wide price for balancing participation that is composed of the overall uncertainty (net-injection variance), the tightness of the generation constraints as well as the tightness of the voltage constraints relative to the implicit voltage variance. We show that the value of balancing participation decreases if a participating producer has strong influence on the systems voltage magnitudes.

Result 4 (Competitive Equilibrium and Producer Decision). In an auction set-up where scheduled power and balancing participation is auctioneered by a central planner, we can show that local constraints that are subject to uncertainty are internalized by the producer's decision. Global constraints are not part of those decisions which leads to a quantifiable mismatch between the optimal system and the optimal producer outcome.

Accelerated and Robust Analytical Target Cascading for Distributed Optimal Power Flow

Ali Mohammadi, *Student Member, IEEE*, Amin Kargarian, *Member, IEEE*, Farnaz Safdarian, *Student Member*

Abstract—Distributed optimization algorithms are sensitive to the choice of initial values and the level of importance of each term in objective functions. If initial values, in particular, penalty parameters, are not set appropriately and the level of importance of objective terms are not balanced, the algorithm may converge slowly, oscillate around the optimal point, or diverge. This paper presents an accelerated, robust analytical target cascading (AR-ATC) to solve optimal power flow (OPF) distributedly. A function is designed to determine a balancing coefficient with respect to initial values. Incorporating this coefficient in ATC makes a tradeoff between the convergence speed and solution accuracy by adjusting penalty terms with respect to generation cost functions. If multipliers are initialized to large values, the proposed function creates a balancing coefficient to avoid premature convergence or divergence. If multipliers are initialized to small values, the proposed function adjusts them to enhance the convergence speed. We name the proposed algorithm an accelerated, robust ATC since it enhances the solution speed and makes it more robust against initialization. Mathematical justifications and simulation studies are performed to analyze the effectiveness of AR-ATC. Potential applications of the proposed method to other distributed approaches such as ATC with exponential penalty functions and auxiliary problem principle (APP) is also studied numerically.

Index Terms—Analytical target cascading, distributed optimal power flow, distributed optimization, accelerated and robust.

I. INTRODUCTION

A. Background

APPLICATIONS of distributed and decentralized optimization algorithms has seen increased interest in the power system community and many other disciplines [1, 2]. The physical structure of smart power grids is becoming more distributed, and different agents take control responsibility of different parts of the system. Distributed algorithms (for the sake of explanation and brevity, we use the term distributed and omit the term decentralized) are applied to coordinate autonomous agents taking into account their information privacy. In addition, distributed optimization algorithms are considered as an efficient alternative for centralized algorithms for solving large optimization problems.

B. Literature Review

Various distributed optimization algorithms have been reported in the literature [1-8]. We focus on algorithms that have been utilized to solve steady-state problems such as optimal power flow (OPF). In most algorithms, interdependencies between subproblems are modeled in the form of either coupling constraints or coupling variables. Primal decomposition algorithms are, usually, applied to solve problems with coupling variables, and dual decomposition algorithms are used to solve problems with coupling constraints [9]. References [1, 2, 10] review distributed algorithms and their application on power systems. Six most popular algorithms, namely, alternating direction method of multipliers (ADMM) [11, 12], analytical target cascading (ATC) [13], auxiliary problem principle (APP) [14], proximal message passing [15], optimality condition decomposition [16, 17],

consensus+innovation [7], and their application to OPF are discussed in [1]. Applications of distributed algorithms on power system state estimation are discussed in [18]. variables between neighboring nodes in a given network.

II. PROPOSED FUNCTION TO CALCULATE α

It is not straightforward to find the optimal (or even a good enough) value for balancing coefficient α . This coefficient is problem dependent and its optimal value is unknown before

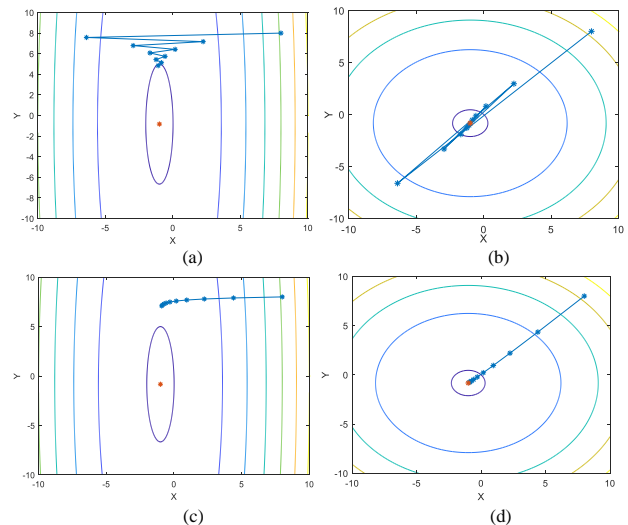


Fig. 1. Contour plot for a) unscaled (step size=0.8), b) scaled (step size=0.8), c) unscaled (step size=0.2) and d) scaled (step size=0.2) problem.

solving the problem. If one select optimality inconsistency constraint as the stopping criteria, the inconsistency constraints will be satisfied after couple of iterations (reach to a feasible point) while the result is not optimal. In contrast, if other cost functions dominate, optimization pays more attention to optimize each term of subproblems' objective function locally and solely while the inconsistency of coupling constraints may vanish slowly. In the other words, optimization find optimal point for each subproblem while they don't have shared variable.

For instance, for OPF with $\omega = 50$, while ALAD takes 100 iterations to reach $rel = 1e - 5$, AR-ALAD takes 75 iterations to obtain the same rel value. Note that the observed rel index fluctuations over the course of iterations are because of compromising between optimality and feasibility.

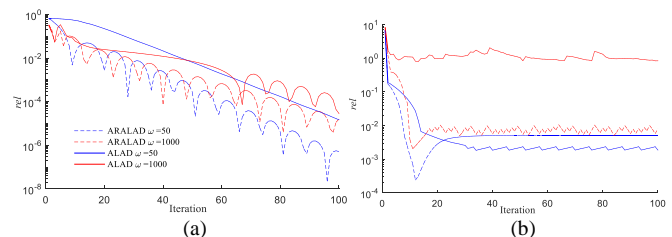


Fig. 6. Relative error versus iteration for a) the OPF problem and b) the mathematical benchmark problem.

Measurement-based Parameter Calibration for a Generic Model for Photovoltaic Generations

Jaemin Moon, Student Member, IEEE
 School of Electrical and Electronic
 Engineering
 Yonsei University
 Seoul, Korea
 Email: jaemin0127@yonsei.ac.kr

Minseung Ko, Student Member, IEEE
 School of Electrical and Electronic
 Engineering
 Yonsei University
 Seoul, Korea
 Email: kms4634500@yonsei.ac.kr

Kyeon Hur, Senior Member, IEEE
 School of Electrical and Electronic
 Engineering
 Yonsei University
 Seoul, Korea
 Email: khur@yonsei.ac.kr

Abstract—This paper study parameter calibration of WECC central station photovoltaic(PV) plant model via measurement-based approaches. Nonlinear optimization algorithm is applied to calibrate PV model parameters. Performance of calibration algorithm is verified with simulation data assumed as measured data.

Keywords—WECC generic PV model, measurement-based approaches, Nonlinear optimization algorithm

I. EQUATIONS

Measurement-based Parameter Calibration find optimal parameters value satisfying the following equation:

$$\min(\mathbf{y} - \mathbf{f}(\mathbf{x}, \mathbf{p}))^2 \quad (1)$$

where \mathbf{y} , \mathbf{f} , \mathbf{x} and \mathbf{p} are respectively measured data, an output vector of the model structure, an input vector of model, and model parameter.

Among the methods for solving (1), Levenberg-Marquardt(LM) algorithm is widely used due to its robust and fast convergence. LM method solve (1) iteratively as update parameter with following equation:

$$\mathbf{p}_{i+1} = \mathbf{p}_i - (\mathbf{J}^T \mathbf{J} + \lambda \mathbf{I})^{-1} \mathbf{J}^T (\mathbf{y} - \mathbf{f}(\mathbf{x}, \mathbf{p}_i)) \quad (1)$$

Where \mathbf{J} , \mathbf{I} , and λ are respectively the Jacobean matrix which is partial derivatives of \mathbf{f} with each parameter, an identity matrix, and a combination coefficient.

II. KEY FIGURE

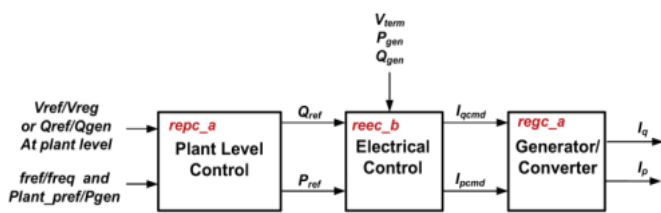


Figure 1. WECC central station PV plant model [1]

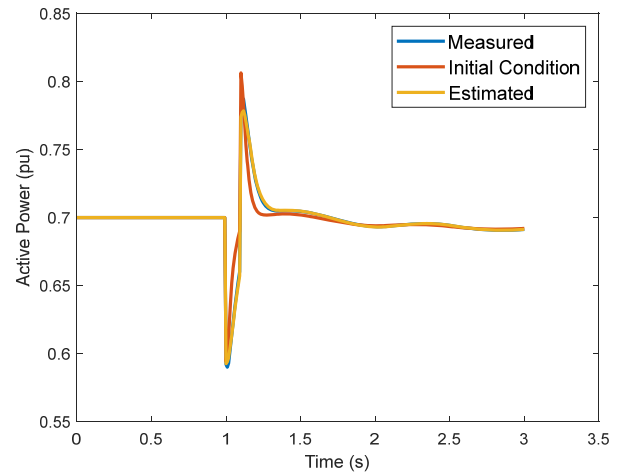


Figure 2. Active power results comparison among measured data, initial parameters, calibrated parameters

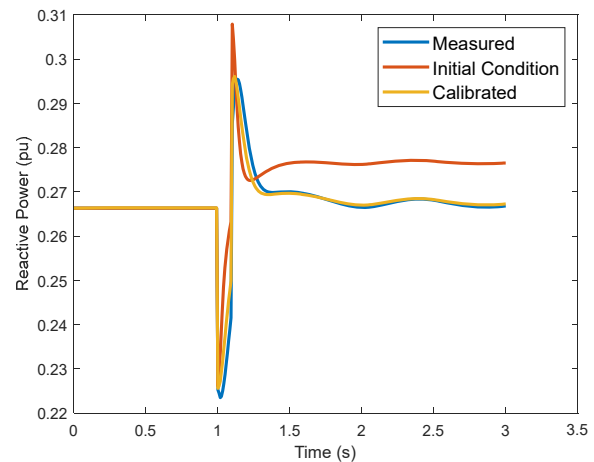


Figure 3. Reactive power results comparison among measured data, initial parameters, calibrated parameters

- [1] R. T. Elliott, A. Ellis, P. Pourbeik, J. J. Sanchez-Gasca, J. Senthil and J. Weber, "Generic photovoltaic system models for WECC - A status report," 2015 IEEE Power & Energy Society General Meeting, Denver, CO, 2015, pp. 1-5

Generative Adversarial Networks for Real-time Stability Assessment of Inverter-based Systems

Gurupraanesh Raman, Xilei Cao, Gururaghav Raman, and Jimmy Chih-Hsien Peng
 Department of Electrical and Computer Engineering, National University of Singapore, Singapore 117583
 Email: gurupraanesh@nus.edu.sg

Abstract—In islanded systems with droop-controlled sources, the droop coefficients need to be tuned in real-time using supervisory control to maintain asymptotic stability. In contrast to offline tuning methods, online stability-region estimation yields non-conservative droop gains in real-time, ensuring good power sharing performance as the operating point varies. The challenge in the traditional stability-region estimation process is its unscalability and $O(n^3)$ computational complexity. In this work, an efficient alternative using conditional Generative Adversarial Networks (cGANs) is described. We demonstrate that the notion of power system stability can be learned by such deep neural networks, and that they can offer a scalable alternative to conventional stability-region estimation methods in islanded distribution systems. The cGANs-based stability assessment is carried out on the islanded IEEE 123 bus test case to validate its advantages.

Index Terms—Distribution system stability, droop control, Generative Adversarial Networks (GANs), supervisory control.

I. APPROACH

The stability region is traditionally determined by evaluating the eigenvalues for a range of droop gains and then classifying each setting as stable/unstable. This process is unscalable and therefore not suitable for online implementation. In this work, conditional Generative Adversarial Networks (cGANs) are used to generate the real-time stability region after offline training over a range of system configurations (e.g., with line faults/switching) and stable droop settings. At the end of the training process, the Generator network can conjure the stability region for any real-time configuration, with the Y_{bus} matrix being the conditional input. The training process is governed by the following equations:

$$\min_G \max_D V(D, G) = \mathbb{E}_{x \sim p_{data}(x)} [\log D(x||y)] + \mathbb{E}_{z \sim p_z(z)} [\log(1 - D(G(z||y)))] \quad (1)$$

The training is stopped when the Chebyshev distance d_c of the generated system configuration from the original configuration becomes less than a threshold value.

$$d_c = \max_z (x_f - G(z)_f) < \epsilon, \quad (2)$$

II. RESULTS AND CONCLUSIONS

An islanded 5-inverter system is derived from the IEEE 123 bus system, which is a 4.16kV, 50 Hz ring system. Each inverter is rated at 1 MVA. The cGANs approach is used to determine the stability-region, and its accuracy is demonstrated in Fig. 1. After the criterion (2) is satisfied, the training is continued to improve the stability region coverage. Comparison of

the running time between cGANs and the traditional method from Table I indicates that the former is about 10 times faster for each system configuration, demonstrating its suitability for online implementation. Moreover from Table II, it is clear that the training process is also scalable with respect to the number of system configurations.

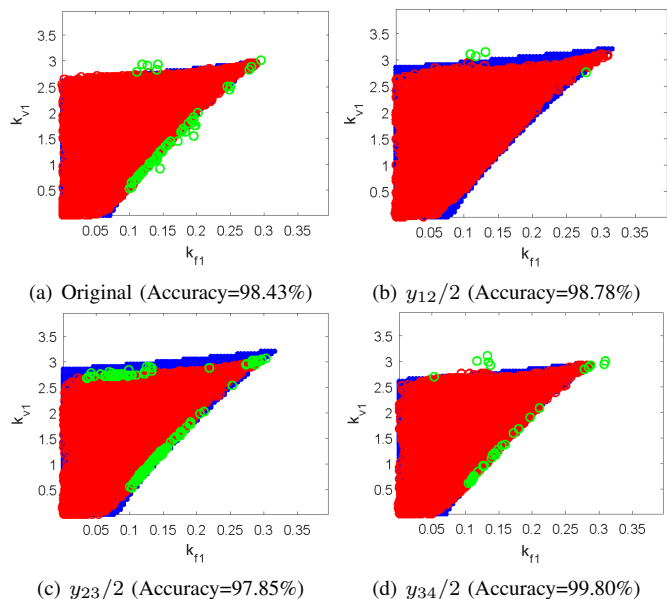


Fig. 1. Stability region from epoch 1907 shown in red for Inverter-1 identified using cGANs for 4 system configurations. Corresponding theoretical regions are indicated in blue, obtained from the traditional method. Green circles denote erroneously projected points of stability by the cGANs method.

TABLE I
 RUNNING TIME FOR 20000 SAMPLES- ACCURACY IN PARENTHESES

Approach	k_f & k_v ($i=2-5$)	Orig. Syst. Time (s)	$y_{12}/2$ Time (s)	$y_{23}/2$ Time (s)	$y_{34}/2$ Time (s)
Traditional	Fixed	14.2336	16.5988	15.1759	14.8897
Traditional	Varied	12.1833	12.3569	12.4272	12.4838
cGANs	Fixed	1.3480	1.3776	1.3343	1.2241
Epoch 1907		(98.43%)	(98.78%)	(97.85%)	(98.03%)
cGANs	Varied	1.2838	1.2896	1.3115	1.2256
Epoch 3994		(100%)	(99.98%)	(99.97%)	(99.80%)

TABLE II
 REQUIRED EPOCHS FOR LEARNING RATE 8×10^{-6}

Number of system configurations	1	2	4
Epochs required for accuracy above 95%	680	695	720
Epochs required for populating whole region	1035	1200	1280

Optimal Operation of UCF Campus Grid with Modeling in MGMS and OPAL-RT

Ivelisse Rivera, Lisian Shehu, Inalvis Alvarez-Fernandez, Wei Sun
 Department of Electrical and Computer Engineering
 University of Central Florida
 Orlando, Florida, United States

ivelisse.rivera@knights.ucf.edu, lisianshehu08@Knights.ucf.edu, alvarezfernandez@knights.ucf.edu, sun@ucf.edu

Abstract - This paper aims to introduce a microgrid model of the University of Central Florida campus grid to analyze how an energy management system determines the optimal mode of operation based on generation, load, and price of energy at any specific time. Data on generation, load and price of energy data have been collected and generated to model the UCF microgrid by utilizing Information Model Management (IMM) and MATLAB Simulink. The collected data and the created model are uploaded into the Microgrid Management System (MGMS) for simulation. Furthermore, real-time data is generated using OPAL-RT technology. Communication is established between OPAL-RT, IMM, and MGMS in order to simulate the microgrid model in real-time. The simulation results will be analyzed to determine how the energy management system can determine the optimal mode of operation in an efficient manner.

I. MICROGRID MODEL OF UCF CAMPUS GRID

University of Central Florida (UCF) campus grid is modeled in MATLAB Simulink. A one-line diagram of UCF's microgrid power system is developed first, based on the UCF power grid diagram provided by Duke Energy. The UCF's microgrid system is composed of two substations, the North and South Substations, which connect to the transmission system at a point of common coupling. The North substation model is composed of three feeder lines, of type 1000 AL, two photovoltaic (PV) devices and twenty-six loads. The PVs are connected to the Parking Garage D and to the UCF Global Building with a generation of 100kW at maximum irradiance. The South substation model consists of three feeder lines of type 1000 AL, two PVs, a combined heat and power (CHP) plant and seventy-two loads. The PVs are connected to Harris Corporation Engineering Center, and to Parking Garage B with a generation of 60kW and 50kW at maximum irradiance, respectively. The CHP plant is connected to the feeder line that provides power to sixty percent of the university, with a generation of 5.5kW.

In order to accurately model UCF's microgrid system, each load contains the building load profile, which updates every 15 minutes. This power data was collected from the Open Energy Information System website for UCF. After the creation of this model in MATLAB Simulink was completed, the model was then prepared for real time execution using OPAL-RT. Furthermore, a digital microgrid model was created in IMM model. In order to accomplish our goal of analyzing how energy management system determines the optimal mode of operation, communication between IMM,

MGMS, and OPAL-RT, was connected through the Distributed Network Protocol (DNP3) communication protocol.

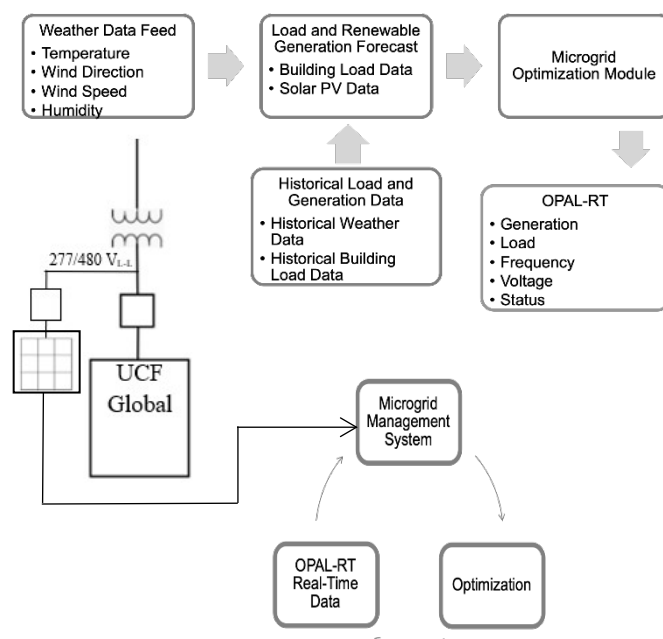


Figure 1: Communication protocol

II. SIMULATION RESULTS

The UCF Simulink Model was ran in OPAL-RT in order to produce real time data. The results of the voltages of some of the buildings located at the North substation were as shown in Table 1.

Table 1: Simulation results of buildings in OPAL-RT

Time (s)	Alumni (kV)	Arts & Humanities (kV)	CFE Arena (kV)	Career Services (kV)	Classroom Bldg. 1 (kV)	Classroom Bldg. 2 (kV)
1	377.27	372.08	368.08	377.27	379.83	377.92
2	377.28	372.08	368.09	377.28	379.83	377.92
3	377.28	372.08	368.08	377.28	379.83	377.92
4	377.29	372.09	368.09	377.29	379.84	377.93

PES Student Program - Schilling, Samuel

Concepts for Acceptance-Friendly AC-DC Transmission Grids

Samuel Schilling, Maren Kuschke, and Kai Strunz
Chair of Sustainable Electric Networks and Sources of Energy (SENSE)
Faculty of Electrical Engineering and Computer Science
Technische Universität Berlin, Berlin, Germany
samuel.schilling@tu-berlin.de, maren.kuschke@tu-berlin.de, kai.strunz@tu-berlin.de

Abstract—The integration of large onshore and offshore wind farms calls for an increase in transmission capacity to transport the generated power towards load centers. Achieving a higher public acceptance for grid extension, the integration of cables is preferred. The realization of AC transmission by cable would require major reactive power compensation, whereas reactive power compensation is not applicable for high voltage direct current (HVDC) transmission. Acceptance can be increased further by bundling infrastructures. The poster examines options for the installation of HVDC cable systems in tunnels parallel to highways. Moreover, a principal operation of an HVDC overlay grid is demonstrated for a scenario with high power transmission.

Index Terms—AC-DC optimal power flow, HVDC transmission, multi-terminal HVDC grid, wind energy integration.

I. INTRODUCTION

A review of high voltage direct current (HVDC) systems and their application in power grids is given in [1]. In current research, the operation of multi-terminal HVDC grids is of particular interest [2], [3]. An integrated AC-DC transmission grid model is developed and studied for normal operation and outages of DC corridors and AC-DC converter stations. Moreover, options for the acceptance-friendly integration of the HVDC overlay grid into existing transport infrastructures are presented.

II. AC-DC TRANSMISSION GRID MODEL

The AC-DC transmission grid model for research purposes is illustrated in Fig. 1. It is assumed that the AC-DC grid is located in Germany, and HVDC cable systems are installed in tunnels along existing highways. The nine-terminal HVDC overlay grid model comprises six North-South corridors and six East-West corridors. Each converter station has a rated power of 6 GVA and consists of several converters connected in parallel. The transmission capacity of the North-South corridors is 10 GW each, while each East-West corridor has a transmission capacity of 5 GW. The optimal power flow of the AC-DC grid model is analyzed for a theoretical transmission scenario with a high power transport from North to South.

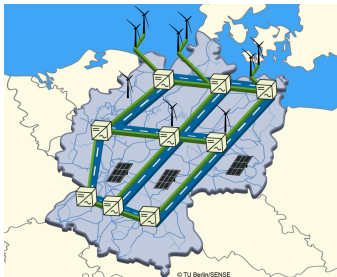


Fig. 1. AC-DC transmission grid model for research purposes.

This work was supported by the German Federal Ministry for Economic Affairs and Energy (BMWi) within the project OVANET (no. 03ET7510A).

III. KEY RESULTS

Demonstrating a principal operation of the HVDC overlay grid, an integrated AC-DC optimal power flow is calculated. For normal operation and outages of DC corridors and converter stations, the line loadings of the HVDC overlay grid model are studied. In addition, the active power injections of converter stations are analyzed. Exemplary results are given in Fig. 2. Furthermore, important aspects considering the installation of HVDC cables along a highway are described. The poster shows options for the acceptance-friendly installation of cables in a tunnel parallel to the highway. For example, the use of highway bridges to overcome obstacles along the route is considered. Fig. 3 illustrates the transition from the tunnel to the bridge.

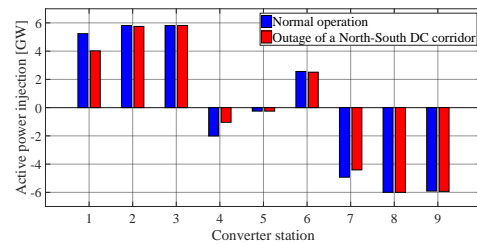


Fig. 2. Active power injections of converter stations for normal operation and outage of a highly loaded North-South DC corridor.



Fig. 3. Schematic illustration of the transition from the tunnel to the bridge.

IV. CONCLUSION

A principal operation of an HVDC overlay grid is demonstrated for a theoretical transmission scenario with a high power transport. An approach for the acceptance-friendly integration of the HVDC overlay grid by bundling infrastructures for energy and transport is addressed. The presented concepts are an important basis for future work in the field of integrated AC-DC power transmission.

REFERENCES

- [1] M. Barnes, D. Van Hertem, S. P. Teeuwssen, and M. Callavik, "HVDC systems in smart grids," *Proceedings of the IEEE*, vol. 105, no. 11, pp. 2082–2098, Nov. 2017.
- [2] K. Meng et al., "Hierarchical SCOPF considering wind energy integration through multi-terminal VSC-HVDC grids," *IEEE Transactions on Power Systems*, vol. 32, no. 6, pp. 4211–4221, Nov. 2017.
- [3] S. Schilling, M. Kuschke, and K. Strunz, "AC-DC optimal power flow implementation: Modeling and application to an HVDC overlay grid," in *IEEE PowerTech*, Manchester, Great Britain, Jun. 2017, pp. 1–6.

A Facility for Physical Simulation of High Impedance Faults in Low Voltage Networks

Anwarul Islam Sifat^{1*}, Joseph Bailey², Kent Hamilton², Fiona J Stevens McFadden², Ramesh Rayudu¹, Arvid Hunze²

¹School of Engineering & Computer Science, Victoria University of Wellington, Wellington, New Zealand

²Robinson Research Institute, Victoria University of Wellington, Gracefield, Lower Hutt, New Zealand

*Email: anwarul.sifat@vuw.ac.nz

Abstract—High impedance fault detection is an active research area, and is important to distribution power system operators. Research to date has focused on new sensor technologies and signal processing schemes to detect these faults. However, development of these schemes requires real fault incident data. Experimental HIF data at low voltage (0.4 kV) are currently unavailable, therefore we have designed a low voltage test facility design to physically simulate HIFs. The facility includes the geometrical representation of actual low voltage distribution lines, as an objective of the facility is for its use in the evaluation of (Giant Magneto-resistance) GMR sensors as a basis for a fault detection system. The initial HIF experimental data collected in this facility demonstrates the capability of the test facility to simulate such faults. The test facility will therefore be beneficial for generating actual data for studying HIF phenomena and for the development of a GMR sensor based detection scheme. This will be the subject of ongoing work.

Keywords—High Impedance Fault, Indoor Test Facility, Test Facility Design, Distribution Network, 400V, Fault Data

I. INTRODUCTION

High Impedance Fault (HIF) detection is a major area of interest within the field of power system fault analysis. Since first reported in 1960, HIF has attracted a lot of research interest, most recently in response to developments in data analytics and pattern recognition algorithms that have the potential for detection algorithms. However, application of such techniques relies on the availability of suitable datasets.

II. KEY EQUATION

For a sensor positioned on the pole, at point $P(x'_0, y'_0, z'_0)$, the magnetic field density due to current through a single overhead conductor is given by,

$$\vec{B}_x = \frac{\mu_0 I}{4\pi} \int_{-D/2}^{D/2} \left[\frac{z'_0 - \frac{1}{c}(\cosh(cy) - 1) + (y - y'_0)\sinh cy}{\left| (x'_0 - x)\hat{i} + (y'_0 - y)\hat{j} + \left(z'_0 - \frac{1}{c}(\cosh(cy) - 1)\right)\hat{k} \right|^3} \right] \hat{i} dy \quad (1)$$

$$\vec{B}_y = \frac{\mu_0 I}{4\pi} \int_{-D/2}^{D/2} \left[\frac{(x'_0 - x)\sinh cy}{\left| (x'_0 - x)\hat{i} + (y'_0 - y)\hat{j} + \left(z'_0 - \frac{1}{c}(\cosh(cy) - 1)\right)\hat{k} \right|^3} \right] \hat{j} dy \quad (2)$$

$$\vec{B}_z = \frac{\mu_0 I}{4\pi} \int_{-D/2}^{D/2} \left[\frac{-(x'_0 - x)}{\left| (x'_0 - x)\hat{i} + (y'_0 - y)\hat{j} + \left(z'_0 - \frac{1}{c}(\cosh(cy) - 1)\right)\hat{k} \right|^3} \right] \hat{k} dy \quad (3)$$

$$\vec{B} = \vec{B}_x + \vec{B}_y + \vec{B}_z \quad (4)$$

III. KEY FIGURES

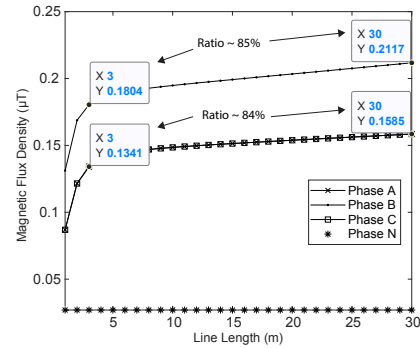


Fig. 1. Resulting Magnetic Flux Density for 30m Overhead Lines

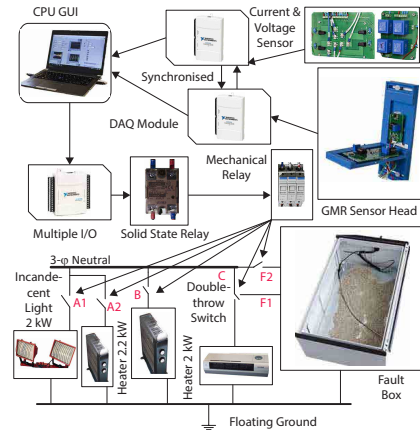


Fig. 2. Control and Data Acquisition System Architecture

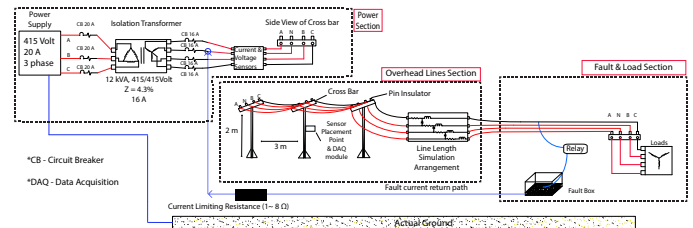


Fig. 3. Test Facility Schematic

Optimal Scheduling of Distributed Energy Resources via Convex Relaxation of ACOPF

Zahra Soltani, *Student Member, IEEE*, Ramin Vakili, *Student Member, IEEE*, and Mojdeh Khorsand, *Member, IEEE*

School of Electrical, Computer, and Energy Engineering, Arizona State University, Tempe, AZ 85287, USA
 Email: zsoltani@asu.edu, rvakili@asu.edu, and mojdeh.khorsand@asu.edu

Abstract— The energy democracy movement is resulting in more and more penetration of energy resources in electric distribution systems. Distributed energy resources (DERs) introduce security and reliability benefits as well as new operational challenges. Also, achieving resilient smart electric grids requires enhancement of operational protocols predominantly for distribution systems. To this end, this paper proposes a resource scheduling model for balanced and unbalanced distribution systems to ensure the economic and secure operation of electric grids. The proposed model accounts for model and limitations of DERs as well as distribution network structure via a convex AC optimal power flow model.

I. INTRODUCTION

The assumptions of DC power flow model are not suitable for the distribution network. AC optimal power flow (ACOPF) problem is NP-hard and highly nonconvex due to the nonlinear power flow equations. Existing approaches for solving the OPF problem are classified into using nonlinear algorithms which search for a local optimal solution of the OPF problem, approximation, and convexification of power flow equations. The former two approaches may not assure global optimality or feasibility of the original ACOPF problem. The latter one, however, provides the ability to check the feasibility and global optimality of ACOPF problem and could find the global optimal solution. For convex relaxations, second-order cone programming is proposed to solve the OPF problem for distribution system based on bus injection and branch flow model in [1] and [2], respectively. In [3], semidefinite programming (SDP) which relies on rank relaxation is discussed for convexifying the feasible set of ACOPF problem. The proposed models in [1]-[3] are designed for the balanced distribution network. However, the distribution networks are highly unbalanced due to unbalanced loads, DERs, and untransposed line segments. Moreover, due to mutual impedance of the line segments, there is a coupling between the phases. Neglecting such couplings can result in inaccuracy and may not reflect physical operation conditions.

This paper designs a resource scheduling tool for balanced and unbalanced distribution systems to enable optimal dispatch of DERs including different types of rooftop PVs, energy storage systems, and responsive loads. Among rooftop PVs, the main focus is on solar resources equipped with smart inverters. The proposed model focuses on identification of the optimal active and reactive power set points of DERs in order to enhance the economic efficiency of distribution system operation. To achieve this goal, an optimization tool based on convex ACOPF is proposed, which accounts for the precise models and related constraints of each of the DER technologies.

II. KEY EQUATIONS

The proposed ACOPF problem is formulated based on convex relaxation methods such as SDP, (1)-(8). Let N be the number of buses and L be the number of lines of radial multiphase

distribution system. The set of phases is denoted by ψ . Three types of rooftop PVs are considered in this paper, where types 1 ($h \in H_1$) and 3 ($h \in H_3$) are able to provide controllable reactive power while type 2 ($h \in H_2$) can only provide active power. Equation (1) represents the objective function including the total cost of energy from grid ($\rho_t^G \cdot P_t^{G,\varphi}$), demand response ($\rho_{l,t}^{RL,\varphi} \cdot P_{l,t}^{RL,\varphi}$), and rooftop PVs ($\rho_{h,t}^{PV1} P_{h,t}^{PV1,\varphi}$, $\rho_{h,t}^{PV2} P_{h,t}^{PV2,\varphi}$, $\rho_{h,t}^{PV3} P_{h,t}^{PV3,\varphi}$). Equations (2) and (4) satisfy active and reactive power balance, where $D_{p,n,t}^\varphi$ and $D_{q,n,t}^\varphi$ denoting the active and reactive power demand at time t and phase φ of bus n , and $\Lambda(n)$ is equal to 1 for $n = 1$, and zero otherwise. V_t is a vector collecting three phase voltages at all the buses. e_l^φ is the standard basis vector of $R^{3N \times 1}$. The reactive power of s^{th} Static Var Compensation (SVC) device at phase φ of bus n is given by $Q_{s,t}^\varphi$. Equation (5) satisfies Schur's component form of feeder thermal constraint where $\phi_{p,lm}^\varphi$ and $\phi_{q,lm}^\varphi$ are defined using (6). The voltage magnitude of each bus at each phase is limited by (8). The proposed method is tested on the IEEE 34-bus system.

$$\text{Min} \sum_{t \in T} (\sum_{\varphi \in \psi} (\rho_t^G \cdot P_t^{G,\varphi} + \sum_{l \in RL} \rho_{l,t}^{RL,\varphi} \cdot P_{l,t}^{RL,\varphi} + \sum_{h \in H_1} \rho_{h,t}^{PV1} P_{h,t}^{PV1,\varphi} + \sum_{h \in H_2} \rho_{h,t}^{PV2} P_{h,t}^{PV2,\varphi} + \sum_{h \in H_3} \rho_{h,t}^{PV3} P_{h,t}^{PV3,\varphi})) \quad (1)$$

Subject to:

$$\Lambda(n) \cdot P_t^{G,\varphi} + \sum_{l \in RL} \rho_{l,t}^{RL,\varphi} P_{l,t}^{RL,\varphi} + \sum_{h \in H_1} \rho_{h,t}^{PV1,\varphi} P_{h,t}^{PV1,\varphi} + \sum_{h \in H_2} \rho_{h,t}^{PV2,\varphi} P_{h,t}^{PV2,\varphi} + \sum_{h \in H_3} \rho_{h,t}^{PV3,\varphi} P_{h,t}^{PV3,\varphi} + \sum_{b \in B} P_{b,t} - D_{p,n,t}^\varphi = \text{Tr}(\frac{1}{2}(Y_n^\varphi + (Y_n^\varphi)^H) \cdot V_t \cdot V_t^H) \quad \forall n \in N, t \in T, \varphi \in \psi \quad (2)$$

$$Y_n^\varphi = e_n^\varphi \cdot (e_n^\varphi)^T \cdot Y \quad (3)$$

$$\Lambda(n) \cdot Q_t^{G,\varphi} + \sum_{l \in RL} \rho_{l,t}^{RL,\varphi} Q_{l,t}^{RL,\varphi} + \sum_{h \in H_1} \rho_{h,t}^{PV1,\varphi} Q_{h,t}^{PV1,\varphi} + \sum_{h \in H_2} \rho_{h,t}^{PV2,\varphi} Q_{h,t}^{PV2,\varphi} + \sum_{s \in S} Q_{s,t}^\varphi - D_{q,n,t}^\varphi = \text{Tr}(\frac{j}{2}(Y_n^\varphi - (Y_n^\varphi)^H) \cdot V_t \cdot V_t^H) \quad \forall n \in N, t \in T, \varphi \in \psi \quad (4)$$

$$\begin{bmatrix} -(S_{lm,max}^\varphi)^2 & \text{Tr}(\phi_{p,lm}^\varphi \cdot V_t \cdot V_t^H) & \text{Tr}(\phi_{q,lm}^\varphi \cdot V_t \cdot V_t^H) \\ \text{Tr}(\phi_{p,lm}^\varphi \cdot V_t \cdot V_t^H) & -1 & 0 \\ \text{Tr}(\phi_{q,lm}^\varphi \cdot V_t \cdot V_t^H) & 0 & -1 \end{bmatrix} \preceq 0 \quad \forall lm \in L, t \in T, \varphi \in \psi \quad (5)$$

$$\phi_{p,lm}^\varphi = \frac{1}{2}(Y_{lm}^\varphi + (Y_{lm}^\varphi)^H), \phi_{q,lm}^\varphi = \frac{j}{2}(Y_{lm}^\varphi - (Y_{lm}^\varphi)^H) \quad (6)$$

$$Y_{lm}^\varphi = \sum_{\rho \in \psi} Y_{(l,m),\rho}^\varphi \cdot e_l^\varphi \cdot (e_l^\varphi)^T - \sum_{\rho \in \psi} Y_{(l,m),\rho}^\varphi \cdot e_l^\varphi \cdot (e_m^\varphi)^T \quad (7)$$

$$(|v_{n,t}^\varphi|^{min})^2 \leq \text{tr}(e_n^\varphi \cdot (e_n^\varphi)^T \cdot V_t \cdot V_t^H) \leq (|v_{n,t}^\varphi|^{max})^2 \quad \forall n \in N, n \geq 2, t \in T, \varphi \in \psi \quad (8)$$

REFERENCES

- [1] R. A. Jabr, "Radial distribution load flow using conic programming," *IEEE Trans. Power Syst.*, vol. 21, no. 3, pp. 1458-1459, Aug. 2006.
- [2] M. Farivar and S. H. Low, "Branch Flow Model: Relaxations and Convexification—Part II," *IEEE Trans. Power Syst.*, vol. 28, no. 3, pp. 2565-2572, Aug. 2013.
- [3] S. H. Low, "Convex Relaxation of Optimal Power Flow—Part I: Formulations and Equivalence," *IEEE Trans. Control Netw. Syst.*, vol. 1, no. 1, pp. 15-27, March 2014.

Power Flow Analysis using Deep Learning Techniques in a Three Phase Unbalanced Distribution Network

Deepak Tiwari, *Student Member, IEEE*, Sarika K. Solanki, *Member, IEEE*,
and Jignesh Solanki, *Member, IEEE*
Electrical and Computer Engineering, West Virginia University

Abstract—Load flow analysis is the most important study performed by utility, required in all stages of power system. This paper discusses the application of deep learning to predict the output of load flow problem for a 3 phase unbalanced distribution system. For problems containing huge data, deep learning is best suited than traditional neural networks. We have formulated this problem as multi output regression model. The training and testing data is generated through OpenDSS MATLAB COM interface. The training data is given to neural network model to train the model. After generating the training dataset, neural network model predict the result for test input data. This is tested on IEEE 4 node test case and results for Radial Basis Function network (RBFnet) and Multi Layer Perceptron (MLP) models are discussed.

Index Terms—Load flow analysis, Deep learning, RBF, MLP, Tensorflow, OpenDSS.

I. INTRODUCTION

Load flow analysis is a performed to determine the steady state operating values in Voltages, currents, power losses. Utilities need to analyze these values very frequently. Due to security issues, utilities do not share exact model of distribution system. In this work, we present a trained neural network which predicts the branch currents, node voltages, angles, power losses with very low error. Such deep neural networks can replace the conventional test cases provided by utilities for research purposes.

Machine learning has numerous application in power system specially data analytics, load forecasting, prediction, fault detection. With advancement in deep learning, it is proven to be important in solving data driven problems in power system. [1] proposed a convolutional neural network classifier for real time fault localization in electric grid. They use the 4 kernels of 5 by 1 with stride 1 and vector data. However they do not identify the exact location of the fault point.

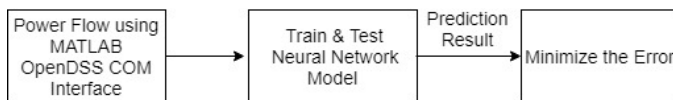


Fig.1 : Problem Architecture

In this work, we used Radial basis function model and Multi layer perceptron. RBF network consists of only three layers: the input, hidden, and output layers, popular network in artificial neural network. RBF uses the feedforward propagation.

The hidden layer received the input data using a non linear function. The output from RBF takes less time in computation as there is only one hidden layer and activation function in hidden layer calculates the euclidean distance between the centroid and the input value.

Multi layer perceptron (MLP) network uses the back propagation. MLP is modeled as a interconnected sets of input, hidden, and output layers. MLP model is developed in TensorFlow for our problem. TensorFlow is an open source software library developed by Google. Deep learning, with more number of hidden layers than ordinary neural network, learns the patterns in available data, used to predict the output.

II. RESULTS

Machine learning main step include: 1) Training 2) Prediction. As shown in figure (1), data is generated using OpenDSS - MATLAB COM interface for IEEE 4 node test case. The power flow is run for 3 years of load data. The source voltage, angles, line parameters are considered as input to the Neural network (NN) model. Nearly 70 % of entire data is used to train the NN model while rest to predict the output. The data is normalized before it is sent to train the model as all the bus voltages and currents differ in range . The output data received from the load flow analysis using COM interface is output of NN model for training.

Scenarios	RBFnet		MLP	
	MSE	MAE	MSE	MAE
Constant PQ Load	0.12 %	0.33 %	0.08 %	0.36 %
Constant Impedance Load	0.11 %	0.33 %	0.08 %	0.36 %
ZIP Load	0.12 %	0.32 %	0.19 %	0.95 %

TABLE I: Results

To calculate the prediction error, parameters like mean absolute error (MAE) and mean squared error (MSE) are used for both the NN models. The % error can be found in table 1. For different types of load scenarios, the MAE and MSE are computed to be very low.

REFERENCES

- [1] Wei Zheng, Desheng Hu, and Jing Wang, Fault Localization Analysis Based on Deep Neural Network, *Mathematical Problems in Engineering*, vol. 2016, Article ID 1820454, 11 pages, 2016.

Power System Stability Enhancement by Demand side Management with considering ZIP and induction motor loads

Jaber Valinejad^a, *Student Member, IEEE*, Mousa Marzband^b, *Senior Member, IEEE*, Junbo Zhao^a, *Member, IEEE*
^a Virginia Tech, US, ^b Northumbria Newcastle University ,UK

Abstract—Load modeling is assumed as one of significant part of power system studies so that inadequate load models can lead to substantially inaccurate simulation outputs leading to an unpleasant event like the Swedish blackout of 1983. In addition to importance of load modelling, demand side management (DSM) can bring numerous benefits such as reduction in the peak load demand, reshaping demand curve, and contributing to the overall system stability. A comprehensive model of the power system including suppliers, utility companies, and consumers with different electrical appliances is presented in this paper. In contrast with the previously proposed power grid models, power consumption and the social pattern of energy usage are considered in this study. The electrical appliances are classified as either responsive/controllable or nonresponsive/uncontrollable devices, according to their distinct constraints with respect to power consumption. All appliances operation patterns are modelled based on their functions in real systems so that DR is implemented to a variety loads encompassing induction type motors as well as polynomial loads to enhance voltage stability. In addition, Voltage stability can be controlled by reactive demand side management so that power electronic devices can inject reactive power to the network. Therefore, in this paper, the new reactive demand side management is proposed.

Index Terms—Demand Response, Stability, Induction Motor, Polynomial Model, Reactive demand side management

I. KEY EQUATIONS

A. polynomial and induction motors loads modeling

$$P_{tr}^{ZIP} = P_{tr}^{ZIP} \left[P_1 \cdot \left(\frac{V_{tr}}{v_r^b} \right)^2 + P_2 \cdot \left(\frac{V_{tr}}{v_r^b} \right) + P_3 \right] \quad (1)$$

$$Q_{tr}^{ZIP} = Q_{tr}^{ZIP} \left[Q_1 \cdot \left(\frac{V_{tr}}{v_r^b} \right)^2 + Q_2 \cdot \left(\frac{V_{tr}}{v_r^b} \right) + Q_3 \right] \quad (2)$$

$$P_{tr}^{IM} = P_{tr}^{IM} \left(R_{1r}^s + \frac{R_{1r}^r}{S_r} \right) \cdot \frac{V_{tr}^2}{(R_{1r}^s + \frac{R_{1r}^r}{S_r})^2 + (X_{1r}^{ys} + X_{1r}^{yr})^2} \quad (3)$$

$$Q_{tr}^{IM} = Q_{tr}^{IM} \cdot (X_{1r}^{ys} + X_{1r}^{yr}) \cdot \frac{V_{tr}^2}{(R_{1r}^s + \frac{R_{1r}^r}{S_r})^2 + (X_{1r}^{ys} + X_{1r}^{yr})^2} \quad (4)$$

B. Real and Reactive DSM

$$P_{tr}^{ZIP/IM,e/p} = \tilde{P}_{tr}^{ZIP/IM,e/p} + \sum_{t'=1} \Delta P_{tr}^{ZIP/IM,e/p} \quad \forall t, r \quad (5)$$

$$Q_{tr}^{ZIP/IM,e/p} = \tilde{Q}_{tr}^{ZIP/IM,e/p} \cdot \frac{\tilde{P}_{tr}^{ZIP/IM,e/p} + \Delta P_{tr}^{ZIP/IM,e/p}}{\tilde{P}_{tr}^{ZIP/IM,e/p}} \quad (6)$$

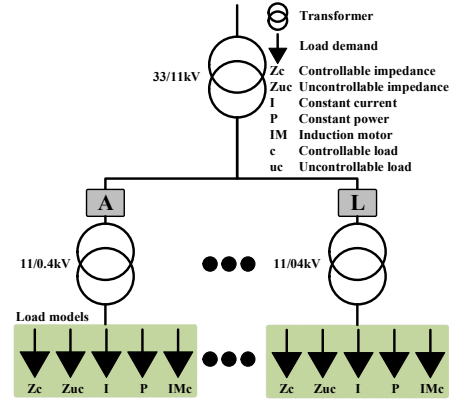


Fig. 1. summary of the network under study

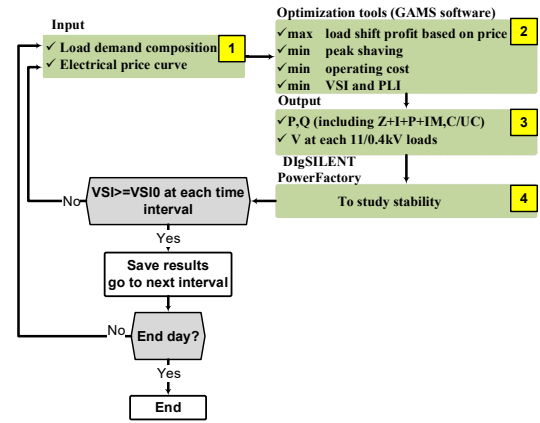


Fig. 2. the stages of executing SMONO framework in the GAMS and DigSILENT environment

II. KEY RESULTS

This IEEE 300 buses including voltage levels of 11, 33, 132, 275, and 400KV is used to implement proposed model.

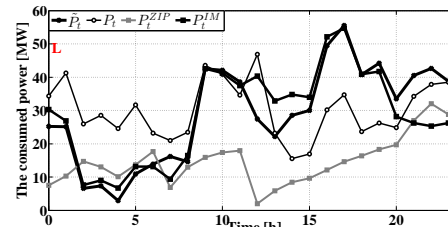


Fig. 3. predicted load demand, total load demand after load shifting, and the value of load demand of ZIP and IM models in different substations

VSC-HVDC Transmission Line Protection Based on Dynamic State Estimation

Binglin Wang¹, Student Member, IEEE, Yu Liu^{1,2,*}, Member, IEEE

1. School of Information Science and Technology, ShanghaiTech University, Shanghai, China, 201210

2. Key Laboratory of Control of Power Transmission and Conversion (SJTU), Ministry of Education, Shanghai, 200240

*Email: liuyu@shanghaitech.edu.cn

Abstract: Voltage Source Converter based High Voltage Direct Current (VSC-HVDC) transmission line protection is of significance for the safe and stable operation of VSC-HVDC systems. In this paper, a dynamic state estimation (DSE) based VSC-HVDC line protection method is proposed. The method is an extension of the current differential protection, considers the distributed shunt capacitance through the line and can be used as the line primary protection. Specifically, the dynamic model that describes all physical laws that the VSC-HVDC line under protection should obey is first established. Afterwards, the consistency between available measurements and the dynamic model is determined by DSE and the line is tripped if the consistency is continuously low for a user-defined period of time. Numerical experiments demonstrate its dependable and fast operation during internal faults, secure refusal of operation during external faults, sensitivity for high impedance faults, robustness towards measurement noises.

Key words: VSC-HVDC transmission line protection, dynamic state estimation, high impedance faults, measurement noise

I. INTRODUCTION

This paper proposes a primary VSC-HVDC line protection method based on Dynamic State Estimation (DSE). The method is an extension of the current differential protection and it considers distributed shunt capacitance through the line. The protection logic is formulated by testing the consistency between the available measurements and the accurate dynamic model of the VSC-HVDC transmission line under protection using the dynamic state estimation procedure.

II. KEY EQUATIONS

The algebraic and differential form of the dynamic model is,

$$\begin{cases} \dot{\mathbf{i}}(t) = \mathbf{A}_1 \cdot \mathbf{x}(t) + \mathbf{B}_1 \cdot d\mathbf{x}(t)/dt \\ \mathbf{0}_{2n-1} = \mathbf{A}_2 \cdot \mathbf{x}(t) + \mathbf{B}_2 \cdot d\mathbf{x}(t)/dt \\ \mathbf{u}(t) = \mathbf{A}_3 \cdot \mathbf{x}(t) + \mathbf{B}_3 \cdot d\mathbf{x}(t)/dt \end{cases} \quad (1)$$

Algebraic form of the dynamic model is,

$$\mathbf{z}(t, t_m) = \mathbf{Y}_{eqx} \cdot \mathbf{x}(t, t_m) - \mathbf{B}_{eq} \quad (2)$$

Weighted least square approach Dynamic state estimation,

$$\mathbf{r}(t, t_m) = \mathbf{Y}_{eqx} \cdot \mathbf{x}(t, t_m) - \mathbf{B}_{eq} - \mathbf{z}(t, t_m) \quad (3)$$

$$\min_{\mathbf{x}(t, t_m)} J(\mathbf{x}) = \mathbf{r}(t, t_m)^T \mathbf{W} \mathbf{r}(t, t_m) \quad (4)$$

$$\hat{\mathbf{x}}(t, t_m) = (\mathbf{Y}_{eqx}^T \mathbf{W} \mathbf{Y}_{eqx})^{-1} \mathbf{Y}_{eqx}^T \mathbf{W} (\mathbf{z}(t, t_m) + \mathbf{B}_{eq}) \quad (5)$$

Quantification of the consistency,

$$\text{test}(t) = \begin{cases} 1, & \hat{J}(t) \geq J_{set} \\ 0, & \hat{J}(t) < J_{set} \end{cases} \quad (6)$$

Criterion of the protection,

$$\text{trip}(t) = \begin{cases} 1, & \int_{t-T_{set}}^t \text{test}(\tau) d\tau = T_{set} \\ 0, & \int_{t-T_{set}}^t \text{test}(\tau) d\tau < T_{set} \end{cases} \quad (7)$$

IV. SIMULATION RESULTS

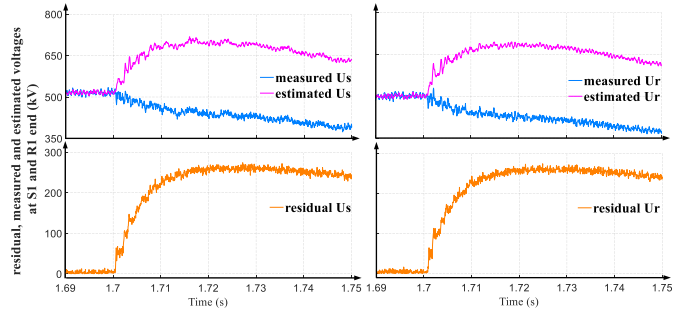


Figure 1. Voltage results: Internal fault event 2

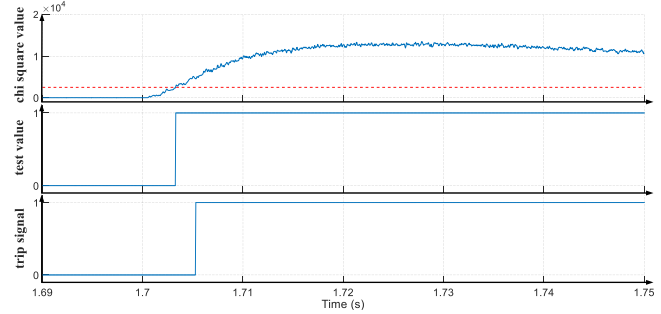


Figure 2. Protection results: Internal fault event 2

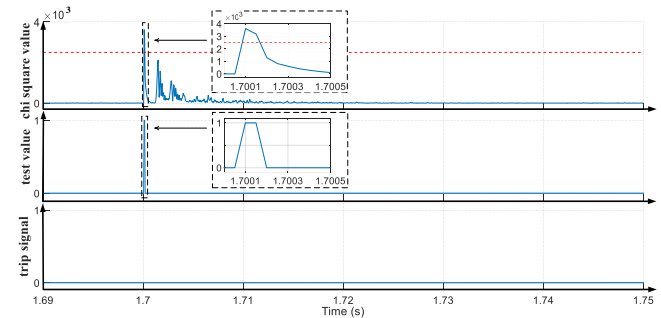


Figure 3. Protection results: External fault event 3

IV. CONCLUSION

Numerical experiments demonstrate that the proposed method can (a) dependably detect and trip internal faults, including high impedance faults; (b) securely ignore system transients such as severe external faults; (c) reliably operate with measurement noises. Therefore, the proposed method can be used as the primary protection of the VSC-HVDC transmission line.

Forming A Markovian Influence Graph from Utility Line Outage Data to Mitigate Cascading

Kai Zhou Ian Dobson Zhaoyu Wang
 Electrical & Computer Engineering
 Iowa State University
 {kzhou,dobson,wzy}@iastate.edu

Alexander Roitershtein
 Statistics
 Texas A&M University
 alexander@stat.tamu.edu

Arka P. Ghosh
 Statistics
 Iowa State University
 apghosh@iastate.edu

Abstract—We use observed transmission line outage data to make a Markovian influence graph that describes the probabilities of transitions between generations of cascading line outages, where each generation of a cascade consists of a single line outage or multiple line outages. The new influence graph defines a Markov chain and generalizes previous influence graphs by including multiple line outages as Markov chain states. The generalized influence graph can reproduce the distribution of cascade size in the utility data. In particular, it can estimate the probabilities of small, medium and large cascades. The influence graph has the key advantage of allowing the effect of mitigations to be analyzed and readily tested, which is not available from the observed data. We exploit the asymptotic properties of the Markov chain to find the lines most involved in large cascades and show how upgrades to these critical lines can reduce the probability of large cascades.

Index Terms—cascading failures, power system reliability, mitigation, Markov, influence graph

I. INTRODUCTION

Cascading outages in power transmission systems can cause widespread blackouts. These large blackouts are infrequent, but are high-impact events that occur often enough to pose a substantial risk to society. The power industry has always analyzed specific blackouts and taken steps to mitigate cascading. However, and especially for the largest blackouts of highest risk, the challenges of evaluating and mitigating cascading risk in a quantitative way remain.

There are two main approaches to evaluating cascading risk: simulation and analyzing historical utility data. Cascading simulations can predict some likely and plausible cascading sequences. However, only a subset of cascading mechanisms can be approximated, and simulations are only starting to be benchmarked and validated for estimating blackout risk. Historical outage data can be used to estimate blackout risk and detailed outage data can be used to identify critical lines. However it is clear that proposed mitigation cannot be tested and evaluated with historical data.

II. PROBLEM STATEMENT

This paper forms a rigorous Markovian influence graph using historical outage data to identify critical lines and test mitigation of large cascades.

We gratefully thank BPA for making the outage data public. The analysis and any conclusions are strictly the author's and not BPA's. We gratefully acknowledge support in part from NSF grants 1609080 and 1735354.

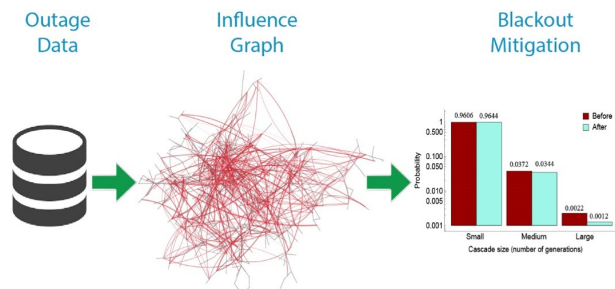


Fig. 1. Overall procedure.

III. THE DISTRIBUTION OF CASCADE SIZES AND ITS CONFIDENCE INTERVAL

The variance of cascade sizes produced by the Markovian influence graph is estimated using the bootstrap method. As

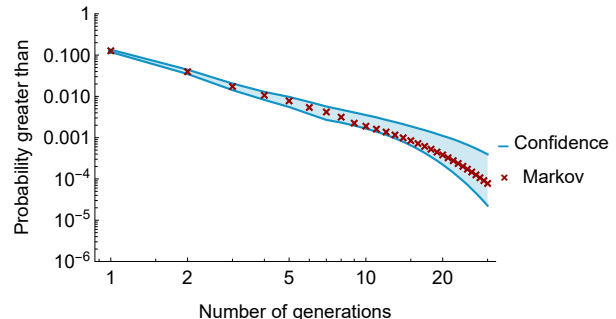


Fig. 2. Survival function of cascade sizes. Red crosses are from Markov chain, and blue lines indicate the 95% confidence interval estimated by bootstrap.

shown in Table I, the probability of large cascades is estimated within a factor of 1.5, which is adequate for the purposes of estimating large cascade risk, since the cost of large cascades is so poorly known: estimates of the direct costs of cascading blackouts vary by more than a factor of 2.

TABLE I
 95% CONFIDENCE INTERVALS USING BOOTSTRAP

cascade size	probability	κ
small (1 or 2 generations)	0.9606	1.005
medium (3 to 9 generations)	0.0372	1.132
large (10 or more generations)	0.0022	1.440

Feasibility Study of Financial P2P Energy Trading in a Grid-tied Power Network

M Imran Azim, S. A. Pourmousavi, Wayes Tushar, and Tapan K. Saha

School of Information Technology and Electrical Engineering,

The University of Queensland, Brisbane, QLD 4072, Australia

E-mail: m.azim@uq.net.au, a.pour@uq.edu.au, w.tushar@uq.edu.au, saha@itee.uq.edu.au

Abstract—This paper studies the applicability of peer-to-peer (P2P) energy trading in a grid-tied network. The main objectives are to understand the impact of the financial P2P energy trading on the network operation, and thus demonstrate the importance of taking various issues related to power network into account while designing a practical P2P trading scheme. To do so, a simple mechanism is developed for energy trading among prosumers without considering any network constraints, as done by many existing studies. Once the trading parameters, such as the energy traded by each prosumer in the P2P market and the price per unit of energy are determined, the developed scheme is tested on a low-voltage (LV) network model to check its feasibility of deployment in a real P2P network. It is shown that although the considered trading scheme is economically beneficial to the participating prosumers compared to the existing incentive mechanisms (such as feed-in-tariff (FiT)), it could be unfit for real deployment due to violating bus voltage limits during multiple P2P trading executed simultaneously. Further, the grid operator may experience financial losses for compensating the losses during P2P transactions.

I. ECONOMIC BENEFITS OF FINANCIAL P2P TRADING

Fig. 1 shows the P2P trading prices for the participants compared to the retail prices and FiT rate. In this study, Buyer 2 and Buyer 1 can save \$3.13 and \$1.5, respectively, in the course of a day. In contrast, Seller 2 earns \$1.24 more at the end of the day, followed by Seller 3 (\$0.3) and Seller 1 (¢8.8).

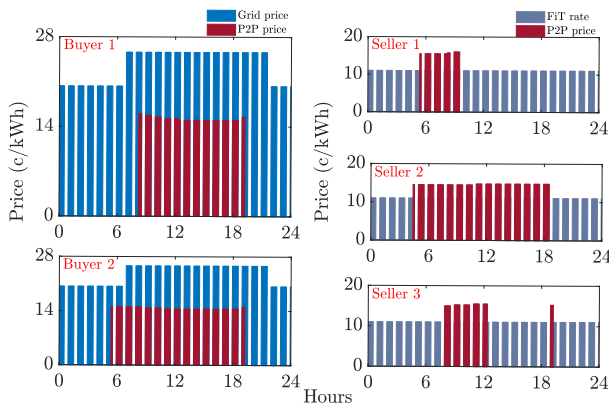


Fig. 1. Financial benefits of P2P trading for all participants.

II. ISSUES WITH PHYSICAL P2P TRADING

A. High Voltage Issue

Fig. 2 reveals that simultaneous P2P transactions can rise the bus voltages beyond the prescribed limit. For instance,

voltage at bus 5 crosses the upper voltage limit while buses 2, 4 and 6 are very close to exceed it as well. Therefore, multiple P2P trading inside a single feeder can cause over-voltage in the network.

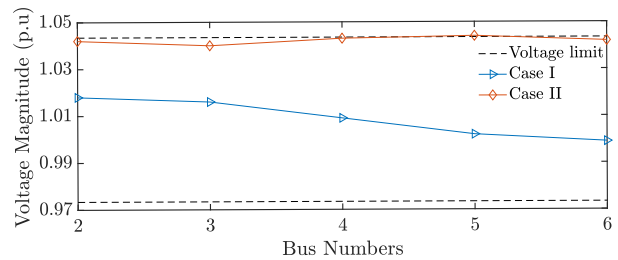


Fig. 2. Bus voltages during multiple P2P trading.

B. Losses Compensation Issue

The trading scenario for a particular time interval, given in Table I, where eight simultaneous P2P transactions are finalised. As is demonstrated in Table I, the total P2P losses is 1.21 kW (4.1% of the total exchanged power) for all transactions. If similar P2P transactions are carried out throughout the year, the grid has to supply 42.4 MW excess power in that year to compensate P2P losses which can cause approximately \$2200-\$2700 financial losses.

TABLE I
DETERMINATION OF P2P TRANSACTION LOSSES

Exchanged Power (kW)	Grid's Losses Compensation (kW)
2.8	1.21
1.4	
3.5	
3.7	
5.0	
4.0	
4.7	
4.9	

For a real LV P2P network with thousands of buses sprawled over a large territory, the transaction losses could be more pronounced. It can be intensified by the fact that anyone from anywhere in the network can join a P2P network to trade energy. Therefore, the amount of losses that has to be compensated by the grid in a real system with significant P2P transactions cannot be ignored. Otherwise, the grid operator may experience substantial financial losses annually.

In summary, a financially attractive P2P trading may not be executed in practice unless power network constraints are considered properly.

A Bi-Level Optimization Formulation of Multilevel Demand Subscription Pricing

Yuting Mou

Center for Operations Research
and Econometrics

Université catholique de Louvain

Email: yuting.mou@uclouvain.be

Anthony Papavasiliou

Center for Operations Research
and Econometrics

Université catholique de Louvain

Email: anthony.papavasiliou@uclouvain.be

Philippe Chevalier

Center for Operations Research
and Econometrics

Université catholique de Louvain

Email: philippe.chevalier@uclouvain.be

Abstract—The modern power system is evolving towards the direction where the penetration of renewable energy is increasingly higher. The intermittency of renewable energy poses more challenges to the power systems. On the one hand, fast-response generators are required for balancing, which results in increased operating costs and emissions. This ultimately undermines the economic and environmental benefits of renewable energy integration. On the other hand, less energy will be produced by conventional generators, whereas the need for capacity remains to supply peak net load. The traditional energy based tariff may fail to reflect consumers true valuation for the capacity increment. These adverse effects can be mitigated by the design novel price plans. In this study, we revisit a multilevel demand subscription pricing policy (MDSP) for electric power, in which a menu to assign different reliability combined with duration for a slice of power is offered. The reliability component in the price menu reflect variation of renewable energy and the needs for capacity increment. Lower reliability corresponds to lower capacity charge, which mobilizes the flexibility of consumers so that the frequent operation of fast-response generators is reduced. The duration component is regarded as the credits consumers purchase for this slice of power. This simple paradigm respects the requirement of consumers for simplicity, privacy and control. We relax many assumptions in the original MDSP theory and develop a bilevel model to integrate the menu design into the day-ahead market. The approach is illustrated on a toy numerical example as well as a large-scale model of the Belgian power market.

I. INTRODUCTION

The increasing integration of renewable energy sources poses challenges to the operation of power systems. It is well-known that there exists substantial flexibility potential on the demand side [1], and with the advances of ICT, it is feasible to implement large-scale demand response for overcoming these challenges. By offering differentiated products, the heterogeneity among the population of consumers can be exploited, thereby mobilizing their flexibility and achieving greater allocative efficiency. Following this stream, many differentiated products are proposed, such as deadline differentiated pricing [2], duration based of service duration-deadline jointly differentiated energy service, etc. Another paradigm based on priority service is proposed in [3], where electricity supply is perceived as a service that can be offered with various degrees of reliability. In this paper, we implement a richer rate structure called multilevel demand subscription

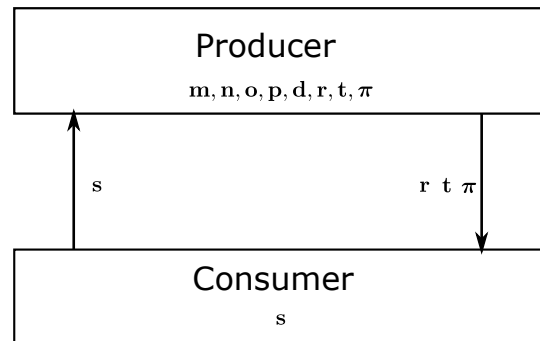


Fig. 1. Interaction between the producer and consumers in the bi-level model.

pricing, that differentiates electric power according to both service reliability and load pattern, using the theory proposed in [6].

II. METHODOLOGY

In this study, we design a MDSP menu as the equilibrium solution to a Stackelberg game where an aggregator moves first with a menu offering, and residential consumers react by selecting menu options and revealing their valuation. The Stackelberg game is modelled as a bi-level optimization problem involving the aggregator and consumers, and then reformulated as a mixed-integer problem. Numerical simulations are also carried out.

REFERENCES

- [1] H. C. Gils, "Assessment of the theoretical demand response potential in europe," *Energy*, vol. 67, pp. 1–18, 2014.
- [2] E. Bitar and S. Low, "Deadline differentiated pricing of deferrable electric power service," in *Decision and Control (CDC), 2012 IEEE 51st Annual Conference on*. IEEE, 2012, pp. 4991–4997.
- [3] S. S. Oren, "A historical perspective and business model for load response aggregation based on priority service," in *System Sciences (HICSS), 2013 46th Hawaii International Conference on*. IEEE, 2013, pp. 2206–2214.
- [4] H.-p. Chao and R. Wilson, "Priority service: Pricing, investment, and market organization," *The American Economic Review*, pp. 899–916, 1987.
- [5] Y. Mou, A. Papavasiliou, and P. Chevalier, "Application of priority service pricing for mobilizing residential demand response in Belgium," in *European Energy Market (EEM), 2017 14th International Conference on the*. IEEE, 2017, pp. 1–5.
- [6] H.-p. Chao, S. S. Oren, S. A. Smith, and R. B. Wilson, "Multilevel demand subscription pricing for electric power," *Energy Economics*, vol. 8, no. 4, pp. 199–217, 1986.

An Incentive Mechanism for Motivating Residents to Participate in Peak Shaving

Jing Tu, Fangxing Li

University of Tennessee, Knoxville
 Dept. of Electrical Engineering and Computer Science
 Knoxville, TN, United States

Abstract—This project proposes an incentive mechanism for motivating residents to participate in peak shaving, especially for the risk averse residents who have smart applications. First, the load models of various appliances considering the user's comfort are established. Second, we put forward a peak shaving incentive mechanism that reflects the contribution of residential power consumption to the peak shaving. The simulation results show that the proposed incentive mechanism can reduce the electricity cost as well as the peak load of residents, and shift the load to the valley load period.

Index Terms-- Demand response, incentive mechanism, smart power consumption, home energy management.

I. MODEL OF HOUSEHOLD APPLICATIONS

There are three kinds of smart applications that are commonly used by residents, as follows:

- 1) Delayable load: the load that can delay its start time, but can't be interrupted once started, such as washing machines, dishwashers, etc.
- 2) Interruptible load: the load that can be interrupted when working, but consume the fixed energy. For example, the electric vehicles.
- 3) Thermostatically controlled load: the load that is used to control temperature based on the one-order thermal transfer model, such as the air conditioners and electric water heaters.

The comfort of delayable load and interruptible load can be measured by the delay time, if we regard the interrupt as a special delay. The comfort of thermostatically controlled load can be measured by deviation of actual temperature and optimum temperature.

Residents try to minimize the weighted sum of a comfort and electricity cost, and then request the task of the applications finished as soon as possible.

II. INCENTIVE MECHANISM

The risk averse residents usually choose time-of-use (TOU) or fixed price instead of real-time price, which lead their smart applications to easily concentrate at the evening or the start time of valley price. So an incentive mechanism that can guide residents to cut peaks and fill valleys is needed.

Firstly the following model is proposed to evaluate the peaking shaving effects of residents:

$$H_{sf} = \frac{\sum_{t=1}^T (P_{user}(t) - \overline{P_{user}})(P_{sys}(t) - \overline{P_{sys}})}{\sqrt{\sum_{t=1}^T (P_{sys}(t) - \overline{P_{sys}})^2}} \quad (1)$$

In (1), $P_{user}(t)$, $P_{sys}(t)$ are the power of a resident and the power system, and $\overline{P_{user}}$, $\overline{P_{sys}}$ are corresponding average of a day. The (1) essentially measures the consistency between resident load curve and normalized system load curve. Besides, it will not change if the resident load curve moves up and down, and will vary in proportion to the resident load, which means fair. The incentive can be calculated as follows:

$$C_{mot} = k \frac{H_{sf}}{H_{sf,base}} \quad (2)$$

And if $C_{mot} < 0$, let $C_{mot} = 0$, so there is no risk for residents.

III. SIMULATION STUDY

In order to verify the proposed incentive mechanism, firstly a typical resident is simulated in this study. The total load of the typical resident is shown in Fig. 1.

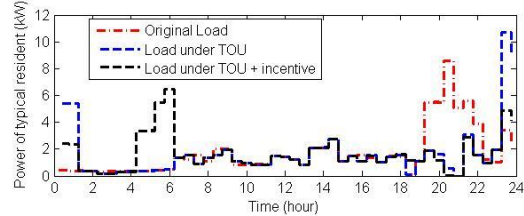


Fig. 1. Load curve of the typical resident under three conditions

And in order to examine its impact on a large number of residents, a community with 1,000 residents who have smart applications is simulated. The total load of the community is shown in Fig. 2.

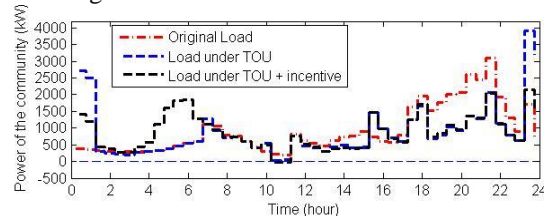


Fig. 2. Load curve of the community under three conditions

As a result, the proposed incentive mechanism effectively reduces the electricity cost & peak load of residents, and shift the load to the valley load period.

Stochastic Optimal Sizing of Micro-Grids Using the Moth-Flame Optimization Algorithm

Soheil Mohseni, Alan C. Brent, Daniel Burmester, Abhi Chatterjee

Sustainable Energy Systems, School of Engineering and Computer Science, Victoria University of Wellington, New Zealand
 Email: {soheil.mohseni, abhi.chatterjee}@ecs.vuw.ac.nz, {alan.brent, daniel.burmester}@vuw.ac.nz

Abstract—Optimal sizing of renewable energy systems should consider the uncertainties associated with various input data to ensure the financial sustainability of developing such systems. This paper proposes a stochastic modelling framework for the optimal sizing of micro-grids (MGs) subject to satisfying a reliability index for supplying the loads. The proposed framework incorporates a model reduction technique, a state-of-the-art meta-heuristic (MH) optimization algorithm, namely the moth-flame optimization algorithm (MFOA), as well as an uncertainty analysis technique using Monte Carlo Simulation (MCS), based on a new scenario reduction process. A MG test system is used to assess the effectiveness of the proposed stochastic framework.

Index Terms—Microgrids, Planning, Reliability, Uncertainty.

I. CHALLENGES IN OPTIMAL SIZING OF MICRO-GRIDS

The optimal sizing problem of the components of MGs is a non-deterministic, polynomial-time hard problem with several sources of nonlinearities and non-convexities involved in its formulation, making it not amenable to exact mathematical optimization algorithms. Therefore, several MHs have been proposed in the literature to solve this problem, yet these, with newly emerged MHs, need to be continuously compared. The other issue that exacerbates the problem in finding optimum solutions for MG components' sizes, is the uncertainty associated with input data. Among the uncertain input data, the climatic and load demand data have the most significant influence on the results for off-grid MG applications, and modelling their uncertainty in the planning phase is a big step toward an accurate representation of real-world scenarios by numeric simulations.

II. KEY TEST SYSTEM AND FRAMEWORK

The MG is equipped with photovoltaic (PV) panels, wind turbines (WTs), a battery bank, an inverter, and an electric vehicle (EV) charging station, whose optimum sizes are under investigation, considering the load and generation uncertainties.

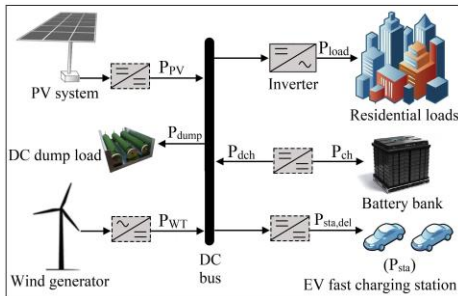


Fig. 1. Schematic diagram of the proposed micro-grid test system.

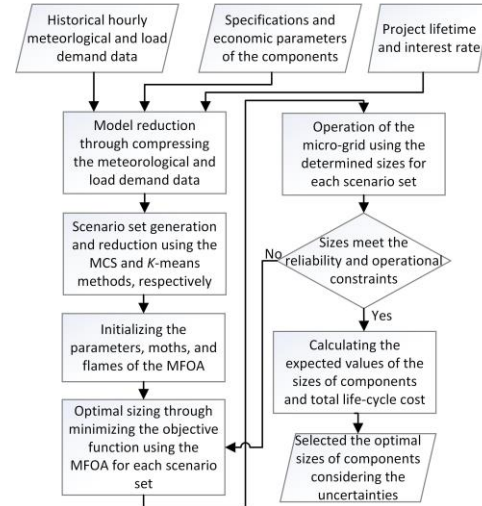


Fig. 2. Flowchart of the proposed stochastic modelling framework.

III. KEY RESULTS AND DISCUSSION

TABLE I. Comparative results of the selected MH algorithms

Algorithm	WTs	PV panels	Battery packs	Inv. [kW]	EV Sta.	TNPC [\$]
MFOA	45	686	59	338	3	4,509,119
GA-PSO	45	689	63	342	4	4,522,083
GA	46	686	81	349	4	4,638,701
PSO	46	689	68	340	4	4,601,573

TABLE II. Comparison of deterministic vs. stochastic results

Case	WTs	PV panels	Battery packs	Inv. [kW]	EV Sta.	TNPC [\$]
Stochastic	51	699	70	351	3	4,821,491
Deterministic	45	686	59	338	3	4,509,119

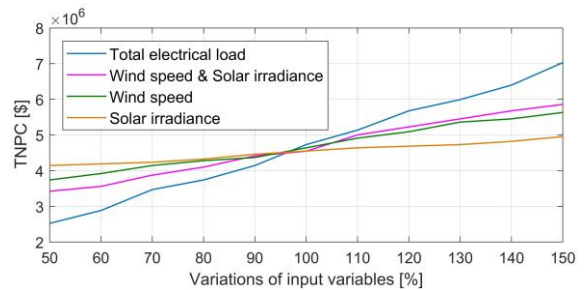


Fig. 3. Sensitivity analyses of the uncertain variables vs. the life-cycle cost.

These findings collectively implicate that: (i) the MFOA outperforms the most prominent MHs in this area, (ii) considering the input uncertainties results in a more rational long-term economic analysis of MGs, and (iii) the influence of an uncertain load demand on the total net present cost (TNPC) is considerably higher than the uncertain climatic data.

A Residential Community Energy Optimization Scheme with Financial Rewards

Avijit Das and Zhen Ni

Electrical Engineering and Computer Science Department

South Dakota State University

Brookings, South Dakota 57006

Email: {avijit.das, zhen.ni}@sdstate.edu

Abstract—Residential load demands have the potential to participate in peak-hour load management to improve power quality and reliability of smart grid. In recent years, incentive-based optimization techniques are proposed as a viable solution where the participants are financially rewarded based on their quantified participation and comfort level. While curtailing the load, existing approaches only consider thermal-related electric appliances to measure the comfort level of the consumer and neglected other major residential appliances which may misguide the controller in terms of consumer comfort level. Thus, the consumers comfort level can get affected which may limit their participation in the program. In this work, we propose a new comfort indicator design to measure the comfort level of the consumer including both thermal and major controllable residential electric appliances. The proposed comfort indicator design is integrated with residential community energy optimization scheme to schedule residential loads efficiently and reward consumers based on their preferences and comfort levels. We investigate both genetic algorithm and mixed integer programming techniques to solve the optimization problem with the goal to minimize the total reward costs of the utility and to maximize the consumers’ comfort level. We have applied our proposed scheme in 10-house residential community test case. The results show that the proposed approach performs efficiently in terms of total financial incentives and average comfort levels, and outperforms other two existing techniques.

I. MODEL DESCRIPTION

Residential community energy management system (CEMS) model and information flow are illustrated in Figure 1.

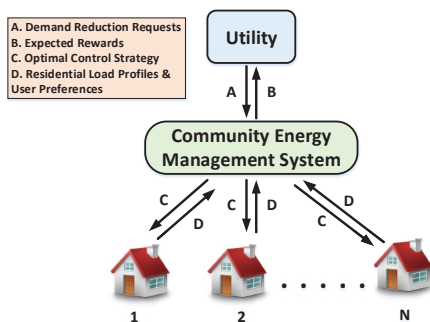


Fig. 1: The community energy management system model and information flow [1].

In the model, the CEMS receives demand reduction request (DRR) from the utility, takes the optimal decision, and executes the decision by controlling residential appliances.

According to the design, the CEMS collects DRR signal from the utility (signal - A), and residential load profiles and user preferences (signal - D). Then, the CEMS generates the optimal scheduling policy (signal - C) for the residential appliances based on user preferences and sends the expected rewards to the utility (signal - B). The rewards are provided based on the measurement of the user comfort level. Any comfort violation causes higher financial rewards to the consumer.

II. SIMULATION RESULTS

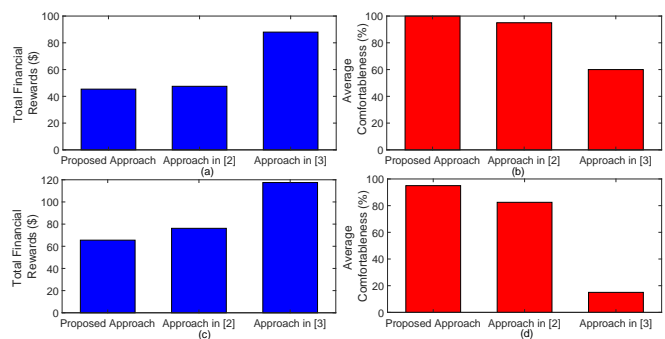


Fig. 2: Results are presented in terms of total financial rewards and average comfortableness. The reference approaches are taken from [2] and [3]. The figures (a) and (b) represent the result comparison in terms of total financial rewards and average comfortableness for approximately 40% demand reduction of the total load. The figures (c) and (d) illustrate the result comparison in terms of total financial rewards and average comfortableness for approximately 55% demand reduction of the total load.

III. CONCLUSION

In this work, a CEMS model is proposed with a new comfort indicator design where both thermal and task based residential appliances are considered. The results show that the proposed scheme schedules the residential loads efficiently and rewards consumers based on their quantified participation.

REFERENCES

- [1] Z. Ni and A. Das, “A new incentive-based optimization scheme for residential community with financial trade-offs,” *IEEE Access*, vol. 6, pp. 57802–57813, 2018.
- [2] Q. Hu, F. Li, X. Fang, and L. Bai, “A framework of residential demand aggregation with financial incentives,” *IEEE Transactions on Smart Grid*, vol. 9, no. 1, pp. 497–505, 2018.
- [3] T. Anandalaskhmi, S. Sathiakumar, and N. Parameswaran, “Peak reduction algorithms for a smart community,” in *2013 International Conference on Energy Efficient Technologies for Sustainability*, pp. 1113–1119, IEEE, 2013.

Validation of Transient Conductor Temperature Model for Ampacity Forecasts

Leanne Dawson, Soheila Karimi, Andy Knight
 Department of Electrical Engineering
 University of Calgary
 Calgary, Canada

Abstract—Dynamic thermal line rating (DTLR) is being investigated as a way to increase the capacity of an existing electrical grid. Presently, most utilities use a static rating, based on reasonable, outer-range environmental conditions. DTLR uses real-time environmental conditions to calculate the actual loadability limit of a transmission line. This research investigates the impact on the thermal capacity of a line if different confidence values for predicted ampacity are used, considering the uncertainty of weather variables. This research will perform transient analysis, using the thermodynamic equations associated with the thermal rating of a transmission line, to quantify the risk associated with selecting different confidence levels within a fuzzy forecast. This research validates this method using conductor temperature measurements.

Index Terms—Dynamic Thermal Rating, Fuzzy Prediction, Conductor Temperature

I. INTRODUCTION

As utilities shift towards implementing more renewable generation to replace traditional thermal generation, more transmission infrastructure is required. Dynamic thermal line rating (DTLR) is being investigated as one potential method to increase the capacity of an existing transmission system. Typically, the thermal rating of an overhead transmission line is determined using static nominal environmental conditions. DTLR uses real-time environmental conditions to update the rating. Both ratings are calculated using a set of thermodynamic equations described in IEEE Standard 738 [1], assuming a maximum allowable conductor temperature. Transmission systems are typically planned in advance, so a predicted DTLR is useful for system operators. Since the thermal capacity is very sensitive to changes in wind speed and direction, the rating can change significantly during a single interval. As the line rating will not change during the interval, with worse environmental conditions, the conductor temperature could increase past the maximum allowable temperature.

II. RESULTS

This analysis uses the fuzzy methods described in [3] to calculate predicted hourly ampacity, based on varying levels of confidence. The ampacity is then used to calculate the conductor temperature, using real-time weather data, shown in Fig. 1. The method used in this analysis is validated using conductor temperature measurements, shown in Fig. 2.

The authors would like to thank AltaLink LP and ATCO Electric for providing the data used in this analysis. This project is financially supported by NSERC, AESO, ATCO Electric and Altalink LP.

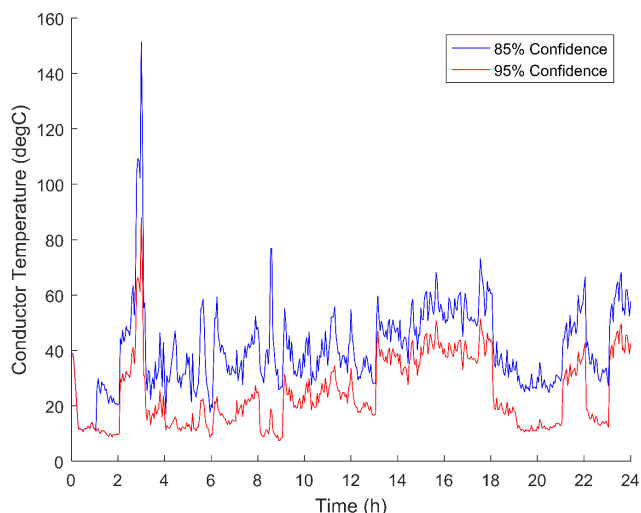


Fig. 1. Transient conductor temperature for 85 and 95% confidence levels

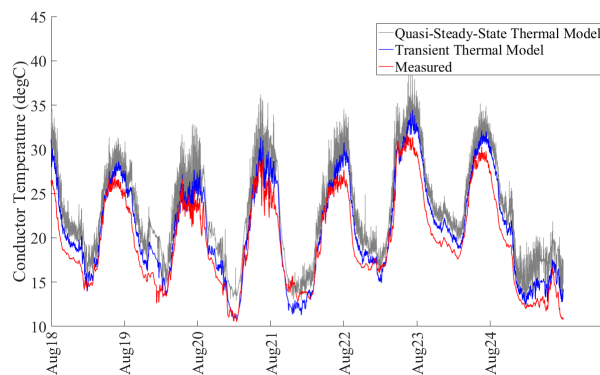


Fig. 2. Comparing transient and quasi-steady-state conductor temperature calculations to measured conductor temperature

REFERENCES

- [1] *IEEE Standard for Calculating the Current-Temperature Relationship of Bare Overhead Conductors*, IEEE Standard 738, 2013.
- [2] A. Michiorri, P. C. Taylor, S. C. E. Jupe, and C. J. Berry, "Investigation into the influence of environmental conditions on power system ratings," *Proc. Inst. Mech. Eng. Part A J. Power Energy*, vol. 223, no. 7, pp. 743757, 2009.
- [3] L. Dawson, S. Karimi, A. Knight, "Quantifying the Risk in Dynamic Thermal Line Rating," in *CIGRE Sessions, Paris*, 2018.

A Realistic One-Year Comparison of Priority Service Versus Real-Time Pricing for Enabling Residential Demand Response

Céline Gérard

*Center for Operations Research and Econometrics,
Université catholique de Louvain
Louvain-la-Neuve, Belgium
Email: celine.gerard@uclouvain.be*

Anthony Papavasiliou

*Center for Operations Research and Econometrics,
Université catholique de Louvain
Louvain-la-Neuve, Belgium
Email: anthony.papavasiliou@uclouvain.be*

Abstract—The recent large-scale integration of renewable energy in electric power systems has led to various challenges in power system operations. Demand response can be used in order to provide additional flexibility to the system to balance the effects of the massive integration of renewable resources. This paper concentrates on the comparison of two approaches for enabling demand response, real-time pricing and priority service pricing. An example of a single household with several appliances over a year is used to assess the effects of these schemes on consumer comfort and electricity charges. The example shows an illustration of (i) a realistic weekly consumption pattern of a residential consumer based on available datasets, (ii) how devices in the household are dispatched by a home energy router considering a certain demand response scheme, and (iii) what consumer welfare losses are relative to the golden standard of real-time pricing.

Index Terms—real-time pricing, priority service, demand response

I. FRAMEWORK

The unprecedented growth of renewable resources has resulted in various challenges in power system operations, due to the unpredictable, highly variable and non-controllable fluctuation of these resources. In order to incorporate more flexibility into the system, demand response paradigms are used to improve the dispatch quality of residential load. In this paper, two different schemes will be analyzed: real-time pricing and priority service pricing. The real-time pricing approach considers consumers as real-time participants into the real-time electricity market that react instantaneously to prices. On the contrary, priority service pricing considers electricity not as a commodity but as a service offered with different levels of supply reliability. In this case, a consumer subscribes to capacity strips of power with a particular reliability from a price menu containing the different options along with their cost. An option with higher reliability is more expensive. For our purpose, we consider a case with only 3 options that corresponds to a color-tagging system that consumers can set for each of their appliances: (i) Green: indicates cheap power that can be interrupted frequently; (ii) Orange: indicates power that can be interrupted under

emergency conditions; (iii) Red: indicates expensive power that cannot be interrupted.

In order to compare these two schemes, we assume that a home energy management system is installed in households which can schedule appliances efficiently under both schemes, while placing minimum decision-making requirements on household consumers. The analysis is then focused on the impact of these two schemes on consumer comfort and expenditures. The effect on consumer comfort is quantified here by means of a frustration measure due to delays on serving power consumption requests.

II. SIMULATION

For each demand response scheme, a heuristic was developed so that the home energy router can place minimum decision-making requirements on the consumer while still managing to solve the problem in an online setting. The online results were also compared with the one obtained beforehand using an optimization program assuming perfect foresight.

The home energy router that we develop is run on a single household with several appliances. Its weekly electricity consumption pattern is created from data provided by the UK-DALE dataset [1]. Moreover, the results are created for an entire year horizon and shows the cost of simplicity incurred by a consumer while choosing the priority service pricing scheme.

ACKNOWLEDGMENT

Céline Gérard is a Research Fellow (Aspirant) of the Fonds de la Recherche Scientifique - FNRS in Belgium. This research has been supported by the ENGIE Chair in Energy Economics and Energy Risk Management and by the ENGIE-Electrabel ColorPower grant.

REFERENCES

- [1] J. Kelly and W. Knottenbelt, "The uk-dale dataset, domestic appliance-level electricity demand and whole-house demand from five uk homes," *Scientific data*, vol. 2, p. 150007, 2015.

Virtual Synchronous Generator model of an Inverter-Based Distributed Generator

Anusha Kandula

Lane department of computer science
and electrical engineering
West virgina university
Morgantown, WV

Sarika Solanki Khushalani

Lane department of computer science
and electrical engineering
West virgina university
Morgantown, WV

Jignesh Solanki

Lane department of computer science
and electrical engineering
West virgina university
Morgantown, WV .

Abstract—Inverter -Based microgrids are gaining more and more importance as they can accommodate various type of Distributed generators (DG’s) effectively and for their superior power quality. Proper control strategies operating such type of DG’s will play a major role in stability of the microgrid. This stability of microgrid can be achieved by introducing virtual inertia into the system. This can be further achieved by control algorithm of inverter and a short-term energy storage system making the DG’s to act as synchronous generator. Thus, can be named as synchronverters or virtual synchronous generators (VSG). Proper Dynamics, implementation and operation of synchronverters will assure good load sharing and stability of the system. In this paper small signal model of a microgrid including VSG is modeled and stability of the system is studied.

Keywords—virtual synchronous generator, synchronverter, electrostatic synchronous generator.

I. INTRODUCTION

The current paradigm in the control of inverters associated with renewable energy sources is to extract maximum power from power source and inject it all into the power grid using controlled inverters. When the penetration of renewable power generators reaches a certain level, such “irresponsible” behavior will become untenable.[1] In responding to the daily increasing share of electricity generated from distributed generator and renewable energy sources, it is important for these sources to feed power to the grid in the form of voltage sources instead of current sources, in a way similar to the conventional generators is particularly true when the grid is weak (or) when an inverter or a microgrid works in the stand-alone mode. Virtual synchronous generator was proposed to work as conventional power generator. The well – established algorithms/theory used to control synchronous generator can still be used in power systems when a significant proportion of generating capacity is inverter based. Such inverters are called as synchronverters. The real and reactive power delivered by VSG connected in parallel can automatically shared by using the well-known frequency and voltage droop mechanisms. Synchronverters can easily be operated in grid connected and stand-alone mode and hence they provide ideal solution for microgrids and smart grids.

II. BASIC PRINCIPLE OF SYNCHRONVERTERS

Figure 1, [3] shows the control diagram of virtual synchronous generator. A typical three-phase voltage source inverter is connected to the grid at the point of common coupling (PCC) through an LC filter, which is composed of the inverter-side inductor L_1 , and filter capacitor C_f . Z_g denotes the grid impedance at the PCC. The power control scheme shown in Figure 2, [3] active and reactive power loops designed to produce essential behavior of a real synchronous

generator, including droop mechanism and inertial characteristics which is important to improve the grid stability.

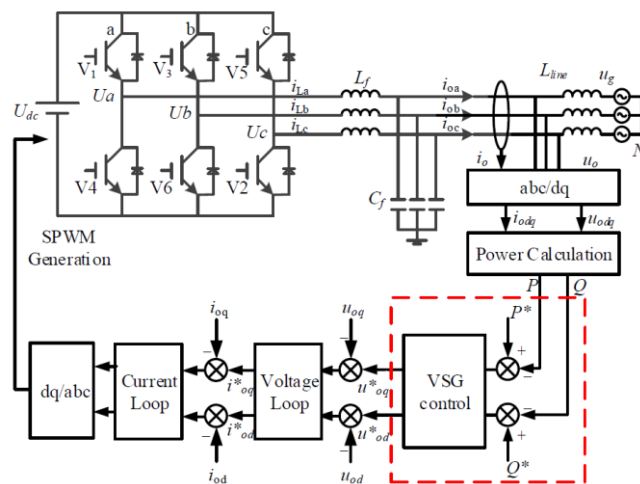


Figure 1: The structure of VSD control

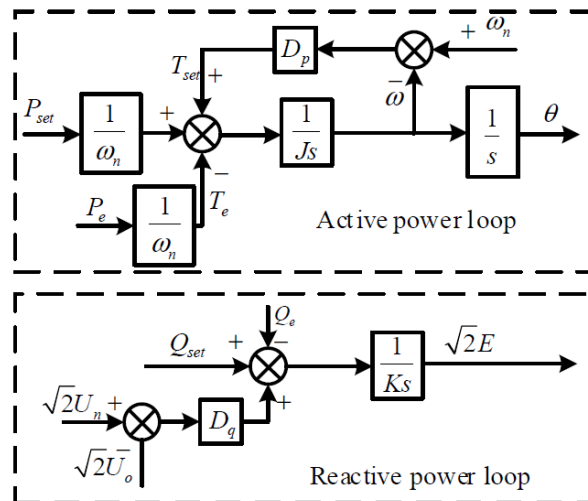


Figure 2: Power loop of VSG control

References

- [1] Q.-C. Zhong and G. Weiss, “Synchronverters: Inverters that mimic synchronous generators”, *IEEE Trans. Ind. Electron.*, vol. 58, no. 4, pp. 1259–1267, Apr. 2011.
- [2] H. Wu *et al.*, “Small-Signal Modeling and Parameters Design for Virtual Synchronous Generators,” in *IEEE Transactions on Industrial Electronics*, vol. 63, no. 7, pp. 4292-4303, July 2016.
- [3] C. Hu, K. Chen, S. Luo, B. Zhou and L. Ding, “Small signal modeling and stability analysis of virtual synchronous generators,” *2017, 20th International Conference on Electrical Machines and Systems (ICEMS)*, Sydney, NSW, 2017, pp. 1-5.

Adaptive Charging Network Research Portal

Zachary J. Lee, Steven H. Low

Division of Engineering and Applied Science, Caltech, Pasadena, CA

Email: zlee, slow@caltech.edu

Abstract—The integration of millions of electric vehicles (EVs) into the grid will require advanced control algorithms. However, a lack of data, simulators and testbeds has hampered research in practical algorithms for EV charging. The Adaptive Charging Network Research Portal addresses this by providing researchers with 1) a publicly accessible dataset of real charging sessions (ACN-Data); 2) a data-driven simulation environment for evaluating EV charging algorithms (ACN-Sim); 3) a framework for field testing online algorithms by controlling real charging stations (ACN-Live). This portal gives researchers the tools they need to develop and evaluate algorithms which work with the grid to efficiently and cost-effectively charge millions of EVs.

I. ADAPTIVE CHARGING NETWORK

In order to study practical EV charging algorithms, our group, in collaboration with PowerFlex Systems, has developed the Adaptive Charging Network (ACN); a framework for large-scale EV charging systems which has been deployed at over 40 sites around the United States.

Our experience building real EV charging systems has led us to study practical issues such as unbalanced three-phase infrastructure and non-ideal EV battery behavior [1]. Motivated by the value of real-world data and realistic simulation in our own research, we have developed and released the ACN Research Portal which is shown in Figure 1. For more information and to access the dataset and code visit <http://ev.caltech.edu>.

II. ACN-DATA

ACN-Data is a publicly accessible dataset which currently includes over 26,000 charging sessions collected from ACNs at Caltech and JPL [2]. Each session includes its arrival time, departure time, energy delivered, and charging port id. We also collect a time series of the control signal and actual charging rate of each session with a resolution of approximately 5 seconds. In addition, for over 12,000 of these sessions we have user information including their anonymized id, predicted departure time and energy request which are collected via a mobile app. The dataset is updated daily with new charging sessions, and will soon contain data from additional sites operated by PowerFlex.

III. ACN-SIM

ACN-Sim is an open-source, high-fidelity, data-driven EV charging simulation environment. This simulator includes realistic models of charging stations, batteries, and electrical infrastructure as well as the ability to play back real scenarios from **ACN-Data** or generate events from statistical models.

This material is based upon work supported by the National Science Foundation Graduate Research Fellowship under Grant No. 1745301, NSF AIR-TT under Grant No. 1602119, and NSF CTT under Grant No. 1637598.

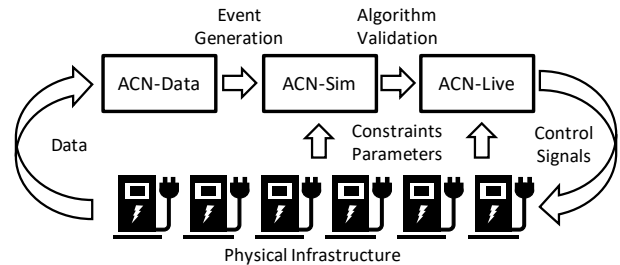


Fig. 1. Overview of the Adaptive Charging Network Research Portal and its integration with the physical ACN.

This simulator provides researchers who may lack access to real EV charging systems with a realistic environment to evaluate their algorithms and test their assumptions. It also provides a common platform on which algorithms can be evaluated head-to-head using scenarios from **ACN-Data**. This allows researchers to better understand and articulate how their work fits into the existing literature.

IV. ACN-LIVE

ACN-Live is a framework to allow field testing of online algorithms using the Caltech ACN. By utilizing the same algorithm interface as **ACN-Sim**, researcher are able to thoroughly test their algorithms in **ACN-Sim** then deploy them to the real testbed with *no code changes*. These field tests help to bridge the gap between theory and practice.

V. CONCLUSION

The ACN Research Portal is a unique collection of data and tools which provide the benefits of the ACN testbed to the wider research community. To our knowledge, **ACN-Data** is the first large-scale, publicly available dataset of workplace/university charging data. As it continues to grow, this dataset will enable researchers to tackle new questions in a data-driven manor. Meanwhile, **ACN-Sim** provides researchers with an easy to use and extensible framework for evaluating their algorithms while making use of **ACN-Data**. Finally, **ACN-Live** is a first-of-its-kind live testbed for EV research which gives researchers the ability to taken control of actual charging stations and demonstrate their algorithms in the wild.

REFERENCES

- [1] Z. J. Lee, D. Chang, C. Jin, G. S. Lee, R. Lee, T. Lee, and S. H. Low, "Large-Scale Adaptive Electric Vehicle Charging," in *IEEE International Conference on Communications, Control, and Computing Technologies for Smart Grids*, Oct. 2018.
- [2] Z. J. Lee, T. Li, and S. H. Low, "ACN-Data: Analysis and Applications of an Open EV Charging Dataset," in *Proceedings of the Tenth International Conference on Future Energy Systems, e-Energy '19*, June 2019. (forthcoming).

A Measurement-based Model for Contingency Analysis Considering Cascading Failures

Rui Ma

Department of Electrical Engineering and Computer Science
Syracuse University
Syracuse, New York, USA
rma102@syr.edu

Sara Eftekharnajad

Department of Electrical Engineering and Computer Science
Syracuse University
Syracuse, New York, USA
seftekha@syr.edu

Abstract—In power systems, contingency analysis (CA) plays a vital role in ensuring reliable system operation. However, the key component of CA, injection shift factor (ISF) that is used to calculate line outage distribution factor (LODF) to estimate the impact of contingencies, is vulnerable to wrong system information, i.e. grid topology, and the conventional risk evaluation of contingencies can not meet the enhanced system security needs from the perspective of cascading failures. In order to address these two concerns of conventional contingency analysis, in this work, a measurement-based contingency analysis model is developed to provide system operators a credible and comprehensive understanding of the power system reliability. With the availability of PMU measurements, a measurement-based ISF estimation method is developed to circumvent the credibility issue of the conventional ISF calculation method, which in turn is used in the developed risk evaluation model to identify risky contingencies in terms of cascading failures.

Index Terms—Cascading failure, contingency analysis, injection shift factor (ISF), risk evaluation

I. MEASUREMENT-BASED CONTINGENCY ANALYSIS

The proposed model utilizes synchronized PMU measurements to estimate ISF, which is a sensitivity factor that reflects the redistribution of power flow for each transmission line when generation or load changes, and then calculates LODF to perform a modified contingency analysis to identify risky contingencies considering the induced cascading failures. Specifically, changes in active power injection and active power flows are used to estimate the ISF, that in turn is utilized to compute LODF and estimate the power flow changes after the occurrences of contingencies. Instead of only evaluating system conditions following contingencies, the potential cascades are taken into consideration to assess the risk of each contingency.

II. KEY RESULTS

The ISF estimation method is tested on the IEEE 57-bus system and the risks of all $N-2$ contingencies are evaluated with the proposed contingency risk evaluation method. The estimation accuracy is illustrated in Fig. 1 and the estimation error is quantified by root mean squared error (RMSE). It can be observed that the proposed ISF estimation method achieves a high accuracy where the largest RMSE is only

This work is supported by the National Science Foundation (NSF) Grant No.1600058.

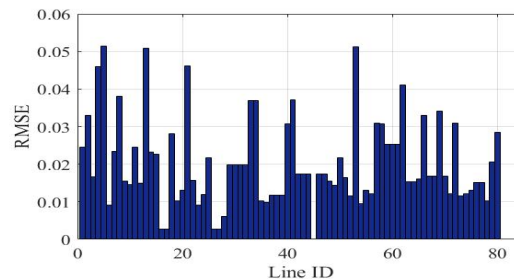


Fig. 1. Estimation accuracy of the proposed ISF estimation method for the IEEE 57-bus system

TABLE I
TOP TEN RISKY $N-2$ CONTINGENCIES IDENTIFIED BY THE DEVELOPED AND THE CONVENTIONAL EVALUATION METHODS FOR THE IEEE 57-BUS SYSTEM

IEEE 57-bus system				
Contingency	Developed evaluation method		Conventional evaluation method	
	Rank	Weight	Rank	Weight
7, 12	1	0.5784	687	0.0006
7, 10	2	0.5704	672	0.0008
3, 8	3	0.2273	2	0.1096
8, 41	4	0.2049	1	0.1162
7, 8	5	0.1567	6	0.0745
8, 67	6	0.1545	3	0.0797
8, 40	7	0.154	5	0.0758
5, 8	8	0.1514	10	0.0719
8, 68	9	0.1489	4	0.0769
8, 18	10	0.1446	7	0.0735

around 0.05. In addition to the estimation accuracy, the top ten risky $N-2$ contingencies obtained from the developed risk evaluation method are given in Table I. The rankings of these ten contingencies in conventional evaluation method that ignores the impact of induced cascades are also given in Table I. It can be observed that most of the top ten risky contingencies obtained from the developed evaluation method also have high rankings in the conventional evaluation method except the two $N-2$ contingencies, that is, losing line 7, line 12 and losing line 7, line 10. Further analysis shows that, compared to other contingencies listed in Table I, the risks of these two sets of contingencies are not high after the occurrences of contingencies. However, if proper actions are not taken to mitigate the contingencies, the induced cascading failures would cause severe adverse impacts on reliable system operation.

Securing Communications and Deployments for Resilient Control Applications using Edge Computing Technology

Zhijie Nie* and Anurag K. Srivastava*

*School of Electrical Engineering and Computer Science, Washington State University, Pullman, WA 99164, USA
 Email: {zhijie.nie, anurag.k.srivastava}@wsu.edu

Abstract—Cyber attack has become one of the major concerns for power system operation. With more and more automated control applications and remedial action schemes (RAS), deployed on wide-area control system (WACS), the environment that applications run on could easily be a target to attackers. Container technology is popular for its rapid deployment and compatibility, which have been leveraged in energy management system (EMS). Recently, these applications are fully supported and ready to be deployed on IoT devices including network switches and routers. In order to enhance the cyber-security for these IoT-enabled assets, an application platform called Resilient Information Application Platform for Smart Grid (RIAPS) is developed and tested with RAS applications, like minimal wind generation curtailment and under-frequency load-shedding. This poster presents the secure communications for RAS applications and the extended features that prevent the deployed environment from malicious attacks.

Index Terms—Edge computing, cyber-physical system, remedial action scheme, analytics platform, synchrophasor

I. INTRODUCTION

Container technology has ushered in the era of lightweight application deployment for IoT devices. State-of-the-art network infrastructures, such as network switches and routers, are employed with container-enabled deployment functionality. For instance, Cisco has put forward IOx application environment using Docker applications across different IoT network devices. For smart grid, by deploying control applications on embedded devices, many automated control services and remedial action schemes can be realized at a low cost. Instead of running applications on a centralized network server, small-scale applications could be distributed on different substations. This alternative solution will benefit from the low network bandwidth, reduction in network propagation delay, and circumvention of the crashing risks on a single computing node.

Unfortunately, network switches and routers are common targets of severe cyber attacks like denial-of-service (DoS) attacks. Many of consumer-class network infrastructures have been publicly reported their cyber vulnerabilities on Common Vulnerabilities and Exposures (CVE) database. To enhance the resiliency for smart grid analytics, the application platform is

The authors would like to thank Advanced Research Projects Agency-Energy (ARPA-E), Power Systems Engineering Research Center (PSERC), and Vanderbilt University for the technical and financial supports in this work.

required to maintain integrity and to secure critical information and when the cyber assets are subject to attacks. RIAPS (Resilient Information Architecture Platform for Decentralized Smart Systems) is developed to improve the resiliency and security for smart grid applications. This poster is going to demonstrate the secure communication and analytics deployment using RIAPS platform with the minimal wind curtailment RAS application, simulated on the hardware-in-the-loop cyber-physical testbed.

Fig. 1 demonstrates our proposed hardware-in-the-loop cyber-physical testbed. RTDS and OPAL-RT simulators are used to simulate the power system in a real-time manner synchronized with external GPS clock. These simulators consist of software PMU modules (GTNET-PMU, C37.118 Slave) that stream phasor data for synchrophasor-based control analytics with precise timestamps. These modules support the TCP/IP transmission under IEEE C37.118 communication protocols. General edge computing devices take advantage of container technology, on which the control applications could be deployed on. However, such IoT infrastructures are communicated through the local area network. Critical information is exposed to risks when there exists a device compromised on the network. The implementation of RIAPS platform leverages three Beaglebone Boards as the distributed computational nodes. Both application deployment and data communication among devices are secured on RIAPS platform. To demonstrate the usage of RIAPS platform, this poster presents an RAS application setup to solve the optimal strategy for wind generation curtailment when the system is subject to operational violations.

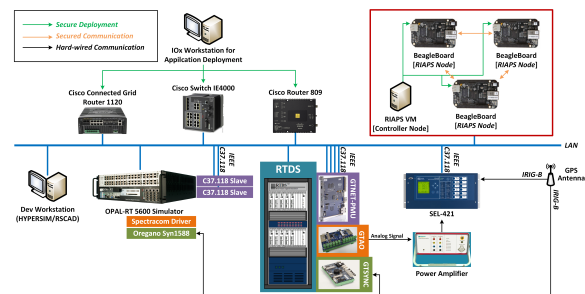


Fig. 1. Secure communications for real-time cyber-physical simulations.

A Hybrid Data-Driven Method for Online Power System Dynamic Security Assessment with Incomplete PMU Measurements

Qiaoqiao Li, Yan Xu

School of Electrical and Electronic Engineering
Nanyang Technological University
Singapore
Email: qiaoqiao001@e.ntu.edu.sg;
xuyan@ntu.edu.sg

Chao Ren

Interdisciplinary Graduate School
Nanyang Technological University
Singapore
Email: renc0003@e.ntu.edu.sg

Junhua Zhao

School of Science and Engineering
Chinese University of Hong Kong
(Shenzhen)
China
Email: fuxiharp@gmail.com

Abstract—With widely deployment of phasor measurement units (PMU), data-driven dynamic security assessment (DSA) has been a promising tool to help power system counteract large disturbance and avoid instability. In case of PMU lost events, the DSA performance may be dramatically degraded. This paper designs a new online DSA model based on hybrid ensemble learning to address the missing data problem. In this method, a set of missing data estimators is proposed to restore the system measurement, and potential inaccurately estimated features are detected in feature validation stage to further ensure the model performance. After excluding inaccurate estimations, the filled-up dataset is provided to support accurate DSA under PMU lost situation. A hybrid ensemble of extreme learning machine (ELM) and random vector functional link networks (RVFL) is designed as learning engine for estimators and DSA classifiers. Simulation results show this approach achieves low estimation error as well as high DSA accuracy and strong robustness.

Index Terms— Data-driven, dynamic Security Assessment, ensemble learning, phasor measurement units.

I. KEY ALGORITHM

A. Extreme Learning Machine (ELM) and Random Vector Functional Link (RVFL)

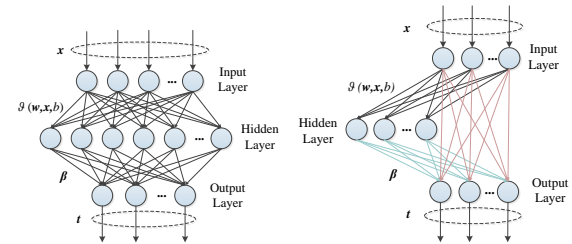


Fig. 1 Structure of ELM and RVFL

$$f_L(x_j) = \sum_{i=1}^L \beta_i \cdot \mathcal{G}(w_i \cdot x_j + b_i) = t_j \quad j=1,2,\dots,N \quad (1)$$

$$H \beta = T \quad (2)$$

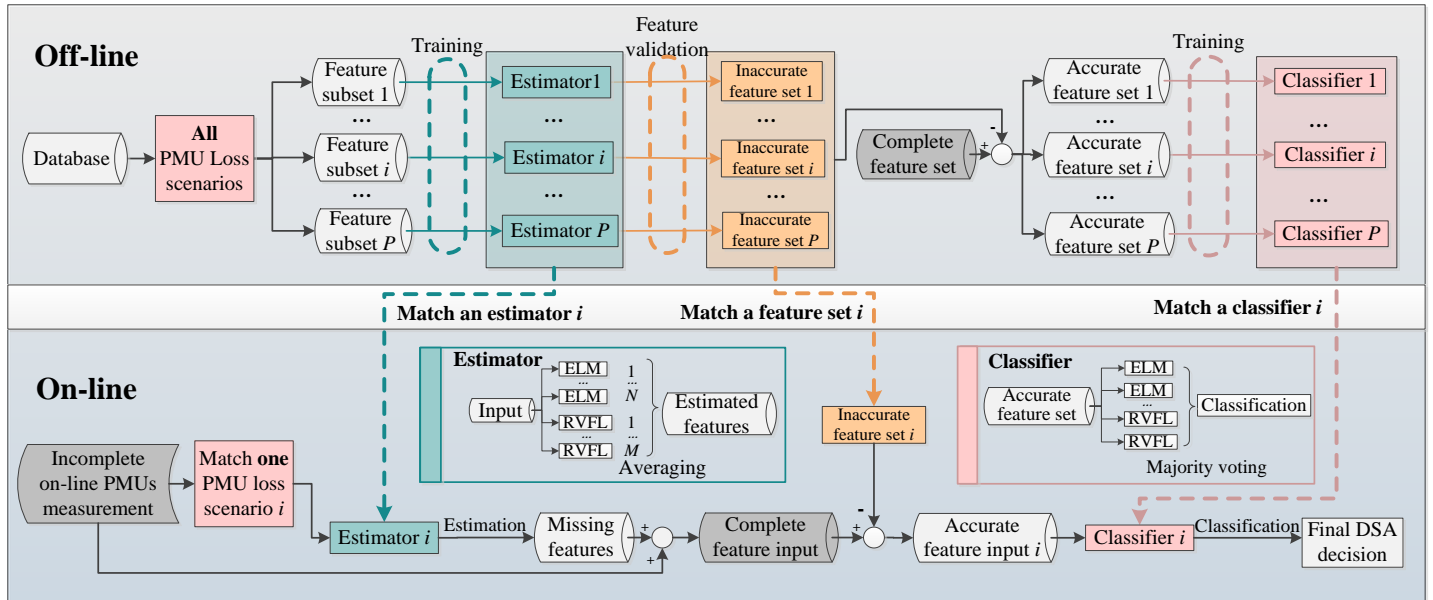


Figure 2 Model design

Assessing the Potential of Large-Scale Energy Storage for Distribution Systems Demand Management

Júlia R. Conceição, Tiago R. Ricciardi, Walmir Freitas
 Department of Systems and Energy
 University of Campinas
 Campinas, SP, Brazil
 {julia.ramos, ricciardi, walmir}@ieee.org

Victor B. Riboldi, Ji Tuo
 Department of Strategy and Innovation
 CPFL Energia
 Campinas, SP, Brazil
 {riboldi, jituo}@cpfl.com.br

Abstract—Distribution systems are traditionally designed to meet a load peak demand, considering its growth in a certain time horizon. The possibility to use Battery Energy Storage Systems (BESS) to shift the load demand from peak to off-peak hours has been receiving increasing attention by distribution utilities. Adequate management of the distribution system loading, propiated by BESS, can rationalize the utilization of its assets and postpone investments related to expansion and/or equipment capacity upgrade. This paper presents a methodology for the assessment of the potential of large-scale BESS for distribution systems demand management. The methodology is then applied for a one-year data set comprising measurement collected by the SCADA from 831 primary feeders served by 175 power transformers of a Brazilian distribution utility. Results indicate that a 2.66 MW/10.54 MWh BESS can alleviate 7.5% of the peak loading for more than 70% of the transformers with capacity exhaustion expected within 10 years.

Index Terms—Demand management, energy storage systems, load curves, peak shaving, smart grids.

I. KEY RESULTS

A simple model to describe the distribution load growth through time is given by:

$$S_n = S_0 \cdot (1 + g)^n \quad (1)$$

where S_n is the demand (MVA) at the end of the n -th year, S_0 is the demand in the year 0, g is the annual growth rate (AGR) and n is the number of years. If system expansion should be accomplished when S_n reaches the limit S_{lim} , then the time until the expansion is needed is given by:

$$n_{exp} = \ln(S_{lim}/S_0)/\ln(1 + g) \quad (2)$$

Peak shaving the transformer loading in the year 0 through the adoption of BESS alternative means a reduction in S_0 , extending the value of n_{exp} and postponing expansion. In order to evaluate such possibility, a case study was presented, in which (i) 15-min time-series measurement data from 175 power transformers collected from the SCADA of a major Brazilian utility were processed; (ii) the utility planning criteria was applied to identify power transformers for which the normal loading limit will be reached in the next 10 years; (iii) BESS were sized for

each transformer to defer their upgrade in 10 years. The case study presented shown that a 2.66 MW/10.64 MWh BESS would be enough for alleviating 7.5% of their planning demand for more than 70% of the transformers analyzed giving them 10 more years before a new expansion alternative is needed. Figure 1 and Table 1 present the results for a single transformer, and Figure 2 presents the results for all the utility transformers with expansion needed in a 10-year horizon.

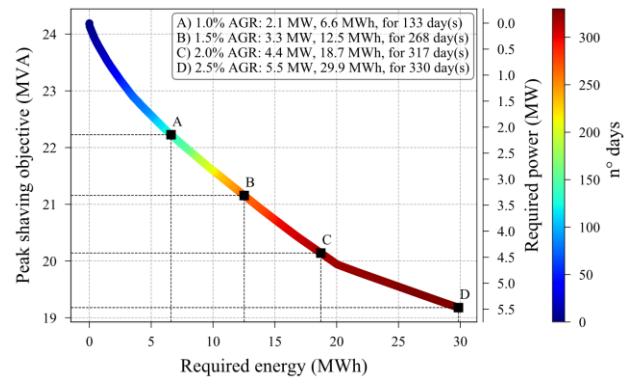


Figure 1. ESS design curve for a selected power transformer.

TABLE I. S_{plan} (%) OF FIGURE 1 TRANSFORMER WITH AND W/O THE BESS.

year	0	1	2	3	4	5	6	7	8	9	10
w/o BESS	90,8	91,7	92,6	93,5	94,5	95,4	96,4	97,3	98,3	99,3	100,3
w/ BESS	83,6	84,4	85,2	86,1	87,0	88,0	88,9	89,9	90,9	91,9	92,9

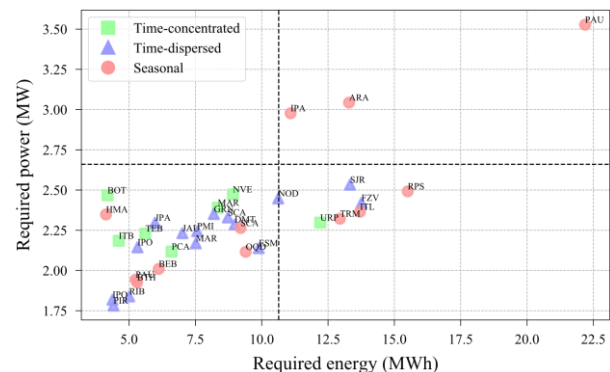


Figure 2. Comparison of BESS sizes for the selected power transformers.

This work has been funded by the Brazilian National Council for Scientific and Technological Development (CNPq) under Grant 162581/2017-3 and by CPFL Energia under the ANEEL R&D program PD-02937-3018/2016.

Distributed Service Restoration in Distribution Networks by DERs Scheduling

Reza Roofegari nejad, *Student Member, IEEE*, Wei Sun, *Member, IEEE*

Department of Electrical and Computer Engineering, University of Central Florida, Orlando, FL USA

r.roofegari@knights.ucf.edu, sun@ucf.edu

Abstract—The resilience of modern power systems has been constantly threatened by various natural disasters and man-made attacks. Under those threats, fast and automatic restoration actions are critical to restore system to normal condition and prevent from additional disastrous consequences. Smart grid technologies, such as distributed energy resources (DERs) and microgrids, provide both opportunities and challenges for the restoration procedure. This study develops a distributed service restoration (DSR) for unbalanced active distribution networks based on alternating direction method of multipliers (ADMM). The step-by-step restoration actions are provided to dispatch DERs and distribution system control devices, as well as the power of boundary substation bus. Accordingly, the restoration problem is formulated as a convex problem by considering various operational constraints, component modeling, and three-phase unbalanced power flow equations. Then, the problem is decomposed into subproblems for each node by applying ADMM-DSR; and solves through each agent by exchanging limited information with neighboring nodes in an iterative procedure. The developed models and algorithms are validated and demonstrated through testing on IEEE test feeders.

Index Terms—Alternating direction method of multipliers (ADMM), bidirectional distributed energy resources, service restoration.

I. INTRODUCTION

One of the key features of resilient power systems is enabling self-healing capabilities such as automatic restoration in distribution systems. The restoration procedure should clearly delineates the actions and responsibilities for different system participants. Accordingly, distribution system restoration has been modeled as centralized combinatorial optimization problem. However, this approach requires central controllers being available in distribution networks to collect data from all participants and send out control decisions in a centralized manner. But this communication structure is costly and likely to suffer from single point failure. Also, it is restricted by the information privacy of various entities. Furthermore, the centralized structure is challenging in adopting to system changes such as integration of DERs. Consequently, the distributed optimization and control are promising solutions in developing modern power system scheme. Therefore, this study developed a distributed service restoration based on ADMM approach in which the original problem is decomposed for each agent while the optimum is guaranteed.

II. THE FRAMEWORK OF ADMM-DSR

Distribution service restoration can be categorized into emergency service restoration and blackout service restoration. The emergency service restoration includes isolation of faulted

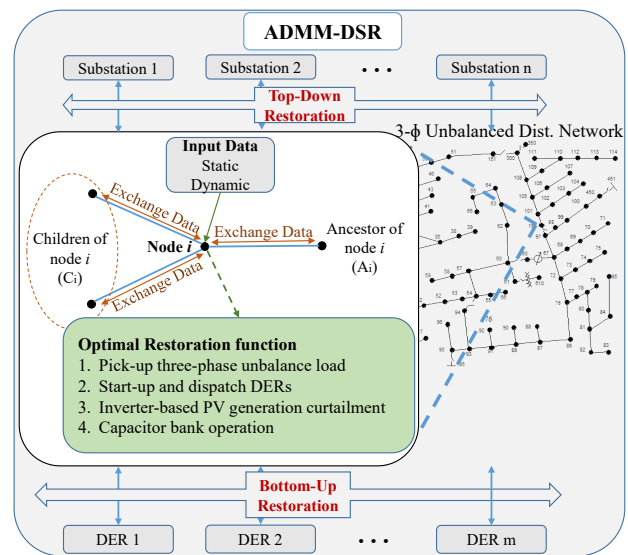


Fig. 1. The proposed ADMM-DSR framework.

area and restoration of un-faulted out-of-service area. However, in the blackout service restoration, distribution networks are totally without power. Accordingly, the DSR depends on the bulk power system restoration, including start-up of generators, energization of lines and distribution substations, and then performs load restoration in distribution systems. This study focuses on load restoration phase, which aims to minimize outage impacts by finding the optimal set of loads to be restored, considering their priorities.

The framework of the proposed ADMM-DSR is shown in Fig. 1. the distributed approach is based upon local optimization process, where only limited information is exchanged among neighboring agents or intelligent nodes. Accordingly, a Lagrange function based on centralized restoration formulation is designed which is separable for each agent. Then, based on the iterative procedure of ADMM algorithm, the optimal restoration plan can be achieved as: 1) each node optimizes its primary variables such as load pick-up, 2) each node optimizes its primary variables such as perception of neighboring nodes voltage. These auxiliary variables are used to enforce boundary constraints, such as power flow equations among neighboring nodes. 3) Lagrange multipliers are updated based on the results from previous steps. This procedure is continued until satisfying stopping criteria and achieving the optimum restoration plan for whole network.

Meter and Device Placement for Duke Energy Distribution Circuits

Shelby Tomassi, Andrew Simms, Matthew Tauber, Ajani Nisbett
William States Lee College of Engineering
University of North Carolina at Charlotte
Charlotte, USA

stomassi@uncc.edu, asimms3@uncc.edu, mtauber1@uncc.edu, anisbett@uncc.edu

Abstract— Research shall be conducted on Duke Energy’s Distribution Management System (DMS) software in the Duke Energy Smart Grid Laboratory. The project first covers the placing of voltage meters and later lead into the placing of Integrated Volt/Var Control (IVVC) devices using the results of meter placement. The process of meter placement will be carried out by conducting sensitivity analysis on switches across a Duke circuit in DMS. This analysis will provide insight as to which switch placements are more sensitive than others within the circuit.

Keywords—*Integrated Volt/Var Control(IVVC), Self-Optimizing Grid(SOG), 4-3-2 Rule, Sensitivity, Distribution System, NetworkX*

I. INTRODUCTION

Many distribution circuits use rules for where integrated volt/var control (IVVC) devices need to be placed to improve the reliability and efficiency of the circuit. Devices used in IVVC are capacitor banks and voltage regulators. Duke Energy uses the 4-3-2 rule to place Self Optimizing Grid (SOG) devices which states that every 400 customers, 3 miles, or 2MW of power usage a device needs to be placed. A second method that can be used to place devices is sensitivity analysis. Sensitivity analysis takes the points along the feeder where the change in voltage over the change in power is highest and states that a device needs to be placed at that location. The results of the 4-3-2 rule will be compared to the results of the sensitivity analysis to determine if the 4-3-2 rule is the best way to place IVVC devices along a circuit as well.

II. WORK COMPLETED

A. Sensitivity Analysis of Switches

A Duke Energy Circuit was simulated through the Distribution Management System (DMS). The main goal of testing and analysis on this circuit was to examine where sensitive areas on the circuit may lie. The group used Python scripts to carry out analysis.

All external switches were queried for within the circuit and established in a list. For each switch, the voltage and real power levels were monitored and recorded on an hour-by-hour basis for an entire day. The change in voltage and real power was then calculated at each change in hour. These values were then placed into a Jacobian Matrix and these measurements could be used to calculate sensitivity. It was then calculated for each hour of the

day. An average sensitivity was then calculated for each switch with respect to the entire day.

The team has conducted several types of tests in order to capture all types of sensitive areas along a Distribution Circuit and a yearly average. These included adding a Photovoltaic (PV) source, turning off all capacitor banks, and using just a normal feeder. All of these tests were compared against the 4-3-2 rule and against each other as well.

B. Mapping Different Device Placement Rulesets

With an externals file containing data for every device on a certain Duke Energy circuit, this circuit could be mapped out and analyzed for research purposes. The circuit would be created with NetworkX, a Python library that would establish nodes and edges in the code. These nodes and edges would effectively create a spider web of information that could be analyzed later. The goal of this mapping was to see where devices should be placed using Duke Energy’s 4-3-2 Rule.

The first thing created in NetworkX was the backbone of the circuit, also known as the three phase lines. These three phase lines connected nodes together. From these nodes, other devices such as single-phase lines, switches, and transformers. The important data for these devices would be taken from the externals file, such as customers on a transformer or power used by a switch. This data was added up as a total of either customers or megawatts for the smaller circuit, and then sent back to the backbone node in the larger circuit. This process was repeated for every backbone node.

With all nodes in the backbone containing customer and power data, and all edges in this circuit containing length data, the 4-3-2 rule could be analyzed for the circuit.

ACKNOWLEDGMENT

The team would like to thank Duke Energy for providing the Smart Grid Lab space in EPIC for us to conduct our research. We would also like to thank our Industry Supporters Gregg Borachok, Brent Seward, Christina Hostetter, Kevin Fox, Andrew Justen from Duke Energy. Along with our UNCC Faculty Mentors Valentina Cecchi and Sukumar Kamalasan. This project would not have been possible or successful without any of them.

Load Management in a building with BESS and HVAC scheduling

Divya T. Vedullapalli, *Student Member, IEEE*

Ramtin Hadidi, *Member, IEEE*

The Department of Electrical and Computer Engineering
Clemson University
Clemson, USA
dvedull, rhadidi @ clemson.edu

John Ruiz

conEdison Battery Storage
Milwaukee, WI
ruizj @ conedceb.com

Abstract — This project will discuss and validate a demand management algorithm for battery energy storage systems and HVAC scheduling using the Model Predictive Control (MPC). Behind-the-meter energy storage system (BESS) is used for modifying the load shape and minimizing the demand charge of a building. Thermal mass of the building can also be utilized to store the heat/cool energy and HVAC is scheduled to minimize power consumption during peak times. Initially this paper works with optimizing BESS using MPC and compares with regular optimization. Later HVAC is modelled mathematically to be able to use in optimization. Finally, battery and HVAC schedules are co-optimized to minimize the annual electricity bill without causing thermal discomfort to the residents of the building.

Index Terms— Battery energy storage system (BESS), Demand charge management, Model Predictive Control (MPC), Optimization

I. INTRODUCTION

To avoid installation of capacity with increasing demand of electricity, utilities employ Time-of-Use (TOU) pricing schemes for energy and/or include demand charges during peak hours. A battery can be utilized to shift the load partially during peak to off-peak time and reduce the electricity cost. A building’s thermal mass can be used as a virtual battery to store the heat energy by pre-cooling or pre-heating during off-peak hours and reducing the power consumption during peak hours. The goal of the demand side management algorithm is to determine the optimal schedule of battery and HVAC set-points for minimizing electricity cost while satisfying customers’ load, battery operating conditions and without causing thermal discomfort.

II. OPTIMIZATION FORMULATION

$$\text{Min} [\rho_E(k) \quad \rho_{D1}(k) \quad \rho_{D2}(k) \quad \rho_{D3}(k) \quad 0 \quad 0] \begin{bmatrix} P(k) \\ P_{Shave1} \\ P_{Shave2} \\ P_{Shave2} \\ T_z(k) \\ T_{SP}(k) \end{bmatrix} \quad (1)$$

s.to.

$$A_p(z)P(k) - B_p(z) \begin{bmatrix} T_{SP}(k) \\ T_{amb}(k) \end{bmatrix} = 0 \quad (2)$$

$$A_T(z)T_z(k) - B_T(z) \begin{bmatrix} T_{SP}(k) \\ T_{amb}(k) \end{bmatrix} = 0 \quad (3)$$

$$lb \leq T_z(k) \leq ub \quad (4)$$

$$0 \leq P(k) \leq P_{Peak} \quad (5)$$

$$lb \leq T_{SP}(k) \leq ub \quad (6)$$

III. SAMPLE RESULTS

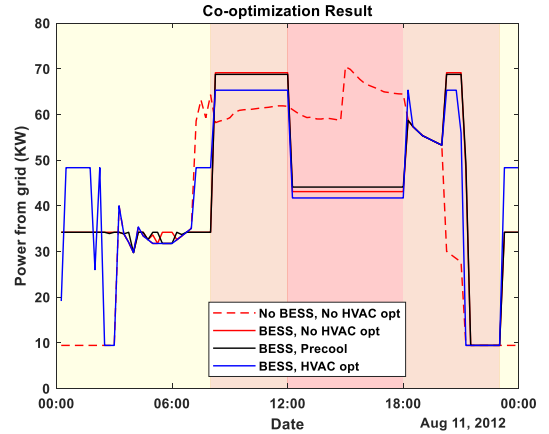


Fig 2. Total building power with co-optimization

TABLE I. ANNUAL ELECTRICITY BILL COMPARISON

Bill Component	No Optimization	HVAC Optimization	Co optimization
Off-peak Energy (\$)	5,242	5,246	7,567
Mid-peak Energy (\$)	18,965	19,251	22,965
Peak Energy (\$)	38,401	36,134	22,386
Off-peak Demand (\$)	3,549	3,556	2,391
Mid-peak Demand (\$)	7,384	7,765	7,792
Peak Demand (\$)	19,713	18,420	9,640

Electric Vehicle Aggregator Modeling and Control for Frequency Regulation

Mingshen Wang, Fangxing Li

Department of Electrical Engineering and Computer Science, the University of Tennessee, Knoxville, TN 37996, USA.
mwang38@utk.edu, fli6@utk.edu

Abstract—With the integration of renewable energy in the power system, the electric vehicles are suggested to be an alternative for frequency regulation. The existing models that managed a large quantity of electric vehicles for centralized control achieved high accuracy at the expense of the heavy calculation workload and the high requirement for real-time communication. This paper develops a state space model that provides a probability to realize the real-time power control of aggregated EVs with the high accuracy and calculation efficiency but the low requirement for real-time communication. The state space model, a reduced model based on the state space method, accurately describes the aggregated electric vehicles with different connecting states and various state of charge (SOC) states. Considering the heterogeneous charging characteristics and the random traveling behaviors of electric vehicles, the state space model realizes the state transition prediction and the regulation capacity estimation with the Markov state transition method, which has much higher calculation efficiency than the existing models. The state space model is used for the frequency regulation, and the SOC adaptive coefficient is implemented to derive the identical control signal and improve the prediction accuracy.

I. MODELING FRAMEWORK

A. SOC-State Model of an Individual EV

The SOC-state model considering connecting states:

$$S_i(k+1) = \begin{cases} S_i(k) - P_i(k) \cdot \eta_{c,i} \cdot T / Q_i, & P_i(k) < 0, \text{ CS} \\ S_i(k), & P_i(k) = 0, \text{ IS} \\ S_i(k) - P_i(k) / \eta_{d,i} \cdot T / Q_i, & P_i(k) > 0, \text{ DS} \end{cases} \quad (1)$$

where k is the time step; S_i is the SOC of EV i ; P_i is the charging power; CS/IS/DS is abbreviation of Charging State/Idle State/Discharging State; S_i is the battery capacity.

B. State Transition of EVA

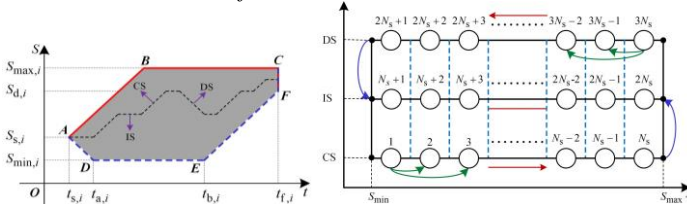


Fig. 1. Operation area of an EV. Fig. 2. State space of aggregated EVs.

The state transition of EVs in one time step:

$$\mathbf{x}(k+1) = \mathbf{A}\mathbf{x}(k) \quad (2)$$

where \mathbf{A} is a $(3N_s \times 3N_s)$ matrix and is derived to describe the transition of the EVs from one state interval to another; \mathbf{x} is $(3N_s \times 1)$ state vector.

Markov estimation method and analytical method can be used to obtain the \mathbf{A} (State Transition Matrix).

C. State Space Model of EVA

$$\begin{cases} \mathbf{x}(k+1) = \mathbf{A}\mathbf{x}(k) + \mathbf{B}\mathbf{u}(k) \\ \mathbf{y}(k) = \mathbf{C}\mathbf{x}(k) \end{cases} \quad (3)$$

where \mathbf{u} is a input vector that indicates responding modes; \mathbf{y} is a output vector; \mathbf{A} is transition matrix; \mathbf{B}/\mathbf{C} is constant matrixes.

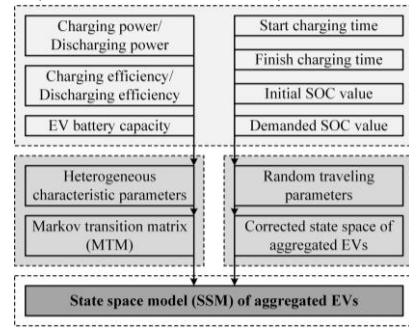


Fig. 3. Framework of the state space model of aggregated EVs.

II. FREQUENCY CONTROL WITH STATE SPACE MODEL

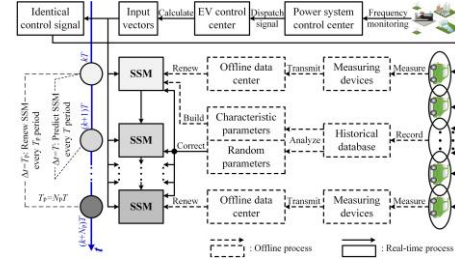


Fig. 4. Frequency regulation strategy.

III. STUDY RESULTS

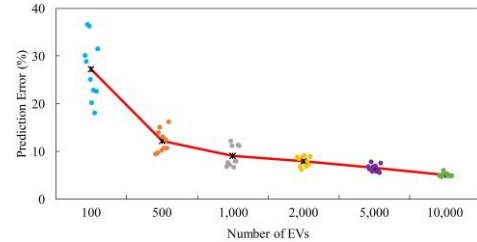


Fig. 5. Prediction errors for EV aggregator.

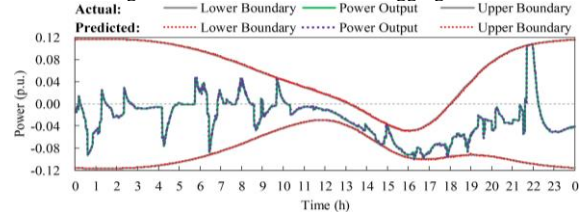


Fig. 6. Power profiles of EVA without SOC adaptive coefficient. The SSM realizes the real-time power control of EV aggregator with the high accuracy and calculation efficiency.

A Semi-Supervised Deep Transfer Learning Architecture for Energy Disaggregation

Shengyi Wang, Liang Du

Department of Electrical and Computer Engineering
Temple University
Philadelphia, PA, United States
Email: {shengyi.wang, ldu}@temple.edu

Qun Zhou

Department of Electrical and Computer Engineering
University of Central Florida
Orlando, FL, United States
Email: qun.zhou@ucf.edu

Abstract—Energy disaggregation is the problem of estimating individual load consumption profiles from an aggregated waveform. Most existing methods ignore the discrepancy of load profile distributions within different sources, which may lead to robustness issues. Furthermore, limit amount of labeled data is a bottleneck for all existing literature. This paper proposed a deep transfer learning based method for energy disaggregation. Each load has its own disaggregator, which consists of a feature extractor and a regressor. Unlike existing methods, a semi-supervised learning using deep domain adaptation is proposed, which can align the energy data distribution to some extent by utilizing both the labeled and the unlabeled data. Tests were carried out on a publicly available dataset. It can be shown that the proposed architecture can effectively improve energy disaggregation performance and enhance the robustness.

I. INTRODUCTION

This paper proposed a novel architecture for energy disaggregation using deep domain adaptation. The disaggregator for each load consists of a feature extractor and a regressor. The former can automatically achieve useful feature representation using CNN blocks. The latter can map abstract features to a target output signal using a sequence-to-point fully-connected layer. The proposed model is pre-trained in a supervised way and then incorporates unlabeled test data into the training process in a semi-supervised way by introducing an adaptive layer. Contributions of this paper are summarized as follows.

- Proposes a deep-learning based architecture with semi-supervised training, which can shrink the distribution discrepancy from different energy sources;
- Introduces an adaptive layer which can regularize model parameters to reduce the risk of overfitting;
- Incorporates unlabeled test data into the training process to lower the demand of high amount of labeled data.

II. DOMAIN ADAPTIVE DISAGGREGATOR

The proposed disaggregator consists of a feature extractor and a regressor. In the feature extractor, 1D-CNN layers are used to automatically capture time-invariant features such as power levels. In the regressor, fully connected (FC) layers are used to map each input sequence of features to an output point. In order to enhance the robustness and reduce the risk of overfitting, the proposed architecture is trained in a semi-supervised manner using deep domain adaptation. To

TABLE I
THE MEAN ABSOLUTE ERROR (MAE) (WATT) FOR PECAN STREET DATA. BEST RESULTS ARE SHOWN IN BOLD. DA(-): WITHOUT DOMAIN ADAPTATION; DA(+): WITH DOMAIN ADAPTATION.

	3367→545	8669→3367	545→8669	Average
da(-) [ev]	603.766	375.457	560.317	513.180
da(+) [ev]	581.641	345.741	545.693	491.025
da(-) [dry]	17.771	38.417	14.120	23.436
da(+) [dry]	18.671	30.225	12.057	20.318
da(-) [ref]	70.653	63.367	61.285	65.102
da(+) [ref]	66.126	63.351	59.437	62.971
da(-) [fur]	192.425	92.620	147.271	144.105
da(+) [fur]	176.584	85.783	149.050	137.139

TABLE II
THE NORMALIZED SIGNAL AGGREGATE ERROR (SAE) FOR PECAN STREET DATA. BEST RESULTS ARE SHOWN IN BOLD. DA(-): WITHOUT DOMAIN ADAPTATION; DA(+): WITH DOMAIN ADAPTATION.

	3367→545	8669→3367	545→8669	Average
da(-) [ev]	0.227	0.039	0.287	0.184
da(+) [ev]	0.138	0.198	0.333	0.223
da(-) [dry]	0.178	0.600	0.268	0.349
da(+) [dry]	0.115	0.016	0.060	0.064
da(-) [ref]	0.528	0.171	0.098	0.266
da(+) [ref]	0.264	0.095	0.025	0.128
da(-) [fur]	0.143	1.026	1.375	0.848
da(+) [fur]	0.304	0.909	1.391	0.868

start with, the model is pre-trained in a supervised manner to minimize the regression loss. It is important to learn general features for 1D-CNN layers. Then a two-stream architecture is deployed for domain adaptation. One stream operates on the source domain and the other on the target domain. It is assumed that both source and target data has similar general features. Therefore, they share the same feature extractor. Meanwhile, after the pre-trained step is completed, the weights in the feature extractor are "frozen", i.e., they will not be updated in the remaining steps.

III. EXPERIMENTS AND RESULTS

The final results can be given in Table I and Table II.

Using Power Transfer Distribution Factors in Subproblems of Distributed Unit Commitment

Shaobo Zhang, *Student Member, IEEE*, and Kory W. Hedman, *Member, IEEE*

School of Electrical, Computer, and Energy Engineering, Arizona State University, Tempe, AZ 85287, USA

Abstract—Distributed algorithms based on Alternating Direction Method of Multipliers (ADMM) have been proposed to reduce the time of solving network-constrained unit commitment (UC) problems. In these algorithms, a power system is partitioned into regions, and the UC problem is decoupled into subproblems accordingly, which are solved in parallel. However, in the subproblems, all the proposed algorithms model the network constraints inside each subproblem with auxiliary phase angle variables. In power systems where only a small percentage of transmission lines are congested, another formulation using power transfer distribution factors (PTDFs) usually solves much faster, because it has less decision variables and constraints. In this work, a subproblem formulation using PTDFs is proposed for the distributed unit commitment algorithm. To quantify the difference in computation performance, numerical simulations are performed on a Polish 3012-bus system.

I. METHODOLOGY

In centralized unit commitment (UC) problems with a formulation using power distribution factors (PTDFs), each transmission line constraint is coupled with generators in different regions, which makes it difficult to apply distributed algorithm directly. Thus, the proposed PTDF subproblem formulation of distributed UC uses the same coupling variables as the b-theta formulation in [1]: the phase angles at boundary buses, and the power flow on tie lines. However, the variables that represent the phase angles of the internal buses of each region in the formulation [1] are eliminated using regional PTDFs in the proposed formulation. In addition to the regional PTDFs, the proposed formulation needs the sensitivity matrix of the phase angle variables at the boundary buses to the power injections at each generator and load bus, which can be computed offline from the nodal admittance matrix. The proposed formulation of network constraints for region v is:

$$\sum_{g \in G} P_g + \sum_{k \in K_{tie}} \delta_k P_{v,k}^{tie} = \sum_{b \in B} d_b \quad (1)$$

$$\begin{aligned} -F_k^{max} &\leq \sum_{b \in B} PTDF_{k,b}^v \left(\sum_{g \in G(b)} P_g + \sum_{k \in K_{tie}(b)} \delta_k P_{v,k}^{tie} - d_{b,t} \right) \\ &\leq F_k^{max}, \forall k \in K \end{aligned} \quad (2)$$

$$\begin{aligned} \theta_{v,i} &= \sum_{b \in B} \frac{\partial \theta_{v,i}}{\partial P_{inj,b}} \left(\sum_{g \in G(b)} P_g + \sum_{k \in K_{tie}(b)} \delta_k P_{v,k}^{tie} - d_b \right) \\ &+ \theta_{v,ref}, \forall i \in \mathcal{N}_v^{BB} \end{aligned} \quad (3)$$

$$P_{v,k}^{tie} = B_k (\theta_{v,from} - \theta_{v,to}), \forall k \in K_{tie} \quad (4)$$

$$-F_k^{max} \leq P_{v,k}^{tie} \leq F_k^{max}, \forall k \in K_{tie}. \quad (5)$$

Constraint (1) is the regional power balance constraint. Constraint (2) is the branch power flow limit constraint using

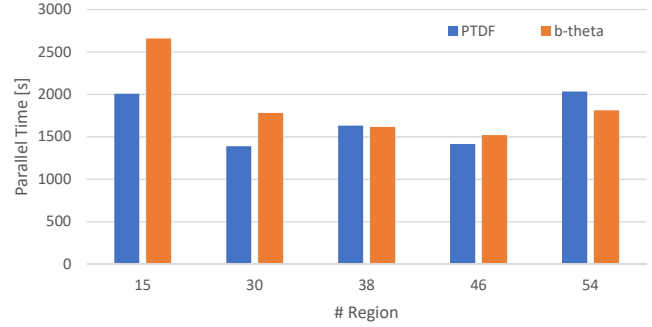


Fig. 1. Parallel time of ADMM-CR plus the first ADMM Bin+ and Bin-cycle.

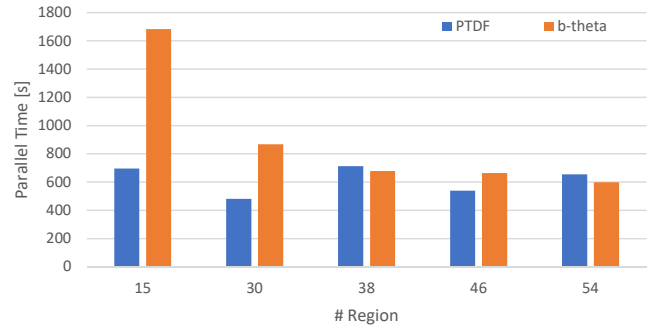


Fig. 2. Parallel time of the first ADMM Bin+ and Bin-cycle.

regional PTDFs. Constraint (3) connects the power injection and the phase angle at the boundary buses using the sensitivity information. $\delta_k \in \{1, -1\}$ represents the direction of tie line k . \mathcal{N}_v^{BB} is the set of boundary buses.

II. SIMULATION RESULTS

A 3012-bus test system from [1] is used in the simulations, and 24-hour hourly UC problems are solved. The system is partitioned by METIS with contiguous option. Only transmission lines that are close to power flow limits using the solution of a centralized UC without network constraints are included. Figure 1 and 2 show that the computational time of the proposed formulation is significantly lower than the formulation used in [1] when the system is partitioned into large regions (the number of regions is small). When the number of regions is large, the difference is small. However, in that case, it can be shown that the distributed algorithm generally takes more iterations to converge.

REFERENCES

- [1] Mohammad Javad Feizollahi, Mitch Costley, Shabbir Ahmed, and Santiago Grijalva. Large-scale decentralized unit commitment. *International Journal of Electrical Power and Energy Systems*, 73:97–106, 2015.

Active and Reactive Power Management of Single Phase Distribution Power Inverters Using Droop Control Based on MIMO Identification

Robin Bisht, *Student Member, IEEE*, Sukumar Kamalasan, *Member, IEEE*,

Abstract—This poster presents a modified power management technique on distributed power inverters based on modified droop equations. The traditional droop technique using P - f and Q - V control law has been implemented to share power between inverters before. Issues arise when power flow in distribution systems do not abide by the traditional droop equations, and active power availability is not reliable. A modified droop control has to be implemented that encompasses the coupling effect of R and X to the active and reactive power flowing through the power inverter. Inverter control topology comprises of the d - q frame active and reactive power control as the inner loop, and the outer loop is responsible for generating virtual active and reactive powers using the impedance matrix, considering the X/R ratio of different networks and/or output filter impedances. This scheme also provides voltage and frequency support during adverse grid conditions by altering the power flow from the inverter. The approach is tested on IEEE 123-bus system.

Index Terms— d - q control, micro-grids, power sharing, stability, single phase inverters, islanding mode.

I. INTRODUCTION

Droop in high voltage transmission is based on P - ω and Q - V droop, and the power sharing problem was solved using this traditional equations. We know that in low voltage networks the R/X ratios are different than that of the transmission systems, hence changing the relation between P , ω , Q and V [1]. The power flowing out of the DER into the network, has a coupling effect on the ω and V . This information will facilitate the generation necessity from the DER [2]. Grid-connected inverters are responsible for the active and reactive power flowing into the network, the outer loop in this paper presents a traditional active and reactive power control for the power inverter.

II. SYSTEM CONFIGURATION AND BACKGROUND THEORY ON MODIFIED DROOP CONTROL

The simulation model contains the DC and AC module of the circuit with the inverter interconnecting the two modules. The DC module contains the PV array with a DC-DC converter, and the Battery with DC-DC converter which is responsible to maintain the DC-link voltage constant. The AC module is the IEEE 123-bus system which acts as the grid to the PV-Battery-inverter systems. Three of these inverter systems have been connected on different points of the 123-bus systems as seen in figure 1.

The inverter active (P) and reactive (Q) power can be expressed as:

$$P = \left(\frac{V_i V_g \cos(\delta - \delta_g)}{Z} - \frac{V_g^2}{Z} \right) \frac{R}{Z} + \frac{V_i V_g \sin(\delta - \delta_g)}{Z} \frac{X}{Z} \quad (1a)$$

$$Q = \left(\frac{V_i V_g \cos(\delta - \delta_g)}{Z} - \frac{V_g^2}{Z} \right) \frac{X}{Z} - \frac{V_i V_g \sin(\delta - \delta_g)}{Z} \frac{R}{Z} \quad (1b)$$

The active and reactive power can be represented as:

$$P = P' \left(\frac{R}{Z^2} \right) + Q' \left(\frac{X}{Z^2} \right) \quad (2a)$$

$$Q = P' \left(\frac{X}{Z^2} \right) - Q' \left(\frac{R}{Z^2} \right) \quad (2b)$$

Where P' and Q' are the virtual active and reactive power components. The equations can be linearized around the nominal values of V_{i0} and δ_0 .

$$\begin{bmatrix} \Delta P \\ \Delta Q \end{bmatrix} = \begin{bmatrix} X/Z & -R/Z \\ R/Z & X/Z \end{bmatrix} \cdot \begin{bmatrix} \Delta(V/Kv) \\ \Delta(f/Kf) \end{bmatrix} \quad (3)$$

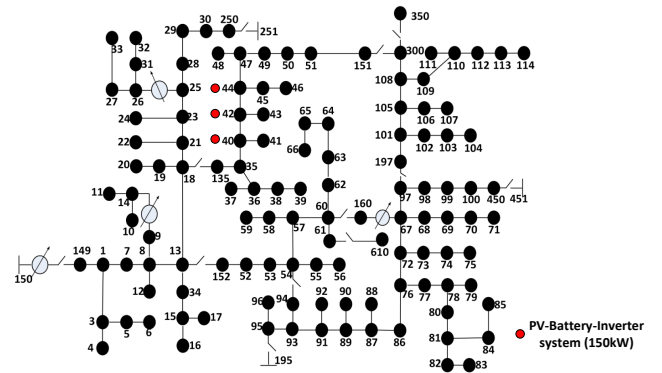


Fig. 1. Active power transfer by the inverter, load and the grid respectively

Equation (3) validates the power coupling and aided by the addition of multiple input and multiple output identification technique can dictate the power of each inverter based on voltage and frequency deviation at any particular bus.

REFERENCES

- [1] J. Liu, Y. Miura, and T. Ise, "Comparison of dynamic characteristics between virtual synchronous generator and droop control in inverter-based distributed generators," *IEEE Transactions on Power Electronics*, vol. 31, no. 5, pp. 3600–3611, May 2016.
- [2] J. C. Vasquez, R. A. Mastromauro, J. M. Guerrero, and M. Liserre, "Voltage support provided by a droop-controlled multifunctional inverter," *IEEE Transactions on Industrial Electronics*, vol. 56, no. 11, pp. 4510–4519, Nov 2009.

PMU Measurement based Synchronous Generator Speed Deviation Signals for PSS Controls

¹Paranietharan Arunagirinathan, *Student Member, IEEE*, ^{1,2}Ganesh K. Venayagamoorthy, *Senior Member, IEEE*

¹Real-Time Power and Intelligent Systems Laboratory,

Holcombe Department of Electrical and Computer Engineering, Clemson University, Clemson, SC 29634, USA

²Eskom Centre of Excellence in HVDC Engineering, University of KwaZulu-Natal, Durban, South Africa

parani@ieee.org, and gkumar@ieee.org

Abstract—Power system oscillations undamped are vulnerable to reliable operation of the electric grid. In history, poorly damped low frequency rotor oscillations have caused system blackouts or brownouts. Synchronous generators are equipped with oscillation damping devices such as power system stabilizers (PSSs). The commonly used input signals for PSSs are rotor speed deviation or frequency deviation. The availability of remote synchronized system measurements from phasor measurement units (PMUs) is used in power system monitoring and control applications. PMU measurement based synchronous generator speed deviation signals are studied in this paper. A two-area four machine benchmark power system integrated with a utility scale PV power plant has been simulated on a real-time digital simulator (RTDS) platform for this study. The results are obtained for different PMU reporting rates and compared the physical and simulation based PMU responses.

Index Terms—PMUs, power system, RTDS, rotor speed deviations, synchronous generators.

I. INTRODUCTION

Phasor measurement unit (PMU) technology brings the system wide measurements for power system monitoring and sophisticated controller design. PMU measured synchronized measurements are hundred times faster compared to supervisory control and data acquisition (SCADA). PMU measurements are compliance to IEEE standard C37.118.2014 [1]. PMU measurements have been used in numerous power system applications including power plant model validation, state estimation, event analysis, oscillation detection and analysis, system islanding detection etc, [2], [3]. Also there are PMU data driven control center monitoring and visualization tools have been developed. In [4] synchrophasor measurements based power system electromechanical modes and damping ratios are displayed to assist control center operators. Power system stabilizer (PSS) input signal from RSCAD [5] simulation PMU and physical PMU devices are studied on a benchmark test power system shown in Fig. 1.

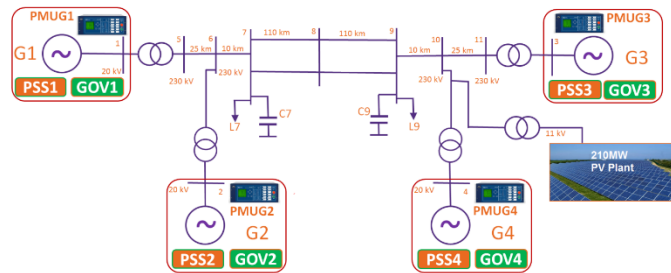


Fig 1. Two-area test system with PMUs

PMUs are configured with different reporting rates such as 30Hz, 60Hz, etc. PMU estimated speed deviation measurements are fed to PSSs in a loop to study the differences during the steady state and transient conditions of the system. System disturbances studied are line-to-ground short circuit placed at bus 8 and a sudden PV power variation.

II. REFERENCES

- [1] *IEEE Standard for Synchrophasor Measurements for Power Systems*, IEEE Std C37.118.1-2011 (Revision of IEEE Std C37.118-2014), 2014.
- [2] A. G. Phadke and J. S. Thorp, *Synchronized Phasor Measurements and Their Applications*, New York: Springer Science+Business Media, LLC, 2008.
- [3] I. Kamwa and R. Grondin, "PMU Configuration for System Dynamic Performance Measurement in Large Multiarea Power Systems," *IEEE Transactions on Power Systems*, vol. 17, no. 2, pp. 385-394, 2002.
- [4] P. Arunagirinathan and G. K. Venayagamoorthy, "Situational Awareness in an Electric Utility's Control Center of its Generators' Damping Capabilities," in *IEEE Power & Energy Society Innovative Smart Grid Technologies Conference (ISGT)*, Washington DC, 2017.
- [5] "RTDS Technologies," [Online]. Available: <https://www.rtds.com/>. [Accessed 12 October 2018].

This work is supported in part by US National Science Foundation (NSF) under grants #1312260 and the Duke Energy Distinguished Professor Endowment Fund. Any opinions, findings and conclusions or recommendations expressed in this material are those of the author(s) and do not necessarily reflect the views of National Science Foundation and Duke Energy.

Scalable Demand Response Scheme with Limited Information Flow

Pramod Herath, *Student Member, IEEE*, Ganesh K. Venayagamoorthy, *Senior Member, IEEE*
Real-Time Power and Intelligent Systems (RTPIS) Laboratory
The Holcombe Dept. of Electrical and Computer Engineering
Clemson University, SC 29634, USA
Emails: {Pramod.u.herath, gkumar}@ieee.org

Abstract— In this research, a large-scale demand response management scheme for residential customer is introduced that makes use of a hierarchically-structured demand response aggregator called ‘Service Provider’ which controls the demand response at different levels of the power system. The direct-control demand response scheme limits the amount of information flow to a limited ‘neighborhood’. The hierarchical nature of the service provider enables the scheme to be easily scalable.

Index terms-- Demand response; Particle Swarm Optimization, service provider, smart neighborhood.

INTRODUCTION

The increasing volatility of the power system due to the large scale integration of renewable energy as well as the ever increasing demand for electric power means that demand response is an essential component of the future smartgrid. Demand response paves way to effectively utilize the existing power generation sources as well as other infrastructure making it both economical as well as environmentally friendly.

Although demand response resources are available in both industrial and commercial/residential sectors, demand response participation in the residential sector is quite low. The reasons include the lack of incentives, privacy concerns, lack of awareness among the customers, and other infrastructure concerns. Yet one third of the total electricity usage is attributed to residential section. In this research a distributed demand response management scheme is introduced, which adopts a direct load control method but still could limit the outflow of personal data to a small pocket of households. The scalable DR structure is made up of several entities: the Home Energy Management System (HEMS), the “Smart Neighborhood” and the “Service Provider” (SP). The following paragraphs describe each of these entities in detail.

A. Home Energy Management System

The HEMS controls the energy usage of the home. HEMS collects the user data from the customer and creates a flexibility schedule for the home. Which it then forwards to the local Service Provider and then awaits an energy schedule

from the service provider. HEMS is also in charge of buying energy and selling unused energy according to its policies.

B. Smart Neighborhood

The Smart Neighborhood is a collection of co-operative set of households which are geographically close to each other. The number of households that belong to the same neighborhood is limited. In our study, this number is limited to twenty households. A Smart Neighborhood entity falls under the control of a Service Provider. The Smart Neighborhood is the only entity that shares individual power consumption data among themselves. The appliances of the members of a Smart Neighborhood is allowed to be controlled by the Service Provider.

C. Service Provider

The service provider[1,2] is the hierarchical structure that controls the demand response scheme. The service provider is essentially the lowest level of a service provider controls a smart neighborhood. The task of the lowest level service provider is to control the loads of the neighborhood as well as to aggregate the demand response flexibility of the neighborhood. Once aggregated, the total flexibility is then passed on to the upper level service provider, which, is in control of a set of such service providers. The upper level service provider would then create higher level demand response schedules by taking the flexibilities of each lower level service provider into account. This hierarchy could expand into any number of levels depending on the number of households available for the demand response. This paper contributes by introducing algorithms that the service provider could use to optimize the demand response scheduling of the service provider as well as by introducing algorithms that could optimize demand response in higher levels.

REFERENCES

- [1] P. U. Herath et al., "Computational Intelligence-Based Demand Response Management in a Microgrid," in *IEEE Transactions on Industry Applications*, vol. 55, no. 1, pp. 732-740, Jan.-Feb. 2019.
- [2] P. Herath and G. K. Venayagamoorthy, "A service provider model for demand response management," *2016 IEEE Symposium Series on Computational Intelligence (SSCI)*, Athens, 2016, pp. 1-8.

Data-Driven Frequency Sensitivity Analysis for Utility-Scale PV Plants

Ali Arzani¹ and Ganesh K. Venayagamoorthy^{1,2}

¹Real-Time Power and Intelligent System Laboratory, Clemson University, SC, USA

²School of Engineering, University of KwaZulu-Natal, Durban, South Africa

aarzani@g.clemson.edu and gkumar@ieee.org

I. RESULTS & DISCUSSION

Solar irradiance step/ramp events can lead to frequency issues at PCC, affecting grid frequency. Taking into account solar irradiance step/ramp events is crucial for PV-VSI control and real-time dispatch operations of PV plants. It will assist the balancing authority in the control area to better understand and deal with solar irradiance step/ramp events and the challenges it introduces in terms of intermittency and variability of PV power generation at PCC. In order to counteract the frequency deviations injected to PCC from utility-scale PV plant operation during such inclement weather conditions, situational awareness on these PV generated frequency deviations seems to be a necessity to TSOs in the control area. That is to take proper measures in regulating the PV bus frequency in few seconds and in a cost-effective manner. Thus, characterization of the

frequency droop from utility-scale PV plant operation and identification of its power-frequency characteristics curve has been accomplished in multiple steps in this research.

Centralized and geographically distributed utility-scale PV plants operation at different solar irradiance levels and under changing meteorological conditions is analyzed through obtained data of Fig. 1, in order to derive a systematic data-driven method for characterizing the variations in power system frequency originating from the PV plant(s) operation. The empirical method is formulated to compensate for each PV-bus unique frequency variations due to variations in injected PV power at different irradiance levels and locations in the control area. The algorithm is implemented on bulk energy storage systems, such as SmartParks as summarized in Fig. 2 for novel adaptive PFACS in the smart grid.

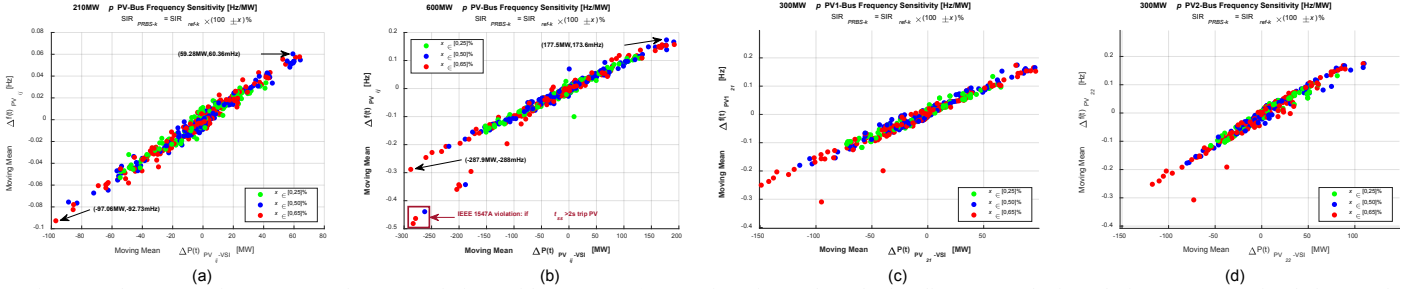


Fig. 1 PV bus power-frequency steady-state variations with respect to $(P_{PVref,k} \int f_{PVref})$ i.e. under solar irradiance perturbations during 1800sec. simulation run for all $SIR_{ref}=100:100:1000W/m^2$. (a) centralized $210MW_p$ PV plant, (b) centralized $600MW_p$ PV plant, (c) distributed PV plants ($2 \times 300MW_p$)

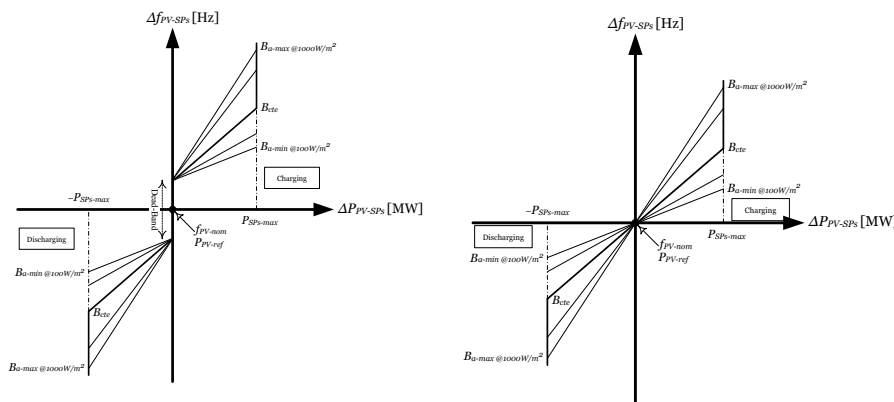


Fig. 2 Aggregate PV-ESS steady-state adaptive frequency droop characteristics curves and formulation for PFACS at PV-ESS PCC.

$$\overline{\Delta B}_k^{PV} = + \frac{\sum_{n=1}^m \Delta B_k^{PV} (4,x)}{m}, \forall: \begin{cases} SIR_{ref,k} = 100k, k = 1, 2, \dots, 10 \\ SIR_{pRBS_k} = SIR_{ref,k} \cdot (100 \pm x)\% \\ x \in \{[0, 25]\%, [0, 50]\%, [0, 65]\%\} \end{cases}$$

$$\Delta f_{PV} (\Delta P_{PV}) = \overline{\Delta B}_k^{PV} \cdot (\Delta P_{PV})$$

$$B_{cte}^{PV} + \sum SP_{ij} = B_{cte}^{SP_{ij}} \sqrt{B_{cte}^{SP_{ij}}} + \overline{\Delta B}_k^{PV}$$

$$PV_{ij} + \sum SP_{ij}: \text{Area (i) Aggregate PV - SmartParks}$$

$$B_{cte}^{SP_{ij}} = \begin{cases} B_{cte}^{SP_1} & \text{if } B_{cte}^{SP_1} = \dots = B_{cte}^{SP_n} = B_{cte}^{SP} \\ \sum_{n=1}^{N_{SP_{ij}}} \frac{P_{nom}^{SP_n}}{B} & \text{if } B_{cte}^{SP_1} \neq \dots \neq B_{cte}^{SP_n} \end{cases}$$

Renewable Distributed Energy Resources Impact on the Macroeconomics Under Net-metering Policy

Mohannad Alkhrajah¹², Bader Alaskar², Abdullah Alsubaie³, Carlos Batlle Lopez⁴⁵

¹Electrical and Computer Engineering Department, Georgia Institute of Technology, Atlanta, GA, USA

²Center for Complex Engineering Systems, King Abdulaziz City for Science and Technology, Riyadh, Saudi Arabia

³Water and Energy Research Institute, King Abdulaziz City for Science and Technology, Riyadh, Saudi Arabia

⁴Institute for Research in Technology, Comillas Pontifical University

⁵MIT Energy Initiative

Email: malkhrajah@kacst.edu.sa

Abstract—Green energy initiatives and the continuous cost reduction of renewable energy resources lead to a steady growth rate of renewable distributed energy resources (DER), especially rooftop solar photovoltaic (PV). One of the most common policies deployed by power system operators is net metering. The objective of this study is to evaluate the economic impact of high penetration of rooftop solar PV under the net metering policy. A dynamic network-based model is proposed to simulate the impact of rooftop solar PV from the customers, utilities, and government perspective. A case study is shown to assess the economic impact with different rooftop solar PV penetration in Riyadh City, Saudi Arabia using the proposed model. One-year datasets of customers' consumption, power grid operation cost, and fuel prices are used to evaluate the economic impact. The model can show the overall energy cost, grid operation cost, and government fuel subsidies at different solar PV penetration levels.

I. INTRODUCTION

The penetration of renewable distributed energy generation (DER) has been increased significantly in recent years. The high deployment rate of DER especially rooftop solar PV is mainly derived by the cost of renewable energy resources and the global direction to reduce the dependency on fossil fuel-based generation to reduce carbon emissions [1]. Many regulators around the world implement net metering policy for rooftop solar PV, where a predefined price is set for selling and purchasing energy. Although rooftop solar PV systems became economically feasible for customers, the overall cost of energy may increase due to high penetration level. Technical challenges related to availability, protection and thermal limit of the power system components in addition to other technical issues are expected to emerge due to the high deployment of DER [1]. The economic value of installing rooftop PV under the net metering policy may attract customers to install rooftop solar PV. Damping excess energy in the morning equivalent to the absorbed energy in the evening, customers with rooftop PV might utilize the power grid free of charge. The consequences of this behavior might affect low-income customers who can't afford to install rooftop solar PV by charging them more to compensate for the power grid cost. In that case, the cost of the grid and energy will be carried by the utilities and other customers without rooftop solar PV [2].

II. METHODOLOGY

In this poster, a dynamic network model is proposed to simulate and evaluate the economic impact of implementing net metering for the deployment of rooftop PV on the current power system. Two coupled dynamic networks are constructed to model financial and energy transactions. Entities with similar function are aggregated and represented

in a single node in the two networks, and each arc represents the dynamic financial and energy transactions between two nodes. Six different entities are considered; government, fuel suppliers, generation companies, system operators, distribution companies and customers. The government are included in this model to reflect government subsidies. Two categories of customers are considered; early adopters and users with no rooftop solar PV. Fig. 1 shows the two networks represent the financial and energy flows.

III. CASE STUDY

A case study is shown for Riyadh City, Saudi Arabia, where a net metering policy is applied to show the economic impact. Actual data of the customers' consumption in Riyadh city, fuel prices, grid operation costs are used to model the economic impact. Several scenarios are simulated using the proposed model, and the result shows that high DER penetration will lead to a decrease in government subsidies due to the reduction in subsidized fossil fuel demand. However, the overall cost of energy is expected to increase which might lead to an increase in energy prices for the customers.

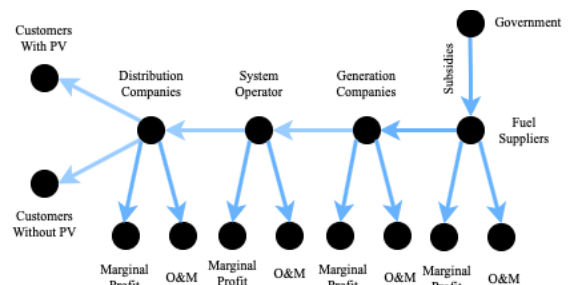


Fig. 1. Dynamic network for the financial transactions

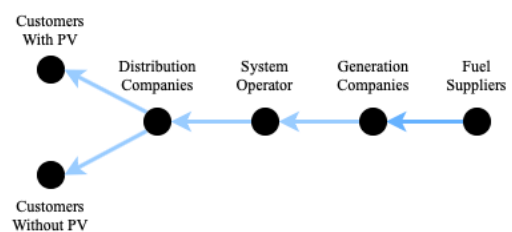


Fig. 2. Dynamic network for the energy flow

REFERENCES

- [1] I. Perez-Arriaga, et al., "Utility of the Future," MIT Energy Initiative, Dec 2016
- [2] I. Adjali, et al., "Can Adoption of Rooftop Solar PV Panels Trigger a Utility Death Spiral? A Tale of Two Cities", King Abdullah Petroleum Studies and Research Center (KAPSARC), May 20

Federation based Cyber Physical Security (CPS) Testbed for Wide-Area Protection and Control in Smart Grid

Vivek Kumar Singh, Manimaran Govindarasu
Department of Electrical & Computer Engineering
Iowa State University, Ames, IA, USA
(Email: vsingh@iastate.edu, gmani@iastate.edu)

Don Porschet, Morris Berman, Edward Shaffer
U.S Army Research Laboratory
Adelphi, MD, USA

Abstract— Cyber Physical Security (CPS) testbed plays a vital role in the development, evaluation, and validation of novel technologies to secure the critical infrastructure like smart grid and to make it attack-resilient. It works as a driving force to accelerate the transition of state-of-the art research works to the industrial products by experimental testing and verification. Most of the published works are based on the traditionally isolated CPS testbeds which do not provide a realistic platform and requires significant investment in money, resources and system modelling. This project aims to go beyond the isolated testbed and develop the sophisticated, federated testbed to provide realistic attack-defense platform. In this project, we present a testbed federation architecture for CPS security/resiliency experimentation by leveraging the resources available at Iowa State University's Power Cyber (ISU) and the US Army Research Laboratory (ARL). Specifically, we have focused on the wide-area protection and control, also known as automatic generation control (AGC) and remedial actions scheme (RAS), which are required to maintain the stability and reliability of smart grid. In this work, we have developed the cyber physical federated testbed where the ARL's testbed is working as multiple substations and the control center is operating at the ISU. We also shows the prototype implementation and demonstration, where the control center receives the power system measurements which are further processed by the anomaly detector to identify possible anomalies including cyber-attacks in real-time.

Communication-free voltage regulation of distribution power grids

Rayan El Helou, *Student Member, IEEE*, Le Xie, *Senior Member, IEEE*,

Abstract—We tackle voltage regulation in distribution networks and propose a novel approach in which nodes in the network do not need to communicate with each other to ensure voltage stability. More specifically, each node/bus is treated as an agent which can only measure the local voltage and decide what amount of reactive power to inject at the same location. We show that under such constraints, there is a closed form expression for the stability region of the control policies that can ensure that all voltage levels approach desired value. We also develop theory regarding the independence of agents and prove some properties of this region.

I. INTRODUCTION

In the presence of Distributed Energy Resources (DERs), such as solar and wind, the operating conditions in a distribution network tend to heavily fluctuate causing undesired voltage deviations. To address this, the same DERs, which provide the capability to supply real power, can also provide reactive power injection which can help regulate the voltage. This can be achieved through inverter control and local sensing [1]. Given the ability to inject reactive power, the natural question is how to control it, and how to manage the communication and control across the entire network? One of the most recent efforts to tackle this issue is introduced by Qu and Li [2]. In their work, a distributed control method is proposed in which each agent communicates with one-hop-away neighbors, and provides both local measurements along with auxiliary variables that help the agents coordinate and strategize their control so that all the nodes achieve desired voltage levels. Our contribution is to prove that we can still achieve desired voltage levels but without the need for communication between agents.

II. VOLTAGE RESPONSE TO REACTIVE POWER INJECTION

In [2], the following model is shown as a linear approximation to describe how injection of reactive power can affect the voltage level across the network. Note that our results from Figure 1 is based on simulation of the full nonlinear power flow model.

$$\mathbf{v} = X\mathbf{q} + \mathbf{v}_0 \quad (1)$$

where \mathbf{v} is the vector of squared voltages at all the nodes and \mathbf{v}_0 is the operating voltage under no changes in reactive power. \mathbf{q} is the amount of reactive power injected at all the buses and X is a constant system-wide parameter that is determined by the line parameters.

III. PROPOSED CONTROL ALGORITHM

We propose that if each agent i receives only local measurement v_i , and appropriately selects control policy scalar g_i , then by applying the following control, all bus voltages approach desired value.

$$\Delta q_i = g_i(v_{des} - v_i) \quad (2)$$

We show how to select the appropriate g_i for each agent i and prove that the stability region (the set of g_i 's that ensure system stability) is convex, and even if some agents do not inject input, the voltage level of other agents can still be stabilized. Moreover, we prove that under a given set of control policies that do stabilize the system, if some agents reduce their g_i value (control policy gain) at a given time, this provides a more relaxed (expanded) stability region for the other agents.

This not only allows for the lack of need of communication between agents, but it also allows the designer of the control policies to test under only 1 scenario which is when all agents are assumed to be active. Then, if each agent uses this dispatched design as a boundary to their g_i value, we know that all voltages can still be stabilized even if individual g_i values are varied within boundary. Therefore, agents do not need to be aware of each others' activities.

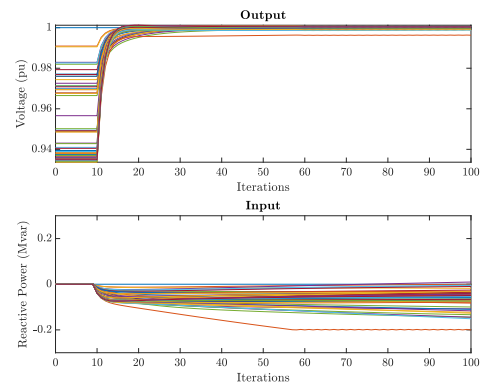


Fig. 1. Communication-free control by injection of reactive power.

REFERENCES

- [1] J. W. Smith, W. Sunderman, R. Dugan, and B. Seal, "Smart inverter volt/var control functions for high penetration of PV on distribution systems," in *2011 IEEE/PES Power Systems Conference and Exposition*. IEEE, mar 2011. [Online]. Available: <https://doi.org/10.1109/psce.2011.5772598>
- [2] G. Qu and N. Li, "Optimal distributed feedback voltage control under limited reactive power," 2018.

Optimal Control for Load Ensembles in Smart Buildings

Ali Hassan, Yury Dvorkin

Department of Electrical and Computer Engineering, Tandon School of Engineering,
New York University, New York, NY, USA, (ah3909,dvorkin)@nyu.edu

Abstract—A large number of distributed energy resources (DERs) such as PV arrays, thermostatically controlled loads (TCLs), energy storage units are being deployed in modern distribution grids. This massive integration of DERs can compromise the reliability of the power systems and challenge the economies of day to day operations due to their intermittent nature. From the technical perspective, such challenges include multi-directional power flows, volatile power injections and voltage fluctuations. One way to deal with such challenges is to explore the potential of behind the meter demand response (DR) resources. DR enrolls flexible loads to provide various grid support services without sacrificing comfort levels of electricity consumers significantly. Controllable electrical and heat appliances in a residential and commercial building can provide significant flexibility to electrical and heat distribution systems by adjusting their consumption to help meeting operational system limits and alleviate overloads. They are usually controlled by an aggregator (has a very large number of similar devices) who serves as a mediator between the distribution system operators (DSO) and TCLs Fig. 1.

Index Terms—Markov Decision Process, Ensemble, Building, Flexibility, Demand Response

I. MODEL SUMMARY

We propose to model an ensemble of heat and electrical appliances as a discrete time, discrete space Markov Decision Process (MDP) [1]. The MDP is well suited for capturing stochastic dynamics of individual appliances, computationally scalable to accommodate thousands of homogeneous appliances in each ensemble and have computational and analytic tractability rendered by solution techniques based on dynamic programming. These properties make MDP a suitable choice to model the such ensembles. Fig. 2 represents an ensemble which is discretized in 8 states. Furthermore, we use linearly solvable MDP (LS-MDP) method, which has no explicit actions as in traditional MDP, and control consists in changing a predefined default probability distribution over next states. The optimal policy obtained with the LS-MDP is not a mapping of states to action variables, but a next-state distribution which minimizes the accumulated state costs of the agent traversing the state-space, while minimizing a divergence cost between the controlled (transition decisions made by the aggregator) and default probability distributions (driven by comfort levels of consumers).

We construct a Markov Process (MP) to represent the energy consumption of building appliances to assess the building flexibility. First, the physical building model is used to characterize the MP using the default probability transition matrix.

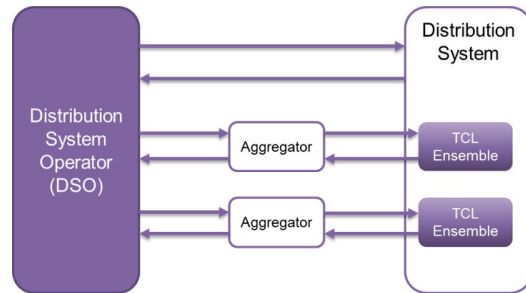


Figure 1. Schematic representation of a hierarchical load control strategy

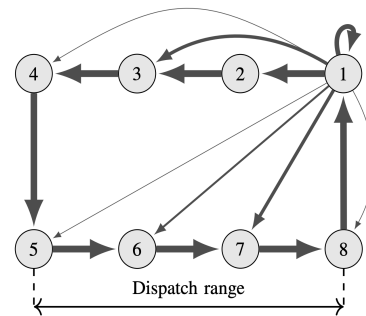


Figure 2. A Markovian representation of the ensemble of electrical or heat appliances with eight discrete states displaying all possible transitions from state 1.

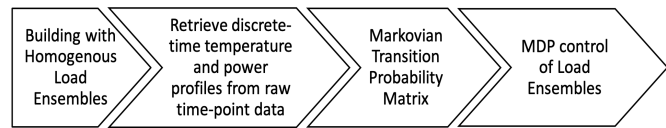


Figure 3. Markov Decision Process in the Context of A Portfolio of Buildings.

Based on this MP, we formulate the Markov Decision Process that can in turn be used to optimally control electric and heat appliances within buildings either by the local utility, or third-party aggregators, or building managers. This process is illustrated in Fig. 3 and presented in detail in our paper in [2].

REFERENCES

- [1] A. Hassan, R. Mieth, M. Chertkov, D. Deka, and Y. Dvorkin, "Optimal load ensemble control in chance-constrained optimal power flow," *IEEE Transactions on Smart Grid*, pp. 1–1, 2018.
- [2] R. Pop, A. Hassan, K. Bruninx, M. Chertkov, and Y. Dvorkin, "A markov process approach to ensemble control of smart buildings," *2019 IEEE PowerTech, Milan, Italy*, July 2019 (Accepted).

Automated Switching Operation for Resilience Enhancement of Distribution Systems

Mohammad Mehdi Hosseini, Amarachi Umunnakwe, Masood Parvania
 Department of Electrical and Computer Engineering
 University of Utah, Salt Lake City, UT 84112
 Emails: {mehdi.hosseini, amarachi.t.umunnakwe, masood.parvania}@utah.edu

Abstract—This paper proposes a model to assess and quantify the impacts of automated fault location, isolation and service restoration (FLISR) on resilience of power distribution systems against wide-spread failure events (e.g., natural disasters). The proposed model includes defining and formulating six probabilistic metrics that capture the capability of FLISR system in fast restoration of load after outage scenarios. In addition, this paper elaborates the contribution of different automation components, such as fault locators and remotely-controlled switches, to each of the proposed metrics. The proposed model is utilized to assess the resilience of a three-feeder test distribution system against hurricane. The numerical results show that the proposed metrics reflect the impacts of different automation strategies on enhancing resilience of the system, which provide critical information for making decisions on implementing the resilience enhancement strategies in distribution systems.

Index Terms—Power system resilience metrics, distribution automation, fault location, isolation and service restoration.

I. CONTRIBUTIONS & HIGHLIGHTS

This paper proposes a set of six probabilistic resilience metrics to assess the dynamics of load served during the outage scenarios after an extreme event and quantify the various impacts of automated fault location, isolation and service restoration operation on the resilience of power distribution systems. In addition, this paper evaluates the impacts of automation devices (e.g., automated fault locators and switches) and their automation level on each of the proposed metrics and identifies the metrics in which each component has the most impact. The results are valuable in decision making on installing automation equipment, as well in optimizing device location or planning of distribution automation. Comparison of the proposed metrics with existing ones show the usefulness of the presented model in resilience assessment of automated distribution systems. The proposed probabilistic metrics include Expected Maximum Load Loss, Expected Load Interruption Rate, Expected Automatic Restoration Time, Expected Load Restored by Automation, Expected Repair Time, and Expected Energy Not Served.

II. APPLICATION IN RESILIENCY EVALUATION

The proposed metrics are able to reflect the rapid and automatic operation of FLISR in fast system reconfiguration following an incident. Contribution of fault indicators and automatic switches as well as the level of automation in

resilience of distribution systems are evaluated using the proposed metrics. Numerical studies on a three-feeder test distribution system demonstrate the impacts of different automation cases on resilience of the system against a simulated hurricane. The results indicate that automated fault location and service restoration substantially improves the resilience metrics. The switching speed during service restoration is the most critical parameter of FLISR impacting the metrics. Applying higher levels of automation and reclosing capability in switches in the system substantially reduced the switching time and the resulting resilience metrics. To check the applicability of our metric framework, we assumed a hurricane passes by the test system and a total of 5000 hurricane scenarios are simulated for a 24-hour horizon. The operation of the FLISR system is evaluated for each outage scenario on the test feeder, and the outage times and interrupted loads are calculated. The resilience metrics are calculated for the test system for four cases with different automation devices and different FLISR schemes. The resulting curves of the expected load served during the hurricane in different cases are shown Fig. 1. Fig. 2 demonstrates how the expected components of our metric framework is extracted from scenarios of one of the cases.

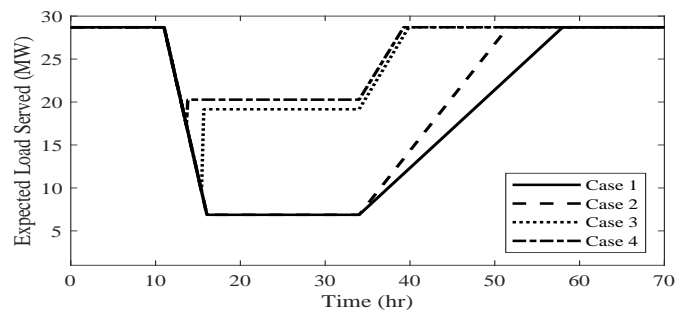


Fig. 1. Expected load served in the study cases

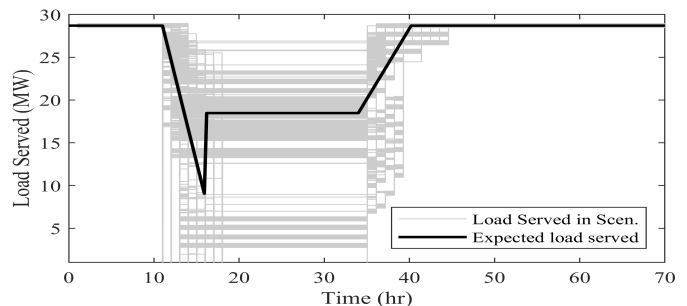


Fig. 2. Expected load served, and load served in scenarios – Case 3

Automated Transformation of IEC 61850 Substation Models to IEC 61499 Applications

Tin Rabuzin*, Francisco de Lima*, Yiming Wu†, and Lars Nordström*

*Department of Electric Power and Energy Systems, KTH Royal Institute of Technology, Stockholm, Sweden

† Vattenfall Services Nordic, Sweden

Abstract—Increasing numbers of substation automation systems (SASs) are designed using the IEC 61850 standard. Even though IEC 61850 standardizes information modelling, applications residing in IEDs still need to be manually configured. This work proposes a top-down approach to SAS design workflow which involves automated transformation of IEC61850 models to IEC 61499 applications. These applications can then be deployed using minimal manual engineering work.

Index Terms—substation automation systems, model transformation

I. PROBLEM FORMULATION

Design and deployment of SASs is a complex process involving both hardware and software supplied by different vendors. In order to allow for interoperability within substations, IEC 61850 standardises modelling of elements of SASs and defines a set of communication protocols which allow unambiguous exchange of information between those elements. The basic building blocks of a substation’s information model are Logical Nodes (LNs) such as a PTOC LN for an overcurrent protection. One can view a IEC 61850 information model as a collection of logical nodes. The model, however, does not completely define functionality of LNs, nor their interconnections apart from the ones requiring the use of the aforementioned communication protocols. The lack of this modelling information obscures parts of the functionality of a SAS.

The standard IEC 61499 arose from the domain of industrial automation systems. One of the benefits it provides is a modelling approach for distributed control applications using a basic execution unit called a function block (FB). Therefore, a parallel can be drawn between the IEC 61850 and IEC 61499 where one can map an IEC 61850 model to an IEC 61499 application model, and LNs to FBs. However, a missing piece of the puzzle is, as was mentioned before, the information about the logical interconnections of different LNs. The missing piece is what we are trying to address in this work.

II. PROPOSED WORKFLOW

The system operators tend to reuse designs of the substations [1]. In some cases, there are predefined design rules which vary depending on the parameters of the substations, e.g. voltage levels, number of bays, etc. The proposed workflow will thus exploit these rules and fill the information void caused by the lack of the interconnections in the IEC 61850

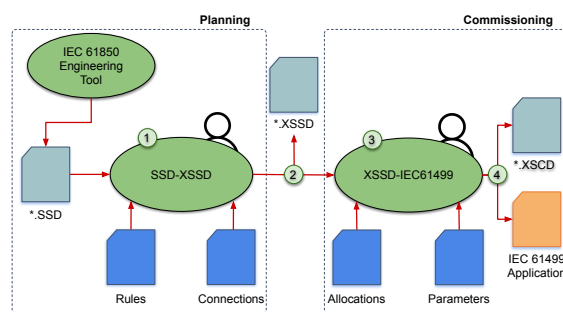


Fig. 1. Proposed workflow

models. The steps of the workflow shown in Fig. 1 are as follows:

- 1) The planning group designs a single line diagram (SLD) in IEC 61850 engineering tool and exports it in the form of an *.SSD file. They import it into the transformation tool along with a library of desired FBs corresponding to the LNs to be used in the substation. Standard configuration rule list describing a generic utility design guideline and substation-specific connection lists are imported.
- 2) The tool processes these files and creates an extended SSD file (*.XSSD) which, in addition to SLD, contains interconnections between all of the LNs, i.e. FBs. This file is then delivered to commissioning engineers.
- 3) They import the *.XSSD file, a file specifying allocations of LNs to specific IEDs in a substation and a list of parameters for all of the protection functions.
- 4) The tool generates the IEC 61499 application which can then be deployed on the IEDs and exports the extended SCD file containing the complete IEC61850 model of the substation and the IEC 61499 application model.

In order to validate the workflow, an open-source transformation tool and a library of FBs were developed. A substation model was transformed and tested on a 4DIAC runtime environment with hardware-in-the-loop simulation [2].

REFERENCES

- [1] “Technical requirements - relay protection line bay 145 kV” E.ON Elnät, Sweden 2017.
- [2] T. Strasser *et al.*, “Framework for Distributed Industrial Automation and Control (4DIAC),” *2008 6th IEEE International Conference on Industrial Informatics*, Daejeon, 2008, pp. 283-288.

Prevention of Cascading Failures in Stressed Power System using Energy Functions

Abhishek Banerjee, *Student Member, IEEE*, and Rajesh Kavasseri, *Senior Member, IEEE*

Abstract—In stressed power systems, relay misoperations could be possible when high loadings are misinterpreted as faults. A typical event that aggravates a cascade is a trip decision by distance relays to faults in zone 3. We examine the use of energy functions as a discriminant in such scenarios to supervise the action of distance relays, in particular, to distinguish between load encroachment and zone 3 faults. This approach is guided by the line energy function component W_{25} . The idea is to use the energy function component W_{25} as an identification tool that will help improvise tripping decisions for the distance relays. We plan to monitor the activity of W_{25} in such events and use it as an input variable of a supervisory control system. The corresponding action will be able to avert the misoperation of relays, thus limiting the cascade.

Index Terms—Blackout, Energy Functions, Relay misoperation, Supervisory Protection, Stressed Power System

I. INTRODUCTION

CASCADING failures in bulk power systems has been a major topic of research. Real time monitoring of the stressed power system can play a major role in dissecting a cascading sequence. Energy functions are intrinsically tied to their physical subsystems and serve as pointers to exactly pinpoint the location of the fault. This unique feature of energy functions enable it as an useful feature extraction tool as explored in [1], [2]. Since it is independent of relay settings, it can be potentially be used as an alternative index to monitor and supervise the actions of distance relays in response to critical system events.

II. SELECTING ENERGY COMPONENT

We consider the models for the system dynamics and measurements in the form of (1),

$$x_{k+1} = f_k(x_k, w_k), \quad y_k = h_k(x_k, v_k) \quad (1)$$

where w_k and v_k are white independent noise processes with known pdf ($N(0,R)$), used for the particle filter design, refer to [1]. The relative change in magnetic energies stored in the transmission lines is captured by the P.E. component W_{25} [1]. This component can be calculated using (2),

$$W_{25} = -1/2 \sum_{i=1}^N \sum_{j=1}^N B_{ij} (V_i V_j \cos(\phi_{ij}) - V_{i0} V_{j0} \cos(\phi_{ij0})) \quad (2)$$

here, $B_{ij} = \text{Imag}(Y_{ij})$, where Y_{ij} is the system bus admittance matrix and $\phi_{ij} = \phi_i - \phi_j$. The subscript "0" here denotes the pre-fault values.

A. Banerjee and R. Kavasseri are with Department of Electrical & Computer Engineering, North Dakota State University, Fargo, ND, USA (e-mail: abhishek.banerjee@ndus.edu, rajesh.kavasseri@ndus.edu).

III. RESULTS AND FUTURE WORK

Fig. 1 (a) indicates the change in W_{25} due to the fault is very high as opposed to relay misoperation. Two similar scenarios were simulated in zone 3 of the relay, as shown in Fig. 1 (b), but further away from the previous distance. We observe that W_{25} peaks instantly after the fault is simulated, whereas the relay misoperation shows comparatively lesser deviation. It can be observed that W_{25} shows significant changes with respect to different locations in zone 3 of the relay, for both the events.

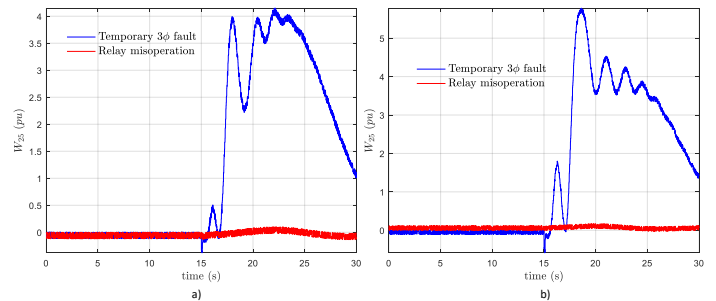


Fig. 1. Change in W_{25} subject to temporary 6-cycle, 3ϕ fault and relay misoperation between (a) bus 26-28, (b) bus 26-27 in IEEE 39-bus New England test system, simulated at $t=15s$.

We plan to emulate a real-time cascade on hardware setup in the future, shown in Fig. 2 and use the proposed supervisory control variable to arrest the progression of the cascade.



Fig. 2. Integrated setup for real-time testing of the proposed approach on blackout sequence

REFERENCES

- [1] R. G. Kavasseri, Y. Cui and S. M. Brahma, "A new approach for event detection based on energy functions," 2014 IEEE PES General Meeting, National Harbor, MD, 2014, pp. 1-5.
- [2] A. Banerjee, M. Maharjan and R. G. Kavasseri, "Fault Mapping in Multi-machine Power Systems by Principal Component Sensitivity-An Energy Function Perspective," 2018 North American Power Symposium (NAPS), Fargo, ND, 2018, pp. 1-6.

Machine-Learning based Advanced Situational Awareness: Prediction of Event Propagation

Paroma Chatterjee, *Student Member, IEEE*, Ramin Vakili, *Student Member, IEEE*, and Mojdeh Khorsand, *Member, IEEE*
 School of Electrical, Computer and Energy Engineering, Arizona State University, Tempe, AZ, USA
pchatte6@asu.edu, rvakili@asu.edu and mojdeh.khorsand@asu.edu

Response of a power system to disturbances depends on dynamics of the system and settings of protection schemes. As such, improving situational awareness requires simultaneous assessment of system’s dynamic characteristics as well as analysis of protection scheme behavior.

Prior analysis confirmed that protection and control schemes play major roles during blackouts; 70% of blackouts involve hidden failures of protection schemes [1]-[2]. Conventional methods for analyzing dynamic performance and protection system behavior are too slow for real-time implementation of situational awareness. Furthermore, these methods need complete information about system topology and state variables. This paper proposes an approach based on machine-learning (ML) algorithms to predict system response in terms of generator coherency and relay operation after the occurrence of a disturbance. The proposed approach can assist power system operators in making faster and more informed decisions about system status and essential remedial actions, by predicting the outcome of an event and system response in advance in order to hedge against cascading outages.

After the occurrence of an event, depending upon its severity and proximity, a single/group of generators may lose synchronism with each other and/or the rest of the system, and form coherent groups. Apart from the initial operation of distance relays due to the fault, loss of synchronism may result in voltage dips across multiple lines, due to a local or widespread power swing. This results in additional line protection operation. In case of events, where the generation in an area is not sufficient to supply all the loads, load-shedding relays, under-frequency (UFLS) and under-voltage (UVLS), start operating. Discrete load shedding nature of UVLS and UFLS relays can further exacerbate system condition by causing larger supply and demand unbalance. Adequate remedial action schemes need to be initiated to prevent cascading outages and uncontrolled islanding.

This paper proposes ML based approaches to predict coherent groups of generators as well as distance relay and UFLS and UVLS relay operations with high level of confidence in advance. These attributes are utilized to identify the impact of the initial event as it spreads through the system and help the operator make an informed decision in the shortest possible time.

With the advancements made in power system monitoring, there is an overwhelming amount of data being produced. Utilizing this data and its underlying patterns, ML-based data analytics has proven to be an effective tool for analysis and control of modern power systems. This paper uses supervised learning methods such as logistic regression (LR), support vector machine (SVM), artificial neural network (ANN), and random forest (RF) to predict generator coherency and relay operations based on phasor measurement unit (PMU) data. Once the algorithms are trained using multiple contingency scenarios (simulated during offline studies and/or historic data), they can be used

for online prediction of post-contingency system behavior. Moreover, moving window-based learning has been utilized to train the algorithms to predict the events that are about to unfold based on the current conditions. The following flowchart outlines the role of ML in this paper.

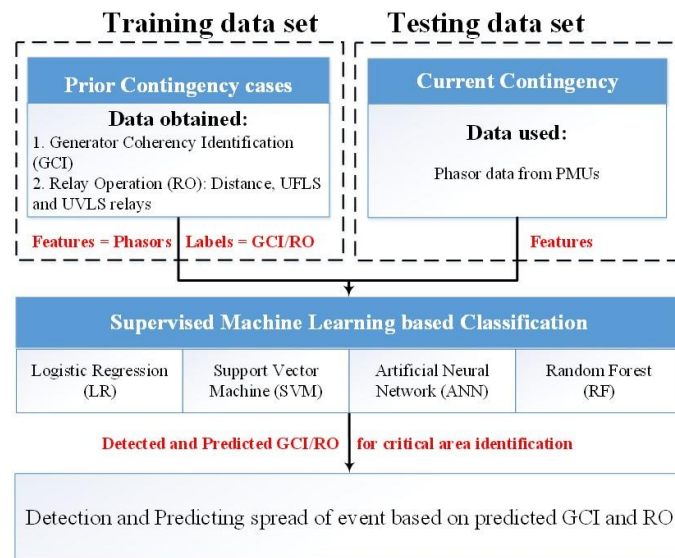


Fig. 1. Flowchart depicting the role of ML in advancing situational awareness

For this paper, an equivalent WECC system was used as a test case. Multiple $N-k$ contingencies, such as the outage of the WECC’s California-Oregon Intertie (COI), was modeled under different operating conditions, such as altered topology or changed dispatch. The ultimate goal of this paper is to not only detect the area affected by the fault in real-time ($t = 1 \text{ sec}$ in Fig. 2), but also be able to predict the spread of the event in advance ($t = 2.5 \text{ sec}$ in Fig. 2).

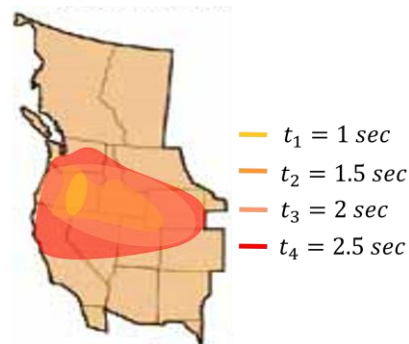


Fig. 2. An $N-3$ contingency case simulated in mini-WECC (120 bus system) for identifying the spread of the event

REFERENCES

- [1] P. Pourbeik, P. S. Kundur, and C. W. Taylor, “The anatomy of a power grid blackout,” *IEEE Power and Energy Magazine*, September 2006
- [2] M. K. Hedman, “Analytical approaches for identification and representation of critical protection systems in transient stability studies,” Ph.D. dissertation, School of Elect. Comput. & Energy Eng., Arizona State Univ., Tempe, AZ, USA, May 2017

An Early-recognition Algorithm of Power Systems Oscillation Detection based on Measurement Data

Hwanhee Cho and Byongjun Lee*
 School of Electric Engineering
 Korea University
 Seoul, Republic of Korea
 leeb@korea.ac.kr

Abstract—This paper proposes, an improvement of power system oscillation detection method and its implementation of oscillation monitoring system using power system measurements. The implemented monitoring systems are based on the nonlinear dynamics, represented on time-series 2-D plane, circulating oscillatory behavior is extracted from the data set. Moreover, Poincare surfaces are constructed and resampled by examining along the trajectory to determine impact of the oscillation to the system. Using proposed method, features of the oscillation can be identified and the early-recognition index can be provided. The oscillation monitoring system is tested on the IEEE 2nd benchmark test system to show fast detection features of the proposed algorithm and PMU example data of low frequency event is carried out to demonstrate practical application of algorithm.

Index Terms—Phasor measurement units, Power system measurements, Series compensation, Subsynchronous resonance, Time series analysis.

I. KEY CONCEPTS

The proposed method introduces the geometrical approach of dynamic system to detect measured values. Figure 1 shows key algorithm structure for the proposed algorithm. If the voltage is acquired from the system, the output is oscillation index and frequency of the oscillation.

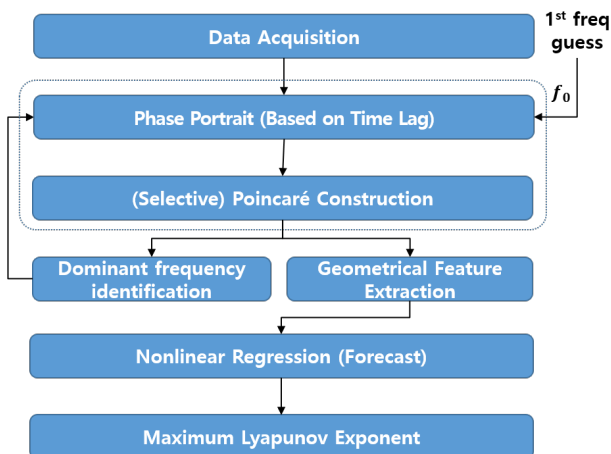
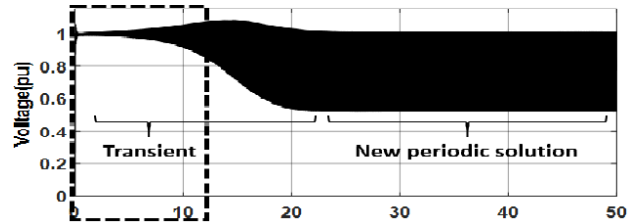


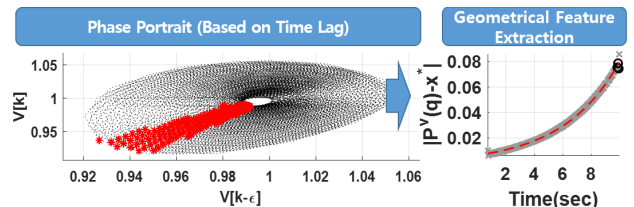
Fig. 1. Flowchart describing conceptual principle of the proposed algorithm.

II. KEY RESULTS

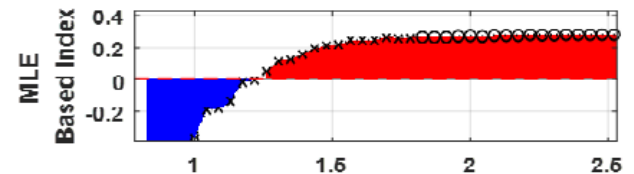
Figures below shows key results applying the proposed method at IEEE 2nd benchmark system.



(a) Voltage measured at fault location for 55% of compensation.



(b) Phase portrait and Poincaré construction(left) and geometrical feature extraction(right).



(c) Nonlinear oscillation detecting index based on the MLE (result of +0.250), the true detection time based on nonlinear regression is 1.8 second.

Fig. 2. Example of entire process for early-recognizing oscillation detection.

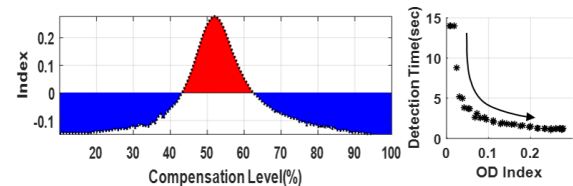


Fig. 3. The full scale compensation level scanning using proposed oscillation detection method(left) and inverse time characteristic of the detection algorithm(right).

III. SUMMARY

Positive MLE based index and the accuracy of the regression is high enough. System shows growing oscillatory behavior or unstable system.

GMD Mitigation Techniques in Power Systems

Pooria Dehghanian, *Student Member, IEEE*, and Thomas J. Overbye, *Fellow, IEEE*

Abstract— Geomagnetic disturbance (GMD) engenders significant threats to the power system infrastructures, potentially resulting in the bulk high-voltage power transformers half-cycle saturation, excessive system reactive power losses, and transformer over-heating, among others. This poster studies the mitigation techniques against the destructive impacts of geomagnetically induced currents (GICs) on the power grid. A hot-spot temperature analysis is conducted to identify the overheated transformers following a GMD event, and then a topology control approach is accomplished as a control mechanism to mitigate the overheating concerns. Additionally, generation re-dispatch process is selected as a first-aid control action to maintain the voltage and operating reserve requirements. All the control actions are tested on large-scale synthetic 2000-bus test system facing a GMD event, where the performance of the mitigation solutions is evaluated.

Keywords—geomagnetic disturbances (GMD); hotspot temperature; transformer; geomagnetic induced current (GIC), mitigation.

I. INTRODUCTION

When a GMD event occurs, GICs are injected into the grounding points of the power transformers resulting in additional reactive power consumption due to loss of magnetic flux and a local voltage drop accordingly. Moreover, due to the injection of GICs into the transformer core and windings, transformers overheating might occur. Hence, implementing practical solutions to mitigate the GIC’s impacts on the power grid is an urgent need. According to the literature, the most common mitigation practices are the generation re-dispatch, topology control (line, shunt and capacitor switching), and GIC blocking device deployment [1]. This poster practices a study of GMD mitigation process such as generation re-dispatch and reactive power control. We also provide a solution to alleviate the possible overheated transformers through network partitioning and topology control actions. The developed GIC model is founded based on the effective GIC current (for heating issue) and neutral current (for Var loss analysis) characterized by uniform earth conductivity. The corresponding temperature impacts are studied through a sensitivity analysis approach implemented in both normal and contingency scenarios.

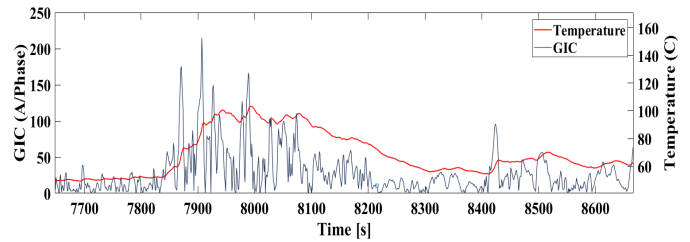


Figure 1. Transformer temperature response vs. GIC.

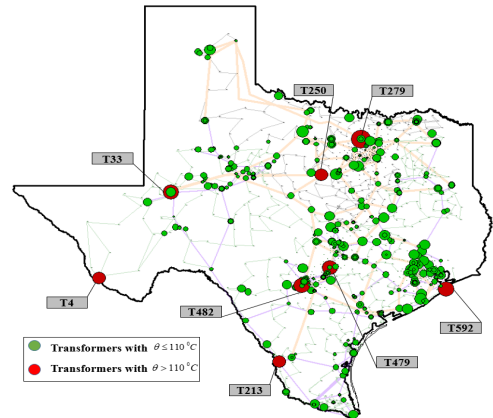


Figure 2. Identification of overheating transformers following a GMD event.

alleviate the transformer temperature rise above the thresholds prescribed by the IEEE standards [3].

III. GENERATION RE-DISPATCH OPERATING PROCEDURES

Figure 3 illustrates the overall procedure for the GMD-targeted protection and control. One GMD mitigation approach is to continuously monitor the transformer neutral current and, if the GIC measurements exceed the corresponding operating limit (~ 10 A) for about 10 minutes at one GIC-monitored transformer, an optimal re-dispatch action (as a corrective tool) would be initiated for the sake of re-routing the electricity flow across the network. Moreover, a contingency analysis is conducted in this study to further investigate the application of remedial actions on alleviation of the GMD aftermaths.

II. THERMAL MONITORING OF GIC-IMPACTED TRANSFORMERS

A. Approximate Transformer Heating Model

In order to infer the transformer heating response, an asymptotic thermal behavior is developed using the available NERC metallic hotspot thermal data to a DC-step injected current [2]. The impulse response of the transformer heating is found from the step unit function. The benchmark GMD E-field data from the case in 1989 is utilized to assess the corresponding GIC values as the input to the heating function. The heating function is closely dependent on transformer characteristics such as cooling constant.

B. Case Study and Control Actions

The proposed heating model will be demonstrated on the large-scale synthetic 2000-bus test case, shown in Fig. 2, to identify the vulnerable overheating transformers across the grid. Then, the remedial actions (network reconfiguration) will be implemented in both normal and contingency scenarios to

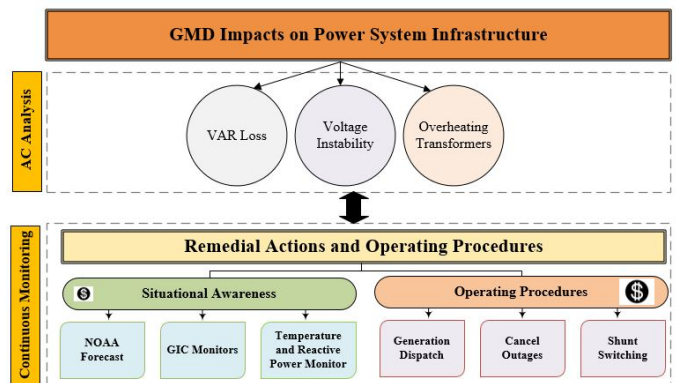


Figure 3. Overall GMD situational awareness and mitigation procedures.

REFERENCES

- [1] “Procedures for Solar Magnetic Disturbances Which Affect Electric Power Systems,” Developed by NPCC project C-15, 2007.
- [2] “Screening criterion for transformer thermal impact assessment”. Developed by the NERC project 2013-03.
- [3] “IEEE standard for general requirements for liquid-immersed distribution, power, and regulating transformers,” in *IEEE Std. C57.12.00-2015*.

Sequential Detection of Forced Oscillations in Power Systems using the CUSUM Procedure

Sanjay Hosur, *Student Member, IEEE*, Dongliang Duan, *Member, IEEE*
 Department of Electrical and Computer Engineering, University of Wyoming
 Laramie, Wyoming, USA

Abstract—The widespread deployment of Phasor Measurement Units (PMUs) makes it possible to monitor the power system operating conditions on-line in near real time. The FOs have a negative impact on the estimation of system modes and mode shapes when not properly accounted for. In this poster, the change-point detection decision statistics based upon the output-only covariance subspace method proposed in our previous work [1] is used in a sequential detection method, the cumulative sum (CUSUM) procedure, to achieve better detection performance.

Index Terms—Power system dynamics, synchrophasor data analysis, change-point detection, subspace-driven output-only system identification

I. KEY EQUATIONS

The same system model used in our previous work [1] is used here. The introduction of FOs basically means a change in the signal space, hence a change in the mean of the residue. In practice, it is not always possible to know the mean μ_1 after the change, especially in the case of on-line testing. Thus, two tests are run in parallel with introduction of minimum jump magnitude v_m that is chosen *a priori*. The stopping rules can be defined as:

When the mean **increases** after the change:

$$U_0 = 0 \quad (1)$$

$$U_n = \sum_{k=1}^n (y_n - \mu_0 - \frac{v_m}{2}) \quad (2)$$

$$m_n = \min_{0 \leq k \leq n} U_k \quad (3)$$

$$g_n^+ \stackrel{\text{def}}{=} U_n - m_n \quad (4)$$

$$\text{alarm when } g_n^+ > \lambda \quad (5)$$

When the mean **decreases** after the change:

$$T_0 = 0 \quad (6)$$

$$T_n = \sum_{k=1}^n (y_n - \mu_0 + \frac{v_m}{2}) \quad (7)$$

$$M_n = \max_{0 \leq k \leq n} T_k \quad (8)$$

$$g_n^- \stackrel{\text{def}}{=} M_n - T_n \quad (9)$$

$$\text{alarm when } g_n^- > \lambda \quad (10)$$

where λ is the threshold.

This work was in part supported by the Department of Energy under grant DE-SC0012671. Email: shosur@uwyo.edu, dduan@uwyo.edu.

II. RESULTS

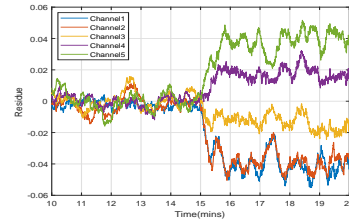


Fig. 1. The plot of the residue.

The simulation results are shown for a simplified system with 2 modes of the minniWECC selected as the poles. The modes are: 1) Montana Mode: a frequency at 0.549 Hz and a damping ratio of 7%; 2) BC Mode: a frequency at 0.626 Hz and a damping ratio of 2%. This is the same simplified system we used in our earlier work [1]. Fig. 1 shows the 5 channel residue and Fig. 2 shows the CUSUM statistics and CUSUM decision statistics. From these figures we see the FO is detected around the 15th minute as expected.

REFERENCES

- [1] S. Hosur and D. Duan, "Subspace-driven output-only based change-point detection of low-amplitude forced oscillations in power systems," in *2018 IEEE/PES Transmission and Distribution Conference and Exposition (T&D)*. IEEE, 2018, pp. 1–5.

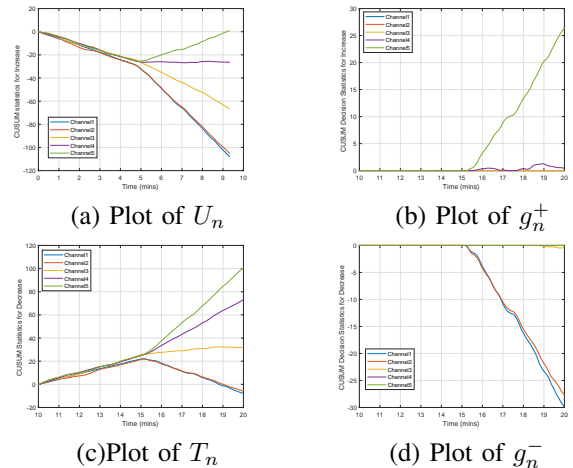


Fig. 2. The CUSUM statistics and CUSUM Decision statistics

An Unsupervised Learning Framework for Event Detection, Type Identification and Localization Using PMUs Without Any Historical Labels

Haoran Li, Yang Weng

Department of Electrical, Computer and Energy Engineering
Arizona State University, Tempe, AZ, USA
Email: {lhaoran,yang.weng}@asu.edu

Evangelos Farantatos, Mahendra Patel

Electric Power Research Institute
Palo Alto, CA, USA
Email: {efarantatos,mpatel}@epri.com

Abstract—The power system requires new monitoring and controls due to changes both at the generation side as well as the load side. Synchrophasor technology with synchronized and high-resolution measurements provided by Phasor Measurement Units (PMUs) has been recognized as a key contributing technology for advanced situational awareness, including event identification, where the application of machine learning techniques is a hot topic recently. However, recent methods focus on supervised learning techniques that require event records, which may be unavailable due to labeling cost. Even if labels exist, the uneven labeled data may cause biased learning models. To address these challenges, an unsupervised learning approach is proposed for conducting fast event identification. Specifically, a highly sensitive and accurate change-point detection method is firstly introduced for finding events via data distribution changes. After detection, event type identification is achieved via a two-stage information filtering. In stage 1, we use cluster number in principal component analysis (PCA) to split the event types. In stage 2, we narrow down the type by evaluating cluster compactness for measuring event severity. Finally, we solve the event localization problem based on a hierarchical clustering to group PMUs with significant changes across change points. Numerical results show fast and robust performances of the proposed methods for different events at different locations.

Power System Fundamental Frequency Estimation Using Unscented Kalman Filter

Cheng Qian, *Graduate Student Member, IEEE*, Mladen Kezunovic, *Life Fellow, IEEE*

Dept. of Electrical and Computer Engineering
Texas A&M University, College Station, TX
peterqiancheng@tamu.edu, kezunov@ece.tamu.edu

Abstract—Fundamental frequency is one of the most vital metrics of the power grid. Numerous frequency estimation techniques have been proposed, which are based on parameterization of deterministic signal models. Cautions should be taken since uncertainties such as noise are common in raw waveform measurements, and will propagate into estimation results. In order to mitigate the adverse impact of measurement noise, most recently, Kalman filter-based approaches were promoted, and are giving promising results. Nevertheless, conventional Kalman filter or extended Kalman filter have limited performance due to the high nonlinearity of the underlying state equations. In order to adapt to nonlinearity, this paper proposed a technique that leverages the Unscented Kalman Filter (UKF). The paper also introduces an approach that employs three-phase measurements to improve the overall frequency estimation accuracy. Simulation results show that the proposed UKF-based approach achieves extremely high fundamental frequency calculation accuracy despite severe noise interference.

Index Terms—Frequency estimation, Kalman filter, uncertainty, unscented Kalman filter, power system measurement

I. METHODS AND KEY EQUATIONS

A. Three-Phase Waveform Models

Denote phase A voltage as x_k , phase B voltage as y_k , and phase C voltage as z_k .

$$x_k = A \cdot \cos(\omega k \Delta t + \phi_0) \quad (1a)$$

$$x_{k+1} = A \cdot \cos[\omega(k+1)\Delta t + \phi_0] \quad (1b)$$

$$x_{k+2} = A \cdot \cos[\omega(k+2)\Delta t + \phi_0] \quad (1c)$$

It can be proven that:

$$x_{k+2} + x_k = 2x_{k+1} \cdot \cos(\omega \Delta t) \quad (2)$$

Similarly, for phase B and C:

$$y_{k+2} + y_k = 2y_{k+1} \cdot \cos(\omega \Delta t) \quad (3a)$$

$$z_{k+2} + z_k = 2z_{k+1} \cdot \cos(\omega \Delta t) \quad (3b)$$

Moreover, it can be observed that:

$$y_k = x_k \cos\left(-\frac{2}{3}\pi\right) + \frac{x_k \cos(\omega \Delta t) - x_{k-1}}{\sin(\omega \Delta t)} \sin\left(-\frac{2}{3}\pi\right) \quad (4a)$$

$$z_k = x_k \cos\left(\frac{2}{3}\pi\right) + \frac{x_k \cos(\omega \Delta t) - x_{k-1}}{\sin(\omega \Delta t)} \sin\left(\frac{2}{3}\pi\right) \quad (4b)$$

B. State-Space Models

In order to fit into the framework of UKF, the signal models in Eq. (1)-(4) should be reformulated to state-space representation.

$$x_{1,k} = x_k, x_{2,k} = x_{k-1}, x_{3,k} = \omega \Delta t \quad (5a)$$

$$y_{1,k} = x_k, y_{2,k} = y_k, y_{3,k} = z_k \quad (5b)$$

$$x_{1,k+1} = -x_{2,k} + 2x_{1,k} \cos(x_{3,k}) \quad (5c)$$

$$x_{2,k+1} = x_k = x_{1,k} \quad (5c)$$

$$x_{3,k+1} = x_{3,k} \quad (5d)$$

$$y_{1,k+1} = x_{1,k+1} \quad (5e)$$

$$y_{2,k+1} = x_{1,k+1} \cos\left(\frac{2}{3}\pi\right) \quad (5f)$$

$$- \frac{x_{1,k+1} \cos(x_{3,k+1}) - x_{2,k+1}}{\sin(x_{3,k+1})} \sin\left(\frac{2}{3}\pi\right)$$

$$y_{3,k+1} = x_{1,k+1} \cos\left(\frac{2}{3}\pi\right) \quad (5g)$$

$$+ \frac{x_{1,k+1} \cos(x_{3,k+1}) - x_{2,k+1}}{\sin(x_{3,k+1})} \sin\left(\frac{2}{3}\pi\right)$$

II. KEY RESULTS

TABLE I. SUMMARY OF FREQUENCY ESTIMATION BIAS

Case Details	UKF-Single Phase	UKF-Three Phase
Steady-state unbalanced	$< 1 \times 10^{-5}$ Hz	$< 5 \times 10^{-6}$ Hz
Steady-state harmonics	$< 1 \times 10^{-6}$ Hz	$< 1 \times 10^{-6}$ Hz
Amplitude modulation	$< 5 \times 10^{-6}$ Hz	$< 2 \times 10^{-6}$ Hz
Phase modulation	$< 1 \times 10^{-6}$ Hz	$< 1 \times 10^{-6}$ Hz
Frequency ramping	$< 1 \times 10^{-6}$ Hz	$< 1 \times 10^{-6}$ Hz

TABLE II. INFLUENCE OF SIGMA POINT SELECTION ON BIASES IN FREQUENCY ESTIMATION

Case Details	20dB Noise	40dB Noise
$\alpha = 1 \times 10^{-3}$ $\beta = 2, \kappa = 0$	5×10^{-4} Hz	5×10^{-4} Hz
$\alpha = 0.1$ $\beta = 2, \kappa = 0$	$< 5 \times 10^{-7}$ Hz	$< 5 \times 10^{-7}$ Hz
$\alpha = 0.1$ $\beta = 4, \kappa = 0$	1.5×10^{-6} Hz	5×10^{-7} Hz
$\alpha = 0.1$ $\beta = 2, \kappa = 2$	5×10^{-7} Hz	5×10^{-7} Hz

Scalable Coordinated Control of Energy Storage Systems for Enhancing Power System Angle Stability

Mohammadali Rostami, *Student Member, IEEE*, Saeed Lotfifard, *Member, IEEE*

Abstract—In this paper a scalable wide area control scheme using distributed model predictive control (DMPC) is proposed to enhance the angle stability of power systems following large disturbances. In this regard, dynamic model of the local subsystems in the multi-area power system is developed for the model predictive controller and each subsystem is controlled by the associated controller. The controller of each subsystem exchanges minimum information with the controllers of neighboring subsystems to reach the final result. The proposed controller works based on optimality condition decomposition (OCD) to coordinate the subsystems. In the proposed wide area control system, the available actuators are mechanical power and field voltage controller of synchronous generator, and energy storage systems (ESS) which are able to provide synchronizing power support. The simulation results demonstrate the effectiveness of the proposed method to improve the angle stability of power systems subsequent to severe disturbances in the system.

I. INTRODUCTION

Dynamic stability is an important factor that needs to be considered for reliable and secure operation of electric power grids. Effective control schemes support the synchronism of generators after severe disturbances in modern power systems that are operated closer to their stability limits. With the increasing deployment of fast communication systems and fast responding devices, it is possible to utilize smart grid technologies in a coordinated approach for improving rotor angle stability of the network by developing appropriate system-wide emergency control schemes. In this paper, a wide area control system using MPC is proposed to enhance the angle stability of power systems by controlling fast responding ESSs and synchronous generators. To assure the scalability of the proposed methodology, it is implemented in a distributed structure. The dynamic model of subsystems in the multi-area power system is developed locally and local controllers solve their own MPC using local models and measurements and exchange information with neighboring subsystems controllers to reach final results. It is assumed that the power system is already decomposed to local subsystems and optimality condition decomposition (OCD) method is employed to coordinate the local MPC problems in each subsystem. The schematic of the distributed network and control links is depicted in Fig .1.

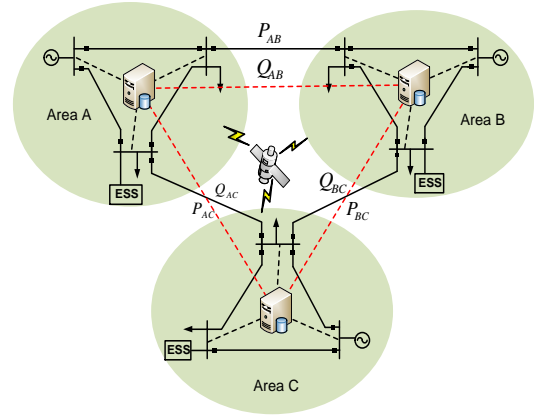


Fig. 1. Power system partitioned to non-overlapping subsystems

II. RESULTS SUMMARY

To demonstrate the performance of the proposed DMPC-based angle stability controller, it is applied to the 68-bus test system. The rotor angle of generators with and without proposed controller are plotted in Fig. 2 and 3. As the results shows the proposed MPC-based stability controller is able to stabilize the system and bring back the generators to synchronism.

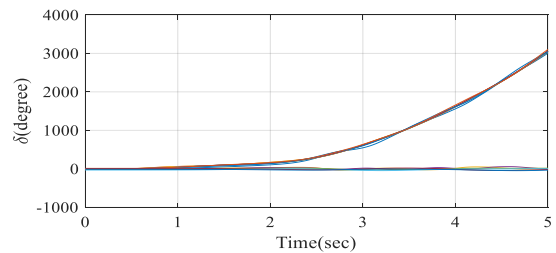


Fig. 2. Rotor angle of generators with conventional controls

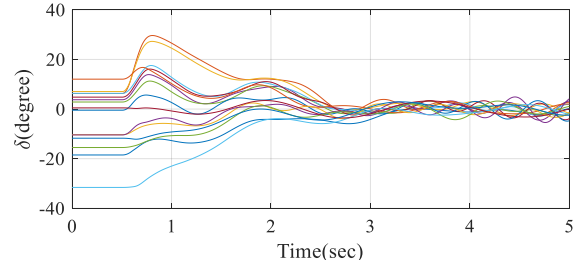


Fig. 3. Rotor angle of generators with proposed MPC-based controller

Effective Scenario Selection for Preventive Stochastic Unit Commitment during Hurricanes

Yuanrui Sang and Mostafa Sahraei-Ardakani
 Department of Electrical and Computer Engineering
 University of Utah
 Salt Lake City, USA
 {yuanrui.sang, mostafa.ardakani}@utah.edu

Jiayue Xue and Ge Ou
 Department of Civil and Environmental Engineering
 University of Utah
 Salt Lake City, USA
 {jiayue.xue, Ge.Ou}@utah.edu

Abstract—In 2017, four hurricanes made U.S. landfalls, leading to millions of customer outages. Our previous work shows that weather forecast can be used to estimate the failure of transmission lines during hurricanes; these failure estimations can be effectively used in stochastic optimizations and guide preventive operation to reduce outages. However, the large number of possible contingency scenarios, caused by hurricanes, makes preventive operation extremely computationally burdensome. The problem can be practically solved with only a small number of representative scenarios. Thus, the effectiveness of preventive operation would directly depend on the scenario selection process. This paper examines two scenario selection methods, which eliminate (a) the unlikely and (b) the inconsequential scenarios. Simulation studies were carried out on IEEE 118-bus system, mapped to the Texas transmission network, using Hurricane Harvey wind data. This study sheds light on the effective selection of an appropriate number of scenarios with acceptable computational complexity.

I. METHODOLOGY

In this study, part of the IEEE 118-bus test system was mapped to the Texas transmission system, and the wind speed during Hurricane Harvey was used to calculate the transmission line failure rate during the hurricane. Results showed that 22 lines could fail, and there was a total of 4,194,304 contingency scenarios. Running a stochastic preventive operation model over such a large number of contingency scenarios is computationally intractable; thus, this study aims at comparing two methods for scenario selection, namely, the probability-based method and the importance-sampling-based method. In the probability-based method, the scenarios with the highest probabilities were selected. In the importance-sampling-based method, the likelihood of selecting a scenario is proportional to its contribution to the objective of the stochastic optimization problem [1].

II. KEY RESULTS

Results showed that the expected dispatch cost, including high penalty costs for lost load and over-generation, obtained under each unit commitment solution, decreases with the increasing number of scenarios. The expected dispatch cost converges to a certain level as the number of scenarios increase. With an extremely small number of scenarios, such as one scenario, neither of the two methods is guaranteed to select a representative scenario set. With a relatively small number of scenarios, the importance sampling method is more effective; but when the number of scenarios is large enough for expected dispatch cost to converge, both scenario selection methods are similar in effectiveness. With similar effectiveness, the probability-based selection method is preferred, because it is much easier to implement compared to the importance sampling method. The computational complexity is highly correlated to the number of

scenarios considered; thus, it is ideal to use the number of scenarios right at the convergence of expected dispatch costs. However, in case that only a relatively small number of scenarios can be chosen due to the limitation of computational resources, the importance sampling method is more effective than the probability-based method in general.

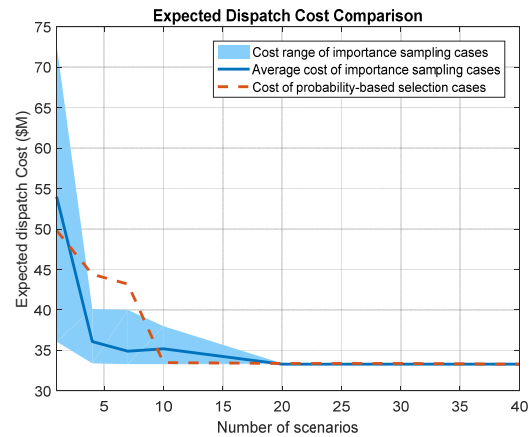


Fig. 1. Comparison of expected cost considering all possible scenarios

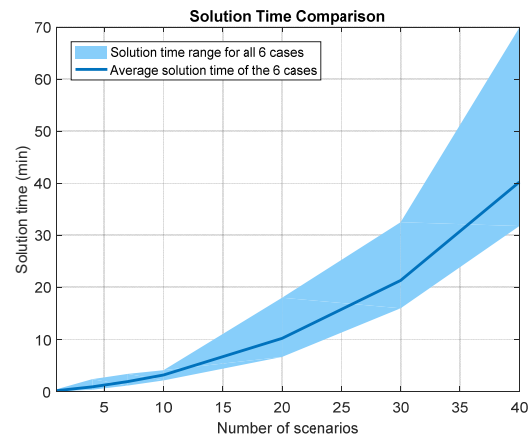


Fig. 2. Solution time comparison under different numbers of scenarios

REFERENCES

- [1] Y. Sang, M. Sahraei-Ardakani, J. Xue and G. Ou, "Effective Scenario Selection for Preventive Stochastic Unit Commitment during Hurricanes," in proc. 2018 IEEE International Conference on Probabilistic Methods Applied to Power Systems (PMAPS), Boise, ID, 2018, pp. 1-6.

Data Driven Oscillation Source Detection in an Islanded Unbalanced Microgrid Using Innovative Ensemble Learning

Hasan UI Banna, *Student Member, IEEE*, Sarika Khushalani Solanki, *Senior Member, IEEE*, and Jignesh Solanki, *Senior Member, IEEE*

Abstract—Islanded microgrid experiences various stability issues due to low physical inertia which also makes it susceptible to Oscillations resulting from loads perturbation and unpredictable renewable energy sources. This work identifies the source location of these oscillations using measurements, offline estimation and classification models. The performance of these offline models is ranked for each reported feature to use highly ranked models during online stage. The proposed framework named as credibility search ensemble learning (CSEL) would be tested and validated in an islanded unbalanced microgrid. The reliability and robustness of the proposed framework would also be checked against measurement noise as well as for partially observable system.

Index Terms—Ensemble learning, power oscillations, support vector machine, random forest classifier.

I. INTRODUCTION

The necessity of reducing environmental pollution caused by the production of electricity is inevitable. A microgrid could fulfill this need by implementing clean energy production. It consists of distributed energy resources (DERs), energy storage, loads and controllers. A microgrid can be operated in grid-connected mode as well as in islanded (standalone) mode where it serves a small geographical area. Compared to grid-connected mode, a microgrid in islanded mode may experience various stability issues. Further, lack of spinning reserves and low physical inertia make its dynamic response quicker than conventional rotating machines. This increases islanded microgrid’s susceptibility towards oscillations resulting from highly fluctuating loads, intermittent renewable sources or malfunctioning of feedback controllers [1]. These oscillations may cause increased losses, power quality degradation, increased EMI and converter overloading [2]. Hence, detection and real time analysis of these oscillations is inevitable. In our previous works, we investigated the detection of power oscillations in a transmission system utilizing data mining based approach. Data mining models such as support vector machine (SVM), random forest classifier (RF), extreme learning machine (ELM) etc. can provide computationally efficient solutions which are needed for oscillation source detection. While there are no current technologies that exist related to the detection of oscillations source in islanded microgrid using ensemble of data mining techniques according to our knowledge, we do not rule out emerging technologies.

II. PROPOSED OSCILLATION SOURCE DETECTION

Individual classification models $\{Y_{SVM}, Y_{DT}, Y_{RF}\}$ are trained offline for data $D = \{(\{x_{11}, x_{12}, x_{13}, \dots, x_{1N}\}, y_1), (\{x_{21}, x_{22}, x_{23}, \dots, x_{2N}\}, y_1), \dots\}$.

Algorithm 1: Proposed CSEL Algorithm

Input:

- a) $\{X_1, X_2, \dots, X_M\} \leftarrow$ Input Feature vectors for offline training
- b) $F_i : \langle V, \theta, \delta, \omega \rangle$ are the streams of features
- c) $\{Y_{SVM}, Y_{DT}, Y_{RF}\} \leftarrow$ Available classifiers for offline credibility determination for individual feature X_i
- d) $\{W_1, W_2, \dots, W_t\} \leftarrow$ online real-time testing stream

Output:

- a) $Y_{Di} : \langle Y_1, Y_2, \dots, Y_M \rangle$ for each D_i
- b) $Y_f \leftarrow$ final oscillation source location

```

1: for t < no. of features+1
2:   for c = 3
3:     K-fold validation with  $\langle Y_{SVM}, Y_{DT}, Y_{RF} \rangle$  end for
4:   record  $Y_{Di}$  for each iteration
5: end for offline training ends
6: retrieve  $\langle Y_1, Y_2, \dots, Y_M \rangle$  from offline training
7:  $\{(W_1, Y_1), (W_2, Y_2), \dots, (W_t, Y_t)\}$  real-time testing
8: final aggregation  $Y_f = f(Y_{Di})$ 
9: Output  $Y_f \leftarrow$  oscillation source location
    
```

Fig. 1: Proposed algorithm

$\{(\{x_{M1}, x_{M2}, x_{M3}, \dots, x_{MN}\}, y_M)\}$. An ensemble of these classification models, whose individual decisions are combined by weighted approach explained above locates the source of oscillation using online measurements. This credibility search ensemble learning approach is explained in detail in Fig. 1. PMU measurement set $X = \{X_1, X_2, X_3, \dots, X_N\}$ with feature vector $X_i = \{V, \theta, \delta, \omega\}$ and classification models $\{Y_{SVM}, Y_{DT}, Y_{RF}\}$ with relatively high prediction accuracy are validated using k-fold cross validation. The classification model that has maximum accuracy, for each feature during offline validation, is selected as credible model during online source localization stage. The final decision $\pi = f\{Y_1, Y_2, \dots, Y_K\}$, contains possible locations of oscillation source obtained by aggregating weighted decisions of each classification model. Fig. 2 shows the mis-classification rate of the considered classifiers during offline validation stage.

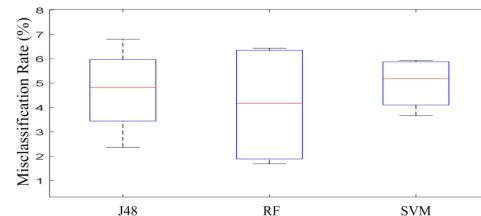


Fig. 2: Box plots of misclassification rate for individual models

REFERENCES

- [1] A. M. Bouzid, J. M. Guerrero, A. Cheriti, M. Bouhamida, P. Sicard, and M. Benganem, A survey on control of electric power distributed generation systems for microgrid applications, *Renew. Sustain. Energy Rev.*, vol. 44, pp. 751766, 2015.
- [2] Saghaei, Hadi, et al. "Power oscillation damping in standalone microgrids using integrated series compensator." 2012 Twenty-Seventh IEEE Applied Power Electronics Conference and Exposition (APEC), 2012.

An Improved Cumulant Method for Probabilistic Load Flow Calculation

Wang Chenxu¹, Tang Fei^{1*}, Zhao Hongsheng², Zhou Yixi¹, Liu Chang¹, Wang Feifei¹,

¹School of Electrical Engineering and Automation Wuhan University Wuhan, 430072, China

²Economic and Technology Research Institute of State Grid Hubei Electric Power Company, 430077, Wuhan, China

Email: tangfei@whu.edu.cn

Abstract—This paper proposes an improved cumulant method for probabilistic load flow calculation. The proposed method combined cumulant method and K-means clustering technique. Firstly, the output power of wind farms is divided into several clusters by K-means technique. Then, the conventional cumulant method is performed in each cluster to obtain the probability distributions of output random variables. Finally, the probabilistic load flow results are obtained by integrating probability distributions of output random variables and corresponding weight of each cluster. The performance of the proposed method is evaluated on a modified IEEE 30-bus system. The simulation results demonstrate that the proposed method could yield accurate results with a low computational burden, and it also overcomes the limitation of existing series expansion methods to approximate multimodal probability distributions.

Index Terms—probabilistic load flow; cumulant; wind power; K-means clustering

I. INTRODUCTION

The uncertainties brought by the great proliferation of renewable energy sources (RES) have a great impact on power systems. By means of the appropriate modeling of uncertainties, probabilistic load flow (PLF) [1] could provide more valuable results, e.g. the likelihood that a bus voltage falls outside its respective permissible limit. However, with the large-scale RES integrated with the power system, traditional PLF techniques are not suitable and suffer from several drawbacks such as computational burden, sensitive accuracy to the complexity of systems, and incapability of approximating multimodal probability distribution. The motivation of this research is developing a cumulant-based method that adequate for the PLF calculations of power systems with a high proliferation of RES.

II. METHODOLOGY

The proposed method consists of two parts: the K-means technique and cumulant method [2]. The procedure of the proposed method can be stated briefly as follow:

- i. Calculate the moment of input variables in the i -th cluster and convert moment to cumulant;
- ii. Perform cumulant method with each cluster;
- iii. Calculate the cumulant of output RVs;
- iv. Reconstruct the probability distribution of output variables through expansion series;
- v. Repeat form step i-v to get the probability distribution of output variables in each clusters.

Finally, the entire probability distribution of outputs

can be calculated by integrating the probability distribution of output random variables and corresponding weight of each cluster.

III. KEY RESULTS

The performance of the proposed method is verified in IEEE 30-bus system. The parameters of wind farms are shown in TABLE I. The wind speeds are modelled as Weibull distribution with $c=8.0$ and $k=2.2$. The correlation factor of the wind speed of each wind farm is shown in (1). The results are compared with SRSMCS and LHSMCS [3]. The simulation results are shown in Fig. 1.

TABLE I. PARAMETERS OF THE WIND FARMS

Bus	Parameters			
	P_r (MW)	V_{ci} (m/s)	V_r (m/s)	V_{co} (m/s)
4	30	3	15	25
12	30	3	15	25
21	25	3	15	25

$$\rho = \begin{bmatrix} 1 & 0.9 & 0.7 \\ 0.9 & 1 & 0.7 \\ 0.7 & 0.7 & 1 \end{bmatrix} \quad (1)$$

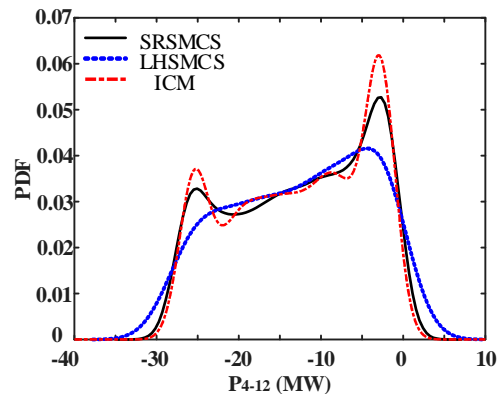


Fig. 1 PDF curves of P₄₋₁₂

REFERENCES

- [1] B. Borkowska, "Probabilistic load flow," *IEEE Trans. Power App. Syst.*, vol. PAS-93, no. 3, pp. 752–755, May/June 1974.
- [2] J. Usaola *et al.*, "Probabilistic load flow with wind production uncertainty using cumulants and Cornish-Fisher expansion," *Int. J. Electr. Power Energy Syst.*, vol. 31, no. 9, pp. 474–481, Oct. 2009.
- [3] Y. Chen, J. Wen, and S. Cheng, "Probabilistic load flow method based on Nataf transformation and latin hypercube sampling," *IEEE Trans. Sustain. Energy*, vol. 4, no. 2, pp. 294–301, Apr. 2013.